

**Tropical Basidiomycota – a prolific source of novel natural
products with prominent biological activities**

Von der Naturwissenschaftlichen Fakultät
der Gottfried Wilhelm Leibniz Universität Hannover

zur Erlangung des Grades

Doktorin der Naturwissenschaften (Dr. rer. nat.)

genehmigte Dissertation

von

Tian Cheng, M.Sc. (China)

2020

Referent: Prof. Dr. Russell J. Cox

Korreferent: Prof. Dr. Marc Stadler

Korreferent: Prof. Dr. Peter Spiteller

Tag der Promotion: 03.09.2020

Vorveröffentlichungen der Dissertation

Teilergebnisse aus dieser Arbeit wurden mit Genehmigung der Fakultät für Lebenswissenschaften, vertreten durch den Mentor der Arbeit, in folgenden Beiträgen vorab veröffentlicht:

Publikationen

1. Cheng T., Chepkirui C., Decock C., Matasyoh J.C., Stadler M., Sesquiterpenes from an Eastern African medicinal mushroom belonging to the genus *Sanghuangporus*. *J. Nat. Prod.*, 2019, **82**: 1283-1291.
2. Chepkirui C.*, Cheng T.*, Sum W.C., Matasyoh J.C., Decock C., Praditya D.F., Wittstein K., Steinmann E., Stadler M., Skeletocutins A-L: antibacterial agents from the Kenyan wood-Inhabiting basidiomycete, *Skeletocutis* sp. *J. Agric. Food. Chem.*, 2019, **67**: 8468-8475. (*co-first author)
3. Cheng T., Chepkirui C., Decock C., Matasyoh J.C., Stadler M., Skeletocutins M-Q: biologically active compounds from the fruiting bodies of the basidiomycete *Skeletocutis* sp. collected in Africa. *Beilstein. J. Org. Chem.*, 2019, **15**: 2782-2789.
4. Chepkirui C., Cheng T., Matasyoh J.C., Decock C., Stadler M., An unprecedented spiro [furan-2,1'-indene]-3-one derivative and other nematicidal and antimicrobial metabolites from *Sanghuangporus* sp. (Hymenochaetaceae, Basidiomycota) collected in Kenya. *Phytochem. Lett.*, 2018, **25**:141-146.
5. Chepkirui C., Sum W.C., Cheng T., Matasyoh J.C., Decock C., Stadler M., Aethiopinolones A-E, new pregnenolone type steroids from the East African basidiomycete *Fomitiporia aethiopica*. *Molecules*, 2018, **23**: e369.
6. Phukhamsakda C., Macabeo A.P.G., Huch V., Cheng T., Hyde K.D., Stadler M., Sparticolins A-G, biologically active oxidized spirodioxynaphthalene derivatives from the ascomycete *Sparticola junci*. *J. Nat. Prod.*, 2019, **82**: 2878-2885.
7. Sandargo B., Chepkirui C., Cheng T., Chaverra-Munoz L., Thongbai B., Stadler M., Hüttel S., Biological and chemical diversity go hand in hand: Basidiomycota as source of new pharmaceuticals and agrochemicals. *Biotechnol. Adv.*, 2019, **37**: 107344.

Conference Talks

1. Cheng T. Exploitation of the secondary metabolites from tropical Basidiomycota. *9th Annual Retreat, HZI Graduate School, Quedlinburg, Germany (2018)*
2. Cheng T. Characterization of the secondary metabolites from tropical Basidiomycota. *H2020-RISE Workshop “GoMyTRi”, Bangkok, Thailand (2018)*
3. Cheng T. Novel bioactive secondary metabolites from tropical Basidiomycota. *International Conference of Deutsche Gesellschaft für Mykologie (DGfM), Möhnesee, Germany (2018)*
4. Cheng T. Study of the bioactive secondary metabolites from tropical Basidiomycota. *10th Annual Retreat, HZI Graduate School, Braunschweig, Germany (2019)*

Conference Posters

1. Cheng T. Characterization of novel bioactive compounds from tropical Basidiomycota. *8th Annual Retreat, HZI Graduate School, Harzhöhe, Goslar – Hahnenklee, Germany (2017)*
2. Cheng T. Exploitation of novel secondary metabolites from Kenyan Basidiomycota. *HZI 10th International PhD Symposium, Braunschweig, Germany (2017)*
3. Cheng T. Biologically active compounds from tropical Basidiomycota. *Fungal Autumn School: Introduction to fungal diversity, cultivation and determination of fungi, Freudenstadt, Germany (2017)*
4. Cheng T. Characterization of novel secondary metabolites from tropical Basidiomycota. *HZI 11th International PhD Symposium, Braunschweig, Germany (2018)*
5. Cheng T. Exploitation of Kenyan tropical Basidiomycota for bioactive secondary metabolites. *3rd European Conference on Natural Products, Frankfurt, Germany (2018)*
6. Cheng T. Kenyan Basidiomycota-a great resource of novel bioactive compounds. *18th congress of European Mycologists, Warsaw-Białowieża, Poland (2019)*

Acknowledgment

First of all, I want to give my cordial gratitude to my dear supervisor Prof. Dr. Marc Stadler, you are the most open-hearted man I have ever met. I still remember the first time I contacted you via email to ask for a chance to be a PhD student in your group, what the group was doing was so interesting for me even though I have a different background. After your patient explanation and kind guidance, I did encourage myself to do research in Germany. I am so grateful that you gave me the chance even you didn't know much about me. From that time, I did believe that an exciting adventure into Fungi is waiting for me and I will have a super nice mentor. Thank you for your encouragements, they really made me braver in the lab and gave me the chance to explore the beautiful science. Your mentorship is an invaluable gift for me and I am sure it will be a light tower in my life.

I also want to thank my co-supervisor Prof. Dr. Russell J. Cox for your professional supervision when I stayed in Hannover. I also want to thank the members of my thesis committee Russell and Prof. Dr. Alice C. McHardy for the valuable advice that made my project successful.

I am also grateful to my colleagues and all the co-authors Clara, Winnie, Josphat, Kathrine, Dimas, and Eike whom and I had a great pleasure working with.

I would also like to thank Dr. Cony Decock who collected the fungal specimens studied in this thesis, and your advice for my manuscripts.

For the girls at B2.77 office: Clara, I really thank you for your help and guidance. Birthe, thank you for your kindness forever. Zeljka, Khadija, and Lucile, your passion and power to life encourage me a lot in the last years. Thank you all for accompanying me.

I also would like to thank Dongsong and Eric for their support during my stay in Hannover.

I want to thank all the current and former members of MWIS. You made my time in Braunschweig and HZI great.

Thank you, Christel, Esther, Wera, and all the technicians from MWIS for your support with NMR, MS, Maxis service, and cytotoxicity tests. Thank you, Katja and the technicians from BMWZ for your kindness to prepare media and solutions.

I would like to thank the bachelor student Darius, thank you for the hard work when you were around.

Thank you, Jennifer, Noppol, Tonny, Bank, and Aey, thank you for the happiness you brought during our stay in Thailand.

Kung, Wilawan and Whitney, I am missing the nice lunch breaks with you, thank you for the nice time you brought without a doubt.

I would like to acknowledge the financial support from CSC (201606870045) for funding my stay here in Germany. I would also like to acknowledge the financial support from the European Union under the Rise project “GoMYTRi” during my stay in Thailand.

Many thanks to my family for their support and all Chinese friends for all the happy times at parties and sports. Finally, I would like to thank my husband for accompanying me all the time.

Contents

Acknowledgment	iii
Abstract	viii
Abbreviations and Units	x
Declaration of Contribution to the Publications	xi
1. Introduction.....	1
1.1 History of Antibiotics and Antimicrobial Resistance.....	1
1.2 Natural Products from Fungi	7
1.3 Agrochemicals and Drug Candidates from Basidiomycota.....	9
1.4 Biosynthesis of Secondary Metabolites in Basidiomycota.....	16
1.5 Aim of the Thesis	18
2. Experimental Section.....	20
2.1 Chemicals	20
2.2 Media, Buffers and Solutions	21
2.3 Enzyme and Antibiotics.....	26
2.4 Specimen Collection and Isolation	26
2.5 Fungal Identification.....	26
2.6 Agar Diffusion Assay for Preliminary Screening.....	27
2.7 Cultivation and Extraction of Small Scale Fermentation	27
2.8 Antimicrobial Assay for Small Scale Crude Extracts	28
2.9 Analytical LC-MS	28
2.10 Analytical GC-MS	29
2.11 Scale-up Fermentation and Extraction	29
2.12 Purification of Compounds by Preparative LC-MS	29
2.13 Structure Elucidation	30
2.14 Bioactivity Tests for Pure Compounds.....	31
2.14.1 Serial Dilution Assay.....	31
2.14.2 Biofilm Inhibition Assay	31
2.14.3 Nematicidal Assay.....	32
2.14.4 Cytotoxicity Assay	32
2.14.5 Leucine Aminopeptidases Inhibition Assays	33
2.14.6 Inhibitory Effects on HCV Infectivity.....	33
2.15 Microbial Strains Used for Biosynthesis	34

2.16	Molecular Biology Methods for Biosynthesis.....	34
2.16.1	Oligonucleotides.....	34
2.16.2	Polymerase Chain Reaction (PCR).....	35
2.16.3	RNA Extraction and cDNA Preparation	35
2.16.4	Construction of Vectors In this Thesis	35
2.16.5	Agarose Gel Electrophoresis	35
2.16.6	DNA Purification from Gel or PCR	36
2.16.7	Isolation of Plasmid DNA from <i>E. coli</i>	36
2.16.8	Isolation of Plasmid DNA from <i>S. cerevisiae</i>	36
2.16.9	Cloning Procedure	36
2.17	Transformation of Chemically Competent <i>Escherichia coli</i> Cells.....	37
2.17.1	Growth of <i>E. coli</i> Strain.....	37
2.17.2	Transformation	37
2.18	Transformation of Competent <i>Saccharomyces cerevisiae</i> Cells	37
2.18.1	Growth of <i>S. cerevisiae</i> Strain.....	37
2.18.2	Transformation	37
2.19	PEG-mediated Transformation of <i>Aspergillus oryzae</i> NSAR1	38
2.19.1	Growth of <i>A. oryzae</i> Strain.....	38
2.19.2	Transformation	38
3.	Results and Discussion.....	40
3.1	Secondary Metabolites from <i>Sanghuangporus</i> species	40
3.1.1	Sesquiterpenes from <i>Sanghuangporus</i> sp. (MUCL 56354).....	40
3.1.2	Unprecedented Metabolite from <i>Sanghuangporus</i> sp. (MUCL 55592)	43
3.2	Antibacterial Agents from <i>Skeletocutis</i> sp. (MUCL 56074)	44
3.2.1	Antibacterial Agents from Liquid Cultures of <i>Skeletocutis</i> sp.	44
3.2.2	Undescribed Metabolites from Fruiting Bodies of <i>Skeletocutis</i> sp.	48
3.3	Pregnenolone Type steroids from <i>Fomitiporia aethiopica</i> (MUCL 56047)	50
3.4	Novel Metabolites from <i>Heimiomyces</i> sp. (MUCL 56078)	51
4.	Additional Project - Illudin Biosynthesis in <i>Omphalotus olearius</i>	56
4.1	Introduction	56
4.1.1	Biological Activity	56
4.1.2	Biosynthesis of Illudins – <i>status quo</i>	58
4.2	Project Aims	65
4.3	Results	65
4.3.1	Analysis of Potential Illudin Biosynthetic Gene Clusters	65
4.3.2	Heterologous Expression of the Illudin BGC in <i>A. oryzae</i>	68

5. Conclusion and Discussion	74
6. References	77
7. Appendices.....	91
8. Publications of the thesis	94

Abstract

The phylum Basidiomycota constitutes the second-largest higher taxonomic group of the Kingdom Fungi after the Ascomycota and comprises *ca* 35,000 species (Halling *et al.*, 1997). They have been proved to be a considerable resource for novel natural products. However, only a small number (~ 2%) of these fungi have been cultured and studied for their potential of producing useful secondary metabolites. The combination of extensive fieldwork, morphology study, phylogeny analysis, biotechnology process, and analytical chemistry resulted in a high discovery rate of novel metabolites. The research in this thesis focuses on the characterization of bioactive secondary metabolites from basidiomycetes originated from Kenyan Kakamega tropical forest and Mount Elgon national reserve. Twenty-seven strains were cultivated in three standard media. Extractions from both mycelia and supernatant were screened by antimicrobial assays and LCMS analysis (Appendix). Five strains were selected for scale-up fermentation, which led to the identification of forty-three previously undescribed bioactive compounds together with several known compounds. Among these, four compounds were identified with new carbon skeletons. In addition, the extraction and isolation of fruiting bodies from one fungus also resulted in the discovery of five unknown secondary metabolites.

Thirteen previously undescribed metabolites, (6*R*,7*S*,10*R*)-7,10-epoxy-7,11-dimethyldodec-1-ene-6,11-diol and twelve sesquiterpenes elgonenes A-L together with the known compound *p*-coumaric were isolated from *Sanhuangporus* sp. (MUCL56354). Most of these exhibited weak antimicrobial effects and cytotoxicity (**publication 1**). A new phelligradin L together with the other six nematocidal and antimicrobial secondary metabolites 3,14-bihispidinyl, hispidin, ionylideneacetic acid, phellidine E, phellidine D, and 1*S*-(2*E*)-5-[(1*R*)-2,2-dimethyl-6-methylidenecyclohexyl]-3-methylpent-2-enoic acid were isolated and characterized from another *Sanhuangporus* sp. (MUCL55592, **publication 4**). Tyromycin A and twelve previous undescribed derivatives, skeletocutins A-L, were identified from *Skeletocutis* sp. (MUCL56074). These showed selective activities against Gram-positive bacteria, while skeletocutin J weakly inhibited the formation of biofilm of *Staphylococcus aureus*. The antiviral activity against HCV of tyromycin A is also reported in **publication 2**. Five further tyromycin A derivatives skeletocutins M-Q were isolated from *Skeletocutis* sp. fruiting bodies (**publication 3**). Five new pregnenolone type steroids aethiopinolones A–E were isolated from the mycelial culture of *Fomitiporia aethiopica* (MUCL56047). These compounds exhibited moderate cytotoxic effects against various human cancer cell lines (**publication 5**). From *Heimiomyces* sp. (MUCL56078), seven novel compounds were isolated and four of them with new carbon skeletons. The determination of their stereochemistry is ongoing. The compounds

isolated from MUCL56078 exhibited activity against Gram-positive bacteria and moderate cytotoxicity.

Even though a fraction of basidiomycetes obtained from the fieldwork have been studied extensively in the past three years, a large number of novel chemical molecules with bioactivities could already be identified. This indicating Basidiomycota have the potential to be a promising source for novel secondary metabolites, which may lead to the discovery of new antibiotics and other useful compounds.

Key words: Secondary metabolites; Basidiomycota; HPLC.

Abbreviations and Units

BGC	biosynthetic gene cluster
BLAST	basic local alignment search tool
CD	circular dichroism
cDNA	complementary DNA
ESI	electrospray ionization
EtOAc	ethyl acetate
EtOH	ethanol
HCV	hepatitis C virus
HIV	human immunodeficiency virus
HPLC	high performance liquid chromatography
HR-ESIMS	high-resolution electrospray ionization mass spectrometry
ITS	internal transcribed spacer region of the ribosomal DNA
LCMS	liquid chromatography-mass spectrometry
LSU	large subunit of the ribosomal DNA
M	molar
MeOH	methanol
MIC	minimal inhibitory concentration
mRNA	messenger RNA
MRSA	methicillin-resistant <i>Staphylococcus aureus</i>
MS	mass spectrometer/spectrometry
MW	molecular weight
NMR	nuclear magnetic resonance
NRPS	nonribosomal peptide synthetase
PCR	polymerase chain reaction
RAxML	randomized accelerated maximum likelihood
RP	reversed phase
TFA	trifluoroacetic acid
UV	ultraviolet
w/v	weight per volume
YMG	yeast malt glucose

Declaration of Contribution to the Publications

The contribution of Tian Cheng (TC) and the co-workers to the publications listed above were as follows:

Publication 1

The first author TC identified the specimen to genus by sequencing the ITS and blasting the ITS to the database in NCBI. The fermentation of the fungus, downstream processing, extraction, chromatographic isolation of compounds, and the following biological activity evaluation were done by the first author TC. CC elucidated the structure of compounds and wrote the structure elucidation part in the manuscript. The biological characterization and isolation part of the manuscript were written by TC. CD and JCM collected the specimen and helped to check the manuscript.

Publication 2

The shared first author TC identified the specimen to genus by sequencing the ITS and blasting the ITS to the database in NCBI. The fermentation of the fungus, downstream processing, extraction, and chromatographic isolation of compounds were done by the TC with assistance from WCM. All the biological activity assays were done by TC, except “Inhibitory Effects on HCV Infectivity” which was done by DFP. The shared first author CC elucidated the structures of the compounds and wrote the manuscript except for the biological characterization and isolation part, which were written by TC. CD and JCM collected the specimen and helped to check the manuscript. KW and ES helped to check the manuscript.

Publication 3

The first author TC identified the specimen to genus by sequencing the ITS and blasting the ITS to the database in NCBI. The extraction, chromatographic isolation of compounds, and the following biological activity evaluation were done by the first author TC. CC elucidated the structures of the compounds. The biological characterization and chemical isolation part of the manuscript were written by TC, the structure elucidation part was written by CC. CD and JCM collected the specimen and helped to check the manuscript.

Publication 4

The first author CC carried out small-scale fermentation of the fungus and screened the extracts for bioactivities. Furthermore, LC-MS analysis of the extracts and database search to identify the new metabolites were carried out by CC. Scale-up of fermentation, downstream processing,

extraction, and chromatographic isolation of the compounds were done by CC. Structure elucidation and manuscript writing were also done by CC. TC helped with the bioassay tests. JCM facilitated the collection of the specimen and helped with proofreading of the manuscript. DC collected, isolated, and identified the producing organism and helped with proofreading of the manuscript.

Publication 5

The shared first author CC carried out the LC-MS analysis of the extracts and the database search to identify the new metabolites. Chromatographic isolation of the compounds was done by CC. Structure elucidation and manuscript writing were done by CC. WCS helped with the fermentation and isolation of compounds. JCM facilitated the collection of the specimen, experiment guidance, and helped with proofreading of the manuscript. TC helped with the biological characterization. DC collected, isolated, and identified the producing organism and helped with proofreading of the manuscript.

Publication 6

The shared first author CP collected the specimen and carried out the LC-MS analysis of the extracts and the database search to identify the new metabolites. Chromatographic isolation of the compounds, as well as their biological characterization, were done by CP. Structure elucidation and related manuscript writing were done by APGM. KDH helped with proofreading of the manuscript. VH and TC helped with the biological characterization.

Publication 7

TC wrote the “Genomics and molecular biology of secondary metabolite biosynthesis in Basidiomycota” part, “Biotechnology of products from Basidiomycota” was written by LCM, and “Brief overview about the taxonomy of the Basidiomycota” was written by BT. The shared first author BS and CC wrote the major part of the manuscript. MS and SH supervised the progress of the project and helped to finalize the manuscript draft.

MS supervised the progress of the project and helped to finalize all the manuscripts drafts.

1. Introduction

1.1 History of Antibiotics and Antimicrobial Resistance

The first natural antibiotic, mycophenolic acid (**Figure 1**), was discovered by the Italian physician and microbiologist Bartolomeo Gosio from “*Penicillium glaucum*” (currently valid name *P. brevicompactum*) in 1893 (Gosio, 1896). Mycophenolic acid is a member of the class of 2-benzofurans and possesses weak and non-selective antibacterial activity. Mycophenolic acid is a potent, reversible, non-competitive inhibitor of inosine-5'-monophosphate dehydrogenase (IMPDH), an enzyme essential to the *de novo* synthesis of guanosine-5'-monophosphate (GMP) from inosine-5'-monophosphate (IMP). The use of mycophenolic acid leads to a relatively selective inhibition of DNA replication in T cells and B cells (Harvey *et al.*, 2011; Nijkamp and Parnham, 2011). Until 1994, the 2-(morpholin-4-yl)ethyl ester of mycophenolic acid was approved by the US Food and Drug Administration (FDA) as an immunosuppressant to prevent transplant rejection (Wu, 1994). At the beginning of the 1910s, chemist Alfred Bertheim synthesized the first man-made antibacterial agent arsphenamine (Salvarsan) in Paul Ehrlich's lab. Salvarsan (**Figure 1**) was the first chemotherapeutic compound and was marketed as a drug for the treatment of syphilis (Vernon, 2019).

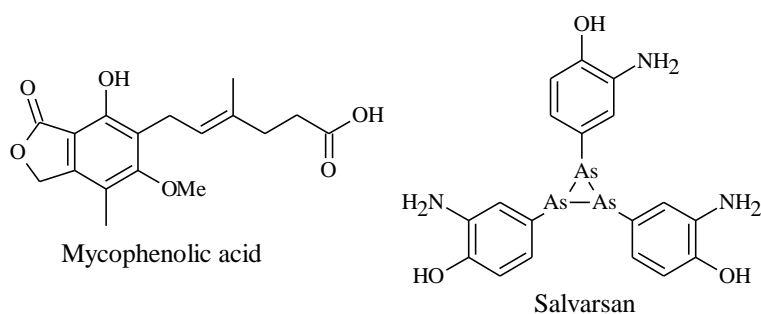


Figure 1. Chemical structures of mycophenolic acid and salvarsan.

The well-known antibiotic penicillin was first discovered by Alexander Fleming from “*Penicillium rubens*” (Houbraken *et al.*, 2011). After early trials in treating sepsis and human wounds, the collaborations with pharmaceutical companies were motivated by the outbreak of the Second World War, which ensured the mass production of penicillin. In 1945, penicillin (nicknamed “the wonder drug”) was no longer an exclusive medication for the military (Cully, 2014). Cephalosporin C (**Figure 2**), discovered by Giuseppe Brotzu from “*Cephalosporium acremonium*” (currently valid name *Sarocladium strictum*) as the first member of the

cephalosporins (a sub-class of β -lactams) in 1945. Its structure inspired numerous synthetic efforts on the designation of analogues from antibacterial drugs, arose with cefalotin (**Figure 2**) being the first clinically approved cephalosporin antibacterial agent (Bo, 2000; Newton and Abraham, 1955). Penicillin G (**Figure 2**) and cephalosporin C are representatives of the important class of β -lactams, they primarily act against Gram-positive bacteria by inhibiting the synthesis of the peptidoglycan layer of the bacterial cell wall (Fisher *et al.*, 2005).

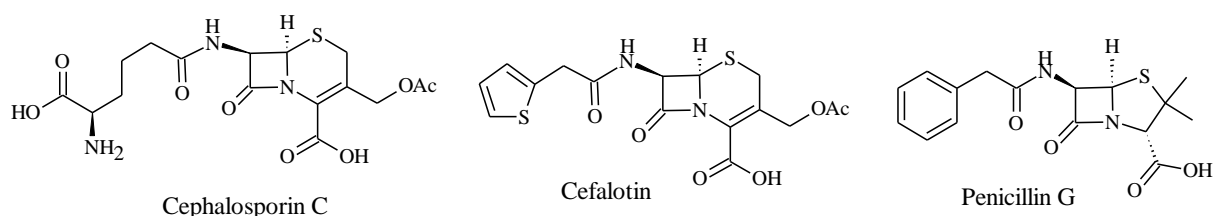


Figure 2. Chemical structures of β -lactams.

Prontosil (**Figure 3**), an antibacterial drug of sulfonamide group, was synthesized by Bayer chemists Josef Klarer and Fritz Mietzsch and marketed in 1935 (Domagk, 1935). Antibacterial sulfonamides (**Figure 3**) act as competitive inhibitors of the enzyme dihydropteroate synthase (DHPS), an enzyme involved in the synthesis of folate. They are therefore bacteriostatic and inhibit the growth and multiplication of bacteria (Zhao *et al.*, 2016).

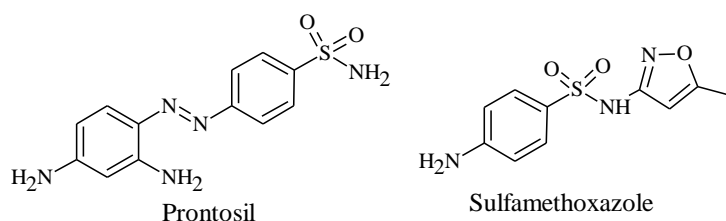


Figure 3. Chemical structures of sulfonamide drugs.

Another milestone in the history of antibiotics was the discovery of streptomycin (**Figure 4**) from *Streptomyces griseus* as the first aminoglycoside antibiotic, with antimicrobial activities against Gram-positive and Gram-negative bacteria (Jones *et al.*, 1944; Schatz *et al.*, 1944). Gentamicin (**Figure 4**), was discovered from the fermentation products of *Micromonospora purpurea* in 1963, it was used as a topical treatment for burns initially and introduced into intravenous (IV) usage in 1971 (Dean, 2012; Weinstein *et al.*, 1963). Aminoglycosides act as inhibitors of protein synthesis in bacteria by binding bacterial 30S or 50S ribosomal subunit,

inhibiting the translocation of the peptidyl-tRNA from the A-site to the P-site, and also causing misreading of mRNA (Serio *et al.*, 2018).

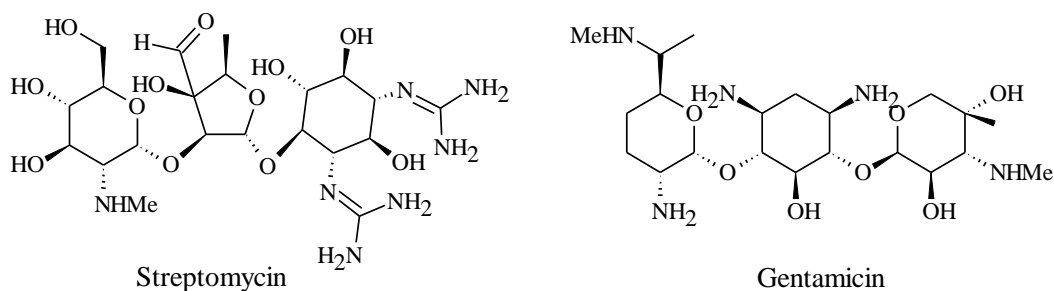


Figure 4. Chemical structures of aminoglycoside antibiotics.

Tetracyclines are one of the most important classes of antibiotics. The first member in this class aureomycin (today known as chlortetracycline, **Figure 5**, Duggar, 1948) was isolated from *Streptomyces aureofaciens* and approved for clinical use in 1948 (Chopra and Roberts, 2001). Soon thereafter, several other members of the tetracycline family were isolated, including oxytetracycline (**Figure 5**) from *Streptomyces Rimosus* and tetracycline (**Figure 5**) from *Streptomyces aureofaciens* (Clardy *et al.*, 2009). Tetracycline antibiotics are protein synthesis inhibitors and work by suppressing the initiation of translation (Chukwudi, 2016).

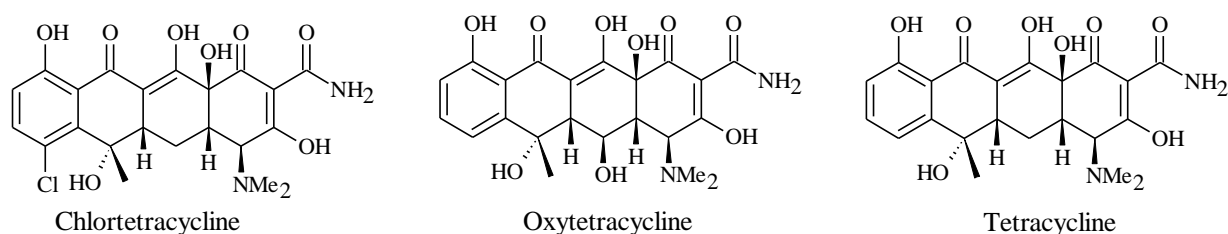


Figure 5. Chemical structures of teracyclines.

The 1950s was the start of the golden age for novel antibiotics, and among the most prominent were the erythromycins. Erythromycins A (**Figure 6**) and B (**Figure 6**) were isolated from *Saccharopolyspora erythraea* in 1952 and marketed with the name Ilotycin in the same year as a mixture (Mcguire *et al.*, 1952). Erythromycins can bind to the 23S ribosomal RNA molecule in the 50S subunit of the bacterial ribosome. This causes a blockage in the protein synthesis and subsequent structure and function processes that are critical for life or replication (Farzam and Quick, 2020). Later on, the ketolide family of antibacterial agents arose from the erythromycin class through semisynthetic studies. Telithromycin (**Figure 6**) was derived from erythromycin

A and marketed in Europe (2001) as an antibacterial drug (Johnson, 2001; Jones and Biedenbach, 1997). Ketolides have a mechanism of action very similar to erythromycin A from which they have been derived (Zhanel *et al.*, 2002).

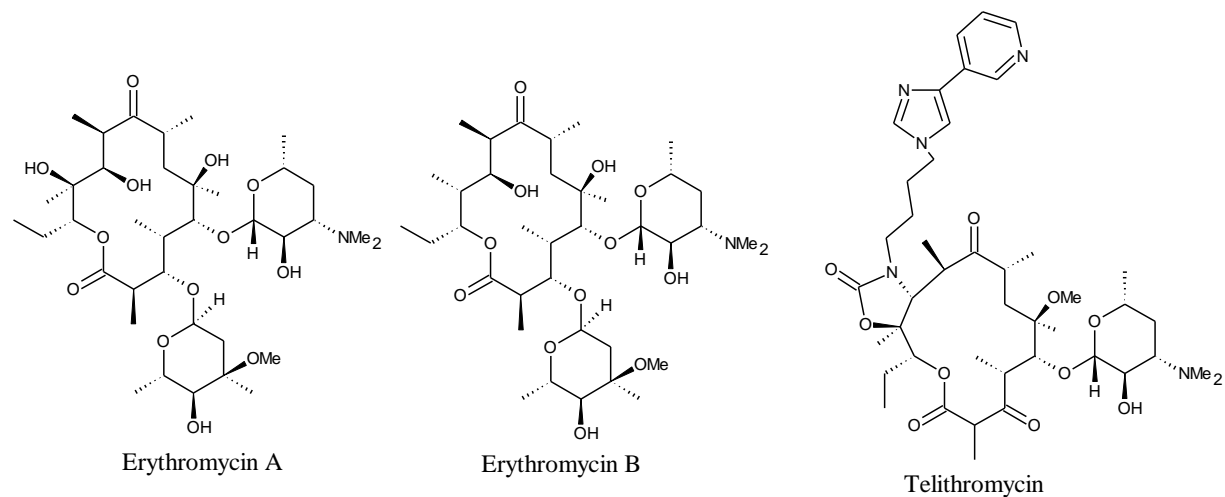


Figure 6. Chemical structures of erythromycins and telithromycin.

Soon after the discovery of the erythromycins, another family of powerful antibiotics, the glycopeptides, were discovered. Vancomycin (**Figure 7**) was isolated from *Strep. orientalis* (currently valid name *Amycolatopsis orientalis*) in 1953 (Griffith, 1981; Moellering, 2006) as the first member of this class. Telavancin (**Figure 7**) was derived semisynthetically from vancomycin. It is an antibacterial drug belonging to the class of lipoglycopeptides. The bactericidal properties of vancomycin and telavancin are derived from the inhibition of bacterial cell wall synthesis by binding to the D-Ala-D-Ala terminus of peptidoglycan in the growing cell wall. They also disrupt bacterial membranes by depolarization (Das *et al.*, 2017).

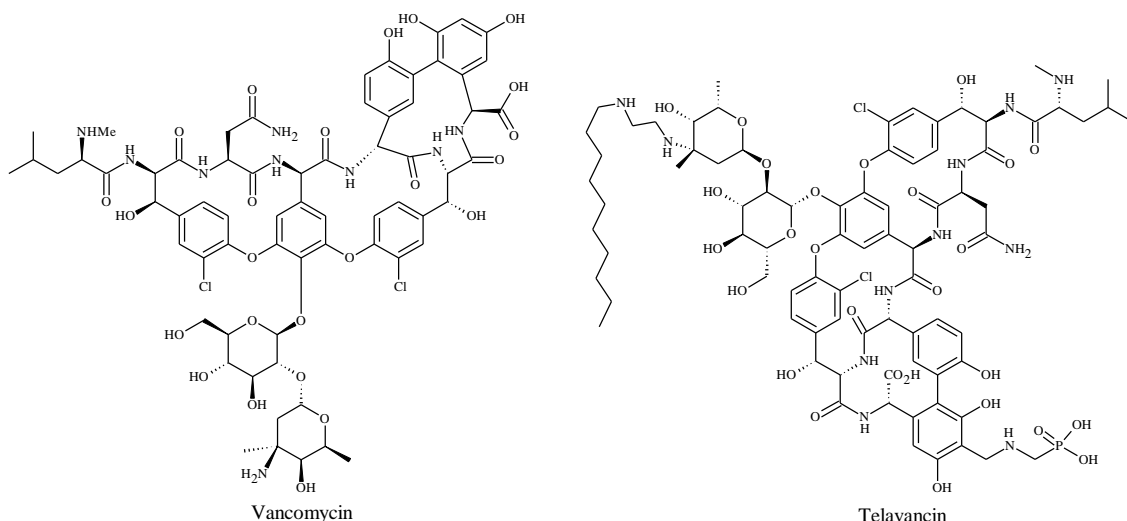


Figure 7. Chemical structures of vancomycin and telavancin.

Ansamycins are a group of macrolactam cytotoxic antibiotics, among which the early members named rifamycins were isolated from *Strep. mediterranei* (now *Amycolatopsis rifamycinica*) in 1959 (Sensi *et al.*, 1959). Rifampicin (**Figure 8**) was approved by the Food and Drug Administration (FDA) in 1971 for the treatment of tuberculosis (Sensi, 1983). The activity of rifamycins relies on the inhibition of bacterial DNA-dependent RNA biosynthesis, which in turn inhibits protein biosynthesis (Pimentel, 2016).

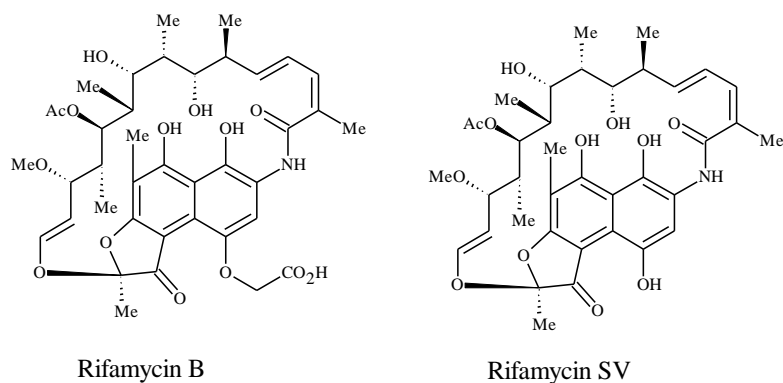


Figure 8. Chemical structures of rifamycins.

The 1940s-1960s were the golden era for antibiotics. Most of the antibiotics we use as medicines in present-day were discovered and marketed in that age. However, antibiotic-resistant bacteria that can survive antibiotic treatment are becoming more and more common (Newman and Cragg, 2020). Even before the extensive use of penicillin, some observations suggested that penicillin antibiotics could be destroyed by an enzyme from bacteria (Abraham

and Chain, 1940). Shortly thereafter, penicillin resistance became a serious clinical problem during the 1950s. But new beta-lactam antibiotics were discovered and developed in response to restrain the resistance problem (Sengupta *et al.*, 2013; Spellberg and Gilbert, 2014).

The first cases of methicillin-resistant *Staphylococcus aureus* (MRSA) were identified in the UK in 1961 and in the US in 1968 (Johnson, 2011). It is prevalent all over the world now and is resistant to the entire class of β -lactams (Kumarasamy *et al.*, 2010). Unfortunately, resistance has eventually occurred to nearly all antibiotics that have been developed. Even for antibiotics like vancomycin, which was introduced for the treatment of methicillin resistance in both *S. aureus* and coagulase-negative staphylococci got ineffective in some cases (Cooper and Shlaes, 2011; Srinivasan *et al.*, 2002). What makes the situation even worse is the number of new antibiotics approved has been steadily declining.

Studies have indicated the direct relationship between the overuse of antibiotics and the emergence of resistant bacterial strains (Read and Woods, 2014). Inappropriately prescribed antibiotics have exposed patients to potential complications of antibiotic therapy and also contribute to the promotion of resistant bacteria (Lushniak, 2014). Additionally, antibiotics used for the purpose of promoting growth and preventing infection of livestock affect the environmental microbiome. Resistant bacteria from animals could potentially be transferred to humans and result in resistance against antibiotics (Bartlett *et al.*, 2013). To face the growing antibiotic resistance crisis, policymakers have been pushing for the careful use of antibiotics, while researchers have been searching for treatments that could effectively fight antibiotic-resistant bacteria (Bush *et al.*, 2011).

According to the National Institute of Health, up to 80% of human microbial infections are associated with biofilms (Jamal *et al.*, 2018), *e.g.* endocarditis, cystic fibrosis, periodontitis, rhinosinusitis, osteomyelitis, non-healing chronic wounds, meningitis, and kidney infections. Human pathogens commonly known to be involved in biofilm-associated infections include *Staphylococcus epidermidis*, *Staphylococcus aureus*, *Pseudomonas aeruginosa*, *Escherichia coli* and *Candida albicans* (Gupta *et al.*, 2016; Paharik and Horswill, 2016; Rimondini *et al.*, 2016). Compounds with the ability to inhibit the formation of biofilms are thought to avoid the rapid evolution of resistance since unlike antibiotics they do not pose a fatal threat to microorganisms. Such compounds could operate as adjunctive agents in combination therapy with antibiotics (Li and Webster, 2018).

1.2 Natural Products from Fungi

The fungal kingdom represents an invaluable source of bioactive natural products, which have long been exploited in various contexts, ranging from crop protection to human disease (Bills and Gloer, 2016; Sandargo *et al.*, 2019a). Fungal natural products have been used as pharmaceuticals against various diseases and contain the potential for innovative drugs (Stadler and Hoffmeister, 2015). The most well-known natural products are penicillins originally derived from *Penicillium* molds (Fleming, 1929), which were among the first medications to be effective against many bacterial infections. Fusidic acid (**Figure 9**), derived from the mold *Ramularia coccinea*, is a steroid-like antibiotic inhibited protein synthesis by preventing the turnover of elongation factor G (EF-G), which resulted in the inhibition of both peptide translocation and ribosome disassembly (Fernandes, 2016).

Griseofulvin (**Figure 9**) was one of the first antifungal agents, isolated from *Penicillium griseofulvum* and marketed for the treatment of dermatophytosis (Grove *et al.*, 1952). Echinocandins and pneumocandins (**Figure 9**) are important fungicidal agents derived from *Aspergillus rugulovalvus*, *Coleophoma empedri*, and *Zalerion arboricola*, both of them belong to the family of cyclic lipopeptides. The echinocandin lipopeptide, acrophiarin (antibiotic S31794/F-1), circumscribed in a patent in 1979 (Dreyfuss and Tschertter, 1979) and confirmed by Lan *et al.*, (2020) that derived from *Penicillium arenicola* NRRL 8095. Both echinocandins and pneumocandins inhibit β -1,3-glucan synthase and prevent the formation of this class of glucan, an essential component of the fungal cell wall in many fungi (Baguley *et al.*, 1979; Denning, 2002).

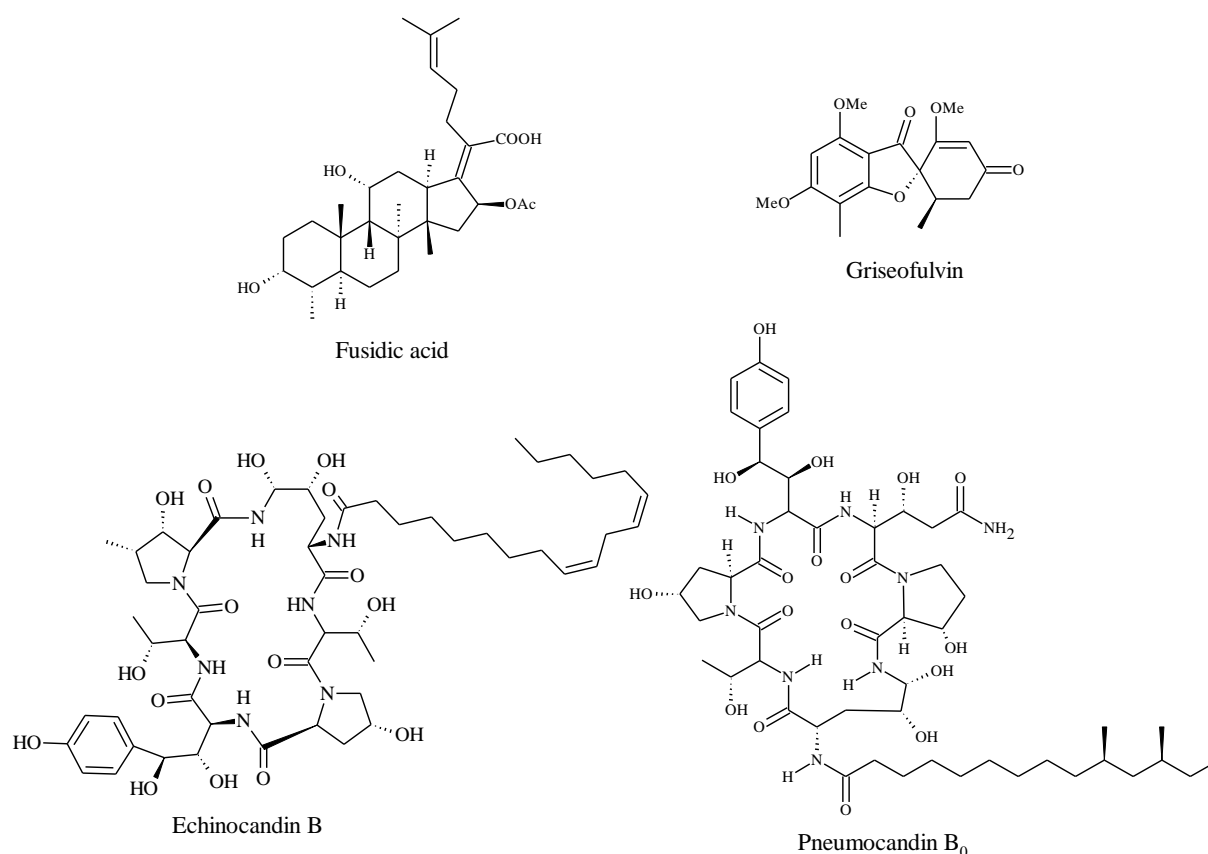


Figure 9. Chemical structures of fusidic acid and three fungicidal agents.

Apart from the antimicrobial properties of fungal natural products, alternative activities are known. For instance, the nonribosomal peptide cyclosporin A (**Figure 10**) is a notable immunosuppressant clinically adopted for organ transplantation (Borel, 1990; Thomson *et al.*, 1984), initially derived from *Tolypocladium inflatum* (Borel and Kis, 1991).

The nematicidal PF1022A (**Figure 10**), an *N*-methylated was first reported by Sasaki *et al.*, (1992). A research of Wittstein *et al.*, (2020) proved that PF1022 derivatives and other cyclodepsipeptides are wide-spread in *Rosellinia*. PF1022A has strong anthelmintic properties against gastrointestinal nematodes of different host animals and fully effective against benzimidazole-, levamisole- or ivermectin-resistant nematodes in sheep and cattle (Harder *et al.*, 2003).

Another clinically important medication, statins (**Figure 10**), are the most important class of HMG-CoA reductase inhibitor. They are derived from fungal natural products and contain two types of structures moieties, a hexahydro-naphthalene system, and a β -hydroxylactone system (Hyde *et al.*, 2019). Compactin (mevastatin, ML-236B) was isolated from *Penicillium brevicompactum* and has hypocholesterolemic activity (Brown *et al.*, 1978; Endo *et al.*, 1976).

Later mevinolin was isolated from *Aspergillus terreus* (Alberts *et al.*, 1980). Lovastatin, commercialized derived from *Aspergillus terreus*, was the first statin drug marketed for treating high blood cholesterol and reducing the risk of cardiovascular disease (Bills and Gloer, 2016).

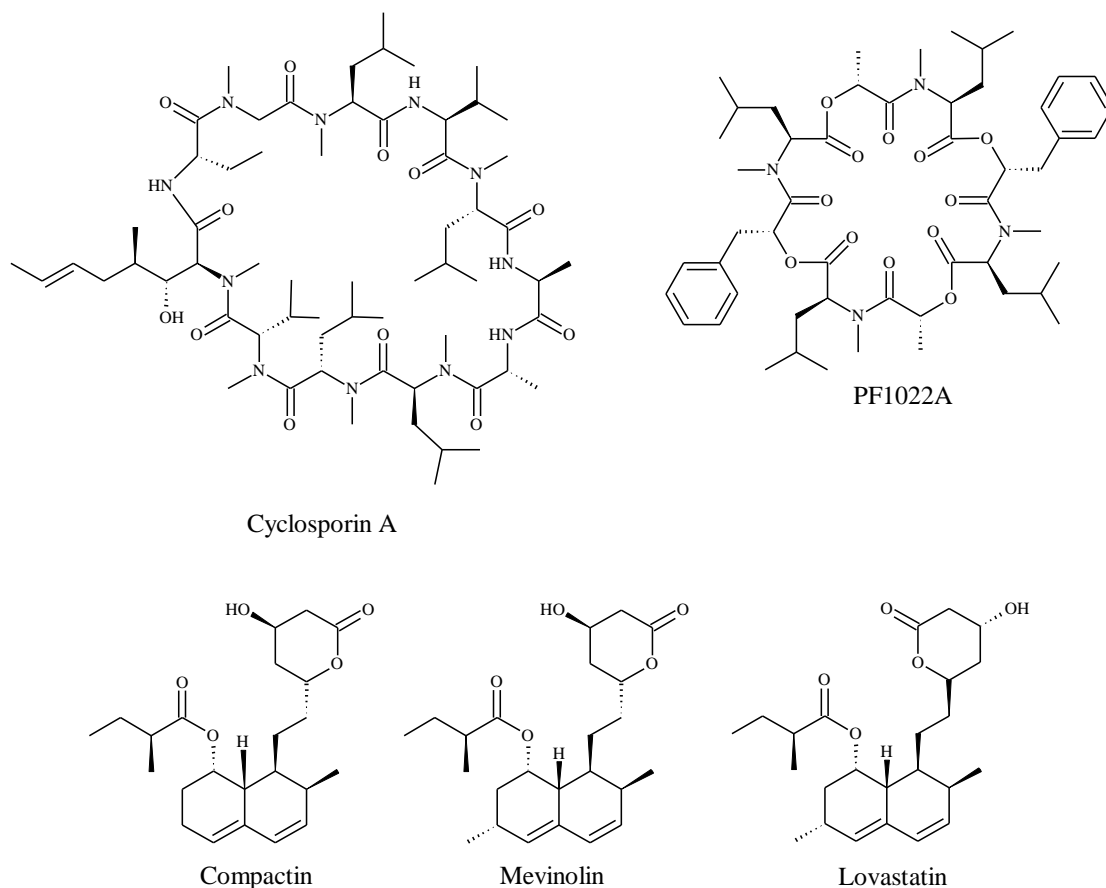


Figure 10. Chemical structures of cyclosporin A, PF1022A and stains.

1.3 Agrochemicals and Drug Candidates from Basidiomycota

A number of very important lead compounds have already been obtained from Basidiomycota, even though they have been less studied for biologically active metabolites than the Ascomycota, which has led to marketed drugs, agrochemicals, and clinical candidates. Strobilurins are a group of naturally occurring antibiotics from the mycelial cultures of various Basidiomycota including *Strobilurus*, *Favolaschia*, *Mycena*, *Oudemansiella*, and *Xerula* (Stadler and Hoffmeister, 2015). These compounds have represented a major development in fungus-based fungicides and served as lead compounds for the agricultural β -methoxyacrylate fungicides (Sauter *et al.*, 1999). Interestingly, new 9-oxo strobilurin derivatives have been identified from *Favolaschia calocera* originating from Kenya (Chepkirui *et al.*, 2016) even after 50 years of intensive studies. By binding to the ubiquinol-oxidation centre (responsible for the

generation of the proton gradient used for ATP synthesis and the transfer of electrons to nitrogenase) in the mitochondrial cytochromes, strobilurins prevent the growth of mycelia and germination of spores (Sauter *et al.*, 1999). Some strobilurins exhibit strong antifungal activity and together with their low cytotoxicity towards mammals and plants, and their relatively easy access by total synthesis has made them promising lead compounds for the development of agricultural fungicides (Anke, 1995). However, since they are “single-target” compounds, it is easy for the pathogens to acquire resistance through single point mutation in the target proteins (Ishii *et al.*, 2001; Vaghefi *et al.*, 2016). Nevertheless, azoxystrobin (**Figure 11**) and kresoxim methyl (**Figure 11**) are still being applied at a large scale in combination with other antifungal agents such as azoles.

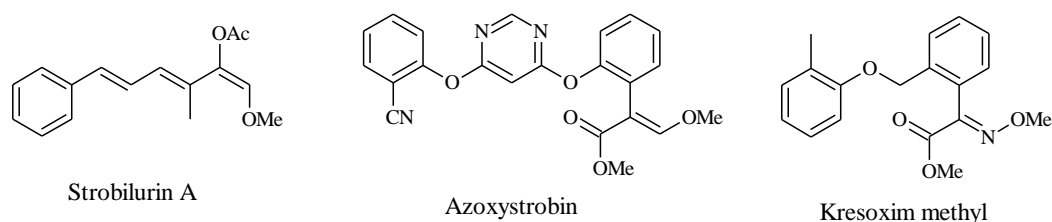


Figure 11. Chemical structures of strobilurins.

Pleuromutilin (**Figure 12**) is another important antibiotic from Basidiomycota, which was first isolated from *Clitopilus passeckerianus* (formerly named *Pleurotus passeckerianus*, Kavanagh *et al.*, 1951), *Drosophila subatrata* (currently valid name: *Parasola conopilus*), *Clitopilus scyphoides*, and some other *Clitopilus* species (Hartley *et al.*, 2009; Kavanagh *et al.*, 1952). Regarding the metabolic stability, gastrointestinal side effects, cardiac safety, and intravenous tolerability, the application of this class of compounds were limited even though their ability against most Gram-positive and some Gram-negative pathogens is quite promising (Novak, 2011; Paukner and Riedl, 2017).

Later on, the semisynthetic pleuromutilin derivatives tiamulin (**Figure 12**) and valnemulin (**Figure 12**) were introduced as veterinary medicine treatment of swine dysentery and enzootic pneumonia in animals (Egger and Reinshagen, 1976a, 1976b). However, due to the unique highly specific mode of action of this class of compounds, the resistance development has been uncommon. Another semisynthetic derivative retapamulin (**Figure 12**) was later marketed as the first approved antibiotic from Basidiomycota for treating skin infections of humans. The recent advances in lead optimization by combing potent antibacterial activity with favorable pharmaceutical properties have led to the synthesis of three further new semisynthetic

pleuromutilin derivatives, BC-3205 (**Figure 12**), and BC-7013 (**Figure 12**) that are currently in clinical trials (Paukner and Riedl, 2017; Prince *et al.*, 2013).

Lefamulin (**Figure 12**), formerly known as BC-3781, is the first systemic pleuromutilin derivative developed for intravenous and oral administration in humans. It is marketed for the treatment of community-acquired bacterial pneumonia since 2019 in the U.S. Lefamulin is highly effective against *Chlamydia trachomatis*, *Mycoplasma genitalium*, and *Neisseria gonorrhoeae* even for multidrug-resistant isolates in antimicrobial activity tests (Bradshaw *et al.*, 2017; Jacobsson *et al.*, 2017). Moreover, lefamulin has demonstrated full activity against methicillin-susceptible and -resistant *Staphylococcus aureus* and β -hemolytic streptococci (Paukner *et al.*, 2013; Sader *et al.*, 2012). Lefamulin prevents the correct positioning of the ribosomal RNA for peptide transfer interfering with bacterial protein synthesis and is unaffected by resistance to other antibiotic classes, such as fluoroquinolones, macrolides, tetracyclines or β -lactams (Long *et al.*, 2006; Yi *et al.*, 2017), which confers a low tendency for the development of bacterial resistance. The marketing authorization application in Europe is under review by Europe marketing authorization (EMA), which will take approximately 12 to 15 months from June of 2019. Once approved by EMA, Lefamulin will receive marketing authorization in all 28 member states of the European Union (EU), as well as in Norway, Liechtenstein, and Iceland (Garrett, 2019).

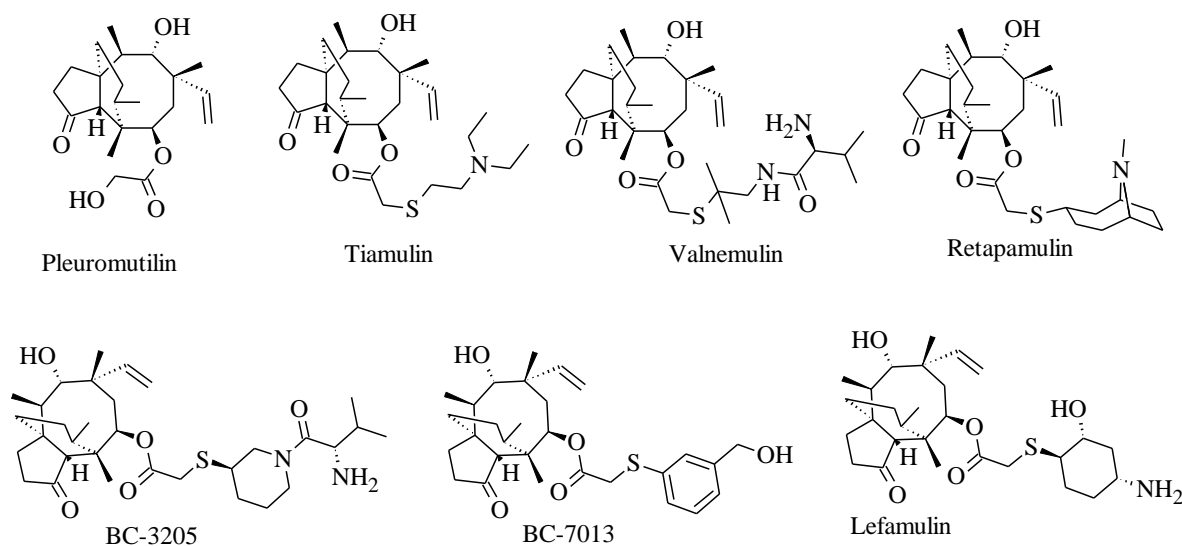


Figure 12. Chemical structures of pleuromutilin and its derivatives.

Further important basidiomycete natural products are the illudins, which are consistently produced by the genera *Omphalotus* (Schobert *et al.*, 2011; Tanasova and Sturla, 2012). These sesquiterpenes possess an unusual cyclopropane ring and exhibit antitumor properties. However,

their high toxicity has restricted potential use as anticancer agents in their natural form (Tanasova and Sturla, 2012). The semisynthetic analogue of illudin S (**Figure 13**), Irofulven (**Figure 13**), is currently under development as an anticancer drug in clinical phase II (Schilder *et al.*, 2010). Interestingly, omphalotin type cyclopeptides were only reported from *Omphalotus* species and co-occur in the cultures with illudins. These compounds exhibited activity against root knot nematodes (Büchel *et al.*, 1998; Mayer *et al.*, 1999). Omphalotin A (**Figure 13**) was first reported from *Omphalotus olearius*. Later on, several derivatives were isolated from the same fungus (Liermann *et al.*, 2009; Sterner *et al.*, 1997).

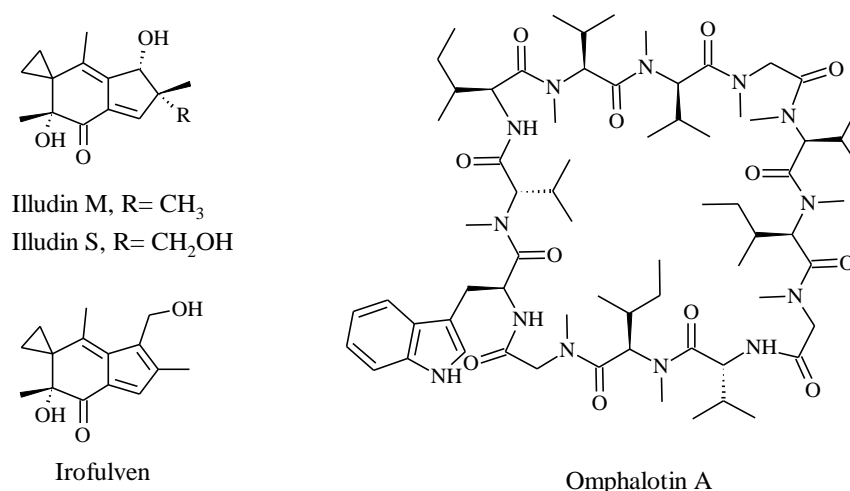


Figure 13. Chemical structures of natural products derived from *Omphalotus* spp. and related analogue.

“*Lingzhi*”, species of genus *Ganoderma*, are fungus in Asian countries and regarded as “panacea” for hundreds of years. The fruiting bodies of “*Lingzhi*” were supposed to treat various diseases such as nephritis, hepatopathy, chronic hepatitis, hypertension and so on (Jong and Birmingham, 1992). The well-known compounds from *Ganoderma* belong to the classes of lanostane-type triterpenoids, ergostane-type steroids, and pentacyclic triterpenes (Richter *et al.*, 2015). These include the cytotoxic triterpenoids such as ganoderic acids, lucidimols, ganodermanondiols, ganoderiols, lucidenic acids, and ganodermanontriols. Ganoderic acids, in particular, ganoderic acids T (**Figure 14**) and DM (**Figure 14**) have been studied for their anticancer activity in detail (De Silva *et al.*, 2013; Liu *et al.*, 2012; Tang *et al.*, 2006).

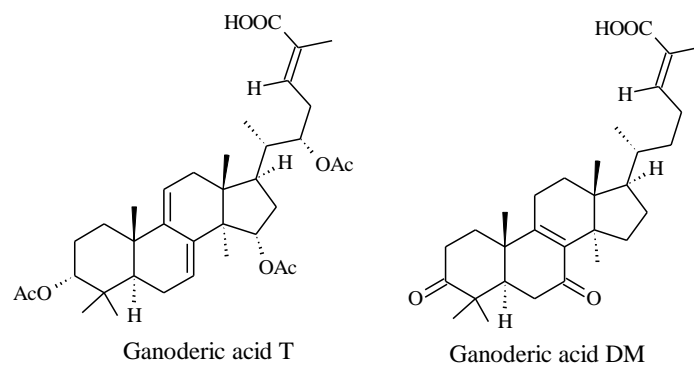


Figure 14. Chemical structures of ganoderic acids.

Blazeispirols (**Figure 15**) are a unique class of spiro-triterpenoids that were isolated from mycelia cultures of *Agaricus* mushrooms (Hirota *et al.*, 1999, 2000, 2002a, 2002b). The blazeispirol derivatives were comprised of two major structural types, represented by blazeispirol A (blazeispirane type) and blazeispirol U (protoblazeispirane type, Hirota *et al.*, 2002b). Prior research on blazeispirols revealed their potential as anti-hypercholesterolemic agents and indicated that they may contain toxic effects on liver function by inhibiting P450 enzymes, especially in case of ovarian cancer (Grothe *et al.*, 2011; Sweet *et al.*, 2013). Moreover, blazeispirol A was proved as a chemotaxonomic marker from the mycelia of the medicinal mushroom *Agaricus subrufescens* (Thongklang *et al.*, 2017).

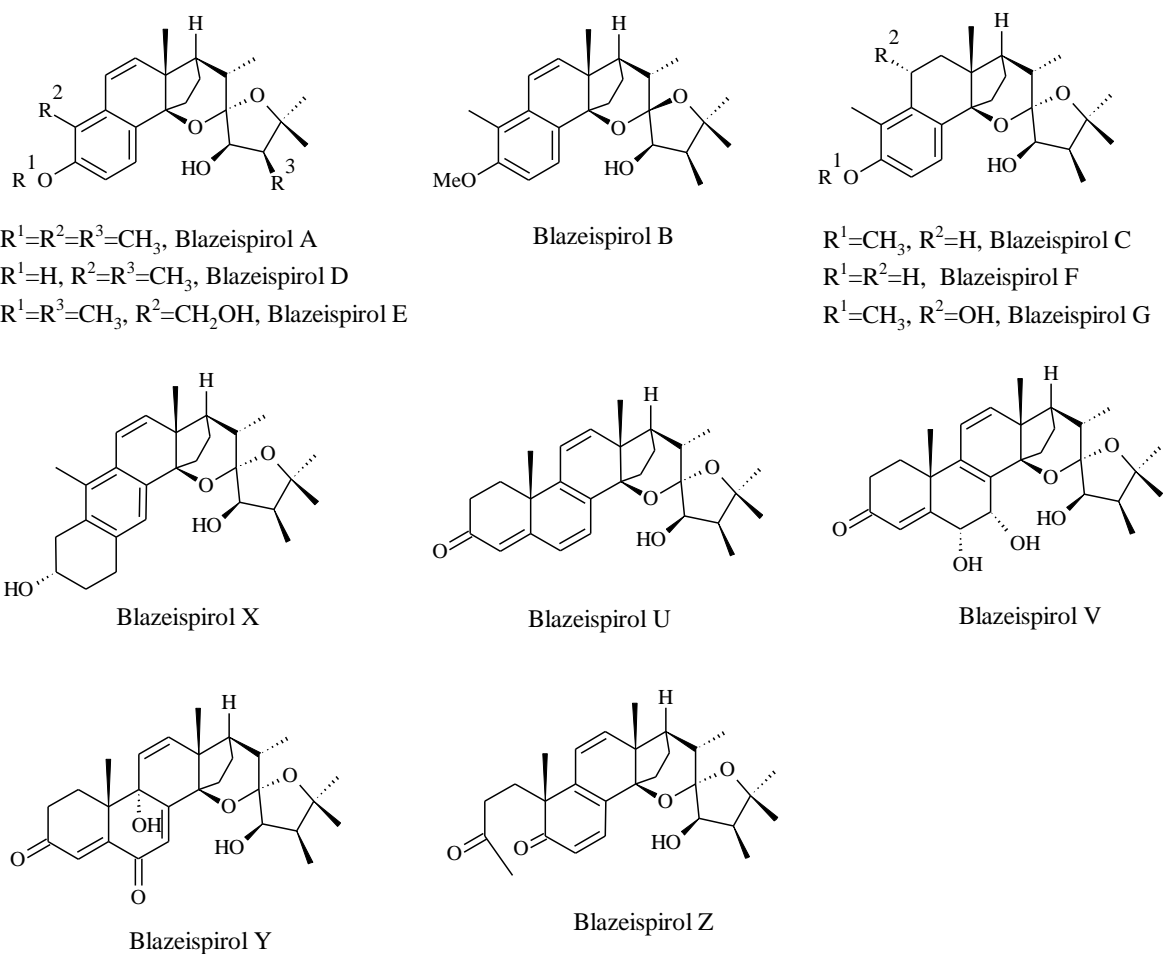


Figure 15. Chemical structure of blazeispirols.

Another two genera, *Inonotus* and *Phellinus*, in the Hymenochaetaceae constitute important medicinal mushrooms. The boundaries between these genera remained unclear until a phylogenetic study and rearrangement of the taxa, which are now being accommodated in the new genera *Sanguangporus* and *Tropicoporus* (Zhou *et al.*, 2016). The respective fungi have been widely used in Asia as traditional medicine for the treatment of cardiovascular disease, tuberculosis, gastrointestinal, as well as diabetes (De Silva *et al.*, 2013; Wasser and Weis, 1999). The metabolites from these mushrooms are mainly hispidin derivatives (**Figure 16**) such as 3,14'-bihispidinyl, phelligridins, and inoscavin that exhibit antioxidant, antimicrobial and cytotoxic effects (De Silva *et al.*, 2013). Another predominant class of metabolites that occurs in these fungi are the sesquiterpenoids such as phellidenes and phellelanes (**Figure 16**) from *Phellinus linteus* (Kobayashi *et al.*, 2010), inonoalliacanes and inonotins from *Inonotus* sp. (Isaka *et al.*, 2017, 2015).

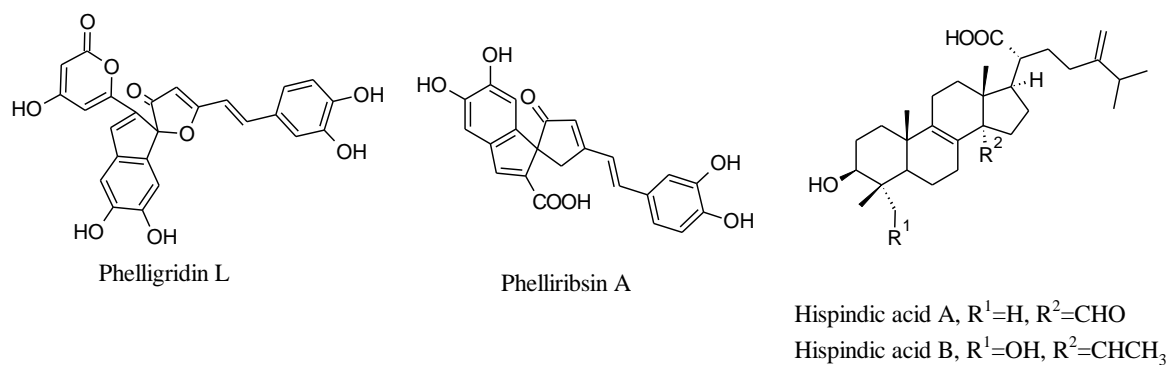


Figure 16. Chemical structures of natural products derived from genus *Inonotus* and *Phellinus*.

The medicinal mushrooms from genus *Hericium* and in particular *Hericium erinaceus* have been used as food supplements and alternative medicine in traditional Chinese medicine for a long time (Thongbai *et al.*, 2015). Metabolites from both fruiting bodies and cultures of *H. erinaceus* exhibit antimicrobial, cytotoxicity, and neurotogenic effects (Kawagishi *et al.*, 1994; Wittstein *et al.*, 2016). Erinacines and hericenones (**Figure 17**) isolated from *H. erinaceus* were investigated for their effects on nerve growth factor (NGF) and brain-derived neurotrophic factor (BDNF), which demonstrated their therapeutic potential for the treatment of Alzheimer's disease. Erinacines are cyathane diterpenoids are produced exclusively in the cultures, while hericenones and isoindolinones are benzofuranone that are produced only in the fruiting bodies (Kawagishi *et al.*, 2006b; Wittstein *et al.*, 2016).

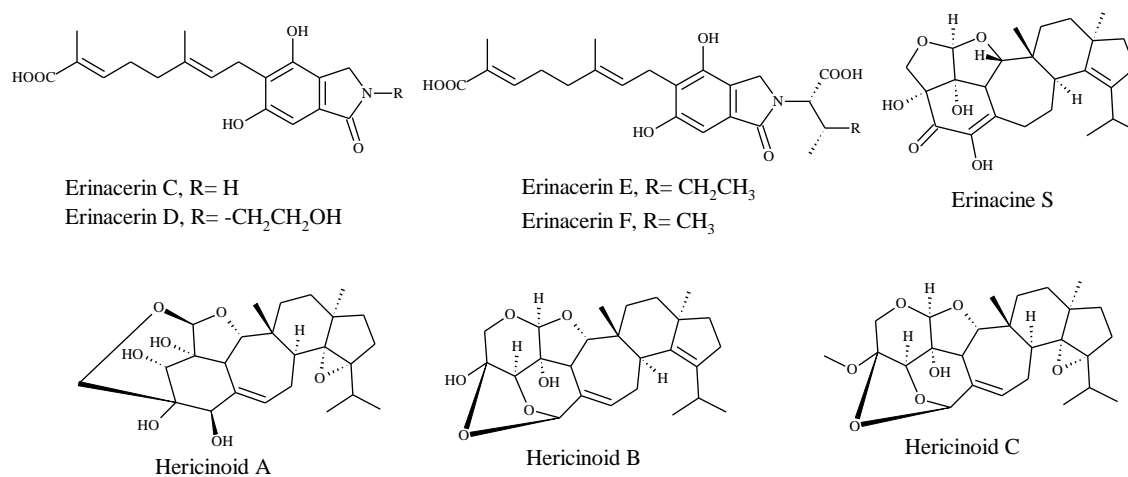


Figure 17. Chemical structures of erinacines and hericenones.

In addition to the aforementioned compounds from valuable basidiomycetes complex, plenty of new metabolites have been isolated from random screening programs in recent years

(Sandargo *et al.*, 2019a). For instance, the cythane diterpenoids pyristriatin A and B from *Cyathus pyristriatus* with moderate antimicrobial and weak cytotoxic activity (Richter *et al.*, 2016). Striatoids A-F from *Cyathus striatus* exhibited dose-dependently enhanced nerve growth factor (NGF)-mediated neurite outgrowth in PC-12 cells (Bai *et al.*, 2015). Laetiporins A and B from *Laetiporus* sp. showed cytotoxicity against various human cancer human cell lines (Chepkirui *et al.*, 2017). Ostalactones A-C from *Stereum ostrea* while ostalactones A and B exhibited moderate activity against human pancreatic lipase (Kang and Kim, 2016). Lentinoids A-D from *Lentinus strigellus* (Vásquez *et al.*, 2018). Pseudohygrophorones A and B from the fruiting bodies of *Hygrophorus abieticola* (Otto *et al.*, 2016). Rosellins A and B from *Mycena rosella* fruiting bodies (Lohmann *et al.*, 2018). The antiviral meroterpenoid rhodatin and sesquiterpenoids rhodocoranes A-E from *Rhodotus palmatus* (Sandargo *et al.*, 2019b). In recent years, the importance of natural products from Basidiomycota has been highlighted (Sandargo *et al.*, 2019a; Schüffler, 2018). This thesis is focused on the chemical diversity and the potential activity of secondary metabolites from tropical fungi.

1.4 Biosynthesis of Secondary Metabolites in Basidiomycota

With the purpose to sequence the genomes of fungi throughout the kingdom, a series of databases have been launched to accelerate the pace of fungal genomics. Examples include the fungal genome initiative (FGI, <https://www.broadinstitute.org/fungal-genome-initiative>, Haas *et al.*, 2011), Mycosm portal from joint genome institute (JGI, <https://mycosm.jgi.doe.gov/mycosm/home>, Grigoriev *et al.*, 2014) and FungiDB (<https://fungidb.org/fungidb/>, Stajich *et al.*, 2012). Taking advantage of the increasing availability of genome sequences, several computational tools like antiSMASH (Blin *et al.*, 2017), SMURF (Khaldi *et al.*, 2010), and NRPS predictor (Röttig *et al.*, 2011) have been developed to identify secondary metabolic gene clusters. However, it is not clear whether they work well in all Basidiomycota genomes because there are too few examples of elucidated pathways for known compounds. Basidiomycetes are much more difficult to work with than ascomycetes because of the very high prevalence of introns which makes gene finding and annotation much more difficult. As discussed by Sandargo *et al.* (2019a), the process of identifying gene clusters currently requires a combination of the use of algorithm platforms with manual annotation.

The first biosynthesis gene cluster (BGC) study on Basidiomycota was dealing with the discovery of six sesquiterpene synthases (*cop1-cop6*) and two cytochrome P450

monooxygenases (*cox1-cox2*) from *Coprinopsis cinerea*. All genes except for *cop5* were cloned and functionally expressed in *Escherichia coli* and/or *Saccharomyces cerevisiae* (Agger *et al.*, 2009; Engels *et al.*, 2008; Jennewein *et al.*, 2013). The BGC of the diterpene pleuromutilin (**Table 1**) from *Clitopilus pseudopinsitus* and *Clitopilus passeckerianus* was recently found to contain seven genes. It was meanwhile expressed heterologously in *Aspergillus oryzae*, giving a significant increase (over 2000%) in the production of pleuromutilin (Alberti *et al.*, 2017; Bailey *et al.*, 2016; Yamane *et al.*, 2017). The erinacine BGC was identified containing three cytochrome P450s (*eriA*, *eriC*, and *eriI*), one GGPPS (*eriE*), two prenyltransferases (*eriF* and *eriG*) and a UDP-glycosyltransferase (*eriJ*) (Liu *et al.*, 2019).

In addition to terpenoids, the biosynthesis of metabolites from other compound classes has also been elucidated. The alkaloid psilocybin isolated from the genus *Psilocybe* has long been used for medicinal and religious purposes by native people of Mexico and British teenagers (Andersson *et al.*, 2009). The psilocybin BGC has been identified from *Psilocybe cubensis* and *Psilocybe cyanescens*, including an L-tryptophan decarboxylase (*psiD*), a kinase (*psiK*), an S-adenosyl-L-methionine (SAM)-dependent N-methyltransferase (*psiM*) and a P450 monooxygenase (*psiH*) (Fricke *et al.*, 2017).

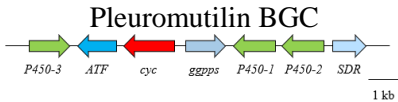
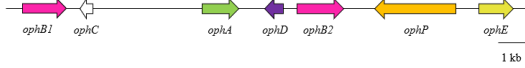
Ramm *et al.* and Van Der Velden *et al.* identified the biosynthetic genes *ophMA* and *ophP* by mining the genome of *Omphalotus olearius* for the BGC of omphalotin A (**Table 1**) and provided the first example of the incorporation of α -N-methylation in a peptide backbone via the RiPP pathway (Ramm *et al.*, 2017; Van Der Velden *et al.*, 2017). RiPP pathway is much different from NRPS biosynthesis of other fungal cyclopeptides and is so far unparalleled in fungi.

The strobilurin BGC was identified from *Strobilurus* spp. (Nofiani *et al.*, 2018), and was shown to encode a highly reducing polyketide synthase with very unusual C-terminal hydrolase and methyltransferase domains. The expression in *Aspergillus oryzae* NSAR1 leads to the formation of prestrobilurin A. The FAD-dependent oxygenase *str9* is responsible for the oxidative rearrangement of prestrobilurin A to form the key β -methoxyacrylate toxophore of the strobilurin fungicides. Two SAM-dependent methyltransferases *str2* and *str3* are required and give the product strobilurin A (Nofiani *et al.*, 2018).

Much of the structural diversity of natural products from Basidiomycota could already be accessed by improving chemical methods and synthetic biology, while the mechanism of the biosynthesis of many molecules from Basidiomycota remains unexplored. For the natural products with notable biological activities and medicinal properties, the elucidation of the

biosynthesis pathways could accelerate the development of these molecules for agricultural and pharmacological applications (Lin *et al.*, 2019).

Table 1. Some published biosynthesis gene clusters

Biosynthesis gene cluster (BGC)	Gene	Putative function	Reference
 <p style="text-align: center;">Pleuromutilin BGC</p>	<i>P450-3</i>	Cytochrome P450	(Bailey <i>et al.</i> , 2016)
	<i>ATF</i>	Acetyltransferase	
	<i>cyc</i>	Terpene Cyclase	
	<i>ggpps</i>	Geranylgeranyl pyrophosphate synthetase (GGs)	
	<i>P450-1</i>	P450 monooxygenase	
	<i>P450-2</i>	P450 monooxygenase	
	<i>SDR</i>	Short-chain dehydrogenase/reductase (SDR)	
 <p style="text-align: center;">Omphalotin A BGC</p>	<i>ophB1</i>	Monooxygenase	(Van Der Velden <i>et al.</i> , 2017)
	<i>ophC</i>	NTF2-like	
	<i>ophA</i>	Methyltransferase	
	<i>ophD</i>	<i>O</i> -Acyltransferase	
	<i>ophB2</i>	Monooxygenase	
	<i>ophP</i>	Prolyloligopeptidase	
	<i>ophE</i>	F-box/RNI-like	

1.5 Aim of the Thesis

The main purpose of this thesis is to screen and identify the active components from the largely neglected basidiomycetes originated from African tropics. In order to clarify the diversity of Basidiomycota and its prosperous chemistry structures, the extensive study of natural products in several basidiomycetes collected from Kenyan tropical rainforest Kakamega and Mount Elgon national reserve was carried on in the past years. Twenty-eight basidiomycetes will be screened for antimicrobial activities and yield in three standard media. Afterward, some strains will be selected for large scale fermentation. The crude extracts from large fermentation will be purified by preparative HPLC, the molecular weight of fractions will be analysed by LC-MS and HR-ESIMS, structures of pure fractions will be elucidated by NMR data. Biological activities of compounds will be tested by a series of tests: antimicrobial, nematicidal, biofilm inhibition, and cytotoxicity assays.

Basidiomycetes that can produce novel compounds with prominent biological activities will be selected for genome sequencing. The illudins are sesquiterpenes with antitumor properties, which have been reported 70 years ago. However, the illudin biosynthetic pathway remains unknown. The side project of this thesis is about elucidation of illudin biosynthesis of *Omphalotus olearius*. The identification of gene clusters will be annotated by software and manual methods. Plasmids will be constructed by homologous recombination in *Saccharomyces cerevisiae*. Heterologous expression of the plasmids will be done in *Aspergillus oryzae*.

2. Experimental Section

2.1 Chemicals

Chemical	Supplier
Acetic acid	Carl Roth
Acetonitrile, HPLC gradient	J.T. Baker
Adenine	Carl Roth
Ammonium sulfate	Carl Roth
Agar	Carl Roth
Calcium carbonate	AppliChem
Calcium chloride	Carl Roth
Casein peptone	Becton dickinson
Complete supplement mixture minus Uracil	Sigma-Aldrich
Cottonseed flour	Sigma-Aldrich
Czapek Dox broth	Duchefa Biochemie
Dichloromethane	J.T. Baker
Dipotassium hydrogen phosphate	AppliChem
Edamin	Oxoid Limited
Ethylenediaminetetraacetic acid	Sigma-Aldrich
Formic acid	Carl Roth
D (+)-Glucose	Cargill Incorporated
D (+)-Glucose Monohydrate	Carl Roth
Glycerol	Carl Roth
Glycine	Sigma-Aldrich
n-Heptane	Carl Roth
Magnesium sulfate heptahydrate	Carl Roth
Molasses	Nordzucker AG
Malt extract	Organotechnie SAS
L-methionine	Carl Roth
MHB medium	AppliChem
D (+)-Maltose	Carl Roth

D-Mannitol	AppliChem
D (+)-Mannose	AppliChem
Methanol	J.T. Baker
Nutrient broth Nr. 2 from Oxoid	Fisher Scientific
Oatmeal	Herrnmühle Reichelsheim, Germany
Polypeptone	Carl Roth
Potassium chloride	J.T. Baker
Potassium dihydrogen phosphate	Carl Roth
Potassium hydroxide	Carl Roth
Sodium nitrate	Carl Roth
Sodium chloride	Sigma-Aldrich
D-sorbitol	Carl Roth
Soy peptone	Oxoid Limited
Sucrose	Carl Roth
Trifluoroacetic	Carl Roth
Trizma base	Carl Roth
Tryptone	Duchefa Biochemie
Milli-Q Water, deionised, ultrapure	Merck KGaA, Darmstadt, Germany
Yeast extract	Becton dickinson
Yeast nitrogen base	Sigma-Aldrich

2.2 Media, Buffers and Solutions

All media, buffers, and solutions were sterilised by autoclaving for 20 min at 120 °C or by a disposable sterile filter (0.45 µm pore size, Roth) and are summarised in **Table 2-5**. Before autoclaving, the pH was measured (inoLab pH 730 pH-meter, WTW/Xylem Analytics Germany Sales GmbH & Co. KG, Weilheim, Germany) and adjusted to the desired pH by slow addition of a 10% solution of KOH or HCl.

Table 2. Media and agar used for fermentation and bioactivity test in this study.

Meida	Ingredients	Composition (g/L)
Casein-peptone soymeal-peptone (CASO)	Casein peptone	17
	Soy peptone	3
	Sodium chloride (NaCl)	5
	Dipotassium hydrogen phosphate	2.5
	D (+)-Glucose	2.5
	PH 7.3 ± 0.2	
MHB agar	MHB medium	
	Agar	15
Nematode agar	Soy peptone	2
	NaCl	1
	Agar	20
Q6 _{1/2}	Glycerol	10
	D (+)-Glucose	2.5
	Cottonseed flour	5
	PH 7.2	
YMG	Malt extract	10
	D (+)-Glucose	4
	Yeast extract	4
	PH 6.3	
YMG agar	YMG medium	
	Agar	15
ZM _{1/2}	Molasses	5
	Oatmeal	5
	Sucrose	4
	Mannitol	4
	D (+)-Glucose	1.5
	Calcium carbonate	1.5
	Edamin	0.5
	Ammonium sulfate	0.5
	PH 7.2	

Table 3. Media and agar used for *E. coli* and *S. cerevisiae* in this study.

Media	Ingredients	Composition [% (v/w)]
LB	NaCl	0.5
	Tryptone	1
	Yeast extract	0.5
LB Agar	LB medium	
	Agar	1.5
YPAD	Yeast extract	1
	Tryptone	2
	D(+)-Glucose Monohydrate	2
	Adenine	0.03
YPAD Agar	YPAD medium	
	Agar	1.5
SM-URA Agar	Yeast nitrogen base	0.17
	(NH ₄) ₂ SO ₄	0.5
	D(+)-Glucose Monohydrate	2
	Complete supplement mixture minus Uracil	0.077
	Agar	1.5

Table 4. Media and agar used for *A. oryzae* in this study.

Media	Ingredients	Composition [% (v/w)]
CZD/S agar	Czapek Dox broth	3.5
	D-sorbitol	18.22
	(NH ₄) ₂ SO ₄	0.1
	L-methionine	0.15
	Adenine	0.05
	Agar	1.5
CZD/S soft agar	Czapek Dox broth	3.5
	D-sorbitol	18.22
	(NH ₄) ₂ SO ₄	0.1
	L-methionine	0.15
	Adenine	0.05
	Agar	0.8
CZD/S1 agar (-met)	Czapek Dox broth	3.5
	D-sorbitol	18.22
	(NH ₄) ₂ SO ₄	0.1
	L-methionine (optional)	0.15
	Agar	1.5
CZD/S1 soft gar (-met)	Czapek Dox broth	3.5
	D-sorbitol	18.22
	(NH ₄) ₂ SO ₄	0.1
	L-methionine (optional)	0.15
	Agar	0.8
DPY	Dextrin from potato starch	2
	Polypeptone	1
	Yeast extract	0.5
	KH ₂ PO ₄	0.5
	MgSO ₄ * H ₂ O	0.05
DPY Agar	DPY medium	
	Agar	2.5
GNB	D(+)-Glucose Monohydrate	2
	Nutrient broth Nr. 2 from Oxoid	3

Table 5. Buffers and solutions used in this study.

Buffers	Ingredients	Composition (g/L)
Glycine-HCl (0,1 M)	Glycine	7.5
	Hydrochloric acid (HCl)	0.832
Hank's	PH 3	
	NaCl	8
	KCl	0.4
	KH ₂ PO ₄	0.06
	D (+)-Glucose	1
	Na ₂ HPO ₄	0.048
	MgSO ₄	0.098
	CaCl	0.14
	NaHCO ₃	0.35
Loading-dye (6 x)	Na ₂ HPO ₄	7.098
	pH 8	
M9	KH ₂ PO ₄	3.0
	Na ₂ HPO ₄	6.0
	NaCl	5.0
	1 mL 1 M MgSO ₄ was added after autoclaving	
PBS	NaCl	8.0
	KCl	0.2
	Na ₂ HPO ₄	1.44
	KH ₂ PO ₄	0.24
10 × SDS running buffer	Tris	3.029
	Glycine	14.413
	SDS	0.1 % (w/v)
	pH 8.3	
TAE buffer	Tris	4.846
	Acetate	1.181
	EDTA	0.292
Solutions	Ingredients	Composition (g/L)
Solution 1	NaCl	46.752
	CaCl ₂	1.110
	Tris-HCl	2.423
	pH 7.5	
Solution 2	PEG 3350	60 % (w/v)
	Tris-HCl	6.057
	NaCl	46.752
	CaCl ₂	1.110

2.3 Enzyme and Antibiotics

Antibiotics stock solutions were prepared in distilled water, ethanol or methanol, and filter sterilized through 0.45 µm syringe filters and stored at – 20 °C. Stock and working concentrations are listed in **Table 6**.

Table 6. Antibiotics used in this study.

Antibiotic	Solvent	Stock concentration (mg/ml)	Working concentration (µg/ml)
Carbenicillin	H ₂ O	50	50
Chloramphenicol	EtOH	30	30
Ciprofloxacin	MeOH	50	150
Hygromycin B	H ₂ O	50	150
Kanamycin	H ₂ O	50	50
Nystatin	MeOH	50	250
Oxytetracycline	MeOH	50	100
Penicillin G	MeOH	50	250
Streptomycin	MeOH	50	250
Tetracyclin	H ₂ O	50	10
Vancomycin	MeOH	50	100

2.4 Specimen Collection and Isolation

The strains of Basidiomycota used in the current thesis and the related publications were collected either from the Kakamega rainforest or Mount Elgon National Reserve in the western part of Kenya. The strains were isolated on YMG agar plates either from spore prints or by incubation of sterile mycelial plugs from the context of the basidiome. Bacteria were prevented to grow by adding the antibiotics, penicillin G, and streptomycin (250 µg/ml) to the YMG medium. The pure cultures have been deposited at MUCL, Louvain-la-Neuve, Belgium and Helmholtz Centre for Infection Research (HZI) in Germany.

2.5 Fungal Identification

The fungal strains were identified by morphological studies and molecular analysis of rDNA (5.8S gene region, the internal transcribed spacers ITS1 and ITS2) and in some cases the D1/D2 domains of the large subunit (LSU). For isolation of DNA from pure cultures, a small amount of mycelium was disrupted with a Precellys 24 homogenizer (Bertin Technologies, France) at a speed of 6000 rpm for 2 × 40 s. The extraction of DNA was performed according to EZ-10 Spin Column Genomic DNA Miniprep kit (Bio Basic Canada Inc., Markham, Ontario, Canada).

Primes ITS1F (Gardes and Bruns, 1993) and ITS4 (White *et al.*, 1990) were used for amplification of the ITS region, LR7 (Vilgalys and Hester, 1990) and NL4 (Reynolds and Taylor, 1993) were used for the LSU amplification. Electrophoresis in 2% agarose gel with a small amount PCR product was used to check the quality. EZ-10 Spin Column PCR Purification Kit (Bio Basic Canada Inc., Markham, Ontario, Canada) was used for purification of the PCR products. The purified amplicons were sent to the department Genome Analytics at the Helmholtz Centre for Infection Research (Braunschweig, Germany) for sequencing. The generated raw data were assembled by the software Geneious 7.1.4 (Biomatters Ltd, Auckland, New Zealand). Afterward, a BLAST (<https://blast.ncbi.nlm.nih.gov/Blast.cgi>) search based on the GenBank database was conducted to obtain the 20 closest hits of the ITS sequence, the phylogenetic relationships were then analyzed by RAxML method (Stamatakis, 2014).

2.6 Agar Diffusion Assay for Preliminary Screening

In the purpose of screening bioactive specimen, small pieces pure fungal cultures cut out by using a cork borer (7 mm) and tested for their antimicrobial activity in an agar diffusion assay, using the following culture media and conditions: YMG and MHB agar plates were used to incubate *Mucor plumbeus* MUCL 49355 and *Bacillus subtilis* DSM 10, respectively. 5×10^4 cells per litre of tested organisms were added in the media before pouring the plates. Five agar plugs from mature cultures were placed on the agar plate in a circle. Ciprofloxacin dissolved in methanol (1.5 mg/ml) was used as positive control and 200 μ L was added on a filter disc for *Bacillus subtilis* DSM10, nystatin used for the positive control of *Mucor plumbeus* MUCL49355 with the same concentration and volume. The filter discs contain antibiotics were placed in the middle of agar plates. The antibacterial and antifungal activities were observed by checking the inhibition around the cultures after 24h and 48h, respectively.

2.7 Cultivation and Extraction of Small Scale Fermentation

Fungal strains exhibited activity in the agar diffusion assay were selected for further screening. For this purpose, the strains were cultivated in three different media: YMG, ZM $_{1/2}$, and Q $_6$ $_{1/2}$. 200 mL of the three media were prepared in 500 mL Erlenmeyer flasks and autoclaved, five pieces cultures (cut by 7 mm cork borer) were inoculated in the media. The cultures were incubated on a rotary shaker (140 rpm) at 23 °C. The growth of cultures was monitored by checking the amount of free glucose with Medi-test glucose/100 (Macherey-Nagel) constantly.

The fermentation process was terminated three days after glucose depletion. Biomass and the culture fluid were separated by filtration with gauze. The mycelium was extracted with 200 mL acetone in an ultrasonic bath for 30 min. The filtrate was evaporated in vacuum at 40 °C, the remaining aqueous residue was diluted with distilled water and extracted with the same amount ethyl acetate and filtered through anhydrous sodium sulphate, the resulting organic phase was evaporated to dryness in vacuum at 40° using a rotary evaporator. The supernatant was extracted by directly adding the same amount of ethyl acetate and subjected to the same procedure as biomass.

2.8 Antimicrobial Assay for Small Scale Crude Extracts

Serial dilution assay was used for evaluation of the antimicrobial activity of the crude extracts from small-scale fermentation. The minimum inhibition concentrations (MIC) against *Bacillus subtilis* DSM 10, *Escherichia coli* DSM 498, *Candida tenuis* MUCL 29892, and *Mucor plumbeus* MUCL 49355 were determined. The starting concentration of the extracts was 300 µg/mL, the assays were conducted with 96-well microtiter plates in MHB medium for bacteria and YMG medium for fungi.

2.9 Analytical LC-MS

The extracts were analysed by HPLC (Ultimate 3000 system, Thermo Fisher Scientific, Waltham, Massachusetts, USA) equipped with a DAD and an ESI-TOF mass spectrometer (Amazon speed, Bruker, Billerica, Massachusetts, USA). An Acquity UPLC BEH C₁₈ column (50 × 2.1 mm, 1.7 µm; Waters, Milford, Connecticut, USA) was used as stationary phase and the temperature was 40 °C, the mobile phase (solvent A: water + 0.1 % formic acid; solvent B: acetonitrile + 0.1 % formic acid) started with isocratic conditions at 5 % solvent B and increased in 20 min to 100% solvent B followed by 10 min isocratic condition with solvent B, the flow rate was 0.6 mL/min and compounds were detected by DAD in the range of 200 - 600 nm. The concentration of the extracts was adjusted to 4.5 mg/mL and 2 µL were injected. The novelty of the compounds in the extracts was determined by comparing the molecular formula and weight obtained from HPLC-MS with the data from the Dictionary of Natural Products (DNP) (Buckingham, 2017).

2.10 Analytical GC-MS

GC-MS analyses were performed on a Thermo ITQ 900 system (Thermo Fisher Scientific Inc., Hudson, NH, USA) equipped with a ZB-5MS column (Phenomenex; dimensions 30m x 0,25mm, film thickness 0,25µm). The samples were collected through a solid phase micro extraction fibre (SPME-fibre; stationary phase Divinylbenzene/Carboxen/PDMS) from the headspace of the samples within 45 min at room temperature. The desorption of samples from SPME-fibre was performed in the PTV injector of the gas chromatograph for 1 min at 230 °C. The temperature gradient was 50 °C for 1 min, 10 °C/min increase rate up to 320 °C, followed by 320 °C for 2 min. The carrier gas was helium, with a column head pressure of 10 psi. The transfer line temperature was set at 250 °C and the ion source at 220 °C. Mass spectra were recorded from m/z 50 to 700. Raw data were converted to cdf-files by Xcalibur 2.1 software (Thermo Scientific), the initial identification of unknown compounds was made by library comparison using the build in NIST-database (version 11).

2.11 Scale-up Fermentation and Extraction

Promising strains were scaled up for fermentation in 25 to 50 flasks with 200 mL medium, the medium was selected depends on both the bioactivities and HPLC-MS results. The mycelia and supernatant were separated via vacuum filtration. The mycelia were extracted with 500 mL of acetone in an ultrasonic bath for 30 min for four times. The extracts were combined and the solvent was evaporated by rotary. The remaining water phase was suspended in 200 mL of distilled water, extracted with the same amount of ethyl acetate three times, and filtered through anhydrous sodium sulphate. The resulting ethyl acetate extract was evaporated to dryness. The supernatant was extracted by adding 5% Amberlite XAD-16N absorbent (Rohm & Haas GmbH, Frankfurt am Main, Germany) and incubated for three hours on a shaker or stirred by a blender. The XAD resin was then filtered and eluted with 500 mL of acetone four times. The resulting acetone extracts were evaporated, and the remaining water phase was extracted with an equal amount of ethyl acetate. The organic phase was dried over anhydrous sodium sulphate and evaporated to dryness.

2.12 Purification of Compounds by Preparative LC-MS

The extracts were filtered using an SPME Strata-X 33 u Polymeric RP cartridge (Phenomenex, Inc., Aschaffenburg, Germany) to get rid of undesired highly hydrophobic compounds, such as

fatty acids. A preparative reverse-phase liquid chromatography system (PLC 2020, Gilson, Middleton, USA) was used for fractionation of the crude extracts, VP Nucleodur 100–5C 18 ec column (250 mm × 40 mm, 7 μm, Macherey-Nagel) was used as a stationary phase. Deionized water (Milli-Q, Millipore, Schwalbach, Germany) with 0.05% trifluoroacetic acid (TFA) (solvent A) and acetonitrile with 0.05% TFA (solvent B) were used as the mobile phase. UV monitoring was carried out at 210, 254, and 350 nm, the flow rate was 40 mL/min. The applied gradients were estimated according to the results of the analytical HPLC data and have been reported in related publications. The purity of the isolated compounds was evaluated by HPLC-DAD-MS and NMR.

Another equipment Waters mass-directed auto purification system was also used for purification of compounds, comprising of a Waters 2767 autosampler, Waters 2545 pump system, a Phenomenex Kinetex Axia column (5 μm, C₁₈, 100 Å, 21.2 × 250 mm) equipped with a Phenomenex Security Guard precolumn (Luna, C₅, 300 Å). Gradient was run over 10 min starting at 10 % acetonitrile/ 90 % HPLC grade water (0.05 % formic acid) and ramping to 90 % acetonitrile. The flow was set to 20 mL/min and the post-column flow was split (100:1) and the minority flow was made up with HPLC grade MeOH + 0.045 % formic acid to 1 mL/min for simultaneous analysis by diode array detector (Waters 2998) in the range 210 to 600 nm and an ELSD detector (Waters 2424) together with mass spectrometry, Waters SQD-2 mass detector, operating simultaneously in ES⁺ and ES⁻ modes between 150 and 1000 *m/z*. Detected peaks were collected into glass test tubes. Combined tubes were evaporated (vacuum centrifuge).

2.13 Structure Elucidation

The exact mass of compounds were determined by high-resolution electrospray ionization mass spectrometry (HR-ESIMS), equipped with an Agilent 1200 series HPLC-UV system (Agilent, Santa Clara, California, USA) combined with an ESI-TOF-MS (Maxis, Bruker, Billerica, Massachusetts, USA), an Acquity UPLC BEH C₁₈ column 2.1 × 50 mm, 1.7 μm, (Waters, Milford, Connecticut, USA) was used. Solvent A: H₂O + 0.1% formic acid; solvent B: acetonitrile + 0.1% formic acid, gradient: 5% solvent B for 0.5 min increasing to 100% solvent B in 19.5 min and then maintaining 100% solvent B for 5 min, flow rate 0.6 mL/min, uv/vis detection 200 – 600 nm. For NMR spectroscopy, a maximum of 10 mg of a pure substance was dissolved in 600 μl deuterated solvent in NMR tube, the smaller amounts (< 1 mg) compounds were dissolved in 300 μl deuterated solvent in a high precision NMR tube (Shigemi Inc, Allison Park, Pennsylvania, USA). NMR spectra were recorded with a Bruker 500 MHz

Avance III spectrometer with a BBFO (plus) SmartProbe (^1H 500 MHz, ^{13}C 126 MHz) and a Bruker 700 MHz Avance III spectrometer with a 5 mm TCI cryoprobe (^1H 700 MHz, ^{13}C 175 MHz). Chemical shifts δ were referenced to the solvents: acetone- d_6 (^1H , $\delta = 2.05$ ppm; ^{13}C , $\delta = 29.3$ ppm), acetonitrile- d_3 (^1H , $\delta = 1.94$ ppm; ^{13}C , $\delta = 1.9$ ppm), chloroform- d (^1H , $\delta = 7.27$ ppm; ^{13}C , $\delta = 77.0$ ppm), pyridine- d_5 (^1H , $\delta = 7.22$ ppm; ^{13}C , $\delta = 123.9$ ppm). Mosher's method (Hoye *et al.*, 2007) was used to determine the absolute stereochemistry. Optical rotations were obtained from a PerkinElmer 241 (Überlingen, Germany) polarimeter. UV spectra were recorded by using a Shimadzu UV-vis spectrophotometer UV-2450. CD spectra were determined with a JASCO spectropolarimeter, model J-815 (JASCO, Pfungstadt, Germany). The structures in this thesis were elucidated by Dr. Clara Chepkirui.

2.14 Bioactivity Tests for Pure Compounds

2.14.1 Serial Dilution Assay

The pure compounds were studied for their antimicrobial activities by serial dilution assay as described in **section 2.8**. Additional microorganisms *Micrococcus luteus* DSM1790, *Mycobacterium smegmatis* DSM43524, MRSA *Staphylococcus aureus* DSM11822, *Staphylococcus aureus* DSM346, *Mucor hiemalis* DSM2656 were included in the test panel.

2.14.2 Biofilm Inhibition Assay

According to the data from the Centre for Disease Control and Prevention Report in 2007, infections from biofilm are a serious threat in hospitals, about 1.7 million infections occur are caused by infections related to biofilms per year. Human pathogens commonly known to be involved in biofilm associated infections include *Staphylococcus epidermidis*, *Staphylococcus aureus*, *Pseudomonas aeruginosa*, *Escherichia coli* and *Candida albicans* (Adam *et al.*, 2002; Khatoon *et al.*, 2018).

In this study, *Staphylococcus aureus* DSM1104 was used in the biofilm inhibition assay and grown in casein-peptone soymeal-peptone (CASO) medium containing 4% glucose with PH 7.0. The concentration of *S. aureus* cell was adjusted to match the turbidity of 0.5 McFarland standard. The assay was performed in 96-well flat bottom plates (Falcon Microplates, USA) by serially diluted compounds from a start concentration of 256 $\mu\text{g}/\text{mL}$ and incubated for 24 h at 37 °C. The supernatant medium was discarded after incubation, the biofilm stained with crystal violet for 15 min and washed with PBS buffer for three times, the dye was solubilized with 30%

acetic acid and incubated at room temperature for 10 - 15 min, the absorbance of the solution was quantified in a plate reader at 550 nm. Methanol was used as negative control; all experiments were carried out in triplicates with two repetitions and cytochalasin B was used as a positive standard (de Carvalho *et al.*, 2016; Yuyama *et al.*, 2018).

2.14.3 Nematicidal Assay

The nematicidal activity against *Caenorhabditis elegans* of all isolated compounds were determined by a slightly modified method according to Stadler *et al.* (1994). *Caenorhabditis elegans* was inoculated on an autoclaved nematode agar plate, the following ingredients were added as sterile filtered solutions: cholesterol (1 mg/mL dissolved in EtOH 0.5 mL), 1M CaCl₂ 1 mL, 1M MgSO₄ 1 mL, 40 mM potassium phosphate buffer 12.5 mL PH 6.8 with living *Escherichia coli* DSM498 (1 mL of a suspension containing approximately 10 cells/mL, pre-inoculated in MHB medium for 12 h at 37 °C) and the plates were incubated at 21 °C for 4 - 5 days. Thereafter, nematodes were washed down from the plates with M9 buffer. Finally, a nematode suspension of approximately 500 nematodes/mL in M9 buffer was prepared and used in the microtiter plate assay. The assay was performed in 24-well microtiter plates at four concentrations (100, 50, 25, and 12.5 µg/ml) for each compound. Ivermectin (Sigma Aldrich) with related concentrations was used as a positive control, while methanol was used as a negative control. The plates were incubated at 20 °C in the dark and nematicidal activity was recorded after 18 h of incubation and expressed as LD₉₀ (*i.e.* concentration causing over 90 % immobility of the nematodes) (Rupcic *et al.*, 2018).

2.14.4 Cytotoxicity Assay

In vitro cytotoxicity (IC₅₀) of the isolated compounds was determined against a panel of mammalian cell lines, including mouse fibroblast L929, HeLa cells KB 3.1, squamous cell carcinoma A431, human breast adenocarcinoma MCF-7, human prostate cancer PC-3 and human lung carcinoma A549. The cell lines L929, KB 3.1 and A549 were cultured in DMEM (Gibco, ThermoFisher Scientific, Hilden, Germany), PC-3 in F12-K (Gibco), MCF-7 and A431 in RPMI (Lonza, Cologne, Germany), all media were supplemented with 10% of fetal bovine serum (Gibco) under 10% CO₂ at 37 °C. The cytotoxicity assay was performed according to using the MTT (3-(4,5-dimethylthiazol-2-yl)-2,5-diphenyltetrazolium bromide) method in 96-well microplates. 60 µL aliquots of serial dilutions from an initial stock with 1 mg/mL in methanol of the test compounds were added to 120 µL aliquots of a cell suspension (5.0 × 10⁴ cells/mL) in 96-well microplates. After 5 days of incubation, MTT assay was performed, and

the absorbance was measured at 590 nm using an ELISA plate reader (Victor, PerkinElmer, Überlingen, Germany). The concentration at the growth of cells was inhibited to 50% of the control (IC₅₀) was obtained from the dose-response curves. Experiments were repeated three times. Epothilone B was used as a positive control, and negative control was methanol (Kuephadungphan *et al.*, 2019). This assay was performed by our technician Wera Collisi.

2.14.5 Leucine Aminopeptidases Inhibition Assays

Hydrolysis of L-Leucine-7-amido-4-methylcoumarin (L-Leu-AMC) by the surface bound aminopeptidases of HeLa (KB3.1) cell lines was evaluated according to the method described by Weber *et al.*, (1992) with slight modifications. KB3.1 cell was grown as monolayer cultures in Dulbecco's Modified Eagle (DMEM) medium containing 10% of fetal calf serum at 37 °C in 24-well multidishes. After three days the confluent monolayers were washed twice with phosphate buffered saline (PBS) and the reaction mixture (450 µL Hank's buffer PH 7.2 containing 50 µM and 100 µM substrate L-Leu-AMC, and compounds dissolved in 50 µL DMSO) was added. After 30 min of incubation at 23 °C, 1 mL of cold 0.2 M glycine-buffer PH 10.5 was added. The amount of hydrolyzed 7-amino-4-methylcoumarin (AMC) was determined in a fluorescence spectrophotometer (excitation/emission: 365/440 nm; Tecan Infinite M200 PRO). Bestatin (Mathé, 1991) and DMSO were used as positive control and negative control, respectively.

2.14.6 Inhibitory Effects on HCV Infectivity

Huh-7.5 cells were inoculated with RLuc Jc1 reporter viruses in the presence of different compounds. Monolayers were washed three times with PBS 4 h later and overlaid with fresh medium without inhibitors. Infected cells were lysed three days later, and reporter virus infection was determined by Renilla luciferase activity. The cell viability was measured by the determination of Firefly luciferase. Huh-7.5 cells stably expressing Firefly luciferase (Huh-7.5 Fluc) were cultured in Dulbecco's modified minimum essential medium (DMEM, Life Technologies Manchester UK) (containing 2 mM/L glutamine, 1× minimum essential medium nonessential amino acids (MEM NEAA, Life Technologies)), 100 µg/mL streptomycin, 100 IU/mL penicillin (Life Technologies), 5 µg/mL blasticidin and 10 % fetal bovine serum). Cells were incubated at 37 °C with 5 % CO₂ supply. Infected cells were lysed and then frozen at -80 °C for 1 h following measurements of Renilla and Firefly luciferase activities on a Berthold Technologies Centro XS3 Microplate Luminometer as indicators of viral genome replication

and cell viability, respectively (Ciesek et al., 2011; Sandargo et al., 2019b). This assay was done by our collaborator from Twincore.

2.15 Microbial Strains Used for Biosynthesis

Table 7. Microbial strains used in this work for heterologous expression.

Strain	Genotype	Reference
BL21 (DE3)	F ⁻ <i>ompT hsdS_B</i> (rB ⁻ , mB ⁻) <i>dcm gal</i> λ(DE3)	Thermo Fisher Scientific
OneShot ccdB survival 2T1 ^R	F ⁻ <i>mcrA</i> Δ(<i>mrr-hsdRMS-mcrBC</i>) Φ80 <i>lacZ</i> ΔM15 Δ <i>lacX74 recA1 ara</i> Δ139 Δ(<i>ara-leu</i>)7697 <i>galU galK rpsL</i> (Str ^R) <i>endA1 nupG fhuA::IS2</i>	Thermo Fisher Scientific
<i>A. oryzae</i> NSAR1	Δ <i>argB sC adeA niaD</i>	Lazarus group, Bristol
<i>S. cerevisiae</i> CEN.PK2	MATa/a <i>ura3-52/ura3-52 trp1-289/trp1-289 leu2-3_112/leu2-3_112 his3 D1/his3 D1MAL2 8C/MAL2-8C SUC2/SUC2</i>	Euroscarf

2.16 Molecular Biology Methods for Biosynthesis

2.16.1 Oligonucleotides

All oligonucleotides used in this work were purchased from Sigma Aldrich and listed in Table 8.

Table 8. Oligonucleotides used in this study.

Oligonucleotide	5'-3' sequence
TCF	TTTCTTTCAACACAAGATCCCAAAGTCAAATGCCGAAACTTTCTACCT
TCR (teno)	GGTTGGCTGGTAGACGTCATATAATCATACCTAGAGCTCAGAAATATCAA
TCR (tadh)	TTCATTCTATGCGTTATGAACATGTTCCCTCTAGAGCTCAGAAATATCAA
P450F (pgpd)	AACAGCTACCCCGCTTGAGCAGACATCACCATGGGTACCAGCATCGCTTC
P450R (teno)	GGTTGGCTGGTAGACGTCATATAATCATACTTACACGACCAGACCGTGGT
P450F (peno)	CGACTGACCAATTCCGCAGCTCGTCAAAGGATGGGTACCAGCATCGCTTC
oxi1F	CAGCTACCCCGCTTGAGCAGACATCACC GGATGTCTGCTCCTGCTTCTTT
oxi1R	ATGTCCATATCATCAATCATGACCGGCGCGTTACACGGAAATCGGGCACC
oxi2F	TTTCTTTCAACACAAGATCCCAAAGTCAAATGTTTTTCATCTAGGGTAGC
oxi2R	TTCATTCTATGCGTTATGAACATGTTCCCTTTATATCTTGAAACCACCAG
oxi3F	AACAGCTACCCCGCTTGAGCAGACATCACCATGTCTGCTCCTTCCACATT
oxi3R	GGTTGGCTGGTAGACGTCATATAATCATACTCAGAACGTTATAGGACACC

2.16.2 Polymerase Chain Reaction (PCR)

PCR was used to amplify DNA fragments. OneTaq® 2 × Master Mix (NEB) with standard buffer was used for screening purposes. For cloning the proofreading Q5® High-Fidelity 2 × Master Mix (NEB) was used. Manufacturers' instructions were followed for both enzymes.

2.16.3 RNA Extraction and cDNA Preparation

The *Omphalotus olearius* strain was inoculated in 100 mL YMG medium in 500 mL flask and incubated in 28 °C at 120 rpm for 5 days. Grown mycelia were harvested by filtration through sterile miracloth, about 100 mg fresh mycelia were processed according to instructions of RNeasy Plant Mini Kit (Qiagen). A digestion step was carried out by the DNase (Qiagen) according to manufacturer instructions to remove genomic DNA. Fresh purified total RNA was used in further steps.

The RevertAid Premium Transcriptase kit (Thermo Fisher Scientific) was used for preparing cDNA from total RNA (Beate Bonsch) using oligo (dT) nucleotides. Manufacturers' instructions were followed.

2.16.4 Construction of Vectors In this Thesis

Construction of fungal and bacterial expression vectors was performed *in vitro* cloning and *in vivo* homologous recombination in *S. cerevisiae*. The expression vectors constructed in this study are listed in **Table 9**.

Table 9. Constructed expression vectors (*A. oryzae*) in this study.

Name	Vector backbone	Oligonucleotides for construction in <i>S. cerevisiae</i>
argTC	pTYGSargB	TCF, TCR (teno)
argTC-P450	pTYGSargB	TCF, TCR (tadh), P450F (pgpd), P450R (teno)
argTC-P450-oxi1	pTYGSargB	TCF, TCR (tadh), P450F (peno), P450R (teno), oxi1F, oxi1R
ade-oxi2-oxi3	pTYGSade	oxi2F, oxi2R, oxi3F, oxi3R

2.16.5 Agarose Gel Electrophoresis

Agarose gel electrophoresis was used to analyse double stranded DNA fragments or RNA samples and was performed using horizontal gel tanks (BioRad) with 1 × TAE buffer. DNA samples were mixed with 6 × loading buffer and loaded on 1% (w/v) agarose gels which contained Roti® -Safe GelStain (1 µl in 40 ml). 1 kb DNA Ladder (New England Biolabs) was

used as a size marker. Electrophoresis was carried out at 80 -120 V for 20 min to 45 min in a Bio-Rad gel chamber containing 1 x TAE running buffer. DNA was visualised under a by the *Molecular Imager Gel doc XR+* (Bio-Rad) system under UV light (312 nm).

2.16.6 DNA Purification from Gel or PCR

Amplified DNA was purified for sequencing or cloning using NucleoSpin® Gel and PCR Clean-up kit (Macherey-Nagel) according to the protocols.

2.16.7 Isolation of Plasmid DNA from *E. coli*

The NucleoSpin® Plasmid kit (Macherey-Nagel) was used to isolate plasmid DNA from an overnight culture of *E. coli*.

2.16.8 Isolation of Plasmid DNA from *S. cerevisiae*

The Zymoprep Yeast Plasmid Miniprep II kit (Zymo Research) was used to isolate plasmid DNA from transformed *S. cerevisiae* cells grown on SM-URA plates. The whole amount of cells was collected and added directly to the lysis buffer provided by the kit. 10 µL ddH₂O was used for the final elution.

2.16.9 Cloning Procedure

Restriction Enzyme Digestion

Restriction enzyme digestions (single or double) were performed according to the manufacturer's protocols (New England Biolabs). Reaction mixtures were incubated at 37 °C in an incubator for 0.5 to 5 h and afterward enzymes were inactivated at 65 °C or 80 °C for 20 min. The resulting fragments were then analysed by agarose gel electrophoresis and purified by the NucleoSpin® Gel and PCR Clean up kit (Macherey-Nagel) as described previously.

Dephosphorylation of Linear DNA and Ligation

In order to prevent self-ligation of linearized plasmids, they were treated with shrimp alkaline phosphatase (SAP). 1 µL of enzyme was added after digestion to the reaction mixture for 1 h at 37 °C. Ligation reactions were performed using T4 DNA ligase. The reaction typically contained 5 × molar excess of DNA inserts. Reaction mixtures were incubated in the fridge (4 °C) overnight followed by inactivation at 65 °C for 20 min.

2.17 Transformation of Chemically Competent *Escherichia coli* Cells

2.17.1 Growth of *E. coli* Strain

E. coli strains were inoculated in liquid LB medium/agar with carbenicillin solution (1 µL/mL) and incubated at 37 °C for 12 – 18 h with 200 rpm. For long term storage glycerol stocks (25 % glycerol) were stored at -80 °C.

2.17.2 Transformation

An aliquot of 50 µL chemically competent *E. coli* cells was defrosted on ice. After the addition of either 1 µL of purified plasmid or 10 µL for a ligation mixture, the mixture was left on ice for 20 min. The heat shock was carried out at 42 °C for 60 s. Afterward, the cells were immediately placed on ice for 3 min, following by the addition of 500 µL of LB medium and 1 h incubation at 37 C, 300 rpm. The cells were spun down for 15 s, most of the supernatant was discard and around 200 µl were spread on LB agar plates with an appropriate antibiotic(s). The plates were incubated overnight in a 37 °C incubator.

2.18 Transformation of Competent *Saccharomyces cerevisiae* Cells

2.18.1 Growth of *S. cerevisiae* Strain

A stock of *S. cerevisiae* CEN.PK2 was spread on a YPAD agar plate and incubated at 30 °C for 72 h. A single colony was used to inoculate in 10 ml liquid YPAD, grown overnight at 30 °C and 200 rpm. *S. cerevisiae* CEN.PK2 transformed with *ura3* containing plasmids was grown on solid or liquid SM–URA agar plate, incubated at 30 °C for 2 - 4 days.

2.18.2 Transformation

Preparation of *S. cerevisiae* competent cells was done using the LiOAc/SS carrier DNA/PEG protocol developed by Gietz and Woods (Gietz and Woods, **2002**). A single colony was inoculated into 10 mL of YPAD medium and grown overnight at 30 °C, 200 rpm. The seed culture was added to 40 mL of YPAD in a 250 mL flask and incubated at 30 °C, 200 rpm, for 4 - 5 h. Cells were then harvested by centrifugation for 5 min at 3000 rpm and washed with 25 mL water, the cell pellet was resuspended in 1 mL water and transferred to a 1.5 mL tube. The

cells were pelleted at $20,000 \times g$ for 15 s, the supernatant was discarded. Afterward the suspension was aliquoted (50 μ L into 1.5 mL tubes each). A solution of ssDNA (Single-Strand Carrier DNA or salmon sperm DNA, 2 mg/mL) was boiled at 95 °C for 5 min and stored on ice until usage. For each transformation the following components were added to the 50 μ L yeast suspension aliquot: 240 μ L PEG solution (50% w/v polyethylene-glycol [PEG] 3350), 36 μ L 1 M LiOAc, 50 μ L ssDNA and up to 34 μ L of DNA (the master mix containing the linearized plasmid and desired inserts in equimolar concentration). Cells were resuspended in the transformation mixture by careful pipetting. The mixture was incubated at 42 °C for 40 min and afterward cells were pelleted at $21,000 \times g$ for 60 s and supernatant was discarded. The cell pellet was gently resuspended in 0.5 mL water, 250 μ L of the mixture was spread over SM-URA plates and incubated at 30 °C for 3 to 4 days.

2.19 PEG-mediated Transformation of *Aspergillus oryzae* NSAR1

2.19.1 Growth of *A. oryzae* Strain

Aspergillus oryzae NSAR1 was grown on DPY agar plates or in DPY medium at 28 °C for 3-7 days (120 rpm). For long term storage, *A. oryzae* spores were collected from plates by adding 3 mL distilled water, mixed with glycerol (final concentration 50 %) and stored at -80 °C.

2.19.2 Transformation

1 mL of *A. oryzaea* spore suspension from a sporulating plate were inoculated into 100 mL GN medium in a 500 mL flask, which was incubated overnight for 28 °C, 110 rpm. The grown mycelia were collected by filtration through sterile miracloth and was incubated in 10 mL protoplasts solution (0.8 M NaCl) containing 10 mg/mL Lysing Enzyme, which was sterilized through a 0.45 μ m syringe filter. After gentle shaking at 30 °C for 2-3 h, protoplasts were released from hyphae strands by gentle pipetting with wide-bore pipette. Afterward the mycelia were collected by filtration through sterile miracloth and centrifugation for 5 min at $3000 \times g$. The resulting supernatant was discarded and collected protoplasts were resuspended in solution 1 (100 μ L per transformation) and 10 μ L of purified plasmid DNA was added. The transformation mixture was incubated on ice for 5 min before adding 1 mL solution 2 and incubated again for 20 min at room temperature. Afterward pre-warmed 5 mL CZD/S (or CZD/S1) soft agar (50 °C) was added to the mixture and overlaid onto prepared CZD/S (or CZD/S1) plates. Plates were incubated at 28 °C for 2-4 days until colonies visible.

Transformants were then further selected twice on CZD/S (or CZD/S1) plates (-methionine) (2nd and 3rd selection plate) to reduce the number of false-positive transformants. From the 3rd selection plates a single colony was picked with a toothpick and grown alone on DPY agar for one week before they were used for fermentation and long-term storage. For fermentation, *A. oryzae* transformants were grown on DPY plates for 5-7 days before spores were collected and used to inoculate in 100 mL DPY medium (500 mL flasks). The inoculated flasks were incubated for 2-4 days at 28 °C shaking at 120 rpm followed by extraction and chemical analysis.

3. Results and Discussion

3.1 Secondary Metabolites from *Sanghuangporus* species

3.1.1 Sesquiterpenes from *Sanghuangporus* sp. (MUCL 56354)

Strain MUCL 56354 was obtained from a specimen that had been collected from Mount Elgon National Reserve in western Kenya, identified as *Sanghuangporus* sp. by morphological study and 5.8S/ITS nrDNA sequence. An initial BLAST search of ITS nucleotide sequence from NCBI database gave KP030787.1 (*Sanghuangporus microcystideus*, Zhou *et al.*, 2016), the closest hit with identity 96%, the next closest hit (JF895464.2 with 93%) belonged to an *Inonotus* species (Zhou *et al.*, 2016). The comparison of the 20 closest ITS BLAST results showed the relationship of MUCL56354, *Sanghuangporus* species, *Inonotus* species and *Phellinus* species (**Figure 18**, Wu *et al.*, 2012; Zhou *et al.*, 2016). Most of the sequences used for phylogenetic analysis are either from the publication of Wu *et al.*, 2012 or Zhou *et al.*, 2016. Based on molecular data we have addressed the strain as *Sanghuangporus* sp. Further taxonomic studies including comparisons with type specimens of related species are ongoing to characterize this strain to the species level. More information about *Sanghuangporus* spp. are stated in the “introduction (Section 1.3)”.

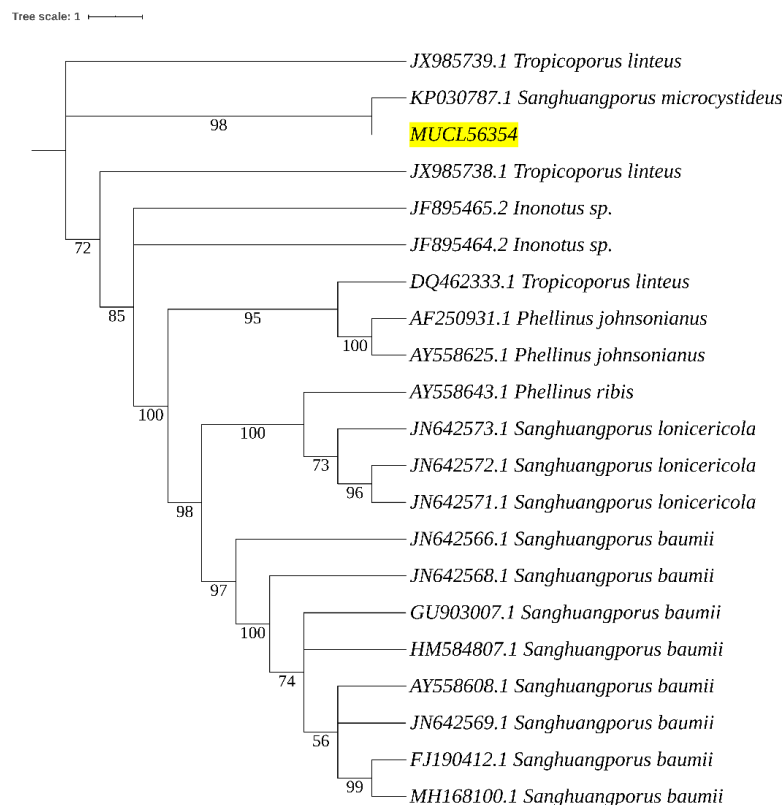


Figure 18. RAXML phylogenetic tree of the MUCL56354 ITS and the 20 closest BLAST results.

A well-grown YMG agar plate of the *Sanghuangporus* sp. culture was cut into small pieces using a 7 mm cork borer, five pieces were inoculated into a 500 mL Erlenmeyer flask containing 200 mL of three media: YM 6.3, Q6 ½, and ZM ½. The cultures were incubated at 23 °C on a rotary shaker (140 rpm). The fermentation was terminated 3 days after glucose depletion. Supernatant and biomass from this fermentation were separated by filtration. The supernatant was extracted by an equal amount of ethyl acetate and evaporated to dryness by means of a rotary evaporator. The mycelia were extracted with 200 mL of acetone in an ultrasonic bath for 30 min and filtered, and the filtrate was evaporated. The remaining water phase was suspended in an equal amount of distilled water, extracted with an equal amount of ethyl acetate, filtered through anhydrous sodium sulphate, and the resulting ethyl acetate extract was evaporated to dryness.

Analysis of the HPLC-MS data of crude extracts from three media and subsequent search in the Dictionary of Natural Products (DNP, https://www.crcpress.com/go/the_dictionary_of_natural_products) revealed the presence of potentially new bioactive metabolites of the production from YMG 6.3 medium and the crude extract exhibited activity against *Bacillus subtilis* with an MIC of 37.5 µg/mL (compared to the positive control ciprofloxacin with 3.1 µg/mL). The strains were inoculated into YMG media in a sterile flask (50 × 200 mL). Extraction from mycelium and supernatant leading to a yield of 151 mg and 369 mg crude extracts, respectively.

The crude extracts from supernatant and mycelia were fractionated by preparative reverse-phase liquid chromatography. Twenty-four fractions were collected according to the observed peaks (F1–F24) from supernatant extracts, and 14 fractions (F1–F14) were collected from the mycelial extracts.

The compounds were then purified by reversed-phase HPLC (solvent A, H₂O + 0.05% TFA; solvent B, ACN + 0.05% TFA) with a preparative HPLC column (Kromasil, MZ Analysentechnik, Mainz, Germany; 250 × 20 mm, 7 µm C₁₈) as stationary phase and a flow rate of 15 mL/min. The related gradients for each compound are listed in (Table 10).

Thirteen previously undescribed metabolites, 6*R*,7*S*,10*R*-7,10-epoxy-7,11-dimethyldodec-1-ene-6,11-diol **1** and twelve sesquiterpenes named elgonenes A–L **2–13**, and the known compound *P*-coumaric acid **14** (Figure 20) were purified. The structure elucidation of compounds was based on 2D NMR spectroscopy, high-resolution mass spectrometry. By searching the structures of identified compounds in SciFinder (<https://scifinder-n.cas.org>), some compounds are closely related compounds named phelilanes: compound **2** and **3** are

structurally related to phelilane D (**Figure 19**) from *Inonotus vaninii* (Yang *et al.*, 2013), a species that is closely related to *Sanghuangporus*; compound **5**, **6**, and **7** have similar structure to phelilane H (**Figure 19**), previously reported from *Phellinus linteus* (currently valid name *Tropicoporus linteus*, Zhou *et al.*, 2016); Compound **8** and **9** are closely related to phelilane E (**Figure 19**) from *Tropicoporus linteus* (Kobayashi *et al.*, 2010). Phelilanes have previously been patented (Kobayashi *et al.*, 2010) as part of the composition of an antibacterial agent that is being marketed for the treatment of ailments as diverse as gastroenteric dysfunction, diarrhea, hemorrhage, cancers, and prevention of periodontal disease and in the form of toothpaste and mouthwash agents in Asia.

Table 10. Details for purification of compounds from *Sanghuangporus* sp. (MUCL56354).

Details for purification of compounds from MUCL56354						
Compound No.	Amount (mg)	Fractions used for purifications	Gradient (solvent B)			
1	0.42	Supernatant fraction F15	52% (5 min)	52–100% (23 min)	100% (5min)	
2, 3, 8/9, and 11	0.28, 0.49, 3.31, and 2.55	Mycelia fraction F12 and supernatant fraction F23	60% (5 min)	60–85% (18 min)	85%–100% (2 min)	100% (5 min)
4,7	1.51, 4.08	Supernatant fraction F18	40% (5 min)	40–80% (18 min)	80%–100% (2 min)	100% (5 min)
5	3.07	Supernatant fraction F17	60% (5 min)	60–100% (23 min)	100% (5 min)	
6	0.89	Supernatant fraction F11	38% (5 min)	38–62% (23 min)	62%–100% (2 min)	100% (5 min)
10	1.34	Supernatant fraction F20	38% (5 min)	38–62% (23 min)	62%–100% (2 min)	100% (5 min)
12	1.2	Mycelia fraction F15	38% (5 min)	38–75% (23 min)	75%–100% (2 min)	100% (5 min)
13	2.17	Supernatant fraction F21 and mycelia fraction F10	55% (5 min)	55–85% (18 min)	85%–100% (2 min)	100% (5 min)
14	6.79	Supernatant fraction F7	34% (5 min)	34–100% (23 min)	100% (5 min)	

Compounds **8/9** (tested as an inseparable mixture), **10**, **11**, and **13** showed weak antimicrobial activity against *Bacillus subtilis*; compounds **8/9** and **13** demonstrated weak activities against *Micrococcus luteus*; compounds **4**, **8/9**, and **13** exhibited weak activities against *Staphylococcus aureus*. Further, most of the tested compounds demonstrated moderate activity against *Mucor hiemalis*, except for compound **7**, which was inactive. In the cytotoxicity assay compounds **4**, **8–11**, and **13** exhibited weak effects against KB 3.1 cells, while compounds **10** and **13** showed weak activity against L929 cells.

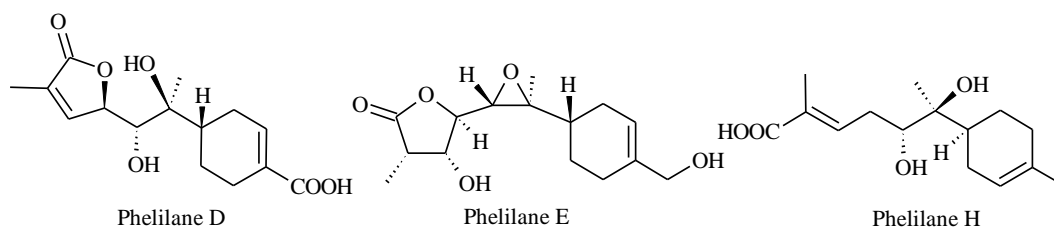


Figure 19. Chemical structures of Phelilanes.

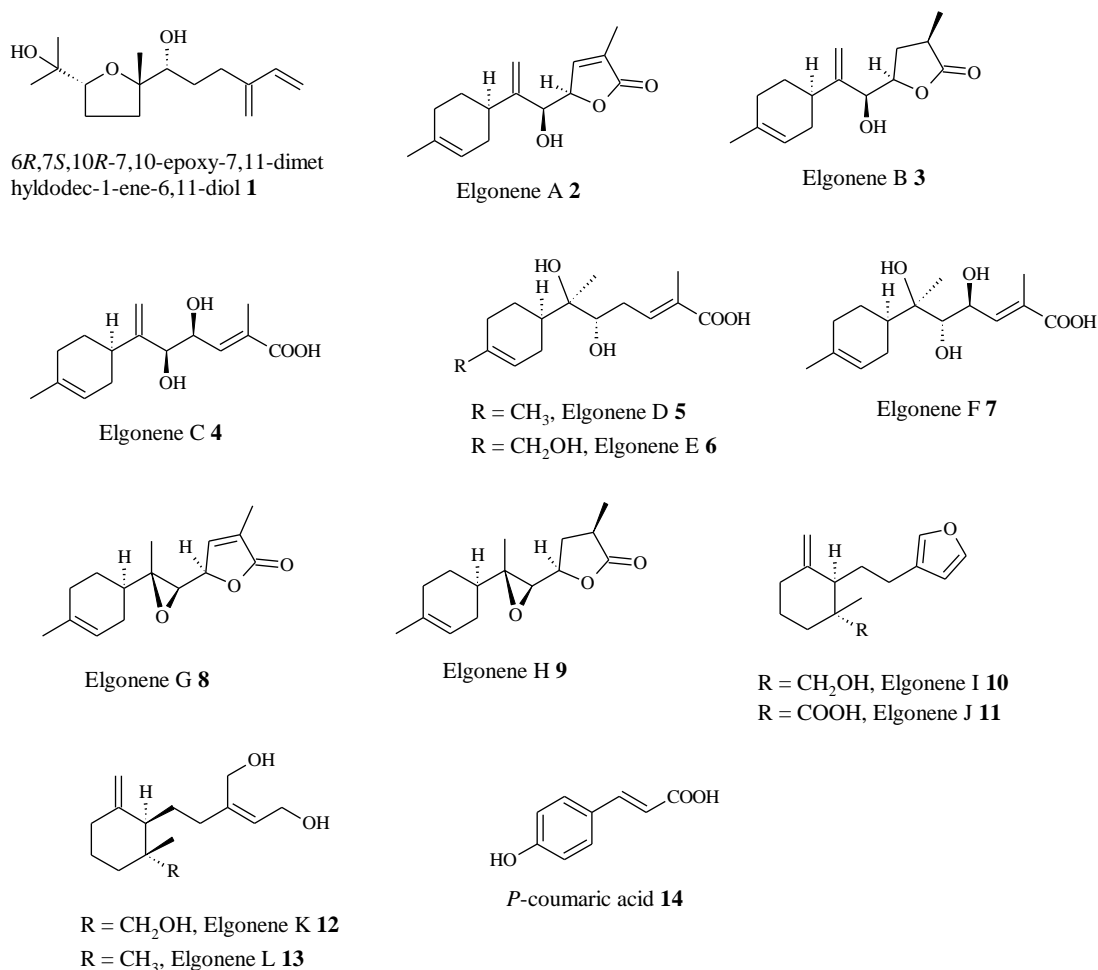


Figure 20. Chemical structures of the secondary metabolites isolated from *Sanghuangporus* sp. (MUCL56354) **publication 1**.

3.1.2 Unprecedented Metabolite from *Sanghuangporus* sp. (MUCL 55592)

Specimen MUCL 55592 collected from Kakamega equatorial rainforest was also identified as *Sanghuangporus* sp. by morphological examination and ITS sequence analysis. ZM ½ medium was selected for the scale-up fermentation with 30 flasks containing 200 mL media in each. Bioassay guided fractionation of supernatant extracts led to the isolation of a new highly oxygenated spiro [furan-2,1'-indine]-3-one derivative named phelligridin L **15**, together with

six known compounds: 3,14'-bihispidinyl **16**, hispidin **17**, ionylideneacetic acid **18**, 1*S*-2*E*-5-[1*R*-2,2-dimethyl-6-methylidencyclohexyl]-3-methylpent-2-enoic acid **19**, phellidene E **20** and phellidene D **21** (**Publication 4, Figure 21**). Compounds **15-19** exhibited moderate antimicrobial activity against various test organisms. Furthermore, compounds **15-17** showed moderate nematocidal activities against *Caenorhabditis elegans* with $LD_{50} \leq 25 \mu\text{g/mL}$, which is the first report about the nematocidal activity of 3,14'-bihispidinyl and hispidin even after research of them for decades.

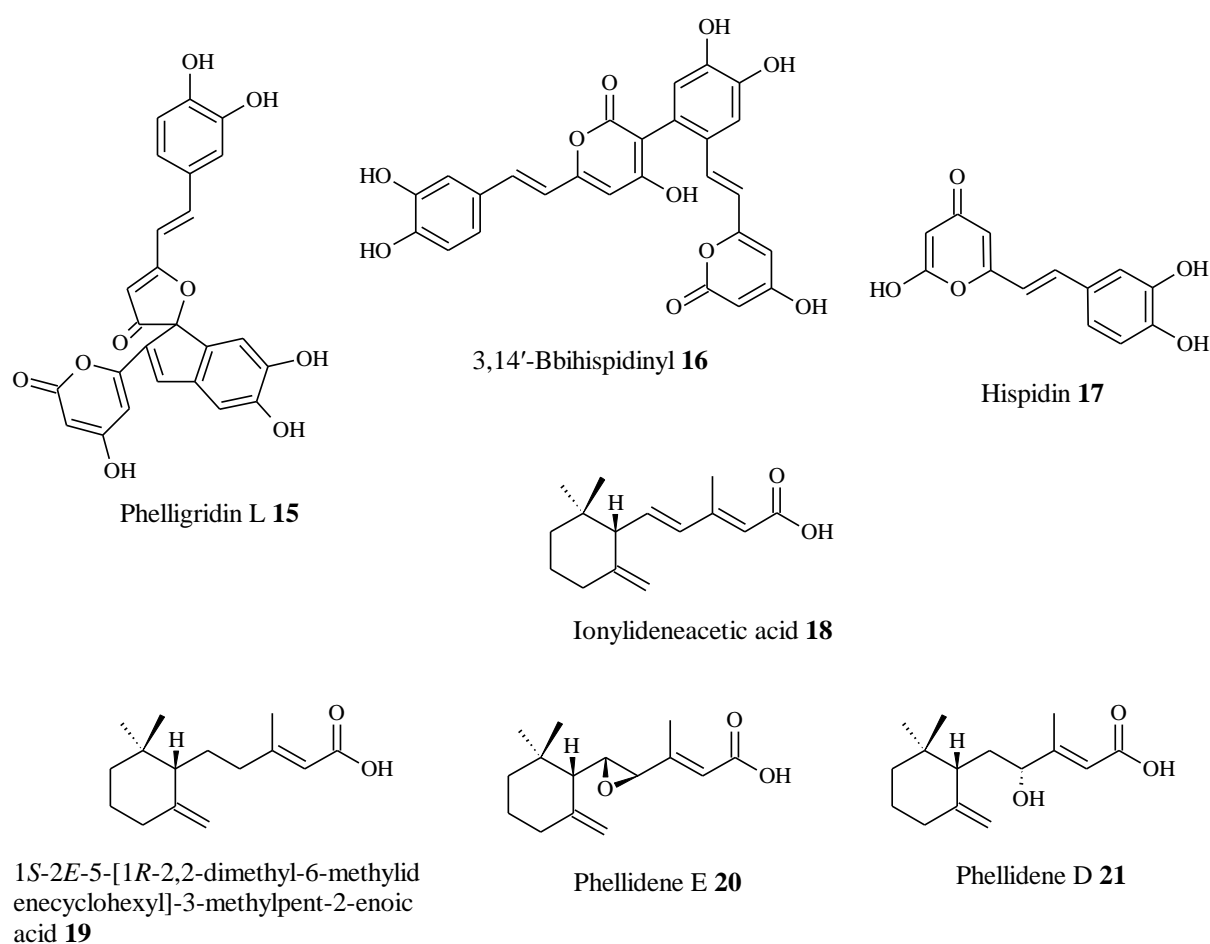


Figure 21. Chemical structures of compounds isolated from *Sanguangporus* sp. (MUCL 55592) **publication 4**.

3.2 Antibacterial Agents from *Skeletocutis* sp. (MUCL 56074)

3.2.1 Antibacterial Agents from Liquid Cultures of *Skeletocutis* sp.

Skeletocutis is a genus of about 40 species in family Polyporaceae (Cui and Dai, 2008). Even though this genus has a worldwide distribution, most of its known species are distributed in the

Northern hemisphere (Cui and Dai, 2008). Like other polypores, species in this genus are known to be saprotrophs that attack dead wood or grow on other fungi. Interestingly, some species have been reported to grow on the dead fruiting bodies of other polypores, giving indications to their mycophilic lifestyle.

YMG medium was used in the scale-up because fermentation in this medium produced the highest volume of metabolites and HPLC-MS results indicated the extracts from 3 standard media are similar. The extraction of supernatant and mycelia led to 610.2 mg and 5.2 g crude extracts, respectively. The extracts were combined since they showed the same metabolite profile by HPLC-MS analysis. The combined extracts were fractionated by preparative HPLC with VP Nucleodur 100-5 C-18 ec column (25 × 40 mm, 7 µm: Macherey- Nagel). 22 fractions (F1-F22) were collected according to the observed peaks. A detailed description of the gradients used for purification of each compound can be found in **Table 11**.

Extensive chromatographic studies of the extract were conducted and led to the isolation of twelve new compounds (**Publication 2**) named skeletocutins A-L **22-26** and **28-34** (**Figure 22**). All of them are derivatives of tyromycin A **27** (Weber *et al.*, 1992), which was originally reported from mycelial cultures of *Tyromyces lacteus* in 1992. Tyromycin A was the first naturally occurring citraconic anhydride derivative with two 3-methyl-maleic anhydride units. The total synthesis of tyromycin A and analogues has been conducted in one step from readily available dicarboxylic acids by Poigny *et al.*, (1998).

Table 11. Details for purification of compounds from liquid cultures of *Skeletocutis* sp. (MUCL56074)

Details for purification of compounds from liquid cultures of MUCL56074						
Compound No.	Amount (mg)	Fractions used for purification	Gradient (solvent B)			
22	40	Fraction F13	68% (5 min)	68–80% (30 min)	80%-100% (5 min)	100% (5 min)
23 and 31	4 and 25.5	Fraction F12	65% (5 min)	65–100% (23 min)	100% (7 min)	
24	9.5	Fraction F16 and F17	75% (5 min)	75–90% (20 min)	90%-100% (2 min)	100% (5 min)
25 and 27	31.2 and 191.1	Fraction F19	86% (5 min)	86–100% (23 min)	100% (7 min)	
26 and 34	17.9 and 62.6	Fraction F18	80% (5 min)	80–100% (23 min)	100% (7 min)	
28	5.9	Fraction F5	50% (5 min)	50–60% (30 min)	60–100% (5 min)	100% (5 min)
29 and 32	4.5 and 19.5	Fraction F9, F10 and F11	65% (5 min)	65–100% (23 min)	100% (7 min)	
30	15.2	Fraction F6 and F7	55% (5 min)	55–65% (30 min)	65–100% (5 min)	100% (5 min)
33	17.1	Fraction F14 and F15	72% (5 min)	72–80% (25 min)	80%-100% (5 min)	100% (5 min)

Among the enzymes bound to the outer surface of mammalian cells, aminopeptidases have been reported as potential targets for immunomodulation of drugs (Drinkwater *et al.*, 2017). Bestatin, the first clinically approved aminopeptidase inhibitor (**Figure 23**), was designed as an immunomodulating agent and is still used for the treatment of lung cancer (Singh *et al.*, 2017). HeLa S3 cells were detected containing aminopeptidases bound to their outer surface which could be easily assayed with L-leucine-7-amido-4-methylcoumarin (Leu-AMC) as substrates (Weber *et al.*, 1992). Tyromycin A was found inhibit both the hydrolyzing activities of Leu-AMC and Bzl-Cys-AMC in HeLa S3 cells with IC₅₀ 31 and 7 µg/mL at 50 µM substrate concentration, respectively (Weber *et al.*, 1992), hence the new analogues were also tested for inhibition of L-Leu-AMC hydrolysis in HeLa (KB 3.1) cells. Bestatin was used as a positive control. Only compounds **26**, **28**, **32**, and **34** were weakly active in this assay with IC₅₀ values in the range 72.3–92.5 and 78.3–118.4 µg/mL when 100 and 50 µM of the substrate were used, respectively, while the positive control bestatin had IC₅₀ 10.8 and 40.9 µg/mL at 100 µM and 50 µM substrate concentration. Even though tyromycin A was previously reported to be active in a similar assay against HeLa S3 cells with IC₅₀ values of 31 µg/mL at 50 µM substrate concentration, an IC₅₀ value >150 µg/mL for this compound was recorded on the HeLa (KB3.1) cells when tested in this study.

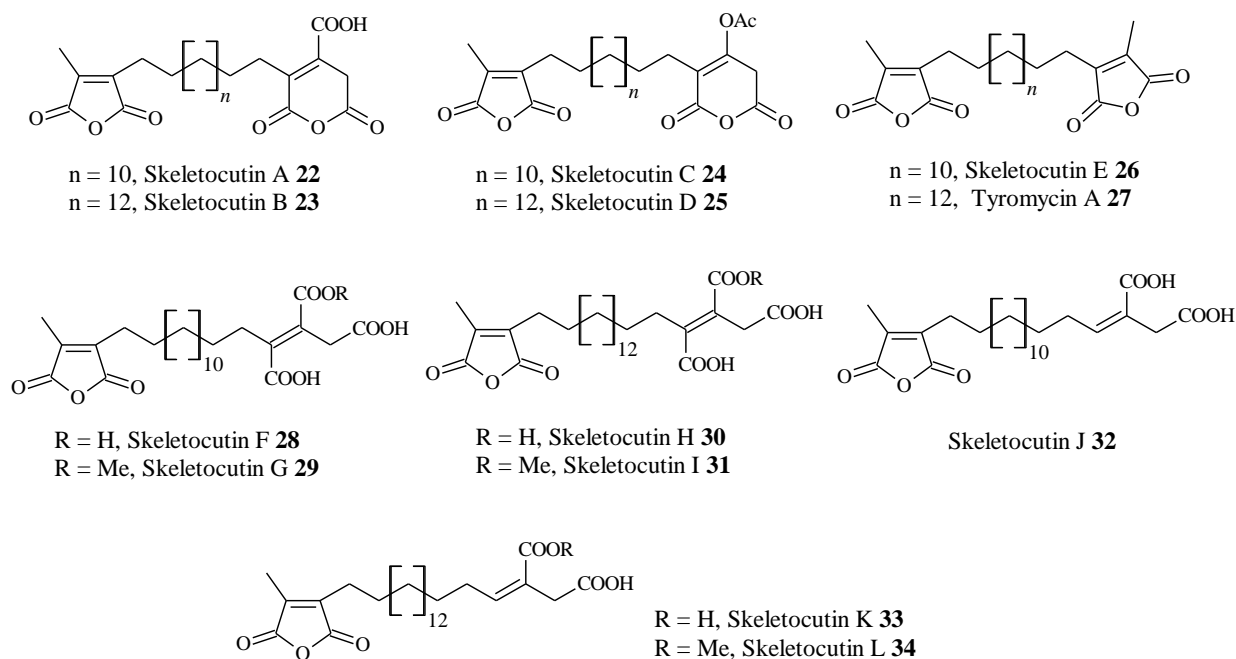


Figure 22. Chemical structures of tyromycin A derivatives isolated from liquid cultures of *Skeletocitis* sp. (MUCL56074) **publication 2**.

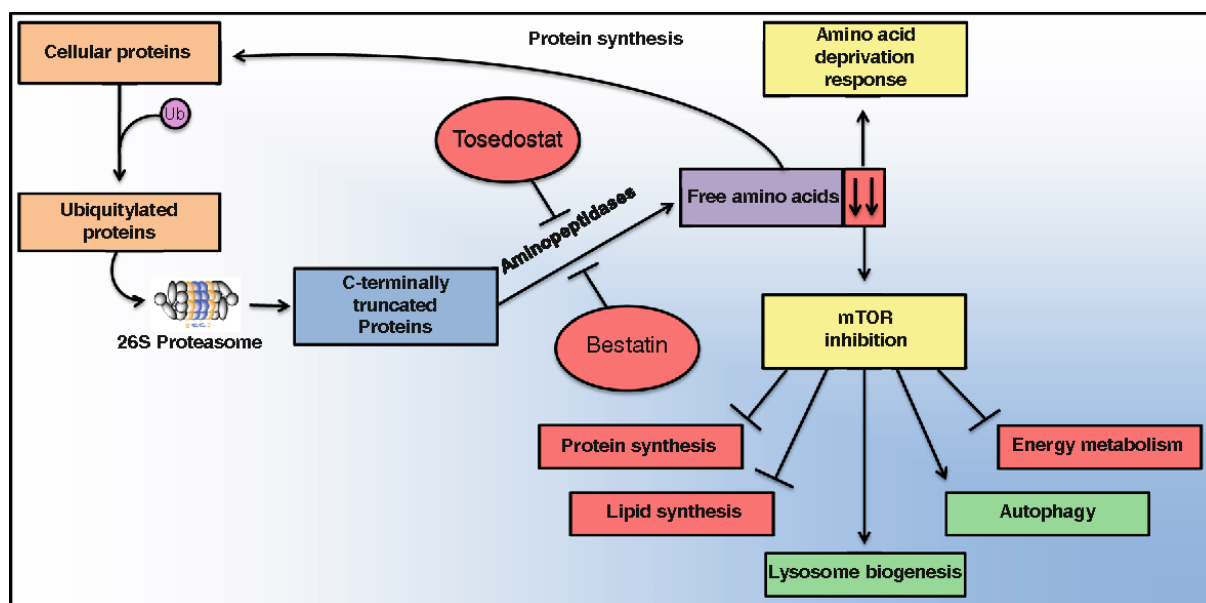


Figure 23. Mechanism of action of aminopeptidase inhibitors bestatin and tosedostat. Aminopeptidase inhibitors elicit two main effects: (1) amino acid deprivation response (AADR) and (2) inhibition of mTOR (Hitzerd *et al.*, 2014).

All compounds except for **28–31** showed moderate activity against *Bacillus subtilis*, *Staphylococcus aureus*, and *Micrococcus luteus* with compounds **22–24**, **26–27**, and **33–34** exhibiting the highest activity in the range of 9.38–37.5 $\mu\text{g/mL}$. Further, the compounds

demonstrated weak activities against MRSA (methicillin-resistant *Staphylococcus aureus*). None of the compounds showed any activity against the tested Gram-negative bacteria nor fungi.

All compounds were also tested for nematicidal activities against *Caenorhabditis elegans* and cytotoxicity against mouse fibroblast (L929) and HeLa (KB 3.1) cell lines but they did not show any significant activities in these assays at concentrations of ≤ 100 $\mu\text{g/mL}$. Compounds that did not show any significant activity (*i.e.* with MIC ≥ 150 $\mu\text{g/mL}$) against *S. aureus* were subjected to the biofilm inhibition assay against *S. aureus* biofilm. Only compound **31** inhibited the formation of the biofilm up to 86% at 256 $\mu\text{g/mL}$ and 28% at 150 $\mu\text{g/mL}$.

Hepatitis C virus (HCV), is one of the major causes of chronic liver disease, with 71 million people infected worldwide. Although curative medications are available for HCV, the majority of infected individuals do not have access to treatment due to the high cost of the treatment. Hence, all of the compounds were tested for their antiviral activity against HCV in a cellular replication assay in human liver cells. Compound **27** strongly inhibited HCV infectivity at the initial concentration of 40 μM while compounds **25** and **26** inhibited HCV with moderate activity. Compounds **22**, **24**, and **34** showed weak activity and the rest of the compounds were not active. All tested compounds except for **27** were found devoid of cytotoxicity on the liver cells. We therefore next evaluated the antiviral activity of **27** against HCV in a dose dependent manner. Compound **27** incubated for 3 days resulted in a dose-dependent inhibition of HCV infectivity with an IC₅₀ 6.6 μM . The green tea molecule epigallocatechin gallate (EGCG, see Ciesek *et al.*, 2011) was used as a positive control.

3.2.2 Undescribed Metabolites from Fruiting Bodies of *Skeletocutis* sp.

A quantity of 9.8 g fruiting bodies was extracted using 500 mL of acetone overnight. Then, the extract was filtered and another 500 mL of acetone was added, this was extracted in an ultrasonic bath for 30 min. The acetone extracts were combined and the solvent evaporated to afford 226 mg of crude extract. The purification *via* preparative HPLC with a VarioPrep (VP) column system packed with NUCLEODUR® 100-5 C₁₈ ec (Machery-Nagel, column size: 25 mm·40 mm, packing: 7 μm), elution gradient: 50% solvent B, increasing solvent B to 100% within 60 min, 100% solvent B for 5 min, flow rate: 40 mL/min, resulted in eight fractions (F1-F8). The further purification (details can be found in **Table 12**) of the fractions with a Kromasil® C₁₈ HPLC column (Nouryon, column size: 250 mm·20 mm, packing: 7 μm , flow rate: 15 mL/min), elution gradient: 45% solvent B for 3 min, increasing solvent B to 100%

within 18 min, 100% solvent B for 4 min, led to the isolation of 5 previously undescribed tyromycin A derivatives, skeletocutins M-Q (**35-39**) and one known compound tyromycin A **27** (**Publication 3**, Weber *et al.*, 1992, **Figure 24**).

Table 12. Details for purification of compounds from fruiting bodies of *Skeletocutis* sp.

Details for purification of compounds from fruiting bodies of <i>Skeletocutis</i> sp.		
Compound No.	amount (mg)	Fractions used for purification
35	4.84	Fraction F6
36	2.26	Fraction F7
37	4.26	Fraction F4
38	2.50	Fraction F1
39	2.87	Fraction F2
27	2.15	Fraction F8

Skeletocutins M-Q **35-39** were devoid of significant activity in antimicrobial, cytotoxic, and nematocidal assays. In the antimicrobial assay, compounds **37** and **39** were observed to interfere with the formation of biofilms commonly produced by *S. aureus*. They were then evaluated for biofilm inhibition activity against *S. aureus*, with a concentration of 256 µg/mL. However, only weak activity with 20 and 56% inhibition of the biofilm, respectively was observed. According to a previous report on the activity of tyromycin A **27** (Weber *et al.*, 1992) to inhibit leucine aminopeptidase in HeLa S3 cells, the isolated compounds were checked in the same assays. Compound **38** exhibited moderate activity, with an IC₅₀ value of 71.1 µg/mL when 50 µM of the substrate was used. Compounds **37** and **39** exhibited weak activities, with IC₅₀ values of >80 µg/mL at 50 and 100 µM substrate concentration, while the positive control bestatin showed stronger activity with IC₅₀ 10.8 and 40.9 µg/mL at 100 µM and 50 µM substrate concentration.

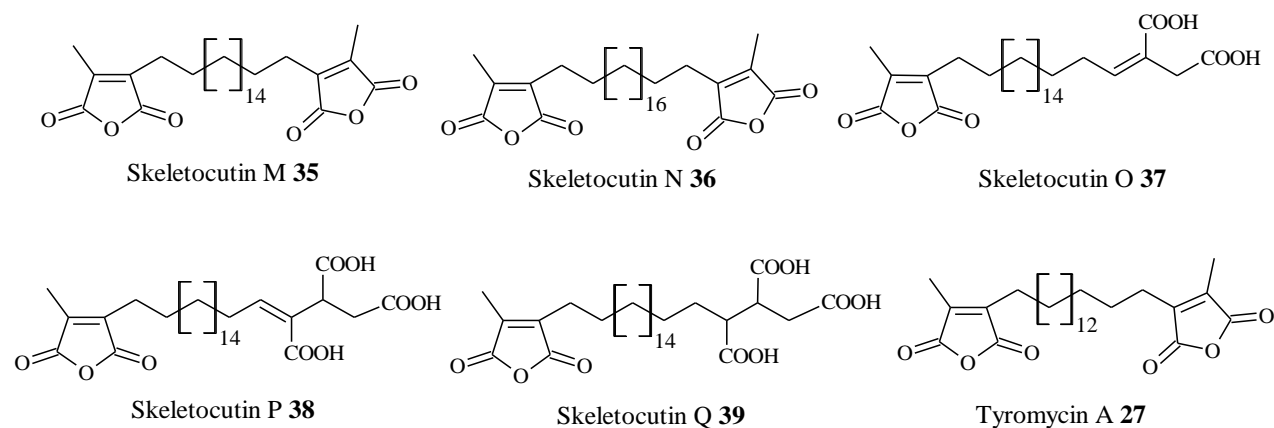


Figure 24. Chemical structures of compounds isolated from fruiting bodies of *Skeletocutis* sp. (MUCL56074) **publication 3**.

The metabolites isolated from fruiting bodies of *Skeletocutis* sp. are closely related to the skelotocutins that were isolated from liquid cultures. There have been relatively few studies on the production of secondary metabolites in mycelial cultures vs fruiting bodies in higher fungi, but so far, there are only a few examples where the same compounds were predominant in both. For instance, in most species hitherto studied of the ascomycete order Xylariales, the fruiting bodies and cultures mostly showed a complementary secondary metabolite production (Helaly *et al.*, 2018). From the current case, it appears that the basidiomes of *Skeletocutis* can be used for chemotaxonomic studies. Investigations of herbarium specimens may not even be helpful for the taxonomic revision of the genus but may lead to the discovery of further, previously undescribed members of the tyromycin/skeletocutin type.

3.3 Pregnenolone Type steroids from *Fomitiporia aethiopica* (MUCL 56047)

Strain MUCL 56047 was identified as *Fomitiporia aethiopica* by morphological studies and ITS sequence analysis. The mycelial culture was fermented in 21 flasks rice media (prepare 90 g rice in 500 mL Erlenmeyer flasks containing 90 mL distilled water and autoclaved twice) at 23 °C for 28 days. The cultures were diced into small pieces and extracted with methanol to afford 800 mg crude extract. The subsequent chromatographic purification of the crude extract led to the identification of 5 previously undescribed pregnenolone type triterpenes aethiopinolones A–E **40-44 (Publication 5, Figure 25)**. They were found devoid of significant nematicidal and antimicrobial activities, however, they exhibited moderate cytotoxic effects against various human cancer cell lines with $8 \leq IC_{50} \leq 70 \mu\text{g/mL}$.

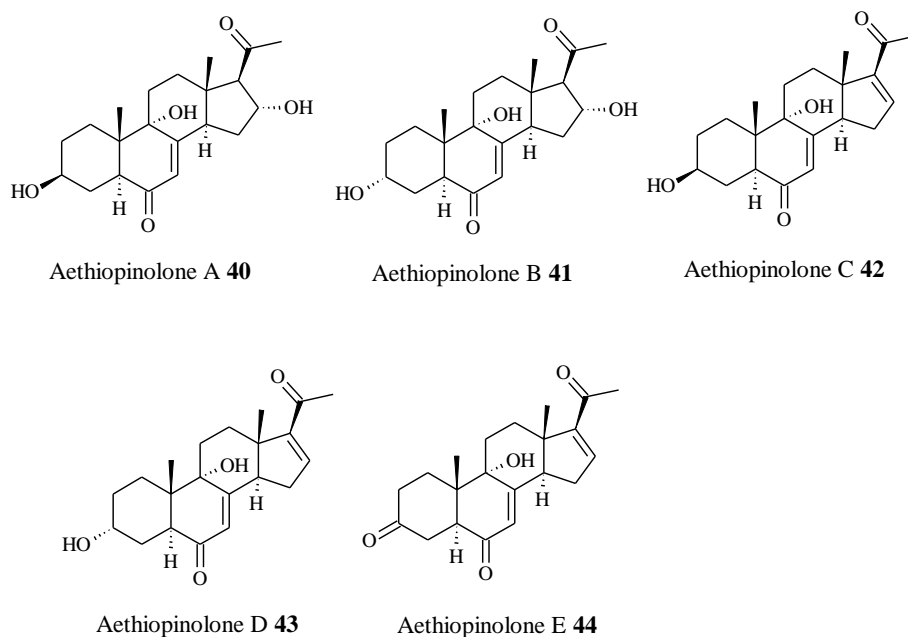


Figure 25. Chemical structures of compounds isolated from *Fomitiporia aethiopica* (MUCL56047) **publication 5.**

3.4 Novel Metabolites from *Heimiomyces* sp. (MUCL 56078)

By comparing the 5.8S/ITS nrDNA sequence and morphological studies, the strain MUCL56078 was assigned tentatively to the genus *Heimiomyces* with a closest hit of 98% query cover to MF100953.1 (*Heimiomyces tenuipes*, Desjardin and Perry, 2018). The next closest hit is KM975407.1 (*Heimiomyces neovelutipes*) with 97% query cover (Cooper and Park, 2014). The comparison of the 20 closest ITS BLAST results showed the relationship of MUCL56078, *Heimiomyces* and *Xeromphalina* (**Figure 26**). *Heimiomyces*, which was described as an independent genus related to *Xeromphalina* (a genus of Agaricales; cf. (Singer, 1959). Singer (1962), later considered *Heimiomyces* as a subgenus of *Xeromphalina* but Horak (1978) studied the macromorphology, micromorphology, and ecology of *Heimiomyces* and *Xeromphalina*, and resurrected *Heimiomyces* again. *Xeromphalina* and *Heimiomyces* are related genera and there are several intermediate species linking the two generic units (Esteve-Raventós *et al.*, 2010). Six sesquiterpenoids and one fungal pigment, xerocomic acid (**Figure 27**), have been isolated and reported from *Xeromphalina* sp. (Liermann *et al.*, 2010).

MUCL56078 was selected for large-scale fermentation in YMG medium since its extracts from the small-scale presented activity against *Bacillus subtilis* at 18.8 µg/mL, 376.2 and 331.3 mg crude extracts were obtained from mycelia and supernatant, respectively. The crude extracts purified by preparative HPLC with elution gradient: 5-100% solvent B in 63 min and thereafter

isocratic condition at 100% solvent B for 5 min. UV detection was carried out at 210, 254, and 350 nm and the flow rate was 40 mL/min. This led to the collection of 14 (F1-F14) and 13 (F1-F13) fractions from supernatant and mycelia, respectively. The further purification of fractions (**Table 13**) resulted in seven novel compounds heimiomycins A-C **45-47**, calamenene derivatives **48-49**, phenanthridine derivative **50**, sesquiterpene **51** and one known compound (17R)-4-hydroxy-17-methylincisterol **52** (Kawagishi *et al.*, 2006a, **Figure 28**). VP Nucleodur 100-10 C₁₈ ec column (Macherey-Nagel, Düren, Germany; 250×10 mm) with flow rate 5 mL/min was used for purification to get compounds **45**, **46** and **51**; preparative HPLC column (Kromasil, MZ Analysentechnik, Mainz, Germany; 250 x 20 mm, 7 µm C₁₈) with flow rate 12 mL/min was used for purification to get compounds **47**, **49**, **50** and **52**; compound **48** was obtained from the fraction purified by preparative Nucleodur Phenyl hexyl column (Macherey-Nagel, Düren, Germany; 250×21 mm, 5 µm) with flow rate 12 mL/min.

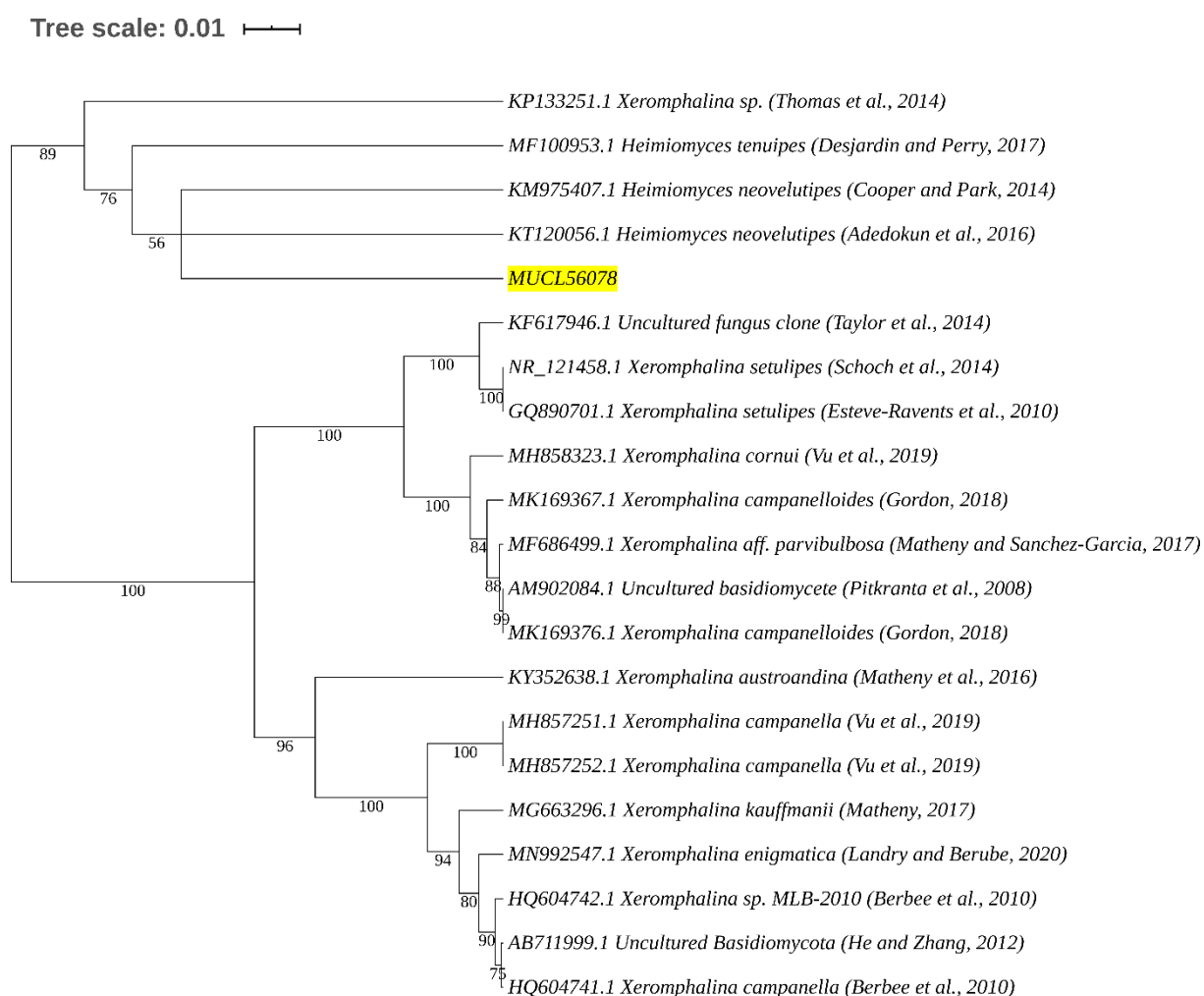


Figure 26. RAxML phylogenetic tree of the MUCL56078 ITS and the 20 closest BLAST results.

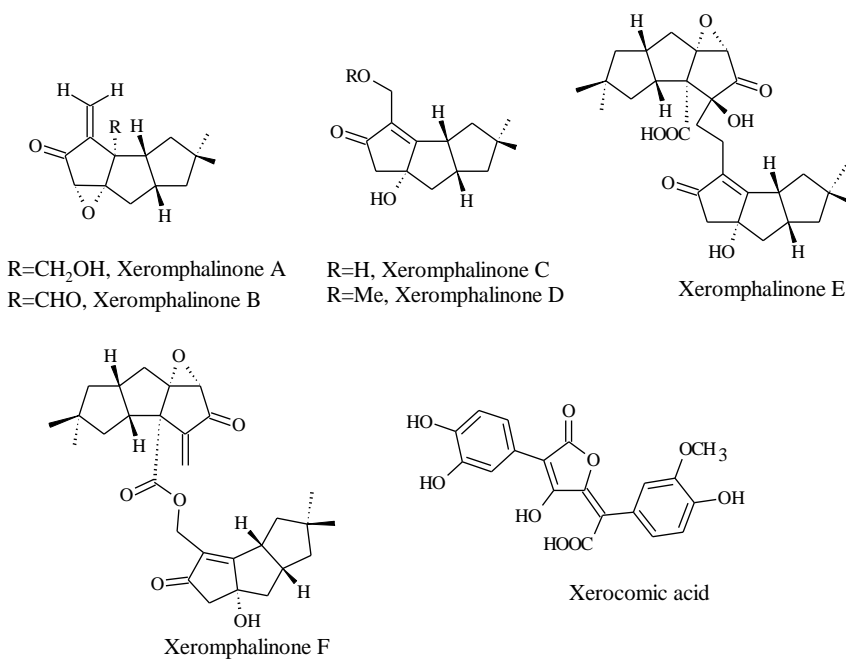


Figure 27. Secondary metabolites isolated from *Xeromphalina* sp. (Liermann *et al.*, 2010).

Table 13. Details for purification of compounds from MUCL56078.

The gradients used for purification of compounds						
Compound No.	amount (mg)	Fractions used for purification	gradient (solvent B)			
45	1.42	Mycelium fraction F9	30% (3 min)	30%-75% (40 min)	75%-100% (5 min)	100% (5 min)
46	4.89	Supernatant fraction F11 and mycelium fraction F8	55% (3 min)	55%-75% (60 min)	75%-100% (5 min)	100% (5 min)
47	3.21	Supernatant fraction F10 and F12	60% (3 min)	60%-80% (63 min)	80%-100% (5 min)	100% (5 min)
48	2.59	Supernatant fraction F7	10% (3 min)	10%-80% (40 min)	80%-100% (5 min)	100% (5 min)
49	1.84	Supernatant fraction F9	35% (3 min)	35%-70% (40 min)	70%-100% (5 min)	100% (5 min)
50	0.69	Mycelium fraction F4 and F5	66% (3 min)	66%-72% (35 min)	72%-100% (5 min)	100% (5 min)
51	0.67	Mycelium fraction F6	25% (3 min)	25%-80% (53 min)	80%-100% (5 min)	100% (5 min)
52	1.05	Supernatant fraction F14	35% (3 min)	35%-100% (53 min)		100% (5 min)

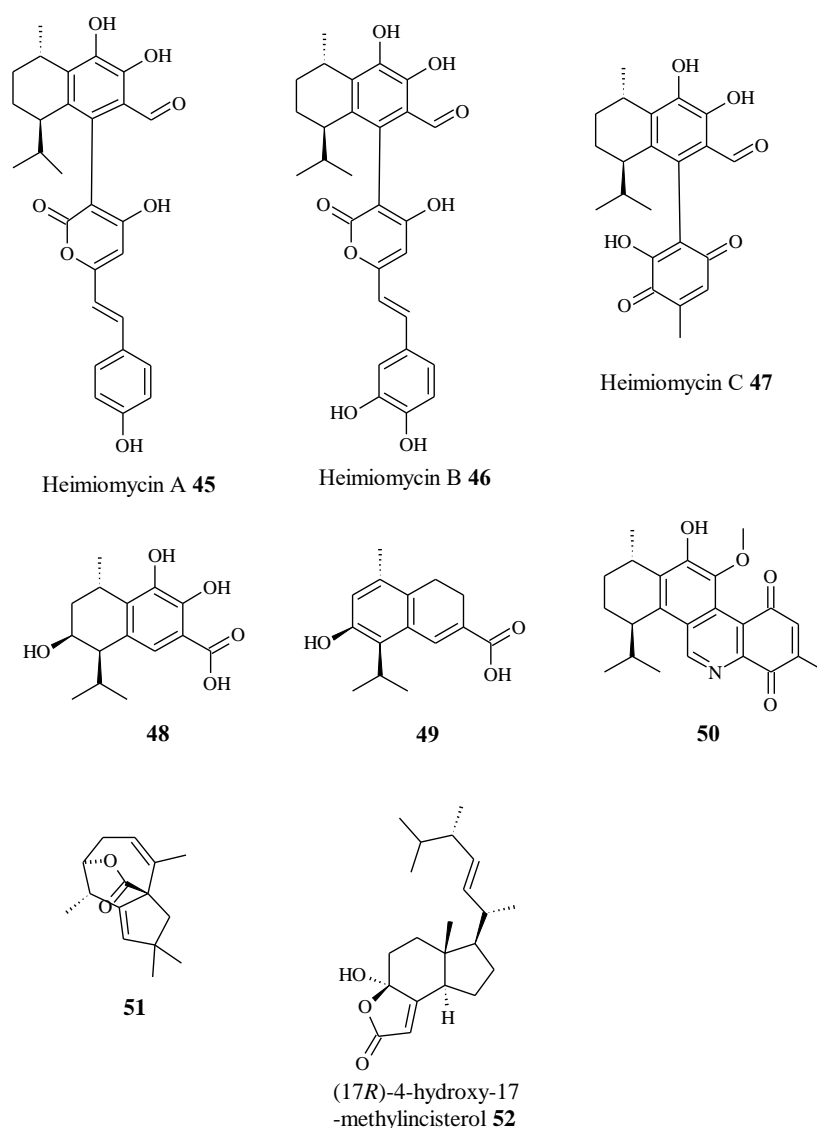


Figure 28. Chemical structures of compounds isolated from *Heimomyces* sp. (MUCL56078).

The antimicrobial activities of compounds **45-52** were assessed by serial dilution assay against bacteria, fungi, and yeast (**Table 14**). Conspicuous is their activity against Gram-positive bacteria *Bacillus subtilis* and *Micrococcus luteus*; filamentous fungi *Mucor hiemalis*. Compound **47** exhibited the most outstanding activity against *M. luteus* with concentration of 3.1 $\mu\text{g/mL}$, while it also inhibits the growth of *B. subtilis* and *M. hiemalis* at 12.5 and 25 $\mu\text{g/mL}$, respectively. Furthermore, the metabolites showed moderate cytotoxicity against the human HeLa cell line and KB 3.1 mouse fibroblast cell line L929 except for compound **48** and **51** (**Table 14**). Compound **52** exhibited the strongest cytotoxicity against KB 3.1 cells at 5.4 μM , while compound **47** inhibited L929 robustly with concentration 5.5 μM . Four compounds **45**,

46, **50** and **51** contain novel carbon skeletons, among them **45** and **46** are two polyketides, **51** is a sesquiterpene. The left part of **50** is a monoterpene, while the right part is polyketide. The structure of **50** is quite unusual, the further plan for this compound is to elucidate the biosynthesis pathway of it. For this, gene clusters that contain both terpene cyclase and PKS are highly interested.

Table 14. Minimum inhibitory concentration (MIC for bacteria and fungi) and half-inhibitory concentrations (IC₅₀ for cell lines) in µg/mL.^[a]

Organisms	MIC (µg/mL)								Reference
	45	46	47	48	49	50	51	52	
<i>Bacillus subtilis</i> DSM10	- ^[b]	100	12.5	-	-	6.3	-	6.3	9.2 ^[c]
<i>Mycobacterium smegmatis</i> DSM44200	-	-	100	-	-	-	-	100	0.6 ^[d]
<i>Micrococcus luteus</i> DSM1790	25	12.5	3.1	100	50	6.3	50	6.3	0.3 ^[c]
<i>Staphylococcus aureus</i> DSM346	100	100	50	100	100	50	50	50	9.2 ^[e]
<i>Mucor hiemalis</i> DSM2656	100	100	25	50	25	50	25	6.3	9.2 ^[f]
<i>Candida albicans</i> DSM1665	-	-	100	-	-	100	-	-	9.2 ^[f]
<i>Pichia anomala</i> DSM6766	100	100	100	-	100	100	-	50	4.6 ^[f]
Cytotoxicity (µM)									
KB3.1	7.6	24.4	16.4	-	45	34.1	-	5.4	8.9×10 ⁻⁵ ^[g]
L929	-	44.7	5.5	-	-	27.3	-	7.2	2.6×10 ⁻³ ^[g]

[a] For MIC, 20 µL of 1.5 mg/mL stock solution (start concentration 100µg/mL) of 33-40 were tested. Cell density was adjusted to 6.7 × 10⁵ cells/mL; 20 µL of methanol was tested as negative control and no activity against tested organisms. For cytotoxicity assay, 6 × 10³ cells/well were selected in 96-well microtiter plates and treated with compounds for 5 days; [b] -, no activity; [c] oxytetracyclin; [d] kanamycin; [e] gentamycin; [f] nystatin; [g] epothilon B.

4. Additional Project - Illudin Biosynthesis in *Omphalotus olearius*

4.1 Introduction

4.1.1 Biological Activity

As stated in the National Cancer Institute (NCI) statistics, about 10 million people die of cancer annually worldwide (Ritchie, 2018). The treatment of cancer is a great challenge for both oncologists and medicinal chemists. Alkylating agents that exert their biological activity by modifying DNA and proteins eventually leading to the death of tumour cells have been a mainstay of cancer therapy ever since the very early days (Singh *et al.*, 2018). Historically, the first examples of such agents were accidentally found among compounds intended for use as poison gas. Derivatives of these are still in clinical use, *e.g.*, the *N*-mustards (chlorambucil, cyclophosphamide), *N*-heterocyclic triazenes (dacarbazine, temozolomide) and *N*-nitrosoureas (BCNU, Carvalho *et al.*, 1998; Eisenbrand *et al.*, 1988; Năstasă *et al.*, 1983). Nature also provided us alkylants with great antitumoral potency: the mitomycins, duocarmycins, and illudins.

The first illudins, illudin M and S, were isolated from culture broths of the bioluminescent jack o' lantern mushroom *Omphalotus olearius* that grows on rotting wood in the east of North America and in mild areas of South and Western Europe (Anchel *et al.*, 1950). Related species producing illudins M and S are *Lampteromyces japonicus* and the Australian ghost fungus (Schobert *et al.*, 2011). The name of illudins M and S derived from their antibacterial activity, illudin M got its name from the activity against *Mycobacterium smegmatis*, while illudin S exhibited activity against *Staphylococcus aureus* (McMorris and Anchel, 1963). Preclinical research revealed that illudins M and S show selective cytotoxicity in leukemia cells and can overcome drug resistance (McMorris *et al.*, 1992). Yet, they turned out to be too toxic in their natural form and with little therapeutic value. Fortunately, they are accessible in gram quantities, which made chemical modification possible aiming at broadening their therapeutic index and at increasing their cancer selectivity. For instance, the oxidation of illudin M with pyridinium dichromate (PDC) afforded dehydroilludin M which showed an improved therapeutic index in animal studies (McMorris *et al.*, 1992, **Figure 29**). HMAF, prepared from illudin S *via* a reverse Prins reaction, displayed a significantly improved therapeutic index and was admitted to clinical trials (McMorris *et al.*, 1996; Schobert *et al.*, 2011, **Figure 29**).

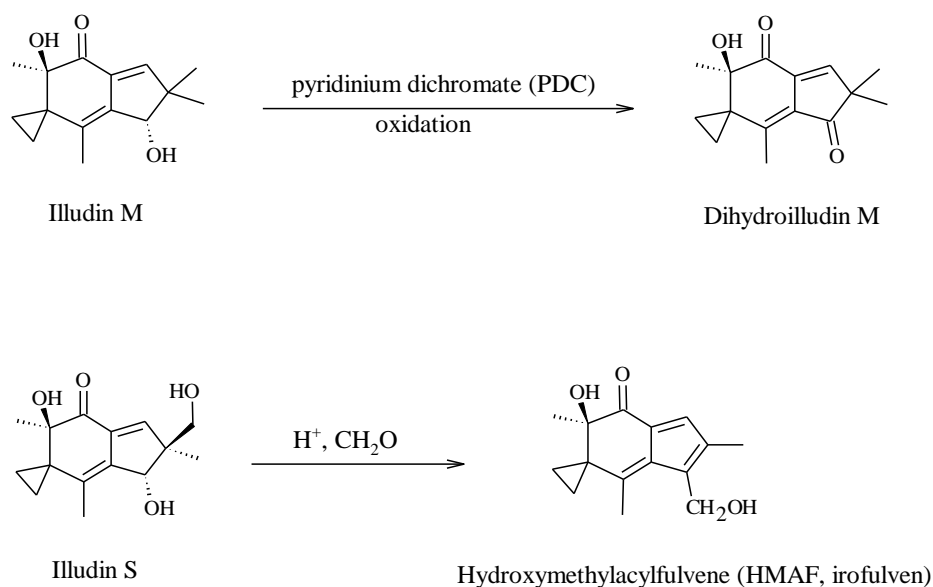


Figure 29. Semi-synthetic analogs of illudin M and S (McMorris *et al.*, 1996).

A number of other illudin-related natural products (**Figure 30**) have been isolated from various basidiomycetes since the discovery of illudin M and S. Illudins A, B, I and J2 exhibit moderate antimicrobial activity against *S. aureus* but are devoid of significant cytotoxicity, except for illudin I, which is highly cytotoxic against HepG2 hepatoma cells (Dufresne *et al.*, 1997; Gonzalez Del Val *et al.*, 2003; Lee *et al.*, 1996). Illudinic acid showed strong antibacterial activity and exhibited moderate cytotoxicity in mammalian cell cultures (Dufresne *et al.*, 1997; Taetle *et al.*, 1987; Twentyman and Luscombe, 1987). A possible biological precursor of illudin M, dihydroilludin M, also isolated from *Omphalotus olearius*, is devoid of significant biological activities (Taetle *et al.*, 1987).

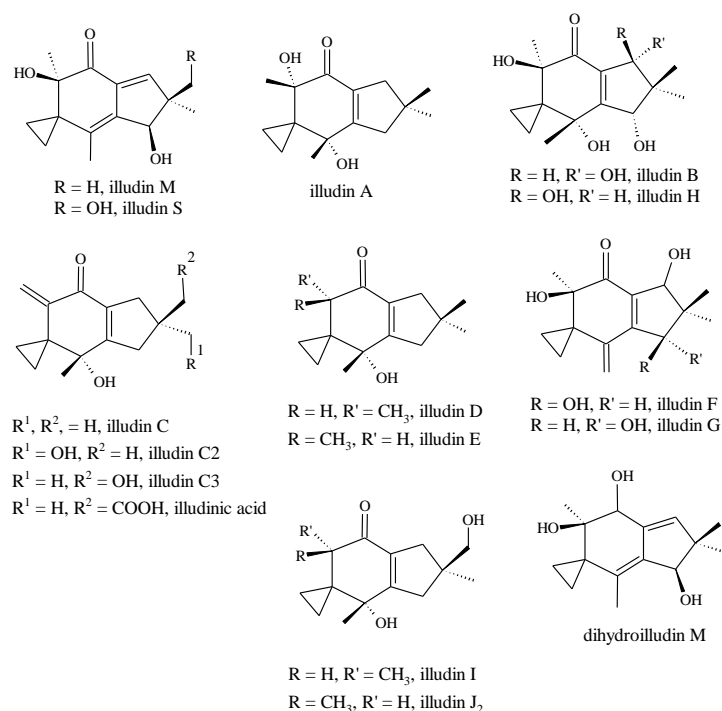


Figure 30. Naturally occurring illudin analogs.

4.1.2 Biosynthesis of Illudins – *status quo*

Since the early 1970s, the investigation of the biosynthesis of illudins has been an area of intense interest and research. Sesquiterpenoids may be classified in terms of the mode of initial cyclisation of farnesyl diphosphate (Hanson *et al.*, 1976). It has been suggested that humulene (α -caryophyllene) may form the first cyclic intermediate in the synthesis of illudin series of metabolites (McMorris and Anchel, 1965).

Feeding studies with labelled mevalonates and acetates and proposed biosynthesis

Terpenoids retain hydrogen atoms derived from mevalonic and acetic acids until the late stages of their biosynthesis (Popják and Cornforth, 1966). The chirality of mevalonate hydrogen atoms in all-*trans*-farnesyl pyrophosphate has been established (**Figure 31**). Accordingly, feeding studies using labelled mevalonates and acetates could provide some information into the mechanism of formation of the carbon skeleton of the illudins.

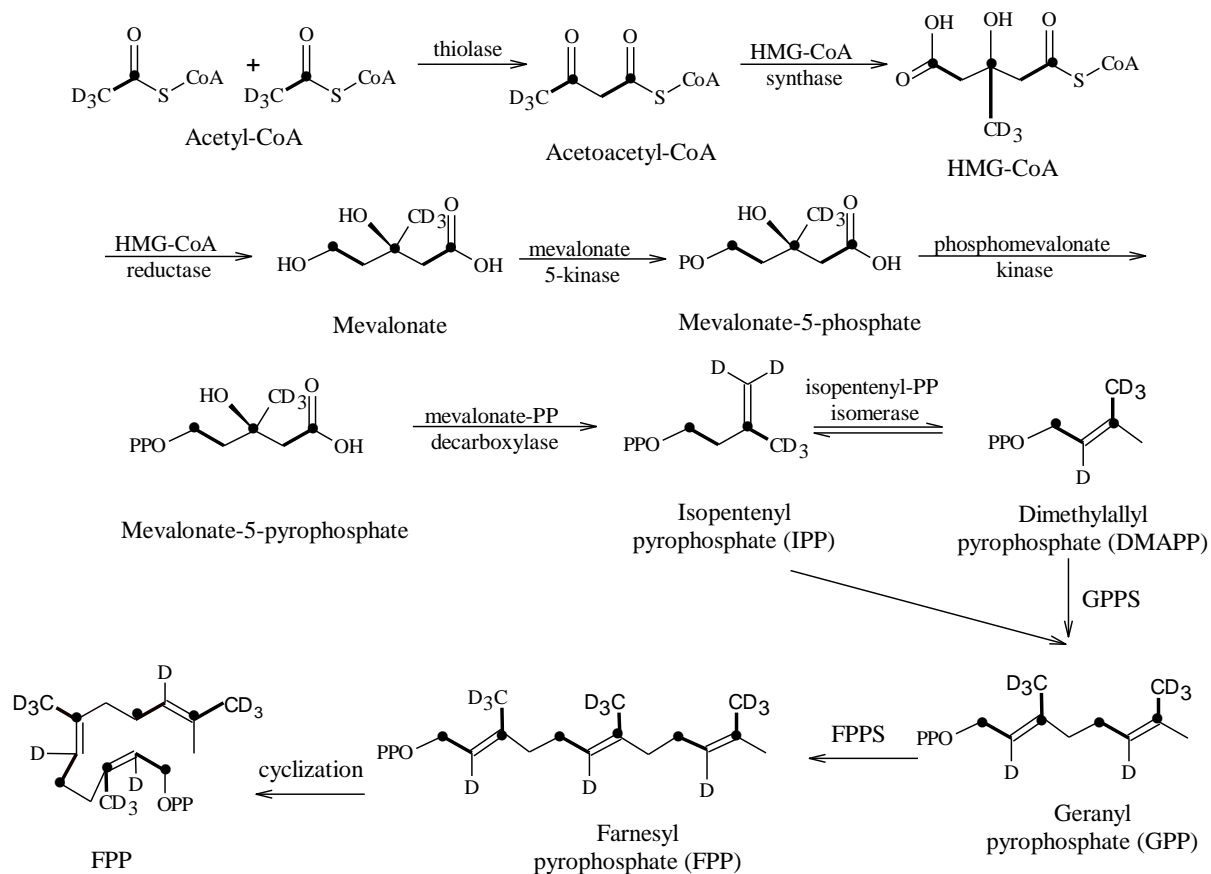


Figure 31. Mevalonate pathway to terpene precursor, from acetate to IPP and DMAPP. • denotes acetate C-1 position, D denotes deuterium.

It has been postulated that illudins are formed biogenetically from farnesyl pyrophosphate (FPP) *via* a primary cyclisation forming a humulene-type intermediate (McMorris and Anchel, 1963). However, it has subsequently been suggested that cyclisation may proceed *via* a protoilludane intermediate after the formation of a humulene ion intermediate (Bradshaw *et al.*, 1982).

Feeding studies with sodium $[1,2-^{13}C]$ - and $[1-^{13}C]$ -acetate determined that C-3 and C-11 of illudin M (**Figure 32**) derived from carbons of an intact acetate unit, defining the stereochemistry of the folding of FPP in the cyclopropane portion of the molecule during biosynthesis (Bradshaw *et al.*, 1978).

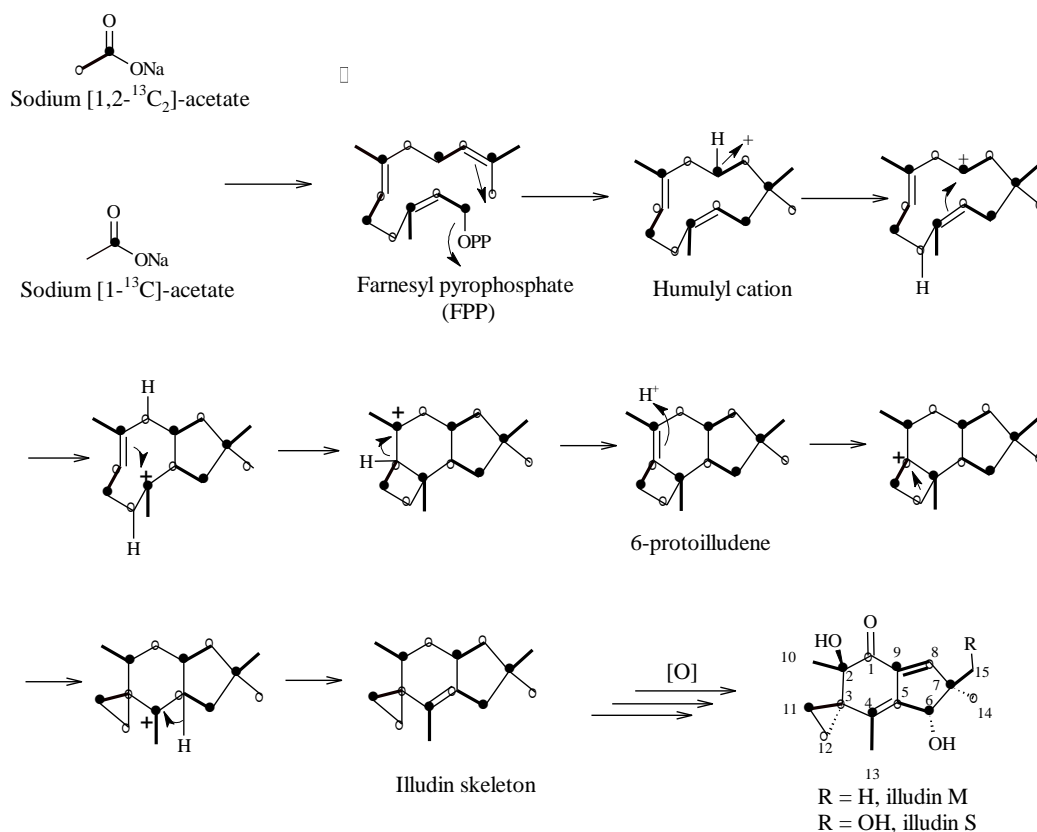
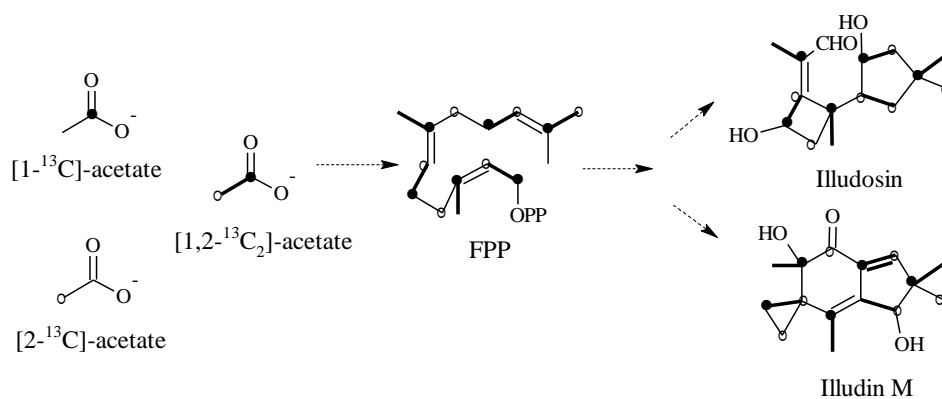


Figure 32. Possible biosynthesis of illudins from FPP. Illudin M and S isolated from the labelling experiment. — denotes pairs of intact acetates coupled atoms in the [1,2-¹³C₂]-acetate experiment, • denotes acetate C-1 position, o denotes acetate C-2 position.

[1-¹³C], [2-¹³C], [1,2-¹³C₂] and [1-¹³C, 2-²H₃]-acetates were employed in labelling experiments in *Omphalotus nidiformis* shake cultures. Incorporation of ¹³C and ²H labels into illudisin and illudin M were observed (Burgess and Barrow, 1999). In the [1-¹³C, 2-²H₃]-acetate feeding experiment, fewer deuterium atoms were incorporated into illudin due to illudin M is less protonated than illudisin (**Figure 33**).



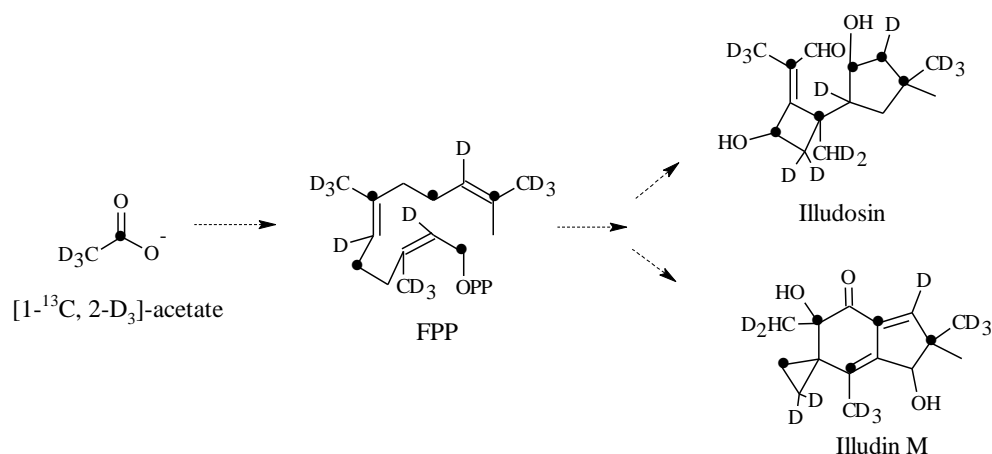


Figure 33. Biosynthetic incorporation of [1- ^{13}C]-, [2- ^{13}C]-, [1,2- $^{13}\text{C}_2$]- and [1- ^{13}C , 2- $^2\text{H}_3$]-acetate into illudisin and illudin M. • denotes acetate C-1 position, o denotes acetate C-2 position, D denotes deuterium.

[5- $^2\text{H}_2$, 5- ^{13}C]- and [2- $^2\text{H}_2$]-mevalonate were fed to *Clitocybe illudens* for studies in the biosynthesis of illudins by applications of ^2H and ^{13}C NMR spectroscopy. One mevalonate proton was lost from C-12 in the cyclopropane region of illudin M. The retention of a ^2H - ^{13}C coupling at H-6 in illudin M indicated that this hydrogen atom is not involved in a hydride rearrangement. This observation can be accommodated by the suggested mechanism of cyclisation *via* a protoilludyl-type intermediate (**Figure 34**, Bradshaw *et al.*, 1982).

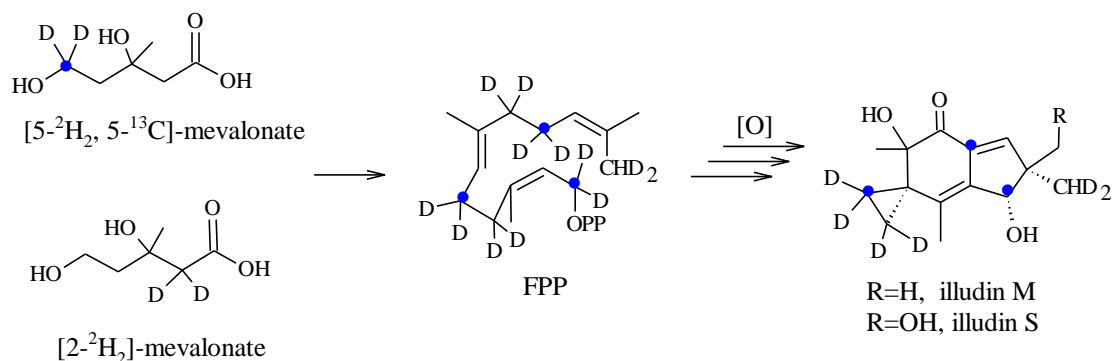


Figure 34. Biosynthetic incorporation of [5- $^2\text{H}_2$, 5- ^{13}C]-, and [2- $^2\text{H}_2$]-mevalonate into illudins M and S. • denotes mevalonate C-5 position, D denotes deuterium.

The biosynthesis of illudin M has been examined by feeding [^3H , ^{14}C]-mevalonates to *Clitocybe illudens*, followed by degradation experiments (Hanson and Marten, 1973). Incorporation of ^{14}C label of [2- $^3\text{H}_2$, 2- ^{14}C]-mevalonate illustrated that three molecules of mevalonate are

incorporated into illudin M. One labelled mevalonoid hydrogen atom from [4(*R*)-4-³H]-mevalonate is incorporated into illudin M (**Figure 35**, Hanson and Marten, 1973).

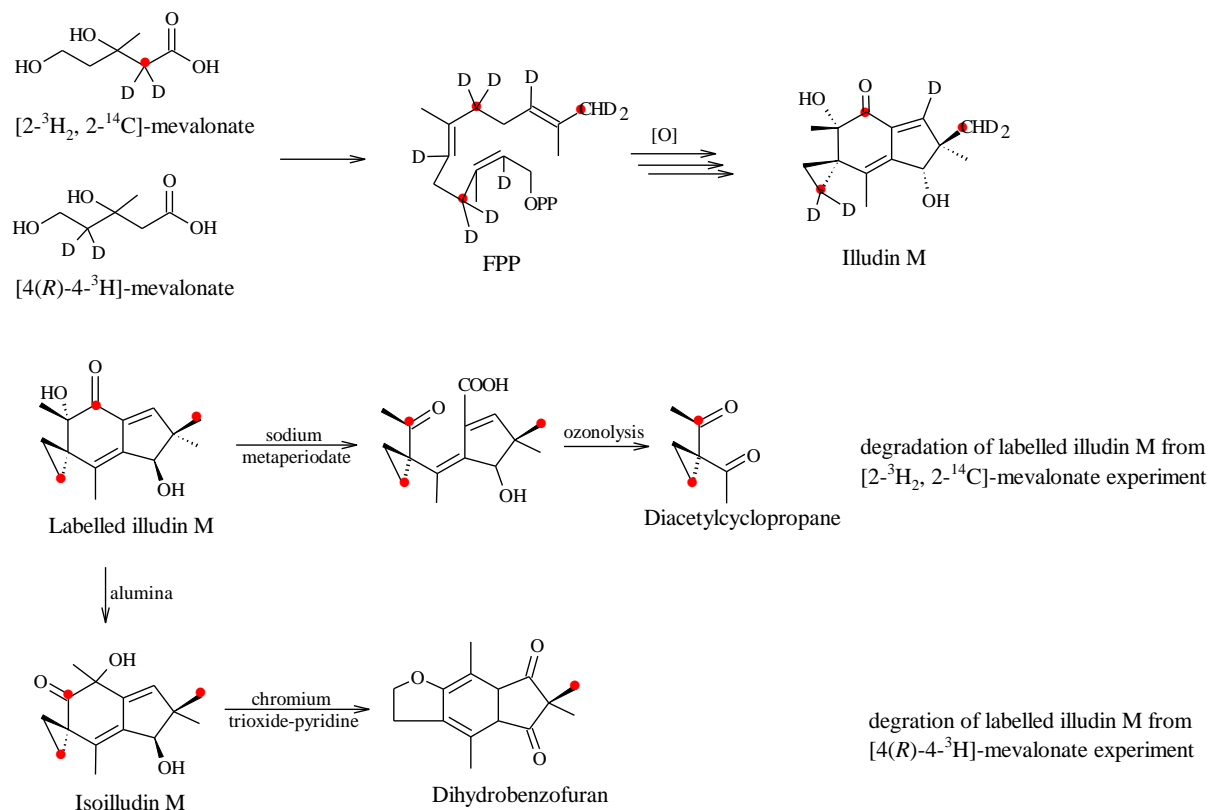


Figure 35. Biosynthetic incorporation of [³H, ¹⁴C]-mevalonate into illudins M and followed degradation experiments. • denotes mevalonate C-2 position, D denotes deuterium.

In order to prove the intermediary role of 6-protoilludene in the biosynthesis of illudins. Morisaki *et al.* (1985) synthesized [13-²H₃]-6-protoilludene and fed it to the growing mycelium of *Omphalotus olearius* (ATCC 11719). The feeding substrate [13-²H₃]-6-protoilludene has been converted to illudins M and S, which indicated 6-protoilludene is the biosynthetic precursor of illudins M and S (**Figure 36**).

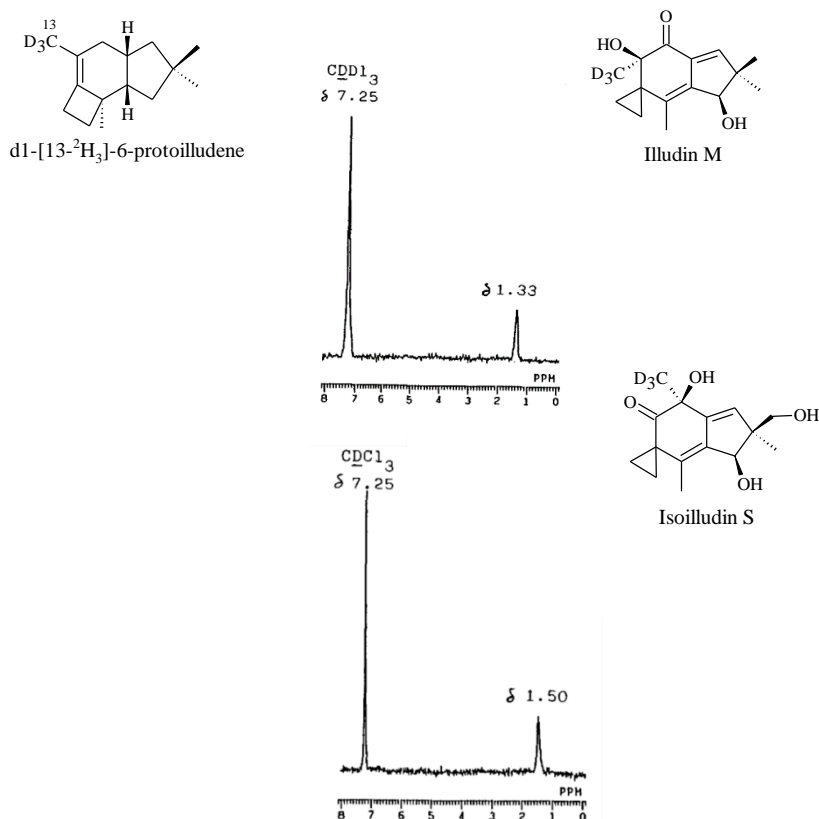


Figure 36. 60 MHz ^2H -NMR spectra of illudin M and isoilludin S derived from deuterated 6-protoilludin in CDCl_3 .

The results of these feeding experiments support a pathway in which cyclisation of farnesyl pyrophosphate generates a humulyl cation. Subsequent ring contraction reactions would give rise to the 6-protoilludene intermediate. Later hydroxylation and oxidation would then generate illudin M and S (**Figure 37**). However, the precise nature and order of the tailoring steps after the protoilludene intermediate are unknown.

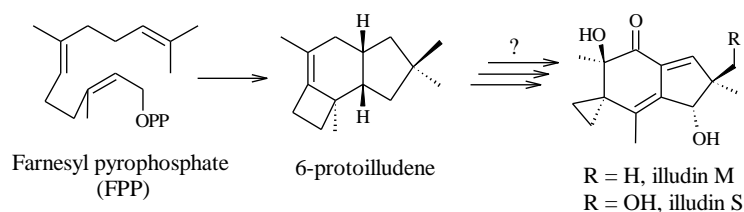


Figure 37. Proposed overall route of illudin biosynthesis.

Gene cluster and proposed biosynthesis of illudin

The investigation of the illudin gene clusters started by Wawrzyn *et al.* (2012). The illudin producing strain *Omphalotus olearius* was sequenced and bioinformatic analyses revealed three

putative BGC for sesquiterpenoid production. Among them, two BGC (*omp6* and *omp7*, **Figure 38**) could be involved in the production of illudins since the direct chemical product of *omp6* and *omp7* was shown to be the precursor of illudins, 6-protoilludene (Wawrzyn *et al.*, 2012). These two clusters contain genes (*omp6* and *omp7*) which encode terpene cyclases, and further numerous genes encoding tailoring proteins involved in oxidation and redox reactions (Wawrzyn *et al.*, 2012). The *omp6* BGC is well defined in roughly 25 kb and includes four P450 monooxygenases and fourteen additional putative genes that include eight putative oxidoreductases, two presumptive transferases, a presumed multiple drug transporter, a GATase1 anthranilate synthase, a polygalactonurase, and two seemingly unrelated enzymes. Contrarily, the *omp7* BGC is much smaller and was reported to contain only a P450 monooxygenase and an FAD binding protein.

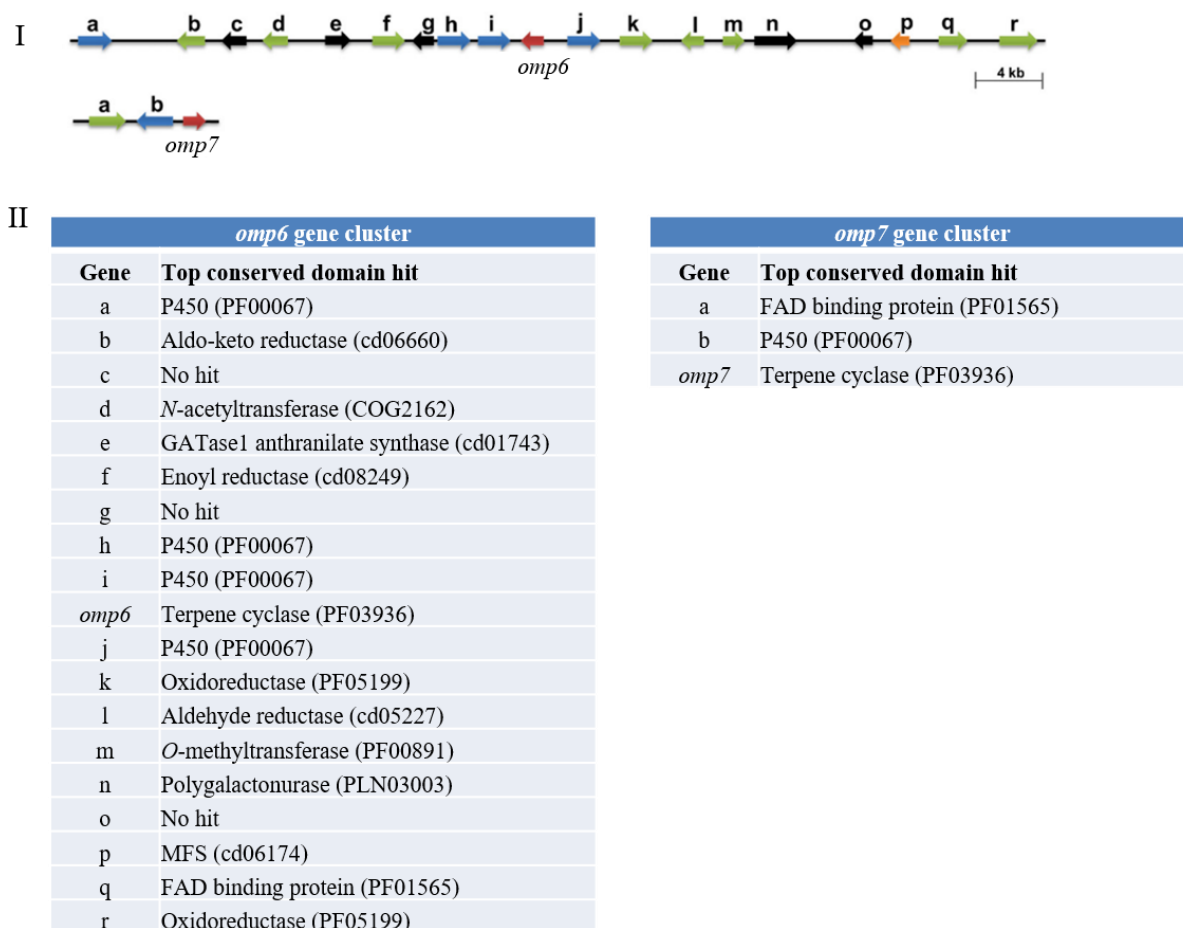


Figure 38. I, organization of genes in *omp6* and *omp7* BGCs; II, overview of predicted protein functions of encoded genes in the two BGC (Wawrzyn *et al.*, 2012).

The genes *omp6*, *omp7* and some of their neighboring putative biosynthetic genes were cloned and expressed in *E. coli* (Wawrzyn *et al.*, 2012). The results suggested that both gene clusters

are functional and expressed in *O. olearius* (Wawrzyn *et al.*, 2012). Synthesis of illudins M and S should involve at least five oxidation steps, which may be catalyzed by P450s and oxidoreductases surrounding *omp6* and *omp7* (Kinder and Bair, 1994). Interestingly, *omp7* showed a 10-fold higher catalytic efficiency than *Omp6* in a kinetic experiment, suggesting that maybe both BGC are important for the biosynthesis of illudins (Wawrzyn *et al.*, 2012).

4.2 Project Aims

Omphalotus olearius is not a genetically amenable fungus that allows examination of biosynthetic functions by gene knockouts (Wawrzyn *et al.*, 2012). Step-wise reconstruction of the biosynthesis reaction sequences in another fungal host such as *Aspergillus oryzae* for functional expression could elucidate the illudin pathways. Later manipulation of the illudin BGC pathway could enable the production of new illudin derivatives with improved bioactivities. But until now there is no molecular evidence for the biosynthetic step of illudins.

Earlier acetate feeding studies showed that 6-protoilludene is a probable biosynthetic precursor of illudins M and S (Morisaki *et al.*, 1985). The aim of this project is elucidation of biosynthesis pathway of illudins from *O. olearius* in a step-wise way, particularly the unusual oxidative and reductive transformations of 6-protoilludene. Therefore, all putative genes involved in illudin biosynthesis should be coexpressed with core terpene cyclase genes (especially P450s and oxidoreductase encoding genes) in the heterologous host *A. oryzae* NSAR1 in order to re-establish illudin production in this ascomycete host.

In vivo characterization of P450 encoding genes by heterologous expression of the illudin BGC in *A. oryzae* NSAR1 should reveal the order of oxidation steps. Using the same methodology should reveal the role of short chain reductases (SDR) and remaining functional genes during the biosynthesis of illudins.

4.3 Results

4.3.1 Analysis of Potential Illudin Biosynthetic Gene Clusters

Based on the available genome sequence of *Omphalotus olearius* from JGI (<https://mycocosm.jgi.doe.gov/Ompol1/Ompol1.home.html>, Wawrzyn *et al.*, 2012), eleven putative sesquiterpene synthases (STS) were identified by both BLAST homology searches

with six STS (*cop1-6*, Wawrzyn *et al.*, 2012) and HMMER (<http://hmmer.org/>) searches with Pfam database (<https://pfam.xfam.org/>). Three STS genes (*omp1*, *omp6*, and *omp7*) are located in biosynthetic gene clusters based on fungiSMASH (<https://fungismash.secondarymetabolites.org/#!/start>) analysis and manual annotation. *Omp6* and *Omp7* (**Figure 38**) were previously proved to be 6-protoilludene synthases by functional characterization after heterologous expression in *E. coli*.

The *Omp7* STS was verified to have a 10-fold higher catalytic efficiency than the *Omp6* STS (Section 5.1.2), which indicates that the small *omp7* gene cluster is a possible gene duplication to boost rate-limiting steps in the biosynthesis of illudins (Wawrzyn *et al.*, 2012). Two scaffolds (Sca034 and Sca146) from a new *O. olearius* genome sequence were provided by a collaborator at the University of Bristol. The BGC derived from these two scaffolds were compared with the *omp6* and *omp7* BGC by ARTEMIS comparison (<https://www.sanger.ac.uk/science/tools/artemis-comparison-tool-act>). The Sca034 and sca146 sequences were shown to overlap with the small *omp7* gene cluster (**Figure 39**).

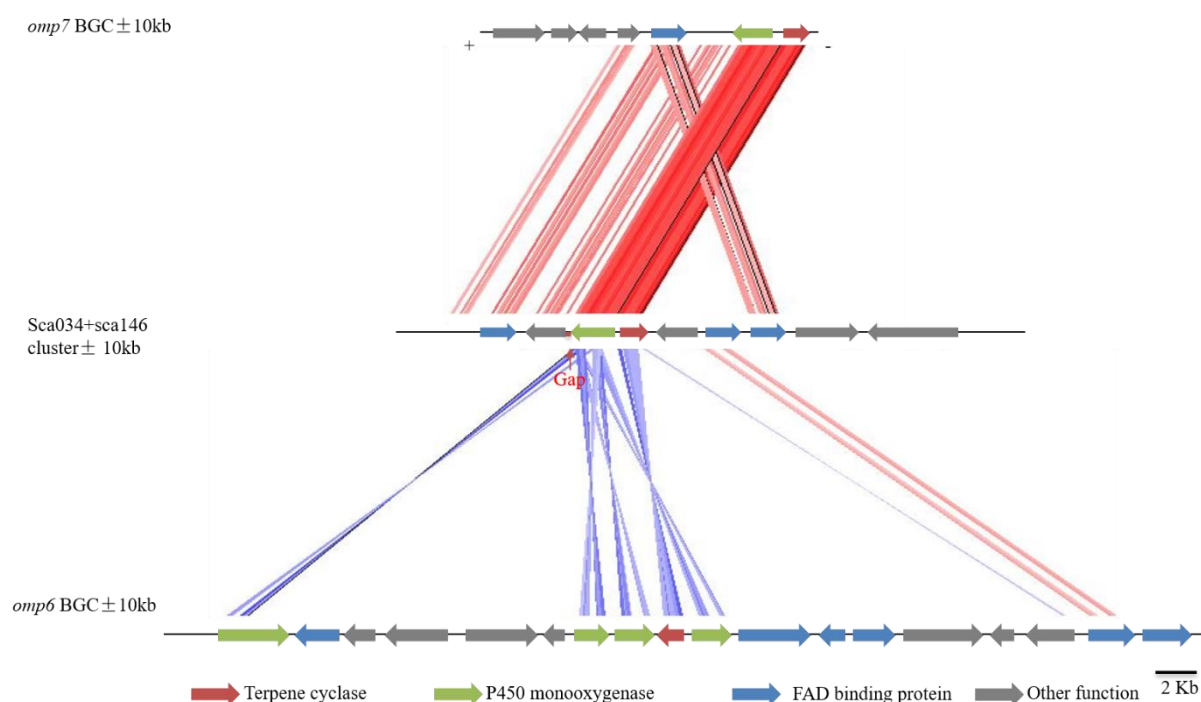


Figure 39. Artemis comparison of the *omp7*, Sca034 + sca146 and *omp6* gene clusters.

The *omp7* gene cluster and the gene cluster derived from Sca034 + sca146 overlap and therefore create a longer gene cluster potentially related to the biosynthesis of illudins, here named as *omp7* BGC (**Figure 42**) and including one terpene cyclase, one P450, and three oxidoreductase genes.

Another illudin BGC named *omp6* BGC (**Figure 39**) is identical to the one reported by Wawrzyn *et al.*, (2012), which contains one terpene cyclase, four P450s, and five oxidoreductase genes. The assumed functions of the genes in these gene clusters were annotated as stated in the UniProtKB database (<https://www.uniprot.org>, **Table 15 & 16**).

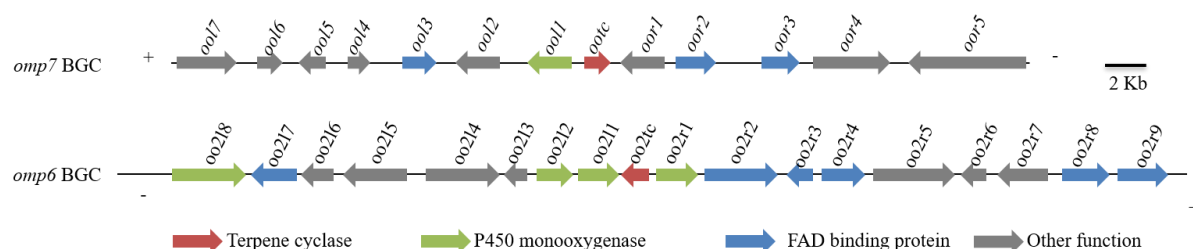


Figure 40. The proposed biosynthesis gene clusters of illudins.

Table 15. The annotation of genes in *omp7* BGC.

Gene	Putative function	InterPro homolog (identity %)	Genbank homolog (identity %)	Reference
<i>ootc</i>	Terpene cyclase	IPR008949 (63)	-	Olson <i>et al.</i> , 2012
<i>ool1</i>	P450	IPR001128 (59)	-	Sipos <i>et al.</i> , 2017
<i>ool2</i>	-	-	-	-
<i>ool3</i>	FAD binding protein	IPR016166 (63)	-	Hess <i>et al.</i> , 2014
<i>ool4</i>	-	-	-	-
<i>ool5</i>	-	-	-	-
<i>ool6</i>	HMG box protein	IPR009071 (73)	XM_008042079.1 (89)	Varga <i>et al.</i> , 2019
<i>ool7</i>	-	-	-	-
<i>oor1</i>	-	-	-	-
<i>oor2</i>	FAD binding protein	IPR016166 (70)	-	Choi <i>et al.</i> , 2018
<i>oor3</i>	FAD binding protein	IPR016166 (66)	CP017346.1 (92)	Riley <i>et al.</i> , 2014
<i>oor4</i>	Na ⁺ solute symporter	IPR038377 (74)	-	Sakamoto <i>et al.</i> , 2016
<i>oor5</i>	AP complex subunit beta	IPR026739 (86)	XM_033680149.1 (95)	Sipos <i>et al.</i> , 2017

Table 16. The annotation of genes in *omp6* BGC.

Gene	Putative function	InterPro homolog (% identity)	Genbank homolog (identity %)	Reference
<i>oo2tc</i>	Terpene cyclase	IPR008949 (84)	-	Mondo <i>et al.</i> , 2018
<i>oo2l1</i>	P450	IPR001128 (55)	-	Floudas <i>et al.</i> , 2012
<i>oo2l2</i>	P450	IPR001128 (65)	-	Olson <i>et al.</i> , 2012
<i>oo2l3</i>	GH131_N protein	-	-	-
<i>oo2l4</i>	Chorismate_bind protein	IPR005801 (74)	-	Mondego <i>et al.</i> , 2008
<i>oo2l5</i>	N-acetyltransferase	IPR001447 (56)	CP036208.1 (90)	Semeiks <i>et al.</i> , 2014
<i>oo2l6</i>	-	-	-	-
<i>oo2l7</i>	Aldo/keto reductase	IPR023210 (83)	-	Semeiks <i>et al.</i> , 2014
<i>oo2l8</i>	P450	IPR001128 (80)	-	Olson <i>et al.</i> , 2012
<i>oo2r1</i>	P450	IPR001128 (84)	-	Nagy <i>et al.</i> , 2016
<i>oo2r2</i>	Aldo/keto reductase	IPR036188 (74)	-	Nagy <i>et al.</i> , 2016
<i>oo2r3</i>	NADP-binding protein	IPR001509 (82)	-	Nagy <i>et al.</i> , 2016
<i>oo2r4</i>	O-methyltransferase	IPR016461 (73)	-	Suzuki <i>et al.</i> , 2012
<i>oo2r5</i>	Glycoside hydrolase protein	IPR002575 (77)	-	Sakamoto <i>et al.</i> , 2016
<i>oo2r6</i>	-	-	-	-
<i>oo2r7</i>	MFS transporter	IPR011701 (70)	-	Varga <i>et al.</i> , 2019
<i>oo2r8</i>	FAD binding protein	IPR016166 (66)	-	Nagy <i>et al.</i> , 2016
<i>oo2r9</i>	GMC oxidoreductase	IPR012132 (75)	-	Olson <i>et al.</i> , 2012

4.3.2 Heterologous Expression of the Illudin BGC in *A. oryzae*

Microbial natural products are a tremendous source of new bioactive chemical entities for drug discovery (Karwehl and Stadler, 2016). Basidiomycota have been playing a secondary role in discovering natural products because they can hardly be isolated from soil samples and their fermentation often requires special protocols (Karwehl and Stadler, 2016). However, numerous natural products with distinct structures have been characterized from both cultures and fruiting bodies of Basidiomycota since the mid-1970s (Chen and Liu, 2017; De Silva *et al.*, 2013). Compared to other microbial producers such as bacteria and filamentous fungi (especially

Ascomycota), Basidiomycota remains greatly undescribed for the discovery and applications of enzymatic machinery in biosynthesis (Sandargo *et al.*, 2019a).

The number of genome sequence data available for Basidiomycota has increased in recent years (Grigoriev *et al.*, 2014). Genome mining has further led to the discovery of numerous uncharacterized metabolic pathways in Basidiomycota. Since many BGC are silent under laboratory conditions or their expression levels are very low, heterologous expression of natural products has gained more interest in the last decades (Zhang *et al.*, 2019). These BGC may encode metabolites with improved biological activities, heterologous expression of them also allow the elucidation of biosynthetic pathways of microorganisms.

For the reconstitution of the desired biosynthetic pathway, the genes from the gene clusters can be amplified from genomic DNA (gDNA) or, if intron splicing might be a problem between distantly related species, from complementary DNA (cDNA). In this project, the genes were amplified from cDNA since the genes from *O. olearius* contain numerous introns.

Vector construction and gene combination for *A. oryzae* transformation

The quadruple auxotrophic host *A. oryzae* NSAR1 is often used as a model host organism for the expression of large BGC (Lazarus *et al.*, 2014). *A. oryzae* NSAR1 is deficient in arginine ($\Delta argB$), adenine (*adeA*⁻), methionine (*sC*⁻) and ammonium (*niaD*⁻) metabolism. Genes involved in BGCs assembled in one or a few multiple gene expression plasmids is performed using homologous recombination in yeast. Using designed pTYGS expression vectors featuring different selection markers (*argB*, *adeA*, *sC*, *niaD*, *ble*^R, *bar*^R) enables the reconstruction of larger biosynthetic pathways by simultaneous expression of multiple genes. Each plasmid possesses four fungal promoter/terminator pairs for gene cloning (*P/T_{adh}*, *P/T_{gpdA}*, *P/T_{eno}*, and *P/T_{amyB}*, **Figure 41**). The first three can be used to add up to three tailoring genes *in vivo* by yeast homologous recombination, which include at least 30 bp homologous overlap sequence that is usually introduced by PCR through tails at the designed oligonucleotides.

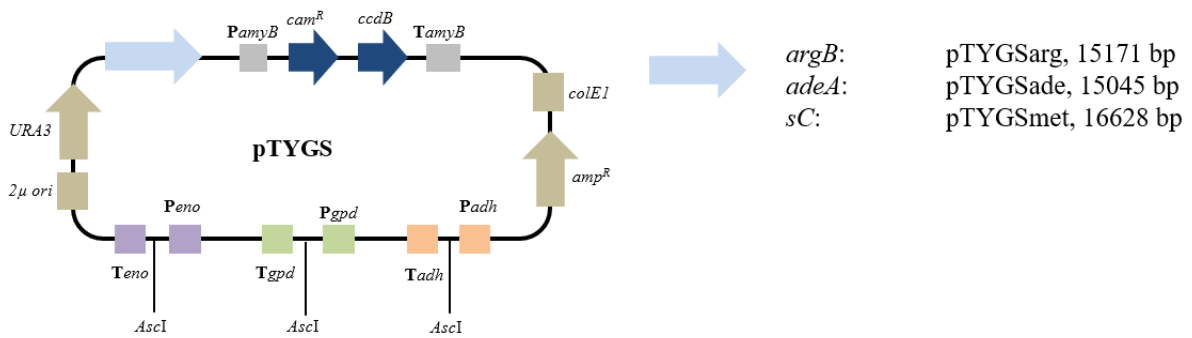


Figure 41. pTYGS vector family used in this thesis.

For selection in *S. cerevisiae*, the vector contains the *URA3* marker to allow growth in the absence of uracil. Transformant colonies contain vector DNA which can be isolated for bacterial transformation and screening. The fungal expression vectors contain a *colE1* origin for replication in *E. coli*, selection of the vector facilitates resistance to chloramphenicol (*cam^R*) and ampicillin (*amp^R*).

In this project, the biosynthesis of illudins starts from *omp7* BGC since the core gene *omp7* has a 10-fold higher catalytic efficiency than *omp6*. The *omp7* BGC encoding a terpene cyclase, a cytochrome P450 monooxygenase, and three FAD-binding oxidoreductases. Plasmids were constructed in different stages (**Figure 42**): (1) pTYGS-Arg-*ootc*; (2) pTYGS-Arg-*ootc-ool1*; (3) pTYGS-Arg-*ootc* + *ool1* + *ool3*, pTYGS-Ade-*oor2* + *oor3*. The plasmids were recombined in yeast and amplified in *E. coli*.

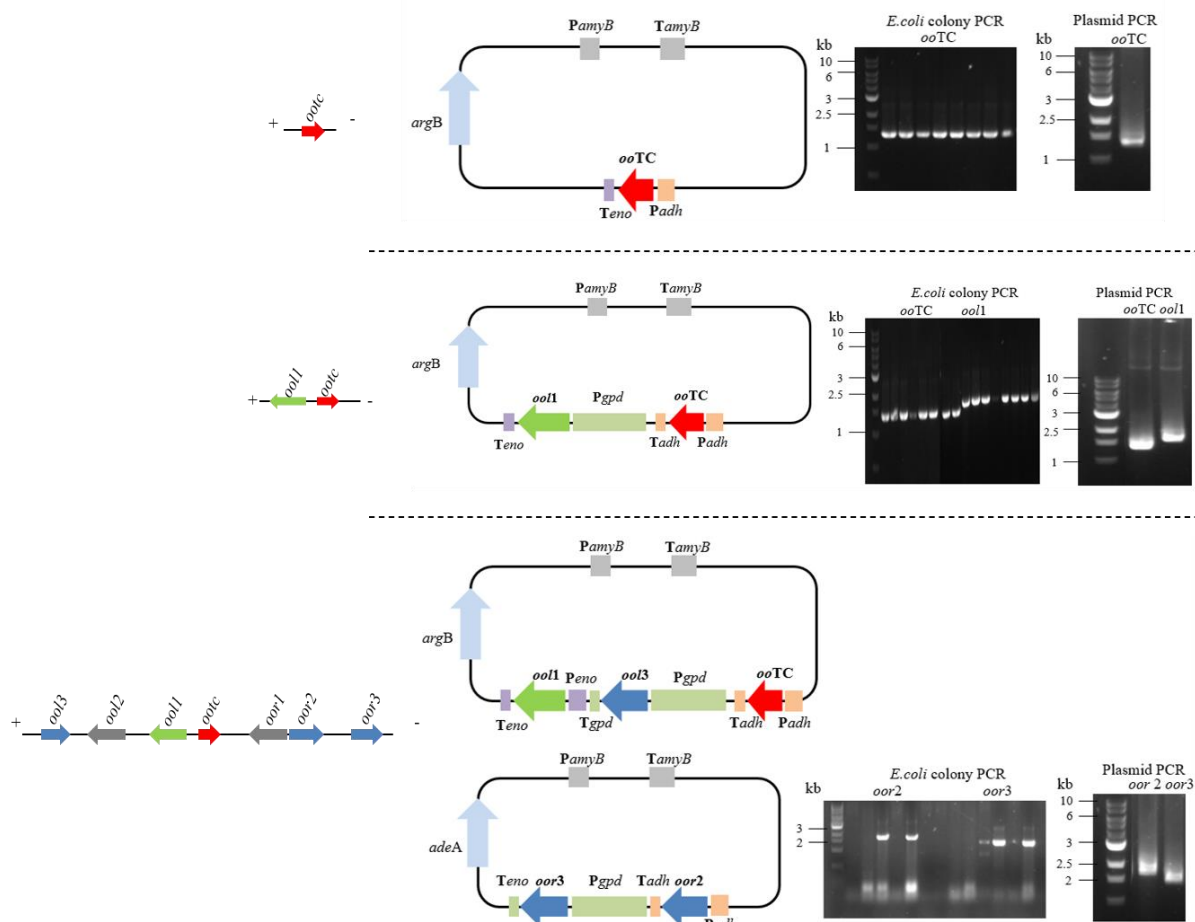


Figure 42. Vectors constructed in this study and PCR results.

Heterologous expression of vectors in *A. oryzae*

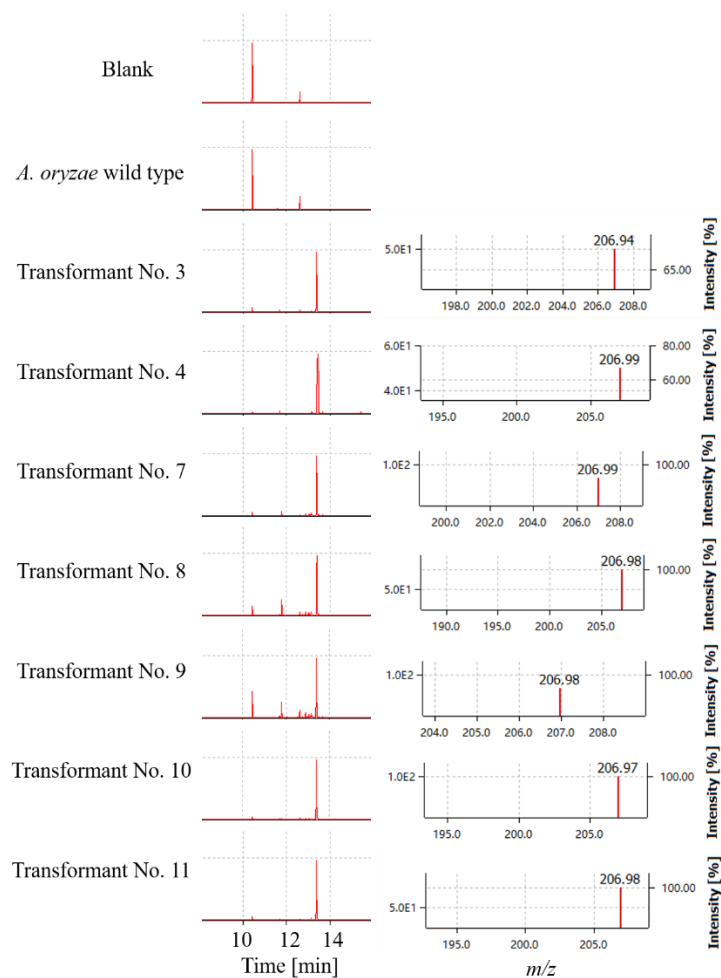
Heterologous expression of constructed vectors in *A. oryzae* NSAR1 led to the acquisition of 14 transformants from the expression of terpene cyclase (*ootc*), 11 transformants from the expression of terpene cyclase (*ootc*) and P450 (*ool1*), and 12 transformants from the expression of terpene cyclase (*ootc*), P450 (*ool1*) and three oxidoreductases (*ool3*, *oor2*, *oor3*). As stated in the introduction (Section 5.1.2), heterologous expression of the core gene *ootc* from illudin *omp7* BGC in *A. oryzae* NSAR1 should lead mainly to the formation of 6-protoilludene, the precursor of illudins (stage 1).

Fourteen transformants from the expression of terpene cyclase (*ootc*) alone were inoculated in 20 mL screw top GC headspace vials that contain 6 mL DPY agar slope. The vials were sent for GCMS (Thermo Scientific ITQ 900 GC/MS) measurements every two days after an initial incubation for four days. The samples were collected through a solid phase microextraction

SPME-fibre from the headspace of the samples within 45 min at room temperature. The desorption of samples from SPME-fibre was performed in the PTV injector of the gas chromatograph for 1 min at 230 °C. The temperature gradient was 50 °C for 1 min, 10 °C/min increase rate up to 320 °C, followed by 320 °C for 2 min.

Obtained raw data were converted to cdf-files by Xcalibur 2.1 software (Thermo Scientific), cdf-files were analysed Openchrom (<https://lablicate.com/platform/openchrom>). Products from the transformants were compared to those from *A. oryzae* NSAR1 controls and blank vials (DPY agar only). Seven out of fourteen transformants showed a new peak in comparison to controls (**Figure 43**). This peak has a mass of 206, which would correspond to a reduced protoilludene or caryophyllene (**Figure 43**). However, these results are consistent with the release of one of many possible C₁₅H₂₄ isomers, followed by reduction (*e.g.* addition of H₂). The purification of this mixture and NMR elucidation will be done in the future since I run out of time for this PhD project.

A



B

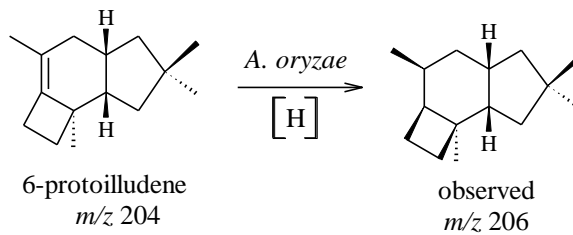


Figure 43. A. Production of transformants from expression of *ootc* detected by GC-MS; **B.** The putative structure of production from expression of *ootc*.

5. Conclusion and Discussion

Antibiotic resistance is an increasing threat to human health, to overcome the resistance of pathogenic bacteria and fungi, the discovery of compounds with new structures and modes of action is needed urgently. Fungi have been proven as a rich source of new and biologically active secondary metabolites, which broadened from saprophytic terrestrial strains to living plants with their endophytes and marine habitats. However, only ~ 5% fungal species have been characterised and most of the collected strains are waiting for identification (Hawksworth, 2011). Tropical rainforests are widely known as the most biologically diverse terrestrial ecosystems on earth (Armstrong, 2018), offering high opportunities for discovering new fungal species. Those give rise to a high probability that tropical rainforests are a promising source for novel structures and active compounds (Reddell and Gordon, 2000).

Most of the metabolites currently in developmental pipelines are derived from ascomycetes, *e.g. Penicillium* and *Aspergillus* species. Basidiomycetes cultures are difficult to handle with respect to large scale production of secondary metabolites since they grow slowly and have low yields. They were therefore neglected for a long time in natural product research and studied less (Hyde *et al.*, 2019). However, interest in basidiomycetes, and the number of new natural products derived from them, has grown considerably due to the unique structures and promising biological activities of metabolites produced by them (Stadler and Hoffmeister, 2015). The main purpose of this project is to screen and identify the active components from the largely neglected basidiomycetes originated from African tropics. In order to clarify the diversity of Basidiomycota and its prosperous chemistry structures, the extensive study of natural products in several basidiomycetes collected from Kenyan tropical rainforest Kakamega and Mount Elgon national reserve was carried on in the past years.

About 200 cultures of basidiomycetes were isolated from the collected species in Kakamega and Mount Elgon national reserve (Chepkirui, 2018), and 27 (see Appendix) among them were screened for antimicrobial activities in three standard media in this project. Five strains and one corresponding fruitbody collection were selected and studied extensively for secondary metabolites, which led to the characterization of over forty undescribed metabolites together with several known secondary metabolites. The undescribed compounds contain various structures and bioactivities. Promisingly, five of them with four novel carbon skeletons.

The previous unprecedented tyromycin A derivatives skeletocutins A-Q isolated from both the liquid cultures and fruiting bodies of *Skeletocutis* sp. and their activities tested in this project enriched the published knowledge of tyromycins. These compounds were evaluated in

antimicrobial, cytotoxicity, biofilm inhibition, nematocidal, leucine aminopeptidases inhibition, and antiviral assays. Notably, the activity inhibits HCV by tyromycin A was reported firstly after 27 years of the discovery of this compound.

Several sesquiterpenes (elgonenes A-L) were obtained from the important traditional Asian medicinal mushroom *Sanghuangporus* sp.. Some of these elgonenes are structurally related to the phelilanes, which were patented as part of an antibacterial agent that is being marketed for the treatment of ailments (Kobayashi *et al.*, 2010). Additionally, elgonenes devoid of the activity or weakly active against tested Gram-positive bacteria and *M. hiemalis*, some of cytotoxic against human cell lines as well. The metabolites derived from *Heimiomyces* sp. are even interesting since five of them contain four novel carbon skeletons, the stereochemistry analysis is ongoing. They exhibited moderate antimicrobial and cytotoxic activities against Gram-positive bacteria and human cell lines, respectively. Further bioactivities evaluation of these compounds could give help for searching the specific and selective targets for them, and the chemical modification may also improve the activities of the reported compounds.

Apart from the natural products mining by fermentation and preparative HPLC approaches from basidiomycetes, the attention at the genetic modification is increasing with the development of genomics technology. Basidiomycetes producing notable biological activities yields could be selected for genome sequencing, gene clusters identifying and heterologous expression. The elucidation of biosynthesis pathway could accelerate the development of natural products for medicinal applications.

With the purpose of identifying agents like alkylants with antitumor activity, the modification of illudins M and S have awakened a lot of interest among academic research since the early 1990s. The dehydroilludin M and HMAF (irofulven), which were modified from illudins M and S, respectively, have shown an improved therapeutic index. However, the biosynthesis of illudins still remains undiscovered.

Three plasmids were constructed based on the sesquiterpene gene cluster *omp7* BGC in this thesis. They were expressed in *A. oryzae* NSAR1. The plasmid contains only one terpene cyclase gene, was expected to produce the proposed precursor of illudins 6-protoilludene. The production of transformants from the expression of *ootc* was detected by GCMS system since the structure of 6-protoilludene make it a volatile compound. Here we obtained a violate with *m/z* 206, which we proposed as the intermediate of illudins. Based on our results and report of Wawrzyn *et al.*, (2012), we presume the biosynthesis pathway of illudins as follows (**Figure 44**).

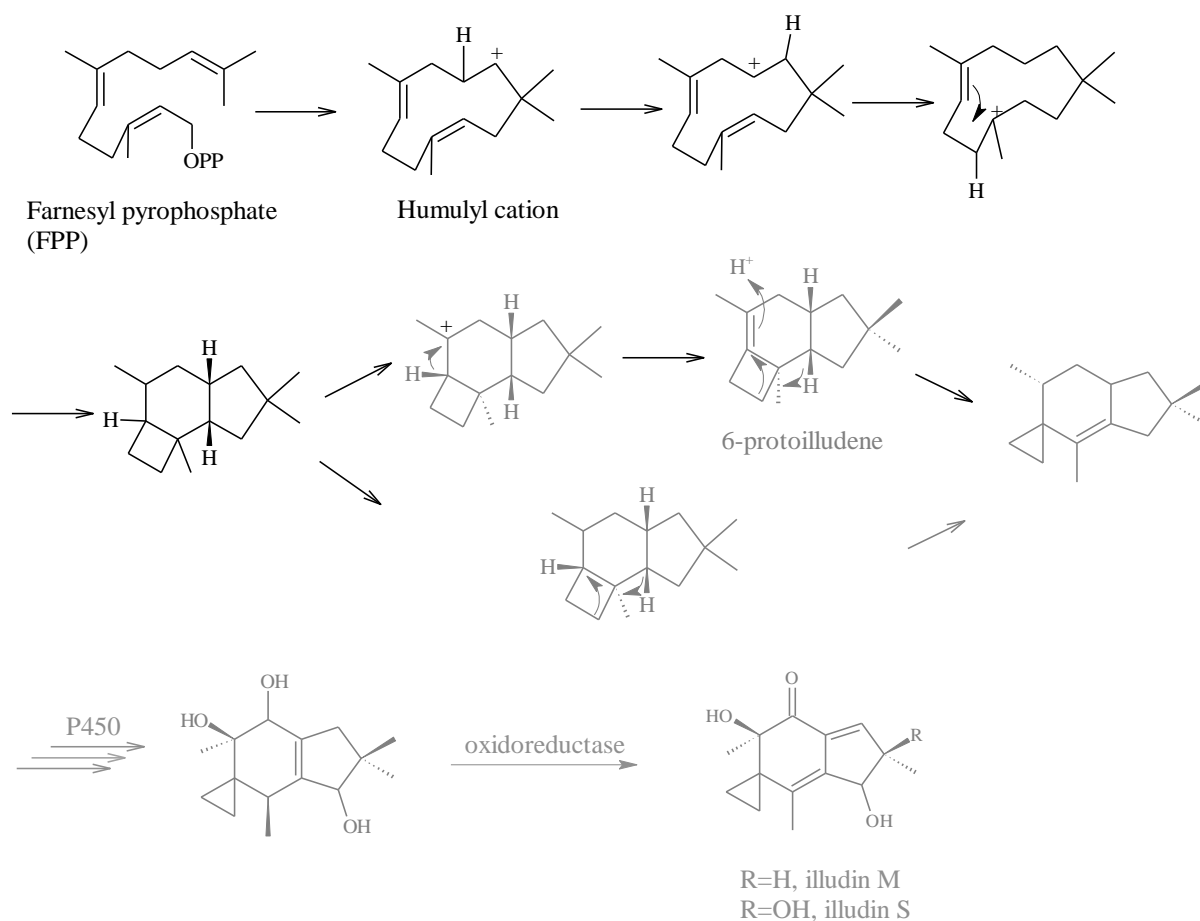


Figure 44. Proposed biosynthesis pathway of illudin. The known steps are in black, proposed steps are in grey.

In future work, the screening of rest transformants from stage 2 and stage 3 would be further investigated in order to understand the oxidation of the precursor in the biosynthesis of illudins. In addition, the research of the second sesquiterpene gene cluster BGC2 annotated from *O. olearius* genome sequence would also help with the elucidation of the biosynthesis pathway of illudins.

6. References

- Abraham, E.P., Chain, E., **1940**. An enzyme from bacteria able to destroy penicillin. *Nature* **146**, 837.
- Adam, B., Baillie, G.S., Douglas, L.J., **2002**. Mixed species biofilms of *Candida albicans* and *Staphylococcus epidermidis*. *J. Med. Microbiol.* **51**, 344–349.
- Agger, S., Lopez-Gallego, F., Schmidt-Dannert, C., **2009**. Diversity of sesquiterpene synthases in the basidiomycete *Coprinus cinereus*. *Mol. Microbiol.* **72**, 1307–1308.
- Alberti, F., Khairudin, K., Venegas, E.R., Davies, J.A., Hayes, P.M., Willis, C.L., Bailey, A.M., Foster, G.D., **2017**. Heterologous expression reveals the biosynthesis of the antibiotic pleuromutilin and generates bioactive semi-synthetic derivatives. *Nat. Commun.* **8**, 1–9.
- Alberts, A.W., Chen, J., Kuron, G., Hunt, V., Huff, J., Hoffman, C., Rothrock, J., Lopez, M., Joshua, H., Harris, E., Patchett, A., Monaghan, R., Currie, S., Stapley, E., Albers-Schonberg, G., Hensens, O., Hirshfield, J., Hoogsteen, K., Liesch, J., Springer, J., **1980**. Mevinolin: A highly potent competitive inhibitor of hydroxymethylglutaryl-coenzyme A reductase and a cholesterol-lowering agent. *Proc. Natl. Acad. Sci. U. S. A.* **77**, 3957–3961.
- Anchel, M., Hervey, A., Robbins, W.J., **1950**. Antibiotic substances from Basidiomycetes+. VII. *Clitocybe illudens*. *Proc. Natl. Acad. Sci. U. S. A.* **36**, 300–305.
- Andersson, C., Kristinsson, J., Gry, Jø., **2009**. Occurrence and use of hallucinogenic mushrooms containing psilocybin alkaloids. *Nordic council of Ministers*. ISBN 978-92-893-1836-5.
- Anke, T., **1995**. The antifungal strobilurins and their possible ecological role. *Can. J. Bot.* **73**, 940–945.
- Armstrong, A.H., **2018**. Tropical rainforest ecosystems, in: international encyclopedia of geography. *Wiley*. 1–16.
- Baguley, B.C., Rommele, G., Gruner, J., Wehrli, W., **1979**. Papulacandin B: an inhibitor of glucan synthesis in yeast spheroplasts. *Eur. J. Biochem.* **97**, 345–351.
- Bai, R., Zhang, C.-C., Yin, X., Wei, J., Gao, J.-M., **2015**. Striatoids A–F, cyathane diterpenoids with neurotrophic activity from cultures of the fungus *Cyathus striatus*. *J. Nat. Prod.* **78**, 783–788.
- Bailey, A.M., Alberti, F., Kilaru, S., Collins, C.M., De Mattos-Shiple, K., Hartley, A.J., Hayes, P., Griffin, A., Lazarus, C.M., Cox, R.J., Willis, C.L., O'Dwyer, K., Spence, D.W., Foster, G.D., **2016**. Identification and manipulation of the pleuromutilin gene cluster from *Clitopilus passeckerianus* for increased rapid antibiotic production. *Sci. Rep.* **6**, 1–11.
- Bartlett, J.G., Gilbert, D.N., Spellberg, B., **2013**. Seven ways to preserve the miracle of antibiotics. *Clin. Infect. Dis.* **56**, 1445–1450.
- Bills, G.F., Gloer, J.B., **2016**. Biologically active secondary metabolites from the fungi. *Microbiol. Spectr.* **4**, 1–32.
- Blin, K., Wolf, T., Chevrette, M.G., Lu, X., Schwalen, C.J., Kautsar, S.A., Suarez Duran, H.G., de los Santos, E.L.C., Kim, H.U., Nave, M., Dickschat, J.S., Mitchell, D.A., Shelest, E., Breitling, R., Takano, E., Lee, S.Y., Weber, T., Medema, M.H., **2017**. antiSMASH 4.0—improvements in chemistry prediction and gene cluster boundary identification. *Nucleic Acids Res.* **45**, W36–W41.
- Bo, G., **2000**. Giuseppe Brotzu and the discovery of cephalosporins. *Clin. Microbiol. Infect.* **6**, 6–8.
- Borel, J.F., **1990**. Pharmacology of cyclosporine (sandimmune). IV. Pharmacological properties *in vivo*. *Pharmacol. Rev.* **41**.

- Borel, J.F., Kis, Z.L., **1991**. The discovery and development of cyclosporine (Sandimmune). *Transplant. Proc.* **23**, 1867–74.
- Bradshaw, A.P.W., Hanson, J.R., Sadler, I.H., **1982**. Studies in terpenoid biosynthesis. Part 26. Applications of ^2H and ^{13}C N.M.R. spectroscopy to the biosynthesis of the illudin sesquiterpenoids. *J. Chem. Soc.* 2445–2448.
- Bradshaw, A.P.W., Hanson, J.R., Siverns, M., **1978**. Biosynthesis of illudin sesquiterpenoids from $[1,2-^{13}\text{C}_2]$ acetate. *J. Chem. Soc. Chem. Commun.* 303–304.
- Bradshaw, C.S., Jensen, J.S., Waites, K.B., **2017**. New horizons in mycoplasma genitalium treatment. *J. Infect. Dis.* **216**, S412–S419.
- Brown, M.S., Faust, J.R., Goldstein, J.L., Kaneko, I., Endo, A., **1978**. Induction of 3-hydroxy-3-methylglutaryl coenzyme A reductase activity in human fibroblasts incubated with compactin (ML-236B), a competitive inhibitor of the reductase. *J. Biol. Chem.* **253**, 1121–1128.
- Büchel, E., Mayer, A., Martini, U., Anke, H., Sterner, O., **1998**. Structure elucidation of omphalotin, a cyclic dodecapeptide with potent nematocidal activity isolated from *Omphalotus olearius*. *Pestic. Sci.* **54**, 309–311.
- Buckingham, J., **2017**. Dictionary of natural products. *CRC. press*.
- Burgess, M.L., Barrow, K.D., **1999**. Biosynthesis of illudosin, a fomannosane-type sesquiterpene, by the Basidiomycete *Omphalotus nidiformis*. *J. Chem. Soc.* 2461–2466.
- Bush, K., Courvalin, P., Dantas, G., Davies, J., Eisenstein, B., Huovinen, P., Jacoby, G.A., Kishony, R., Kreiswirth, B.N., Kutter, E., Lerner, S.A., Levy, S., Lewis, K., Lomovskaya, O., Miller, J.H., Mobashery, S., Piddock, L.J.V., Projan, S., Thomas, C.M., Tomasz, A., Tulkens, P.M., Walsh, T.R., Watson, J.D., Witkowski, J., Witte, W., Wright, G., Yeh, P., Zgurskaya, H.I., **2011**. Tackling antibiotic resistance. *Nat. Rev. Microbiol.* **9**, 894–896.
- Carvalho, E., Iley, J., De Jesus Perry, M., Rosa, E., **1998**. Triazene drug metabolites: Part 15. Synthesis and plasma hydrolysis of anticancer triazenes containing amino acid carriers. *Pharm. Res.* **15**, 931–935.
- Chen, H., Liu, J., **2017**. Progress in the chemistry of organic natural products 110. *Springer.* **107**, 1-102.
- Chepkirui, C., **2018**. Characterization of novel bioactive natural products from tropical basidiomycota. Dissertation.
- Chepkirui, C., Matasyoh, J.C., Decock, C., Stadler, M., **2017**. Two cytotoxic triterpenes from cultures of a Kenyan *Laetiporus* sp. (Basidiomycota). *Phytochem. Lett.* **20**, 106–110.
- Chepkirui, C., Richter, C., Matasyoh, J.C., Stadler, M., **2016**. Monochlorinated calocerins A-D and 9-oxostrobilurin derivatives from the basidiomycete *Favolaschia calocera*. *Phytochemistry* **132**, 95–101.
- Chopra, I., Roberts, M., **2001**. Tetracycline antibiotics: mode of action, applications, molecular biology, and epidemiology of bacterial resistance. *Microbiol. Mol. Biol. Rev.* **65**, 232–260.
- Chukwudi, C.U., **2016**. rRNA binding sites and the molecular mechanism of action of the tetracyclines. *Antimicrob. Agents Chemother.* **60**, 4433-4441.
- Ciesek, S., von Hahn, T., Colpitts, C.C., Schang, L.M., Friesland, M., Steinmann, J., Manns, M.P., Ott, M., Wedemeyer, H., Meuleman, P., Pietschmann, T., Steinmann, E., **2011**. The green tea polyphenol, epigallocatechin-3-gallate, inhibits hepatitis C virus entry. *Hepatology* **54**, 1947–1955.
- Clardy, J., Fischbach, M.A., Currie, C.R., **2009**. The natural history of antibiotics. *Curr. Biol.* **19**, R437-R441.

- Cooper, M.A., Shlaes, D., **2011**. Fix the antibiotics pipeline. *Nature* **472**, 32.
- Cui, B.-K., Dai, Y.-C., **2008**. *Skeletocutis luteolus* sp. nov. from southern and eastern China. *Mycotaxon. Ithaca. Ny.* **104**, 97–101.
- Cully, M., **2014**. Public health: The politics of antibiotics. *Nature* **509**, S16–S17.
- Das, B., Sarkar, C., Das, D., Gupta, A., Kalra, A., Sahni, S., **2017**. Telavancin: a novel semisynthetic lipoglycopeptide agent to counter the challenge of resistant Gram-positive pathogens. *Ther. Adv. Infect. Dis.* **4**, 49–73.
- de Carvalho, M.P., Gulotta, G., do Amaral, M.W., Lünsdorf, H., Sasse, F., Abraham, W.R., **2016**. Coprinuslactone protects the edible mushroom *coprinus comatus* against biofilm infections by blocking both quorum-sensing and murA. *Environ. Microbiol.* **18**, 4254–4264.
- De Silva, D.D., Rapior, S., Sudarman, E., Stadler, M., Xu, J., Aisyah Alias, S., Hyde, K.D., **2013**. Bioactive metabolites from macrofungi: Ethnopharmacology, biological activities and chemistry. *Fungal Divers.* **62**, 1–40.
- Dean, L., **2012**. Gentamicin Therapy and MT-RNR1 Genotype, Medical Genetics Summaries. (<https://www.ncbi.nlm.nih.gov/books/NBK285956/>)
- Denning, D.W., **2002**. Leading articles Echinocandins: a new class of antifungal. *J. Antimicrob. Chemother.* **49**, 889–891.
- Desjardin, D., Perry, B., **2018**. The gymnopoid fungi (Basidiomycota, Agaricales) from the Republic of São Tomé and Príncipe, West Africa. *Mycosphere* **8**, 1317–1391.
- Díaz-Valderrama, J.R., Aime, M.C., **2016**. The cacao pathogen *Moniliophthora roreri* (Marasmiaceae) possesses biallelic A and B mating loci but reproduces clonally. *Heredity (Edinb.)* **116**, 491–501.
- Domagk, G., **1935**. Ein Beitrag zur Chemotherapie der bakteriellen Infektionen. *Dtsch. Medizinische Wochenschrift* **61**, 250–253.
- Dreyfuss, M.M., Tschertter, H., **1979**. Antibiotic S 31794/F-1. US4173629A.
- Drinkwater, N., Lee, J., Yang, W., Malcolm, T.R., McGowan, S., **2017**. M1 aminopeptidases as drug targets: broad applications or therapeutic niche? *FEBS J.* **284**, 1473–1488.
- Dufresne, C., Young, K., Pelaez, F., Gonzalez del Val, A., Valentino, D., Graham, A., Platas, G., Bernard, A., Zink, D., **1997**. Illudinic acid, a novel illudane sesquiterpene antibiotic. *J. Nat. Prod.* **60**, 188–90.
- Duggar, B.M., **1948**. Aureomycin: a product of the continuing search for new antibiotics. *Ann. N. Y. Acad. Sci.* **51**, 177–181.
- Egger, H., Reinshagen, H., **1976a**. New pleuromutilin derivatives with enhanced antimicrobial activity. II. Structure-activity correlations. *J. Antibiot. (Tokyo)*. **29**, 923–927.
- Egger, H., Reinshagen, H., **1976b**. New pleuromutilin derivatives with enhanced antimicrobial activity. I. Synthesis. *J. Antibiot. (Tokyo)*. **29**, 915–922.
- Eisenbrand, G., Berger, M.R., Fischer, J., Schneider, M.R., Tang, W., Zeller, W.J., **1988**. Development of more selective anti-cancer nitrosoureas. *Anticancer. Drug Des.* **2**, 351–9.
- Endo, A., **1979**. Monacolin K, a new hypocholesterolemic agent produced by a *Monascus* species. *J. Antibiot. (Tokyo)*. **32**, 852–854.
- Endo, A., Kuroda, M., Tsujita, Y., **1976**. ML-236A, ML-236B, and ML-236C, new inhibitors of cholesterol synthesis produced by *Penicillium citrinum*. *J. Antibiot. (Tokyo)*. **29**, 1346–1348.

- Engels, B., Dahm, P., Jennewein, S., **2008**. Metabolic engineering of taxadiene biosynthesis in yeast as a first step towards Taxol (Paclitaxel) production. *Metab. Eng.* **10**, 201–206.
- Esteve-Raventós, F., Moreno, G., Manjón, J.L., Alvarado, P., **2010**. *Xeromphalina setulipes* (hygrophoroid clade, Agaricales), a new *Mediterranean* species. *Mycol. Prog.* **9**, 575–583.
- Farzam, K., Quick, J., **2020**. Erythromycin, StatPearls. *StatPearls Publishing*. (<https://www.ncbi.nlm.nih.gov/books/NBK532249/>).
- Fernandes, P., **2016**. Fusidic acid: A bacterial elongation factor inhibitor for the oral treatment of acute and chronic staphylococcal infections. *Cold Spring Harb. Perspect. Med.* **6**, a025437.
- Fisher, J.F., Meroueh, S.O., Mobashery, S., **2005**. Bacterial resistance to beta-lactam antibiotics: compelling opportunism, compelling opportunity. *Chem. Rev.* **105**, 395–424.
- Fleming, A., **1929**. On the antibacterial action of cultures of a *Penicillium*, with special reference to their use in the isolation of *B. influenzae*. *Br. J. Exp. Pathol.* **10**, 226–236.
- Floudas, D., Binder, M., Riley, R., Barry, K., Blanchette, R.A., Henrissat, B., Martínez, A.T., Otilar, R., Spatafora, J.W., Yadav, J.S., Aerts, A., Benoit, I., Boyd, A., Carlson, A., Copeland, A., Coutinho, P.M., De Vries, R.P., Ferreira, P., Findley, K., Foster, B., Gaskell, J., Glotzer, D., Górecki, P., Heitman, J., Hesse, C., Hori, C., Igarashi, K., Jurgens, J.A., Kallen, N., Kersten, P., Kohler, A., Kües, U., Kumar, T.K.A., Kuo, A., LaButti, K., Larrondo, L.F., Lindquist, E., Ling, A., Lombard, V., Lucas, S., Lundell, T., Martin, R., McLaughlin, D.J., Morgenstern, I., Morin, E., Murat, C., Nagy, L.G., Nolan, M., Ohm, R.A., Patyshakuliyeva, A., Rokas, A., Ruiz-Dueñas, F.J., Sabat, G., Salamov, A., Samejima, M., Schmutz, J., Slot, J.C., John, F.S., Stenlid, J., Sun, H., Sun, S., Syed, K., Tsang, A., Wiebenga, A., Young, D., Pisabarro, A., Eastwood, D.C., Martin, F., Cullen, D., Grigoriev, I. V., Hibbett, D.S., **2012**. The paleozoic origin of enzymatic lignin decomposition reconstructed from 31 fungal genomes. *Science (80-)*. **336**, 1715–1719.
- Fricke, J., Blei, F., Hoffmeister, D., **2017**. Enzymatic synthesis of psilocybin. *Angew. Chemie Int. Ed.* **56**, 12352–12355.
- Gardes, M., Bruns, T.D., **1993**. ITS primers with enhanced specificity for basidiomycetes - application to the identification of mycorrhizae and rusts. *Mol. Ecol.* **2**, 113–118.
- Garrett, D., **2019**. Nabriva therapeutics announces European medicines agency (EMA) validation of marketing authorization application for lefamulin nasdaq:NBRV. *Nabriva. Therapeutics*.
- Gietz, R.D., Woods, R.A., **2002**. Transformation of yeast by lithium acetate/single-stranded carrier DNA/polyethylene glycol method. *Methods Enzymol.* **350**, 87–96.
- Gonzalez Del Val, A., Platas, G., Arenal, F., Orihuela, J.C., Garcia, M., Hernandez, P., Royo, I., De Pedro, N., Silver, L.L., Young, K., Vicente, M.F., Pelaez, F., **2003**. Novel illudins from *Coprinopsis episcopalis* (syn. *Coprinus episcopalis*), and the distribution of illudin-like compounds among filamentous fungi. *Mycol. Res.* **107**, 1201–1209.
- Gosio, B., **1896**. Ricerche batteriologiche e chimiche sulle alterazioni del mais: contributo all'etiologia della pellagra. *Tip. delle. mantellate* **7**, 825–849.
- Griffith, R.S., **1981**. Introduction to vancomycin. *Rev. Infect. Dis.* **3**, S200–S204.
- Grigoriev, I. V., Nikitin, R., Haridas, S., Kuo, A., Ohm, R., Otilar, R., Riley, R., Salamov, A., Zhao, X., Korzeniewski, F., Smirnova, T., Nordberg, H., Dubchak, I., Shabalov, I., **2014**. MycoCosm portal: gearing up for 1000 fungal genomes. *Nucleic Acids Res.* **42**, D699–D704.
- Grothe, T., Stadler, M., Köpcke, B., Roemer, E., Bitzer, J., Wabnitz, P., Küper, T., **2011**. Terpenoid spiro ketal compounds with LXR agonists activity, their use and formulations with them. *U.S. Pat. Appl.* No. 13/994 447.

- Grove, J.F., Macmillan, J., Mulholland, T.P.C., Thorold Rogers, M.A., **1952**. Griseofulvin. part IV. structure. *J. Chem. Soc.* 3943–3945.
- Gupta, P., Sarkar, S., Das, B., Bhattacharjee, S., Tribedi, P., **2016**. Biofilm, pathogenesis and prevention—a journey to break the wall: a review. *Arch. Microbiol.* **198**, 1-15.
- Haas, B.J., Zeng, Q., Pearson, M.D., Cuomo, C.A., Wortman, J.R., **2011**. Approaches to fungal genome annotation. *Mycology* **2**, 118–141.
- Halling, R.E., Hawksworth, D.L., Kirk, P.M., Sutton, B.C., Pegler, D.N., **1997**. Ainsworth and Bisby's dictionary of the Fungi. *Mycologia* **89**, 821.
- Hanson, J.R., Marten, T., **1973**. Incorporation of [2-³H₂]- and [4(R)-4-³H]-mevalonoid hydrogen atoms into the sesquiterpenoid illudin M. *J. Chem. Soc. Chem. Commun.* **4**, 171–172.
- Hanson, J.R., Marten, T., Nyfeler, R., **1976**. Studies in terpenoid biosynthesis. Part XV. Biosynthesis of the sesquiterpenoid illudin M. *J. Chem. Soc. Perkin 1.* 876–880.
- Harder, A., Schmitt-Wrede, H.P., Krücken, J., Marinovski, P., Wunderlich, F., Willson, J., Amliwala, K., Holden-Dye, L., Walker, R., **2003**. Cyclooctadepsipeptides - An anthelmintically active class of compounds exhibiting a novel mode of action. *Int. J. Antimicrob. Agents* **22**, 318–331.
- Hartley, A.J., De Mattos-Shiple, K., Collins, C.M., Kilaru, S., Foster, G.D., Bailey, A.M., **2009**. Investigating pleuromutilin-producing *Clitopilus* species and related basidiomycetes. *FEMS Microbiol. Lett.* **297**, 24–30.
- Harvey, R.A., Clark, M.A., Finkel, R., Rey, J.A., Whalen, K., **2011**. Pharmacology (Lippincott's Illustrated Reviews) 5th. ISBN-13: 978-1451113143.
- Hawksworth, D., **2011**. A new dawn for the naming of fungi: impacts of decisions made in Melbourne in July 2011 on the future publication and regulation of fungal names. *MycoKeys* **1**, 7–20.
- Hedden, P., Sponcel, V., **2015**. A century of gibberellin research. *J. Plant Growth Regul.* **34**, 740-760.
- Helaly, S.E., Thongbai, B., Stadler, M., **2018**. Diversity of biologically active secondary metabolites from endophytic and saprotrophic fungi of the ascomycete order *Xylariales*. *Nat. Prod. Rep.* **35**, 992–1014.
- Hess, J., Skrede, I., Wolfe, B.E., Butti, K. La, Ohm, R.A., Grigoriev, I. V., Pringle, A., **2014**. Transposable element dynamics among asymbiotic and ectomycorrhizal amanita fungi. *Genome Biol. Evol.* **6**, 1564–1578.
- Hirotsu, M., Hirotsu, S., Takayanagi, H., Yoshikawa, T., **1999**. Blazeispirol A, an unprecedented skeleton from the cultured mycelia of the fungus *Agaricus blazei*. *Tetrahedron Lett.* **40**, 329–332.
- Hirotsu, M., Hirotsu, S., Yoshikawa, T., **2000**. Blazeispirol X and Y, two novel carbon skeletal sterols from the cultured mycelia of the fungus *Agaricus blazei*. *Tetrahedron Lett.* **41**, 5107–5110.
- Hirotsu, M, Sai, K., Hirotsu, S., Yoshikawa, T., **2002a**. Blazeispirols B, C, E and F, des-A-ergostane-type compounds, from the cultured mycelia of the fungus *Agaricus blazei*. *Phytochemistry* **59**, 571–577.
- Hirotsu, M, Sai, K., Kaneko, A., Asada, Y., Yoshikawa, T., **2002b**. Biosynthetic studies on blazeispirane and protoblazeispirane derivatives from the cultured mycelia of the fungus *Agaricus blazei*. *Tetrahedron* **58**, 10251–10257.
- Hirotsu, M, Sai, K., Nagai, R., Hirotsu, S., Takayanagi, H., Yoshikawa, T., **2002c**. Blazeispirane and protoblazeispirane derivatives from the cultured mycelia of the fungus *Agaricus blazei*. *Phytochemistry* **61**, 589–595.

- Hitzerd, S.M., Verbrugge, S.E., Ossenkoppele, G., Jansen, G., Peters, G.J., **2014**. Positioning of aminopeptidase inhibitors in next generation cancer therapy. *Amino. Acids*. **46**, 793-808.
- Houbraken, J., Frisvad, J.C., Samson, R.A., **2011**. Fleming's penicillin producing strain is not *Penicillium chrysogenum* but *P. rubens*. *IMA Fungus* **2**, 87–95.
- Hoye, T.R., Jeffrey, C.S., Shao, F., **2007**. Mosher ester analysis for the determination of absolute configuration of stereogenic (chiral) carbinol carbons. *Nat. Protoc.* **2**, 2451.
- Hyde, K.D., Xu, J., Rapior, S., Jeewon, R., Lumyong, S., Niego, A.G.T., Abeywickrama, P.D., Aluthmuhandiram, J.V.S., Brahamaanage, R.S., Brooks, S., Chaiyasen, A., Chethana, K.W.T., Chomnunti, P., Chepkirui, C., Chuankid, B., de Silva, N.I., Doilom, M., Faulds, C., Gentekaki, E., Gopalan, V., Kakumyan, P., Harishchandra, D., Hemachandran, H., Hongsanan, S., Karunarathna, A., Karunarathna, S.C., Khan, S., Kumla, J., Jayawardena, R.S., Liu, J.K., Liu, N., Luangharn, T., Macabeo, A.P.G., Marasinghe, D.S., Meeks, D., Mortimer, P.E., Mueller, P., Nadir, S., Nataraja, K.N., Nontachaiyapoom, S., O'Brien, M., Penkhrue, W., Phukhamsakda, C., Ramanan, U.S., Rathnayaka, A.R., Sadaba, R.B., Sandargo, B., Samarakoon, B.C., Tennakoon, D.S., Siva, R., Sriprom, W., Suryanarayanan, T.S., Sujarit, K., Suwannarach, N., Suwunwong, T., Thongbai, B., Thongklang, N., Wei, D., Wijesinghe, S.N., Winiski, J., Yan, J., Yasanthika, E., Stadler, M., **2019**. The amazing potential of fungi: 50 ways we can exploit fungi industrially. *Fungal Divers.* **97**, 1-136.
- Isaka, M., Sappan, M., Supothina, S., Srichomthong, K., Komwijit, S., Boonpratuang, T., **2017**. Alliaceane sesquiterpenoids from submerged cultures of the basidiomycete *Inonotus* sp. BCC 22670. *Phytochemistry* **136**, 175–181.
- Isaka, M., Yangchum, A., Supothina, S., Boonpratuang, T., Choeyklin, R., Kongsaree, P., Prabpai, S., **2015**. Aromadendrane and cyclofarnesane sesquiterpenoids from cultures of the basidiomycete *Inonotus* sp. BCC 23706. *Phytochemistry* **118**, 94–101.
- Ishii, H., Fraaije, B.A., Sugiyama, T., Noguchi, K., Nishimura, K., Takeda, T., Amano, T., Hollomon, D.W., **2001**. Occurrence and molecular characterization of strobilurin resistance in cucumber powdery mildew and downy mildew. *Phytopathology* **91**, 1166–1171.
- Jacobsson, S., Paukner, S., Golparian, D., Jensen, J.S., Unemo, M., **2017**. *In vitro* activity of the novel pleuromutilin lefamulin (BC-3781) and effect of efflux pump inactivation on multidrug-resistant and extensively drug-resistant *Neisseria gonorrhoeae*. *Antimicrob. Agents. Chemother.* **61**, e01497-17.
- Jamal, M., Ahmad, W., Andleeb, S., Jalil, F., Imran, M., Nawaz, M.A., Hussain, T., Ali, M., Rafiq, M., Kamil, M.A., **2018**. Bacterial biofilm and associated infections. *J. Chinese. Med. Assoc.* **81**, 7-11.
- Jennewein, S., Engels, B., Grothe, T., Stadler, M., **2013**. Protoilludene synthase. US20130204034A1.
- Johnson, A.P., **2011**. Methicillin-resistant *Staphylococcus aureus*: The European landscape. *J. Antimicrob. Chemother.* **66**, iv43–iv48.
- Johnson, A.P., **2001**. Telithromycin. Aventis pharma. *Curr. Opin. Investig. drugs* **2**, 1691–1701.
- Jones, D., Metzger, H.J., Schatz, A., Waksman, S.A., **1944**. Control of gram-negative bacteria in experimental animals by streptomycin. *Science*. **100**, 103–105.
- Jones, R.N., Biedenbach, D.J., **1997**. Antimicrobial activity of RU-66647, a new ketolide. *Diagn. Microbiol. Infect. Dis.* **27**, 7–12.
- Jong, S.C., Birmingham, J.M., **1992**. Medicinal benefits of the mushroom *Ganoderma*. *Adv. Appl. Microbiol.* **37**, 101–134.

- Kang, H.-S., Kim, J.-P., **2016**. Ostalactones A–C, β - and ϵ -lactones with lipase inhibitory activity from the cultured basidiomycete *Stereum ostrea*. *J. Nat. Prod.* **79**, 3148–3151.
- Karwehl, S., Stadler, M., **2016**. Exploitation of fungal biodiversity for discovery of novel antibiotics. *Curr. Top. Microbiol. Immunol.* **398**, 303–338.
- Kavanagh, F., Hervey, A., Robbins, W.J., **1952**. Antibiotic substances from basidiomycetes: IX. *Drosophila subatrata* (Batsch Ex Fr.) Quel. *Proc. Natl. Acad. Sci.* **38**, 555–560.
- Kavanagh, F., Hervey, A., Robbins, W.J., **1951**. Antibiotic substances from basidiomycetes: VIII. *Pleurotus Multilus* (Fr.) Sacc. and *Pleurotus Passeckerianus* Pilat. *Proc. Natl. Acad. Sci.* **37**, 570–574.
- Kawagishi, H., Akachi, T., Ogawa, T., Masuda, K., Yamaguchi, K., Yazawa, K., Takahashi, M., **2006a**. Chaxine A, an osteoclast-forming suppressing substance, from the mushroom *Agrocybe chaxingu*. *Heterocycles* **69**, 253–258.
- Kawagishi, H., Masui, A., Tokuyama, S., Nakamura, T., **2006b**. Erinacines J and K from the mycelia of *Hericium erinaceum*. *Tetrahedron* **62**, 8463–8466.
- Kawagishi, H., Shimada, A., Shirai, R., Okamoto, K., Ojima, F., Sakamoto, H., Ishiguro, Y., Furukawa, S., **1994**. Erinacines A, B and C, strong stimulators of nerve growth factor (NGF)-synthesis, from the mycelia of *Hericium erinaceum*. *Tetrahedron Lett.* **35**, 1569–1572.
- Khalidi, N., Seifuddin, F.T., Turner, G., Haft, D., Nierman, W.C., Wolfe, K.H., Fedorova, N.D., **2010**. SMURF: Genomic mapping of fungal secondary metabolite clusters. *Fungal Genet. Biol.* **47**, 736–741.
- Khatoun, Z., McTiernan, C.D., Suuronen, E.J., Mah, T.-F., Alarcon, E.I., Alarcon Bacterial, E.I., **2018**. Bacterial biofilm formation on implantable devices and approaches to its treatment and prevention. *Heliyon* **4**, e01067.
- Kinder, F.R., Bair, K.W., **1994**. Total synthesis of (\pm)-illudin M. *J. Org. Chem.* **59**, 6965–6967.
- Kobayashi, Y., Ino, C., Hirotsu, M., **2010**. Oral cavity composition containing *Phellinus linteus*-derived sesquiterpene derivatives. JP20100475.
- Kuephadungphan, W., Macabeo, A.P.G., Luangsa-ard, J.J., Tasanathai, K., Thanakitpipattana, D., Phongpaichit, S., Yuyama, K., Stadler, M., **2019**. Studies on the biologically active secondary metabolites of the new spider parasitic fungus *Gibellula gamsii*. *Mycol. Prog.* **18**, 135–146.
- Kumarasamy, K.K., Toleman, M.A., Walsh, T.R., Bagaria, J., Butt, F., Balakrishnan, R., Chaudhary, U., Doumith, M., Giske, C.G., Irfan, S., Krishnan, P., Kumar, A. V., Maharjan, S., Mushtaq, S., Noorie, T., Paterson, D.L., Pearson, A., Perry, C., Pike, R., Rao, B., Ray, U., Sarma, J.B., Sharma, M., Sheridan, E., Thirunarayan, M.A., Turton, J., Upadhyay, S., Warner, M., Welfare, W., Livermore, D.M., Woodford, N., **2010**. Emergence of a new antibiotic resistance mechanism in India, Pakistan, and the UK: A molecular, biological, and epidemiological study. *Lancet. Infect. Dis.* **10**, 597–602.
- Lan, N., Perlatti, B., Kvitek, D.J., Wiemann, P., Harvey, C.J.B., Frisvad, J., An, Z., Bills, G.F., **2020**. Acrophiarin (antibiotic S31794/F-1) from *Penicillium arenicola* shares biosynthetic features with both *Aspergillus* - and *Leotiomyces* -type echinocandins. *Environ. Microbiol.* 1–20.
- Lazarus, C.M., Williams, K., Bailey, A.M., **2014**. Reconstructing fungal natural product biosynthetic pathways. *Nat. Prod. Rep.* **31**, 1339–1347.
- Lee, I.K., Jeong, C.Y., Cho, S.M., Yun, B.S., Kim, Y.S., Yu, S.H., Koshino, H., Yoo, I.D., **1996**. Illudins C2 and C3, new illudin C derivatives from *Coprinus atramentarius* ASI20013. *J. Antibiot. (Tokyo)*. **49**, 821–2.

- Li, B., Webster, T.J., **2018**. Bacteria Antibiotic Resistance: New challenges and opportunities for implant-associated orthopaedic infections HHS public access. *J Orthop Res* **36**, 22–32.
- Liermann, J.C., Opatz, T., Kolshorn, H., Antelo, L., Hof, C., Anke, H., **2009**. Omphalotins E-I, five oxidatively modified nematocidal cyclopeptides from *Omphalotus olearius*. *European J. Org. Chem.* **2009**, 1256–1262.
- Liermann, J.C., Schüffler, A., Wollinsky, B., Birnbacher, J., Kolshorn, H., Anke, T., Opatz, T., **2010**. Hirsutane-type sesquiterpenes with uncommon modifications from three basidiomycetes. *J. Org. Chem.* **75**, 2955–2961.
- Lin, H.C., Hewage, R.T., Lu, Y.C., Chooi, Y.H., **2019**. Biosynthesis of bioactive natural products from Basidiomycota. *Org. Biomol. Chem.* **17**, 1027–1036.
- Liu, J., Shimizu, K., Tanaka, A., Shinobu, W., Ohnuki, K., Nakamura, T., Kondo, R., **2012**. Target proteins of ganoderic acid DM provides clues to various pharmacological mechanisms. *Sci. Rep.* **2**, 905.
- Lohmann, J.S., von Nussbaum, M., Brandt, W., Mülbradt, J., Steglich, W., Spiteller, P., **2018**. Rosellin A and B, two red diketopiperazine alkaloids from the mushroom *Mycena rosella*. *Tetrahedron* **74**, 5113–5118.
- Long, K.S., Hansen, L.H., Jakobsen, L., Vester, B., **2006**. Interaction of pleuromutilin derivatives with the ribosomal peptidyl transferase center. *Antimicrob. Agents Chemother.* **50**, 1458–1462.
- Lushniak, B.D., **2014**. Antibiotic resistance: a public health crisis. *Public Health Rep.* **129**, 314–316.
- Mathé, G., **1991**. Bestatin, an aminopeptidase inhibitor with a multi-pharmacological function. *Biomed. Pharmacother.* **45**, 49–54.
- Mayer, A., Kilian, M., Hoster, B., Sterner, O., Anke, H., **1999**. *In-vitro* and *in-vivo* nematocidal activities of the cyclic dodecapeptide omphalotin A. *Pestic. Sci.* **55**, 27–30.
- Mcguire, J.M., Bunch, R.L., Anderson, R.C., Boaz, H.E., Flynn, E.H., Powell, H.M., Smith, J.W., **1952**. Ilotycin, a new antibiotic. *Antibiot. Chemother.* **2**, 281–283.
- McMorris, T.C., Anchel, M., **1965**. Fungal metabolites. The structures of the novel sesquiterpenoids illudin-S and -M. *J. Am. Chem. Soc.* **87**, 1594–1600.
- McMorris, T.C., Anchel, M., **1963**. The structures of the basidiomycete metabolites illudin S and illudin M. *J. Am. Chem. Soc.* **85**, 831–832.
- McMorris, T.C., Kelner, M.J., Wang, W., Estes, L.A., Montoya, M.A., Taetle, R., **1992**. Structure-activity relationships of illudins: analogs with improved therapeutic index. *J. Org. Chem.* **57**, 6876–6883.
- McMorris, T.C., Kelner, M.J., Wang, W., Yu, J., Estes, L.A., Taetle, R., **1996**. (Hydroxymethyl) acylfulvene: an illudin derivative with superior antitumor properties. *J. Nat. Prod.* **59**, 896–899.
- Moellering, R.C., **2006**. Vancomycin: a 50-year reassessment. *Clin. Infect. Dis.* **42**, S3–S4.
- Mondego, J.M.C., Carazzolle, M.F., Costa, G.G.L., Formighieri, E.F., Parizzi, L.P., Rincones, J., Cotomacci, C., Carraro, D.M., Cunha, A.F., Carrer, H., Vidal, R.O., Estrela, R.C., García, O., Thomazella, D.P.T., de Oliveira, B. V., Pires, A.B.L., Rio, M.C., Araújo, M.R.R., de Moraes, M.H., Castro, L.A.B., Gramacho, K.P., Gonçalves, M.S., Neto, J.P.M., Neto, A.G., Barbosa, L. V., Gultinan, M.J., Bailey, B.A., Meinhardt, L.W., Cascardo, J.C.M., Pereira, G.A.G., **2008**. A genome survey of *Moniliophthora perniciosa* gives new insights into Witches' Broom Disease of cacao. *BMC. Genomics* **9**, 1–25.
- Moore, T.C., Moore, T.C., **1974**. Extraction and bioassay of gibberellins from *Fusarium moniliforme*, in: Research experiences in plant physiology. *Springer Berlin Heidelberg*, 229–245.

- Morisaki, N., Furukawa, J., Kobayashi, H., Iwasaki, S., Nozoe, S., Okuda, S., **1985**. Conversion of 6-protoilludene into illudin-M and -S by *Omphalotus olearius*. *Tetrahedron. Lett.* **26**, 4755–4758.
- Nagy, L.G., Riley, R., Tritt, A., Adam, C., Daum, C., Floudas, D., Sun, H., Yadav, J.S., Pangilinan, J., Larsson, K.H., Matsuura, K., Barry, K., Labutti, K., Kuo, R., Ohm, R.A., Bhattacharya, S.S., Shirouzu, T., Yoshinaga, Y., Martin, F.M., Grigoriev, I. V., Hibbett, D.S., **2016**. Comparative genomics of early-diverging mushroom-forming fungi provides insights into the origins of lignocellulose decay capabilities. *Mol. Biol. Evol.* **33**, 959–970.
- Năstăsă, V., Sunel, V., Dăneț, D., Dăneț, R., **1983**. Experimental study on the antitumoral activity of some N-mustards derivatives of the L-asparagic acid. *Rev. Med. Chir. Soc. Med. Nat. Iasi* **87**, 619–622.
- Newman, D.J., Cragg, G.M., **2020**. Natural products as sources of new drugs over the nearly four decades from 01/1981 to 09/2019. *J. Nat. Prod.* **83**, 770-803.
- Newton, G.G.F., Abraham, E.P., **1955**. Cephalosporin C, a new antibiotic containing sulphur and D- α -aminoadipic acid. *Nature* **175**, 548.
- Nijkamp, F.P., Parnham, M.J., **2011**. Principles of Immunopharmacology, *Basel: Birkh user Verlag*. ISBN 978-3-0346-0136-8.
- Nofiani, R., de Mattos-Shiple, K., Lebe, K.E., Han, L.C., Iqbal, Z., Bailey, A.M., Willis, C.L., Simpson, T.J., Cox, R.J., **2018**. Strobilurin biosynthesis in basidiomycete fungi. *Nat. Commun.* **9**, 1–11.
- Novak, R., **2011**. Are pleuromutilin antibiotics finally fit for human use? *Ann. N. Y. Acad. Sci.* **1241**, 71–81.
- Olson,  ., Aerts, A., Asiegbu, F., Belbahri, L., Bouzid, O., Broberg, A., Canb ack, B., Coutinho, P.M., Cullen, D., Dalman, K., Deflorio, G., van Diepen, L.T.A., Dunand, C., Duplessis, S., Durling, M., Gonthier, P., Grimwood, J., Fossdal, C.G., Hansson, D., Henrissat, B., Hietala, A., Himmelstrand, K., Hoffmeister, D., H ogberg, N., James, T.Y., Karlsson, M., Kohler, A., K ies, U., Lee, Y.H., Lin, Y.C., Lind, M., Lindquist, E., Lombard, V., Lucas, S., Lund en, K., Morin, E., Murat, C., Park, J., Raffaello, T., Rouz e, P., Salamov, A., Schmutz, J., Solheim, H., St ahlberg, J., V el ez, H., de Vries, R.P., Wiebenga, A., Woodward, S., Yakovlev, I., Garbelotto, M., Martin, F., Grigoriev, I. V., Stenlid, J., **2012**. Insight into trade-off between wood decay and parasitism from the genome of a fungal forest pathogen. *New Phytol.* **194**, 1001–1013.
- Otto, A., Porzel, A., Schmidt, J., Brandt, W., Wessjohann, L., Arnold, N., **2016**. Structure and absolute configuration of pseudohygrophorones A 12 and B 12 , alkyl cyclohexenone derivatives from *Hygrophorus abieticola* (Basidiomycetes). *J. Nat. Prod.* **79**, 74–80.
- Paharik, A.E., Horswill, A.R., **2016**. The Staphylococcal biofilm: adhesins, regulation, and host response, in: virulence mechanisms of bacterial pathogens. *ASM. Press.* **4**, 529–566.
- Paukner, S., Riedl, R., **2017**. Pleuromutilins: potent drugs for resistant bugs-mode of action and resistance. *Cold Spring Harb. Perspect. Med.* **7**, 1–16.
- Paukner, S., Sader, H.S., Ivezic-Schoenfeld, Z., Jonesb, R.N., **2013**. Antimicrobial activity of the pleuromutilin antibiotic BC-3781 against bacterial pathogens isolated in the SENTRY antimicrobial surveillance program in 2010. *Antimicrob. Agents Chemother.* **57**, 4489–4495.
- Phukhamsakda, C., Ariyawansa, H.A., Phillips, A.J.L., Wanasinghe, D.N., Bhat, D.J., McKenzie, E.H.C., Singtripop, C., Camporesi, E., Hyde, K.D., **2016**. Additions to *Sporormiaceae*: introducing two novel genera, *Sparticola* and *Forliomyces*, from *Spartium*. *Cryptogam. Mycol.* **37**, 75–97.
- Pimentel, M., **2016**. Review article: Potential mechanisms of action of rifaximin in the management of irritable bowel syndrome with diarrhoea. *Aliment. Pharmacol. Ther.* **43**, 37-49.

- Poigny, S., Guyot, M., Samadi, M., **1998**. One-step synthesis of tyromycin A and analogues. *J. Org. Chem.* **63**, 1342–1343.
- Popják, G., Cornforth, J.W., **1966**. Substrate stereochemistry in squalene biosynthesis: The first Ciba medal lecture. *Biochem. J.* **101**, 553.b4-568.
- Prince, W.T., Ivezic-Schoenfeld, Z., Lell, C., Tack, K.J., Novak, R., Obermayr, F., Talbot, G.H., **2013**. Phase II clinical study of BC-3781, a pleuromutilin antibiotic, in treatment of patients with acute bacterial skin and skin structure infections. *Antimicrob. Agents Chemother.* **57**, 2087–2094.
- Ramm, S., Krawczyk, B., Mühlenweg, A., Poch, A., Mösker, E., Süßmuth, R.D., **2017**. A self-sacrificing *N*-methyltransferase is the precursor of the fungal natural product omphalotin. *Angew. Chemie Int. Ed.* **56**, 9994–9997.
- Read, A.F., Woods, R.J., **2014**. Antibiotic resistance management. *Evol. Med. Public Heal.* **2014**, 147.
- Reddell, P., Gordon, V., **2000**. “Lessons from nature”: can ecology provide new leads in the search for novel bioactive chemicals from tropical rainforests? *Roy. Soc. Chem.* 205–212.
- Reynolds, D.R., Taylor, J.W., **1993**. The fungal holomorph: mitotic, meiotic and pleomorphic speciation in fungal systematic. *CAB Int.* ISBN-13: 978-0851988658.
- Reynolds, H.T., Vijayakumar, V., Gluck-Thaler, E., Korotkin, H.B., Matheny, P.B., Slot, J.C., **2018**. Horizontal gene cluster transfer increased hallucinogenic mushroom diversity. *Evol. Lett.* **2**, 88–101.
- Richter, C., Helaly, S.E., Thongbai, B., Hyde, K.D., Stadler, M., **2016**. Pyristriatins A and B: pyridino-cyathane antibiotics from the basidiomycete *Cyathus cf. striatus*. *J. Nat. Prod.* **79**, 1684–1688.
- Richter, C., Wittstein, K., Kirk, P.M., Stadler, M., **2015**. An assessment of the taxonomy and chemotaxonomy of *Ganoderma*. *Fungal Divers.* **71**, 1–15.
- Riley, R., Salamov, A.A., Brown, D.W., Nagy, L.G., Floudas, D., Held, B.W., Levasseur, A., Lombard, V., Morin, E., Otiillar, R., Lindquist, E.A., Sun, H., LaButti, K.M., Schmutz, J., Jabbour, D., Luo, H., Baker, S.E., Pisabarro, A.G., Walton, J.D., Blanchette, R.A., Henrissat, B., Martin, F., Cullen, D., Hibbett, D.S., Grigoriev, I. V., **2014**. Extensive sampling of basidiomycete genomes demonstrates inadequacy of the white-rot/brown-rot paradigm for wood decay fungi. *Proc. Natl. Acad. Sci. U. S. A.* **111**, 9923–9928.
- Rimondini, L., Cochis, A., Varoni, E., Azzimonti, B., Carrassi, A., **2016**. Biofilm formation on implants and prosthetic dental materials, in: Handbook of bioceramics and biocomposites. *Springer. Cham.* 991–1027.
- Ritchie, H., **2018**. How many people in the world die from cancer? *Our World Data.* (<https://ourworldindata.org/how-many-people-in-the-world-die-from-cancer>)
- Röttig, M., Medema, M.H., Blin, K., Weber, T., Rausch, C., Kohlbacher, O., **2011**. NRPSpredictor2—a web server for predicting NRPS adenylation domain specificity. *Nucleic. Acids. Res.* **39**, W362–W367.
- Rupcic, Z., Chepkirui, C., Hernández-Restrepo, M., Crous, P., Luangsa-ard, J., Stadler, M., **2018**. New nematicidal and antimicrobial secondary metabolites from a new species in the new genus, *Pseudobambusicola thailandica*. *MycoKeys* **33**, 1–23.
- Sader, H.S., Biedenbach, D.J., Paukner, S., Ivezic-Schoenfeld, Z., Jonesa, R.N., **2012**. Antimicrobial activity of the investigational pleuromutilin compound BC-3781 tested against gram-positive organisms commonly associated with acute bacterial skin and skin structure infections. *Antimicrob. Agents Chemother.* **56**, 1619–1623.

- Sandargo, B., Chepkirui, C., Cheng, T., Chaverra-Muñoz, L., Thongbai, B., Stadler, M., Hüttel, S., **2019a**. Biological and chemical diversity go hand in hand: Basidiomycota as source of new pharmaceuticals and agrochemicals. *Biotechnol. Adv.* **37**, 107344.
- Sandargo, B., Michehl, M., Praditya, D., Steinmann, E., Stadler, M., Surup, F., **2019b**. Antiviral meroterpenoid rhodatin and sesquiterpenoids rhodocoranes A-E from the wrinkled peach mushroom, *Rhodotus palmatus*. *Org. Lett.* **21**, 3286–3289.
- Sasaki, T., Takagi, M., Yaguchi, T., Miyadoh, S., Okada, T., Koyama, M., **1992**. A new anthelmintic cyclodepsipeptide, PF1022A. *J. Antibiot. (Tokyo)*. **45**, 692–697.
- Sauter, H., Steglich, W., Anke, T., **1999**. Strobilurins: evolution of a new class of active substances. *Angew. Chemie Int. Ed.* **38**, 1328–1349.
- Schatz, A., Bugle, E., Waksman, S.A., **1944**. Streptomycin, a substance exhibiting antibiotic activity against Gram-positive and Gram-negative bacteria. *Exp. Biol. Med.* **55**, 66–69.
- Schilder, R.J., Blessing, J.A., Shahin, M.S., Miller, D.S., Tewari, K.S., Muller, C.Y., Warshal, D.P., McMeekin, S., Rotmensch, J., **2010**. A phase 2 evaluation of irifulven as second-line treatment of recurrent or persistent intermediately platinum-sensitive ovarian or primary peritoneal cancer: A gynecologic oncology group trial. *Int. J. Gynecol. Cancer.* **20**, 1137-1141.
- Schobert, R., Knauer, S., Seibt, S., Biersack, B., **2011**. Anticancer active illudins: recent developments of a potent alkylating compound class. *Curr. Med. Chem.* **18**, 790–807.
- Schöffler, A., **2018**. Secondary metabolites of basidiomycetes. *Physiol. Genet.* 231–275.
- Semeiks, J., Borek, D., Otwinowski, Z., Grishin, N. V., **2014**. Comparative genome sequencing reveals chemotype-specific gene clusters in the toxigenic black mold *Stachybotrys*. *BMC Genomics* **15**, 590.
- Sengupta, S., Chattopadhyay, M.K., Grossart, H.P., **2013**. The multifaceted roles of antibiotics and antibiotic resistance in nature. *Front. Microbiol.* **4**, 47.
- Sensi, P., **1983**. History of the development of rifampin. *Rev. Infect. Dis.* **5**, S402–S406.
- Sensi, P., Margalith, P., Timbal, M.T., **1959**. Rifomycin, a new antibiotic; preliminary report. *Farm. Sci* **14**, 146–147.
- Serio, A.W., Keepers, T., Andrews, L., Krause, K.M., **2018**. Aminoglycoside Revival: review of a historically important class of antimicrobials undergoing rejuvenation. *EcoSal Plus.* **8**, 1–20.
- Singer, R., **1959**. Type studies on Agarics IV. 1). 133-151.
- Singh, R., Williams, J., Vince, R., **2017**. Puromycin based inhibitors of aminopeptidases for the potential treatment of hematologic malignancies. *Eur. J. Med. Chem.* **139**, 325–336.
- Singh, R.K., Kumar, S., Prasad, D.N., Bhardwaj, T.R., **2018**. Therapeutic journey of nitrogen mustard as alkylating anticancer agents: Historic to future perspectives. *Eur. J. Med. Chem.* **151**, 401-433.
- Sipos, G., Prasanna, A.N., Walter, M.C., O'Connor, E., Bálint, B., Krizsán, K., Kiss, B., Hess, J., Varga, T., Slot, J., Riley, R., Bóka, B., Rigling, D., Barry, K., Lee, J., Mihaltcheva, S., LaButti, K., Lipzen, A., Waldron, R., Moloney, N.M., Sperisen, C., Kredics, L., Vágvölgyi, C., Patrignani, A., Fitzpatrick, D., Nagy, I., Doyle, S., Anderson, J.B., Grigoriev, I. V., Güldener, U., Münsterkötter, M., Nagy, L.G., **2017**. Genome expansion and lineage-specific genetic innovations in the forest pathogenic fungi *Armillaria*. *Nat. Ecol. Evol.* **1**, 1931–1941.
- Spellberg, B., Gilbert, D.N., **2014**. The future of antibiotics and resistance: a tribute to a career of leadership by John Bartlett. *Clin. Infect. Dis.* **59**, S71–S75.

- Srinivasan, A., Dick, J.D., Perl, T.M., **2002**. Vancomycin resistance in *Staphylococci*. *Clin. Microbiol. Rev.* **15**, 430–438.
- Stadler, M., Hoffmeister, D., **2015**. Fungal natural products-the mushroom perspective. *Front. Microbiol.* **6**, 1–4.
- Stadler, M., Mayer, A., Anke, H., Sterner, O., **1994**. Fatty acids and other compounds with nematocidal activity from cultures of basidiomycetes. *Planta Med.* **60**, 128–132.
- Stajich, J.E., Harris, T., Brunk, B.P., Brestelli, J., Fischer, S., Harb, O.S., Kissinger, J.C., Li, W., Nayak, V., Pinney, D.F., Stoeckert, C.J., Roos, D.S., **2012**. FungiDB: an integrated functional genomics database for fungi. *Nucleic Acids Res.* **40**, D675–D681.
- Stamatakis, A., **2014**. RAxML version 8: a tool for phylogenetic analysis and post-analysis of large phylogenies. *Bioinformatics* **30**, 1312–1313.
- Sterner, O., Etzel, W., Mayer, A., Anke, H., **1997**. Omphalotin, a new cyclic peptide with potent nematocidal activity from *Omphalotus olearius*. II. Isolation and structure determination. *Nat. Prod. Lett.* **10**, 33–38.
- Suzuki, H., MacDonald, J., Syed, K., Salamov, A., Hori, C., Aerts, A., Henrissat, B., Wiebenga, A., VanKuyk, P.A., Barry, K., Lindquist, E., LaButti, K., Lapidus, A., Lucas, S., Coutinho, P., Gong, Y., Samejima, M., Mahadevan, R., Abou-Zaid, M., de Vries, R.P., Igarashi, K., Yadav, J.S., Grigoriev, I. V., Master, E.R., **2012**. Comparative genomics of the white-rot fungi, *Phanerochaete carnosae* and *P. chrysosporium*, to elucidate the genetic basis of the distinct wood types they colonize. *BMC Genomics* **13**, 444.
- Sweet, E.S., Standish, L.J., Goff, B.A., Andersen, M.R., **2013**. Adverse events associated with complementary and alternative medicine use in ovarian cancer patients. *Integr. Cancer Ther.* **12**, 508–516.
- Taetle, R., Jones, O.W., Honeysett, J.M., Abramson, I., Bradshaw, C., Reid, S., **1987**. Use of nude mouse xenografts as preclinical screens. Characterization of xenograft-derived melanoma cell lines. *Cancer* **60**, 1836–41.
- Tanasova, M., Sturla, S.J., **2012**. Chemistry and biology of acylfulvenes: sesquiterpene-derived antitumor agents. *Chem. Rev.* **112**, 3578–3610.
- Tang, W., Liu, J.W., Zhao, W.M., Wei, D.Z., Zhong, J.J., **2006**. Ganoderic acid T from *Ganoderma lucidum* mycelia induces mitochondria mediated apoptosis in lung cancer cells. *Life Sci.* **80**, 205–211.
- Thomson, A.W., Whiting, P.H., Simpson, J.G., **1984**. Cyclosporine: immunology, toxicity and pharmacology in experimental animals. *Agents Actions* **15**, 306–327.
- Thongbai, B., Rapior, S., Hyde, K.D., Wittstein, K., Stadler, M., **2015**. *Hericium erinaceus*, an amazing medicinal mushroom. *Mycol. Prog.* **14**, 1–23.
- Thongklang, N., Thongbai, B., Chamyuang, S., Callac, P., Chukeatirote, E., Hyde, K.D., Wittstein, K., Stadler, M., **2017**. Blazeispirol A, a chemotaxonomic marker from mycelia of the medicinal mushroom *Agaricus subrufescens*. *Chiang Mai J. Sci.* **44**, 298–308.
- Twentyman, P.R., Luscombe, M., **1987**. A study of some variables in a tetrazolium dye (MTT) based assay for cell growth and chemosensitivity. *Br. J. Cancer* **56**, 279–285.
- Vaghefi, N., Hay, F.S., Kikkert, J.R., Pethybridge, S.J., **2016**. Genotypic diversity and resistance to azoxystrobin of cercospora beticola on processing table beet in New York. *Plant Dis.* **100**, 1466–1473.

- Van Der Velden, N.S., Kälin, N., Helf, M.J., Piel, J., Freeman, M.F., Künzler, M., **2017**. Autocatalytic backbone *N*-methylation in a family of ribosomal peptide natural products. *Nat. Chem. Biol.* **13**, 833–835.
- Varga, T., Krizsán, K., Földi, C., Dima, B., Sánchez-García, M., Sánchez-Ramírez, S., Szöllösi, G.J., Szarkándi, J.G., Papp, V., Albert, L., Andreopoulos, W., Angelini, C., Antonín, V., Barry, K.W., Bougher, N.L., Buchanan, P., Buyck, B., Bense, V., Catcheside, P., Chovatia, M., Cooper, J., Dämon, W., Desjardin, D., Finy, P., Geml, J., Haridas, S., Hughes, K., Justo, A., Karasiński, D., Kautmanova, I., Kiss, B., Kocsubé, S., Kotiranta, H., LaButti, K.M., Lechner, B.E., Liimatainen, K., Lipzen, A., Lukács, Z., Mihaltcheva, S., Morgado, L.N., Niskanen, T., Noordeloos, M.E., Ohm, R.A., Ortiz-Santana, B., Ovrebo, C., Rácz, N., Riley, R., Savchenko, A., Shiryayev, A., Soop, K., Spirin, V., Szebenyi, C., Tomšovský, M., Tulloss, R.E., Uehling, J., Grigoriev, I. V., Vágvölgyi, C., Papp, T., Martin, F.M., Miettinen, O., Hibbett, D.S., Nagy, L.G., **2019**. Megaphylogeny resolves global patterns of mushroom evolution. *Nat. Ecol. Evol.* **3**, 668–678.
- Vásquez, R., Rios, N., Solano, G., Cubilla-Rios, L., **2018**. Lentinoids A–D, new natural products isolated from *Lentinus strigellus*. *Molecules* **23**, 773.
- Vernon, G., **2019**. Syphilis and Salvarsan. *Br. J. Gen. Pract.* **69**, 246.
- Vilgalys, R., Hester, M., **1990**. Rapid genetic identification and mapping of enzymatically amplified ribosomal DNA from several *Cryptococcus* species. *J. Bacteriol.* **172**, 4238–4246.
- Wasser, S.P., Weis, A.L., **1999**. Therapeutic effects of substances occurring in higher basidiomycetes mushrooms: a modern perspective. *Crit. Rev. Immunol.* **19**, 32.
- Wawrzyn, G.T., Quin, M.B., Choudhary, S., López-Gallego, F., Schmidt-Dannert, C., **2012**. Draft genome of *Omphalotus olearius* provides a predictive framework for sesquiterpenoid natural product biosynthesis in basidiomycota. *Chem. Biol.* **19**, 772–783.
- Weber, W., Semar, M., Anke, T., Bross, M., Steglich, W., **1992**. Tyromycin A: a novel inhibitor of leucine and cysteine aminopeptidases from *Tyromyces lacteus*. *Planta Med.* **58**, 56–59.
- Weinstein, M.J., Luedemann, G.M., Oden, E.M., Wagman, G.H., Rosselet, J.P., Marquez, J.A., Coniglio, C.T., Charney, W., Herzog, H.L., Black, J., **1963**. Gentamicin, a new antibiotic complex from *Micromonospora*. *J. Med. Chem.* **6**, 463–464.
- White, T.J., Bruns, T., Lee, S., Taylor, J., **1990**. Amplification and direct sequencing of fungal ribosomal RNA genes for phylogenetics. *PCR Protoc.* **2**, 315–322.
- Wittstein, K., Cordsmeier, A., Lambert, C., Wendt, L., Sir, E.B., Weber, J., Wurzler, N., Petrini, L.E., Stadler, M., **2020**. Identification of *Rosellinia* species as producers of cyclodepsipeptide PF1022 A and resurrection of the genus *Dematophora* as inferred from polythetic taxonomy. *Stud. Mycol.* **96**, 1–16.
- Wittstein, K., Rascher, M., Rupcic, Z., Löwen, E., Winter, B., Köster, R.W., Stadler, M., **2016**. Corallocins A–C, nerve growth and brain-derived neurotrophic factor inducing metabolites from the mushroom *Hericium coralloides*. *J. Nat. Prod.* **79**, 2264–2269.
- Wu, J.C., **1994**. Mycophenolate mofetil: molecular mechanisms of action. *Perspect. Drug Discov. Des.* **2**, 185–204.
- Wu, S., Dai, Y., Hattori, T., Yu, T., Wang, D., Parmasto, E., Chang, H., Shih, S., **2012**. Species clarification for the medicinally valuable “*Sanghuang*” mushroom. *Bot. Stud.* **53**, 135–149.
- Yamane, M., Minami, A., Liu, C., Ozaki, T., Takeuchi, I., Tsukagoshi, T., Tokiwano, T., Gomi, K., Oikawa, H., **2017**. Biosynthetic machinery of diterpene pleuromutilin isolated from basidiomycete fungi. *ChemBioChem* **18**, 2317–2322.
- Yang, J., Wang, N., Yuan, H.S., Hu, J.C., Dai, Y.C., **2013**. A new sesquiterpene from the medicinal fungus *Inonotus vaninii*. *Chem. Nat. Compd.* **49**, 261–263.

- Yi, Y., Fu, Y., Dong, P., Qin, W., Liu, Y., Liang, J., Shang, R., **2017**. Synthesis and biological activity evaluation of novel heterocyclic pleuromutilin derivatives. *Molecules* **22**, 996.
- Yuyama, K.T., Wendt, L., Surup, F., Kretz, R., Chepkirui, C., Wittstein, K., Boonlarpradab, C., Wongkanoun, S., Luangsa-Ard, J., Stadler, M., Abraham, W.R., **2018**. Cytochalasins act as inhibitors of biofilm formation of *Staphylococcus aureus*. *Biomolecules* **8**, 1–13.
- Zhanel, G.G., Walters, M., Noreddin, A., Vercaigne, L.M., Wierzbowski, A., Embil, J.M., Gin, A.S., Douthwaite, S., Hoban, D.J., **2002**. The ketolides: A critical review. *Drugs*. **62**, 1771-1804.
- Zhang, J.J., Yamanaka, K., Tang, X., Moore, B.S., **2019**. Direct cloning and heterologous expression of natural product biosynthetic gene clusters by transformation-associated recombination. *Methods. Enzymol.* **621**, 87–110.
- Zhao, Y., Shadrack, W.R., Wallace, M.J., Wu, Y., Griffith, E.C., Qi, J., Yun, M.K., White, S.W., Lee, R.E., **2016**. Pterin–sulfa conjugates as dihydropteroate synthase inhibitors and antibacterial agents. *Bioorganic Med. Chem. Lett.* **26**, 3950–3954.
- Zhou, L.W., Vlasák, J., Decock, C., Assefa, A., Stenlid, J., Abate, D., Wu, S.H., Dai, Y.C., **2016**. Global diversity and taxonomy of the *Inonotus linteus* complex (Hymenochaetales, Basidiomycota): *Sanghuangporus* gen. nov., *Tropicoporus excentrodendri* and *T. guanacastensis* gen. et spp. nov., and 17 new combinations. *Fungal Divers.* **77**, 335–347.

7. Appendices

Spirodioxynaphthalene derivatives from *Sparticola junci* (MFLUCC 15-0030)

The ascomycete *Sparticola junci* Phukhamsakda, Camporesi & K.D. Hyde represents the ex-type strain of this species, was collected and isolated from a dead branch of *Spartium junci* (Phukhamsakda *et al.*, 2016). Five plugs mycelium from a 20-day old *Sparticola junci* in YMG agar plate were used for preparing seed cultures (500 mL flask containing 200mL YMG media and incubated on a shaker at 23 °C and 140 rpm). After 30 days, the seed cultures were homogenized by using an Ultra Turrax and 10 mL of them were inoculated in each of the 30 × 500 mL flasks with 200mL Q6 ½ medium, all of them incubated in same condition as seed cultures for 21 day. The extraction of supernatant and mycelia yielded 3g of a brown syrup. The purification by preparative HPLC led to the characterization of 7 highly oxygenated and functionalized spirodioxynaphthalene natural products sparticolins A-G **53-59** (**Publication 6, Figure 45**). Among them, Sparticolin B and sparticolin G exhibited inhibitory activity against various Gram-positive bacteria and fungi. All other sparticolins were only weakly active against *Staphylococcus aureus* and also showed weak activities against the nematode *Caenorhabditis elegans*. Sparticolin B and sparticolin G also showed moderate cytotoxic activities against seven mammalian cell lines.

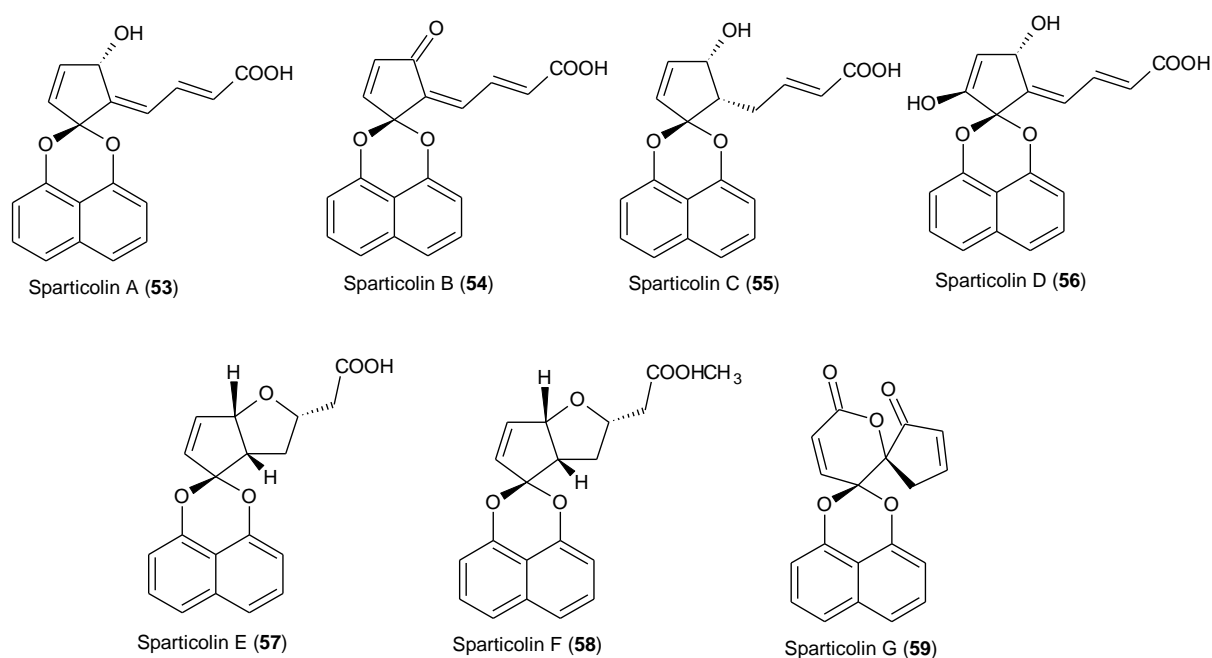


Figure 45. Chemical structures of compounds isolated from *Sparticola junci* (**publication 6**).

Table 17. Basidiomycetes screened in this project

Strain code	Name	bioactivity screening results of extracts from small scale fermentation
MUCL56056	<i>Abortiporus</i> sp. Nov	weak antibacterial and moderate antifungal activity
MUCL56348	<i>Antrodia</i> sp. Nov	weak antifungal activity and potential to inhibit the formation of <i>B. subtilis</i>
MUCL56349	<i>Antrodia</i> sp. Nov	potential to inhibit the formation of <i>B. subtilis</i>
MUCL56350	<i>Antrodia</i> sp. Nov	potential to inhibit the formation of <i>B. subtilis</i>
MUCL56165	<i>Asterostroma</i> sp.	moderate antifungal activity
MUCL56166	<i>Asterostroma</i> sp.	moderate antifungal activity
MUCL55600	<i>Fuscoporia</i> sp.	moderate antifungal activity
MUCL55606	<i>Fuscoporia</i> sp.	weak antibacterial and moderate antifungal activity
MUCL56038	<i>Fuscoporia</i> sp.	moderate antifungal activity
MUCL56351	<i>Gloeophyllum</i> sp.	weak antifungal activity and potential to inhibit the formation of <i>B. subtilis</i>
MUCL56368	<i>Haploporus</i> sp.	no activity
MUCL56369	<i>Haploporus</i> sp.	no activity
MUCL56078	<i>Heimiomyces</i> sp.	strong antibacterial activity
MUCL55557	<i>Lentinus</i> sp.	moderate antifungal activity
MUCL55560	<i>Lentinus</i> sp.	moderate antifungal activity
MUCL55566	<i>Lentinus</i> sp.	moderate antifungal activity
MUCL55578	<i>Lentinus</i> sp.	moderate antifungal activity
MUCL56028	<i>Perenniporia</i> sp.	no activity
MUCL56044	<i>Perenniporia</i> sp.	no activity
MUCL56346	<i>Rigidoporus ulmarius</i>	weak antibacterial and moderate antifungal activity
MUCL56354	<i>Sanghuangporus</i> sp.	moderate antibacterial activity
MUCL56345	<i>Sanghuangporus</i> sp.	weak antibacterial activity
MUCL56347	<i>Sanghuangporus</i> sp.	weak antibacterial activity
MUCL56352	<i>Sanghuangporus</i> sp.	weak antibacterial activity
MUCL55598	<i>Schizoporia</i> sp.	weak antifungal activity
MUCL56036	<i>Schizoporia</i> sp.	weak antifungal activity
MUCL56074	<i>Skeletocutis</i> sp.	strong antibacterial activity

>MUCL56354 ITS nrDNA sequence

GACTGCGGAAGGATTATCGAGCTTTTTGAAAGCGAGACTTGTTGCTGGCGCGTGGAACG
CGCATGTGCACGGTTTTTCGCGCTCAAATCCATCTCTTTAAACCCCGCCTTAACCCGGCCA
AAGTTAGTAGTCTTTTTGGGGTTTGTGGTTTGTAGTAAATCAGTAGAAAGGTGAAATCG
GGTGAGCTTACTTACCCGGTAGTAATCTTTTGAACGTCGAAAGCAAAGGCGAAACGATCT
TCTCCCTATTCCTCCGTTTCGGGCGAAGGCTTTGGCTTGTGTGTGTTATTATACAAACACCT
TTAATTGTCTTTGTGAATGTATTTGCTCCTTGTGGGCGAAAATAAATACAACCTTTCAACAA
CGGATCTCTTGGCTCTCGCATCGATGAAGAACGCAGCGAAATGCGATAAGTAATGTGAAT
TGCAGAATTCAGTGAATCATCGAATCTTTGAACGCACCTTGCGCCCTTGGTATTCCGAG
GGGCATGCCTGTTTGTGAGTGTGATGTTAATCTCAAACCGCTAGTCTTTCTTAATTGAAGGGC
TTTGTGAGTTTGGACTTGGAGGCTTCATTGCTGGCGTGGGGGTTCCCTTTTCGGGAGGACTT
CGTCCGGCTCCTCTTAAATGCATTAGCTGGGCTTTGGCTCGCGTTTACGGTGTAAATAGTTA
ATTCCATTACCAAGGAACGCTTGCCTTACGGGCCTGCTTCTAATCGTCCGCATCGTCGGA
CAAGGAGCTGTTGTTGCTCCTTCTTGACCCCTTTGACTCAAATCAGGTAGGACTACCCGCT
GAACTTAAGCT

>MUCL56074 ITS nrDNA sequence

ATATGCTTAAGTTCAGCGGGTAGTCCTACCCGATTTGAGGTGCAGATGTCAAAGATTAT
TACAATCTGTCTTAAAAGACAACCTAGAAGCGGAATTCATACATGTGCTTAGACAGCTAC
AGCGTAGACAATTATCACACTGAAGCTAGACCTGAGCAAAGATTTCCAGCTAATATATTC
AAGAGGAGCAGATTTTACTAAACCTGCAAAGAGACCTCCAAATCCAAAGCACCAACA
TCATCAAAAAATGAAGAGGGCTTTGAGAATACCATGACACTCAAACGGGCATGCCCTTCG
GAATACCAAAGGGCGCAAGTTGCGTTCAAAGATTCGATGATTCCTGAATTCTGCAATTC
ACATTACTTATCGCATTTCGCTGCGTTCTTCATCGATGCGAGAGCCAAGAGATCCGTTGCT
AAAAGTTATATATAATGCGTTATTTAAGCGCAAGAGACATTCATGATACAGCGTGTGTGA
ATGAAACATAGGAAGGCGTCAACAACCTAGAGAGGAACCTAAGTTCTTCTCCTGTATCAAC
CATCCTACAATATGTGCACAGGTGTTAAAGATGAGTTGGATTTGAGCGAAGCGTGCACAT
GCCCCGAAAGGCCAGCTACAACCTCTTTCAAAGACTCGATAATGATCCTTCCGCAGGTTCC
ACCTACGGAAACCTTGTTACGACTTTTACTTCC

>MUCL56078 ITS nrDNA sequence

GAGGAAGTAAAAGTCGTAACAAGGTTTCCGTAGGTGAACCTGCGGAAGGATCATTATTG
AATTGAAACCGTTGGGCTGTTTGTGCTGGCTCGTCACAGAGCATGTGCACGCTCTTCGACTTC
TCCCAATTTTCCACCTGTGCACCTCTTGTAGTTCCATTGGTGAAAGGGAAGGCGAAACGA
GTAGTCGTCCCTCGAACCTCTGGTCCTATGTCTTTTACACACTATTGTATGTCTAGAATGT
CTTTGTGGGCTTAGCCATAAAACGCGACGCCTTATAAACTTAATACAACCTTTCAACAACG
GATCTCTTGGCTCTCGCATCGATGAAGAACGCAGCGAAATGCGATAAGTAATGTGAATTG
CAGAATTCAGTGAATCATCGAATCTTTGAACGCACCTTGCGCCCTTGGTATTCCGAGGG
GCATGCCTGTTTGTGAGTGCATTAAATTCTCAACTCCTCCGGCTTTTTTTGGGCTGGTTGGG
GCTTGGATGTGAGGGTTTGTGCGGGCCTCTTCTGAGGTGCGCTCCCTTTAAATGCATTAGC
GGAACGTCTTCGTGGACCCCGTGCACCTTGGTGTGATAATTATCTACGCCTCACTGACTTGA
AGCGAAATGGTTCAGCTCTCTAATCGTCTTCGGACAATGACTTGACAATTTGACCTCAAA
TCAGGTAGGACTACCCGCTGAACTTAAGCATATCA

> MUCL56047 ITS nrDNA sequence

TTGAGGCAAGGGTCAAAAATGGTTTAAAGGTAACAGAGTACCTGTCTGACACATAGGCAG
ACTATTGGAAGCAGACAGTCTAAGTAAGCACTGGTGAATATAGATAGAAAACCTATTACA
CCAAACAATGCGAACTACAGTCCAGCTAATGCATTTGAGAGGAGCCGATACAGACAGTA
CCAGCATAACATATTGCCTCCAAGTCCAAGCCCCTTCTTCAATTAAGAAAAAGAGGATTGA
GAATTACATGACACTCAAACAGGCATGCCCTCGGAATACCAAGGGGCGCAAGGTGCGT
TCAAAGATTCGATGATTCCTGAATTCTGCAATTCACATTACTTATCGCATTTTCGCTGCGT
TCTTCATCGATGCGAGAGCCAAGAGATCCGTTGTTGAAAGTTGTATATTTGTATTTTCGCTC

ACAGGAGCATTACACATTCACAGGAACAAGAAAATGTTTGTATAGGTAAAAGTCAAAGT
GTTTCATAGTAAGTAAAGCCAAGAT CATTACTACTGCCAGAAGGGGTACCC

>MUCL55592I5 ITS nrDNA sequence

CATTATCGAGTTTTTTGAAGCGAAGACTTGTTGCTGGCGTGAAAATAAATCTTCGCGCATG
TGCACGGCCTTCGCGCTCAAATCCAACCTCAAACCACCCCTGTGCACCTATATGTCGCGAG
TCGAAGTTAGTAGTCTGAGGTTCTTGTAAGTAATCGGTAGGAAGGCGAAAGCGAGTGGG
AGTAGTCTTACTCGTTAGGTAACCTTTTGAAAATGAAAGCGAGTGCCTCGGGTGAAGACT
CTCGGCTTGTGTTGTTAT

>MUCL55592I3-I4 ITS nrDNA sequence

ATTCAGTGAATCATCGAATCTTTGAACGCACCTTGCGCGCCTTGGTATTCCGAGGGGCAT
GCCTGTTTGAGTGTGCATGTTAATCTCAAACCGCCCGTCTTTTCTTAATTGTGAAGGGCTTG
CGGTTTGGACTTGGAGGGTACTGCCGGCGTCCCTTCCCTTCGAGGGGGGGTTCGGCTCCT
CTTAAATATATTAGCTGGGTTTTGGCTCGCGTTTACGGTGTAATAGTTGATTCCGTTCCACC
AACGAGCGCTTGCCTGACGAGCCTGCTTCTAGTCGTCCGCGTCGTCTGACAAGGAGATAA
AACACCTTGACCTCAAATCA

8. Publications of the thesis

Sesquiterpenes from an Eastern African Medicinal Mushroom Belonging to the Genus *Sanghuangporus*

Tian Cheng,[†] Clara Chepkirui,[†] Cony Decock,[‡] Josphat Clement Matasyoh,[§] and Marc Stadler^{*,†,‡,§}

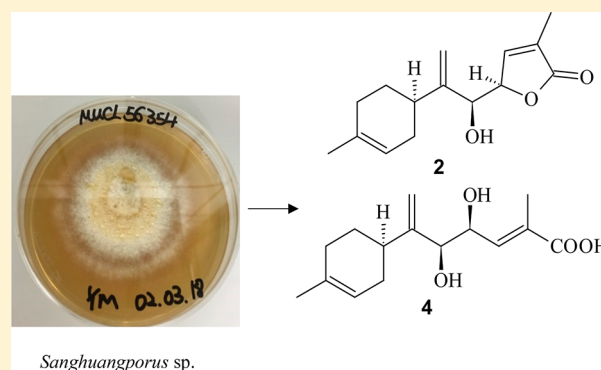
[†]Department of Microbial Drugs, Helmholtz Centre for Infection Research (HZI), and German Centre for Infection Research (DZIF), Partner Site Hannover/Braunschweig, Inhoffenstrasse 7, 38124 Braunschweig, Germany

[‡]Mycothèque de l'Université Catholique de Louvain (BCCM/MUCL), Place Croix du Sud 3, B-1348 Louvain-la-Neuve, Belgium

[§]Department of Chemistry, Faculty of Sciences, Egerton University, P.O. Box 536, 20115, Njoro, Kenya

Supporting Information

ABSTRACT: During the course of searching for new anti-infective and other biologically active secondary metabolites from Kenyan basidiomycetes, 13 previously undescribed metabolites, (6*R*,7*S*,10*R*)-7,10-epoxy-7,11-dimethyldodec-1-ene-6,11-diol (**1**) and 12 sesquiterpenes named elgonenes A–L (**2**–**13**), and the known compound *P*-coumaric acid (**14**) were isolated from a basidiomycete collected in Mount Elgon Natural Reserve. The producing organism represents a new species of the genus *Sanghuangporus*, which is one of the segregates of the important traditional Asian medicinal mushrooms that were formerly known as the “*Inonotus linteus*” complex. The structure elucidation of compounds **1**–**13**, based on 2D NMR spectroscopy, high-resolution mass spectrometry, and other spectral methods, and their antibacterial, antifungal, and cytotoxic activities are reported.



The phylum Basidiomycota comprises the mushroom-forming fungi and various other organisms that represent a considerable part of the global biodiversity. Recent molecular ecology studies have revealed huge diversity of fungi in different habitats, including soil, plants, and invertebrates.¹ Unfortunately, most of these fungi and especially the majority of the species from tropical areas have neither been cultured nor studied for potential beneficial traits such as the production of antibiotics or other useful secondary metabolites.² For the last four years, we have embarked on an extensive study of the secondary metabolites of basidiomycetes collected from Kenya's tropical rain forests, Kakamega and Mount Elgon National Reserves. This study has resulted in the discovery of novel structurally diverse metabolites.^{3–8} The genus *Sanghuangporus* in the family Hymenochaetaceae and the order Hymenochaetales belongs to the group of medicinal mushrooms commonly known as the *Inonotus linteus* complex (also referred to as the *Phellinus linteus* complex). This complex consists of species originally described in the genera *Phellinus* and *Inonotus*, which were eventually transferred to *Inonotus* based on molecular studies.⁹ Although the species of the *I. linteus* complex were placed in the genus *Inonotus*, their perennial basidiomes with a dimittic hyphal system distinguish the complex from other species in the genus. This has led to the segregation of this group to accommodate the *I. linteus* complex in the new genera *Sanghuangporus* and *Tropicoporus*.¹⁰ These medicinal mushrooms have been used as folk medicines in Asian countries for thousands of years, in particular for the

treatment of hemorrhage, hemostasis, and diseases related to menstruation. The species *Phellinus linteus* (*Tropicoporus linteus*) in particular has been used in traditional Chinese medicine because of its therapeutic effects on various ailments including tumor, diabetes, inflammation, and obesity.^{9,11}

The novel phelligrudin L together with the four known sesquiterpenes ionylideneacetic acid, 1*S*-(2*E*)-5-[(1*R*)-2,2-dimethyl-6-methylidenecyclohexyl]-3-methylpent-2-enoic acid, and phellidines D and E were reported previously from a study of *Sanghuangporus* sp. (MUCL55592).⁵ In the study reported here a fungal strain identified as *Sanghuangporus* sp. (MUCL56354) was examined for the production of bioactive metabolites. Herein, we describe the isolation, structure elucidation, and biological evaluation of 13 previously undescribed secondary metabolites (**1**–**13**) and *P*-coumaric acid (**14**).

RESULTS AND DISCUSSION

The strain MUCL 56354 was identified by comparison of morphological characteristics and sequencing of the 5.8S/ITS nrDNA,¹² as described in the **Experimental Section**. A BLAST search in GenBank confirmed the generic affinities of the strain to the genus *Sanghuangporus* in the Hymenochaetaceae by a closest hit to KP030787.1 (*Sanghuangporus microcystideus*) with 96% identity (cf. Figure 109 in the **Supporting**

Received: December 22, 2018

Published: April 19, 2019

Chart 1

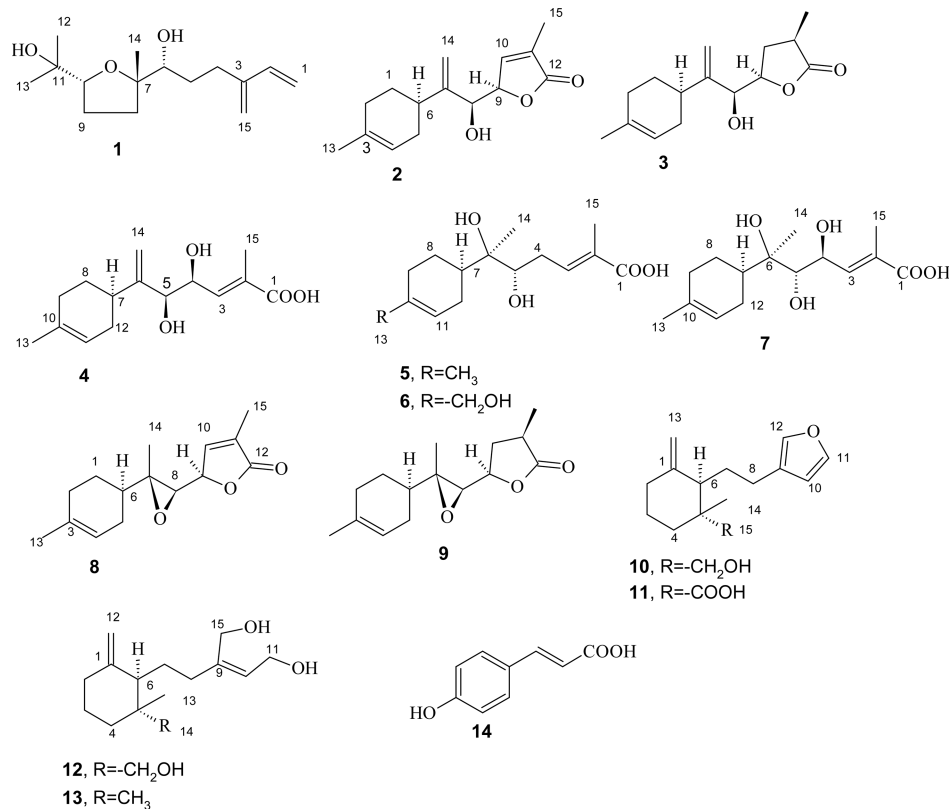


Table 1. NMR Spectroscopic Data for Compound 1 (¹H 700 MHz, ¹³C 175 MHz in Acetone-*d*₆), Compounds 2 and 3 (¹H 700 MHz, ¹³C 175 MHz, in CDCl₃), and Compound 4 (¹H 500 MHz, ¹³C 125 MHz, in CDCl₃)

no.	1		2		3		4	
	¹³ C	¹ H/HSQC	¹³ C	¹ H/HSQC	¹³ C	¹ H/HSQC	¹³ C/DEPT	¹ H/HSQC
1	113.8, CH ₂	5.05, dd (17.64, 1.08) 5.30, dd (17.64, 1.08)	29.4, CH ₂	1.55, m 1.88, m	31.5, CH ₂	2.02, m 2.06, m	170.6, C	
2	139.9, CH	6.39, dd (17.64, 10.76)	30.6, CH ₂	1.99, m 2.07, m	30.6, CH ₂	1.98, m 2.05, m	130.3, C	
3	147.8, C		133.9, C		133.9, C		140.1, CH	6.87, br d (8.82)
4	29.2, CH ₂	a: 2.23, m b: 2.55, m	120.2, CH	5.41, m	120.2, CH	5.40, m	69.9, CH	4.53, dd (8.82, 4.52)
5	31.9, CH ₂	a: 1.42, m b: 1.69, m	31.6, CH ₂	2.05, m 2.12, m	29.4, CH ₂	1.49, m 1.86, m	76.4, CH	4.34, d (4.52)
6	77.2, CH	3.50 dd (17.64)	36.9, CH	2.14, m	36.9, CH	2.05, m	152.7, C	
7	86.9, C		152.1, C		151.1, C		36.8, CH	2.12, m ^a
8	32.7, CH ₂	a: 1.50, m b: 2.12, m	73.3, CH	4.41, d (4.30)	71.9, CH	4.54, br s	29.6, CH ₂	1.49, m 1.84, m
9	27.3, CH ₂	1.87, m 1.97, m	82.3, CH	4.95, m	78.9, CH	4.49, ddd (3.44, 6.29, 9.84)	30.6, CH ₂	1.98, m ^a 2.04, m ^a
10	85.5, CH	3.79, t (7.42)	145.3, CH	7.07, m	29.4, CH ₂	1.95, m 2.20, m	133.7, C	
11	71.7, C		131.7, C		35.5, CH	2.68, m	120.5, CH	5.41, m
12	26.6, CH ₃	1.07, s	173.9, C		179.4, C		31.6, CH ₂	^a 1.99, m ^a 2.08, m
13	27.8, CH ₃	1.20, s	23.4, CH ₃	1.67, s	23.4, CH ₃	1.66, s	23.4, CH ₃	1.66, s
14	23.7, CH ₃	1.11, s	111.4, CH ₂	5.15, br s 5.27, br s	110.8, CH ₂	5.07, s 5.28, s	111.3, CH ₂	5.07, s 5.22, s
15	116.2, CH ₂	a: 5.04, s b: 5.05, s	10.9, CH ₃	1.96, t (1.94)	15.1, CH ₃	1.30, s	13.0, CH ₃	1.92, s

^aPeaks overlapping with other peaks.

Table 2. NMR Spectroscopic Data for Compound 5 (¹H 500 MHz, ¹³C 125 MHz in Acetone-*d*₆), Compound 6, (¹H 500 MHz, ¹³C 125 MHz in Methanol-*d*₄), and Compounds 7–9 (¹H 700 MHz, ¹³C 175 MHz in CDCl₃)

no.	5		6		7		8		9	
	¹³ C/ DEPT	¹ H/HSQC	¹³ C/ DEPT	¹ H/ HSQC	¹³ C/ DEPT	¹ H/HSQC	¹³ C	¹ H/HSQC	¹³ C	¹ H/HSQC
1	169.2, C		171.8, C		171.0, C		24.6, CH ₂	1.48, m 1.88, m	24.5, CH ₂	1.48, m 1.86, m
2	128.9, C		129.9, C		130.3, C		29.8, CH ₂	1.98, m	29.9, CH ₂	1.98, m
3	142.4, CH	6.99, m	142.7, CH	6.98, m	141.5, CH	6.89, dd (8.93, 1.18)	134.1, C		134.1, C	
4	31.8, CH ₂	2.32, m 2.59, m	32.0, CH ₂	2.31, m 2.58, m	69.9, CH	4.73, dd (8.82, 6.45)	119.5, CH	5.35, m	119.6, CH	5.35, m
5	75.2, CH	3.68, dd (2.59, 9.92)	75.6, CH	3.64, m	74.9, CH	3.72, d (6.45)	27.0, CH ₂	1.86, m 2.00, m	27.1, CH ₂	1.86, m 2.05, m
6	75.6, C		76.7, C		77.4, C		41.4, CH	1.40, m	41.6, CH	1.40, m
7	41.3, CH	1.77, m	42.3, CH	1.79, m	40.7, CH	1.74, m	64.2, C		64.1, C	
8	24.6, CH ₂	1.34, m 1.81, m	27.7, CH ₂	1.36, m ^a 1.84, m ^a	23.5, CH ₂	1.35, m 1.81, m	61.1, CH	2.57, d (8.39)	63.1, CH	2.80, d (7.96)
9	31.7, CH ₂	1.93, m	27.7, CH ₂	2.04, m ^a 2.13, m ^a	30.6, CH ₂	1.98, m ^a 2.04, m ^a	78.1, CH	4.63, dt (1.77, 8.50)	75.2, CH	4.17, ddd (5.83, 7.96, 13.55)
10	133.9, C		138.5, C		133.8, C		147.1, CH	7.22, m	35.5, CH ₂	1.88, m 2.64, tt (5.81, 8.60)
11	122.3, CH	5.38, m	123.8, CH	5.67, m	120.5, CH	5.40, m	130.9, C		35.0, CH	2.69, m
12	26.7, CH ₂	2.01, m ^a 2.16, m ^a	26.7, CH ₂	2.04, m ^a 2.20, m ^a	25.6, CH ₂	2.05, m ^a 2.09, m ^a	173.6, C		179.1, C	
13	23.6, CH ₃	1.61, br s	67.4, CH ₂	3.91, s	23.3, CH ₃	1.66, s	23.4, CH ₃	1.64, br s	23.4, CH ₃	1.64, br s
14	19.8, CH ₃	1.16, s	19.2, CH ₃	1.17, s	19.8, CH ₃	1.31, s	13.9, CH ₃	1.38, s	13.9, CH ₃	1.31, s
15	12.8, CH ₃	1.81, d (1.22)	12.9, CH ₃	1.84, s	13.0, CH ₃	1.96, s	10.8, CH ₃	1.97, d (1.72)	15.2, CH ₃	1.33, d (6.88)

^aPeaks overlapping with other peaks.

Information). Further taxonomic studies including comparisons with type specimens of related species are ongoing to characterize this strain to the species level, but it constitutes an undescribed taxon according to the data presently available.

The extracts of the strain (MUCL56354) exhibited activity against *Bacillus subtilis* with an MIC 37.5 µg/mL (compared to the positive control ciprofloxacin at MIC 3.1 µg/mL). Extensive chromatography of the extracts led to the bioactivity-guided isolation of 13 previously undescribed compounds and the known *P*-coumaric acid, the latter of which was identified by comparing its NMR data with those reported in the literature.¹³

Compound **1** was obtained from the supernatant as a yellow oil with the molecular formula C₁₅H₂₆O₃ deduced from the HR-ESIMS data. The ¹³C NMR spectroscopic data of **1** revealed the presence of 15 carbon signals, which were further identified as three methyl, six methylene, three methine, and three nonprotonated carbons (one sp² carbon and two sp³ oxygenated carbons) from the DEPT NMR data. The ¹H NMR spectrum revealed three methyl singlets resonating at δ 1.07 (H₃-12), 1.11 (H₃-14), and 1.20 (H₃-13). A doublet and triplet resonating at δ 3.50 and 3.79 attributed to oxygenated methines were also recorded. HMBC correlations of H₂-1 to C-2/C-3, H₂-15 to C-2/C-4, and H₂-5 to C-3/C-4/C-6/C-7 along with the COSY correlations of H₂-1 to H-2 and H₂-5 to H₂-4/H-6 confirmed the first side chain in the molecule attached at C-7. The methyl protons H₃-14 showed HMBC correlations to C-6/C-7/C-8, while methylene protons H₂-9 correlated with C-7/C-8/C-10/C-11. Cross-peaks were recorded between H₂-8 and H₂-9 in the COSY spectra. The chemical shifts of C-7 (δ 86.9) and C-10 (δ 85.5) and the HMBC correlation of H-10 to C-7 indicated that these carbons

were connected via an oxygen bridge forming the oxolane. The methyl group protons H₃-12 showed HMBC correlations to C-11/C-10/C-13. Based on the molecular formula of **1** and the chemical shift of C-11 (δ 71.7), it was determined that a hydroxy group was attached to this carbon. Cross-peaks were also observed in the ROESY spectra between H₃-14 and H-6/H_b-5/H_a-8, H-6 and H_b-5/H₃-4/H_a-8, and H_a-9 and H₃-8/H-10. The closely related compounds neroplofulol and 7,10-epoxy-3,7,11-trimethyldodec-2-ene-1,6,11-triol have been reported from the plant *Oplopanax horridus* and the actinobacterium *Streptomyces scopuliridis*, respectively.^{14,15} The relative stereochemistry at C-10 for this class of compounds was reported to be significantly impacted by the orientation of 14-Me and the 2-hydroxysopropyl moiety. According to Inui et al.,¹⁴ a chemical shift of C-10 (about δ 85 ppm) indicates the *anti*-orientation of these two substituents because of the *γ*-gauche effect caused by an alkyl substituent at C-6. For the case where the two substituents are in the *syn*-orientation, the C-10 is shifted downfield by around 3.3 ppm. Based on these literature data and the ROESY correlations observed by us, the relative stereochemistry of **1** was assigned as 6*R**, 7*S**, 10*R**. The absolute stereochemistry of **1** was consequently assigned by derivatization with both *R*- and *S*-MTPA chloride to their corresponding *S*- and *R*-MTPA esters.¹⁶ The C-5/C-4 methylene protons gave positive values, while the H₃-14/H₂-8/H₂-9 gave negative values for the Δδ_{SR} = δ(*S*-MTPA ester) – δ(*R*-MTPA ester) (see Table 1 in the Supporting Information). Therefore, the absolute stereochemistry at C-6 was assigned as *R* and the absolute configurations of the other stereocenters were assigned as 7*S* and 10*R*. The structure of **1** was concluded to be (6*R*,7*S*,10*R*)-7,10-epoxy-7,11-dimethyldodec-1-ene-6,11-diol (**1**).

Table 3. NMR Spectroscopic Data for Compound 10 (^1H 500 MHz, ^{13}C 125 MHz in Acetone- d_6), Compound 11 (^1H 700 MHz, ^{13}C 175 MHz in Acetone- d_6), Compound 12 (^1H 500 MHz, ^{13}C 125 MHz in CDCl_3), and Compound 13 (^1H 700 MHz, ^{13}C 175 MHz in CDCl_3)

no.	10		11		12		13	
	$^{13}\text{C}/\text{DEPT}$	$^1\text{H}/\text{HSQC}$	$^{13}\text{C}/\text{DEPT}$	$^1\text{H}/\text{HSQC}$	$^{13}\text{C}/\text{DEPT}$	$^1\text{H}/\text{HSQC}$	$^{13}\text{C}/\text{DEPT}$	$^1\text{H}/\text{HSQC}$
1	150.1, C		148.8, C		150.1, C		149.1, C	
2	33.0, CH_2	2.03, m ^a 2.16, m	34.5, CH_2	2.03, m 2.25, m ^a	33.0, CH_2	2.03, m 2.16, m ^a	32.3, CH_2	2.03, m 2.06, m
3	24.2, CH_2	1.53, m ^a	25.2, CH_2	1.59, m ^a 1.66, m	23.6, CH_2	1.56, m ^a	23.6, CH_2	1.53, m ^a
4	31.7, CH_2	1.34, m ^a 1.59, m	34.8, CH_2	1.56 ^a 1.95, td (4.62, 8.44)	33.1, CH_2	1.29, m ^a ^a 1.63, m	36.1, CH_2	1.23, m ^a 1.47, m ^a
5	40.1, C		49.3, C		40.0, C		34.9, C	
6	49.3, CH	2.06, m ^a	49.1, CH	2.66, dd (2.37, 11.4)	45.5, CH	2.12, dd (2.90, 11.75)	53.8, CH	1.73, dd (3.01, 11.19)
7	27.2, CH_2	1.68, m 1.75, m	28.4, CH_2	1.58, m ^a 1.75, m	22.9, CH_2	1.63, m ^a	24.8, CH_2	1.50, m ^a 1.63, m
8	23.9, CH_2	2.21, m ^a 2.40, m	23.9, CH_2	2.27, m ^a 2.47, m	34.4, CH_2	2.03, m 2.16, m ^a	34.4, CH_2	1.90, m 2.13, m
9	126.4, C		126.1, C		143.6, C		144.5, C	
10	111.9, CH	6.35, br s	111.9, CH	6.34, br s	127.9, CH	5.62, t (6.87)	126.1, CH	5.64, t (6.88)
11	143.7, CH	7.44, br s	143.7, CH	7.43, br s	58.5, CH_2	4.14, dd (12.36, 6.87) 4.22, m ^a	58.7, CH_2	4.24, br d (6.88) 4.28, dd (3.44, 6.88) ^a
12	139.8, CH	7.34, br s	139.8, CH	7.34, br s	108.8, CH_2	4.59, s 4.86, s	109.2, CH_2	4.56, s 4.78, s
13	109.8, CH_2	4.60, s 4.81, s	109.8, CH_2	4.69, s 4.87, s	19.1, CH_3	0.74, s	26.4, CH_3	0.85, s
14	21.6, CH_3	0.82, s	19.8, CH_3	1.06, s	69.5, CH_2	3.29, d (11.29) 3.56, d (11.29)	28.4, CH_3	0.92, s
15	68.6, CH_2	3.23, d (10.76) 3.50, d (10.76)	178.5, C		60.7, CH_2	4.05, s 4.23, s	61.2, CH_2	4.18, s 4.19, s

^aPeaks overlapping with other peaks.

Compound 2 was isolated as a yellow oil from both the supernatant and the mycelia. The HR-ESIMS data revealed the molecular formula to be $\text{C}_{15}\text{H}_{20}\text{O}_3$ with six degrees of unsaturation. Two methyl peaks at δ 1.67 (H_3 -13) and 1.96 (H_3 -15) and two olefinic singlets at δ 5.15 and 5.27 were recorded in the ^1H NMR spectrum. A total of 15 carbons, two methyl groups, four methylene groups, five methine groups, and four nonprotonated carbons could be identified from the ^{13}C and DEPT NMR data. In the HMBC spectrum correlations of H-9 to C-10/C-11/C-12/C revealed the dihydrofuran part of the molecule. Correlations of H_3 -15 to C-10/C-11/C-12 were also observed in the HMBC spectra. Further, HMBC correlations of H-8 to C-6/C-7/C-9/C-10/C-14 were observed. Cross-peaks in the COSY spectrum were also recorded between H-9 and H-8/H-10. The position of the vinyl group was confirmed from the HMBC correlations of H_2 -14 to C-6/C-7/C-8. The COSY correlations of H_2 -1 to H-6/ H_2 -2 and H_2 -5 to H-6/H-4 along with the HMBC correlations of H_3 -13 to C-2/C-3/C-4 confirmed the cyclohexyl part of the molecule connected through C-6. ROESY correlations were observed between H-8 and H-6/H-9. The absolute stereochemistry of 2 was assigned by derivatization with *R* and *S* MTPA chloride. The $\Delta\delta_{\text{SR}} = \delta(\text{S-MTPA ester}) - \delta(\text{R-MTPA ester})$ for protons neighboring C-8 (see Table 2 in the Supporting Information) led to the *S*-configuration assignment at C-8 and consequently the assignment of 6*R* and 9*R* for the other respective stereocenters.

Compound 3, with the molecular formula $\text{C}_{15}\text{H}_{22}\text{O}_3$ and five degrees of unsaturation deduced from HR-ESIMS data, was isolated from both the supernatant and the mycelial extracts. Analysis of the 1D and 2D NMR data for 3 revealed a similar structure to 2 with the double bond at C-10 missing in compound 3. Analysis of the ^{13}C NMR data for 3 indicated the absence of the olefinic C-10 occurring at δ 145.3 and the C-11 (131.7) in compound 2 and a methylene and methine signals at δ 29.4 and 35.5, respectively, were observed. The H_3 -15 (δ 1.30) showed HMBC correlation to C-10 (δ 29.4)/C-11 (δ 35.5)/C-12 (δ 179.4). Additional ROESY correlations between H-9 and H-11 were also observed. Since compounds 2 and 3 were obtained as congeners, the absolute stereochemistry of 3 was assigned as 6*R*, 8*S*, 9*R*, and 11*R*. Compounds 2 and 3 are structurally related to phelilane D from *Inonotus vaninii*,¹⁷ i.e., a species that is closely related to *Sanguangporus*.

Compound 4 was isolated as a yellow oil only from the supernatant. The HR-ESIMS data revealed the molecular formula to be $\text{C}_{15}\text{H}_{22}\text{O}_4$ with five degrees of unsaturation. Analysis of the 1D and 2D NMR data suggested a structure closely related to compound 2. Similar COSY, HMBC, and ROESY correlations were observed except for the HMBC correlations of H-4 to C-1, which was missing in 4, indicating that this compound had an open end chain instead of the dihydrofuran in 2. This was in agreement with the HR-ESIMS data, which showed the presence of four oxygen atoms for this molecule. The olefinic double bond between C-2 and C-3 was

assigned an *E*-configuration because of the upfield shifts of C-15 (δ 13.0). ROESY correlations of H-7 suggested that this compound shared the same *R*-configuration with **2** at C-7; hence the stereochemistry of this molecule was assigned as 4*S*, 5*S*, and 7*R*. This compound is closely related to 2-methyl-6-(4-methyl-3-cyclohexen-1-yl)-2,6-heptadienoic acid, (*E*)-(9*CI*), previously reported in the patent by Kobayashi et al. *Tropicoporus linteus*.¹⁸

Compound **5** was isolated as a yellow oil from the supernatant extract. It had the molecular formula $C_{15}H_{24}O_4$ and showed four degrees of unsaturation as established from the HR-ESIMS data. Three methyl singlets at δ 1.16 (H₃-14), 1.61 (H₃-13), and 1.81 (H₃-15) were observed in the ¹H NMR spectrum. Further, three methyl, four methylene, four methane, and four nonprotonated carbons (three sp² carbons and one oxygenated sp³ carbon) were identified from the ¹³C and DEPT NMR data. HMBC correlations of H₃-15 to C-1/C-2/C-3, H-5 to C-3/C-4/C-6/C-14, and H₃-14 to C-5/C-6/C-7 established the structure of the side chain. COSY correlations were also observed between H-4 and H-3/H-5. Similar COSY and HMBC correlations making up the cyclohexyl moiety connected to the side chain through C-7 in compounds **1**, **2**, and **3** were also established for this compound. The double bond at C-2 was assigned as *E* based on the upfield shift of C-15 (δ 12.8). ROESY correlations H-14 to H-7/H₂-4 (δ 2.32)/H₂-12 (δ 2.01) indicated that these protons were on the same side of the plane. On the other hand cross-peaks were observed between H-5 and H₂-4 (δ 2.59)/H₂-12 (δ 2.16) in the ROESY spectra. To assign the absolute stereochemistry, both *S*- and *R*-MTPA ester derivatives of **5** were prepared from *R*- and *S*-MTPA chloride, respectively. The $\Delta\delta_{SR} = \delta(S\text{-MTPA ester}) - \delta(R\text{-MTPA ester})$ for protons neighboring C-5 gave negative values for the C-4 methylene protons (-0.005 and -0.008) and positive values for H₃-14 and H-7, i.e., $+0.003$ and $+0.012$, respectively (Table 3 in the SI). Therefore, the absolute stereochemistry at C-5 was assigned as *S*, and consequently the other centers were assigned as 6*R*, 7*R*. Phellilane H, previously reported from *Phellinus linteus* (current valid name *Tropicoporus linteus*¹⁰), has a similar structure to **5** but a different stereochemistry.¹⁸

Compound **6**, with the molecular formula $C_{15}H_{24}O_5$ and four degrees of unsaturation deduced from HR-ESIMS data, was isolated from supernatant extracts. Analysis of the 1D and 2D NMR data for **6** indicated a similar structure to **5** with the C-13 methyl group missing in compound **6**, but an oxymethylene peak at δ 67.4 (C-13) was recorded instead. The H₂-13 (δ 3.91) showed HMBC correlations to C-9/C-10/C-11.

Compound **7**, which was isolated as a yellow oil only from the supernatant extract, had a molecular formula of $C_{15}H_{24}O_5$ and four degrees of unsaturation established from the HR-ESIMS data. Analysis of the 1D and 2D NMR data for **7** indicated a similar structure to that of **5** with the C-4 methylene group replaced by an oxymethine signal resonating at δ 69.9. COSY correlations between the oxymethine proton (δ 4.73) and H-3/H-5 were observed. Furthermore, a correlation of this proton (H-4) to C-2/C-3/C-5/C-6 could be established in the HMBC spectra. In the ROESY spectra of **7**, similar correlations to those observed for **5** were recorded. In addition, cross-peaks in the ROESY spectra of **7** were recorded between H-4 and H₃-14/H-7. Thus, the 4*S*, 5*S*, 6*R*, and 7*R* configurations were concluded for this molecule. The comparison of the circular dichroism (CD) spectra of **5** and

7 supported this conclusion, as the electronic circular dichroism (ECD) curves of these compounds were comparable in the range of 204–240 nm (positive Cotton effect registered) (Figure 1). Compounds **6** and **7** are also closely related to phellilane H.¹⁸

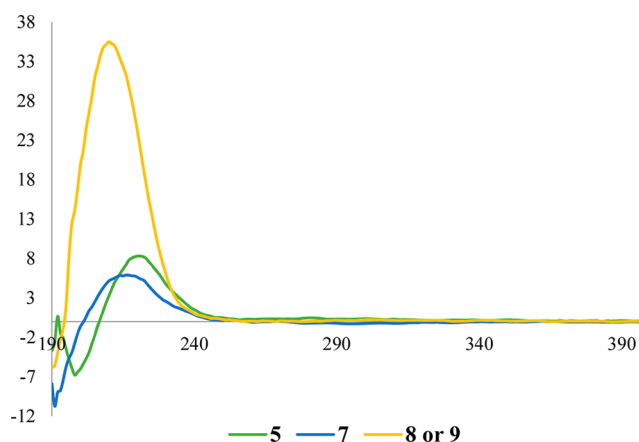


Figure 1. ECD spectra of compounds **5**, **7**, and **8/9** in ethanol.

Compounds **8** and **9** were isolated as yellow oils from both the supernatant and mycelial extracts. The mixture of the two compounds (ratio 2:1) could not be separated, but their NMR data were clearly resolved and, thus, their structures could be determined independently. HR-ESIMS data revealed their molecular weights as $C_{15}H_{20}O_3$ and $C_{15}H_{22}O_3$ for compounds **8** and **9**, respectively.

For compound **8** HMBC correlations of H₃-15 to C-10/C-11/C-12, H-9 to C-7/C-8/C-10/C-11/C-12, and H₃-14 to C-6/C-7/C-8 together with the COSY correlations of H-9 to H-8/H-10 confirmed one part of the structure. The chemical shift of C-9 (δ 78.1) and the HMBC correlations of H-9 to C-12 suggested that C-9 and C-12 were linked via an oxygen bridge, forming a dihydrofuran. Similar HMBC and COSY correlations making up the cyclohexyl part of the molecules already described above for the congeners were also recorded for this molecule. Based on the chemical shifts of the C-7 (δ 64.2) and C-8 (δ 61.1) an epoxide was concluded to be in the molecule.

The 1D and 2D NMR data of **9** were similar to those of **8**, with the difference being the absence of the olefinic bond between C-10 and C-11. For both compounds ROESY correlations of H₃-14 to H-6/H-8/H-9 and H-8 to H-6/H-9 were observed and cross-peaks were recorded between H-9 and H-11 in the ROESY spectra of **9**. These correlations revealed that these compounds had the same stereochemistry as **5** at C-5 and C-6. The stereochemistry of this molecule was thus assigned as 6*R*, 7*R*, 8*R*, and 9*R*. Comparison of the CD spectra of the mixture of compounds **8/9** with that of **5** supported this assignment, as only a positive Cotton effect in the range of 194–240 nm was observed for the mixture (Figure 1). Therefore, the structures of **8** and **9** were unambiguously established as (9*R*)-11-methyl-9-[(7*R*,8*R*)-7-methyl-6-[(6*R*)-3-methylcyclohex-3-en-6-yl]oxiran-8-yl]furan-12-one and (9*R*,11*R*)-11-methyl-9-[(7*R*,8*R*)-7-methyl-6-[(6*R*)-3-methylcyclohex-3-en-6-yl]oxiran-8-yl]oxolan-12-one, respectively. These two compounds are closely related to phellilane E from *Tropicoporus linteus*.¹⁸

Compound **10**, with the molecular formula $C_{15}H_{22}O_2$ and five degrees of unsaturation determined from the HR-ESIMS

data, was obtained as a yellow oil only from the supernatant extract. One methyl, seven methylene, four methane, and three nonprotonated carbons (two sp^2 carbons and one sp^3 carbon) were identified in the ^{13}C and DEPT NMR spectra. COSY correlations of H₂-3 to H₂-2/H₂-4, as well as the HMBC correlations of H₂-13 to C-1/C-2/C-6 and H₃-14/H₂-15 to C-4/C-5/C-6, confirmed the cyclohexane ring part in the molecule. Further cross-peaks in the COSY spectra between H₂-7 and H-6/H₂-8 were established. In the HMBC spectra H₂-8 showed correlations to C-6/C-7/C-9/C-10/C-12, H-10 to C-9/C-11/C-12, and H-12 to C-9/C-10/C-11. Based on the chemical shift of C-11 (δ 143.7) and C-12 (δ 139.8) the two carbons were linked via an oxygen bridge forming the furan. Hence the structure was elucidated as {5-[9-(furan-9-yl)ethyl]-5-methyl-1-methylidencyclohexyl}methanol.

Compound **11** was isolated as a yellow oil from both the supernatant and mycelia extracts. The HR-ESIMS data revealed the molecular formula to be C₁₅H₂₀O₃ with 6 degrees of unsaturation. The 1D and 2D NMR data for **11** revealed a similar structure to **10** except that the oxymethylene group at δ 68.6 (C-15) in **10** was missing and a carboxylic acid peak at δ 178.5 (H-15) was observed instead. The H₃-14 correlated to this carbon in the HMBC spectra. Interestingly, compounds **10** and **11** are somewhat structurally related to dihydropallescensin-2 from the defensive organs of the nudibranch *Tyrinna nobilis*.¹⁹

Compound **12** was isolated as a yellow oil from the supernatant with the molecular formula C₁₅H₂₆O₃ established from the HR-ESIMS data. 1D and 2D NMR data for **12** indicated a structure similar to **10** with the open end chains instead of the furan. Two oxymethylene carbons at δ 58.5 (C-11) and 60.7 (C-15) were identified in the ^{13}C /DEPT NMR data. HMBC correlations of the diastereotopic protons H₂-11 (δ 4.14, 4.22) to C-9/C-10 and H₂-15 (δ 4.05, 4.23) to C-8/C-9/C-10 were observed. The olefinic bond between C-9 and C-10 was assigned the *Z*-configuration because of the ROESY correlations of H-10 (δ 5.62) to the diastereotopic protons H₂-8 (δ 2.03, 2.16). Therefore, the structure was unambiguously determined to be (9*Z*)-9-{9-[(5-(hydroxymethyl)-5-methyl-1-methylidencyclohexyl)ethyl]but-9-ene-11,15-diol}.

Compound **13** was obtained as a yellow oil from both supernatant and mycelia extracts with the molecular formula C₁₅H₂₆O₂ determined from the HR-ESIMS data. The 1D and 2D NMR data indicated a similar structure to that of compound **12** with the difference being the substituents at C-5. The C-14 hydroxymethyl group in **12** was replaced with a methyl group (δ 28.4). The structure of **13** was therefore concluded to be (9*Z*)-9-{9-[(5,5-dimethyl-1-methylidencyclohexyl)ethyl]but-9-ene-11,15-diol}. The absolute stereochemistry of **13** at C-6 was assigned as *S* from comparison of its optical rotation ($[\alpha]_D^{20}$ +7.9 in methanol) to that of the known compound dihydropallescensin-2 ($[\alpha]_D^{20}$ +6.0 in chloroform), which has the same stereocenter.²⁰ To determine the stereochemistry at C-6 for compounds **10** and **11**, CD spectra of these three compounds were measured. While a negative Cotton effect was observed in the range of 190–220 nm of the ECD curve of compound **13** in EtOH, a positive Cotton effect was recorded for **10** and **11** (opposite that of **13**) in the same region, suggesting a 6*R*-configuration for these two compounds (Figure 2). H₃-14 and H-6 did not correlate in the ROESY spectra, and therefore, a 5*R*-configuration was concluded for these compounds. Com-

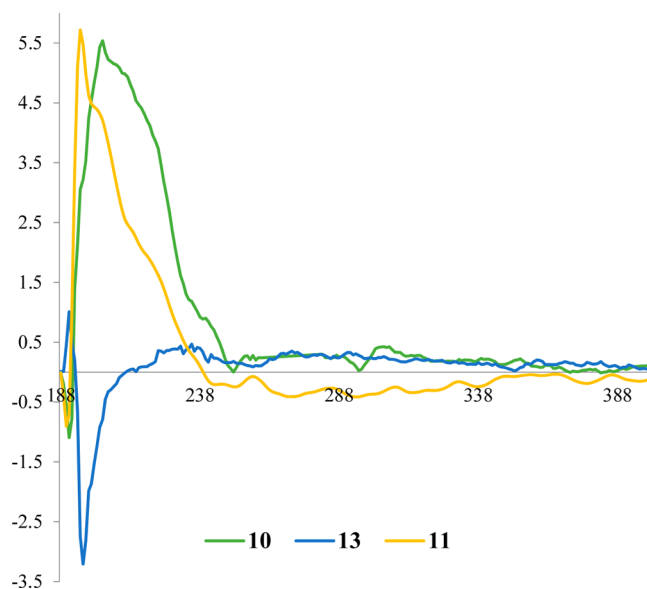


Figure 2. ECD spectra of compounds **10**, **11**, and **13** in ethanol.

pounds **12** and **13** are closely related to *trans*- γ -monocyclofarnesol.²¹

As already mentioned above, some closely related compounds named phelilanes have previously been patented from *Tropicoporus linteus* as part of the composition of an antibacterial agent that is being marketed for the treatment of ailments as diverse as gastroenteric dysfunction, diarrhea, hemorrhage, cancers, and prevention of periodontal disease and in the form of toothpaste and mouthwash agents in Asia.¹⁸ These compounds have to the best of our knowledge never been published in peer-reviewed papers, but a comparison of their spectral data proved helpful.

Compounds **4**, **5**, and **7–14** were evaluated for their antimicrobial activity (Table 4). Metabolites **1–3** and **6** were not tested because they were produced in small quantities (0.42, 0.28, 0.49, and 0.89 mg for each) and they were used in the pretest bioassay (serial dilution assay tested for *Bacillus subtilis*, *Escherichia coli*, and *Candida albicans*). Compounds **8/9** (tested as an inseparable mixture, see above), **10**, **11**, and **13** showed weak antimicrobial activity against *Bacillus subtilis*; compounds **8/9** and **13** demonstrated weak activities against *Micrococcus luteus*; compounds **4**, **8/9**, and **13** exhibited weak activities against *Staphylococcus aureus*. Further, most of the tested compounds demonstrated moderate activity against *Mucor hiemalis*, except for compound **7**, which was inactive. No activity against Gram- bacteria or yeast was observed. In the cytotoxicity assay **4**, **8–11**, and **13** exhibited weak effects against KB 3.1 cells, while **10** and **13** showed weak activity against L929 cells.

Notably, none of the isolated metabolites has reached the initially observed MIC of the crude extracts. Therefore, we cannot exclude cumulative effects. However, it might also be possible that we have lost some potent components due to its instability during the isolation procedure or that some of the minor congeners we obtained that were not tested for lack of material could be more active.

EXPERIMENTAL SECTION

General Experimental Procedures. CD spectra were determined with a JASCO spectropolarimeter, model J-815 (JASCO, Pfungstadt, Germany). Optical rotations were recorded on a

Table 4. Antimicrobial and Cytotoxic Activities of Compounds 4–14^a

test organisms	4	5	7	8/9	10	11	12	13	14	reference	
MIC ($\mu\text{g/mL}$)											
Gram-Positive Bacteria											
<i>Bacillus subtilis</i> DSM 10	–	–	–	100	75	75	–	100	–	ciprofloxacin	3.1
<i>Micrococcus luteus</i> DSM 1790	–	–	–	100	/	–	–	100	–	oxytetracycline	0.4
<i>Mycobacterium smegmatis</i> DSM 43524	–	–	–	–	/	–	–	–	–	kanamycin	0.4
<i>Staphylococcus aureus</i> DSM 346	100	–	–	100	/	–	–	100	–	oxytetracycline	0.4
Filamentous Fungi											
<i>Mucor hiemalis</i> DSM 2656	100	50	–	100	/	50	50	25	50	nystatin	16.7
Cytotoxicity IC ₅₀ (μM)											
Cell Lines											
L929	/	/	/	–	59.8	–	–	117.5	–	epothilon B	0.00275
KB3.1	172.9	/	/	144.5	27.8	141	–	79.8	–	epothilon B	6.5×10^{-5}

^a– no activity; / not tested; starting concentrations for antimicrobial assay and cytotoxicity assay were 300 and 37 $\mu\text{g/mL}$, respectively.

PerkinElmer (Überlingen, Germany) 241 MC polarimeter. NMR spectra were recorded on Bruker 700 spectrometers with a 5 mm TXI cryoprobe (¹H 700 MHz, ¹³C 175 MHz, ¹⁵N 71 MHz) and Bruker AV III-600 (¹H 600 MHz, ¹³C 150 MHz) spectrometers. HR-ESIMS mass spectra were measured by using an Agilent 1200 series HPLC-UV system (column 2.1 \times 50 mm, 1.7 μm , C₁₈ Acquity UPLC BEH (waters), solvent A (H₂O + 0.1% formic acid); solvent B (AcCN + 0.1% formic acid), gradient: 5% B for 0.5 min increasing to 100% in 19.5 min and then maintaining 100% B for 5 min, flow rate 0.6 mL/min, UV/vis detection 200–600 nm combined with ESI-TOF-MS (Maxis, Bruker)) [scan range 100–2500 *m/z*, capillary voltage 4500 V, dry temperature 200 °C]. UV spectra were recorded by using a Shimadzu UV-2450 UV–vis spectrophotometer.

Fungal Material. The fungal specimen was collected by C. Decock and J. C. Matasyoh from Mount Elgon National Reserve, located in the western part of Kenya (1°7'6" N, 34°31'30" E) in April 2016 from wood. A dried specimen and the corresponding mycelial culture, which was obtained from the contents of the basidium, were deposited at MUCL, Louvain-la-Neuve, Belgium, under the accession number MUCL 56354.

DNA was extracted from the culture of MUCL 56354 by using the EZ-10 spin column genomic DNA miniprep kit (Bio Basic Canada Inc., Markham, Ontario, Canada) as described previously.¹² A Precellys 24 homogenizer (Bertin Technologies, France) was used for cell disruption at a speed of 6000 rpm for 2 \times 40 s. Standard primers ITS 1f and NL4 were used for the DNA region amplification by following the protocol by Otto et al.²²

Small-Scale Fermentation. *Sanghuangporous* sp. MUCL56354 was cultivated in three different liquid media: YM 6.3, Q6_{1/2}, and ZM_{1/2} (media compositions see Supporting Information). A well-grown culture from a YM agar plate (YM supplemented with 1.5% agar, pH = 6.3) was cut into small pieces using a cork borer (7 mm), and five pieces were inoculated into a 500 mL Erlenmeyer flask containing 200 mL of the three media. The cultures were incubated at 23 °C on a rotary shaker (140 rpm). The growth of the fungus was monitored by measuring the amount of free glucose using Diastix Harnzuckerstreifen (Bayer). The fermentation was terminated 3 days after glucose depletion.

Scale-up of Fermentation. Analysis of the HPLC-MS data and subsequent search in the Dictionary of Natural Products database²³ revealed the presence of potentially new bioactive metabolites in the YM 6.3 medium, and this was selected for scale-up. A well-grown YM agar plate of mycelial culture was cut into small pieces using a 7 mm cork border and five pieces inoculated into larger batches of sterile flasks (in total 10 L) by following the original protocol.

Preparation of the Extracts. Supernatant and biomass from small-scale fermentation were separated by filtration. The supernatant resulting from an ethyl acetate extract was evaporated to dryness by means of a rotary evaporator. The mycelia were extracted with 200 mL of acetone in an ultrasonic bath for 30 min and filtered, and the filtrate was evaporated. The remaining water phase was suspended in

an equal amount of distilled water, extracted with an equal amount of ethyl acetate, and filtered through anhydrous sodium sulfate, and the resulting ethyl acetate extract was evaporated to dryness.

The mycelia and supernatant from the large-scale fermentation were separated via vacuum filtration. The mycelia were extracted with 4 \times 500 mL of acetone in an ultrasonic bath for 30 min. The extracts were combined and the solvent was evaporated by means of a rotary evaporator. The remaining water phase was suspended in 200 mL of distilled water, extracted with 3 \times 500 mL of ethyl acetate, and filtered through anhydrous sodium sulfate. The resulting ethyl acetate extract was evaporated to dryness, leaving a brown solid (151 mg). The supernatant was extracted by adding 5% Amberlite XAD-16N absorbent (Rohm & Haas Deutschland GmbH, Frankfurt am Main, Germany) and incubation of the resin overnight on a shaker. The Amberlite resin was then filtered and eluted with 4 \times 500 mL of acetone. The resulting acetone extract was evaporated, and the remaining water phase was extracted with an equal amount of ethyl acetate. The organic phase was dried by sodium sulfate and evaporated to dryness, and a brown extract (369 mg) was obtained.

Isolation of Compounds 1–14. The extract was filtered using a SPME Strata-X 33 u Polymeric RP cartridge (Phenomenex, Inc., Aschaffenburg, Germany). The supernatant and mycelia crude extracts were fractionated by preparative reverse-phase liquid chromatography (PLC 2020, Gilson, Middleton, WI, USA). The VP Nucleodur 100–5C 18 ec column (250 mm \times 40 mm, 7 μm , Macherey-Nagel) was used as stationary phase. Deionized water (Milli-Q, Millipore, Schwalbach, Germany) with 0.05% trifluoroacetic acid (TFA) (solvent A) and acetonitrile with 0.05% TFA (solvent B) were used as the mobile phase. The elution gradient used 5–100% solvent B over 45 min and thereafter isocratic conditions at 100% solvent B for 10 min. UV monitoring was carried out at 210, 254, and 350 nm, and the flow rate was 40 mL/min. Twenty-four fractions were collected according to the observed peaks (F1–F24) from supernatant extracts, and 14 fractions (F1–F14) were collected from the mycelial extracts.

Fraction F15 of the supernatant was further purified by reversed-phase HPLC (solvent A (H₂O + 0.05% TFA)/solvent B (ACN + 0.05% TFA), elution gradient: 52–100% solvent B for 23 min, followed by maintaining isocratic conditions at 100% for 5 min with a preparative HPLC column (Kromasil, MZ Analysentechnik, Mainz, Germany; 250 \times 20 mm, 7 μm C₁₈) as stationary phase and a flow rate of 15 mL/min, to afford compound 1 (0.42 mg; equivalent to 0.1% of the crude extract). Unless stated otherwise, the same column was used for the purification of the other fractions. Fraction F12 and supernatant fraction F23 were combined and purified with a gradient of 60–85% solvent B for 18 min, followed by a gradient shift from 85% to 100% in 2 min and isocratic conditions at 100% for 5 min to afford compounds 2 (0.28 mg; 0.05%), 3 (0.49 mg; 0.1%), 8/9 (3.31 mg; 0.65%), and 11 (2.55 mg; 0.5%). Application of the elution gradient of 40–80% solvent B for 18 min, followed by gradient shift from 80% to 100% in 2 min and maintaining isocratic conditions

100% for 5 min, yielded compound 4 (1.51 mg; 0.4%) and compound 7 (4.08 mg; 1.1%) from fraction F18 of the supernatant. Compound 5 (3.07 mg; 0.8%) was purified from supernatant fraction F17 with the following elution gradient: 60–100% solvent B for 23 min, followed by isocratic conditions at 100% B for 5 min. Compound 6 (0.89 mg; 0.25%) was purified from supernatant fraction F11 by application of the following gradient: 38–62% solvent B for 23 min, followed by gradient shift from 62% to 100% in 2 min and isocratic gradient 100% for 5 min. The same gradient was used to isolate compound 10 (1.34 mg; 0.35%) from supernatant fraction F20. Fraction F15 of the supernatant was purified using the elution gradient 38–75% solvent B for 23 min, followed by a gradient shift from 75% to 100% in 2 min and isocratic conditions of 100% solvent B for 2 min to afford compound 12 (1.2 mg; 0.3%). Compound 13 (2.17 mg; 0.4%) was obtained from purification of supernatant fraction F21 and mycelia fraction F10 with the gradient 55–85% solvent B for 18 min, followed by 2 min gradient shift from 85% to 100% and finally isocratic conditions at 100% B for 5 min. The known compound 14 (6.79 mg; 2%) was purified from supernatant fraction F7 with the elution gradient 34–100% solvent B for 23 min, followed by isocratic elution with 100% B for 5 min.

Antimicrobial Assay. Minimum inhibitory concentrations (MIC) were determined in serial dilution assays using different test microorganisms. The assays were conducted in 96-well plates in Mueller Hinton Broth (comprising beef infusion solids, 2.0 g/L; casein hydrolysate, 17.5 g/L; starch, 1.5 g/L) for bacteria and YM medium for filamentous fungi and yeasts, as described earlier.²⁴

Cytotoxicity Assay. In vitro cytotoxicity (IC₅₀) of compounds 3, 4, and 8–14 were evaluated against mouse fibroblast L929 and HeLa (KB-3.1) cell lines according to the method described earlier.⁶

(6*R*,7*S*,10*R*)-7,10-Epoxy-7,11-dimethyldec-1-ene-6,11-diol (1): $[\alpha]_{\text{D}}^{20} +40.7$ (c 1.075, MeOH); UV (MeOH, c 0.125) λ_{max} (log ϵ) 222 (3.828); HR-ESIMS m/z 255.1954 [M + H]⁺, calcd for C₁₅H₂₇O₃ 255.1960.

(9*R*)-9-[(8*S*)-8-Hydroxy-7-[(6*R*)-3-methylcyclohex-3-en-6-yl]prop-7-en-8-yl]-11-methylfuran-12-one (elgonene A (2)): $[\alpha]_{\text{D}}^{20} +82.3$ (c 1.0, MeOH); UV (MeOH, c 0.125) λ_{max} (log ϵ) 222 (3.879); HR-ESIMS m/z 249.1486 [M + H]⁺, calcd for C₁₅H₂₁O₃ 249.1490.

(9*R*,11*R*)-9-[(8*S*)-8-Hydroxy-7-[(6*R*)-3-methylcyclohex-3-en-6-yl]prop-7-en-8-yl]-11-methylloxolan-12-one (elgonene B (3)): $[\alpha]_{\text{D}}^{20} +14.3$ (c 1.0, MeOH); UV (MeOH, c 0.125) λ_{max} (log ϵ) 230 (3.659); HR-ESIMS m/z 251.1641 [M + H]⁺, calcd for C₁₅H₂₃O₃ 251.1647.

(2*E*,4*S*,5*S*)-4,5-Dihydroxy-2-methyl-6-[(7*R*)-10-methylcyclohex-10-en-7-yl]hepta-2,6-dienoic acid (elgonene C (4)): $[\alpha]_{\text{D}}^{20} +25.9$ (c 2.0, MeOH); UV (MeOH, c 0.125) λ_{max} (log ϵ) 281 (2.589), 203 (3.849); HR-ESIMS m/z 267.1588 [M + H]⁺, calcd for C₁₅H₂₃O₃ 267.1596.

(2*E*,5*S*,6*R*)-5,6-Dihydroxy-2-methyl-6-[(7*R*)-10-methylcyclohex-10-en-7-yl]hept-2-enoic acid (elgonene D (5)): $[\alpha]_{\text{D}}^{20} -12.2$ (c 1.99, MeOH); UV (MeOH, c 0.1) λ_{max} (log ϵ) 197 (3.986); HR-ESIMS m/z 269.1743 [M + H]⁺, calcd for C₁₅H₂₅O₄ 269.1752.

(2*E*,5*S*,6*R*)-5,6-Dihydroxy-6-[(7*R*)-10-(hydroxymethyl)cyclohex-10-en-7-yl]-2-methylhept-2-enoic acid (elgonene E (6)): $[\alpha]_{\text{D}}^{20} +61.1$ (c 1.49, MeOH); UV (MeOH, c 0.0) λ_{max} (log ϵ) 218 (3.890); HR-ESIMS m/z 285.1694 [M + H]⁺, calcd for C₁₅H₂₅O₅ 285.1702.

(2*E*,4*S*,5*S*,6*R*)-4,5,6-Trihydroxy-2-methyl-6-[(7*R*)-10-methylcyclohex-10-en-7-yl]hept-2-enoic acid (elgonene F (7)): $[\alpha]_{\text{D}}^{20} -20.5$ (c 1.29, MeOH); UV (MeOH, c 0.05) λ_{max} (log ϵ) 212 (4.103); HR-ESIMS m/z 285.1695 [M + H]⁺, calcd for C₁₅H₂₅O₅ 285.1702.

(9*R*)-11-Methyl-9-[(7*R*,8*R*)-7-methyl-6-[(6*R*)-3-methylcyclohex-3-en-6-yl]oxiran-8-yl]furan-12-one (elgonene G (8)): UV (MeOH, c 0.125) λ_{max} (log ϵ) 216 (3.879); HR-ESIMS m/z 249.1486 [M + H]⁺, calcd for C₁₅H₂₁O₃ 249.1490.

(9*R*,11*R*)-11-Methyl-9-[(7*R*,8*R*)-7-methyl-6-[(6*R*)-3-methylcyclohex-3-en-6-yl]oxiran-8-yl]oxolan-12-one (elgonene H (9)): UV (MeOH, c 0.125) λ_{max} (log ϵ) 216 (3.879); HR-ESIMS m/z 251.1639 [M + H]⁺, calcd for C₁₅H₂₃O₃ 251.1647.

{(5*R*,6*R*)-5-[9-(Furan-9-yl)ethyl]-5-methyl-1-methylidenecyclohexyl}methanol (elgonene I (10)): $[\alpha]_{\text{D}}^{20} -11.9$ (c

2.0, MeOH); UV (MeOH, c 0.125) λ_{max} (log ϵ) 228 (3.8453); HR-ESIMS m/z 235.1689 [M + H]⁺, calcd for C₁₅H₂₃O₂ 235.1698.

(5*R*,6*R*)-5-[9-(Furan-9-yl)ethyl]-5-methyl-1-methylidenecyclohexane-5-carboxylic acid (elgonene J (11)): $[\alpha]_{\text{D}}^{20} +11.9$ (c 3.6, MeOH); UV (MeOH, c 0.25) λ_{max} (log ϵ) 277(2.894), 216 (3.834); HR-ESIMS m/z 249.1483 [M + H]⁺, calcd for C₁₅H₂₁O₃ 249.1490.

(9*Z*)-9-[(9-[(5*R*,6*R*)-5-(Hydroxymethyl)-5-methyl-1-methylidenecyclohexyl]ethyl]but-9-ene-11,15-diol (elgonene K (12)): $[\alpha]_{\text{D}}^{20} +10.8$ (c 10.41, MeOH); UV (MeOH, c 0.125) λ_{max} (log ϵ) 203 (3.849); HR-ESIMS m/z 255.1954 [M + H]⁺, calcd for C₁₅H₂₇O₃ 255.1960.

(9*Z*)-9-[(9-[(6*S*)-5,5-Dimethyl-1-methylidenecyclohexyl]ethyl]but-9-ene-11,15-diol (elgonene L (13)): $[\alpha]_{\text{D}}^{20} +7.9$ (c 1.24, MeOH); UV (MeOH, c 0.25) λ_{max} (log ϵ) 213 (3.634); HR-ESIMS m/z 239.2002 [M + H]⁺, calcd for C₁₅H₂₇O₂ 239.2011.

■ ASSOCIATED CONTENT

📄 Supporting Information

The Supporting Information is available free of charge on the ACS Publications website at DOI: [10.1021/acs.jnatprod.8b01086](https://doi.org/10.1021/acs.jnatprod.8b01086).

Experimental procedures, 1D and 2D NMR data, LCMS data, 5.8S/ITS DNA sequence of the producing organism (PDF)

■ AUTHOR INFORMATION

✉ Corresponding Author

*Tel (M. Stadler): +49 531 6181-4240. Fax: +49 531 6181 9499. E-mail: marc.stadler@helmholtz-hzi.de.

ORCID

Marc Stadler: 0000-0002-7284-8671

Notes

The authors declare no competing financial interest.

■ ACKNOWLEDGMENTS

We are grateful to W. Collisi for conducting the cytotoxicity assays, C. Kakoschke for recording NMR data, and C. Schwager and E. Surges for recording HPLC-MS data. Financial support by the “ASAFEM” Project (grant no. IC-070) under the ERAfrica Programme of the European Commission to J.C.M and M.S. and personal Ph.D. stipends from the China Scholarship Council (CSC), the German Academic Exchange Service (DAAD), and the Kenya National Council for Science and Technology (NACOSTI) to T.C. and C.C., respectively, are gratefully acknowledged.

■ REFERENCES

- (1) Tedersoo, L.; Bahram, M.; Pölme, S.; Kõljalg, U.; Yorou, N. S.; Wijesundera, R.; Villarreal Ruiz, L.; Vasco-Palacios, A. M.; Thu, P. Q.; Suija, A.; Smith, M. E.; Sharp, C.; Saluveer, E.; Saitta, A.; Rosas, M.; Riit, T.; Ratkowsky, D.; Pritsch, K.; Pöldmaa, K.; Piepenbring, M.; Phosri, C.; Peterson, M.; Parts, K.; Pärtel, K.; Otsing, E.; Nouhra, E.; Njounkou, A. L.; Nilsson, R. H.; Morgado, L. N.; Mayor, J.; May, T. W.; Majuakim, L.; Lodge, D. J.; Lee, S. S.; Larsson, K. H.; Kohout, P.; Hosaka, K.; Hiiesalu, I.; Henkel, T. W.; Harend, H.; Guo, L. D.; Greslebin, A.; Grelet, G.; Geml, J.; Gates, G.; Dunstan, W.; Dunk, C.; Drenkhan, R.; Deamaley, J.; De Kesel, A.; Dang, T.; Chen, X.; Buegger, F.; Brearley, F. Q.; Bonito, G.; Anslan, S.; Abell, S.; Abarenkov, K. *Science* **2014**, *346*, 1052–1053.
- (2) Sandargo, B.; Chepkirui, C.; Cheng, T.; Chaverra-Munoz, L.; Thongbai, B.; Stadler, M.; Hüttel, S. *Biotechnol. Adv.* **2019**, DOI: [10.1016/j.biotechadv.2019.01.011](https://doi.org/10.1016/j.biotechadv.2019.01.011).
- (3) Chepkirui, C.; Richter, C.; Matasyoh, J. C.; Stadler, M. *Phytochemistry* **2016**, *132*, 95–101.

- (4) Chepkirui, C.; Matasyoh, J. C.; Decock, C.; Stadler, M. *Phytochem. Lett.* **2017**, *20*, 106–110.
- (5) Chepkirui, C.; Cheng, T.; Matasyoh, J. C.; Decock, C.; Stadler, M. *Phytochem. Lett.* **2018**, *25*, 141–146.
- (6) Chepkirui, C.; Sum, C. W.; Cheng, T.; Matasyoh, J. C.; Decock, C.; Stadler, M. *Molecules* **2018**, *23*, 369.
- (7) Chepkirui, C.; Yuyama, K. T.; Wanga, L. A.; Decock, C.; Matasyoh, J. C.; Abraham, W. R.; Stadler, M. *J. Nat. Prod.* **2018**, *81*, 778–784.
- (8) Mudalungu, C. M.; Richter, C.; Wittstein, K.; Abdalla, M. A.; Matasyoh, J. C.; Stadler, M.; Süßmuth, R. D. *J. Nat. Prod.* **2016**, *79*, 894–898.
- (9) Hsieh, P. W.; Wu, J. B.; Wu, Y. C. *BioMedicine* **2013**, *3*, 106–113.
- (10) Zhou, L. W.; Vlasák, J.; Decock, C.; Assefa, A.; Stenlid, J.; Abate, D.; Wu, S. H.; Dai, Y. C. *Fungal Divers.* **2016**, *77*, 335–347.
- (11) Chen, H.; Tian, T.; Miao, H.; Zhao, Y. Y. *Fitoterapia* **2016**, *113*, 6–26.
- (12) Wendt, L.; Sir, E. B.; Kuhnert, E.; Heitkämper, S.; Lambert, C.; Hladki, A. I.; Romero, A. I.; Luangsa-ard, J. J.; Srikitikulchai, P.; Peršoh, D.; Stadler, M. *Mycol. Prog.* **2018**, *17*, 115–154.
- (13) Inamatsu, K. *Soil Sci. Plant Nutr.* **1968**, *14*, 62–67.
- (14) Inui, T.; Wang, Y.; Nikolic, D.; Smith, D. C.; Franzblau, S. G.; Pauli, G. F. *J. Nat. Prod.* **2010**, *73*, 563–567.
- (15) Li, L.; Liu, R.; Han, L.; Jiang, Y.; Liu, J.; Li, Y.; Yuan, C.; Huang, X. *Magn. Reson. Chem.* **2016**, *54*, 606–609.
- (16) Hoye, T. R.; Jeffrey, C. S.; Shao, F. *Nat. Protoc.* **2007**, *2*, 2451.
- (17) Yang, J.; Wang, N.; Yuan, H. S.; Hu, J. C.; Dai, Y. C. *Chem. Nat. Compd.* **2013**, *49*, 261–263.
- (18) Kobayashi, Y.; Ino, C.; Hirotsu, M. Japanese Patent JP2010047512, 2010.
- (19) Fontana, A.; Muniain, C.; Cimino, G. *J. Nat. Prod.* **1998**, *61*, 1027–1029.
- (20) Thompson, J. E.; Walker, R. P.; Wratten, S. J.; Faulkner, D. J. *Tetrahedron* **1982**, *38*, 1865–1873.
- (21) Ludwiczuk, A.; Odrzykoski, I. J.; Asakawa, Y. *Phytochemistry* **2013**, *95*, 234–241.
- (22) Otto, A.; Laub, A.; Wendt, L.; Porzel, A.; Schmidt, J.; Palfner, G.; Becerra, J.; Krüger, D.; Stadler, M.; Wessjohann, L.; Westermann, B.; Arnold, N. *J. Nat. Prod.* **2016**, *79*, 929–938.
- (23) Buckingham, J. *Chapman & Hall, Chemical Database*; CRC: Boca Raton, FL, USA, 2017.
- (24) Rupčić, Z.; Chepkirui, C.; Hernández-Restrepo, M.; Crous, P.; Luangsa-ard, J. J.; Stadler, M. *MycoKeys* **2018**, *33*, 1–23.

Skeletocutins A-L: Antibacterial Agents from the Kenyan Wood-Inhabiting Basidiomycete, *Skeletocutis* sp.

Clara Chepkirui,^{†,^} Tian Cheng,^{†,^} Winnie Chemutai Sum,[‡] Josphat Clement Matasyoh,[§] Cony Decock,[⊥] Dimas F. Praditya,^{||,#,∇} Kathrin Wittstein,[†] Eike Steinmann,^{||,#} and Marc Stadler^{*,†,Ⓛ}

[†]Department of Microbial Drugs, Helmholtz Centre for Infection Research (HZI), German Centre for Infection Research (DZIF), Partner Site Hannover/Braunschweig, Inhoffenstrasse 7, 38124 Braunschweig, Germany

[‡]Department of Biochemistry, Egerton University, P.O. BOX 536, 20115 Njoro, Kenya

[§]Department of Chemistry, Faculty of Sciences, Egerton University, P.O. Box 536, 20115 Njoro, Kenya

[⊥]Mycothèque de l' Université Catholique de Louvain (BCCM/MUCL), Place Croix du Sud 3, B-1348 Louvain-la-Neuve, Belgium

^{||}Department of Molecular and Medical Virology, Ruhr-University Bochum, 44801 Bochum, Germany

[#]TWINCORE—Centre for Experimental and Clinical Infection Research (Institute of Experimental Virology) Hanover, Feodor-Lynen-Str. 7-9, 30625 Hannover, Germany

[∇]Research Center for Biotechnology, Indonesian Institute of Science, Jl. Raya Bogor KM 46, Cibinong 16911, Indonesia

S Supporting Information

ABSTRACT: Fermentation of the fungal strain *Skeletocutis* sp. originating from Mount Elgon Natural Reserve in Kenya, followed by bioassay guided fractionation led to the isolation of 12 previously undescribed metabolites named skeletocutins A-L (1–5 and 7–13) together with the known tyromycin A (6). Their structures were assigned by NMR spectroscopy complemented by HR-ESIMS. Compounds 1–6 and 11–13 exhibited selective activities against Gram-positive bacteria, while compound 10 weakly inhibited the formation of biofilm of *Staphylococcus aureus*. The isolated metabolites were also evaluated for inhibition of L-leucine aminopeptidase, since tyromycin A had previously been reported to possess such activities but only showed weak effects. Furthermore, all compounds were tested for antiviral activity against Hepatitis C virus (HCV), and compound 6 moderately inhibited HCV infectivity with an IC₅₀ of 6.6 μM.

KEYWORDS: *polyporaceae, secondary metabolites, basidiomycota, structure elucidation*

■ INTRODUCTION

Tropical rainforest ecosystems represent a treasure trove of biological heritage, and the vast majority of its biodiversity still remain unexploited. The constant chemical innovations that exist in these habitats may be driven by the active evolutionary race, making tropical species a rich source for new bioactive molecules.¹ Fungi represent a considerable proportion of the total biodiversity in these ecosystems, but the majority of the tropical fungi remain unstudied for production of bioactive secondary metabolites. We have recently started to explore Basidiomycota from Kenya's rain forests, Kakamega and Mount Elgon National Reserve and have already reported several novel bioactive secondary metabolites from new or rare species. Those include the calocerins and the new 9-oxo strobilurins from *Favolaschia calocera*, the antibiotic laxitextines from *Laxitextum incrustatum*, the biofilm inhibitors named microporenic acids from *Microporus* sp. and the triterpenes, laetiporins and aethiopilonones from *Laetiporus* sp. and *Fomitiporia aethiopica*, respectively.^{2–6} Two strains of *Sanghuangporus* were also evaluated, and numerous bioactive compounds were discovered in their cultures.^{7,8} The current study deals with another basidiomycete, *Skeletocutis* sp. (MUCL56074) and the identification and characterization of its bioactive secondary metabolites.

Skeletocutis is a genus of about 40 species in family Polyporaceae. Even though this genus has a worldwide distribution, most of its known species are distributed in the Northern Hemisphere.⁹ Like other polypores, species in this genus are known to be forest pathogens causing white rot in a diverse array of woody plants. Interestingly, some species have been reported to grow on the dead fruiting bodies of other polypores, giving indications to their mycophilic lifestyle. Those include *Skeletocutis brevispora* and *Skeletocutis chrysellia*, which were reported from dead basidiomes of *Phellinidium ferrugineofusum* and *Phellinus chrysoloma*, respectively.¹⁰ Phylogenetically, *Skeletocutis* is closely related to the genus *Tyromyces*, and in recent phylogenetic studies, the two genera clustered together in the “*Tyromyces* clade” on a branch lying outside of the core polyporoid clade.^{11–13}

Herein we report the isolation, structure elucidation and bioactivities of 12 new compounds that are the first secondary metabolites known from *Skeletocutis*, and for which we propose the trivial names skeletocutins A-L accordingly.

Received: April 27, 2019

Revised: July 9, 2019

Accepted: July 16, 2019

Published: July 16, 2019

MATERIAL AND METHODS

General Experimental Procedures. NMR spectra were recorded with Bruker 700 spectrometer with 5 mm TXI cryoprobe (^1H 700 MHz, ^{13}C 175 MHz, ^{15}N 71 MHz) and Bruker AV II-500 (^1H 500 MHz, ^{13}C 125 MHz) spectrometers. HR-ESIMS mass spectra were recorded with Agilent 1200 series HPLC-UV system (column 2.1 \times 50 mm, 1.7 μm , C18 Acquity UPLC BEH (waters), solvent A: H_2O + 0.1% formic acid; solvent B: AcCN + 0.1% formic acid, gradient: 5% B for 0.5 min increasing to 100% in 19.5 min and then maintaining 100% B for 5 min, flow rate 0.6 mL/min, UV-vis detection 200–600 nm combined with ESI-TOF-MS (Maxis, Bruker)) [scan range 100–2500 m/z , capillary voltage 4500 V, dry temperature 200 $^\circ\text{C}$]. UV spectra were recorded by using a Shimadzu UV-2450 UV-vis spectrophotometer.

Fungal Material. The fungal specimen was collected by Decock and Matasyoh from Mount Elgon National Reserve, located in the western part of Kenya (1 $^\circ$ 7'6" N, 34 $^\circ$ 31'30" E). Dried specimen and corresponding cultures were deposited at MUCL, Louvain-la-Neuve, Belgium, under the accession number MUCL 56074. The genus was determined by morphological studies and comparison of the internal transcribed spacer (ITS)-nrDNA sequences with those of other Basidiomycota deposited in GenBank.

For molecular phylogenetic studies, DNA was extracted by using the EZ-10 Spin Column Genomic DNA Miniprep kit (Bio Basic Canada Inc., Markham, Ontario, Canada) as described previously.^{14,17} Precellys 24 homogenizer (Bertin Technologies, France) was used for cell disruption at a speed of 6000 rpm for 2 \times 40 s. Standard primers ITS 1f and NL4 were used for amplification of the 5.8S/ITS nrDNA regions according to the protocol of Lambert et al.¹⁶

Small-Scale Fermentation. *Skeletocutis* sp. MUCL56074 was cultivated in 3 different liquid media: YMG 6.3, Q6 1/2 and ZM 1/2 (media compositions see Supporting Information). A well grown culture from a YMG agar plate (YMG supplemented with 1.5% agar, pH 6.3) was cut into small pieces using a cork borer (7 mm) and five pieces were inoculated in a 500 mL Erlenmeyer flask containing 200 mL of the three media. The cultures were incubated on a rotary shaker (140 rpm) at 24 $^\circ\text{C}$. The growth of the fungus was monitored by constantly checking the amount of free glucose using Medi-test Glucose (Macherey-Nagel). The fermentation was terminated 2 days after glucose depletion.¹⁷

Scale-up of Fermentation. LC-MS dereplication was carried out by comparing the masses of the detected peaks and their molecular formula obtained from HRMS data with those in the Dictionary of natural products (<http://dnp.chemnetbase.com>). Several new compounds in the three media screened were detected in both the extracts from mycelia and supernatants. Preliminary LC-MS results indicated that similar metabolites were produced in all the three media but YMG medium produced the highest amount of metabolites, this medium was used in the scale-up. A well-grown YMG agar plate of mycelial culture was cut into small pieces using 7 mm cork border and five pieces inoculated into 500 mL sterile flasks containing 200 mL (25 flasks).

Preparation of the Extracts. Supernatant and biomass from small scale fermentation were separated by filtration. The supernatant was extracted with equal amount of ethyl acetate and filtered through anhydrous sodium sulfate. The resulting ethyl acetate extract was evaporated to dryness by means of rotary evaporator. The mycelia were extracted with 200 mL of acetone in ultrasonic bath for 30 min, filtered, and the filtrate evaporated. The remaining water phase was mixed with equal amount of distilled water, extracted with equal amount of ethyl acetate, and filtered through anhydrous sodium sulfate and dried by evaporator.

The mycelia and supernatant from the large scale fermentation were separated via vacuum filtration. The mycelia were ultrasonicated for 30 min with 4 \times 500 mL of acetone. The extracts were combined and evaporated and the remaining water phase was suspended in 200 mL distilled water and extracted 3 times with 500 mL ethyl acetate. The organic layer was filtered and evaporated to dryness, leaving brown solid extract (610.2 mg). 5% Amberlite XAD-16N adsorbent

(Rohm & Haas Deutschland GmbH, Frankfurt am Main, Germany) was added to the supernatant and shook overnight. The Amberlite resin was then filtered and eluted with 4 \times 500 mL of acetone. The resulting extract was evaporated and the remaining water phase was extracted three times with equal amount of ethyl acetate. The organic phase was dried by to afford 5.2 g of extract.

Isolation of Compounds 1–13. The extracts from mycelia and supernatant were combined and filtered using an SPME Strata-X 33 u Polymeric RP cartridge (Phenomenex, Inc., Aschaffenburg, Germany). The extract was then fractionated by preparative reverse phase liquid chromatography (PLC 2020, Gilson, Middleton, USA), using VP Nucleodur 100-5 C-18 ec column (25 \times 40 mm, 7 μm : Macherey-Nagel). Deionized water (Milli-Q, Millipore, Schwalbach, Germany) with 0.05% TFA (solvent A) and acetonitrile with 0.05% TFA (solvent B) were used as mobile phase. Elution gradient: 50% solvent B increased to 100% in 60 min and finally isocratic conditions at 100% solvent B for 5 min. The flow rate was 40 mL/min and UV detection was carried out at 210, 254, and 350 nm. A total of 22 fractions were collected according to the observed peaks (F1–F22). Detailed description of the methods can be found in the SI.

Antimicrobial Assays. Compounds 1–13 were evaluated for antimicrobial activity (minimum inhibition concentrations, MIC) in serial dilution assays against several test microorganisms (Table 5) according to our previous research.^{14,15} The assays were conducted in 96-well plates in Mueller-Hinton broth (MHB) media for bacteria and YMG media for filamentous fungi and yeasts.

Cytotoxicity Assays. Compounds 1–13 were evaluated in the cytotoxicity assay against mouse fibroblasts (L929) and HeLa (KB3.1) cell lines as described previously.¹⁷

Biofilm Inhibition Assay. *Staphylococcus aureus* DSM1104 was grown overnight in casein-peptone soymeal-peptone (CASO) medium containing 4% glucose with pH7.0. The *S. aureus* cell concentration was adjusted to match the turbidity of 0.5 McFarland standard. The assay was performed in 96-well flat bottom plates (Falcon Microplates, U.S.A.) as previously described.¹⁸ Methanol was used as negative control; all experiments were carried out in triplicates and cytochalasin B was used as a standard (cf. Yuyama et al.¹⁹)

Nematicidal Assay. The nematicidal activity against *Caenorhabditis elegans* was performed in 24-well microtiter plates as previously described.²⁰ Ivermectin and methanol were used as positive and negative control, respectively. The results were expressed as LD₉₀.

Leucine Aminopeptidases Inhibition Assays. Hydrolysis of *L*-leucine-7-amido-4-methylcoumarin (*L*-Leu-AMC) by the surface bound aminopeptidases of HeLa (KB3.1) cell lines was evaluated according to the method described by Weber et al.²¹ with slight modifications. KB3.1 cells were grown as monolayer cultures in Dulbecco's Modified Eagle (DMEM) medium containing 10% of fetal calf serum at 37 $^\circ\text{C}$ in 24-well multidishes. After 3 days the confluent monolayers were washed twice with phosphate buffered saline (PBS) and the reaction mixture (450 μL Hank's buffer PH 7.2 containing 50 μM and 100 μM substrate *L*-Leu-AMC, and compounds dissolved in 50 μL DMSO) was added. After 30 min of incubation at 23 $^\circ\text{C}$, 1 mL of cold 0.2 M glycine-buffer PH 10.5 was added. The amount of hydrolyzed 7-amino-4-methylcoumarin (AMC) was determined in a fluorescence spectrophotometer (excitation/emission: 365/440 nm; Tecan Infinite M200 PRO). Bestatin²² and DMSO were used as positive control and negative control, respectively.

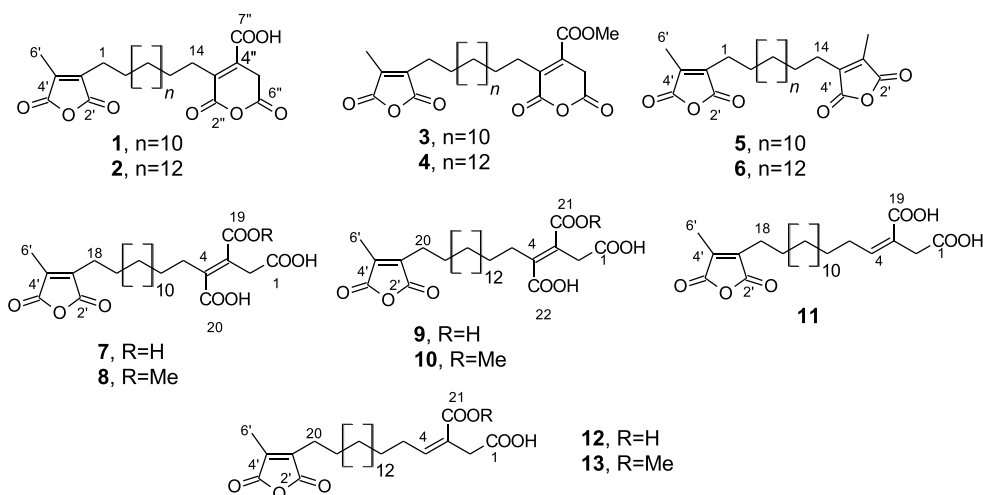
Inhibitory Effects on HCV Infectivity. Compounds 1–13 were tested for antiviral activity against Hepatitis C virus (HVC) as previously described.^{23,24} Detailed information can be found in the SI.

RESULTS AND DISCUSSION

As described in the Experimental section, the strain MUCL56074 was assigned to the genus *Skeletocutis* by morphological studies and sequencing of the rDNA (5.8S gene region and ITS). The BLAST result from GenBank confirmed the identity of this fungus to genus *Skeletocutis* in the Polyporaceae family. The closest hit was the DNA sequence with GenBank acc no KY953026.1 (*Skeletocutis*

Table 1. NMR Data (^1H 500 MHz and ^{13}C 125 MHz) in CDCl_3 for **1** and **2** and (^1H 500 MHz and ^{13}C 125 MHz) in $\text{Acetone-}d_6$ for **3** and **4**

no.	1		2		3		4	
	^{13}C	$^1\text{H}/\text{HSQC}$	^{13}C	$^1\text{H}/\text{HSQC}$	^{13}C	$^1\text{H}/\text{HSQC}$	^{13}C	$^1\text{H}/\text{HSQC}$
1	24.4, CH_2	2.46 (t), $J = 7.78$ Hz	24.4, CH_2	2.45 (t), $J = 7.78$ Hz	24.8, CH_2	2.50 (t), $J = 7.63$ Hz	24.1, CH_2	2.50 (t), $J = 7.48$ Hz
2	27.5, CH_2	1.60 (m)	27.6, CH_2	1.59 (m)	28.3, CH_2	1.60 (m)	28.2, CH_2	1.60 (m)
3–12/ 3–14	29.4–29.6, CH_2	1.26–1.32 (m)	29.1–29.9, CH_2	1.26–1.32 (m)	29.3–30.3, CH_2	1.28–1.36 (m)	29.4–30.3, CH_2	1.28–1.34 (m)
13/15	27.5, CH_2	1.62 (m)	27.6, CH_2	1.59 (m)	28.3, CH_2	1.61 (m)	28.3, CH_2	1.61 (m)
14/16	24.9, CH_2	2.50 (t), $J = 7.63$ Hz	27.6, CH_2	24.9 (t), $J = 7.63$ Hz	25.2, CH_2	2.57 (t), $J = 7.63$ Hz	25.2, CH_2	2.56 (t), $J = 7.78$ Hz
2'	165.9, C		165.9, C		167.2, C		167.2, C	
3'	144.8, C		144.8, C		145.0, C		145.0, C	
4'	140.5, C		140.4, C		141.8, C		141.8, C	
5'	166.3, C		166.3, C		167.4, C		167.4, C	
6'	9.5, CH_3	2.08 (s)	9.5, CH_3	2.07 (s)	9.6, CH_3	2.08 (s)	9.6, CH_3	2.08 (s)
2''	165.1, C		165.9, C		166.7, C		166.7, C	
3''	148.0, C		148.0, C		148.0, C		148.0, C	
4''	135.6, C		135.6, C		137.9, C		137.9, C	
5''	29.0, CH_2	3.57 (s)	29.1, CH_2	3.57 (s)	39.9, CH_2	3.68 (s)	30.1, CH_2	3.68 (s)
6''	165.1, C		165.9, C		166.4, C		166.4, C	
7''	171.5, C		171.3, C		169.0, C		169.1, C	
					52.6, OCH_3	3.7 (s)	52.9, OCH_3	3.7 (s)

**Figure 1.** Chemical structures of compounds **1**–**12**.

nivea) with 96.99% identity (see Figure S106, Supporting Information), from which no metabolites had hitherto been reported.

The extracts from small scale fermentation of *Skeletocutis* sp. (strain MUCL 56074) exhibited good antibacterial activity (4.68 $\mu\text{g}/\text{mL}$) against *Bacillus subtilis*. Moreover, analyses of the secondary metabolite profiles by HPLC-MS pointed toward the presence of several hitherto unknown compounds. Therefore, extensive chromatographic studies of the extract as described in the Experimental Section were conducted and finally led to the isolation of 12 new compounds named skelotocutins A–L. Their characteristics are reported further below.

Compound **1** (skelotocutin A) with the molecular formula $\text{C}_{25}\text{H}_{34}\text{O}_8$ and nine degrees of unsaturation deduced from the HR-ESIMS spectrum was isolated as a white solid. The ^{13}C NMR spectroscopic data of **1** (Table 1) revealed the presence of 25 carbon signals, which could further be classified into one

methyl carbon, 15 methylene carbons and nine nonprotonated carbons (including five attached to heteroatoms) in the DEPT NMR spectrum. The HMBC correlations of $\text{H}_3\text{-6}'$ (δ 2.08) to $\text{C-3}''/\text{C-4}''/\text{C-5}''$ and $\text{H}_2\text{-1}$ to $\text{C-2}''/\text{C-3}''/\text{C-4}''$ confirmed the maleic anhydride moiety in the molecule. The presence of the glutaric anhydride moiety was revealed by HMBC correlations of $\text{H}_2\text{-14}$ (δ 2.50) to $\text{C-2}''/\text{C-3}''/\text{C-4}''$ and $\text{H}_2\text{-5}''$ (δ 3.57) to $\text{C-3}''/\text{C-4}''/\text{C-6}''$. Further, HMBC correlations of $\text{H-5}''$ to $\text{C-7}''$ confirmed the position of the $\text{C-7}''$ carboxylic acid substituent. COSY correlations of $\text{H}_2\text{-1}$ triplet (δ 2.46) to $\text{H}_2\text{-2}$ (δ 1.60) and $\text{H}_2\text{-13}$ (δ 1.62) to $\text{H}_2\text{-14}$ triplet (δ 2.50) were also observed. A multiplet resonating between (δ 1.26–1.32) was attributed to the remaining ten methylene groups of the tetradecamethylene chain in the molecule. This was further confirmed by the integration of the multiplet, which gave an integral value of 20, confirming the 20 methylene protons or C-3 to C-12. The connection of the tetradecamethylene chain to the maleic and glutaric anhydride moieties was confirmed by

HMBC correlations of H₂-1/H₂-2 to C-3' and H₂-13/H₂-14 to C-3'', respectively. Therefore, the structure of **1** was unambiguously concluded to be 5''-[14-(4'-methyl-2,5-dioxo-2,5-dihydrofuran-3-yl)tetradecyl]-2'',6''-dioxo-2'',6''-dihydropyran-4''-carboxylic acid (Figure 1).

Compound **2**, which had the molecular formula C₂₇H₃₈O₈ derived from HR-ESIMS data, was isolated as white solid. 1D and 2D NMR data of **2** pointed to a similar structure as **1** with the difference being the size of the carbon chain in the molecule. The multiplet occurring at δ 1.26–1.32 for the methylene groups (C-3-C-14) in **2** gave an integral value of 24 indicating a hexadecamethylene chain in the molecule instead of the tetradecamethylene chain elucidated for compound **1**. This was further supported by the fact that the two molecules mass difference was 28, which is equivalent to the mass of two methylene groups. The structure of **2** was therefore concluded to be 5''-[16-(4'-methyl-2',5'-dioxo-2',5'-dihydrofuran-3'-yl)-tetradecyl]-2'',6''-dioxo-2'',6''-dihydropyran-4''-carboxylic acid that we propose the trivial name skeletocutin B.

Compound **3** (skeletocutin C) with the molecular formula C₂₆H₃₆O₈ and 9 degrees of unsaturation and compound **4** with molecular formula C₂₈H₄₀O₈ and 9 degrees of unsaturation were obtained as yellow solid and white solid, respectively. Analysis of the ¹³C NMR spectra of **2** revealed a structure closely related to that of **1** with the difference being methoxy group signal occurring at δ 52.6. The methoxy group proton (δ 3.70) showed HMBC correlations to C-7'' (δ 169.0). Similarly, for compound **4** (skeletocutin D), the 1D and 2D NMR data indicated a similar structure as **2** with the difference being a methoxy group (δ 52.9) whose proton (δ 3.70) showed a HMBC correlation to C-7'' (δ 169.1).

Compound **5** (skeletocutin E), which was obtained as yellow oil, had the molecular formula C₂₄H₃₄O₆ and eight degrees of unsaturation. The ¹³C NMR spectrum of **5** showed only 12 signals which indicates that the compound consisted of two identical halves. A methyl singlet resonance at δ 2.07 (H₃-6') along with methylene groups triplet and quintet occurring at δ 2.45 (H₂-1/H₂-14) and δ 1.57 (H₂-2/H₂-13) respectively were observed in the ¹H NMR spectrum (Table 2). HMBC correlations of the C-6' methyl group proton (δ 2.07) to C-3'/C-4'/C-5' and H₂-1/H₂-14 to C-2'/C-3'/C-4' confirmed the maleic anhydride moiety in the molecule. Integration of the methyl singlet (H₃-6') gave an integral value of 6 confirming the presence of two maleic anhydride groups. The multiplet occurring between δ 1.26–1.32 was attributed to the

remaining ten methylene groups of carbon chain. The integral value of 20 obtained for this multiplet confirmed the chain length. Cross peaks in the HMBC spectrum between the H₂-1/H₂-14 and H₂-2/H₂-13 and C-3' confirmed the connection of the chain to the two maleic anhydride and therefore confirming the structure of **5** to be 1,14-bis [4'-methyl-2',5'-dioxo-3'-furyl] tetradecane. Compound **5** has been reported before as a product of chemical synthesis, but to the best of our knowledge it has never before been isolated from a natural source. The published MS data and ¹H and ¹³C NMR data reported for the synthetic product matched our own findings.²⁵

Compound **6** was isolated as white crystalline solid. The HR mass spectrum revealed the molecular formula to be C₂₆H₃₈O₆ with nine degrees of unsaturation. This compound was identified as tyromycin A by comparing its NMR and HR-MS data previously reported from *Tyromyces lacteus*, which belongs to the same family (Polyporaceae) as *Skeletocutis*.²¹ An efficient one-step synthesized of this compound using double radical decarboxylation has also been reported.²⁵

Compound **7** (skeletocutin F) with the molecular formula C₂₅H₃₆O₉ and eight degrees of unsaturation was isolated as yellow solid. Analysis of the 1D and 2D NMR data of **7** (Table 3) indicated the presence of the maleic anhydride like in the other compounds described above. Further, the HMBC correlations of H₂-18 (δ 2.39) to C-2'/C-3'-C4' confirmed the linkage of this moiety to the 14-carbon chain in the molecule. The three carboxylic acid moieties for the tricarboxylic acid part of the molecule had resonance at δ 171.5 (C-1), 171.4 (C-19), and 170.2 (C-20) in the ¹³C NMR spectrum. Cross peaks in the HMBC spectrum were observed between H₂-2 and C-1/C-3/C-4/C-19. HMBC correlations of H₂-5 to C-3/C-4/C-20 confirmed the connection of the tricarboxylic acid moiety to the chain and the position of C-20. The COSY correlations of H₂-5 to H₂-6 and H₂-18 to H₂-17 were also recorded. The olefinic bond between C-3 and C-4 was assigned the *E* configuration due to the absence of cross peaks in the ROESY spectra between the C-2 and C-5 methylene protons. The integration of the multiplet signal at δ 1.23–1.30 indicated ten additional methylene groups and hence the compound was identified as 3*E*-18-(4'-methyl-2',5'-dioxo-2',5'-dihydrofuran-3'-yl) octadecane-1,2,3-tricarboxylic acid.

Compound **8** (skeletocutin G) with molecular formula C₂₆H₃₈O₉ and 8 degrees of unsaturation was isolated as white solid. The ¹³C NMR spectra of **8** revealed a structure closely related to that of **7** with the difference being methoxy group, indicated by a signal occurring at δ 52.8. The methoxy group proton (δ 3.74) showed HMBC correlations to C-19 (δ 171.8).

Compound **9** (skeletocutin H), which was designated the molecular formula C₂₇H₄₀O₉ from the HRMS data was obtained as white solid. The 1 and 2D NMR data indicated a similar structure as **7** with the difference being the size of the carbon chain. The multiplet occurring at δ 1.28–1.36 for the methylene groups C-7-C-18 gave an integral value of 24 indicating icosane-1,2,3-tricarboxylic acid in the molecule instead of the octadecane-1,2,3-tricarboxylic acid elucidated in compound **7**.

Compound **10** (skeletocutin I) with molecular formula C₂₈H₄₂O₉, 1 and 2D NMR data indicated a similar structure as **9** with the difference being a methoxy group (δ 52.5) whose proton (δ 3.74) showed HMBC correlation to C-21 (δ 170.6).

Table 2. NMR Data (¹H 500 MHz and ¹³C 125 MHz) in CDCl₃ for **5** and (¹H 500 MHz and ¹³C 125 MHz) in DMSO for **6**

no.	5		6	
	¹³ C/HSQC	¹ H	¹³ C/HSQC	¹ H
1/14/16	24.4, CH ₂	2.45 (t), J = 7.78 Hz	23.6, CH ₂	2.40 (t), J = 7.53 Hz
2/13/15	3, CH ₂	1.57 (p), J = 7.78 Hz	26.7, CH ₂	1.48 (p), J = 7.53 Hz
3–12/14	29.1–29.6, CH ₂	1.26–1.32 (m)	28.6–29.0, CH ₂	1.23–1.29 (m)
2'	165.9, C		166.2, C	
3'	144.8, C		143.4, C	
4'	140.4, C		140.8, C	
5'	166.3, C		166.4, C	
6'	9.5, CH ₃	2.08 (s)	9.2, CH ₃	1.99 (s)

Table 3. NMR Data (^1H 500 MHz and ^{13}C 125 MHz) in DMSO for **7** (^1H 500 MHz and ^{13}C 125 MHz) in Acetone- d_6 for **9** and (^1H 500 MHz and ^{13}C 125 MHz) in CDCl_3 for **8** and **10**

7		8		9		10			
no.	$^{13}\text{C}/\text{HSQC}$	^1H	$^{13}\text{C}/\text{HSQC}$	^1H	no.	$^{13}\text{C}/\text{HSQC}$	^1H	$^{13}\text{C}/\text{HSQC}$	^1H
1	171.5, C		170.7, C		1	171.9, C		172.3, C	
2	36.9, CH_2	3.30 (s)	36.5, CH_2	3.60 (s)	2	37.4, CH_2	3.56 (s)	36.5, CH_2	3.61 (s)
3	128.0, C		128.1, C		3	129.5, C		128.2, C	
4	143.5, C		145.8, C		4	144.9, C		145.9, C	
5	30.4, CH_2	2.53 (t), $J = 7.9$ Hz	31.5, CH_2	2.72 (t), $J = 7.93$ Hz	5	31.9, CH_2	2.70 (t), $J = 7.93$ Hz	31.5, CH_2	2.73 (t), $J = 7.78$ Hz
6	28.1, CH_2	1.36 (q), $J = 6.71$ Hz	28.7, CH_2	1.54 (m)	6	29.5, CH_2	1.52 (br p), $J = 7.50$ Hz	28.7, CH_2	1.53 (m)
7/16	28.6–29.0, CH_2	1.2–1.30 (m)	29.2–29.7, CH_2	1.26–1.36(m)	7/18	29.3–30.4, CH_2	1.28–1.36 (m)	29.2–29.6, CH_2	1.25–1.31 (m)
17	26.9, CH_2	1.48 (q), $J = 7.48$ Hz	27.6, CH_2	1.57 (m)	19	28.3, CH_2	1.59 (br p), $J = 7.48$ Hz	27.7, CH_2	1.57 (m)
18	23.6, CH_2	2.39, (s), $J = 7.48$ Hz	24.4, CH_2	2.45 (s), $J = 7.71$ Hz	20	24.8, CH_2	2.50, (s), $J = 7.63$ Hz	24.4, CH_2	2.46, (t), $J = 8.09$ Hz
19	171.4, C		171.8, C		21	169.0, C		171.6, C	
20	170.2, C		171.6, C		22	170.5, C		171.8, C	
2'	166.2, C		165.9, C		2'	167.2, C		165.9, C	
3'	143.5, C		144.8, C		3'	145.0, C		144.8, C	
4'	140.9, C		140.4, C		4'	141.8, C		140.5, C	
5'	166.4, C		166.3, C		5'	167.4, C		166.3, C	
6'	9.2, CH_3	1.99 (s)	9.5, CH_3	2.08 (s)	6'	9.6, CH_3	2.08 (s)	9.5, CH_3	2.08 (s)
			52.8, OCH_3	3.74 (s)				52.5, OCH_3	3.74 (s)

Table 4. NMR Data (^1H 500 MHz and ^{13}C 125 MHz) in CDCl_3 CDCl_3 for **11–13**

11			12			13			
no.	$^{13}\text{C}/\text{HSQC}$	^1H	no.	$^{13}\text{C}/\text{HSQC}$	^1H	$^{13}\text{C}/\text{HSQC}$	^1H	$^{13}\text{C}/\text{HSQC}$	^1H
1	176.3, C		1	177.2, C		171.2, C			
2	32.1, CH_2	3.37 (s)	2	32.1, CH_2	3.37 (s)	31.8, CH_2	3.36 (s)		
3	124.4, C		3	124.5, C		124.6, C			
4	148.9, CH	7.11 (t), $J = 7.48$ Hz	4	148.9, CH	7.12 (t), $J = 7.48$ Hz	148.8, CH	7.10 (t), $J = 7.63$ Hz		
5	29.2, CH_2	2.23 (q), $J = 7.48$ Hz	5	29.1, CH_2	2.22 (q), $J = 7.48$ Hz	28.7, CH_2	2.21 (q), $J = 7.63$ Hz		
6	28.3, CH_2	1.47 (p), $J = 7.48$ Hz	6	28.3, CH_2	1.47 (p), $J = 7.48$ Hz	28.3, CH_2	1.47 (p), $J = 7.63$ Hz		
7–16	29.2–29.6, CH_2	1.26–1.31 (m)	7–18	29.1–29.6, CH_2	1.26–1.31 (m)	29.4–2.6, CH_2	1.26–1.32(m)		
17	27.5, CH_2	1.58 (P), $J = 7.63$ Hz	19	27.5, CH_2	1.58 (p), $J = 7.55$ Hz	27.6, CH_2	1.58 (p), $J = 7.32$ Hz		
18	24.4, CH_2	2.46, (t), $J = 7.63$ Hz	20	24.4, CH_2	2.45, (t), $J = 7.55$ Hz	24.4, CH_2	2.45, (t), $J = 7.32$ Hz		
19	171.9, C		21	172.4, C		171.2, C			
2'	165.9, C		2'	165.9, C		165.9, C			
3'	144.8, C		3'	144.8, C		144.8, C			
4'	140.4, C		4'	140.4, C		140.4, C			
5'	166.3, C		5'	166.3, C		166.3, C			
6'	9.5, CH_3	2.07 (s)	6'	9.5, CH_3	2.07 (s)	9.5, CH_3	2.07 (s)		
						52.1, OCH_3	3.69 (s)		

Compound **11** (skeletalocutin J), which was assigned the molecular formula $\text{C}_{24}\text{H}_{36}\text{O}_7$ from the HRMS data, was isolated as white oil. Analysis of the 1D and 2D NMR data suggested a structure closely related to that of **7**, with the difference being the absence of the tricarboxylic acid moiety and the presence of a dicarboxylic acid moiety instead. HMBC correlations of H_2 -2 to C-1/C-3/C-4/C-19, H-4 to C-2/C-19/C-5/C-6 and H_2 -5 to C-3/C-4/C-6 were observed. Further, COSY correlations of H_2 -5 to H-4/ H_2 -6 were also recorded. The olefinic bond between C-4 and C-5 was assigned the *cis* configuration because of the small coupling constant of 7.48 Hz recorded. Therefore, the structure of **11** was concluded to be (3*Z*)-3-[6-(4'-methyl-2',5'-dioxo-2',5'-dihydrofuran-3'-yl)pentadecene]butanedioic acid.

Compound **12** (skeletalocutin K) which was isolated as yellow oil, had molecular formula $\text{C}_{26}\text{H}_{40}\text{O}_7$ deduced from the HR mass spectrum. The 1 and 2 D NMR data revealed a similar structure as **11** but the integration of the methylene groups' multiplet occurring between δ 1.26–1.31 gave an integral value of 24 suggesting a 16 carbon chain. Also, the mass difference between these two compounds is 28 i. e two methylene groups. Hence, the structure of **12** was unambiguously assigned as (3*Z*)-3-[6-(4'-methyl-2',5'-dioxo-2',5'-dihydrofuran-3'-yl)heptadecene]butanedioic acid (Table 4).

Compound **13** (skeletalocutin L), which was designated the molecular formula $\text{C}_{27}\text{H}_{42}\text{O}_7$ from the HRMS data was isolated as yellow oil. The 1D and 2 D NMR data indicated a similar structure as **12** with the difference being a methoxy group (δ

Table 5. Antimicrobial Activities of Compounds 1–13

organism	MIC ($\mu\text{g/mL}$)									
	1	2	3	4	5	6	11	12	13	ref
<i>Bacillus subtilis</i> DSM10	150	18.75	37.5	75	18.75	9.375	300		18.75	3.1 ^a
MRSA <i>Staphylococcus aureus</i> DSM11822	150	150	300	300	150	150	150	75	75	0.4 ^b
<i>Staphylococcus aureus</i> DSM346	37.5	300	150	150	37.5	150	150	37.5	18.75	6.7 ^c
<i>Micrococcus luteus</i> DSM20030	150				150	150		150	37.5	0.4 ^c

^aCiprofloxacin. ^bVancomycin. ^cOxytetracycline.

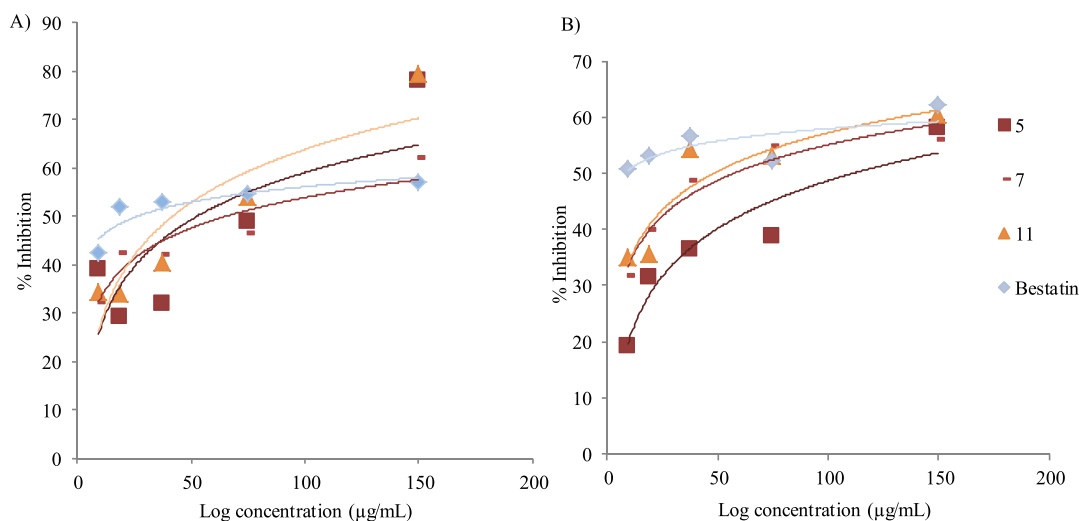


Figure 2. Inhibition of hydrolysis of leu-AMC (A) concentration of L -Leu-AMC: 100 μM and (B) concentration of L -Leu-AMC: 50 μM .

52.1). The protons of the methoxy group (δ 3.69) showed a HMBC correlation to C-21 (δ 171.2).

Biological Activity. Compounds 1–13 were evaluated for their antimicrobial activity against different organisms (Table 5). All tested compounds except for 7–10 showed moderate activity against *Bacillus subtilis*, *Staphylococcus aureus*, and *Micrococcus luteus* with compounds 1–3, 5–6, and 12–13 exhibiting the highest activity in the range of 9.38–37.5 $\mu\text{g/mL}$. Further, the compounds demonstrated weak activities against MRSA (methicillin resistant *Staphylococcus aureus*). Neither of the compounds showed any activity against the tested Gram negative bacteria (*Chromobacterium violaceum*, *Escherichia coli*, *Mycobacterium smegmatis*, and *Pseudomonas aeruginosa*) nor fungi (*Candida albicans*, *Candida tenuis*, *Mucor plumbeus*, and *Pichia anomala*).

All compounds were also tested for nematicidal activities against *Caenorhabditis elegans* and cytotoxicity against mouse fibroblast (L929) and HeLa (KB 3.1) cell lines but they did not show any significant activities in these assays at concentrations ≤ 100 $\mu\text{g/mL}$ and 37 $\mu\text{g/mL}$, respectively. Compounds that did not show any significant activity (i.e with MIC ≥ 150 $\mu\text{g/mL}$) against *S. aureus* were subjected to the biofilm inhibition assay against *S. aureus* biofilm. Only compound 10 inhibited the formation of the biofilm up to 86% at 256 $\mu\text{g/mL}$ and 28% at 150 $\mu\text{g/mL}$. Tyromycin A (6) was reported before as an inhibitor of leucine aminopeptidase in HeLa S3 cells,²¹ hence the novel analogues were also tested for inhibition of L -Leu-AMC hydrolysis in HeLa (KB 3.1) cells. Only compounds 5, 7, 11, and 13 were weakly active in this assay with IC₅₀ values in the range 72.3–92.5 and 78.3–118.4 $\mu\text{g/mL}$ when 100 and 50 μM of the substrate were used, respectively (Figure 2 and Table 6). Even though tyromycin A

Table 6. Inhibition of L -Leu-AMC by the Metabolites from *Skeletocutis* sp

compounds	IC ₅₀ ($\mu\text{g/mL}$)	
	substrate (100 μM)	substrate (50 μM)
5	84	118.4
7	92.5	89.7
11	72.3	78.3
13	88.7	113.9
bestatin	10.8	40.9

(6) was previously reported to be active in a similar assay against HeLa S3 cells with IC₅₀ values of 31 $\mu\text{g/mL}$ at 50 μM substrate concentration, an IC₅₀ value >150 $\mu\text{g/mL}$ for this compound was recorded on the HeLa (KB3.1) cells when tested in this study.

Furthermore, all of the compounds were tested for their antiviral activity against hepatitis C virus (HCV), which is one of the major causes of chronic liver disease, with 71 million people infected worldwide. Although curative medications are available for HCV, the majority of infected individuals do not having an access to treatment due to high cost of the treatment. In a cellular replication assay to evaluate antiviral activity against HCV in human liver cells (Figure 3), compound 6 strongly inhibited HCV infectivity at the initial concentration 40 μM while compounds 4 and 5 inhibited HCV with moderate activity. Compounds 1, 3 and 13 showed weak activity and the rest of compound were not active. All tested compounds except for 6 were found devoid of cytotoxicity on the liver cells. We therefore next evaluated the antiviral activity of 6 against HCV in a dose dependent manner. As depicted in Figure 3C, incubation of 6 for 3 days

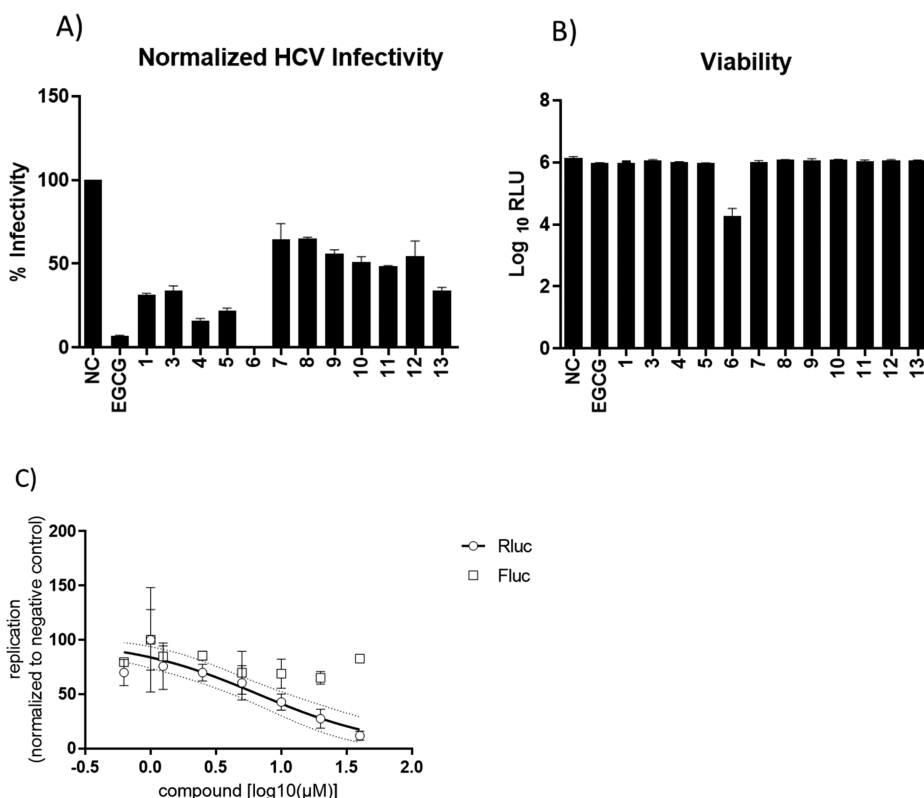


Figure 3. Antiviral activity of compound 1-13 against Hepatitis C virus (HCV). Huh-7.5 cells were inoculated with RLuc-Jc1 reporter viruses in the presence of the compounds. The inoculum was removed 4 h later and monolayers were washed three times with PBS and overlaid with fresh medium containing no inhibitors. Infected cells were lysed 3 days later, and reporter virus infection was determined by the *Renilla* luciferase activity (A). The cell viability was measured by determination of *Firefly* luciferase (B), which is stably expressed in the target cells. Dose-dependent inhibition of HCV infectivity was observed after treatment with compound 6 for 3 days (C).

resulted in a dose-dependent inhibition of HCV infectivity with a 50% inhibitory concentration (IC_{50}) of 6.6 μ M. The green tea molecule epigallocatechin gallate (EGCG) was used as positive control.²⁴

Skeletocutin A (1). White solid; UV (MeOH) $\lambda_{max}(\log \epsilon)$ 209 (4.54), 257 (3.02); ESIMS m/z 947 [2 M + Na]⁺, 485 [M + Na]⁺, 463 [M + H]⁺, 445 [M + H - H₂O]⁺; HRMS m/z 463.2330 [M + H]⁺ (calcd for C₂₅H₃₅O₈, 463.2331).

Skeletocutin B (2). White solid; UV (MeOH) $\lambda_{max}(\log \epsilon)$ 206 (4.54), 256 (3.02); ESIMS m/z 1003 [2 M + Na]⁺, 513 [M + Na]⁺, 491 [M + H]⁺, 473 [M + H - H₂O]⁺; HRMS m/z 491.2646 [M + H]⁺ (calcd for C₂₇H₃₉O₈, 491.2645).

Skeletocutin C (3). Yellow solid; UV (MeOH) $\lambda_{max}(\log \epsilon)$ 215 (4.65), 256 (3.17); ESIMS m/z 975 [2 M + Na]⁺, 499 [M + Na]⁺, 477 [M + H]⁺, 459 [M + H - H₂O]⁺; HRMS m/z 477.2470 [M + H]⁺ (calcd for C₂₆H₃₇O₈, 477.2488).

Skeletocutin D (4). White solid; UV (MeOH) $\lambda_{max}(\log \epsilon)$ 222 (4.39), 253 (3.61); ESIMS m/z 1031 [2 M + Na]⁺, 527 [M + Na]⁺, 505 [M + H]⁺, 487 [M + H - H₂O]⁺; HRMS m/z 505.2798 [M + H]⁺ (calcd for C₂₈H₄₁O₈, 505.2801).

Skeletocutin E (5). Yellow oil; UV (MeOH) $\lambda_{max}(\log \epsilon)$ 207 (4.39), 253 (3.65); ESIMS m/z 859 [2 M + Na]⁺, 441 [M + Na]⁺, 419 [M + H]⁺, 401 [M + H - H₂O]⁺; HRMS m/z 419.2429 [M + H]⁺ (calcd for C₂₄H₃₅O₆, 419.2433).

Tyromycin A (6). White crystalline solid; UV (MeOH) $\lambda_{max}(\log \epsilon)$ 214 (3.74), 256 (3.62); ESIMS m/z 915 [2 M + Na]⁺, 469 [M + Na]⁺, 447 [M + H]⁺, 429 [M + H - H₂O]⁺; HRMS m/z 447.2738 [M + H]⁺ (calcd for C₂₆H₃₉O₆, 447.2746).

Skeletocutin F (7). Yellow solid; UV (MeOH) $\lambda_{max}(\log \epsilon)$ 215 (4.48), 252 (3.08); ESIMS m/z 983 [2 M + Na]⁺, 503 [M + Na]⁺, 481 [M + H]⁺, 463 [M + H - H₂O]⁺; HRMS m/z 481.2422 [M + H]⁺ (calcd for C₂₅H₃₇O₉, 481.2437).

Skeletocutin G (8). White solid; UV (MeOH) $\lambda_{max}(\log \epsilon)$ 214 (4.20), 253 (4.33); ESIMS m/z 1011 [2 M + Na]⁺, 517 [M + Na]⁺, 495 [M + H]⁺, 477 [M + H - H₂O]⁺; HRMS m/z 495.2576 [M + H]⁺ (calcd for C₂₆H₃₉O₉, 495.2594).

Skeletocutin H (9). White solid; UV (MeOH) $\lambda_{max}(\log \epsilon)$ 227 (4.09), 256 (3.68); ESIMS m/z 1039 [2 M + Na]⁺, 531 [M + Na]⁺, 509 [M + H]⁺, 491 [M + H - H₂O]⁺; HRMS m/z 509.2746 [M + H]⁺ (calcd for C₂₇H₄₁O₉, 509.2750).

Skeletocutin I (10). White solid; UV (MeOH) $\lambda_{max}(\log \epsilon)$ 218 (4.28), 255 (3.40); ESIMS m/z 1067 [2 M + Na]⁺, 545 [M + Na]⁺, 523 [M + H]⁺, 505 [M + H - H₂O]⁺; HRMS m/z 523.2904 [M + H]⁺ (calcd for C₂₈H₄₃O₉, 523.2907).

Skeletocutin J (11). White oil; UV (MeOH) $\lambda_{max}(\log \epsilon)$ 218 (4.27), 256 (3.87); ESIMS m/z 895 [2 M + Na]⁺, 459 [M + Na]⁺, 437 [M + H]⁺, 419 [M + H - H₂O]⁺; HRMS m/z 437.2519 [M + H]⁺ (calcd for C₂₄H₃₇O₇, 437.2539).

Skeletocutin K (12). Yellow oil; UV (MeOH) $\lambda_{max}(\log \epsilon)$ 216 (4.505), 253 (4.02); ESIMS m/z 951 [2 M + Na]⁺, 487 [M + Na]⁺, 465 [M + H]⁺, 447 [M + H - H₂O]⁺; HRMS m/z 465.2850 [M + H]⁺ (calcd for C₂₆H₄₁O₇, 465.2852).

Skeletocutin L (13). Yellow oil; UV (MeOH) $\lambda_{max}(\log \epsilon)$ 218 (4.21), 259 (3.97); ESIMS m/z 979 [2 M + Na]⁺, 501 [M + Na]⁺, 479 [M + H]⁺, 461 [M + H - H₂O]⁺; HRMS m/z 479.2993 [M + H]⁺ (calcd for C₂₇H₄₃O₇, 479.3008).

■ ASSOCIATED CONTENT

Supporting Information

The Supporting Information is available free of charge on the ACS Publications website at DOI: 10.1021/acs.jafc.9b02598.

Experimental procedures, 1D and 2D NMR data, LCMS data, 5.8S/ITS DNA sequence of the producing organism (PDF)

■ AUTHOR INFORMATION

Corresponding Author

*Tel: +49-53161814240. Fax: +49-53161819499. E-mail: marc.stadler@helmholtz-hzi.de.

ORCID

Marc Stadler: 0000-0002-7284-8671

Author Contributions

^C.C. and T.C. contributed equally to this work.

Notes

The authors declare no competing financial interest.

■ ACKNOWLEDGMENTS

We are grateful to W. Collisi for conducting the cytotoxicity assays, C. Kakoschke for recording NMR data, and C. Schwager and E. Surges for recording HPLC-MS data. Financial support by the "ASAFEM" Project (Grant no. IC-070) under the ERAfrica Programme of the European Commission to C.D., J.C.M., and M.S. is gratefully acknowledged. Personal Ph.D. stipends from the German Academic Exchange Service (DAAD), the Kenya National Council for Science and Technology (NACOSTI), and the China Scholarship Council (CSC), to C.C., D.P., and T.C., respectively, are gratefully acknowledged.

■ REFERENCES

- (1) Sandargo, B.; Chepkirui, C.; Cheng, T.; Chaverra-Muñoz, L.; Thongbai, B.; Stadler, M.; Hüttel, S. Biological and chemical diversity go hand in hand: Basidiomycota as source of new pharmaceuticals and agrochemicals. *Biotechnol. Adv.* **2019**, S0734, 30011–30014, DOI: 10.1016/j.biotechadv.2019.01.011.
- (2) Chepkirui, C.; Richter, C.; Matasyoh, J. C.; Stadler, M. Monochlorinated calocerins A-D and 9-oxostrobilurin derivatives from the basidiomycete *Favolaschia calocera*. *Phytochemistry* **2016**, 132, 95–101.
- (3) Mudalungu, C. M.; Richter, C.; Wittstein, K.; Abdalla, M. A.; Matasyoh, J. C.; Stadler, M.; Süßmuth, R. D. Laxitextines A and B, cyathane xylosides from the tropical fungus *Laxitextum incrustatum*. *J. Nat. Prod.* **2016**, 79, 894–898.
- (4) Chepkirui, C.; Matasyoh, J. C.; Decock, C.; Stadler, M. Two cytotoxic triterpenes from cultures of a Kenyan *Laetiporus* sp. (Basidiomycota). *Phytochem. Lett.* **2017**, 20, 106–110.
- (5) Chepkirui, C.; Yuyama, K. T.; Wanga, L. A.; Decock, C.; Matasyoh, J. C.; Abraham, W.-R.; Stadler, M. Microporenic acids A-G, biofilm inhibitors, and antimicrobial agents from the basidiomycete *Microporus* species. *J. Nat. Prod.* **2018**, 81, 778–784.
- (6) Chepkirui, C.; Sum, W. C.; Cheng, T.; Matasyoh, J. C.; Decock, C.; Stadler, M. Aethiopinolones A-E, new pregnenolone type steroids from the East African basidiomycete *Fomitiporia aethiopica*. *Molecules* **2018**, 23, 369.
- (7) Cheng, T.; Chepkirui, C.; Decock, C.; Matasyoh, J. C.; Stadler, M. Sesquiterpenes from an Eastern African medicinal mushroom belonging to the genus *Sanguangporus*. *J. Nat. Prod.* **2019**, 82, 1283–1291.
- (8) Chepkirui, C.; Cheng, T.; Matasyoh, J. C.; Decock, C.; Stadler, M. An unprecedented spiro [furan-2,1'-indene]-3-one derivative and other nematocidal and antimicrobial metabolites from *Sanguangporus*

sp. (Hymenochaetaceae, Basidiomycota) collected in Kenya. *Phytochem. Lett.* **2018**, 25, 141–146.

(9) Cui, B.-K.; Dai, Y.-C. *Skeletocutis luteolus* sp. nov. from southern and eastern China. *Mycotaxon* **2008**, 104, 97–101.

(10) Ryvardeen, L.; Melo, I. Poroid fungi of Europe. *Synopsis Fungorum* **2017**, 37.

(11) Yao, Y.-J.; Pegler, D. N.; Chase, M. W. Application of ITS (nrDNA) sequences in the phylogenetic study of *Tyromyces* s.l. *Mycol. Res.* **1999**, 103, 219–229.

(12) Kim, S.-Y.; Park, S.-Y.; Jung, H.-S. Phylogenetic classification of *Antrrodia* and related genera based on ribosomal RNA internal transcribed spacer sequences. *J. Microbiol. Biotechnol.* **2001**, 11, 475–481.

(13) Floudas, D.; Hibbett, D. S. Revisiting the taxonomy of *Phanerochaete* (Polyporales, Basidiomycota) using a four gene dataset and extensive its sampling. *Fungal Biol.* **2015**, 119, 679–719.

(14) Richter, C.; Helaly, S. E.; Thongbai, B.; Hyde, K. D.; Stadler, M. Pyriatriatins A and B: pyridino-cyathane antibiotics from the basidiomycete *Cyathus cf. striatus*. *J. Nat. Prod.* **2016**, 79, 1684–1688.

(15) Wendt, L.; Sir, E. B.; Kuhnert, E.; Heitkämper, S.; Lambert, C.; Hladki, A. I.; Romero, A. I.; Luangsa-Ard, J. J.; Srikitikulchai, P.; Peršoh, D.; Stadler, M. Resurrection and emendation of the Hypoxylaceae, recognised from a multigene phylogeny of the Xylariales. *Mycol. Prog.* **2018**, 17, 115–154.

(16) Lambert, C.; Wendt, L.; Hladki, A. I.; Stadler, M.; Sir, E. B. *Hypomontagnella* (Hypoxylaceae): a new genus segregated from *Hypoxylon* by a polyphasic taxonomic approach. *Mycol. Prog.* **2019**, 18, 187–201.

(17) Kuhnert, E.; Surup, F.; Herrmann, J.; Huch, V.; Müller, R.; Stadler, M. Rickenyls A-E, antioxidative terphenyls from the fungus *Hypoxylon rickii* (Xylariaceae, Ascomycota). *Phytochemistry* **2015**, 118, 68–73.

(18) Yuyama, K. T.; Chepkirui, C.; Wendt, L.; Fortkamp, D.; Stadler, M.; Abraham, W.-R. Bioactive compounds produced by *Hypoxylon fragiforme* against *Staphylococcus aureus* biofilms. *Microorganisms* **2017**, 5, 80.

(19) Yuyama, K. T.; Wendt, L.; Surup, F.; Kretz, R.; Chepkirui, C.; Wittstein, K.; Boonlarppradab, C.; Wongkanoun, S.; Luangsa-Ard, J.; Stadler, M.; Abraham, W. R. Cytochalasins act as inhibitors of biofilm formation of *Staphylococcus aureus*. *Biomolecules* **2018**, 8, 129.

(20) Rupcic, Z.; Chepkirui, C.; Hernández-Restrepo, M.; Crous, P.; Luangsa-Ard, J.; Stadler, M. New nematocidal and antimicrobial secondary metabolites from a new species in the new genus, *Pseudobambusicola thailandica*. *Myckeys* **2018**, 33, 1–23.

(21) Weber, W.; Semar, M.; Anke, T.; Bross, M.; Steglich, W. Tyromycin A: A novel inhibitor of leucine and cysteine aminopeptidases from *Tyromyces lacteus*. *Planta Med.* **1992**, 58, 56–59.

(22) Mathé, G. Bestatin, an aminopeptidase inhibitor with a multi-pharmacological function. *Biomed. Pharmacother.* **1991**, 45, 49–54.

(23) Sandargo, B.; Michehl, M.; Praditya, D.; Steinmann, E.; Stadler, M.; Surup, F. Antiviral meroterpenoid rhodatin and sesquiterpenoids rhodocoranes A-E from the wrinkled peach mushroom. *Org. Lett.* **2019**, 21, 3286–3289.

(24) Ciesek, S.; von Hahn, T.; Colpitts, C. C.; Schang, L. M.; Friesland, M.; Steinmann, J.; Manns, M. P.; Ott, M.; Wedemeyer, H.; Meuleman, P.; Pietschmann, T. The green tea polyphenol, epigallocatechin-3-gallate, inhibits hepatitis C virus entry. *Hepatology* **2011**, 54, 1947–1955.

(25) Poigny, S.; Guyot, M.; Samadi, M. One-step synthesis of tyromycin A and analogues. *J. Org. Chem.* **1998**, 63, 1342–1343.



Skeletocutins M–Q: biologically active compounds from the fruiting bodies of the basidiomycete *Skeletocutis* sp. collected in Africa

Tian Cheng¹, Clara Chepkirui¹, Cony Decock², Josphat C. Matasyoh³ and Marc Stadler^{*1}

Full Research Paper

Open Access

Address:

¹Department of Microbial Drugs, Helmholtz Centre for Infection Research (HZI), German Centre for Infection Research (DZIF), Partner Site Hannover/Braunschweig, Inhoffenstraße 7, 38124 Braunschweig, Germany, ²Mycothèque de l' Université Catholique de Louvain (BCCM/MUCL), Place Croix du Sud 3, B-1348 Louvain-la-Neuve, Belgium and ³Department of Chemistry, Faculty of Science, Egerton University, P.O. Box 536, 20115, Egerton, Kenya

Email:

Marc Stadler* - Marc.Stadler@helmholtz-hzi.de

* Corresponding author

Keywords:

basidiomycete; polyporaceae; secondary metabolites; structure elucidation

Beilstein J. Org. Chem. **2019**, *15*, 2782–2789.

doi:10.3762/bjoc.15.270

Received: 20 July 2019

Accepted: 05 November 2019

Published: 19 November 2019

Associate Editor: K. N. Allen

© 2019 Cheng et al.; licensee Beilstein-Institut.

License and terms: see end of document.

Abstract

During the course of screening for new metabolites from basidiomycetes, we isolated and characterized five previously undescribed secondary metabolites, skeletocutins M–Q (**1–5**), along with the known metabolite tyromycin A (**6**) from the fruiting bodies of the polypore *Skeletocutis* sp. The new compounds did not exhibit any antimicrobial, cytotoxic, or nematocidal activities. However, compound **3** moderately inhibited the biofilm formation of *Staphylococcus aureus* (*S. aureus*), while compounds **3** and **4** performed moderately in the L-leucine-7-amido-4-methylcoumarin (L-Leu-AMC) inhibition assay. These compounds represent the first secondary metabolites reported to occur in the fruiting bodies by *Skeletocutis*. Interestingly, tyromycin A (**6**) was found to be the only common metabolite in fruiting bodies and mycelial cultures of the fungus, and none of the recently reported skeletocutins from the culture of the same strain were detected in the basidiomes.

Introduction

Over the past years, we have been studying the secondary metabolites of African Basidiomycota that were collected in rainforests and mountainous areas of Western Kenya. These species were new to science, and proved to be a prolific source of unprecedented natural compounds showing a set of prominent biological activities [1-3].

The present study deals with the comparison of the secondary metabolites located in the basidiomes (fruiting bodies) of another, putatively new species belonging to the genus *Skeletocutis*, strain MUCL56074. We have recently reported the known metabolite tyromycin A (**6**), together with 12 unprecedented congeners for which we proposed the trivial names

skeletocutins A–L, which were obtained from a liquid culture of the same fungus [4]. A preliminary characterization of the producer organism suggested that it belongs to a new species because neither DNA sequence data in the public domain nor morphological characteristics matched the previously reported species, as compared to the literature. The genus *Skeletocutis* (of the Polyporaceae) consists of approximately 40 species, which grow as a crust on the surface of collapsing wood [5] and mostly occur in the temperate climate zones.

In our preceding study, the fungal specimen MUCL56074 has been assigned to the genus *Skeletocutis* by comparison of morphological features and 5.8S/ITS rDNA sequences, as reported previously [4]. Strain MUCL56074 represents a hitherto undescribed species, which will be formally described in a separate paper in a mycological journal, pending the examination of type material of related species. In view of a potential application of chemotaxonomic methodology, the basidiomes of the fungus were checked for the presence of secondary metabolites for later comparison with herbarium specimens of other species by HPLC–diode array detection (HPLC–DAD)–MS. Surprisingly, we detected further members of the skeletocutin family that were not present in the cultures. The current paper is dedicated to the description of their isolation as well as biological and physicochemical characterization.

Results and Discussion

The fruiting bodies of the fungal specimen MUCL56074 were extracted with acetone and subsequently purified via preparative HPLC, which led to the isolation of five previously undescribed secondary metabolites, **1–5** ($t_R = 17.8, 18.8, 15.7, 14.0,$

and 14.3 min, respectively), and one known compound, namely tyromycin A (**6**, $t_R = 16.8$ min) [6] (Figure 1).

Compound **1** (Table 1 and Figure 2), named skeletocutin M, was isolated as a yellow solid. Its molecular formula was determined to be $C_{28}H_{42}O_6$, with eight degrees of unsaturation, by HRESIMS. Signals for $m/z = 475.3054, 497.2868,$ and 971.5839 , corresponding to the ions $[M + H]^+, [M + Na]^+,$ and $[2M + Na]^+$, respectively, were also recorded in the mass spectrum. A singlet resonating at $\delta = 2.08$ ppm for the methyl protons $H_{3-6'}$ and a triplet and quintet resonating at $\delta = 2.50$ and 1.59 ppm, respectively, for the methylene groups, were recorded in the 1H NMR spectrum. Further, the ^{13}C NMR spectrum revealed only 14 signals instead of 28, as indicated by the molecular formula, suggesting that the molecule consisted of two identical halves.

Determination of HMBC correlations between the C-6' methyl protons ($\delta = 2.08$ ppm) and C-3'/4'/5' as well as between $H_{2-1/18}$ and C-2'/3'/4' confirmed the presence of a maleic anhydride moiety in the molecule. Integration of the singlet for the C-6' methyl group in the 1H NMR spectrum gave a value of 6, indicating the presence of two maleic anhydride functions. The multiplet at $\delta = 1.28–1.36$ ppm was assigned to the remaining 14 methylene units making up the carbon chain. Integration of this multiplet gave a value of 28, confirming the length of the chain. The connection of this chain to two maleic anhydride units was confirmed by HMBC correlations between the protons $H_{2-1/2/17/18}$ and C-3' ($\delta = 144.9$ ppm). Additionally, long-range correlations between the protons H_{2-1} and $H_{3-6'}$ were observed in the COSY spectrum. Therefore, the structure

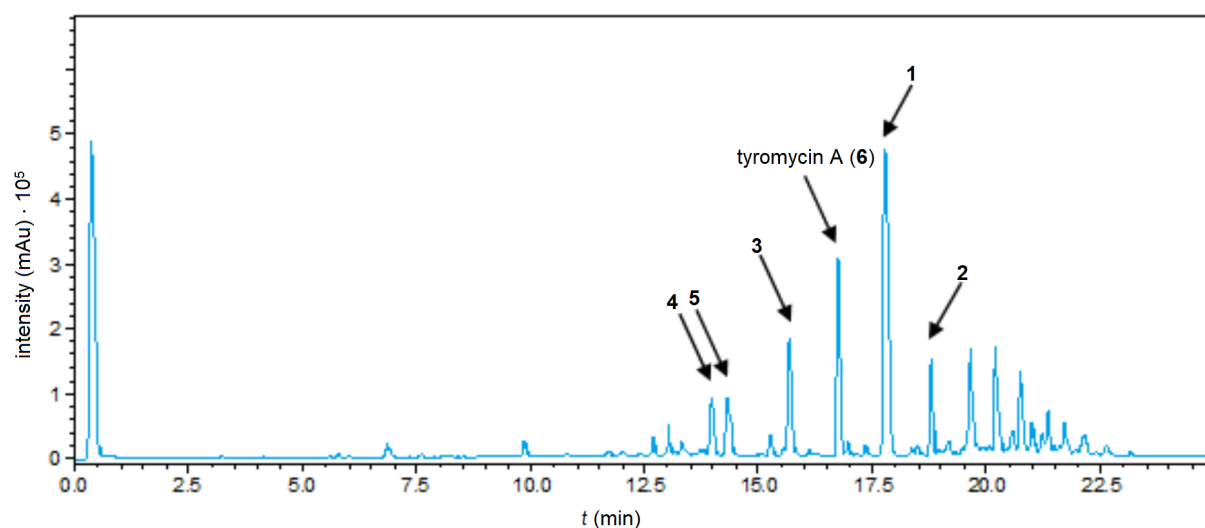
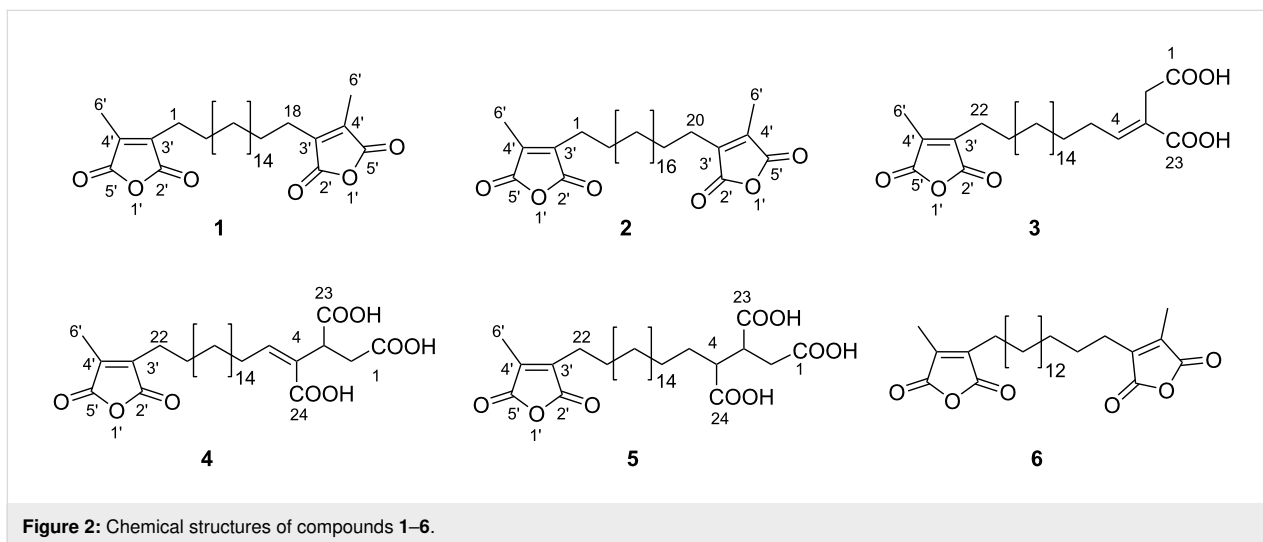


Figure 1: HPLC–UV chromatogram of the extract from fruiting bodies of *Skeletocutis* sp. (detection wavelength $\lambda = 190–600$ nm).

Table 1: ^1H and ^{13}C NMR data for **1** (in acetone- d_6) and **2** (in CDCl_3).

Position	1		2	
	$^{13}\text{C}/\text{DEPT}$	^1H	$^{13}\text{C}/\text{DEPT}$	^1H
1/18 (1) or 1/20 (2)	24.8, CH_2	2.50 (t), $J = 7.6$ Hz	24.4, CH_2	2.46 (t), $J = 7.6$ Hz
2/17 (1) or 2/19 (2)	28.2, CH_2	1.59 (p), $J = 7.6$ Hz	27.6, CH_2	1.58 (p), $J = 7.6$ Hz
3–16 (1) or 3–18 (2)	29.4–29.8, CH_2	1.28–1.36 (m)	29.2–29.7, CH_2	1.26–1.32 (m)
2'	167.1, C		165.9, C	
3'	144.9, C		144.8, C	
4'	141.7, C		140.4, C	
5'	167.4, C		166.3, C	
6'	9.6, CH_3	2.08 (s)	9.5, CH_3	2.08 (s)

**Figure 2:** Chemical structures of compounds **1**–**6**.

of natural product **1** was unambiguously concluded to be 1,18-bis[4'-methyl-2',5'-dioxo-3'-furyl]octadecane.

Compound **2** (skeletocutin N, Table 1 and Figure 2) was obtained as a white solid, with the molecular formula $\text{C}_{30}\text{H}_{46}\text{O}_6$ and eight degrees of unsaturation determined from HRESIMS data. The 1D and 2D NMR data for **2** revealed a similar structure to **1**, with the difference being the size of the carbon chain in the molecule. A value of 32 obtained from the integration of the C-3–C-18 multiplet ($\delta = 1.26$ – 1.32 ppm) led to the conclusion that **2** had an icosane chain instead of the octadecane chain elucidated for skeletocutin M (**1**).

Compound **3** (skeletocutin O, Table 2 and Figure 2), isolated as a yellow oil, had the molecular formula $\text{C}_{28}\text{H}_{44}\text{O}_7$ and seven degrees of unsaturation, deduced from HRESIMS data. Signals for $m/z = 493.3163$ ($[\text{M} + \text{H}]^+$), 515.2980 ($[\text{M} + \text{Na}]^+$), 475.3058 ($[\text{M} + \text{H} - \text{H}_2\text{O}]^+$), and 1007.6067 ($[2\text{M} + \text{Na}]^+$) were also recorded by HRESIMS. A singlet for a methyl group

($\delta = 2.08$ ppm, H_3 -6'), along with another singlet ($\delta = 3.37$ ppm, H_2 -2), a quintet ($\delta = 1.58$ ppm, H_2 -21), a triplet ($\delta = 2.45$ ppm, H_2 -22) for three methylene groups, and a triplet for a methine unit ($\delta = 7.13$ ppm, H-4) were observed in the ^1H NMR spectrum of **3**. Analysis of 1D and 2D NMR data for **3** indicated a similar structure to **1**, with a difference being the absence of one maleic anhydride moiety, which was replaced by a dicarboxylic acid motif and an olefinic bond between position C-3 ($\delta = 124.5$ ppm) and C-4 ($\delta = 148.9$ ppm). Resonances for the carbon atoms of the carboxylic acid moieties occurred at $\delta = 176.8$ ppm (C-1) and 172.0 ppm (C-23). The dicarboxylic acid function could be elucidated through HMBC correlations between H_2 -2 and C-1/3/4/23, H-4 and C-23/3, as well as H_2 -5 and C-3. Further cross peaks between H_2 -5 and H_2 -6/H-4 were observed in COSY spectra, which confirmed the linkage of the dicarboxylic acid motif to the chain at C-3. The diastereotopic protons H_2 -2 ($\delta = 3.37$) showed ROESY correlations to H_2 -5 ($\delta = 2.23$ ppm), but no correlations between H_2 -2 and H-4 ($\delta = 7.13$ ppm) were recorded. Therefore, the configuration of

Table 2: ^1H and ^{13}C NMR data for **3** (in CDCl_3) and compounds **4** and **5** (in $\text{DMSO}-d_6$).

	3		4		5	
Position	$^{13}\text{C}/\text{DEPT}$	^1H	$^{13}\text{C}/\text{DEPT}$	^1H	$^{13}\text{C}/\text{DEPT}$	^1H
1	176.8, C		174.5, C		174.3, C	
2	32.1, CH_2	3.37 (s)	35.8, CH_2	2.23 (dd), $J = 16.3, 5.8$ Hz 2.92 (dd), $J = 16.3, 7.8$ Hz	33.6, CH_2	2.29 (dd), $J = 16.6, 2.4$ Hz 2.53 (m) ^a
3	124.5, C		39.6, CH	3.86 (dd), $J = 7.8, 5.8$ Hz	42.8, CH	2.83 (ddd), $J = 10.5, 6.7,$ 3.4 Hz
4	148.9, CH	7.13 (t), $J = 7.6$ Hz	131.9, C		46.1, CH	2.50 (m) ^a
5	29.12, CH_2	2.23 (m)	144.7, CH	6.74 (t), $J = 7.4$ Hz	28.6, CH_2	1.56 (m)
6	28.3, CH_2	1.48 (m)	28.5, CH_2	2.19 (q), $J = 7.4$ Hz	28.6, CH_2	1.35 (m)
7			28.5, CH_2	1.38 (m)		
8–20	29.3–29.7, CH_2	1.26–1.31 (m)	29.1–29.5, CH_2	1.23–1.26 (m)	28.82–29.0, CH_2	1.23–1.26 (m)
21	27.6, CH_2	1.58 (p), $J = 7.6$ Hz	27.3, CH_2	1.48 (p), $J = 7.5$ Hz	26.9, CH_2	1.49 (p), $J = 8.0$ Hz
22	24.4, CH_2	2.45 (t), $J = 7.6$ Hz	24.1, CH_2	2.39 (t), $J = 7.5$ Hz	23.6, CH_2	2.40 (t), $J = 8.0$ Hz
23	172.0, C		173.8, C		172.9, C	
24			167.8, C		174.7, C	
2'	165.9, C		166.7, C		166.2, C	
3'	144.8, C		143.9, C		143.4, C	
4'	140.4, C		141.3, C		140.8, C	
5'	166.3, C		166.9, C		166.4, C	
6'	9.3, CH_3	2.08 (s)	9.7, CH_3	1.99 (s)	9.2, CH_3	2.00 (s)

^aOverlapping signals.

the olefinic bond between C-3 and C-4 was assigned (*E*)-configuration. As such, the structure of **3** was concluded to be (*E*)-2-(19-(4'-methyl-2',5'-dioxo-2',5'-dihydrofuran-3'-yl)nonadecylidene)butanedioic acid.

Compound **4** (Table 2 and Figure 2), named skeletocutin P, was isolated as a white solid. Its molecular formula was established to be $\text{C}_{29}\text{H}_{44}\text{O}_9$, with eight degrees of unsaturation, from HRESIMS data. Peaks for $m/z = 537.3058$ ($[\text{M} + \text{H}]^+$), 559.2877 ($[\text{M} + \text{Na}]^+$), 519.2953 ($[\text{M} + \text{H} - \text{H}_2\text{O}]^+$), and 1095.5860 ($[\text{2M} + \text{Na}]^+$) were observed in the mass spectrum. The 1D and 2D NMR data of **4** were similar to those of **3**, with the difference being the presence of a tricarboxylic acid moiety instead of a dicarboxylic acid motif at one end of the chain. The three carboxylic acid functions of the molecule had resonances at $\delta = 174.5$ (C-1), 173.8 (C-23), and 167.8 ppm (C-24) in the ^{13}C NMR spectrum. The HMBC correlations between H_2 -2 and C-1/3/4/23 as well as H-5 and C-3/24 and the COSY correlations between H_2 -2 and H-3 confirmed the tricarboxylic acid moiety in the molecule. COSY correlations between H_2 -6 and

H_2 -5/7 confirmed the linkage of this moiety to the rest of the molecule. The absence of ROESY correlations between H-5 and H-3 but the presence of such between the protons H-3 and H_2 -6 indicated (*Z*)-configuration of the olefinic bond between C-4 and C-5. Therefore, the structure of **4** was unambiguously elucidated as (*Z*)-21-(4'-methyl-2',5'-dioxo-2',5'-dihydrofuran-3'-yl)henicos-3-ene-1,2,3-tricarboxylic acid.

Compound **5** (skeletocutin Q, Table 2 and Figure 2), with the molecular formula $\text{C}_{29}\text{H}_{46}\text{O}_9$ and seven degrees of unsaturation, as established from HRESIMS data, was obtained as a yellow solid. Analysis of 1D and 2D NMR data of **5** indicated a similar structure to **4**, with saturation of the olefinic bond between C-4 and C-5. In the ^{13}C NMR spectrum of **5**, the signals that had occurred at $\delta = 144.7$ and 131.9 ppm for compound **4** were missing, and instead, a methylene signal at $\delta = 28.5$ ppm (C-5) and a methine signal at $\delta = 46.1$ ppm (C-4) were recorded. HMBC correlations were observed between H-4 ($\delta = 2.50$ ppm) and C-2/3/23/24 as well as H_2 -5 ($\delta = 1.56$ ppm) and C-4/C6/24. Furthermore, COSY correlations between H-3

and H₂-2/H-4 as well as H₂-5 and H-4/H₂-6 could be recorded. Hence, **5** was concluded to be 21-(4'-methyl-2',5'-dioxo-2',5'-dihydrofuran-3'-yl)henicosane-1,2,3-tricarboxylic acid.

Tyromycin A (**6**), a closely related compound to the metabolites **1**–**5**, has been reported before, and was isolated from the cultures of the same fungus (i.e., the corresponding mycelial culture of the specimen that was the subject of the present study [4]) and originally from *Tyromyces lacteus* [6]. In these two cases, **6** was reported to be the major component of the culture extracts. Even though this compound is occurring in fruiting bodies, in this case, skeletocutin M (**1**) was the major component instead of tyromycin A (**6**). The two molecules **1** and **6** differ in their chain length, with the former having an 18-carbon chain instead of a 16-carbon chain, as in **6**.

The isolated compounds **1**–**6** were evaluated for antimicrobial, cytotoxic, and nematocidal activities, as described in the Experimental section. However, compounds **1**–**5** were devoid of activity in these assays, whereas tyromycin A (**6**) and skeletocutin A–L had been reported before to be active against several Gram-positive bacteria [4], namely *Bacillus subtilis* (*B. subtilis*), *S. aureus*, methicillin-resistant *S. aureus* (MRSA), and *Micrococcus luteus* (*M. luteus*). In the antimicrobial assay, compounds **3** and **5** were observed to interfere with the forma-

tion of biofilms commonly associated with *S. aureus*. When compounds **3** and **5** were evaluated for biofilm inhibition activity against *S. aureus*, they showed only weak activity with 20 and 56% inhibition of the biofilm, respectively, at a concentration 256 µg/mL. Tyromycin A (**6**) was previously reported to be an inhibitor of leucine aminopeptidase in HeLa S3 cells [6]. Accordingly, all compounds **1**–**5** were tested for their inhibition activity against hydrolysis of L-leucine-7-amido-4-methylcoumarin (L-Leu-AMC). Compound **4** exhibited moderate activity, with an IC₅₀ value of 71.1 µg/mL (Table 3 and Figure 3) when 50 µM of the substrate was used. Compounds **3** and **5** exhibited weak activities, with IC₅₀ values of >80 µg/mL at 50 and 110 µM substrate concentration. Although tyromycin A (**6**) was previously reported to be active in a similar assay against HeLa S3 cells, with IC₅₀ values of 31 µg/mL at 50 µM substrate concentration, an IC₅₀ value >150 µg/mL for this compound was recorded on the HeLa (KB3.1) cells during this cytotoxicity study [6].

Conclusion

In summary, five previously undescribed tyromycin A derivatives **1**–**5** could be isolated from *Skeletocutis* sp. fruiting bodies. These metabolites are closely related to the skelotocutins that were previously reported as isolates from liquid cultures. Compounds **3** and **5** were observed to weakly inhibit the biofilm for-

Table 3: Inhibition of L-Leu-AMC hydrolysis by the metabolites **1**–**5**.

Substrate (c)	IC ₅₀ (µg/mL)						Bestatin [12]
	1	2	3	4	5	6	
L-Leu-AMC (50 µM)	–	–	89.6	71.1	153.2	138.4	10.8
L-Leu-AMC (100 µM)	–	–	130.4	102.3	225.3	–	40.9

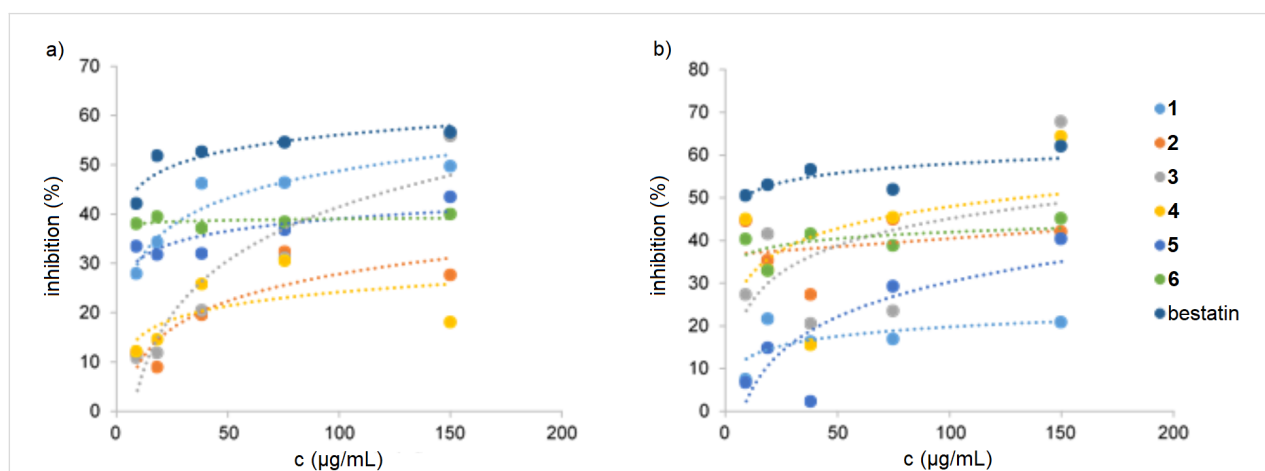


Figure 3: Inhibition Leu-AMC hydrolysis. a) c (L-Leu-AMC) = 100 µM. b) c (L-Leu-AMC) = 50 µM.

mation by *S. aureus* and constrain inhibitory activity of L-Leu-AMC hydrolysis in KB 3.1 cells. There have been relatively few studies on the production of secondary metabolites in mycelial cultures vs fruiting bodies in higher fungi, but so far, there are only few examples where the same compounds were predominant in both. For instance, in most species hitherto studied of the ascomycete order Xylariales, the fruiting bodies and cultures mostly showed a complementary secondary metabolite production [7]. In the current case, it appears that the basidiomes of *Skeletocutis* can be used for chemotaxonomic studies. Investigations of herbarium specimens may not even be helpful for the taxonomic revision of the genus but may even lead to the discovery of further, previously undescribed members of the tyromycin/skeletocutin type.

Experimental

General information

NMR spectra were recorded with a Bruker 500 MHz spectrometer at frequencies of 500.130 (^1H NMR) and 125.758 MHz (^{13}C NMR). HRESIMS spectra were recorded after purification with an Agilent 1200 series HPLC–UV system (column size: 2.1 mm–50 mm, packing: 1.7 μm , Waters ACQUITY UPLC BEH C18 sorbent, solvent A: H_2O + 0.1% formic acid, solvent B: acetonitrile + 0.1% formic acid, elution gradient: 5% solvent B for 0.5 min, increasing solvent B to 100% within 19.5 min, 100% solvent B for 5 min, flow rate: 0.6 mL/min, UV–vis detection at $\lambda = 200\text{--}600$ nm) and ESI–TOF–MS analysis (maXis™ system, Bruker, scan range: 100–2500 m/z , capillary voltage: 4500 V, drying temperature: 200 °C). UV–vis spectra were recorded with a Shimadzu UV-2450 UV–vis spectrophotometer. The chromatogram in Figure 1 was recorded on a Bruker Agilent 1260 Infinity Series equipped with DAD and an ESI ion trap mass spectrometer (amaZon speed ion trap, Bruker).

Fungal material

The fungal specimen was collected by C. Decock and J. C. Matasyoh in the Mount Elgon National Reserve [4]. The dried specimen and corresponding cultures were deposited in the MUCL collection (MUCL accession number: 56074).

Extraction of the crude extract

A quantity of 9.8 g fruiting bodies were extracted using 500 mL of acetone overnight. Then, the extract was filtered and another 500 mL of acetone were added. This was extracted in an ultrasonic bath for 30 min. The extracts were combined and the solvent evaporated to afford 226 mg of crude extract.

Isolation of compounds 1–6

The crude extract (vide supra) was filtered using solid-phase microextraction (SPME) with a Strata™-X 33 μm Polymeric

Reversed Phase (RP) cartridge (Phenomenex). The extract was fractionated by preparative RP chromatography (RPC) using a PLC 2020 purification system (Gilson). A VarioPrep (VP) column system packed with NUCLEODUR® 100-5 C18 ec was used as stationary phase (Machery-Nagel, column size: 25 mm–40 mm, packing: 7 μm). Deionized water, obtained from a Milli-Q® water purification system (Millipore), + 0.05% TFA (solvent A) and acetonitrile + 0.05% TFA (solvent B), respectively, were used as mobile phases (elution gradient: 50% solvent B, increasing solvent B to 100% within 60 min, 100% solvent B for 5 min, flow rate: 40 mL/min, UV–vis detection at 210, 254, and 350 nm). Eight fractions (F1–F8) were collected, in accordance with the observed signals.

F1 was further purified by RPC using solvent A and solvent B (elution gradient: 45% solvent B for 3 min, increasing solvent B to 100% within 18 min, 100% solvent B for 4 min). A Kromasil® C18 HPLC column (Nouryon, column size: 250 mm–20 mm, packing: 7 μm , flow rate: 15 mL/min) was used as stationary phase. This led to the isolation of compound **4** (2.50 mg). Using the same column and elution gradient, **5** (2.87 mg) was purified from F2, compound **3** (4.26 mg) from F4, compound **1** (4.84 mg) from F6, compound **2** (2.26 mg) from F7, and tyromycin A (**6**, 2.15 mg) was obtained from F8.

Physicochemical data for compounds 1–5

Skeletocutin M (**1**): yellow solid (4.84 mg). UV (MeOH) λ_{max} , (log ϵ): 220 nm (4.26); HRESIMS (m/z): $[\text{M} + \text{H}]^+$ calcd for $\text{C}_{28}\text{H}_{43}\text{O}_6$, 475.3054; found, 475.3059.

Skeletocutin N (**2**): white solid (2.26 mg). UV (MeOH) λ_{max} , (log ϵ): 214 (4.84), 254 nm (5.02); HRESIMS (m/z): $[\text{M} + \text{H}]^+$ calcd for $\text{C}_{30}\text{H}_{47}\text{O}_6$, 503.3374; found, 503.3373.

Skeletocutin O (**3**): yellow oil (4.26 mg). UV (MeOH) λ_{max} , (log ϵ): 220 nm (3.87); HRESIMS (m/z): $[\text{M} + \text{H}]^+$ calcd for $\text{C}_{28}\text{H}_{45}\text{O}_7$, 493.3163; found, 493.3165.

Skeletocutin P (**4**): white solid (2.50 mg). $[\alpha]_{\text{D}}^{20} +12$ (c 0.0025, MeOH); UV (MeOH) λ_{max} , (log ϵ): 222 nm (5.14); HRESIMS (m/z): $[\text{M} + \text{H}]^+$ calcd for $\text{C}_{29}\text{H}_{45}\text{O}_9$, 537.3058; found, 537.3064.

Skeletocutin Q (**5**): yellow solid (2.87 mg). $[\alpha]_{\text{D}}^{20} +8.7$ (c 0.001, MeOH); UV (MeOH) λ_{max} , (log ϵ): 206 (4.49), 256 nm (4.65); HRESIMS (m/z): $[\text{M} + \text{H}]^+$ calcd for $\text{C}_{29}\text{H}_{47}\text{O}_9$, 539.3215; found, 539.3220.

Antimicrobial assay

Minimum inhibitory concentrations (MIC) were determined in serial dilution assays using several microorganisms, as de-

scribed previously [8,9]. Herein, Gram-positive bacteria used were *B. subtilis* DSM10, MRSA DSM11822, *S. aureus* DSM346, *M. luteus* DSM20030, and *Mycobacterium smegmatis* (*M. smegmatis*) ATCC700084, Gram-negative bacteria were *Escherichia coli* (*E. coli*) DSM498, *Chromobacterium violaceum* (*C. violaceum*) DSM30191, and *Pseudomonas aeruginosa* (*P. aeruginosa*) PA14. Moreover, the filamentous fungus *Mucor plumbeus* (*M. plumbeus*) MUCL49355 and the yeasts *Candida tenuis* (*C. tenuis*) MUCL29892, *Pichia anomala* (*P. anomala*) DSM6766, and *Candida albicans* (*C. albicans*) DSM1665 were applied. The assays were conducted in 96-well plates and Mueller–Hinton Broth (MHB) for bacteria, or yeast, malt, and glucose (YMG) medium for filamentous fungus and yeasts.

Cytotoxicity assay

In vitro cytotoxicity, using IC₅₀ values as a measure, was evaluated against mouse fibroblasts cell line L929 and HeLa (KB3.1) cells and carried out according to our previous reports [8,9].

Inhibition of biofilm formation

The assay was performed in Falcon® 96-well flat bottom plates as previously described [10]. *S. aureus* DSM1104 was enriched overnight to reach 0.5 McFarland standard turbidity in casein-peptone soymeal-peptone (CASO) medium containing 4% glucose at pH 7.0 for biofilm formation. Methanol was used as negative control, while tetracycline was used as positive control. All experiments were made in triplicates.

Nematicidal activity assay

The nematicidal activity of isolated compounds against *Caenorhabditis elegans* (*C. elegans*) was performed in 24-well microtiter plates as previously described [11]. Ivermectin was used as positive control and methanol was used as negative control. The results are expressed as LD₉₀ values.

Inhibition of leucine aminopeptidases

Hydrolysis of L-Leu-AMC by the surface-bound aminopeptidases of KB3.1 cells was assayed based on the method from Weber and co-workers [6] with slight modifications. KB3.1 cells were grown as monolayer cultures in Dulbecco's modified Eagle's medium (DMEM) containing 10% fetal calf serum at 37 °C in 24-well multidishes. After three days, the confluent monolayers were washed twice with phosphate buffered saline (PBS), and the reaction mixture (450 µL Hanks' buffer at pH 7.2 containing 50 or 100 µM substrate L-Leu-AMC, compounds dissolved in 50 µL DMSO) was added. After being incubated at 23 °C for 30 min, 1 mL cold 0.2 M glycine buffer at pH 10.5 was added. The amount of hydrolyzed 7-amino-4-methylcoumarin (AMC) was measured in a Tecan Infinite M200 PRO fluorescence spectrophotometer (excitation and

emission at λ = 365 and 440 nm, respectively). Bestatin [12] and DMSO were used as positive and negative control, respectively.

Supporting Information

Supporting Information File 1

HRESIMS data, NMR spectra of metabolites, media composition for incubation of microorganisms, and ITS sequences of the producing strain.

[<https://www.beilstein-journals.org/bjoc/content/supplementary/1860-5397-15-270-S1.pdf>]

Acknowledgements

We are grateful to W. Collisi for conducting the cytotoxicity assays, C. Kakoschke for recording NMR data, and C. Schwager as well as E. Surges for recording HPLC–MS data. Financial support by the ASAFEM project (Grant no. IC-070) under the ERAfrica Programme of the European Commission (EC) to J. C. M. and M. S. as well as personal Ph.D. stipends from the China Scholarship Council (CSC), the German Academic Exchange Service (DAAD), and the Kenya National Council for Science and Technology (NACOSTI) to T. C. and C. C., respectively, are gratefully acknowledged.

ORCID® iDs

Tian Cheng - <https://orcid.org/0000-0001-7733-981X>

Cony Decock - <https://orcid.org/0000-0002-1908-385X>

Marc Stadler - <https://orcid.org/0000-0002-7284-8671>

Preprint

A non-peer-reviewed version of this article has been previously published as a preprint doi:10.3762/bxiv.2019.74.v1

References

- Sandargo, B.; Chepkirui, C.; Cheng, T.; Chaverra-Muñoz, L.; Thongbai, B.; Stadler, M.; Hüttel, S. *Biotechnol. Adv.* **2019**, *37*, No. 107344. doi:10.1016/j.biotechadv.2019.01.011
- Schöffler, A. Secondary Metabolites of Basidiomycetes. In *Physiology and Genetics - Selected Basic and Applied Aspects*, 2nd ed.; Anke, T.; Schöffler, A., Eds.; Springer: Cham, 2018; Vol. 15, pp 231–275. doi:10.1007/978-3-319-71740-1_8
- Yin, X.; Yang, A.-A.; Gao, J.-M. *J. Agric. Food Chem.* **2019**, *67*, 5053–5071. doi:10.1021/acs.jafc.9b00414
- Chepkirui, C.; Cheng, T.; Sum, W. C.; Matasyoh, J. C.; Decock, C.; Praditya, D. F.; Wittstein, K.; Steinmann, E.; Stadler, M. *J. Agric. Food Chem.* **2019**, *67*, 8468–8475. doi:10.1021/acs.jafc.9b02598
- Floudas, D.; Hibbett, D. S. *Fungal Biol.* **2015**, *119*, 679–719. doi:10.1016/j.funbio.2015.04.003
- Weber, W.; Semar, M.; Anke, T.; Bross, M.; Steglich, W. *Planta Med.* **1992**, *58*, 56–59. doi:10.1055/s-2006-961390

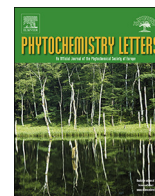
7. Helaly, S. E.; Thongbai, B.; Stadler, M. *Nat. Prod. Rep.* **2018**, *35*, 992–1014. doi:10.1039/c8np00010g
8. Kuhnert, E.; Surup, F.; Herrmann, J.; Huch, V.; Müller, R.; Stadler, M. *Phytochemistry* **2015**, *118*, 68–73. doi:10.1016/j.phytochem.2015.08.004
9. Sandargo, B.; Michehl, M.; Praditya, D.; Steinmann, E.; Stadler, M.; Surup, F. *Org. Lett.* **2019**, *21*, 3286–3289. doi:10.1021/acs.orglett.9b01017
10. Yuyama, K. T.; Chepkirui, C.; Wendt, L.; Fortkamp, D.; Stadler, M.; Abraham, W.-R. *Microorganisms* **2017**, *5*, No. 80. doi:10.3390/microorganisms5040080
11. Rupcic, Z.; Chepkirui, C.; Hernández-Restrepo, M.; Crous, P.; Luangsa-ard, J.; Stadler, M. *MycKeys* **2018**, *33*, 1–23. doi:10.3897/mycokeys.33.23341
12. Mathé, G. *Biomed. Pharmacother.* **1991**, *45*, 49–54. doi:10.1016/0753-3322(91)90122-a

License and Terms

This is an Open Access article under the terms of the Creative Commons Attribution License (<http://creativecommons.org/licenses/by/4.0>). Please note that the reuse, redistribution and reproduction in particular requires that the authors and source are credited.

The license is subject to the *Beilstein Journal of Organic Chemistry* terms and conditions: (<https://www.beilstein-journals.org/bjoc>)

The definitive version of this article is the electronic one which can be found at:
[doi:10.3762/bjoc.15.270](https://doi.org/10.3762/bjoc.15.270)



An unprecedented spiro [furan-2,1'-indene]-3-one derivative and other nematicidal and antimicrobial metabolites from *Sanghuangporus* sp. (Hymenochaetaceae, Basidiomycota) collected in Kenya

Clara Chepkirui^a, Tian Cheng^a, Josphat Matasyoh^b, Cony Decock^c, Marc Stadler^{a,*}

^a Department of Microbial Drugs, Helmholtz Centre for Infection Research and German Centre for Infection Research (DZIF), Partner Site Hannover/Braunschweig, Inhoffenstrasse 7, 38124 Braunschweig, Germany

^b Egerton University, Department of Chemistry, P.O BOX 536, 20115, Njoro, Kenya

^c Mycothèque de l' Université catholique de Louvain (BCCM/MUCL), Place Croix du Sud 32 bte L7.05.06, B-1348 Louvain-la-Neuve, Belgium

ARTICLE INFO

Keywords:

Hymenochaetaceae
Secondary metabolites
Basidiomycota
Medicinal mushroom
Structure elucidation

ABSTRACT

Bioassay guided fractionation of extracts derived from submerged cultures of a *Sanghuangporus* sp. (i.e., the genus that was until recently referred to as the “*Inonotus linteus* complex” of medicinal mushrooms) originating from Kenya led to the isolation of a new spiro [furan-2,1'-indene]-3-one derivative, for which we propose the trivial name phelligrudin L (1) together with the known compounds 3,14'-bihispidinyl (2), hispidin (3), ionylideneacetic acid (4), 1S-(2E)-5-[(1R)-2,2-dimethyl-6-methylidene-cyclohexyl]-3-methylpent-2-enoic acid (5), phellidine E (6) and phellidine D (7). Compounds 1–3, showed moderate nematicidal activity against *Caenorhabditis elegans* with LD₅₀ of 12.5 µg/m. The nematicidal activity of 3, 14'-bihispidinyl and hispidin (1, 2) has not been reported before. Furthermore, compounds 1–5 demonstrated moderate antimicrobial activity against various test organisms.

1. Introduction

Fungi have been recognized as source of structurally unique and bioactive metabolites (Karwehl and Stadler, 2016). The fungal diversity in the tropical rainforest ecosystems has been underexplored, since the majority of the fungal species found in these habitats have not been described nor has their chemistry been studied. In an effort to document this diversity and its rich chemistry, we embarked on extensive study of the secondary metabolite production of several basidiomycetes collected from Kenya's tropical rain forest Kakamega. Novel structurally diverse and bioactive metabolites like laetiporins, calocerins, 9-oxotrobinurins, laxitextines, microporenic acids and aethiopinolones are some of the metabolites that we have reported recently (Chepkirui et al., 2018a, 2018b, 2017, 2016; Mudalungu et al., 2015) from our ongoing study.

The present paper deals with a species belonging to the genus *Sanghuangporus* (Hymenochaetaceae), whose extracts from mycelial cultures had shown prominent antimicrobial effects during the course of the aforementioned study. The specimen was collected from the Kakamega Nature Reserve, a spot of rain forest at medium elevation in Kenya. The genus *Sanghuangporus* was erected for the “*Inonotus linteus*

complex”, and several additional species from the Paleotropics previously included in *Phellinus* (Zhou et al., 2015). It originally included *S. alpinus*, *S. baumii*, *S. lonicericola*, *S. lonicerinus*, *S. microcystideus*, *S. sanghuang*, *S. vaninii*, *S. weigela*, *S. weirianus* and *S. zonatus* (Zhou et al., 2015). Three more species have been added later, viz. *S. ligneus*, *S. pilatii* and *S. quercicola* (Ghobad-Nejhad, 2015; Tomsovsky, 2015; Zhu et al., 2017). The Asian species have been referred to in the literature as medicinal mushrooms. Only one species in the genus, *S. microcystideus*, has been reported from Eastern Africa (Zhou et al., 2015). In this study we report the isolation, structure elucidation and biological activities of secondary metabolites from another African *Sanghuangporus* sp., which probably represents an undescribed species.

2. Experimental section

2.1. General experimental procedure

Optical rotations were determined with a Perkin-Elmer (Überlingen, Germany) 241 spectrometer; UV spectra were recorded with a Shimadzu (Duisburg, Germany) UV-vis spectrophotometer UV-2450. NMR spectra were recorded with a Bruker (Bremen, Germany) Ascend

* Corresponding author.

E-mail addresses: Clara.Chepkirui@helmholtz-hzi.de (C. Chepkirui), Tian.Cheng@helmholtz-hzi.de (T. Cheng), josphat2001@yahoo.com (J. Matasyoh), cony.decock@uclouvain.be (C. Decock), marc.stadler@helmholtz-hzi.de (M. Stadler).

<https://doi.org/10.1016/j.phytol.2018.04.022>

Received 23 February 2018; Received in revised form 5 April 2018; Accepted 6 April 2018
1874-3900/ © 2018 Phytochemical Society of Europe. Published by Elsevier Ltd. All rights reserved.

700 spectrometer with 5 mm TXI cryoprobe (^1H 700 MHz, ^{13}C 175 MHz) and Bruker AV II-600 (^1H 500 MHz, ^{13}C 150 MHz) spectrometers. HR-ESI-MS mass spectra were recorded with a Bruker (Bremen, Germany) Agilent 1200 series HPLC-UV system (column 2.1×50 mm, $1.7 \mu\text{m}$, C18 Waters Acquity UPLC BEH, solvent A: $\text{H}_2\text{O} + 0.1\%$ formic acid; solvent B: $\text{AcCN} + 0.1\%$ formic acid, gradient: 5% B for 0.5 min increasing to 100% B in 19.5 min and then maintaining 100% B for 5 min, flow rate $0.6 \text{ mL}/\text{min}$, (UV-vis detection 200–600 nm) combined with ESI-TOF-MS (Maxis, Bruker) [scan range 100–2500 m/z , capillary voltage 4500 V, dry temperature 200°C]. Chemicals and solvents were obtained from AppliChem GmbH, Avantor Performance Materials, Carl Roth GmbH & Co. KG and Merck KGaA in analytical and HPLC grade.

2.2. Fungal material

The specimen MUCL 55592 was collected from Kakamega equatorial rainforest, located in the western part of Kenya ($0^\circ17'3.19''\text{N}$ $34^\circ45'8.24''\text{E}$) by C. Decock on Feb. 17, 2015. The dried herbarium specimen and culture are deposited at MUCL, Louvain-la-Neuve, Belgium (designation no. MUCL 55592). The fungus was identified as a species of the genus *Sanghuangporus* by morphological examination and sequencing of the rDNA (5.8S gene region, the internal transcribed spacer (ITS) and part of the nuclear ribosomal large subunit (nLSU).

DNA extraction was performed as reported previously (Wendt et al., 2018) with the EZ-10 Spin Column Genomic DNA Miniprep kit (Bio Basic Canada Inc., Markham, Ontario, Canada). A Precellys 24 homogenizer (Bertin Technologies, France) was used for cell disruption at a speed of 6000 rpm for 2×40 s. The gene regions were amplified with primers ITS 1f and NL4 for sequencing of the rDNA (5.8S gene region, the internal transcribed spacer ITS1 and ITS2). Genomic DNA Miniprep kit (Bio Basic Canada Inc., Markham, Ontario, Canada). The gene regions were amplified with primers ITS 1f and ITS4 for ITS and LROR and LR7 for nLSU.

2.3. Fermentation

Sanghuangporus sp. was cultivated in 500 mL Erlenmeyer flask containing 200 mL of the three different liquid media YMG, Q6 $\frac{1}{2}$ and ZM $\frac{1}{2}$ (for details on the composition of these media see Supplementary information). These three media were selected because previous studies had revealed that they were optimal for attaining complementary secondary metabolites profiles in filamentous fungi (Bitzer et al., 2008). A well grown culture grown on an YMG agar plate was cut into small pieces using a cork borer (7 mm) and five pieces inoculated in each flask. The cultures were incubated at 23°C on a rotary shaker (140 rpm). The growth of the fungus was monitored by constantly checking the amount of free glucose (using Bayer Diastix Harnzuckerstreifen). The fermentation was terminated five days after glucose depletion.

2.4. Extraction of crude extracts from small scale fermentation

The supernatant and the mycelia from the small scale fermentation were separated by filtration. The supernatant was extracted with equal amount of ethyl acetate and filtered through anhydrous sodium sulphate. The resulting ethyl acetate extract was evaporated to dryness by means of rotary evaporator. The mycelia were extracted with 200 mL of acetone in ultrasonic bath for 30 min, filtered and the filtrate evaporated. The remaining water phase was suspended in equal amount of distilled water and subjected to same procedure as the supernatant. The mycelia and supernatant crude extracts from the three media HRMS were measured. Analysis of the MS spectra by comparing the masses of the detected peaks and their molecular formula obtained from HRMS with those in the data base (Dictionary of natural products) led to the identification of the new compound on the ZM $\frac{1}{2}$ supernatant crude

extract (Dictionary of Natural Products on DVD, 2017).

2.5. Scale-up fermentation

A well-grown seven days old YMG agar plate of the mycelial culture was cut into small pieces using a 7 mm cork borer and five pieces inoculated in 500 mL Erlenmeyer flask containing 200 mL (30 flasks) of ZM $\frac{1}{2}$ medium. The culture was incubated at 23°C on a rotary shaker (140 rpm). The growth of the fungus was monitored by constantly checking the amount of free glucose (using Bayer Diastix Harnzuckerstreifen). The fermentation was terminated five days after glucose depletion.

2.6. Isolation of compounds 1–7

The supernatant culture crude extracts (700 mg) were fractionated using preparative reverse phase liquid chromatography (PLC 2020, Gilson, Middleton, USA). VP Nucleodur 100-5C 18 ec column (250×40 mm, $7 \mu\text{m}$: Macherey-Nagel) used. Deionized water (Milli-Q, Millipore, Schwalbach, Germany) (solvent A) and acetonitrile (solvent B) were used as the mobile phase. The elution gradient used was 5–100% solvent B in 52 min and thereafter isocratic condition at 100% solvent B for 10 min. UV detection was carried out at 210, 254 and 350 nm and flow rate $35 \text{ mL}/\text{min}$. Five fractions (F1–F5) were collected according to the observed peaks.

Fraction F1 and F2 were further purified by reversed phase LC (solvent A/solvent B), elution gradient 20–30% solvent B for 30 min followed by gradient shift from 35 to 100% in 3 min and finally isocratic condition at 100% solvent B for 5 min with a preparative Nucleodur Phenyl hexyl column (Macherey-Nagel, Düren, Germany; 250×21 mm, $5 \mu\text{m}$) as stationary phase and a flow rate of $15 \text{ mL}/\text{min}$, to afford compound 1 (3 mg) and compound 3 (50 mg). Using the same column and a modified elution gradient (25–45% solvent B for 30 min fraction) F3 was purified to afford 45 mg of 2. Fractions F4 and F5 were purified by reversed phase HPLC (solvent A/solvent B), elution gradient 78–100% solvent B for 25 min followed by isocratic condition at 100% solvent B for 5 min with a preparative (Kromasil, MZ Analysentechnik, Mainz, Germany) 250×20 mm $7 \mu\text{m}$ C-18 column as stationary phase to give compound 4 (125 mg) and 5 (10 mg). The same separation and purification conditions were applied to the mycelial culture. Compound 6 (5 mg) and 7 (2 mg) were purified from F4 by reverse phase LC (solvent A/solvent B), elution gradient 65–85% solvent B for 20 min followed by gradient shift from 85 to 100% in 3 min and finally isocratic condition at 100% solvent B for 5 min with a preparative HPLC column (Kromasil, 250×20 mm, $7 \mu\text{m}$ C-18) as stationary phase.

2.7. Antimicrobial assay

Minimum Inhibition Concentrations (MIC) against different test organisms were determined in serial dilution assay as described previously by Teponno et al. (2017), against *Candida tenuis* MUCL 29982, *Mucor plumbeus* MUCL 49355, *Escherichia coli* DSM498 and *Bacillus subtilis* DSM10 and *Micrococcus luteus* DSM 1790. The assays were carried out in 96-well microtiter plates in YMG medium for filamentous fungi and yeasts and MH for bacteria. The stock solution concentration was $300 \mu\text{g}/\text{mL}$.

2.8. Nematicidal assay

Compounds 1–5 were assessed for nematicidal activity against *Caenorhabditis elegans* according to Rupcic et al. (2018) and Kuephadungphan et al. (2017) with slight modification. *Caenorhabditis elegans* were inoculated monoxenically on nematode agar at room temperature for 4–5 days. Thereafter, nematodes were washed down from the plates with M9 buffer. The final nematodes concentration was adjusted to 500 nematodes/mL of M9 buffer. Assay was performed in

24-well microtiter plate at four different concentration (100, 50, 25 and 12, 5 μmL) of each compound. Ivermectin was used as the positive control and methanol as a negative control. The plates were incubated at 20 °C in the shaker in the dark and nematocidal activity was recorded after 18 h of incubation and expressed as a LD_{50} .

3. Results and discussion

The fungal strain *Sanghuangporus* sp. (MUCL 55592) was identified to generic level by sequencing parts of the rDNA (5.8S gene region, including the internal transcribed spacers (ITS1 and ITS2) and part of the large subunit (LSU) as described in the Experimental. A BLAST search in GenBank confirmed the identity affinities of this strain with members of *Sanghuangporus* since the most homologous sequences were derived from this genus. This was in agreement with the morphological features of the basidiomata. Currently, further taxonomic studies are ongoing to assess whether MUCL 55592 constitutes a new species; still a bulk of *Inonotus* and *Phellinus* species need to be re-evaluated in a modern taxonomic scheme.

Sanghuangporus sp. MUCL 55592 was investigated for active secondary metabolites as its crude extract exhibited antimicrobial activity against *Bacillus subtilis*. Analysis of the HPLC–MS data and subsequent search in public databases such as the Dictionary of Natural Products (Dictionary of Natural Products on DVD, 2017), revealed the presence of a potentially new metabolite. The secondary metabolite profile of the crude extracts is shown in (Fig. 1). Bioassay guided fractionation led to the isolation of one new compound of the phelligridin family named phelligridin L (1) together with known compounds: 3, 14'-bihispidinyl (2), hispidin (3), ionylideneacetic acid (4), 1S-(2E)-5-[(1R)-2,2-dimethyl-6-methylidene-cyclohexyl]-3-methylpent-2-enoic acid (5), phellidine E (6) and phellidine D (7) (Fig. 2) (Klaar and Steglich, 1977; Edwards et al., 1961; Kobayashi et al., 2010). The known compounds were identified by comparing their NMR and HR-MS data with those reported in the literature.

Phelligridin L was isolated as a brown powder. The molecular formula $\text{C}_{25}\text{H}_{16}\text{O}_9$ with 18° of unsaturation was deduced from the HRMS data. Furthermore, the ion peaks $[\text{M} + \text{H}]^+$ at m/z 461.0871, $[\text{M} + \text{Na}]^+$ at m/z 483.0690 and $[2\text{M} + \text{H}]^+$ at m/z 921.1660 were identified in the HR mass spectrum. The ^1H NMR spectrum revealed 6 singlets, 4 doublets and one doublet of doublets attributed to aromatic and/or olefinic protons. From the ^{13}C and DEPT/HSQC NMR spectra 11 methines and 14 quaternary carbons were identified (Table 1).

The HMBC correlations (Fig. 3) of H-3 to C-2, C-5 and H-5 (δ_{H} 5.72)

to C-3, C-4, C-6, C-2' established the 4,6-disubstituted pyrone moiety in the molecule. Although C-3 (δ_{C} 90.4) and C-5 (δ_{C} 100.9) were missing in the ^{13}C spectra their existence was confirmed from the HSQC and HMBC correlations of H-5 (Fig. 4). The oxygenated substituents were attached to C-2 (δ_{C} 163.0), C-4 (δ_{C} 174.8) and C-6 (δ_{C} 156.3) based on their chemical shifts. Further HMBC correlations of H-3' (δ_{H} 7.63) to C-6, C-7'a, C-1', C-3'a, H-4' (δ_{H} 6.93) to C-7'a, C-3', C-6' and H-7' (δ_{H} 6.62) to C-3'a, C-5', C-1' unambiguously established the disubstituted-5',6'-dihydroxyindene moiety. The chemical shifts of the quaternary carbons C-5' (148.4) and C-6' (δ_{C} 148.1) indicated that these carbons were oxygenated. The long range HMBC correlations of H-5 to C-2' and H-3' to C-6 confirmed the linkage of the pyrone moiety to the indene moiety part of the molecule through C-2' and C-6 bond.

The HMBC correlations of a doublet occurring at δ_{H} 7.16 (H-4'') with a coupling constant 1.94 Hz to C-2'', C-5'', C-6'', C-8'', a doublet H-7'' (δ_{H} 6.80, $J = 8.17$ Hz) to C-3'', C-5'', C-6'' and a doublet of doublets H-8'' (δ_{H} 7.07, $J = 1.94, 8.17$ Hz) to C-4'', C-2'', C-6'' observed pointed to a 1,2,4-trisubstituted benzene ring. Based on their chemical shifts δ_{C} 147.2 and δ_{C} 150.5 for C-5'' and C-6'' respectively, hydroxyl groups were attached to these carbons. Further HMBC correlations of H-1'' (δ_{H} 7.01) to C-3'', C-5'', 4'' and H-2'' to C-4'', C-8'', C-5'' were observed. Cross peaks between H-1'' and H-2'' were also observed in the COSY spectrum with the olefinic bond between them being *trans* because of the large coupling constant of 15.92 Hz recorded. From these HMBC and COSY correlations a *trans*-5'', 6''-dihydroxystyryl moiety was elucidated.

The singlet at δ_{H} 6.08 (H-4'') long range HMBC correlations to C-1', C-3'', C-5'', C-1'' were recorded thus establishing the connection of C-1' to C-5'' through C-3'' and C-4''. The HMBC correlations of H-4'' to C-5'', C-1'' and H-4'' to C-1' established the connection between this part of the molecule to the *trans*-5'', 6''-dihydroxystyryl moiety and the disubstituted-5', 6'-dihydroxyindene moiety respectively. The molecular formula of compound 1 had been established from the HRMS data as $\text{C}_{25}\text{H}_{16}\text{O}_9$, and the 18° of unsaturation, to these 25 carbons, 16 hydrogens, 8 oxygens and 17° of unsaturation have been accounted for. Therefore based on the chemical shifts of C-5'' (δ_{C} 188.0) and C-1' (δ_{C} 96.9) and the molecular formula, C-1' and C-5'' were connected via an oxygen atom establishing the spiroindene moiety in the molecule. Therefore the structure of compound 1 was elucidated as 5',6'-dihydroxy-2'-(4-hydroxy-2-oxo-2H-pyran-6-yl)-5-[(E)-2-(4-hydroxy-phenyl) ethenyl]-3H-spiro[furan-2,1'-inden]-3-one.

Phelligridin L (1) is closely related to other naturally occurring antioxidant and cytotoxic agents such as phelligridin G, phelligridin E

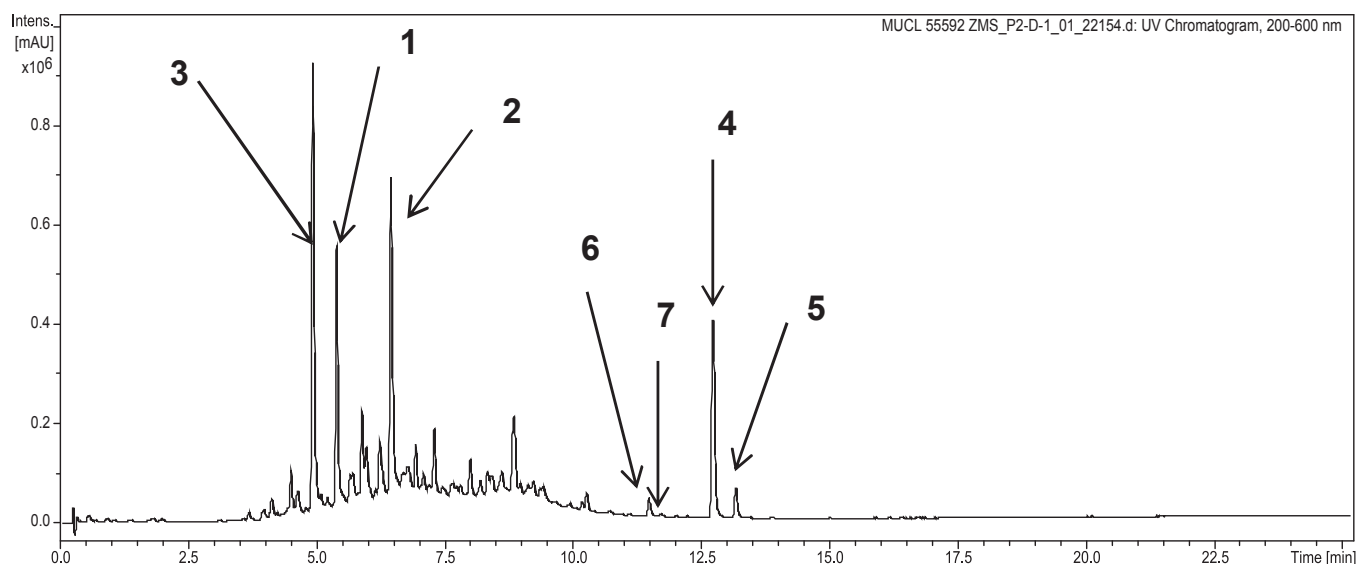


Fig. 1. “HPLC profile (chromatogram recorded of the total UV/Vis adsorption between 200–600 nm)” of the crude extract from the supernatant of *Sanhuangporus* sp.

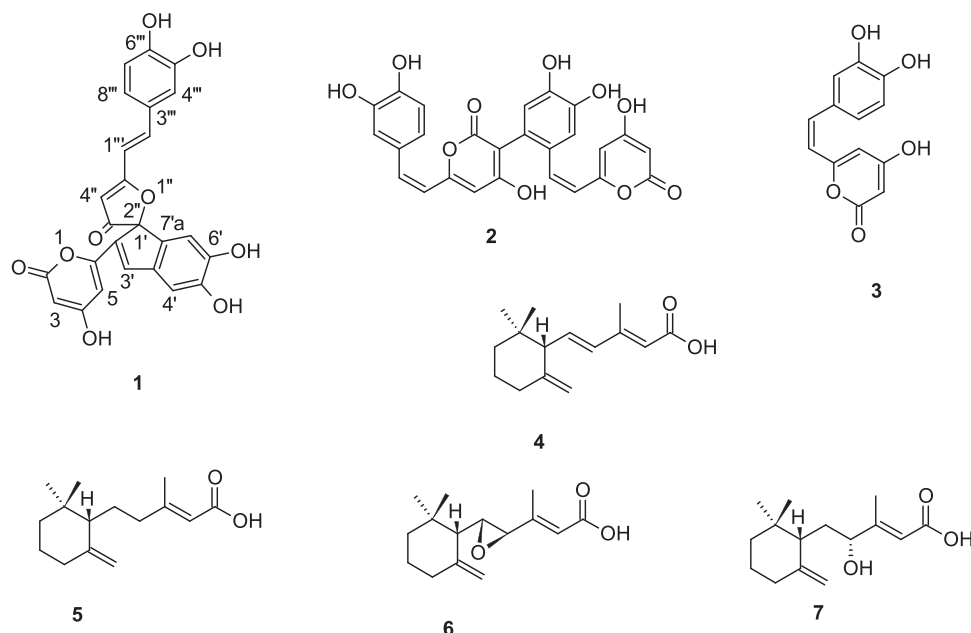


Fig. 2. Chemical structures of 1–7.

Table 1

^1H and ^{13}C data of phelligridin L (1) recorded in methanol- d_4 (^1H 700 MHz, ^{13}C 150 MHz).

No	δ_{C}	DEPT	δ_{H}
2	163.0	C	
3	90.4	CH	5.34
4	174.8	C	
5	100.9	CH	5.72 (s)
6	156.3	C	
1'/2''	96.9	C	
2'	134.7	C	
3'	141.4	CH	7.63 (s)
3a'	134.4	C	
4'	112.1	CH	6.93 (s)
5'	148.4	C	
6'	148.1	C	
7'	110.5	CH	6.62 (s)
7a'	136.1	C	
3''	201.6	C	
4''	104.5	CH	6.08 (s)
5''	188.0	C	
1'''	113.4	CH	7.01 (d), $J = 15.92$ Hz
2'''	143.9	CH	7.60 (d), $J = 15.92$ Hz
3'''	128.3	C	
4'''	115.7	CH	7.16 (d), $J = 1.94$ Hz
5'''	141.4	C	
6'''	150.5	C	
7'''	116.8	CH	6.80 (d), $J = 8.17$ Hz
8'''	124.0	CH	7.07 (dd), $J = 1.94, 8.17$

and inoscavin A (Wang et al., 2005; Mo et al., 2004; Kim et al., 1999). Like the above mentioned compounds phelligridin L was optically inactive. The biogenetic formation of the chiral centre at C-1' of the spiroindene moiety has been reported before to be nonstereo-selective (Wang et al., 2005).

The nematocidal effects of compounds 1–7 on *Caenorhabditis elegans* are shown in Table 2. Compounds 1 and 3 showed moderate nematocidal activity with LD_{50} of 12.5 $\mu\text{g}/\text{mL}$. Compound 2 exhibited a weak effect with LD_{50} of 50 $\mu\text{g}/\text{mL}$. The other compounds 4–7 did not show any significant nematocidal effects on *C. elegans*. Although the biological activities of hispidin (3), and 3, 14'-Bihispidinyl (2) have already been studied for decades, to the best of our knowledge their nematocidal activities have not been reported. Furthermore 1–7 were tested for

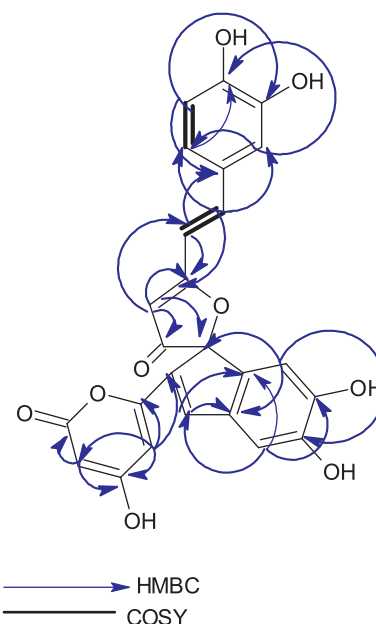


Fig. 3. HMBC and COSY correlations of 1.

antimicrobial activities against various test organisms (Table 2). Compound 1 and 3 were found to be active against *Micrococcus luteus* with MIC of 25 $\mu\text{g}/\text{mL}$ and 100 $\mu\text{g}/\text{mL}$ respectively. Further 4–5 demonstrated non selective antibacterial and antifungal activities. Antimicrobial activities of these two compounds have been reported before (Kobayashi et al., 2010). However, when studied by us, phelligridins D and E exhibited no significant antimicrobial activities at concentrations up to 100 $\mu\text{g}/\text{mL}$. This observation may relate to the different test organism and protocols used by us in comparison to the aforementioned reference.

4. Conclusion

Sanguangporus sp. belongs to the *Inonotus linteus* complex of medicinal mushrooms. A new highly oxygenated spiro [furan-2,1'-indine]-3-one derivative (1) together with six known compounds were isolated

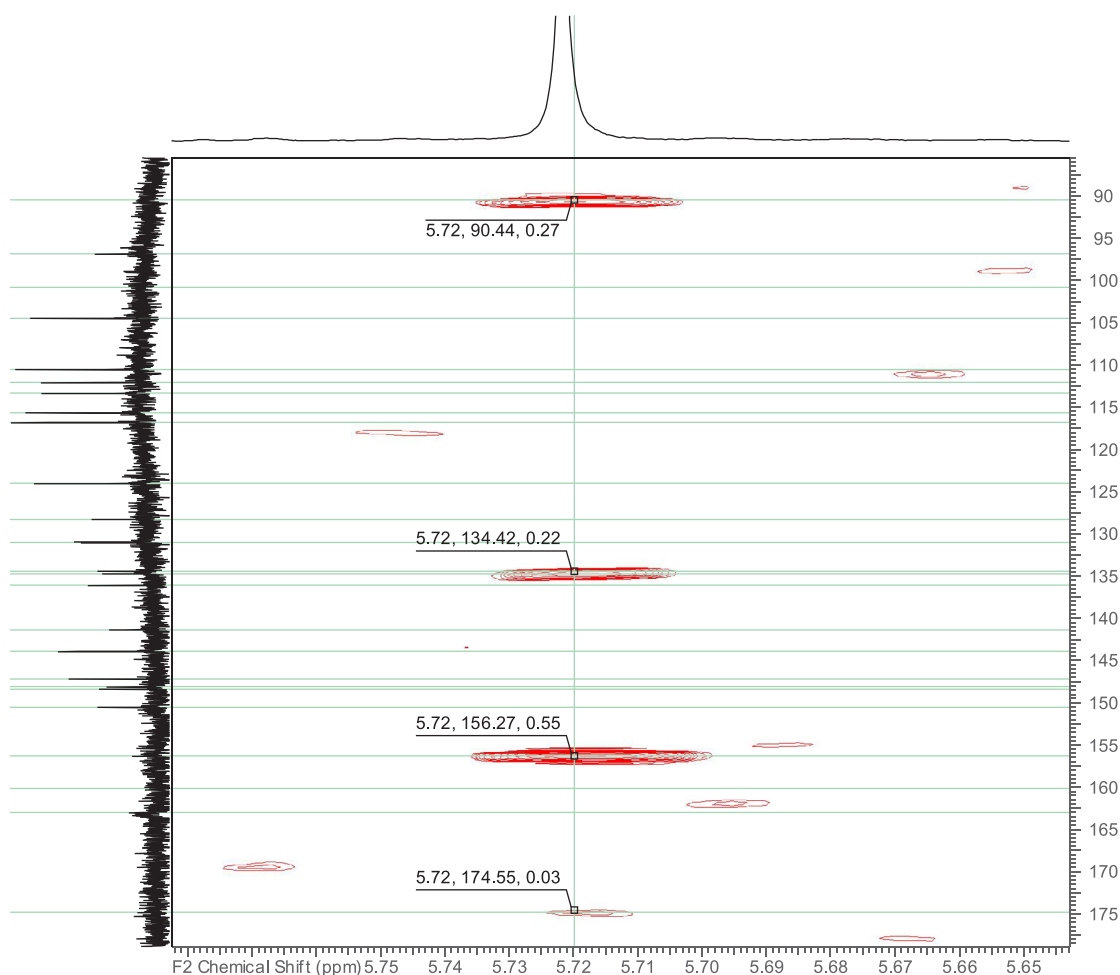


Fig. 4. Extracted part of HMBC spectra of phelligridin L (1) showing H-5 HMBC correlations.

Table 2

Antimicrobial and nematocidal activities of compounds 1–7.

Test strains	1	2	3	4	5	6	7	Reference
Antimicrobial activities MIC (µg/mL)								
<i>Bacillus subtilis</i> DSM 10	/	/	/	6.25	/	/	/	2.3 ^a
<i>Micrococcus luteus</i> DSM 1790	25	25	100	25	≤100	/	/	8.3 ^a
<i>Escherichia coli</i> DSM 498	/	/	/	/	/	/	/	2.3 ^a
<i>Candida tenuis</i> MUCL 29982	/	/	/	50	/	/	/	2.3 ^b
<i>Mucor plumbeus</i> MUCL 49355	100	/	/	12.5	100	/	/	9.4 ^b
Nematocidal activities LD₅₀ (µg/mL)								
<i>Caenorhabditis elegans</i>	12.5	12.5	25	/	/	/	/	≤3.1 ^c

/ No activity; stock solution 100 µg/mL.

^a Ciprofloxacin.

^b Nystatin.

^c Ivermectin.

from *Sanghuangporus* sp. Compounds 1–5 showed moderate antimicrobial activity. Furthermore, compound 1–3 showed moderate nematocidal activities against *C. elegans*. Even though 3,14'-bihispidinyl and hispidin have been studied for several decades their nematocidal activity have not been reported before. Some of the biological activities of hispidin and other hispidin derivatives include antimicrobial, anti-oxidants, cytotoxic, anti-inflammatory and β -secretase inhibition activities (Chen et al., 2016; De Silva et al., 2013; Hsieh et al., 2013; Lee et al., 2006; Lee and Yun, 2011).

5. Chemical data

Phelligridin L (1): Brown powder; UV (MeOH, c = 0.25) λ_{max} (log ϵ) 202 (3.663), 256 (3.3950), 385 (3.646); ¹H NMR (700 MHz, Methanol-d₄) see Table 1, ¹³C NMR (175 MHz, Methanol-d₄) see Table 1; HRESIMS m/z 461.0871 [M + H]⁺ (calcd for C₂₅H₁₇O₆, 461.0872).

Conflict of interest

The authors declare no competing financial interests.

Supplementary information

UV, HRMS data and ¹H, ¹³C, COSY, HSQC, HMBC NMR spectra of metabolites 1 are available as Supporting information. The ITS and LSU sequences of the producing organism are also included.

Acknowledgements

We are grateful to Christel Kakoschke and Cécilia Schwager for their technical support. Financial support by the “ASAFEM” Project (Grant no. IC-070) under the ERAfrica Programme to J.C.M., C.D. and M.S. and a personal PhD stipend by the German Academic Exchange Service (DAAD) and the Kenya National Council for Science and Technology (NACOSTI) to C.C. is gratefully acknowledged (programme-ID: 57139945).

Appendix A. Supplementary data

Supplementary data associated with this article can be found, in the online version, at <https://doi.org/10.1016/j.phytol.2018.04.022>.

References

- Bitzer, J., Læssøe, T., Fournier, J., Kummer, V., Decock, C., Tichy, H.V., Piepenbring, M., Persoh, D., Stadler, M., 2008. Affinities of *Phylacia* and the daldinoid Xylariaceae: inferred from chemotypes of cultures and ribosomal DNA sequences. *Mycol. Res.* 112, 251–270.
- Chen, H., Tian, T., Miao, H., Zhao, Y.Y., 2016. Traditional uses, fermentation, phytochemistry and pharmacology of *Phellinus linteus*: a review. *Fitoterapi* 113, 6–26.
- Chepkirui, C., Richter, C., Matasyoh, J.C., Stadler, M., 2016. Monochlorinated calocerins A–D and 9-oxostrobilurin derivatives from the basidiomycete *Favolaschia calocera*. *Phytochemistry* 132, 95–101.
- Chepkirui, C., Matasyoh, J.C., Decock, C., Stadler, M., 2017. Two cytotoxic triterpenes from cultures of a Kenyan *Laetiporus* sp. (Basidiomycota). *Phytochem. Lett.* 20, 106–110.
- Chepkirui, C., Sum, W.C., Cheng, T., Matasyoh, J.C., Decock, C., Stadler, M., 2018a. Aethiopinolones A–E, new pregnenolone type steroids from the East African basidiomycete *Fomitiporia aethiopica*. *Molecules* 23, 369–378.
- Chepkirui, C., Yuyama, K.T., Wanga, L.A., Decock, C., Matasyoh, J.C., Wolf-Rainer, A., Stadler, M., 2018b. Microporenic Acids A–G, biofilm inhibitors and antimicrobials agents from the basidiomycete *Microporus* sp. *J. Nat. Prod.* <http://dx.doi.org/10.1021/acs.jnatprod.7b00764>. in press.
- De Silva, D.D., Rapior, S., Sudarman, E., Stadler, M., Xu, J., Alias, S.A., Hyde, K.D., 2013. Bioactive metabolites from macrofungi: ethnopharmacology, biological activities and chemistry. *Fungal Divers.* 1 (62), 1–40.
- Dictionary of Natural Products on DVD, 2017. Dictionary of Natural Products on DVD. Chapman & Hall, Chemical Data Base; CRC, Boca Raton, FL.
- Edwards, R.L., Lewis, D.G., Wilson, D.V., 1961. Constituents of the higher fungi. Part I. Hispidin, a new 4-hydroxy-6-styryl-2-pyrone from *Polyporus hispidus* (Bull.) Fr. *JCS* 4995–5003.
- Ghobad-Nejhad, M., 2015. Collections on *Lonicera* in Northwest Iran represent an undescribed species in the *Inonotus linteus* complex (Hymenochaetales). *Mycol. Progress* 14, 90–94.
- Hsieh, P.W., Wu, J.B., Wu, Y.C., 2013. Chemistry and biology of *Phellinus linteus*. *BioMed* 3, 106–113.
- Karwehl, S., Stadler, M., 2016. Exploitation of fungal biodiversity for discovery of novel antibiotics. *Curr. Top. Microbiol. Immunol.* 398, 303–338.
- Kim, J., Yun, B., Shim, Y.K., Yoo, I., 1999. Inoscavin A, a new free radical scavenger from the mushroom *Inonotus xeranticus*. *Tet. Lett.* 40, 6643–6644.
- Klaar, M., Steglich, W., 1977. Pigmented, XXVII isolation of hispidin and 3,14'-Bihispidinyl from *Phellinus pomaceus* (Poriales). *Chem. Ber.* 110, 1058–1062.
- Kobayashi, Y., Asada, Y., Ino, C., Hirotsu, M., 2010. Oral Cavity Composition Containing *Phellinus linteus*-derived Sesquiterpene Derivatives. Japanese Patent JP2010047512.
- Kuephadungphan, W., Helaly, S.E., Daengrot, C., Phongpaichit, S., Luangsa-ard, J.J., Rukachaisirikul, V., Stadler, M., 2017. Akanthopyrones A–D, α -pyrones bearing a 4-O-methyl- β -D-glucopyranose moiety from the spider-associated ascomycete *Akanthomyces novoguineensis*. *Molecules* 22, 1202–1211.
- Lee, I.K., Yun, B.S., 2011. Styrylpyrone-class compounds from medicinal fungi *Phellinus* and *Inonotus* spp., and their medicinal importance. *J. Antibiotics* 64, 349.
- Lee, I.K., Seok, S.J., Kim, W.K., Yun, B.S., 2006. Hispidin Derivatives from the Mushroom *Inonotus xeranticus* and their antioxidant activity. *J. Nat. Prod.* 24 (69), 299–301.
- Mo, S., Wang, S., Zhou, G., Yang, Y., Li, Y., Chen, X., Shi, J., 2004. Phelligrindins C–F: cytotoxic pyrano[4,3-c][2] benzopyran-1,6-dione and furo[3,2-c]pyran-4-one derivatives from the fungus *Phellinus igniarius*. *J. Nat. Prod.* 67, 823–828.
- Mudalungu, C.M., Richter, C., Wittstein, K., Abdalla, A.M., Matasyoh, J.C., Stadler, M., Süßmuth, R.D., 2015. Laxitextines A and B, Cyathane xyloides from the tropical fungus *Laxitextum incrustatum*. *J. Nat. Prod.* 79, 894–898.
- Ruppic, Z., Chepkirui, C., Hernández-Restrepo, M., Crous, P.W., Luangsa-ard, J.J., Stadler, M., 2018. New nematocidal and antimicrobial secondary metabolites from a new species in a new genus, *Pseudobambusicola thailandica*. *MycKeys* 33, 1–23.
- Teponno, R.B., Noumeur, S.R., Helaly, S.E., Hüttel, S., Harzallah, D., Stadler, M., 2017. Furanones and anthranilic acid derivatives from the endophytic fungus *Dendrothyrium variisporum*. *Molecules* 22, 1674–1685.
- Tomsovsky, M., 2015. *Sanghuangporus pilatii*, a new combination, revealed as European relative of Asian medicinal fungi. *Phytotaxa* 239, 82–88.
- Wang, Y., Mo, S., Wang, S., Li, S., Yang, Y., Shi, J., 2005. A unique highly oxygenated pyrano[4,3-c][2] benzopyran-1,6-dione derivative with antioxidant and cytotoxic activities from the fungus *Phellinus igniarius*. *Org. Lett.* 7, 1675–1678.
- Wendt, L., Sir, E.B., Kuhnert, E., Heitkämper, S., Lambert, C., Hladki, A.I., Romero, A.I., Luangsa-ard, J.J., Srikitikulchai, P., Peršoh, D., Stadler, M., 2018. Resurrection and emendation of the Hypoxylaceae: recognised from a multi-gene genealogy of the Xylariales. *Mycol. Prog.* 17, 115–154.
- Zhou, L., Vlasák, J., Decock, C., Assefa, A., Stenlid, J., Abate, D., Wu, S., Dai, Y., 2015. Global diversity and taxonomy of the *Inonotus linteus* complex (Hymenochaetales, Basidiomycota): *Sanghuangporus* gen. nov., *Tropicoporus excentrodendri* and *T. guanacastensis* gen. et spp. nov., and 17 new combinations. *Fungal Divers.* 77, 335–347.
- Zhu, L., Xing, J., Cui, B., 2017. Morphological characters and phylogenetic analysis reveal a new species of *Sanghuangporus* from China. *Phytotaxa* 311, 270–276.

Article

Aethiopinolones A–E, New Pregnenolone Type Steroids from the East African Basidiomycete *Fomitiporia aethiopica*

Clara Chepkirui ^{1,†}, Winnie C. Sum ^{2,†}, Tian Cheng ¹, Josphat C. Matasyoh ³, Cony Decock ⁴ and Marc Stadler ^{1,*} 

¹ Department of Microbial Drugs, Helmholtz Centre for Infection Research and German Centre for Infection Research (DZIF), Partner Site Hannover/Braunschweig, Inhoffenstrasse 7, 38124 Braunschweig, Germany; clara.chepkirui@helmholtz-hzi.de (C.C.); Tian.Cheng@helmholtz-hzi.de (T.C.)

² Department of Biochemistry, Egerton University, P.O. BOX 536, Njoro 20115, Kenya; winsumbt@gmail.com

³ Department of Chemistry, Egerton University, P.O. BOX 536, Njoro 20115, Kenya; josphat2001@yahoo.com

⁴ Mycothèque de l' Université Catholique de Louvain (BCCM/MUCL), Place Croix du Sud 3, B-1348 Louvain-la-Neuve, Belgium; Cony.Decock@uclouvain.be

* Correspondence: marc.stadler@helmholtz-hzi.de; Tel.: +49-531-6181-4240; Fax: 49-531-6181-9499

† These authors contributed equally to this work.

Received: 16 January 2018; Accepted: 8 February 2018; Published: 9 February 2018

Abstract: A mycelial culture of the Kenyan basidiomycete *Fomitiporia aethiopica* was fermented on rice and the cultures were extracted with methanol. Subsequent HPLC profiling and preparative chromatography of its crude extract led to the isolation of five previously undescribed pregnenolone type triterpenes 1–5, for which we propose the trivial name aethiopinolones A–E. The chemical structures of the aethiopinolones were determined by extensive 1D- and 2D-NMR, and HRMS data analysis. The compounds exhibited moderate cytotoxic effects against various human cancer cell lines, but they were found devoid of significant nematicidal and antimicrobial activities.

Keywords: cytotoxicity; fungi; Hymenochaetaceae; triterpenes

1. Introduction

The fungal kingdom includes many species that produce various classes of structurally unique and biologically active metabolites [1,2]. Of interest to us are the largely neglected basidiomycetes and more so, those available from rich untapped sources like the African tropics. During the course of our studies on Kenya's tropical basidiomycetes we have encountered various interesting organisms that yielded new biologically active metabolites such as laetiporins, calocerins, 9-oxostrobilurins and laxitextines [3–5]. Another specimen collected in Kenya was identified as *Fomitiporia aethiopica*, a species that had been first reported from the Ethiopian highlands [6]. The mycelial culture showed an interesting secondary metabolite profile when studied by HPLC-MS. Although the taxonomy of the genus *Fomitiporia* in Africa has been reported, the secondary metabolites of these genus have so far not been studied extensively, even though one of its species is involved in the esca disease syndrome of grapevine [6–8]. The present paper is dedicated to the first investigation of the secondary metabolite production in mycelial cultures of *Fomitiporia aethiopica*.

2. Results and Discussion

2.1. Structure Elucidation

Solid phase fermentation on rice of the strain *Fomitiporia aethiopica* was carried out as described in the Materials and Methods section. In the antimicrobial assay the crude extracts initially showed

activity against *Bacillus subtilis* but the activity was later attributed to fatty-acid like components of the extracts. However, we found some interesting peaks upon analysis of the HPLC-MS data. A subsequent search in the Dictionary of Natural Products database suggested the presence of hitherto undescribed metabolites [9]. Scale-up of fermentation and subsequent preparative chromatography yielded five new triterpenes 1–5, for which we propose the trivial names aethiopinolones A–E.

Aethiopinolone A (1) was isolated as yellow oil with the molecular formula $C_{21}H_{30}O_5$ and seven degrees of unsaturation deduced from the HRMS data. The ^{13}C -NMR spectroscopic data of 1 revealed the presence of 21 carbon signals (Table 1). From the DEPT NMR data three methyl groups, six methylene groups, six methane groups and six quaternary carbons were identified. In the 1H -NMR spectrum, three methyl singlets resonating at δ 0.58 (H₃-18), δ 0.93 (H₃-19) and δ 2.16 (H₃-21) were recorded. Further, peaks at δ 2.71 (H-17), δ 3.50 (H-3) and 4.74 (H-16) attributed to oxygenated methine groups were observed in the 1H -NMR.

Table 1. NMR data for compounds 1 (in acetone- d_6) and 2 (in DMSO- d_6).

Position	1		2	
	δ_C , Type	δ_H (J in Hz)	δ_C , Type	δ_H (J in Hz)
1	30.5, CH ₂	β :1.31, m ^b ; α :1.48, m ^b	24.2, CH ₂	β :1.01, m ^b ; α :2.27, m ^b
2	31.6, CH ₂	β :1.32, m ^b ; α :1.77, m ^b	27.4, CH ₂	α :1.52, m ^b ; β :1.40, m ^b
3	70.3, CH	3.50, tt, (4.5, 11.3)	63.1, CH	3.91, m
4	31.5, CH ₂	β :2.05, m ^b ; α :2.12 m ^b	27.9, CH ₂	β :1.35, m ^b ; α :1.80, m ^b
5	47.2, CH	2.90, dd, (12.2, 3.8)	41.4, CH	3.17 dd, (12.05, 3.9)
6	199.3, C		200.7, C	-
7	124.2, CH	5.48, d, (2.3)	122.6, CH	5.39, d(1.9)
8	160.8, C		160.4, C	
9	74.2, C		72.6, C	
10	42.7, C		41.9, C	
11	28.5, CH ₂	α :1.84, m ^b ; β :2.01, m ^b	26.8, CH ₂	α :1.69, dd, (13.6, 3.9); β :1.78, dd, (13.6, 4.43)
12	35.5, CH ₂	β :1.97, m ^b ; α :2.07, m ^b	34.0, CH ₂	β :1.83, m; α :1.94, m
13	46.8, C		45.6, C	
14	50.1, CH	3.12, ddd, (12.8, 6.7, 2.3)	48.8, CH	3.01, ddd, (12.4, 6.6, 1.9)
15	35.1, CH ₂	β :1.61, m ^b ; α :2.02, m ^b	33.8, CH ₂	α :1.47, m ^b ; α :1.88, m ^b
16	71.6, CH	4.74, bt, (3.0)	69.9, CH	4.55, bt, (3.1)
17	74.3, CH	2.71, d, (6.0)	73.0, CH	2.63, d, (6.1)
18	14.8, CH ₃	0.58, s	14.2, CH ₂	0.46, s
19	17.2, CH ₃	0.93, s	15.8, CH ₃	0.80, s
20	207.6, C		207.7, C	
21	31.9, CH ₃	2.16, s	31.6, CH ₃	2.15, s

^b Signals partially obscured, b- broad.

HMBC correlations of H₃-18 to C-12/C-13/C-14/C-17, H₃-19 to C-1/C-5/C-9/C-10, H-5 to C-3/C-4/C-6/C-9/C-10/C-19, H-14 to C-7/C-8/C-9/C-13/C-15/C-18 and H₃-21 to C-17/C-20 suggested a pregnenolone type of steroids (Figure 1). COSY correlations of H₂-2 to H₂-1/H-3, H₂-4 to H-3/H-5, H₂-11 to H₂-12, H-14 to H₂-15 and H-16 to H₂-15/H-17 further supported these HMBC correlations. Furthermore, cross peaks observed between H-7 and C-5/C-9/C-14 in the HMBC spectrum and long range COSY correlation to H-14 with a coupling constant of 1.9 Hz helped to confirm the position of the double bond.

A network of ROESY correlations were observed between H₃-18 to H₃-19/H₂-12 β /H-15 β /H-16/H₃-21 and H₃-19 to H₃-18/H₂-1 β /H₂-11 β , suggesting that these protons are on the same side of the plane (Figure 2). On the other hand, cross peaks in the ROESY spectra were observed between H-3 to H₂-1 α /H₂-4 α /H₂-2 α /H-5, H-14 to H₂-15 α /H₂-12 α /H-17 and H-17 to H₂-15 α /H-14. For H-3, an α orientation was established based on the coupling constant of 4.52 Hz and 11.3 Hz together with the ROESY correlations of H-3 to H-5/H₂-1 α /H₂-4 α /H₂-2 α . Conversely, H-16 was β oriented as indicated by the small coupling constant of 3.0 Hz and the cross peaks observed between H-16 and

H₃-18/H₂-15β in the ROESY spectrum. The absolute configuration of **1** was finally determined using Mosher's method [10]. The difference in chemical shifts $\Delta\delta^{SR} = (\Delta_s - \delta_R)$ for protons neighboring C-3 gave positive values +0.079, +0.041 and +0.015 for H₂-4α, H₂-4β and H-5 respectively. On the contrary, negative values of $\Delta\delta^{SR}$ i.e., -0.078 (H₂-α), -0.110 (H₂-2β), -0.016 (H-2-1α), -0.061 (H₂-1β) and -0.011 (H₃-19) were obtained. Therefore the absolute configuration of the C-3 stereocenter can be assigned as *S* (Supplementary Information, Table S1). Using C-3 as the reference the other stereocenters were assigned as 5*S*, 9*S*, 10*S*, 13*S*, 14*R*, 16*R* and 17*R*.

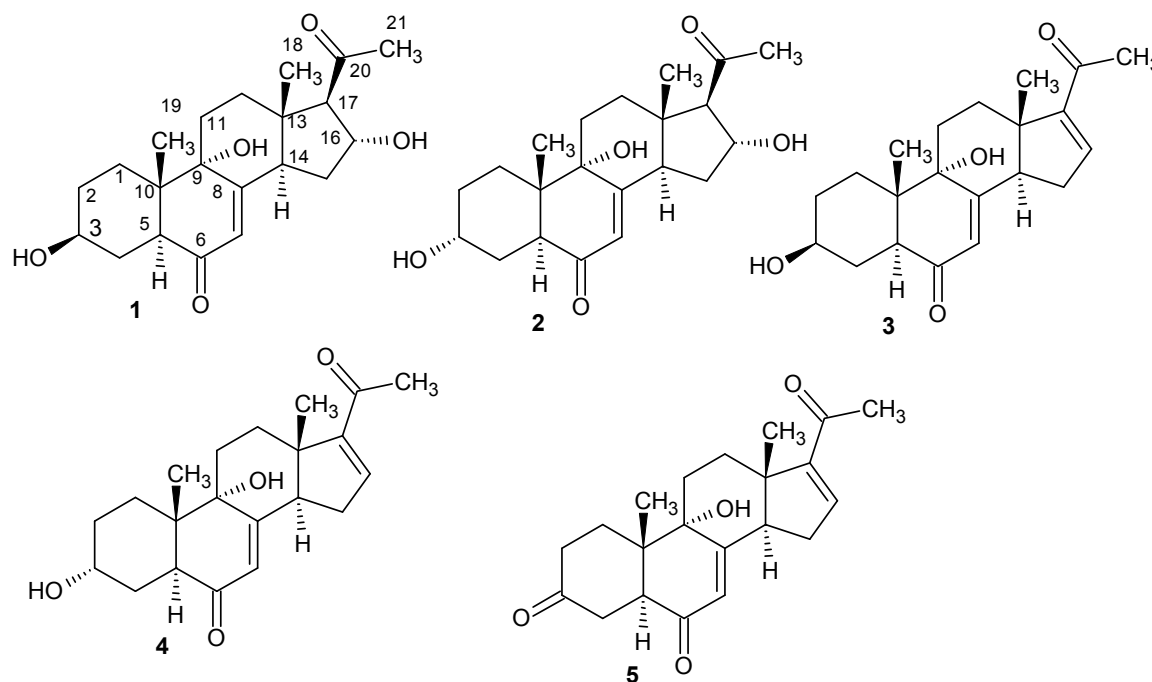


Figure 1. Chemical structures of 1–5.

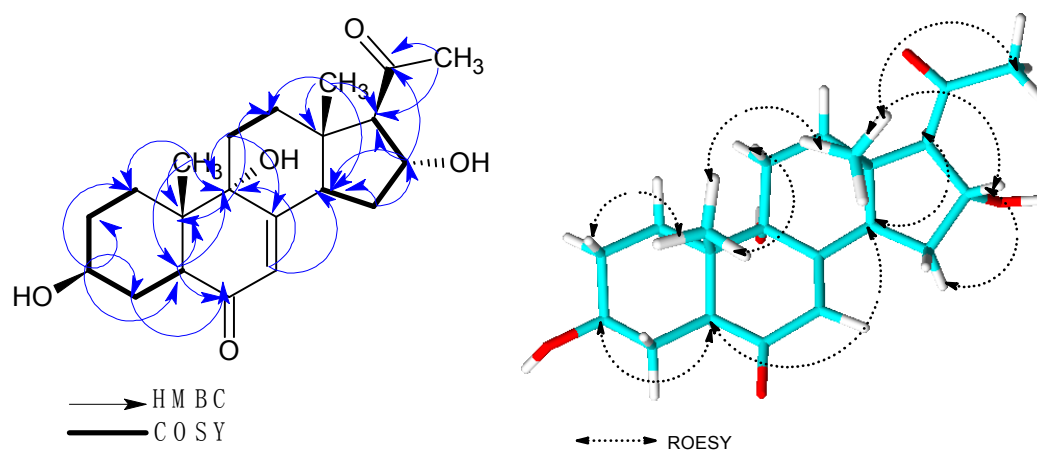


Figure 2. HMBC, COSY and ROESY correlations of **1**.

Aethiopinolone B (**2**) was obtained as a white solid. The molecular formula C₂₁H₃₀O₅ and seven degrees of unsaturation were deduced from the HR mass spectrum. The 1D and 2D-NMR data of **2** suggested that it possesses the same planar structure as **1**, the difference being the stereochemistry at C-3. The ROESY correlation of H-3 to H₃-19 and the OH-3 (δ 4.26) to H-5 pointed to H-3 having β orientation. In the ¹H-NMR spectrum of compound **1** H-3 resonated as a triple triplet while H-3 of compound **2** resonated as multiplet. Furthermore, C-3 was slightly shielded resonating at δ 63.1 as

compared to C-3 of **1**, which occurred at δ 70.3. Consequently the stereochemistry at C-3 was assigned as *R*.

Aethiopinolone C (**3**) with a molecular formula $C_{21}H_{28}O_4$ and eight degrees of unsaturation deduced from HR mass spectrum was further isolated as yellow oil. Analysis of the 1H -NMR revealed the absence of the methine proton at δ 2.71 (H-17) and the oxygenated methine proton δ 4.74 (H-16) which were observed in the 1H -NMR of **1**. Instead an olefinic doublet of doublet resonating at δ 6.91 (H-16) was recorded. In the ^{13}C spectrum new signals at δ 144.3 and δ 155.1 were identified (Table 2). H-16 showed HMBC correlations to C-13/C-14/C-20 and COSY correlations to H₂-15 implying that **3** has similar planar structure as **1** with the difference being the double bond between C-16/C-17. Further, similar ROESY correlations patterns in compounds **1** and **3** were recorded. Derivatization of **3** with both *S* and *R*-MPA chloride gave similar results as **1** for protons neighboring C-3 hence the absolute stereochemistry was assigned as 3*S*, 5*S*, 9*S*, 10*S*, 13*S* and 14*R* (Table S2, SI).

Aethiopinolone D (**4**) was isolated as yellow oil with molecular formula $C_{21}H_{28}O_4$ and eight degrees of unsaturation established from the HRMS data. The 1D and 2D data of **4** indicated that **4** was analogous to **3** with the difference being the stereochemistry at C-3. The same ROESY correlations of H-3 to H₃-19, H-3 multiplicity in the 1H -NMR spectrum and the shielding effect reported in ^{13}C -NMR data of compound **2** were also observed in the ^{13}C -NMR of **4**, evincing the same stereochemistry at C-3 for the two molecules. Esterification of compound **4** with both *S* and *R*-MPA chloride, and subsequent determination of $\Delta\delta^{SR}$ from the resulting esters gave negative values -0.096 , -0.012 and -0.11 for H-5, H₂-4 β and H₂-4 α respectively. Positive values $+0.005$, $+0.162$, $+0.028$ for H-19, H₂-2 β and H₂-2 α respectively were obtained (Supplementary Information, Table S3). Therefore the absolute stereochemistry of compound **4** was assigned as 3*R*, 5*S*, 9*S*, 10*S*, 13*S* and 14*R*.

Aethiopinolone E (**5**) was obtained as yellow oil. The molecular formula $C_{21}H_{26}O_4$ and nine degrees of unsaturation were deduced from the HRMS data. Analysis of the ^{13}C and DEPT NMR data of **5** indicated that it was similar to **3** with the difference being a keto group at position 3. The oxygenated methine signal of compound **3** resonating at δ 70.3 was missing and instead a keto carbonyl group was observed at δ 210.1. HMBC correlations of diastereotopic protons H₂-2 α (δ 2.35), H₂-2 β (δ 2.26), H₂-4 α (δ 2.39), H₂-4 β (δ 2.51), to this carbon supported the assignment.

2.2. Biological Activities

Compounds **1**–**5** were tested for their cytotoxic effects against various mammalian cell lines (Table 3). **3**–**4** showed moderate activity against all the tested cell lines. All compounds apart from **2** showed significant activities against MCF-7 and A431 with IC₅₀ in the range 16–20 μ g/mL and 14–27 μ g/mL respectively. Compound **1** generally showed the strongest activity against the tested cell lines with the highest effects against PC-3 (8 μ g/mL). Compound **2** showed moderate activity only against L929 and KB3.1 cells with IC₅₀ of 45 μ g/mL and 39 μ g/mL respectively. Aside from these cytotoxic activities, compounds **1**–**5** were found devoid of significant antimicrobial and nematocidal effects at concentrations ≤ 300 μ g/mL and ≤ 100 μ g/mL respectively.

Although steroids are rather common in the Basidiomycota, they have not been reported yet from the genus *Fomitiporia*. Studies on *Fomitiporia ellipsoidea* metabolites indicated that this fungus produced a large amount of common ergosterol and its derivatives but this species has since been moved to the genus *Phellinus* (currently valid name: *Phellinus ellipsoidea*) [11,12]. The close relationship between these two genera has seen the transfer of several other species previously assigned to the genus *Phellinus* to the genus *Fomitiporia*, examples being species like *F. erecta*, *F. hartigii*, *F. robusta*, *F. punctata*, *F. hippophaeicola* and *F. pseudopunctata* [13]. Styrylpyrones like the protein kinase C inhibitor, bihispidinyl and hypholomin B, which are common metabolites among the Hymenochaetales, have been reported to occur in some *Fomitiporia* species [14,15].

Table 2. NMR data for compounds 3–5 in acetone-*d*₆.

Pos.	3		4		5	
	δ_C , Type	δ_H (J in Hz)	δ_C , Type	δ_H (J in Hz)	δ_C , Type	δ_H (J in Hz)
1.	30.4, CH ₂	β :1.29, m ^b ; α :1.49, m ^b	25.3, CH ₂	β :1.16, m ^b ; α :2.47, m ^b	32.2, CH ₂	β :1.82, m ^b ; α :1.91, m ^b
2.	30.4, CH ₂	β :1.33 m ^b ; α :1.77, m ^b	28.7, CH ₂	α :1.60, m ^b ; β :1.65, m ^b	37.5, CH ₂	β :2.26, m ^b ; α :2.35, m ^b
3.	70.3, CH	3.47, tt, (4.4, 11.3)	65.0, CH	4.05, m	210.1, CH	
4.	31.5, CH ₂	β :2.10, m ^b ; α :2.13 m ^b	29.2, CH ₂	β :1.54, m ^b ; α :1.97, m ^b	37.6, CH ₂	α :2.39, m ^b ; β :2.51, m ^b
5.	47.3, CH	2.91, dd, (12.2, 3.8)	42.7, CH	3.32, dd, (12.3, 4.1)	49.0, CH	3.30, dd, (12.7, 4.9)
6.	199.4, C		201.1, C		198.4, C	
7.	123.4, CH	5.60, d, (2.1)	123.5, CH	5.58, d, (2.2)	123.1, CH	5.68, d, (2.2)
8.	160.2, C		160.0, C		160.8, C	
9.	74.4, C		74.5, C		74.6, C	
10.	42.8, C		43.4, C		43.1, C	
11.	31.3, CH ₂	α :1.77, m ^b ; β :2.15, m ^b	29.4, CH ₂	β :1.84, m ^b ; α :2.13, m ^b	29.6, CH ₂	α :1.92, m ^b ; β :2.24, m ^b
12.	32.1, CH ₂	β :1.81, m ^b ; α :2.30 m ^b	32.1, CH ₂	β :1.80, m ^b ; α :2.32, m ^b	32.1, CH ₂	β :1.82, m ^b ; α :2.35, m ^b
13.	46.8, C		49.0, C		49.0, C	
14.	52.9, CH	3.11, ddd, (11.6, 6.6, 2.1)	52.7, CH	3.13, ddd, (11.6, 6.5, 2.2)	52.7, CH	3.14, ddd (11.6, 2.2 Hz, 6.2)
15.	31.3, CH ₂	β :2.39, m; α :2.47, m	31.3, CH ₂	β :2.41, m; α :2.47, m	31.3, CH ₂	β :2.42, m; α :2.51, m
16.	144.3, CH	6.91, dd, (1.9, 3.4)	144.3, CH	6.91, dd, (1.9, 3.2)	144.3, CH	6.92, dd, (3.4, 1.9)
17.	155.1, C		155.2, C		155.1, C	
18.	16.4, CH ₃	0.88, s	16.4, CH ₃	0.88, s	16.4, CH ₃	0.91, s
19.	17.2, CH ₃	0.99, s	16.5, CH ₃	0.99, s	16.5, CH ₃	1.24, s
	196.3, C		196.3, C	-	196.3, C	
	27.14, CH ₃	2.25, s	27.2, CH ₃	2.26, s	27.1, CH ₃	2.26, s

^b Signals partially obscured.

Table 3. Cytotoxic activities of compounds 1–5.

Cell Lines	Cytotoxicity IC ₅₀ (µg/mL)					Epothilon B
	1	2	3	4	5	
L929	28	45	40	45	40	0.0014
KB3.1	19	39	35	39	33	0.00022
A431	22	-	27	21	14	0.0006
A549	nt	-	70	52	43	0.005
PC-3	8	-	45	40	39	0.0002
SKOV-3	26	-	38	36	34	0.0014
MCF-7	20	-	18	17	16	0.0004

Not active, nt- not tested.

3. Materials and Methods

3.1. General Experimental Procedures

Optical rotations were determined with a Perkin-Elmer (Überlingen, Germany) 241 spectrometer; UV spectra were recorded with a Shimadzu (Duisburg, Germany) UV-2450 UV-vis spectrophotometer. NMR spectra were recorded with a Bruker (Bremen, Germany) Ascend 700 spectrometer equipped with a 5 mm TXI cryoprobe (¹H-700 MHz, ¹³C-175 MHz) and Bruker AV II-600 (¹H-500 MHz, ¹³C-150 MHz) spectrometers. HR-ESI-MS mass spectra were recorded with a Bruker (Bremen, Germany) Agilent 1260 series HPLC-UV/Vis system (column 2.1 × 50 mm, 1.7 µm, C18 Acquity UPLC BEH (waters), solvent A: H₂O + 0.1% formic acid; solvent B: AcCN + 0.1% formic acid, gradient: 5% B for 0.5 min increasing to 100% B in 19.5 min and then maintaining 100% B for 5 min, flow rate 0.6 mL/min⁻¹, uv/vis detection 200–600 nm combined with ESI-TOF-MS (Maxis, Bruker) [scan range 100–2500 *m/z*, capillary voltage 4500 V, dry temperature 200 °C]. Chemicals and solvents were obtained from AppliChem GmbH (Darmstadt, Germany), Avantor Performance Materials (Arnhem, Netherlands), Carl Roth GmbH & Co. KG (Karlsruhe, Germany) and Merck KGaA (Darmstadt, Germany) in analytical and HPLC grade.

3.2. Fungal Material

The specimen MUCL 56047 was collected from Mount Elgon, located in the western part of Kenya (1°7'6" N, 34°31'30" E) by C. Decock in April 2016 (collection and isolation number KE/16-163). The dried herbarium specimen and culture are deposited at MUCL (Louvain-la-Neuve, Belgium) as MUCL 56047. The fungus was identified as *Fomitiporia aethiopica* by morphological studies and sequencing of the rDNA (5.8S gene region, the internal transcribed spacer ITS1 and ITS2). Genomic DNA Miniprep kit (Bio Basic Canada Inc., Markham, ON, Canada). A Precellys 24 homogenizer (Bertin Technologies, Saint-Quentin-en-Yvelines, France) was used for cell disruption at a speed of 6000 rpm for 2 × 40 s. The gene regions were amplified with primers ITS 1f and ITS 4. Details are given in the Supplementary Material.

3.3. Fermentation

The mycelial culture of MUCL 56047 was subjected to solid state fermentation in rice according to [16] with slight modifications. The rice medium was prepared by weighing 90 g of rice into 500 mL Erlenmeyer flasks containing in 90 mL of distilled water and autoclaved twice. A well-grown YMG agar plate of the mycelial culture was cut into small pieces using a 7 mm cork borer and five plugs inoculated into each of the 21 flasks containing sterile rice media. The cultures were incubated in a dark room at 23 °C for 28 days.

3.4. Extraction

The cultures were diced into smaller pieces with a spatulum and each of the 21 flasks was soaked in 150 mL of methanol overnight. Repeated extraction and filtration in an ultrasonic bath at 40° C for 30 min until an exhausted residue was yielded was carried out. The residue was discarded and

the filtrate evaporated by means of a rotary evaporator. The resulting aqueous phase was suspended in equal amount of distilled water and extracted with equal amount of ethyl acetate four times. The aqueous phase was discarded and the organic phase filtered through anhydrous sodium sulphate. The resulting ethyl acetate extracts were evaporated to dryness by means of rotary evaporator to afford 800 mg of crude product.

3.5. Isolation and Physico-Chemical Characteristics of Compounds 1–5

The crude extract was fractionated using preparative reverse phase liquid chromatography (PLC 2020, Gilson, Middleton, MA, USA). A VP Nucleodur 100-5 C 18 ec column (250 × 40 mm, 7 μm; Macherey-Nagel, Schkeuditz, Germany) was used. Deionized water (Milli-Q, Millipore, Schwalbach, Germany) (solvent A) and acetonitrile (solvent B) were used as the mobile phase. The elution gradient used was 10–100% solvent B in 55 min and thereafter isocratic condition at 100% solvent B for 10 min. UV detection was carried out at 210, 254 and 350 nm. Seven fractions (F1–F7) were collected according to the observed peaks. Fraction F4 was purified by reverse phase LC (solvent A/solvent B), elution gradient 20–35% solvent B for 30 min, followed by a gradient shift from 35% to 100% in 3 min and finally isocratic condition at 100% solvent B for 5 min with a preparative (Kromasil, Mainz, Germany) 250 × 20 mm, 7 μL C-18 column as stationary phase to give compounds **1** (30 mg) and **3** (16 mg). Using the same column and elution gradient 25–40% solvent B for 35 min, fraction F6 was purified to afford 60 mg of compound **2**, as well as 12 mg of **4** and 8 mg of **5**.

Aethiopinolone A (1): Yellow oil; $[\alpha]_D^{25} -13^\circ$ (*c* 0.001, MeOH); UV (MeOH) $\lambda_{\max}(\log \epsilon)$ 236 (3.73); HREIMS *m/z* 363.2166 (calcd. for C₂₁H₃₁O₅, 363.2171); ¹H-NMR (acetone-*d*₆, 700 MHz) and ¹³C-NMR (acetone-*d*₆, 175 MHz) data: see Table 1.

Aethiopinolone B (2): White solid; $[\alpha]_D^{25} -33^\circ$, (*c* 0.001, MeOH); UV (MeOH) $\lambda_{\max}(\log \epsilon)$ 240 (3.77); HREIMS *m/z* 363.2162 (calcd. for C₂₁H₃₁O₅, 363.2171); ¹H-NMR (DMSO, 500 MHz) and ¹³C-NMR (DMSO, 125 MHz) data: see Table 1.

Aethiopinolone C (3): Yellow oil; $[\alpha]_D^{25} +15^\circ$, (*c* 0.001, MeOH); UV (MeOH) $\lambda_{\max}(\log \epsilon)$ 234 (3.45); HREIMS *m/z* 345.2060 (calcd. for C₂₁H₂₉O₄, 345.2065); ¹H-NMR (acetone-*d*₆, 500 MHz) and ¹³C-NMR (acetone-*d*₆, 125 MHz) data: see Table 2.

Aethiopinolone D (4): Yellow oil; $[\alpha]_D^{25} +19^\circ$, (*c* 0.001, MeOH); UV (MeOH) $\lambda_{\max}(\log \epsilon)$ 234 (3.38); HREIMS *m/z* 345.2052 (calcd. for C₂₁H₂₉O₄, 345.2065); ¹H-NMR (acetone-*d*₆, 700 MHz) and ¹³C-NMR (acetone-*d*₆, 175 MHz) data: see Table 2.

Aethiopinolone E (5): Yellow oil; $[\alpha]_D^{25} +10^\circ$, (*c* 0.001, MeOH); UV (MeOH) $\lambda_{\max}(\log \epsilon)$ 238 (3.61); HREIMS *m/z* 343.1901 (calcd. for C₂₁H₂₇O₄, 343.1909); ¹H-NMR (acetone-*d*₆, 700 MHz) and ¹³C-NMR (acetone-*d*₆, 175 MHz) data: see Table 2.

Aethiopinolone A (1) 3-O-(S)-MTPA ester: ¹H-NMR (chloroform-*d*, 700 MHz) δ 7.55 (2H, m, ArH), 7.43 (3H, m, ArH), 5.766 (1H, d, *J* = 2.2 Hz, H-7), 5.016 (1H, tt, *J* = 4.5, 11.8 Hz, H-3), 3.994 (1H, m, H-16), 3.590 (3H, s, OCH₃), 3.040 (1H, m, H-14), 2.985 (1H, dd, *J* = 3.9, 12.3, H-5), 2.472 (1H, d, *J* = 5.8 Hz, H-17), 2.443 (1H, m, 15 α), 2.388 (1H, m, H-4 α), 2.309 (3H, s, H-21), 2.011 (1H, m, H-1 α), 1.945 (1H, m, H-2 α), 1.631 (1H, m, H-4 β), 1.568 (1H, m, H-15 α), 1.515 (1H, m, H-2 β), 1.303 (1H, m, H-1 β), 1.034 (3H, s, H-19), 0.896 (3H, s, H-18). EIMS *m/z* 579.27 (calcd. for C₃₁H₃₈F₃O₇, 579.2569)

Aethiopinolone A (1) 3-O-(R)-MTPA ester: ¹H-NMR (chloroform-*d*, 700 MHz) δ 7.55 (2H, m, ArH), 7.43 (3H, m, ArH), 5.757 (1H, d, *J* = 1.9 Hz, H-7), 5.012 (1H, tt, *J* = 4.7, 11.6 Hz, H-3), 3.994 (1H, m, H-16), 3.570 (3H, s, OCH₃), 3.038 (1H, m, H-14), 2.970 (1H, dd, *J* = 3.9, 12.5, H-5), 2.473 (1H, d, *J* = 5.6 Hz, H-17), 2.446 (1H, m, 15 α), 2.334 (1H, m, H-1 α), 2.309 (1H, m, H-4 α), 2.310 (3H, s, H-21), 2.024 (1H, m, H-2 α), 1.625 (1H, m, H-2 β), 1.569 (1H, m, H-15 α), 1.590 (1H, m, H-4 β), 1.364 (1H, m, H-1 β), 1.045 (3H, s, H-19), 0.897 (3H, s, H-18). EIMS *m/z* 579.29 (calcd. for C₃₁H₃₈F₃O₇, 579.2569)

Aethiopinolone C (3) S-MTPA ester: ¹H-NMR (pyridine-*d*₅, 700 MHz) δ 7.40–7.48 (5H, m, ArH), 6.615 (1H, dd, *J* = 1.9, 3.2, H-16), 5.956 (1H, d, *J* = 2.2 Hz, H-7), 5.290 (1H, tt, *J* = 4.7, 11.6, H-3), 3.528 (1H, dd,

$J = 3.7, 12.3$ Hz, H-5), 3.695 (3H, s, OCH₃), 3.413 (1H, ddd, $J = 1.9, 6.5, 11.6$ Hz, H-14), 2.711 (1H, m, H-4 α), 2.397 (2H, m, H-1), 2.2351 (1H, m, 15 α), 2.238 (1H, m, H-15 β), 2.251 (3H, s, H-21), 1.983 (1H, m, H-2 α), 1.926 (1H, m, H-4 β), 1.556 (1H, m, H-2 β), 1.019 (3H, s, H-19), 0.948 (3H, s, H-18). EIMS m/z 561.28 (calcd. for C₃₁H₃₆F₃O₆, 561.2463)

Aethiopinolone C (3) R-MTPA ester: ¹H-NMR (pyridine-*d*₅, 700 MHz) δ 7.40–7.47 (5H, m, ArH), 6.612 (1H, dd, $J = 1.7, 3.2$, H-16), 5.944 (1H, d, $J = 2.2$ Hz, H-7), 5.287 (1H, tt, $J = 4.5, 11.8$, H-3), 3.506 (1H, dd, $J = 3.9, 12.5$ Hz, H-5), 3.852 (3H, s, OCH₃), 3.399 (1H, ddd, $J = 2.2, 6.0, 11.6$ Hz, H-14), 2.669 (1H, m, H-4 α), 2.418 (2H, m, H-1), 2.2350 (1H, m, 15 α), 2.232 (1H, m, H-15 β), 2.250 (3H, s, H-21), 2.049 (1H, m, H-2 α), 1.846 (1H, m, H-4 β), 1.685 (1H, m, H-2 β), 1.027 (3H, s, H-19), 0.950 (3H, s, H-18). EIMS m/z 561.26 (calcd. for C₃₁H₃₆F₃O₆, 561.2463)

Aethiopinolone D (4) S-MTPA ester: ¹H-NMR (pyridine-*d*₅, 700 MHz) δ 7.40–7.47 (5H, m, ArH), 6.600 (1H, dd, $J = 1.9, 3.4$, H-16), 5.910 (1H, d, $J = 2.2$ Hz, H-7), 5.639 (1H, m, H-3), 3.619 (1H, dd, $J = 4.1, 12.5$ Hz, H-5), 3.850 (3H, s, OCH₃), 3.367 (1H, ddd, $J = 2.2, 6.0, 11.6$ Hz, H-14), 2.657 (1H, 1 β , H-1), 2.530 (1H, m, H-4 α), 2.296 (1H, m, 15 α), 2.222 (1H, m, H-15 β), 2.078 (1H, m, H-2 α), 2.015 (3H, s, H-21), 1.999 (1H, m, H-4 β), 1.741 (1H, m, H-2 β), 1.361 (1H, m, 1 α), 1.067 (3H, s, H-19), 0.971 (3H, s, H-18). EIMS m/z 561.30 (calcd. for C₃₁H₃₆F₃O₆, 561.2463)

Aethiopinolone D (4) R-MTPA ester: ¹H-NMR (pyridine-*d*₅, 700 MHz) δ 7.40–7.47 (5H, m, ArH), 6.600 (1H, dd, $J = 1.7, 3.2$, H-16), 5.945 (1H, d, $J = 2.2$ Hz, H-7), 5.640 (1H, m, H-3), 3.715 (1H, dd, $J = 4.1, 12.2$ Hz, H-5), 3.698 (3H, s, OCH₃), 3.366 (1H, ddd, $J = 1.94, 6.2, 11.8$ Hz, H-14), 2.640 (1H, m, H-4 α), 2.507 (1H, 1 β , H-1), 2.300 (1H, m, 15 α), 2.229 (1H, m, H-15 β), 1.976 (1H, m, H-2 α), 2.015 (3H, s, H-21), 2.011 (1H, m, H-4 β), 1.713 (1H, m, H-2 β), 1.298 (1H, m, 1 α), 1.062 (3H, s, H-19), 0.959 (3H, s, H-18). EIMS m/z 561.29 (calcd. for C₃₁H₃₆F₃O₆, 561.2463)

3.6. Preparation of the (R)- and (S)-MTPA Ester Derivatives

Compound 1 (3 mg) were dissolved in pyridine (6 mL) and transferred into two vials (3 mL each). (R)-(-)- α -Methoxy- α -(trifluoromethyl)phenylacetyl chloride (5 μ L) was added to one of the vials and (S)-(+)- α -methoxy- α -(trifluoromethyl)phenylacetyl chloride (5 μ L) was added into the other vial, and stirred for 1 h. The products were purified by reverse phase LC (acetonitrile (B)/H₂O (A), elution gradient 40–100% solvent B for 25 mins followed by isocratic condition at 100% solvent B for 5 min with a preparative (VP 250/10 NUCLEODUR 100-5 C18 ec, Macherey-Nagel, Schkeuditz, Germany) 250 \times 10 mm, C-18 column as stationary phase and 6mL/min flow rate. ¹H-NMR and ¹H, ¹H COSY of the samples were recorded after wards. Compound 3 and 4 (3 mg each) were dissolved in deuterated pyridine (6 mL) and transferred into two vials (3mL each). (R)-(-)- α -Methoxy- α -(trifluoromethyl)phenylacetyl chloride (5 μ L) was added to one of the vials and (S)-(+)- α -methoxy- α -(trifluoromethyl)phenylacetyl chloride (5 μ L) was added into the other vial, and stirred for 3 h. ¹NMR and ¹H, ¹H COSY of the samples were recorded after wards.

3.7. Antimicrobial Assay

Minimum Inhibition Concentrations (MIC) against different test organisms were determined in serial dilution assay as described previously [17] against *Candida tenuis* MUCL 29982, *Mucor plumbeus* MUCL 49355, *Escherichia coli* DSM498 and *Bacillus subtilis* DSM10. The assays were carried out in 96-well microtiter plates in YMG media for filamentous fungi and yeast and MH for bacteria. The stock solution concentration was 300 μ g/mL.

3.8. Cytotoxicity Assay

In vitro cytotoxicity (IC₅₀) of the pure compounds 1–5 was determined against a panel of mammalian cell lines including mouse fibroblast L929, HeLa (KB-3-1), epidermoid carcinoma cells A431, breast cancer cells MCF-7, prostate cancer cells PC-3 and adenocarcinomic human alveolar basal epithelial cells A549. The cell lines were cultured in DMEM (Gibco, ThermoFisher Scientific,

Hilden, Germany) and MCF-7 in RPMI (Lonza, Cologne, Germany) media, all supplemented with 10% of fetal bovine serum (Gibco) under 10% CO₂ at 37 °C. The cytotoxicity assay was performed according to the MTT (3-(4,5-dimethylthiazol-2-yl)-2,5 diphenyltetrazolium bromide) method in 96-well microplates (ThermoFisher Scientific). Briefly 60 µL aliquots of serial dilutions from an initial stock of 1 mg/mL in MeOH of the test compounds were added to 120 µL aliquots of a cell suspension (5.0×10^4 cells/mL) in 96-well microplates. After 5 days incubation, a MTT assay was performed, and the absorbance measured at 590 nm using an ELISA plate reader (Victor, PerkinElmer, Überlingen, Germany). The concentration at which the growth of cells was inhibited to 50% of the control (IC₅₀) was obtained from the dose response curves. The negative control was methanol.

3.9. Nematicidal Assay

Compounds 1–5 were assessed for nematicidal activity against *Caenorhabditis elegans* according to [18] with slight modifications. *Caenorhabditis elegans* were inoculated monoxenically on nematode agar at room temperature for 4–5 days. Thereafter, nematodes were washed down from the plates with M9 buffer. The final nematodes concentration was adjusted to 500 nematodes/mL of M9 buffer. Assay was performed in 24-well microtiter plate at four different concentration (100, 50, 25 and 12.5 µ/mL) of each compound. Ivermectin was used as the positive control and methanol as a negative control. The plates were incubated at 20 °C in the shaker in the dark and nematicidal activity was recorded after 18 h of incubation and expressed as a LD₉₀.

4. Conclusions

In our continuous search for novel and bioactive compounds from tropical basidiomycetes, we found five novel steroids from mycelial cultures of *Fomitiporia aethiopica*. The metabolites are the first steroids from the genus in the current circumscription, even though triterpenoids and steroids in particular are of widespread occurrence in Basidiomycota. The new metabolites were tested in various bioassays, but only moderate to weak cytotoxic activities were observed, and their biological functions remain obscure. Although closely related pregnane-type steroids have been reported before from *Phellinus igniarius* and the marine alga-derived fungus *Phaeosphaeria spartinae*, such pregnenolone-like compounds are unprecedented in fungal metabolism [19,20]. Accumulating evidence on triterpenoids broad spectrum pharmacological activities coupled with a low toxicity profile has sparked discussion with regard to their application, especially in cancer treatment.

Supplementary Materials: UV, HRMS, ¹H- and ¹³C-NMR, ¹H-¹H COSY, HSQC, and HMBC and ROESY spectra of compounds 1–5 and data on the producing organism are available as Supplementary Material.

Acknowledgments: We are grateful to Wera Collisi, Christel Kakoschke and Cäcilia Schwager for their technical support. Financial support by the “ASAFEM” Project (Grant no. IC-070) under the ERAfrica Programme to J.C.M. and M.S. and a personal PhD stipend by the German Academic Exchange Service (DAAD) and the Kenya National Council for Science and Technology (NACOSTI) to C.C. is gratefully acknowledged (programme-ID: 57139945).

Author Contributions: C.C. contributed to chemical analysis of the extracts, isolation of compounds, structure elucidation and manuscript writing; W.C.S. contributed to fermentation, isolation of compounds and manuscript writing; T.C. contributed to bioactivity assays, isolation and purification; C.D. collected and identified the producing organism, J.C.M. contributed to fungal specimen collection, facilities, chemicals and experiment guidance; M.S. contributed facilities, chemicals and experiment guidance and edited the manuscript.

Conflicts of Interest: The authors declare no conflict of interest.

References

1. Karwehl, S.; Stadler, M. Exploitation of fungal biodiversity for discovery of novel antibiotics. *Curr. Top. Microbiol. Immunol.* **2016**, *398*, 303–338. [[CrossRef](#)] [[PubMed](#)]
2. De Silva, D.D.; Rapior, S.; Sudarman, E.; Stadler, M.; Xu, J.; Aisyah, S.A.; Hyde, K.D. Bioactive metabolites from macrofungi: Ethnopharmacology, biological activities and chemistry. *Fungal Divers* **2013**, *62*, 1–40. [[CrossRef](#)]

3. Chepkirui, C.; Matasyoh, J.C.; Decock, C.; Stadler, M. Two cytotoxic triterpenes from cultures of a Kenyan *Laetiporus* sp. (BasiDOImycota). *Phytochem. Lett.* **2017**, *20*, 106–110. [[CrossRef](#)]
4. Chepkirui, C.; Richter, C.; Matasyoh, J.C.; Stadler, M. Monochlorinated calocerins A–D and 9-oxostrobilurin derivatives from the basidiomycete *Favolaschia calocera*. *Phytochemistry* **2016**, *132*, 95–101. [[CrossRef](#)] [[PubMed](#)]
5. Mudalungu, C.M.; Richter, C.; Wittstein, K.; Abdalla, A.M.; Matasyoh, J.C.; Stadler, M.; Süßmuth, R.D. Laxitextines A and B, Cyathane xylosides from the tropical fungus *Laxitextum incrustatum*. *J. Nat. Prod.* **2015**, *79*, 894–898. [[CrossRef](#)] [[PubMed](#)]
6. Decock, C.; Bitew, A.; Castillo, G. *Fomitiporia tenuis* and *Fomitiporia aethiopica* (BasiDOImycetes, Hymenochaetales), two undescribed species from the Ethiopian highlands: Taxonomy and phylogeny. *Mycologia* **2005**, *97*, 121–129. [[CrossRef](#)] [[PubMed](#)]
7. Amalfi, M.; Yombiyeni, P.; Decock, C. *Fomitiporia* in sub-Saharan Africa: Morphology and multigene phylogenetic analysis support three new species from the Guineo-Congolian rainforest. *Mycologia* **2010**, *102*, 1303–1317. [[CrossRef](#)] [[PubMed](#)]
8. Cloete, M.; Fischer, M.; Mostert, L.; Halleen, F. A novel *Fomitiporia* species associated with esca on grapevine in South Africa. *Mycol. Prog.* **2014**, *13*, 303–311. [[CrossRef](#)]
9. Buckingham, J. *Dictionary of Natural Products on DVD*; Chapman & Hall, Chemical Database, CRC: Boca Raton, FL, USA, 2017.
10. Hoyer, T.R.; Jeffrey, C.S.; Shao, F. Mosher ester analysis for the determination of absolute configuration of stereogenic (chiral) carbinol carbons. *Nat. Protoc.* **2007**, *2*, 2451–2458. [[CrossRef](#)] [[PubMed](#)]
11. Liu, H.B.; Bao, H.Y.; Cui, B.K. Chemical constituents of *Fomitiporia ellipsoidea* fruiting bodies. *Mycosystema* **2011**, *30*, 459–463.
12. Cui, B.-K.; Decock, C. *Phellinus castanopsidis* sp. nov. (Hymenochaetaceae) from southern China, with preliminary phylogeny based on rDNA sequences. *Mycol. Prog.* **2013**, *12*, 341–351. [[CrossRef](#)]
13. Fiasson, J.; Niemelä, T. The Hymenochaetales: A revision of the European poroid taxa. *Karstenia* **1984**, *24*, 14–28. [[CrossRef](#)]
14. Fiasson, J. Distribution of styrylpyrones in the basidiocarps of various Hymenochaetaceae. *Biochem. Syst. Ecol.* **1982**, *10*, 289–296. [[CrossRef](#)]
15. Hilaire, V.K.W.; Hartl, A.; Trinh, T.K.; Hertweck, C. Inotilone and related phenylpropanoid polyketides from *Inonotus* sp. and their identification as potent COX and XO inhibitors. *Org. Biomol. Chem.* **2006**, *4*, 2545–2548. [[CrossRef](#)]
16. Ye, S.D.; Ying, S.H.; Chen, C.; Feng, M.G. New solid-state fermentation chamber for bulk production of aerial conidia of fungal biocontrol agents on rice. *Biotechnol. Lett.* **2006**, *28*, 799–804. [[CrossRef](#)] [[PubMed](#)]
17. Kuephadunphan, W.; Helaly, S.E.; Daengrot, C.; Phongpaichit, S.; Luangsa-ard, J.J.; Rukachaisirikul, V.; Stadler, M. Akanthopyrones A–D, α -pyrones bearing a 4-O-Methyl- β -D-glucopyranose moiety from the spider-associated ascomycete *Akanthomyces novoguineensis*. *Molecules* **2017**, *22*, 1202. [[CrossRef](#)] [[PubMed](#)]
18. Ashrafi, S.; Helaly, S.E.; Schroers, H.J.; Stadler, M.; Richert-Poeggeler, K.R.; Dababat, A.A.; Maier, W. *Ijuhya vitellina* sp. nov., a novel source for chaetoglobosin A, is a destructive parasite of the cereal cyst nematode *Heterodera filipjevi*. *PLoS ONE* **2017**, *12*, e0180032. [[CrossRef](#)] [[PubMed](#)]
19. Yin, R.; Zhao, Z.; Ji, X.; Dong, Z.; Li, Z.; Feng, T.; Liu, J. Steroids and sesquiterpenes from cultures of the fungus *Phellinus igniarius*. *Nat. Prod. Bioprospect.* **2015**, *5*, 17–22. [[CrossRef](#)]
20. Mahmoud, F.E.; Kehraus, S.; König, G.M. Caught between triterpene- and steroid-metabolism: 4a-Carboxylic pregnane-derivative from the marine alga-derived fungus *Phaeosphaeria spartinae*. *Steroids* **2013**, *78*, 880–883. [[CrossRef](#)]

Sample Availability: Samples of the compounds 1–5 are available from the authors.



© 2018 by the authors. Licensee MDPI, Basel, Switzerland. This article is an open access article distributed under the terms and conditions of the Creative Commons Attribution (CC BY) license (<http://creativecommons.org/licenses/by/4.0/>).

Sparticolins A–G, Biologically Active Oxidized Spirodioxynaphthalene Derivatives from the Ascomycete *Sparticola junci*

Chayanard Phukhamsakda,^{†,||} Allan Patrick G. Macabeo,^{‡,§,||} Volker Huch,[⊥] Tian Cheng,[‡] Kevin D. Hyde,[†] and Marc Stadler^{*,‡,||}

[†]Center of Excellence in Fungal Research, Mae Fah Luang University, Chiang Rai 57100, Thailand

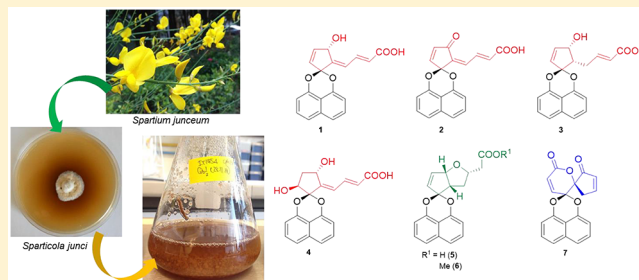
[‡]Department of Microbial Drugs, Helmholtz Centre for Infection Research and German Centre for Infection Research (DZIF), partner site Hannover/Braunschweig, Inhoffenstrasse 7, 38124 Braunschweig, Germany

[§]Laboratory for Organic Reactivity, Discovery and Synthesis (LORDS), Research Center for the Natural and Applied Sciences, University of Santo Tomas, 1015 Manila, Philippines

[⊥]Institut für Anorganische Chemie, Universität des Saarlandes, Campus, Gebäude C 4.1, 66123 Saarbrücken, Germany

Supporting Information

ABSTRACT: To explore the chemical diversity of metabolites from new species of Dothideomycetes, the ex-type strain of *Sparticola junci* was investigated. Seven highly oxygenated and functionalized spirodioxynaphthalene natural products incorporating carboxyalkylidene–cyclopentanoid (1–4), carboxyl-functionalized oxabicyclo[3.3.0]octane (5–6), and annelated 2-cyclopentenone/δ-lactone (7) units, sparticolins A–G, were isolated from submerged cultures of the fungus. Their chemical structures including their relative (and absolute) configurations were established through spectroscopic and X-ray crystallographic analyses. Sparticolin B (2) exhibited inhibitory activity against the Gram-positive bacteria *Bacillus subtilis*, *Micrococcus luteus*, and *Staphylococcus aureus*, while sparticolin G (7) showed antifungal activities against *Schizosaccharomyces pombe* and *Mucor hiemalis*. All other sparticolins were only weakly active against *S. aureus* and also showed weak activities against the nematode *Caenorhabditis elegans*. Compounds 2 and 7 also showed moderate cytotoxic activities against seven mammalian cell lines.



Fungal metabolites have been shown to be a prolific source of novel molecules that can serve as lead candidates for development of pharmaceutical drugs, agrochemical pesticides, and other products for the life science industry.^{1,2} However, the majority of the fungal species still remain untapped for secondary metabolite production, and in particular, newly discovered plant-associated Ascomycota may be a good source of novel chemistry. During a study of the mycobiota of the plant genera *Clematis* and *Spartium*, several new taxa of Dothideomycetes were discovered, and their cultures were studied for secondary metabolite production.³ Several of these strains were subjected to intensive studies, because their extracts showed interesting biological activities in various bioassays. We have recently reported a new terpenoid from a *Rousoella* sp. associated with *Clematis* from Thailand that can significantly inhibit biofilm formation by the human pathogenic bacterium *Staphylococcus aureus*.⁴ In the current study, a type strain of *Sparticola* (Sporormiaceae, Pleosporales)³ from the Spanish broom, *Spartium junceum* (Fabaceae) found in Italy³ was explored for its secondary metabolism and associated biological activity. The present paper reports the isolation, structure elucidation, and biological characterization of seven unpre-

cedented polyketides from the mycelial cultures of *Sparticola junci* Phukhamsakda, Camporesi & K.D. Hyde and represent the first secondary metabolites of the genus *Sparticola*.

RESULTS AND DISCUSSION

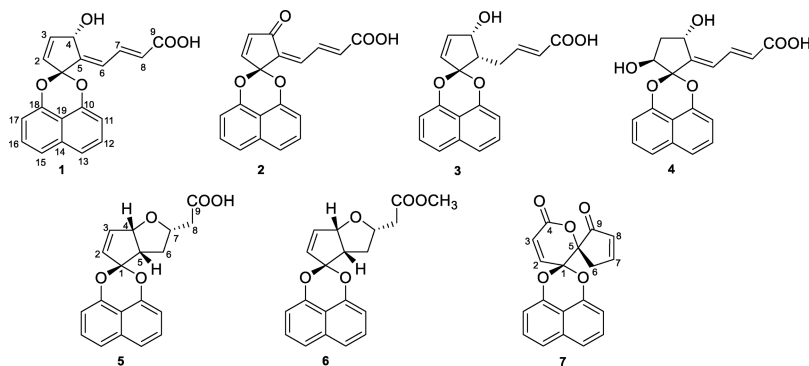
The ethyl acetate extract obtained from the Q61/2 medium⁵ was fractionated by repeated reversed-phase preparative and semipreparative HPLC to afford compounds 1–7.

The NMR spectroscopic data for sparticolins A–G (1–7) suggested that they are new members in the spirodioxynaphthalene natural products family. The common structural moiety present in sparticolins 1–7 is a 1,8-dioxynaphthalene linked to highly functionalized cyclopentanoid, or 5,6-dihydro-2*H*-pyran-2-one (in the case of compound 7) substructures, and can be readily correlated to a spiroketal carbon resonating at approximately 96–113 ppm in the ¹³C NMR spectrum.⁶ The NMR spectroscopic data of the dioxynaphthalene moieties of all seven compounds were almost the same (Tables 1 and 2).

Received: July 10, 2019

Published: October 10, 2019

Chart 1

Table 1. ¹H NMR Spectroscopic Data for Sparticolins A–G (1–7)

position	1 ^a	2 ^a	3 ^a	4 ^b	5 ^a	6 ^b	7 ^b
2	5.97, dd (6.2, 1.3)	7.44, d (6.3)	5.83, dd (6.0, 1.6)	4.51, ddd (5.1, 3.4, 0.8)	5.90, ddd (5.8, 1.0, 0.4)	5.91, dd (5.8, 0.9)	6.64, d (10.3)
3a	6.28, ddd (6.2, 2.3, 0.7)	6.59, dd (6.4, 0.6)	6.15, dd (6.0, 1.7)	2.30, ddd (13.5, 7.6, 3.5)	6.28, dd (5.8, 1.8)	6.27, dd (5.8, 1.8)	6.29, d (10.3)
3b				2.08, ddd (13.5, 7.1, 5.1)			
4	5.43, dd (1.9, 1.7)	-	4.59, dt (5.8, 1.7)	5.14, td (7.3, 2.3)	5.10, ddd (7.1, 1.9, 1.0)	5.10, ddd (7.1, 1.8, 1.0)	-
5	-	-	2.51, ddd (8.2, 6.9, 5.7)	-	3.18, td (9.1, 7.0)	3.19, td (9.1, 7.1)	-
6a	6.75, d (11.8)	7.09, d (11.9)	2.87, dddd (15.1, 8.4, 7.1, 1.6)	6.53, dd (11.7, 2.3)	1.83, m	1.82, m	3.38, dt (22.3, 2.3)
6b			2.75, m				3.02, dt (22.3, 2.3)
7	7.94, dd (15.4, 11.8)	8.61, dd (15.6, 11.8)	7.18, dt (15.5, 7.3)	7.89, dd (15.4, 11.7)	4.29, dtd (9.7, 6.5, 5.2)	4.29, dtd (9.8, 7.3, 5.4)	6.76, dt (7.3, 2.3)
8	6.04, d (15.5)	6.36, d (15.6)	6.04, dt (15.5, 1.5)	5.87, d (15.4)	2.54, d (6.6)	2.58, d (6.5)	6.41, d (7.3)
11	6.89, d (7.5)	6.99, d (7.6)	6.91, d (7.5)	7.01, d (7.5)	6.86, d (7.5)	6.92, d (7.6)	7.03, d (7.6)
12	7.40, dd (8.3, 7.5)	7.49, dd (8.4, 7.6)	7.41, dd (8.3, 7.5)	7.44, dd (8.5, 7.5)	7.42, dd (8.4, 7.5)	7.43, dd (8.3, 7.6)	7.49, dd (8.4, 7.6)
13	7.49, d (8.5)	7.61, d (8.4)	7.49, d (8.3)	7.52, d (8.5)	7.50, d (8.4)	7.50, d (8.3)	7.61, d (8.4)
14	-	-	-	-	-	-	-
15	7.49, d (8.5)	7.61, d (8.4)	7.49, d (8.3)	7.52, d (8.5)	7.50, d (8.4)	7.50, d (8.3)	7.61, d (8.4)
16	7.40, dd (8.3, 7.5)	7.49, dd (8.4, 7.6)	7.41, dd (8.3, 7.5)	7.44, dd (8.5, 7.5)	7.42, dd (8.4, 7.5)	7.43, dd (8.3, 7.5)	7.49, dd (8.4, 7.6)
17	6.89, d (7.5)	6.99, d (7.6)	6.89, d (7.5)	6.93, d (7.5)	6.92, d (7.5)	6.90, d (7.56)	7.00, d (7.6)
9-OMe	-	-	-	-	-	3.66, s	-

^a500 MHz, MeOH-*d*₄. ^b700 MHz, MeOH-*d*₄.

Discussion of the structure elucidation of the 1,8-naphthalene moiety is provided for sparticolin A (1) to serve as a general example. Discussion of the structures of sparticolins B–G (2–7) focused on the remaining portions of each molecule, especially the relative configurations of derivatives possessing multiple chiral centers using 2D-ROESY.

Sparticolin A (1) was obtained as an amorphous powder, and its molecular formula established as C₁₉H₁₄O₅ from HR-ESI-MS, implying 13 degrees of unsaturation.

Detailed analysis of the ¹H, ¹³C, and HSQC-DEPT NMR spectroscopic data revealed the presence of a carboxylic acid carbon, a ketal carbon, five nonprotonated aromatic carbons (two oxygenated and three nonoxygenated), six aromatic methines, five olefinic methines, and an oxygenated sp³ methine carbon. In the ¹H–¹H COSY spectrum of 1, homonuclear coupling correlations of H-11/H-17 (δ_H 6.89) with H-12/H-16 (δ_H 7.40) as well as correlations of H-13/H-15 (δ_H 7.49) with H-12/H-16 indicated the presence of two three-proton spin systems corresponding to the C-11 to C-13 and C-15 to C-17

substructures of 1, which displayed *ortho* coupling with *J*-values of 8.5 and 7.5 Hz. The HMBC correlations of H-11/H-17 with C-10/C-18 (δ_C 150.2) and C-19 (δ_C 115.1) and H-13/H-15 with C-14 (δ_C 135.9) and C-19 led to the attachment of both subunits at C-14 and C-19, suggesting the presence of a naphthalene substructure. In addition, the chemical shifts of C-10 and C-18 were indicative of a 1,8-dioxynaphthalene fragment. The remaining part of 1 was constructed through analysis of COSY and HSQC-DEPT spectroscopic data revealing connectivities (bold line) between H-2 → H-3 → H-4 and H-6 → H-7 → H-8 (Figure 1a). HMBC correlations of H-2 (δ_H 5.97) and H-4 (δ_H 5.43) with dioxygenated C-1 (δ_C 108.2) and olefinic C-5 (δ_C 149.4) suggested 1-ketal and 5-*exo*-alkylidene 2-cyclopenten-4-ol moieties, where the 1,8-dioxynaphthalene moiety should be connected to ketal C-1 through *spiro* annelation. Further HMBC correlations of H-6 (δ_H 6.75) with ketal C-1, alcohol C-4 (δ_C 73.0), and alkylidene C-5 and of H-8 (δ_H 6.04) with the C-9 (δ_C 169.9) carboxylic acid carbon allowed the elucidation of the gross planar structure of 1 (Figure

Table 2. ^{13}C NMR Spectroscopic Data^a for Sparticolins A–G (1–7)

position	1 ^b	2 ^b	3 ^b	4 ^c	5 ^b	6 ^c	7 ^c
1	108.2, C	103.7, C	111.1, C	112.6, C	108.2, C	112.6, C	96.3, C
2	130.5, CH	150.8, CH	130.0, CH	73.3, CH	131.6, CH	131.7, CH	138.0, CH
3	141.3, CH	140.6, CH	142.5, CH	41.2, CH ₂	140.8, CH	140.8, CH	125.4, CH
4	73.0, CH	193.8, C	79.3, CH	69.3, CH	87.2, CH	87.4, CH	163.1, C
5	149.4, C	137.5, C	57.4, CH	150.4, C	52.6, CH	52.6, CH	89.2, C
6	128.6, CH	135.8, CH	31.0, CH ₂	129.6, CH	34.3, CH ₂	34.2, CH ₂	42.3, CH ₂
7	141.3, CH	138.2, CH	149.4, CH	141.2, CH	80.2, CH	80.1, CH	138.8, CH
8	126.6, CH	133.8, CH	123.8, CH	125.9, CH	41.2, CH ₂	41.1, CH ₂	128.8, CH
9	169.9, C	169.2, C	170.1, C	170.0, C	174.8, C	173.2, C	207.0, C
10	150.2, C	149.3, C	150.0, C	149.4, C	150.0, C	150.0, C	147.1, C
11	110.3, CH	110.8, CH	110.1, CH	110.5, CH	110.3, CH	110.3, CH	111.4, CH
12	128.6, CH	128.8, CH	128.6, CH	128.6, CH	128.6, CH	128.6, CH	128.9, CH
13	121.9, CH	122.6, CH	121.7, CH	121.8, CH	121.8, CH	121.8, CH	122.8, CH
14	135.9, C	135.8, C	136.0, C	135.9, C	136.1, C	136.2, C	135.8, C
15	121.9, CH	122.6, CH	121.7, CH	121.8, CH	121.7, CH	121.7, CH	122.8, CH
16	128.6, CH	128.8, CH	128.6, CH	128.5, CH	128.6, CH	128.6, CH	128.9, CH
17	110.2, CH	110.8, CH	109.9, CH	110.0, CH	110.1, CH	110.1, CH	110.9, CH
18	150.2, C	149.3, C	149.8, C	149.4, C	149.8, C	149.8, C	146.6, C
19	115.1, C	114.8, C	115.3, C	115.2, C	115.6, C	115.6, C	114.5, C
9-OMe	-	-	-	-	-	52.2	-

^aCarbon multiplicities were deduced from HSQC–DEPT-135 spectra. ^b125 MHz, MeOH-*d*₄. ^c175 MHz, MeOH-*d*₄.

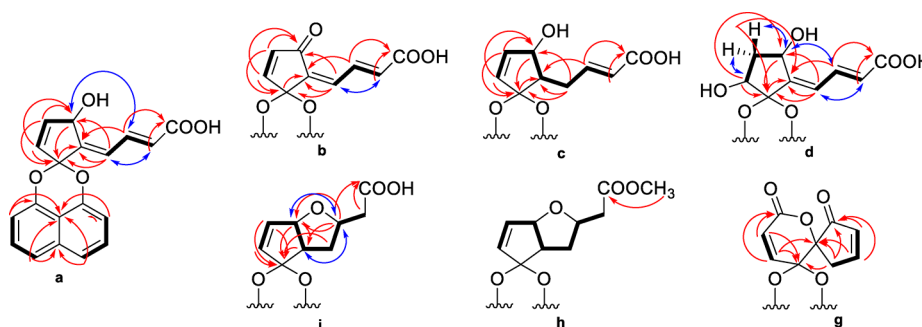


Figure 1. COSY (bold bonds), HMBC (red arrows), and ROESY (blue arrows). Correlations in sparticolins A–G (1–7).

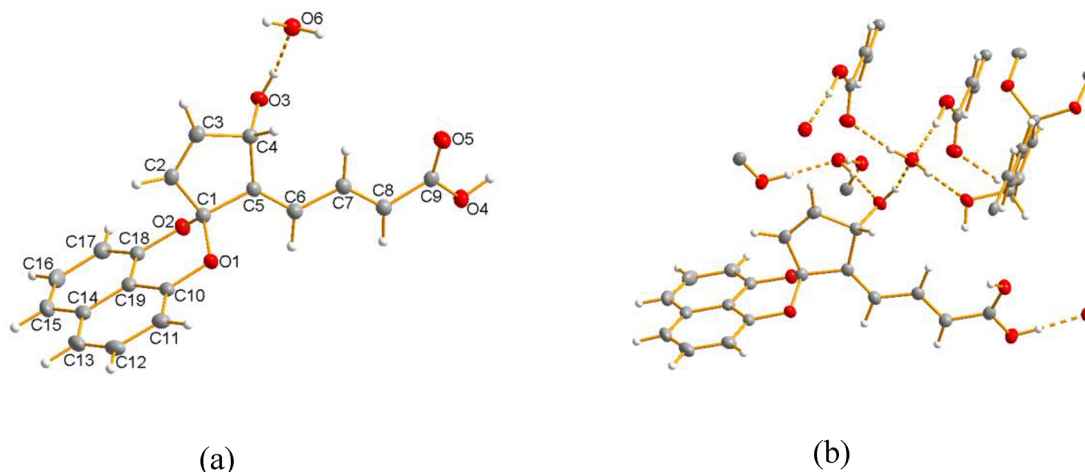


Figure 2. (a) Single crystal X-ray absolute stereostructure of **1**, monohydrate. (b) Hydrogen bond networks of **1** with water in the solid state packing.

1a). The geometric orientations of the protons in the $\Delta^{5(6)}$ and $\Delta^{7(8)}$ diene moiety were deduced to have *trans* relationships on the basis of their vicinal coupling constant ($J_{\text{H-7, H-8}} = 15.5$ Hz) and ROESY correlation. The $\Delta^{5(6)}$ configuration was established as *E* through a ROESY correlation between H-4 and H-7 giving rise to a *5E,7E* geometric configuration in the *exo*-alkyldiene

carboxylic acid moiety (Figure 1a). The absolute configuration at C-4 was deduced to be *S* on the basis of its single crystal X-ray diffraction data (Figure 2). Thus, the structure of **1** was assigned as (2*Z*,4*E*)-4-((*S*)-4-hydroxyspiro[cyclopentane-1,2'-naphtho[1,8-*de*][1,3]dioxin]-2-en-5-ylidene)but-2-enoic acid and hitherto assigned the trivial name, sparticolin A.

Sparticolin B (**2**) was isolated as a brown syrup. The HR-ESI-MS of **2** showed a sodiated molecular ion peak at m/z 343.0754 $[M + Na]^+$, corresponding to the molecular formula $C_{19}H_{12}O_5$, indicating an index of hydrogen deficiency of 14. Detailed analysis of the NMR spectroscopic data (Tables 1 and 2) revealed that compound **2** has nearly the same planar structure as sparticolin A (**1**), differing only by replacement of the sp^3 oxygenated methine at C-4, with a conjugated ketone unit (δ_C 193.8). This observation was supported by an isolated H-2 \rightarrow H-3 spin system deduced from the COSY spectrum, and HMBC correlations of H-2 (δ_H 7.44) and H-3 (δ_H 6.59) with the C-1 dioxygenated carbon (δ_C 103.7), ketone C-4, and C-5 alkylidene (δ_C 137.5) (Figure 1b). The relative configurations of the diene at C-5 and C-7 were deduced to be *E* based on coupling constant analysis and comparison to compound **1**. Thus, the structure of **2** was elucidated as shown, and the compound was assigned the name, sparticolin B.

Sparticolin C (**3**) was isolated as a light yellow syrup, and its molecular formula was established as $C_{19}H_{16}O_5$ by HR-ESI-MS in conjunction with the analysis of its 1H and ^{13}C NMR spectroscopic data (Tables 1 and 2). Its index of hydrogen deficiency was determined to be 12. In addition to signals for a 1,8-dioxynaphthalene unit, detailed analysis of the 1H , ^{13}C , and HSQC-DEPT NMR data (Tables 1 and 2) revealed the presence of additional signals due to one carboxylic acid, one doubly oxygenated nonprotonated sp^3 carbon, four olefinic methines, one oxygenated methine, an additional sp^3 hybridized methine, and a methylene carbon. The COSY spectrum showed the presence of an eight-proton spin system (Figure 1c) corresponding to the C-2 to C-8 unit in **3**. The chemical shifts in the 1H and ^{13}C spectra along with the COSY NMR data revealed the loss of the typical alkylidene at C-5 of the cyclopentenol moiety present in **1** and **2**. The gross structure of **3** was constructed based on the key HMBC correlations of H-5 and H₂-6 with C-1 and of H-7 and H-8 with carboxyl carbon C-9. The vicinal coupling constant ($^3J_{H-4,H-5} = 5.7\text{--}5.8\text{ Hz}$)⁷ between H-4 and H-5 revealed a *cis* configuration at C-4 and C-5 (Figure 1c). Thus, compound **3** was identified as shown and assigned the name, sparticolin C.

Sparticolin D (**4**) was obtained as a light yellow syrup, and its molecular formula was established as $C_{19}H_{16}O_6$ based on HR-ESI-MS data, implying 12 degrees of unsaturation. Examination of its 1H and ^{13}C NMR spectroscopic data (Tables 1 and 2) revealed the presence of a carboxylic acid, a ketal, four olefinic carbons (three of which were protonated), two oxygenated methines, and a methylene carbon. Analysis of its COSY spectrum showed correlations for two spin systems, H-2 \rightarrow H₂-3 \rightarrow H-4 and the typical three-proton spin-system, H-6 \rightarrow H-7 \rightarrow H-8, which is also present in sparticolins A (**1**) and B (**2**) for the *exo*-alkylidene moiety (Figure 1d). Comparison of the 1H and ^{13}C NMR spectroscopic data (Tables 1 and 2) of **4** with those of **1**–**3** along with the COSY and HMBC data revealed the replacement of olefinic C-2 and C-3 by a carbinol, C-2 (δ_C 73.3) connected to a methylene, C-3 (δ_C 41.2). HMBC correlations of H-2 with C-1 and C-5 and H-4 with C-5 allowed the elucidation of a 1-dioxy-2,4-dihydroxycyclopentanoid substructure. The connection of the carboxylated *exo*-alkylidene to the latter substructure was established by HMBC correlations of H-6 with C-1 and C-5 (Figure 1d). The relative configuration of compound **4** was established through analysis of 1H – 1H NMR coupling constants and ROESY data. The $^3J_{H-2,H-3a}$ coupling constant ($\sim 5\text{ Hz}$) indicated that the 2-OH must adopt an equatorial orientation, while the $^3J_{H-3a/H-3b,H-4}$ coupling

constant ($\sim 7\text{ Hz}$) suggested that the 4-OH is axially oriented.^{7a} This implies that **4** has a *trans* relative configuration for hydroxylated, C-2 and C-4. Strong ROESY correlations were also observed between H-2 and H-3b and H-3a and H-4. In addition, a ROESY correlation between H-4 and H-7 was also noted, pointing to a C-5–C-6 olefin configuration similar to that of **1** and **2** (Figure 1d). Thus, **4** was established as (2*E*,4*E*)-4-((2*S**,4*S**)-2,4-dihydroxyspiro[cyclopentane-1,2'-naphtho-[1,8-de][1,3]dioxin]-5-ylidene)but-2-enoic acid and assigned the name, sparticolin D.

Sparticolin E (**5**) was obtained as a reddish-brown syrup. Its molecular formula was determined to be $C_{19}H_{16}O_5$ by HR-ESI-MS analysis reflecting 12 degrees of unsaturation, which was also supported by the 1H and ^{13}C NMR spectroscopic data (Tables 1 and 2). Apart from a set of ^{13}C NMR chemical shifts characteristic of the 1,8-dioxynaphthalene moiety similar to those of **1**–**4**, the spectra of **5** showed additional signals for a carboxylic acid, a ketal, two olefinic methines, three sp^3 methines (including two oxygenated functionalities), and two methylene carbons. The construction of the upper subunit was facilitated by analysis of 1H – 1H COSY and HMBC spectra. Analysis of the COSY spectroscopic data led to the identification of a nine-proton spin system (Figure 1) corresponding to the C-2–C-8 unit (Figure 1e). Key HMBC correlations of H-2, H-3, H-4, and H-5 with dioxygenated carbon C-1 allowed the elucidation of a C-4/C-5 disubstituted 2-cyclopentene moiety linked to 1,8-dioxynaphthalene through a spiroketal junction. Annulation of a tetrahydrofuran moiety at C-4 and C-5 in the cyclopentene substructure forming a 1-oxabicyclo[3.3.0]octane was established on the basis of HMBC correlations of H-4 with C-7 and those of H-7 with C-4. Finally, HMBC correlations of H-7 and H-8 with carboxylic acid C-9 completed the planar structure of sparticolin E (**5**) (Figure 1e). The *cis* relationship between H-4 and H-5 was depicted through a $\sim 7\text{ Hz}$ vicinal coupling constant ($^3J_{H-4,H-5}$).⁸ A ROESY correlation of H-7 with H-4 and H-5 enabled assignment of the relative configurations of the chiral carbons as 4*S**, 5*R**, and 7*S**. Thus, compound **5** was assigned the structure as shown.

Compound **6** (sparticolin F) was isolated as a brownish solid. An HR-ESI-MS analysis gave a molecular ion at m/z 339.1230 $[M + H]^+$, which was consistent with the molecular formula $C_{20}H_{19}O_5$, indicating 12 degrees of unsaturation. Analysis of the 1D and 2D NMR spectroscopic data of **6** showed structural and stereochemical similarities with sparticolin E (**5**) except for the appearance of an additional oxygenated methyl group resonating at δ_C 52.2. HMBC correlation of the singlet at δ_H 3.66 with carboxyl carbon C-9 indicated that **6** must be the methyl ester derivative of **5** (Figure 1f). This is supported by a 14 amu difference in their molecular masses.

Sparticolin G (**7**) was obtained as an optically active light yellow oil, and its molecular formula was determined to be $C_{19}H_{12}O_5$ by HR-ESI-MS analysis. This observation was consistent with the number of carbon signals (19) observed in the ^{13}C NMR spectra (Table 2) and was indicative of an index of hydrogen deficiency of 14. In addition to signals corresponding to a *spiro*-annulated 1,8-dioxynaphthalene moiety, detailed examination of the 1H , ^{13}C , and HSQC-DEPT NMR spectroscopic data (Tables 1 and 2) revealed additional resonances corresponding to chemical shifts of an ester carbon, a ketone, a ketal, four olefinic methines, an oxygenated nonprotonated sp^3 carbon, and an sp^3 methylene carbon. The COSY correlation and chemical shifts observed for H-2 (δ_H 6.64)/H-3 (δ_H 6.29) and H₂-6 (δ_H 3.02; δ_H 3.38)/H-7 (δ_H

Table 3. Antibacterial, Antifungal, and Nematicidal Activities of 1–7

tested organisms	strain no.	MIC [$\mu\text{g/mL}$]							reference ^a
		1	2	3	4	5	6	7	
fungi									
<i>Candida albicans</i>	DSM 1665	–	–	–	–	–	–	33.3	8.3 (N)
<i>Mucor hiemalis</i>	DSM 2656	–	16.7	–	–	–	–	2.1	4.2 (N)
<i>Pichia anomala</i>	DSM 6766	–	–	–	–	–	–	66.6	8.3 (N)
<i>Rhodoturulula glutinis</i>	DSM 10134	–	33.3	–	–	–	–	16.7	1.0 (N)
<i>Schizosaccharomyces pombe</i>	DSM 70572	–	33.3	–	–	–	–	8.3	8.3 (N)
bacteria									
<i>Bacillus subtilis</i>	DSM 10	–	4.2	–	–	–	–	33.3	2.4 (O)
<i>Chromobacterium violaceum</i>	DSM 30191	–	–	–	–	–	–	–	4.1 (O)
<i>Escherichia coli</i>	DSM 1116	–	–	–	–	–	–	–	33.3 (O)
<i>Micrococcus luteus</i>	DSM 1790	–	8.3	–	–	–	–	66.6	4.2 (O)
<i>Mycobacterium smegmatis</i>	ATCC 700084	–	–	–	–	–	–	66.6	4.1 (K)
<i>Pseudomonas aeruginosa</i>	DSM PA14	–	–	–	–	–	–	–	1.0 (G)
<i>Staphylococcus aureus</i>	DSM 346	66.6	4.2	66.6	66.6	66.6	66.6	16.7	2.1 (O)
nematode									
<i>Caenorhabditis elegans</i>	–	50	50	25	50	50	12.5	nt	1.0 (I)

^aPositive drug controls: K = kanamycin, N = nystatin, O = oxytetracyclin hydrochloride, I = ivermectin. Em dash (–): No activity observed at concentrations of 66 $\mu\text{g/mL}$. nt: not tested.

Table 4. Cytotoxicity of 1–7 against Mammalian Cell Lines

cell line	IC ₅₀ [μM]							epothilone B
	1	2	3	4	5	6	7	
mouse fibroblast L929	–	0.6	–	–	52.4	114.9	0.6	1.4×10^{-3}
HeLa cells KB3.1	–	0.8	40.1	–	61.7	70.7	1.2	8.9×10^{-5}
human breast adenocarcinoma MCF-7	–	0.4	–	–	–	–	0.4	2.4×10^{-4}
human lung carcinoma A549	–	2.2	–	–	–	–	1.6	6.9×10^{-5}
human prostate cancer PC-3	–	0.9	–	–	–	–	0.4	1.6×10^{-3}
ovarian carcinoma SKOV-3	–	0.6	–	–	–	–	0.3	2.8×10^{-4}
squamous cell carcinoma A431	–	0.2	–	–	–	–	0.1	7.9×10^{-5}

^aThe in vitro cytotoxicity test of sparticolins A–G (1–7) was conducted against seven mammalian cell lines, with epothilone B as a positive control. The starting concentration for the cytotoxicity assay was 300 $\mu\text{g/mL}$, and substances were dissolved in MeOH (1 mg/mL). MeOH was used as the negative control and showed no activity against the tested mammalian cell lines. Results were expressed as IC₅₀: half maximal inhibitory concentration (μM). Em dash (–): no inhibition.

6.76)/H-8 (δ_H 6.41) along with HMBC correlations of H-2 and H-3 with carboxyl ester C-4 and of H-7 and H-8 with ketone C-9 indicated the presence of α,β -unsaturated carbonyl moieties. Complete elucidation of the *spiro*-annelated δ -lactone/2-cyclopenten-1-one substructure was achieved via HMBC correlations of H-2 and H-3 with ketal carbon C-1 and oxygenated tertiary carbon C-5, of H₂-6 and H-7 with C-5, and of H₂-6 with C-1 (Figure 1f). The gross structure of 7 was elucidated by connecting the 1,8-dioxynaphthalene subunit to dioxxygenated C-1, fashioning a second *spiro* junction. Thus, the structure of compound 7 was assigned as shown.

While most spirobisnaphthalene derivatives have been isolated from fungi, several have been detected from plant sources.⁹ The first example of a 19 carbon-containing *nor* derivative bearing a *spiro*-nonadiene skeleton, spiromamakone A, was isolated as an optically inactive compound from an unidentified nonsporulating endophytic fungus.¹⁰ The profound antimicrobial and cytotoxic activities of spiromamakone A sparked explorations especially in the fields of complex molecule synthesis^{11,12} and medicinal chemistry.¹³ An additional related structure, spiropressione A, was reported from the Sporormiaceae fungus *Preussia* sp.^{14,15} However, it was later found to be identical to spiromamakone A through synthetic efforts.¹² To our knowledge, sparticolins A–F (1–7) are the first secondary

metabolites reported from the genus *Sparticola*. The modification of moieties in the upper rim of each structure is unprecedented in polyketide metabolites, specifically among the spirodioxynaphthalene class of natural products.

Sparticolins A–G (1–7) were evaluated for their antimicrobial, cytotoxic,¹⁶ and nematicidal activities.¹⁷ All compounds showed weak inhibition against *Staphylococcus aureus* except sparticolin B (2), which also exhibited inhibitory activity against other Gram-positive bacteria such as *Bacillus subtilis* and *Micrococcus luteus* and some fungal strains (Table 3).

Sparticolin G (7) showed broad spectrum antifungal activities with inhibitory activities against *Schizosaccharomyces pombe* and *Mucor hiemalis* with greater or equal potency compared to the positive control nystatin and showed weaker effects against *Candida albicans*, *Pichia anomala*, and *Rhodoturulula glutinis* as well as some Gram-positive bacteria (Table 3). Compounds 1–5 showed very weak nematicidal activity, while compound 6 was moderately active against *C. elegans*, and compound 7 was not tested due to insufficient material.

Interestingly, compounds 2 and 7 also showed moderately strong cytotoxic activities against seven mammalian cell lines (Table 4). The presence of electrophilic α,β -unsaturated carbonyl functionalities such as a 2-cyclopentenone in 2 and a

2H-pyran-2-one/2-cyclopentenone hybrid in **7** may explain the observed biological activities.

EXPERIMENTAL SECTION

General Experimental Procedures. Specific optical rotations ($[\alpha]_D$) were measured on a PerkinElmer 241 polarimeter in a 100 × 2 mm cell at 22 °C. UV–vis spectra were obtained on a Shimadzu UV-2450 spectrophotometer with 1 cm quartz cells. Nuclear magnetic resonance (NMR) spectra were acquired either on a Bruker AV II-500 MHz (^1H 500 MHz, ^{13}C 120 MHz) spectrometer or a Bruker Ascend 700 MHz spectrometer with a 5 mm TXI cryoprobe (^1H 700 MHz, ^{13}C 175 MHz). In all cases, spectra were acquired at 25 °C (unless otherwise specified) in solvents as specified in the text, with referencing to residual ^1H or ^{13}C signals in the deuterated solvents. HR-ESI mass spectra were measured using an Agilent 1200 series HPLC-UV system in combination with an ESI-TOF-MS (Maxis, Bruker) [column 2.1 × 50 mm, 1.7 μm , C18 Acquity UPLC BEH (Waters), solvent A: 95% 5 mM ammonium acetate buffer (pH 5.5, adjusted with 1 M acetic acid) with 5% acetonitrile, solvent B: 95% acetonitrile with 5% 5 mM ammonium acetate buffer]. Elution was achieved using a gradient from 10% solvent B increasing to 100% solvent B within 30 min, maintaining 100% B for another 10 min, $R_f = 0.3 \text{ mL min}^{-1}$, UV detection 200–600 nm].

Identity of the Producer Strain. The ascomycete *Sparticola junci* Phukhamsakda, Camporesi & K.D. Hyde, which represents the ex-type strain of the species, was isolated from a dead branch of *Spartium junci*, and its characteristics have previously been described in detail by Phukhamsakda et al.³ The holotype specimen and the ex-type culture are deposited at the culture collection of Mae Fah Luang University, Chiang Rai, Thailand, under the designation numbers MFLU 15-1405 and MFLUCC 15-0030, respectively. The GenBank accession number of the fungal barcode (5.8S gene region, the internal transcribed spacer ITS1 and ITS2) is provided as NR_154428.

Production, Extraction, Isolation, and Structure Characterization of 1–7. A 20 day old *Sparticola junci* mycelium grown on a yeast–malt glucose (YMG) agar plate (1% malt extract, 0.4% glucose, 0.4% yeast extract, 2% agar, pH 6.3) was used to prepare a seed culture. Five plugs of well-grown mycelium were inoculated in 500 mL Erlenmeyer flasks containing 200 mL of YMG media and incubated on a rotary shaker at 24 °C and 140 rpm for 30 days. The seed cultures were homogenized mechanically using an Ultra Turrax. Subsequently, 10 mL of seed culture was transferred to each of the 30 × 500 mL sterilized Erlenmeyer flasks with 200 mL of Q6 1/2 medium⁵ (6 L) and incubated on a rotary shaker (21 days, 24 °C, 140 rpm). Fermentation was terminated 6 days after glucose depletion (glucose strip test). The mycelia and supernatant were separated using vacuum filtration, and the mycelia were homogenized and extracted with acetone under ultrasonic conditions. The combined acetone extracts were evaporated in a rotary evaporator (40 °C), and the crude product was suspended in distilled water (300 mL) and extracted with an equal volume of ethyl acetate (5×). The aqueous layer was discarded, and the organic phase was dried over anhydrous Na_2SO_4 and concentrated under reduced pressure to yield 2.2 g of crude ethyl acetate extract. The supernatant was mixed with Amberlite XAD-16 N (30 g per 1 L) and extracted with an equal volume of ethyl acetate (5×) according to a previously described procedure. The resulting ethyl acetate extracts were evaporated to dryness to give 800 mg of crude material. The combined crude extracts from the mycelia and broth yielded 3 g of a brown syrup. The extracts were dissolved in methanol and filtered on an RP solid-phase cartridge (Strata-X 33 mm, polymeric reversed phase; Phenomenex Aschaffenburg, Germany) to yield 2.7 g of crude material.

For the isolation of the compounds, preparative purifications were achieved on a preparative HPLC (Gilson, Middleton, WI, USA) equipped with a GX-271 Liquid Handler, a 172 DAD, and a 305 and 306 pump (with 50SC Piston Pump Head). A VP Nucleodur 100-10 C18 ec column (150 × 40 mm, 7 μm ; Macherey-Nagel) was used as stationary phase. The mobile phase was composed of deionized water (Milli-Q, Millipore, Schwalbach, Germany) with 0.05% trifluoroacetic acid (solvent A) and acetonitrile (AcCN, HPLC grade) with 0.05%

trifluoroacetic acid (solvent B). The crude extract (1.8 g) was initially purified by preparative HPLC using a linear gradient of 15% solvent B for 5 min, 15–100% solvent B for 40 min, and 100% solvent B for 15 min. The fractions were combined peak-wise, according to UV absorptions at 210, 254, and 350 nm to afford 18 pooled fractions. Compound **1** (126 mg) eluted at $t_R = 25.5$ –26.2 min from fraction 13. Fraction 8 (16.6 mg) and fraction 12 (46.9 mg) were further purified using preparative RP-HPLC on a Gemini 10u C18 110A column (250 × 21.20 mm, 10 μm) with the following gradient: 40% to 100% of solvent B in 35 min, followed by 100% solvent B for 15 min. Compound **4** (3.6 mg) eluted at $t_R = 30$ –31 min, and compound **3** (4.1 mg) eluted at $t_R = 12$ –13 min. Fraction 15 (39.2 mg) was rechromatographed using preparative RP-HPLC (solvent system: 40 to 100% of solvent B in 20 min, followed by 100% solvent B for 10 min) to afford compounds **5** (6.1 mg, $t_R = 16.2$ –17.2 min) and **6** (1.0 mg, $t_R = 20.5$ –21 min). Fraction 16 (33.6 mg) yielded compound **2** (2.1 mg, $t_R = 14$ –15 min), and fraction 18 (13.3 mg) yielded compound **7** (2.1 mg, $t_R = 14$ –15 min) using preparative RP-HPLC employing a gradient of solvent B from 20 to 50% in 5 min, followed by 50–80% B in 30 min, 80–100% B in 5 min, and 100% solvent B for 10 additional minutes.

Sparticolin A (1). Sparticolin A (**1**): Colorless crystals (MeOH–water); mp 186 °C (dec.); $[\alpha]_D^{25} = -147$ (c 0.001, MeOH); UV (c 0.01, MeOH) λ_{max} ($\Delta\epsilon$) 225 (4.71), 258 (4.39), 300 (3.97) nm; ^1H and ^{13}C NMR data, Tables 1 and 2; HR-ESI-MS m/z 345.0723 $[\text{M} + \text{Na}]^+$ (calcd for $\text{C}_{19}\text{H}_{14}\text{O}_5\text{Na}$, 345.0733).

Sparticolin B (2). Sparticolin B (**2**): Brown syrup; UV (c 0.01, MeOH) λ_{max} ($\Delta\epsilon$) 225 (4.67), 299 (4.26) nm; ^1H and ^{13}C NMR data, Tables 1 and 2; HR-ESI-MS m/z 343.0574 $[\text{M} + \text{Na}]^+$ (calcd for $\text{C}_{19}\text{H}_{12}\text{O}_5\text{Na}$, 343.0582).

Sparticolin C (3). Sparticolin C (**3**): Light yellow syrup; $[\alpha]_D^{25} = -201$ (c 0.001, MeOH); UV (c 0.01, MeOH) λ_{max} ($\Delta\epsilon$) 226 (4.63), 300 (3.78), 328 (3.52) nm; ^1H and ^{13}C NMR data, Tables 1 and 2; HR-ESI-MS m/z 347.0881 $[\text{M} + \text{Na}]^+$ (calcd for $\text{C}_{19}\text{H}_{16}\text{O}_5\text{Na}$, 347.0889).

Sparticolin D (4). Sparticolin D (**4**): Light yellow syrup; $[\alpha]_D^{25} = -287$ (c 0.001, MeOH); UV (c 0.01, MeOH) λ_{max} ($\Delta\epsilon$) 225 (4.64), 260 (4.23) nm; ^1H and ^{13}C NMR data, Tables 1 and 2; HR-ESI-MS m/z 363.0834 $[\text{M} + \text{Na}]^+$ (calcd for $\text{C}_{19}\text{H}_{16}\text{O}_6\text{Na}$, 363.0839).

Sparticolin E (5). Sparticolin E (**5**): Reddish-brown syrup; $[\alpha]_D^{25} = -115$ (c 0.001, MeOH); UV (c 0.01, MeOH) λ_{max} ($\Delta\epsilon$) 226 (4.63), 300 (3.78), 328 (3.53) nm; ^1H and ^{13}C NMR data, Tables 1 and 2; HR-ESI-MS m/z 325.1066 $[\text{M} + \text{H}]^+$ (calcd for $\text{C}_{19}\text{H}_{17}\text{O}_5$, 325.1070).

Sparticolin F (6). Sparticolin F (**6**): Brownish solid; $[\alpha]_D^{25} = -157$ (c 0.001, MeOH); UV (c 0.01, MeOH) λ_{max} ($\Delta\epsilon$) 226 (4.67), 300 (3.83), 328 (3.59) nm; ^1H and ^{13}C NMR data, Tables 1 and 2; HR-ESI-MS m/z 339.1229 $[\text{M} + \text{H}]^+$ (calcd for $\text{C}_{20}\text{H}_{19}\text{O}_5$, 339.1227).

Sparticolin G (7). Sparticolin G (**7**): Light yellow oil; $[\alpha]_D^{25} = -43$ (c 0.001, MeOH); UV (c 0.03, MeOH) λ_{max} ($\Delta\epsilon$) 224 (4.40), 296 (3.52) nm; ^1H and ^{13}C NMR data, Tables 1 and 2; HR-ESI-MS m/z 321.0762 $[\text{M} + \text{H}]^+$ (calcd for $\text{C}_{19}\text{H}_{13}\text{O}_5$, 321.0757).

X-ray Crystallographic Analysis of Sparticolin A (1).¹⁸

Colorless crystals of **1** were obtained from a MeOH– H_2O solution. The monohydrate of **1** was analyzed with a Bruker D8 Venture diffractometer with a microfocus tube and Cu $K\alpha$ radiation ($\lambda = 1.54178 \text{ \AA}$). APEX3 was used for data collection, SAINT was used for cell refinement and data reduction, and SADABS was used for experimental absorption correction. The structure was solved by intrinsic phasing using SHELXT, while refinement was done by full-matrix least-squares on F^2 using SHELXL-2018/3.^{19–21} The hydrogen atoms were freely refined. The absolute configuration of **1** was solved using anomalous dispersion from Cu $K\alpha$, resulting in a Flack parameter²² of 0.030(2) using Parsons' quotient method. Graphics were drawn using DIAMOND.²³ The structural data have been deposited in the Cambridge Crystallographic Data Center (CCDC No. 1915632).

Crystal data of **1**: $\text{C}_{19}\text{H}_{14}\text{O}_5 \cdot \text{H}_2\text{O}$, $M = 340.32$, orthorhombic system, space group $P2(1)2(1)2(1)$, $a = 5.5027(4) \text{ \AA}$, $b = 7.9285(5) \text{ \AA}$, $c = 36.706(2) \text{ \AA}$, $V = 1601.42(18) \text{ \AA}^3$, $Z = 4$, $d_{\text{calc}} = 11.412 \text{ mg/m}^3$, crystal size = $0.630 \times 0.120 \times 0.057 \text{ mm}^3$, $F(000) = 712$, $\mu(\text{Mo } K\alpha) = 0.885 \text{ mm}^{-1}$, $6.653 < \theta < 80.377^\circ$. The 3909 measurements yielded 3318 independent reflections after equivalent data were averaged. The final

refinement gave $R_1 = 0.0249$ and $wR_2 = 0.0649$ [$I > 2\sigma(I)$]. The absolute structure parameter was 0.03(2).

Cytotoxicity Assay. The cytotoxicity of 1–7 was tested against a panel of mammalian cell lines. The evaluation of in vitro cytotoxicity effects (IC_{50}) was performed with mouse fibroblast cell line L929 and mammalian HeLa KB3.1 cancer cells. Additionally, human ovarian carcinoma (SKOV-3), human prostate cancer (PC-3), human lung carcinoma tissue (A549), human skin squamous cell carcinoma (A431), and human breast adenocarcinoma (MCF-7) were evaluated for compounds 1–7. The cell lines were cultured in DMEM (Gibco, ThermoFisher Scientific, Hilden, Germany) and MCF-7 in RPMI (Lonza, Cologne, Germany) media, all supplemented with 10% fetal bovine serum (Gibco) under 10% CO_2 at 37 °C. The cytotoxicity assays were performed using the MTT (3-(4,5-dimethylthiazol-2-yl)-2,5-diphenyltetrazolium bromide) method in 96-well microplates (ThermoFisher Scientific). Briefly, 60 μ L aliquots of serial dilutions from an initial stock of 1 mg/mL in MeOH of the test compounds were added to 120 μ L aliquots of a cell suspension (5.0×10^4 cells/mL) in 96-well microplates. After 5 days of incubation, an MTT assay was performed, and the absorbance was measured at 590 nm using an ELISA plate reader (Victor, PerkinElmer, Überlingen, Germany). The concentration at which the growth of cells was inhibited to 50% of the control (IC_{50}) was obtained from the dose response curves. Experiments were repeated three times. Epothilone B was used as a positive control, and the negative control was methanol.¹⁶

Antimicrobial Assay. Antimicrobial activities of 1–7 were evaluated in serial dilution assays against various fungal and bacterial strains as given in Table 3, using the broth microdilution method according to our previously described procedures.¹⁶ Gentamicin, kanamycin, and oxytetracyclin were used as positive controls against the Gram-positive and Gram-negative bacteria, respectively. Nystatin was used as a positive control against yeasts and filamentous fungi.¹⁶

Nematicidal Assay. The nematicidal activity of 1–7 against *Caenorhabditis elegans*, monoxenically grown on nematode agar (soy peptone 2 g, NaCl 1 g, agar 20 g, 1000 mL of deionized water; adding 0.5 mL of cholesterol (1 mg/mL EtOH), 1 mL of 1 M $CaCl_2$, 1 mL of 1 M $MgSO_4$, and 12.5 mL of 40 mM potassium phosphate buffer after autoclaving; pH adjusted to 6.8) with living *E. coli* DSM498, at 20 °C for a week, was assessed according to our previously reported protocol with slight modifications. The nematodes were then washed from the plates with M9 buffer, and the buffer was diluted to 500 nematodes/mL. The assay was performed in 24-well microtiter plates at five different concentrations (100, 50, 25, 12.5, and 6.25 μ g/mL) of each compound. Ivermectin was used as the positive control, and methanol was used as the negative control. The plates were incubated at 20 °C in a shaker in the dark, and nematicidal activity was recorded after 18 h of incubation and expressed as an LD_{50} .^{17,24}

■ ASSOCIATED CONTENT

Supporting Information

The Supporting Information is available free of charge on the ACS Publications website at DOI: 10.1021/acs.jnatprod.9b00604.

Description and images of *Sparticola junci* and 1D and 2D NMR spectra of 1–7 (PDF)

X-ray crystallographic data of 1 (CIF)

■ AUTHOR INFORMATION

Corresponding Author

*Tel: +49-531-6181-4267. Fax: +49-531-6181-9499. E-mail: Marc.Stadler@helmholtz-hzi.de. (M.S.)

ORCID

Chayanard Phukhamsakda: 0000-0002-1033-937X

Allan Patrick G. Macabeo: 0000-0001-7972-106X

Kevin D. Hyde: 0000-0002-3407-9517

Marc Stadler: 0000-0002-7284-8671

Author Contributions

||C.P. and A.P.G.M. contributed equally on this work.

Notes

The authors declare no competing financial interest.

■ ACKNOWLEDGMENTS

This work was supported by the Royal Golden Jubilee PhD Program (RGJ) under the Thailand Research Fund (TRF) and the German Academic Exchange Service (DAAD) for a joint TRF-DAAD [PPP 2017–2018] academic exchange grant to K.D.H. and M.S. and the TRF for a personal grant to C.P. (Scholarship number [PHD/0020/2557]). The Alexander von Humboldt Foundation is also greatly acknowledged for the George-Forster postdoctoral research fellowship to A.P.G.M., and T.C. is grateful for a PhD stipend of the China Scholarship Council (CSC). We also thank Ms. Wera Collisi and Ms. Christel Kakoschke for expert technical assistance.

■ REFERENCES

- (1) Bills, G. F.; Gloer, J. B. *Microbiol. Spectr.* **2016**, *4*, 1–32.
- (2) Hyde, K. D.; Xu, J.; Rapior, S.; Jeewon, R.; Lumyong, S.; Niego, A. G. T.; Abeywickrama, P. D.; Aluthmuhandiram, J. V. S.; Brahmanage, R. S.; Brooks, S.; Chaiyasen, A.; Chethana, K. W. T.; Chomnunti, P.; Chepkirui, C.; Chuankid, B.; de Silva, N. I.; Doilom, M.; Faulds, C.; Gentekaki, E.; Gopalan, V.; Kakumyan, P.; Harishchandra, D.; Hemachandran, H.; Hongsan, S.; Karunaratna, A.; Karunaratna, S. C.; Khan, S.; Kumla, J.; Jayawardena, R. S.; Liu, J.-K.; Liu, N.; Luangharn, T.; Macabeo, A. P. G.; Marasinghe, D. S.; Meeks, D.; Mortimer, P. E.; Mueller, P.; Nadir, S.; Nataraja, K. N.; Nontachaiyapoom, S.; O'Brien, M.; Penkhruue, W.; Phukhamsakda, C.; Ramanan, U. S.; Rathnayaka, A. R.; Sadaba, R. B.; Sandargo, B.; Samarakoon, B. C.; Tennakoon, D. S.; Siva, R.; Sriprong, W.; Suryanarayanan, T. S.; Sujarit, K.; Suwannarach, N.; Suwunwong, T.; Thongbai, B.; Thongklang, N.; Wei, D.; Wijesinghe, S. N.; Winiski, J.; Yan, J.; Yasanthika, E.; Stadler, M. *Fungal Diversity* **2019**, *97*, 1–136.
- (3) Phukhamsakda, C.; Ariyawansa, H. A.; Phillips, A. J. L.; Wanasinghe, D. N.; Bhat, D. J.; McKenzie, E. H. C.; Singtripong, C.; Camporesi, E.; Hyde, K. D. *Cryptogam.: Mycol.* **2016**, *37*, 75–97.
- (4) Phukhamsakda, C.; Macabeo, A. P. G.; Yuyama, K.; Hyde, K. D.; Stadler, M. *Molecules* **2018**, *23*, 2190–2197.
- (5) Chepkirui, C.; Matasyoh, J. C.; Decock, C.; Stadler, M. *Phytochem. Lett.* **2017**, *20*, 106–110.
- (6) Cai, Y.-S.; Kurtan, T.; Miao, Z.-H.; Mandi, A.; Komaromi, I.; Liu, H.-L.; Ding, J.; Guo, Y.-W. *J. Org. Chem.* **2011**, *76*, 1821–1830.
- (7) (a) Napolitano, J. G.; Gavin, J. A.; Garcia, C.; Norte, M.; Fernandez, J. J.; Hernandez Daranas, A. *Chem. - Eur. J.* **2011**, *17*, 6338–6347. (b) Chen, H.; Gong, Y.; Gries, R. M.; Plettner, E. *Bioorg. Med. Chem.* **2010**, *18*, 2920–2929. (c) Frelek, J.; Karchier, M.; Madej, D.; Michalak, K.; Rozanski, P.; Wicha, J. *Chirality* **2014**, *26*, 300–306. (d) Clausen, V.; Frydenvang, K.; Koopmann, R.; Jorgensen, L. B.; Abbiw, D. K.; Ekpe, P.; Jaroszewski, J. W. *J. Nat. Prod.* **2002**, *65*, 542–547.
- (8) (a) Enomoto, M.; Kuwahara, S. *J. Org. Chem.* **2006**, *71*, 6287–6290. (b) Che, Y.; Araujo, A. R.; Gloer, J. B.; Scott, J. A.; Malloch, D. J. *Nat. Prod.* **2005**, *68*, 435–438. (c) Yokosuka, A.; Mimaki, Y.; Sashida, Y. *J. Nat. Prod.* **2000**, *63*, 1239–1243.
- (9) Cai, Y.-S.; Guo, Y. W.; Krohn, K. *Nat. Prod. Rep.* **2010**, *27*, 1840–1870.
- (10) Van der Sar, S. A.; Blunt, J. W.; Munro, M. H. G. *Org. Lett.* **2006**, *8*, 2059–2061.
- (11) Tsukamoto, H.; Hanada, S.; Kumasaka, K.; Kagaya, N.; Izumikawa, M.; Shin-ya, K.; Doi, T. *Org. Lett.* **2016**, *18*, 4848–4851.
- (12) Tsukamoto, H.; Hanada, S.; Nomura, Y.; Doi, T. *J. Org. Chem.* **2018**, *83*, 9430–9441.
- (13) Murphy, A. C.; Devenish, S. R. A.; Muscroft-Taylor, A. C.; Blunt, J. W.; Munro, M. H. G. *Biomol. Chem.* **2008**, *6*, 3854–3862.

- (14) Chen, X.; Shi, Q.; Lin, G.; Guo, S.; Yang, J. *J. Nat. Prod.* **2009**, *72*, 1712–1715.
- (15) Van der Sar, S. A.; Lang, G.; Mitova, M. I.; Blunt, J. W.; Cole, A. L. J.; Cummings, N.; Ellis, G.; Munro, M. H. G. *J. Org. Chem.* **2008**, *73*, 8635–8638.
- (16) Kuephadungphan, W.; Macabeo, A. P. G.; Luangsa-ard, J. J.; Tasanathai, K.; Thanakitpipattana, D.; Phongpaichit, S.; Yuyama, K.; Stadler, M. *Mycol. Prog.* **2019**, *18*, 135–146.
- (17) Helaly, S. E.; Ashrafi, S.; Teponno, R. B.; Bernecker, S.; Dababat, A. A.; Maier, W.; Stadler, M. *J. Nat. Prod.* **2018**, *81*, 2228–2234.
- (18) Crystallographic data of compound **1** have been deposited in the Cambridge Crystallographic Data Centre as CCDC 1915632. These data can be obtained free of charge via http://www.ccdc.cam.ac.uk/data_request/cif (or from the CCDC, 12 Union Road, Cambridge CB21EZ, U.K.; fax: +44-1223-336-033; e-mail: deposit@ccdc.cam.ac.uk).
- (19) Sheldrick, G. M. SADABS, Software for empirical absorption correction; University of Gottingen: Gottingen, Germany, 1996.
- (20) Sheldrick, G. M. SHELXTL, Structure determination software programs; Bruker Analytical X-ray System Inc.: Madison, WI, 1997.
- (21) Sheldrick, G. M. *Acta Crystallogr.* **2015**, *C71*, 3–8.
- (22) Flack, H. D. *Acta Crystallogr., Sect. A: Found. Crystallogr.* **1983**, *A39*, 876–881.
- (23) Putz, H.; Brandenburg, K. *Diamond: Crystal and Molecular Structure Visualization*; Crystal Impact.
- (24) Winter, N.; Rupcic, Z.; Stadler, M.; Trauner, D. *J. Antibiot.* **2019**, *72*, 375–383.



Research review paper

Biological and chemical diversity go hand in hand: Basidiomycota as source of new pharmaceuticals and agrochemicals[☆]

Birthe Sandargo^{a,b,1}, Clara Chepkirui^{a,b,1}, Tian Cheng^{a,b}, Lilibeth Chaverra-Muñoz^{a,b}, Benjarong Thongbai^{a,b}, Marc Stadler^{a,b,*}, Stephan Hüttel^{a,b,*}

^a Department of Microbial Drugs, Helmholtz Centre for Infection Research, 38124 Braunschweig, Germany

^b German Center for Infection Research, partner site Hannover-Braunschweig, 38124 Braunschweig, Germany

ARTICLE INFO

Keywords:

Antibiotics
Anticancer agents
Bioprospecting
Biotechnology
Medicinal mushrooms
Natural products
Neurotrophic agents

ABSTRACT

The Basidiomycota constitutes the second largest higher taxonomic group of the Fungi after the Ascomycota and comprises over 30,000 species. Mycelial cultures of Basidiomycota have already been studied since the 1950s for production of antibiotics and other beneficial secondary metabolites. Despite the fact that unique and selective compounds like pleuromutilin were obtained early on, it took several decades more until they were subjected to a systematic screening for antimicrobial and anticancer activities. These efforts led to the discovery of the strobilurins and several hundreds of further compounds that mainly constitute terpenoids. In parallel the traditional medicinal mushrooms of Asia were also studied intensively for metabolite production, aimed at finding new therapeutic agents for treatment of various diseases including metabolic disorders and the central nervous system. While the evaluation of this organism group has in general been more tedious as compared to the Ascomycota, the chances to discover new metabolites and to develop them further to candidates for drugs, agrochemicals and other products for the Life Science industry have substantially increased over the past decade. This is owing to the revolutionary developments in -OMICS techniques, bioinformatics, analytical chemistry and biotechnological process technology, which are steadily being developed further. On the other hand, the new developments in polythetic fungal taxonomy now also allow a more concise selection of previously untapped organisms. The current review is dedicated to summarize the state of the art and to give an outlook to further developments.

1. Introduction

The Basidiomycota (sometimes still referred to by the outdated, invalid term “basidiomycetes”, which has characterized a class) is the second largest division of the Kingdom Fungi after the Ascomycota and comprise ca. 35,000 species (Kirk et al., 2008). The true number of global species, however, is probably much higher, since recent studies relying on methods of molecular ecology (e.g. Tedersoo et al., 2014) have revealed a vast, unexpected diversity in the Basidiomycota as well as in fungi in general. Many species of Basidiomycota, in particular the class Agaricomycetes, produce conspicuous fruiting bodies (basidiomes) and have probably been used as a source of food since early human civilization. Since the edible species are often easily confused with morphologically similar and poisonous mushrooms, the consumption of the latter species may lead to fatalities. For this reason, the evaluation and

identification of the mushroom toxins, such as muscarine and the amanitins, has been the topic of many of the early chemical studies on fungal metabolites (e.g. Wieland and Hallermayer, 1941; Wilkinson, 1961). Curiously, these studies came about at about the same time as the discovery of penicillin, which marked the onset of the “Golden Era of Antibiotics” (Mohr, 2017), and already in the early 1950s, biotechnologists and chemists started to study not only soil-derived molds, bacilli and actinobacteria but even Basidiomycota cultures for production of antibiotics. These efforts have already led to various discoveries of important molecules, including pleuromutilin (1) (Kavanagh, 1947), from which a marketed drug and several developmental candidates have been developed several decades later (see Fig. 1). Further examples of early discovered molecules from cultures of Basidiomycota include pleurotin (Kavanagh, 1947) and the illudins (McMorris and Anchel, 1963), which will also be treated in detail further below.

[☆] This paper is dedicated to Profs. Heidrun and Timm Anke for their great efforts on the discovery of secondary metabolites from Basidiomycota.

* Corresponding authors at: Department of Microbial Drugs, Helmholtz Centre for Infection Research, 38124 Braunschweig, Germany.

E-mail addresses: marc.stadler@helmholtz-hzi.de (M. Stadler), stephan.huettel@helmholtz-hzi.de (S. Hüttel).

¹ These authors contributed equally to this work.

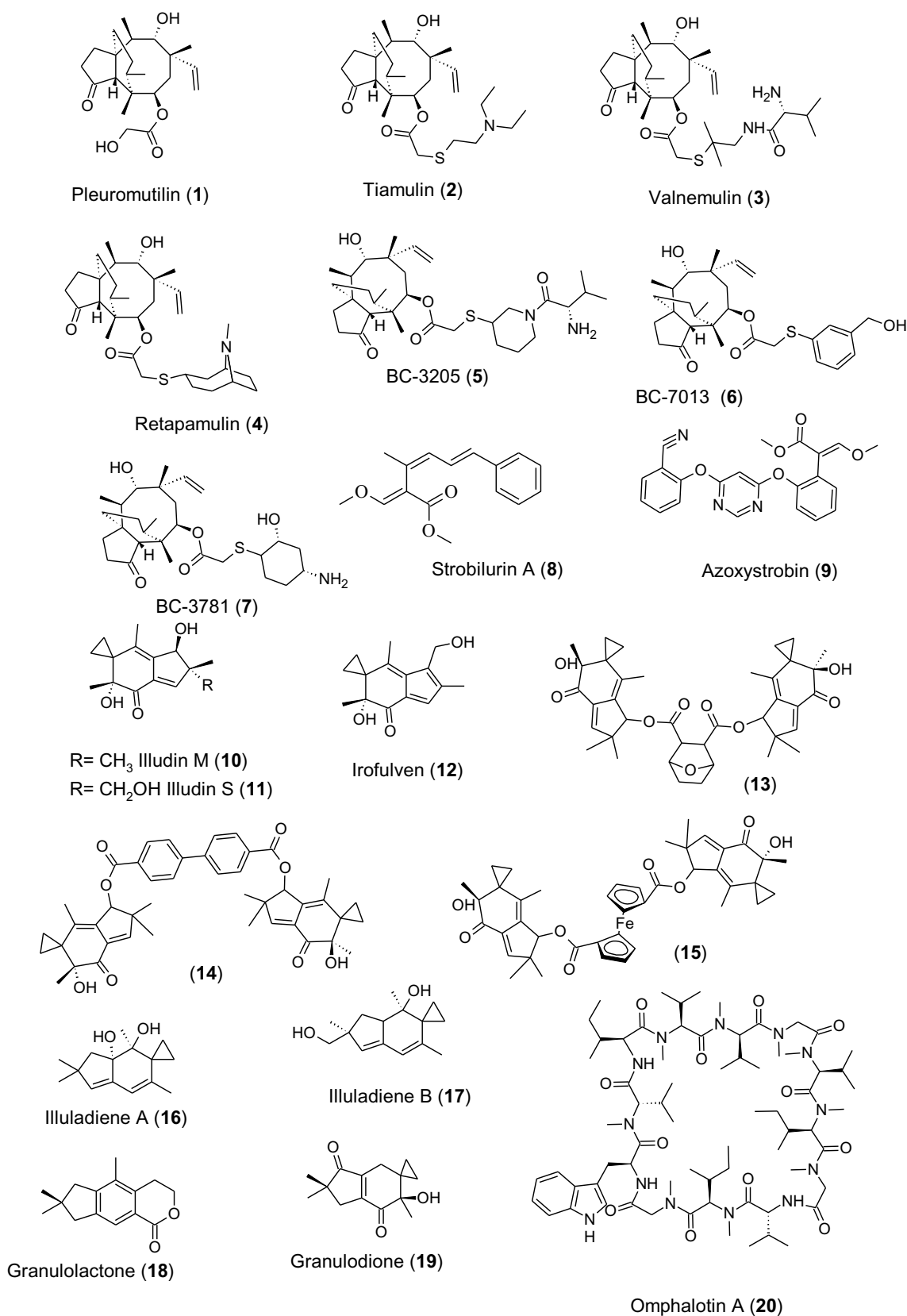


Fig. 1. Chemical structures of compounds used as drug or under development and agrochemicals discovered from Basidiomycota.

During the same period of time (from 1950-1975), hundreds- if not thousands- of researchers have been focusing world-wide on the exploitations of fungi and bacteria for novel lead compounds in many

indications of the Agro and Pharma sectors. Almost all large pharmaceutical and agrochemical companies have been participating in these endeavors, and some of them actually owe their great commercial

success to the respective discoveries because several blockbuster drugs have resulted from natural product screening (Bills and Gloer, 2016). Mostly, these research programs have been following the principle of random screening of soil isolates and were strongly focused on the exploitation of fast-growing organisms like actinobacteria, bacilli and conidial fungi whose fermentation and extraction can easily be standardized. Basidiomycota have been playing a secondary role in these scenarios because they can hardly be isolated from soil samples and their fermentation often requires special protocols (Karwehl and Stadler, 2017). Only since the mid-1970s, triggered by the exciting discovery of the strobilurins (see Fig. 1) by a team of German researchers, have these organisms come more strongly into the focus of natural product based drug discovery. Since then, many new metabolites have been obtained from Basidiomycota, and in the past 15 years, the majority of new compounds were actually reported by Asian scientists, who studied intensively the “medicinal mushrooms” of their countries, as demonstrated in the overview of De Silva et al. (2013). Meanwhile even the biosynthesis of selected molecules produced by Basidiomycota has been evaluated, and the number of fully sequenced genomes of these organisms is steadily increasing, owing to the substantial progress in bioinformatics, genomics and transcriptomics (cf. Hoffmeister and Stadler, 2015). Moreover, sustainable biotechnological processes for the production of these molecules have become available, some of which are even using heterologous hosts. The present review aims to summarize the state of the art of various aspects relating to the discovery of new biologically active compounds from Basidiomycota and their development to market products in a historical context with emphasis on the literature of the past five years.

2. Brief overview about the taxonomy of the Basidiomycota

The Basidiomycota² with an estimate of over 30.000 described species are a phylogenetic sister group of the Ascomycota and presently comprise of four subphyla (Agaricomycotina, Pucciniomycotina, Ustilaginomycotina, and Wallemiomycotina (Zhao et al., 2017; Fig. 2). Out of those, in particular the first mentioned subphylum, which contains almost all fleshy mushrooms, has been tapped for secondary metabolite production. Notably, even in the Agaricomycotina, many species have so far not been made available for studies on the secondary metabolites in culture or for other biotechnological applications. The reason is that Basidiomycota form different guilds (= ecological groups) including ectomycorrhizal fungi, saprotrophs, and pathogens. Some representative species are depicted in Fig. 3. Within the ectomycorrhizal group, as represented by many widely recognized genera for fleshy mushrooms (e.g. *Amanita*, *Boletus*, *Cantharellus*, *Cortinarius*, *Hydnellum*, *Lactarius*, *Sarcodon*, and *Russula* and the respective families like Boletaceae, Russulaceae and Cantharellaceae), a mutualistic relationship between the fungal symbiont and the roots of various plant species exists. The ectomycorrhizal fungi show the strongest relationship to the richness of host plant species (i.e. conifers and deciduous trees) and high soil pH, followed by saprotroph richness than the pathogens (Tedersoo et al. 2014). Surprisingly, the Agaricomycotina make up more than 50% of the total mycobiota that were detected in soil, which should give rise to attempt to make more of their species accessible to studies of their metabolites in culture. In natural habitats, they efficiently degrade lignocellulose, which makes them indispensable for maintenance of the global carbon cycles, but they can often not be taken in artificial axenic culture without the plant symbiont. Therefore, the available studies on their secondary metabolites are so far largely

²The fungal names used in this review are given as proposed in Mycobank, the official fungal nomenclature database of the International Mycological Association (<http://www.mycobank.org>, last accessed on Dec 27 2018). We do not provide the authorities of these names and have in some cases pointed out the synonyms previously used in the literature.

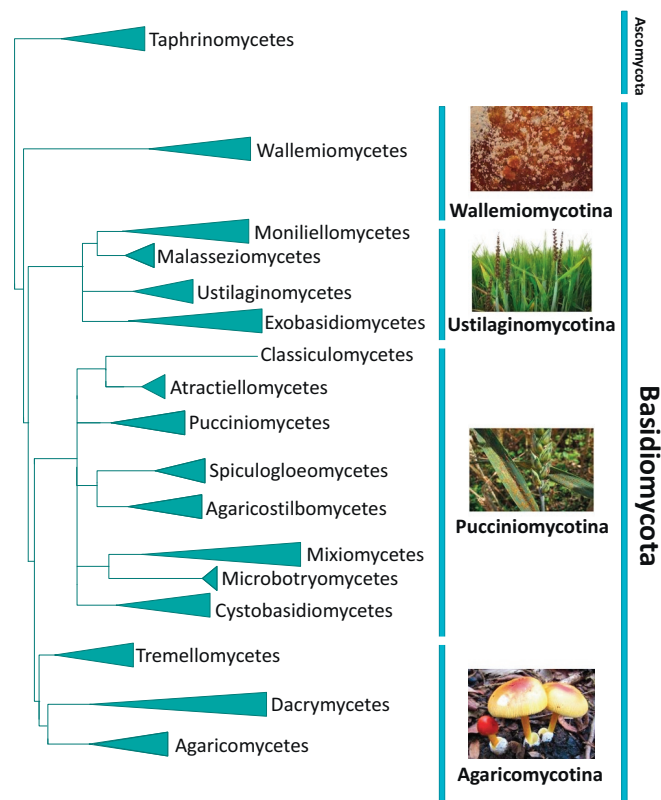


Fig. 2. Scheme illustrating the phylogenetic relationships of Basidiomycota as inferred from recent multi locus genealogies. Modified according to Zhao et al. (2017). The length of the triangles in the phylogenetic tree does not represent the species richness of the classes, but merely refers to the phylogenetic distance.

restricted to their fruiting bodies. As it would lead too far to include all fruiting body metabolites in this review, we refer to the respective papers by Chen and Liu (2017), Schüffler (2018) and De Silva et al. (2013). Remarkably, even the species of some genera that are considered to be saprotrophs, such as *Pluteus* and *Lepiota* are not easy to culture, as their spores fail to germinate in the laboratory. The ecological preferences of numerous Basidiomycota have so far remained obscure and can only now be elucidated by using modern methods of molecular ecology. For instance, some species that were hitherto regarded as saprotrophs, such as *Hygrocybe virginea*, are now suspected to possess hitherto unknown associations with plants, and conducting in-depth studies on their ecology might in the future be rewarding (Tello et al., 2014). However, the endophytic nature of these mushrooms poses a challenge and partially explains why only a few species of *Hygrocybe* have ever been cultivated and studied for secondary metabolites.

While the Wallemiomycotina are a very small taxonomic group and have so far only been studied scarcely, in particular the biotrophic pathogens, and almost the entire subdivision Pucciniomycotina (rust fungi), as well as many members of the Ustilaginomycotina (smut fungi) are also difficult –if not impossible to culture at large scale. Even though several complex protocols for cultivation of rusts and smuts as well as mycorrhizal fungi exist, they often rely on the supplementation of vitamins or even the use of minimal media that do not support sustainable mycelial growth. The reasons for this behaviour are often not clear, but complex, sugar-rich media that easily allow cultivation of saprotrophic fungi will often turn out not to be suitable for cultivation of certain Basidiomycota, and there have been relatively few systematic studies on the nutritional preferences of certain species and genera. As pointed out by Hoffmeister and Stadler (2015), the genomes of the



Fig. 3. Morphological diversity of Basidiomycota. (A) *Turbinellus* sp. (B) *Clavulina* sp. (C) *Agaricus* sp. (D) *Tremella* sp. (E) *Amanita rubrovolvata* (F) *Clavulina* sp. (G) *Clathrus* sp. (H) *Cortinarius* sp. (I) *Hygrocybe* sp. (J) *Tylopilus* sp. (K) *Meripilus giganteus*. (L) *Lactarius* sp.

mycorrhizal fungi were found to harbour numerous genes and gene clusters that seem to encode for the biosynthesis of secondary metabolites. In the future, it may be possible to isolate and characterise the respective products, based on strategies for heterologous expression that are outlined later in the present paper. The DNA can potentially be extracted from the fruiting bodies, or in case of the less fleshy species, by letting their mycelia grow for several months.

3. Secondary metabolites from Basidiomycota

3.1. Important drug candidates and agrochemicals from Basidiomycota

Despite the fact that the Basidiomycota have been much less studied for biologically active metabolites than the Ascomycota, a number of very important lead compounds have already been obtained from them,

which has led to clinical development candidates or even marketed drugs and agrochemicals. We have briefly summarized the history and the state of the art on these compounds in the following paragraphs.

3.1.1. Pleuromutilins are the newest class of antibacterial antibiotics launched on the market

Pleuromutilin (1) is a naturally occurring antibiotic from the culture of the mushroom *Clitopilus passeckerianus* (formerly named *Pleurotus passeckerianus*) and was already discovered several decades ago (Kavanagh, 1947; Kavanagh et al., 1951). This tricyclic diterpenoid was also reported from "*Drosophila subtrata*" (currently valid name: *Parasola conopilus*), *Clitopilus scyphoides*, and some other *Clitopilus* species (Hartley et al., 2009; Kavanagh et al., 1952). Even though the potent activity of pleuromutilin against most Gram-positive and some Gram-negative pathogens was quite promising, at that time resistance to β -lactams antibiotics was not regarded as a critical issue, therefore the interest in antibiotic research including pleuromutilins was limited (Paukner and Riedl, 2018). Questions regarding the metabolic stability, gastrointestinal side effects, cardiac safety and intravenous tolerability to this class of compounds further limited their application in humans (Novak, 2011). However, the semisynthetic pleuromutilin derivatives, tiamulin (2) and valnemulin (3), were introduced to veterinary medicine in 1979 and 1999, respectively, for the treatment of swine dysentery and enzootic pneumonia (Poulsen et al., 2001). Despite the use of pleuromutilins for treatment in veterinary medicine for many years, resistance development has been uncommon. This could be attributed to the unique and highly specific mode of action of this class of compounds, which inhibit protein synthesis in bacteria by binding to the peptidyl transferase component of the 50S subunit of their ribosomes. The wide spread emergence of antimicrobial resistance has renewed the research on the pleuromutilins. Synthetic derivatization of this compound has also resulted in the development of retapamulin (4), a semisynthetic analogue approved for treatment of skin infections in humans, which is the first approved antibiotic drug from the Basidiomycota. The recent advances in lead optimization by combining potent antibacterial activity with favorable pharmaceutical properties have led to the synthesis of three further new semisynthetic pleuromutilin derivatives, BC-3205 (5), BC-7013 (6) and BC-3781 (7) that are currently in clinical trials. BC-3781 is currently at phase II and phase III trial against acute bacterial skin structure infections and community acquired bacterial pneumonia respectively (Paukner and Riedl, 2018; Prince et al., 2013).

3.1.2. Strobilurins are one of the most successful classes of agrochemical fungicides

The strobilurins (Fig. 1) are another important class of compounds from Basidiomycota that have served as lead compounds for the development of the agricultural β -methoxyacrylate fungicides (Sauter et al., 1999). These compounds are known from the mycelial cultures of various Basidiomycota including *Favolaschia*, *Mycena*, *Oudemansiella*, *Strobilurus* and *Xerula* (Hoffmeister and Stadler, 2015). After 50 years of intensive research on this class of compounds it is quite interesting that new derivatives like the 9-oxo strobilurin derivatives reported from *Favolaschia calocera* originating from Kenya (Chepkirui et al., 2016) can still be discovered. Strobilurins prevent mycelial growth and germination of spores by binding to the ubiquinol-oxidation center in the mitochondrial cytochromes, which is responsible for the generation of the proton gradient used for ATP synthesis and the transfer electrons to nitrogenase, consequently blocking electron transfer (Sauter et al., 1999). The fact that some strobilurins exhibit strong antifungal activity coupled with their low cytotoxicity towards mammals and plants, and the relatively easy access by total synthesis made them promising lead compounds for synthesis of agricultural fungicides (Anke, 1995). Although strobilurin analogs were very successful in the market since the late 1990s, resistance to these fungicides developed in populations of plant pathogenic fungi only two years after their introduction to the

market. This was attributed to them being "single-target" compounds, and it is easy for the pathogens to acquire resistance through single point mutation in the target proteins (Ishii et al., 2001; Vaghefi and Hay, 2016; Zhang et al., 2009). Nevertheless, azoxystrobin (9) and kresoxim-methyl are still being applied at large scale in combination with other antifungal agents such as azoles. The fact that even resistances against azoles are now becoming more frequent among both, human and plant pathogens is really frightening because they are presently the only class of environmentally friendly fungicides and also constitute the optimal therapeutic drugs against certain fungal human pathogens. Unfortunately, the pipeline for the development of novel fungicides and antimycotics of the large companies seems to be even more empty than in case of the antibacterial antibiotics. This can in part be attributed to the negligence of natural product-based antifungal agents over the past decades.

3.1.3. The genus *Omphalotus* is a source of potential anticancer drugs and agrochemical pesticides

Species of the genera *Omphalotus* and *Lampteromyces* consistently produce acylfulvene (or illudane) type sesquiterpenes, featuring an unusual cyclopropane ring (Schobert et al., 2011; Tanasova and Sturla, 2012). Illudins M and S (10-11) were the first members of this terpenoid family to be discovered in the 1950s (Kavanagh, 1947). Even though Illudins were studied extensively for their cytotoxicity in various tumor cell types and tumor xenografts, the frequent animal deaths, associated with the high toxicity of illudins, initially restricted their potential use as anticancer agents. However, this stimulated a pursuit for analogues that combine high potency with better therapeutic characteristics (Schobert et al., 2008, 2011; Tanasova and Sturla, 2012). Irofulven, also known as 6-hydroxymethylacylfulvene or HMAF (12), a semisynthetic analogue of illudin S, is currently under development as anticancer drug (Tanasova and Sturla, 2012). More recently, several "new generation" illudin analogs with improved tumor specificity have been synthesized by Schobert and co-workers. The semisynthetic chlorambucil analogs (13-14) were reported to show promising improved specificity toward tumor cells over normal fibroblasts, while M-ferrocene conjugates (15) were found to be more active against melanoma cells as compared to leukemia cell lines or nonmalignant fibroblasts (Knauer et al., 2009; Schobert et al., 2008).

Recently, eight illudanes have also been found in the wood-decaying fungus *Granulobasidium vellereum*, out of which the cytotoxic illuladienes A (16) and B (17) constitute novel natural products (Nord et al., 2015). Two other new illuladane sesquiterpenoids named granulolactone (18) and granulodione (19) were reported later on from the same species (Kokubun et al., 2016). Only granulodione (19) exhibited acaricidal activity against *Tetranychus urticae*, with 83% mortality after 2 h of exposure in a contact activity test.

Curiously, in addition to the illudins, all species hitherto studied of the genus *Omphalotus* also produce cyclopeptides of the omphalotin type with pronounced activities against root knot nematodes like *Meloidogyne incognita* (Mayer et al. 1999). Sterner et al. (1997) first reported omphalotin A (20) from *Omphalotus olearius*. Later, several other derivatives of this compound were isolated from the same fungus (Büchel et al., 1998; Liermann et al., 2009). These compounds co-occur in the cultures with illudins, while the latter compounds are located in both the basidiomes and the mycelia of the fungi.

3.2. Novel biologically active compounds from Basidiomycota

The mushroom-forming fungi have been used for many centuries as remedies of various diseases especially in Asia. Some of these "medicinal mushrooms" in particular are known to be prolific producers of bioactive metabolites and they have been widely exploited (De Silva et al., 2013). The therapeutic benefits of these mushrooms go back in many cases to complex high molecular weight compounds such as polysaccharides, proteins and lipids as active principles, which are not

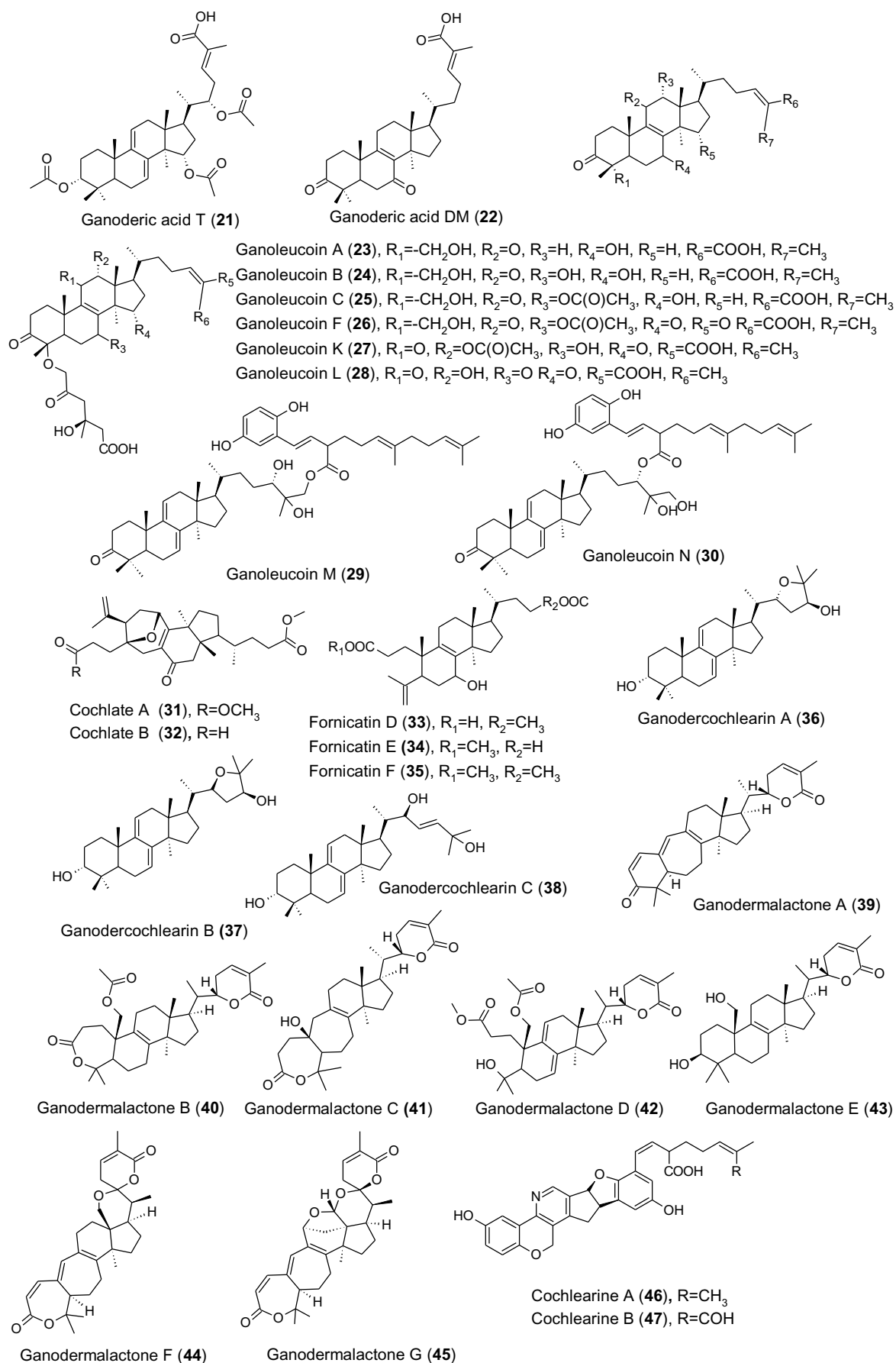


Fig. 4. Chemical structures of compounds isolated from *Ganoderma* species.

being treated here in detail. We instead concentrate on those species that are known to produce compounds with low-molecular weight, such as terpenoids, polyketides, and alkaloids.

3.2.1. Metabolites from *Ganoderma* species

Aside from *Ophiocordyceps sinensis*, which belongs to the Ascomycota and is thus not being treated in detail here, *Ganoderma lingzhi* (previously often falsely reported in the literature as “*G. lucidum*” *sensu lato*) is surely the most important (group of) medicinal mushroom (s). The taxonomy and nomenclature of the Chinese medicinal *Ganoderma* spp. has been heavily disputed among mycologists (Hawksworth, 2005; Richter et al., 2015). Recently, a paper co-authored by several eminent specialists in the taxonomy of the Basidiomycota has been published that will hopefully settle this matter and allow the name *G. lingzhi* to take preference over competing names once and for all (Dai et al., 2017).

In Chinese traditional folk medicine the fruit bodies of *Ganoderma* (aside from the Lingzhi, also other species like *G. sinense* have been used) are regarded as a panacea for all types of diseases due to its demonstrated efficacy as a popular remedy to treat hepatopathy, chronic hepatitis, nephritis, hypertension, hyperlipemia among others diseases (Jong and Birmingham, 1992). Several secondary metabolites have been isolated from different species belonging to this genus (a selection thereof is depicted in Fig. 4). The majority of known secondary metabolites from *Ganoderma* species are largely triterpenoids belong to the class of lanostane-type or ergostane-type and pentacyclic triterpenes (Richter et al., 2015). These include the cytotoxic triterpenoids such as ganoderic acids, lucidimols, ganodermanondiol, ganoderiols, lucidenic acids and ganodermanontriols. The biological activities of these compounds have been discussed at length by De Silva et al. (2013). Ganoderic acid T (21) and a closely related triterpenoid named ganoderic acid DM (22) produced by “*Ganoderma lucidum*” are some of the compounds that have been studied in detail with regard to their application in cancer treatment. Tang et al. (2006) reported that ganoderic acid T induces apoptosis of metastatic lung tumor cells through an intrinsic pathway related to mitochondrial dysfunction. Ganoderic acid DM (22), on the other hand, was shown to inhibit cell proliferation and colony formation in MCF-7 human breast cancer cells and also induced cell cycle (G1) arrest and apoptosis in MCF7 cells (Liu et al., 2012; Wu et al., 2012).

In the past years, several other lanostane triterpenes have been discovered from *Ganoderma* species. From basidiomes of *Ganoderma leucocontextum*, several lanostane triterpenes named ganoleucoins A–P were isolated. Ganoleucoins A–C (23–25), F (26), K–N (27–30) and ganoleucoin O (structure not shown) exhibited inhibitory effects on both HMG-CoA reductase and α -glucosidase in the μ M range (Kai et al., 2015). Peng et al. (2014) also reported several triterpenoids from *G. cochlear*. These include cochlates A (31) and B (32) featuring a 3,4-seco-9,10-seco-9,19-cyclo skeleton, as well as fornicatins D–F (33–35) and ganodercochlearins A–C (36–38). Fornicatins D (33) and F (35) were reported to lower both, the alanine aminotransferase (ALT) and aspartate aminotransferase (AST) levels in HepG2 cells treated with H₂O₂, indicating that they could display in vivo hepatoprotective activities. From “*Ganoderma* sp. KM01”, the ganoderimalactones A–G (39–45) were obtained, but when these compounds were tested against *Plasmodium falciparum*, only ganoderimalactone F showed significant antimalarial activity (Lakornwong et al., 2014). Furthermore, cochlearines A (46) and B (47) along with cochlearoids A–E (48–52) (Fig. 5) were isolated from cultures of *G. cochlear*. Compounds 46, 48 and 50 significantly inhibited the calcium channel Ca_v3.1 TTCC (Zhou et al., 2015). Meroterpenoids named chizhines A (53), B (54) and C (55)–F were reported from “*G. lucidum*” by Luo et al. (2015b). These compounds significantly inhibited the monocyte chemotactic protein 1 (MCP-1) and fibronectin production with chizhine F (56) being the most potent derivative. The nortriterpenes, ganoboninketals A–C (57–59), which feature a rearranged 3,4-seco-27-norlanostane skeleton, were reported to occur in

Ganoderma boninense and showed antiplasmodial activity against *Plasmodium falciparum* and weak cytotoxicity against A549 cells (Ma et al., 2014). A dimeric meroterpenoid applanatumin A (60) with a new hexacyclic skeleton was isolated from “*G. applanatum*” (actually this fungus was probably misidentified because this European species has never been safely recorded from China). In any case, compound (60) exhibited potent antifibrotic activity in TGF- β 1-induced human renal proximal tubular cells (Luo et al., 2015a). In summary, the genus *Ganoderma* appears to be an almost inexhaustible source of novel chemistry, but it is very unfortunate that many of the reports on new compounds do not deal with material that has been identified by specialists and often not even voucher specimens are deposited in the public domain for later verification of the taxonomy.

3.2.2. Metabolites from the *Inonotus linteus* complex

Inonotus and *Phellinus* are two genera in the Hymenochaetaceae that have been traditionally distinguished by the morphology of their basidiomes and are very difficult to separate; hence, the boundaries between these genera always remained unclear. This is the reason why one of the most important groups of medicinal mushrooms was historically referred to alternatively as the *Inonotus linteus* or the *Phellinus linteus* complex. A recent phylogenetic study has resulted in the resolution of this species complex and a rearrangement of those taxa that were formerly placed in *Inonotus* or *Phellinus*, which are now being accommodated in the new genera *Sanguangporus* and *Tropicoporus* (Zhou et al., 2016a).

The respective fungi have been widely used in Asia for the treatment of gastrointestinal cancer, cardiovascular disease, tuberculosis, liver or heart diseases, as well as diabetes as a traditional medicine (de Silva et al., 2013; Solomon and Alexander, 1999). Their characteristic metabolites include unique complex styrylpyrone derivatives like phelligridins and the closely related inoscavins and inonoblins that exhibit antioxidant and cytotoxic effects (De Silva et al., 2013). In the past five years, two additional phelligridin derivatives have been reported. One of them is phelligridin L (61) (Fig. 5) from the cultures of *Sanguangporus* sp. This compound demonstrated moderate antibacterial activity as well as nematocidal activity against *Caenorhabditis elegans* (Chepkirui et al., 2018a). From another medicinal fungus that was previously referred to as *Phellinus ribis* (current name *Phylloporia ribis*) a new spiroindene pigment phelliribsin A (62) with cytotoxic activity against PC12 cells at a concentration of 30 μ M was isolated. This compound was reported together with the known compounds phelligridin F and inoscavin B (Kubo et al., 2014).

Another predominant class of metabolites that occurs in these fungi are the sesquiterpenoids, as evidenced by recent literature. Yin et al. (2014) isolated two tremulanes, i.e., 6 β ,11,12-trihydroxy-tremul-1(10)-ene (63) and 10 β ,12-dihydroxy-tremulene (64) from *P. ignarius*. These sesquiterpenes exhibited different levels of vascular-relaxing activities against KCl-induced vasoconstriction. Exploitation of the well-known medicinal mushroom “*Phellinus linteus*” (currently valid name: *Tropicoporus linteus* (Zhou et al., 2016a) over the years has resulted in the isolation of several bioactive metabolites. These include some antimicrobial sesquiterpenes, which are part of the oral composition of an antibacterial agent used in the treatment or prevention of periodontal disease and related diseases; they are also used in the form of toothpaste, mouthwash and lozenge (Kobayashi et al., 2010). Huang et al. (2013) reported phellilins A–C (65–67) with weak inhibitory activity on superoxide anion generation and elastase release from this fungus. The inonoalliacanes A–I (68–72), which have an alliacane carbon skeleton, were isolated from the culture broth of another *Inonotus* sp. BCC 22670. Inonoalliacane B showed antiviral activity against Herpes Simplex Virus type 1 (Isaka et al., 2017). The same group also reported the isolation of romadendrane sesquiterpenoids named inonotins (including the inonotins A–G; 73–79) from *Inonotus* sp. strain BCC 23706, but failed to detect any bioactivities (Isaka et al., 2015). The related species, *Inonotus obliquus* (commonly known as Chaga mushroom) is used in Chinese

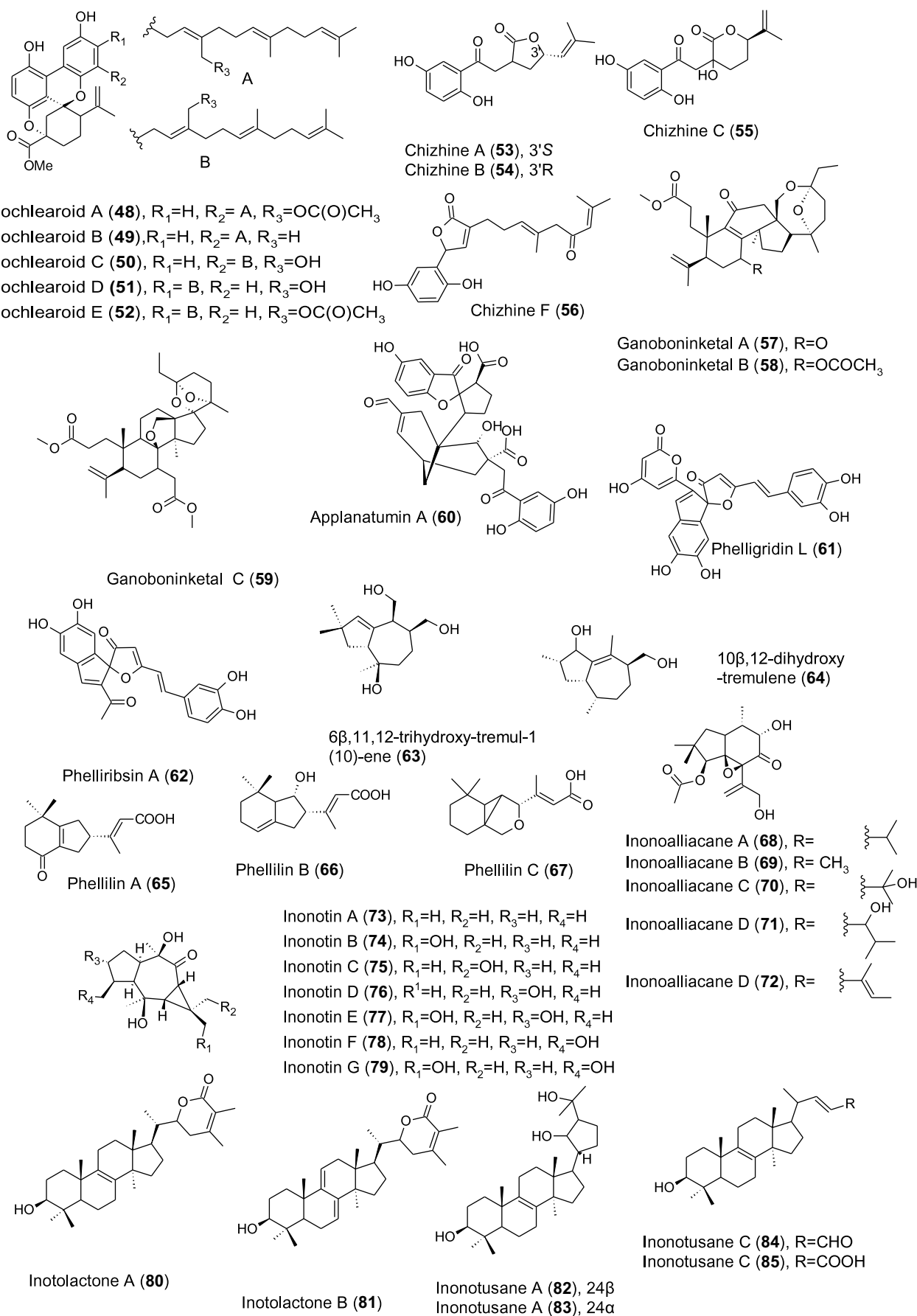


Fig. 5. Chemical structures of compounds isolated from various medicinal mushrooms.

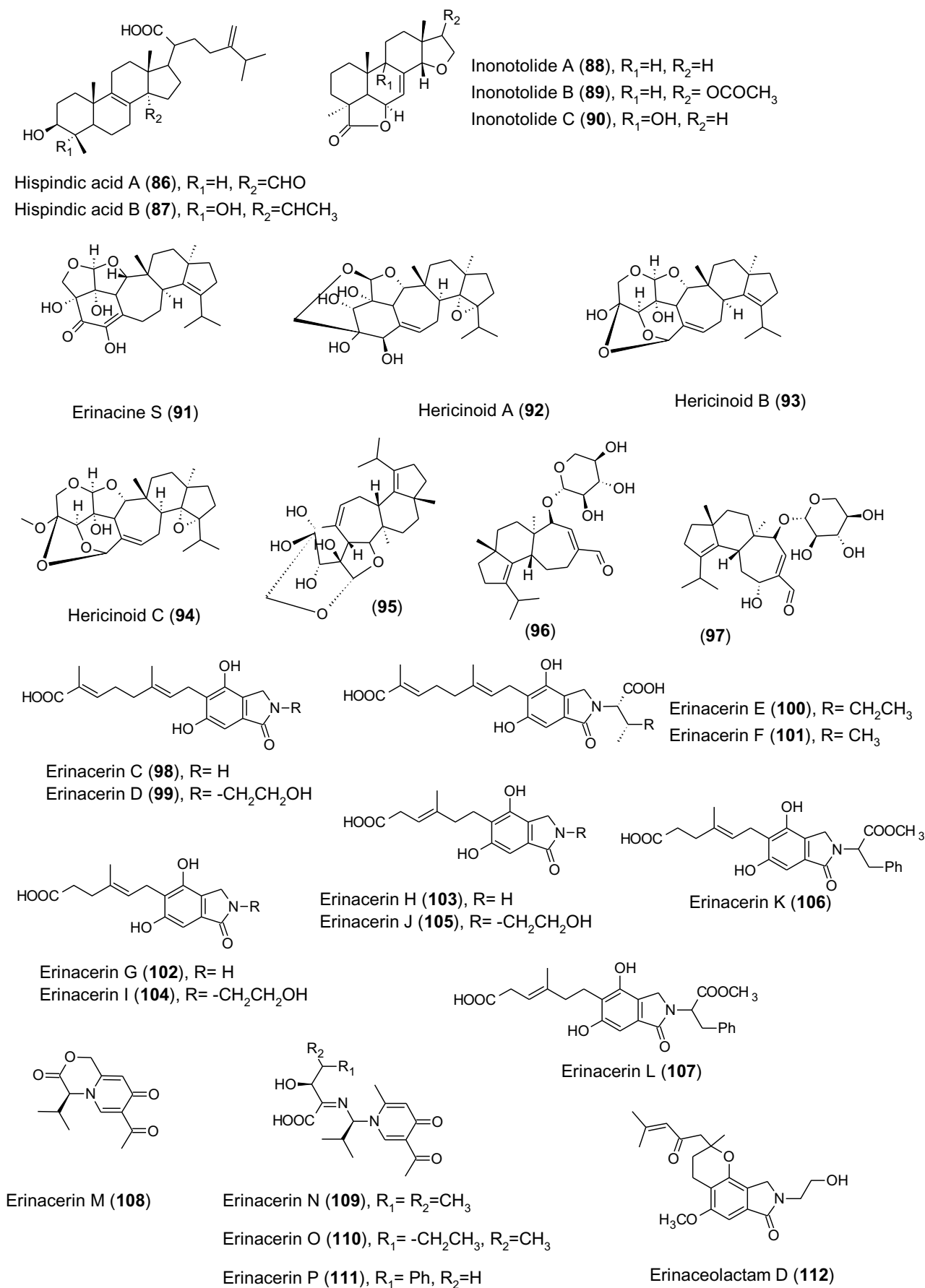


Fig. 6. Chemical structures of compounds isolated from various medicinal mushrooms.

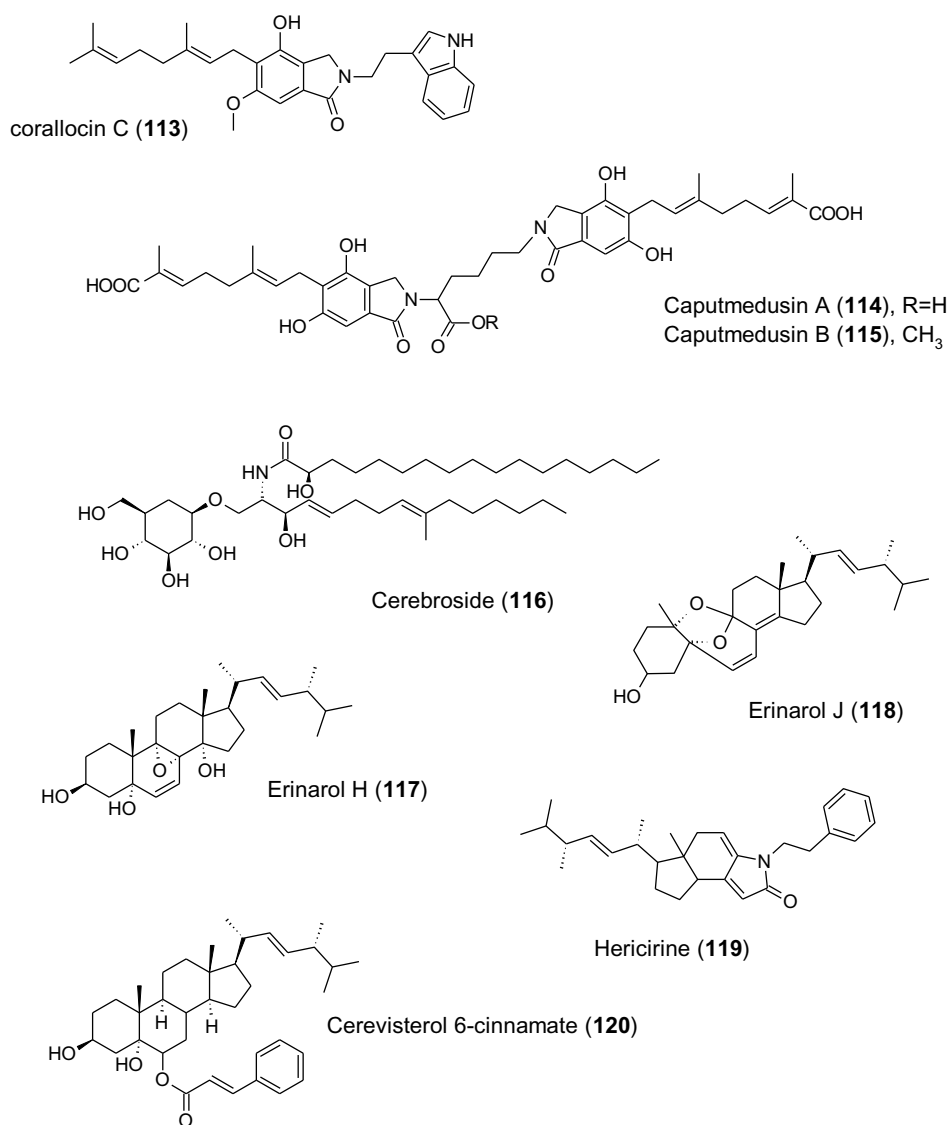


Fig. 7. Chemical structures of compounds isolated from different *Hericium* species.

traditional medicine to treat diabetes and was studied for its secondary metabolite production by Ying et al. (2014). The authors reported lanostane-type triterpenoids bearing α,β -dimethyl, α,β -unsaturated δ -lactone side chains named inotolactones A (80) and B (81). Interestingly, the latter compounds exhibited more potent alpha-glucosidase inhibitory activities than the positive control, i.e., the marketed drug Acarbose (Ying et al., 2014). Furthermore, some closely related terpenoids named inotusanes A–C (82–84) along with 3β -hydroxy-25,26,27-trinorlanosta-8,22E-dien-24-oic acid (85) from the same fungus were reported to exhibit strong cytotoxicity against A549 tumor cell lines and moderate activities against several other cell lines including HT29, HeLa and L1210 (Zhao et al., 2015). Hispidic acids A (86) and B (87) (Fig. 6), which are also lanostane-type triterpenoids, were isolated from *Inonotus hispidus*. They showed stronger activation abilities of melanogenesis and tyrosinase in B16 melanoma cells (Qing et al., 2017). The new isopimarane diterpenoid lactones, inonotolides A–C (88–90) are yet another class of compounds that have been reported from *Inonotus sinensis*. The compounds were evaluated for their cytotoxicity against various cancer cell lines, but they were devoid of activity (Ding et al., 2018).

3.2.3. *Hericium* species and their neurotrophic and other biologically active metabolites

The medicinal mushrooms of the genus *Hericium* and in particular *Hericium erinaceus* have been used in traditional Chinese medicine for a long time as food supplements and alternative medicine (Thongbai et al., 2015). Metabolites with various biological activities including antimicrobial, cytotoxic and neurotogenic effects were isolated from both the fruiting bodies and cultures of these fungi (Kawagishi et al., 1994; Thongbai et al., 2015; Wittstein et al., 2016). Both, the erinacines and hericenones/corallocons were reported to induce nerve growth factor (NGF) and brain-derived neurotrophic factor (BDNF). This illustrates their therapeutic potential for the treatment of Alzheimer's disease and other neurodegenerative disorders by compounds produced by *H. erinaceus* and other species of the genus. Interestingly, the erinacines, which are cyathane diterpenoids, are produced exclusively in the cultures whereas the hericenones and other isoindolinones are prevailing in the basidiomes.

In the past years, several further cyathane diterpenoids from the genus *Hericium* have been reported. Erinacine S (91) (Fig. 6) was isolated from the mycelial ethanol extract of *H. erinaceus*. The amyloid pathology potentials of this compound and erinacine A were studied *in vivo* in mice through a 30-day oral course of erinacines A and S. These

compounds were found to significantly increase the level of insulin-degrading enzyme (IDE) in cerebral cortex thus reducing the AB10-stained plaque burden (Chen et al., 2016). Other cyathane diterpenoids named hericinoids A–C (92–94) and the unnamed compound 95 were isolated from the same fungus. The hericinoids did not enhance neurite outgrowth in PC-12 cells, maybe owing to their moderate cytotoxicity, which was tested against HL-60 cell lines (Chen et al., 2018). Notably, metabolites that have cytotoxic properties will often not show activities in these NGF-induction assays. Compound 95 exhibited moderate antibacterial activities and cytotoxic effects against the human cancer cell lines K562, LANCAP and HEP2 (Zhang et al., 2015). Two additional erinacine derivatives (96–97) along with several known erinacines were isolated from the cultures of this fungus or of the related species *H. flagellum* (Rupcic et al., 2018). The erinacine derivative (96) and several known congeners were found to enhance neurotrophin production in astrocytic cells significantly by acting on Brain-Derived Neurotrophic Factor (BDNF), as well on NGF (Rupcic et al., 2018). These results were confirmed by quantitative PCR, corroborating the morphological studies on the cells, where differentiation was actually observed. However, the biochemical mechanisms leading to these neurotrophic effects remain to be elucidated. Interestingly, Premnath et al. (2018) recently reported the mutacin synthesis inhibitory effects of erinacine C in *Streptococcus mutans*.

Erinacerines are alkaloids that are commonly isolated from both the cultures and fruiting bodies of *H. erinaceus*. The first erinacerines (i.e. erinacerines A and B) were isolated by Yaoita et al. (2005) from the basidiomes, and Wang et al. (2015a) later reported the isolation of erinacerines C–L (98–107) from the cultures of the fungus. Erinacerines D–L (99–107) showed inhibitory activities against α -glucosidase. Structure–activity analysis indicated that the erinacerines side chain and the phenolic hydroxy groups contributed greatly to the α -glucosidase inhibitory activity. Furthermore, erinacerines M–T were also reported to occur in solid cultures of the same fungus. Erinacerines Q–T showed inhibitory activities against both protein tyrosine phosphatase-1B (PTP1B) and α -glucosidase while erinacerines M–P (108–111) showed moderate cytotoxicity against K562 cells and doxorubicin-resistant K562 cells (Wang et al., 2015b). The closely related crinaceolactams A–E (e.g. erinaceolactam D; 112) from *H. erinaceus* were found inactive against the carcinoma cell lines SMMC-7221 and MHCC-97H (Wang et al., 2016). Erinacerine derivatives are apparently genus specific marker metabolites of *Hericium* species. From the medicinal and edible mushroom *Hericium coralloides*, the corallocins A–C (corallocin C (113), Fig. 7) were found to induce NGF and BDNF expression in human 1321N1 astrocytes (Wittstein et al., 2016). Further, isoindolinone-containing meroterpenes dimers, named caputmedusins A–B along with their analogues caputmedusins C–K were reported from *Hericium caput-medusae* cultures. The caputmedusins A (114), B (115) and C showed moderate inhibitory activity against α -glucosidase (Chen et al., 2017a).

There are also a few reports of other constituents of *H. erinaceus* that represent different types of molecules. For example, the erinarols G–J are ergostane-type sterols, isolated from a methanol extract of the dried fruiting bodies of *H. erinaceus*. Erinarols H (117) and J (118) exhibited inhibitory activity against TNF- α secretion (Li et al., 2015). Moreover, an ergosterol conjugation-type alkaloid, hericirine (119), was isolated from the dried fruiting bodies of the Lion's Mane mushroom and reported to significantly inhibit protein expression of iNOS and COX-2 and to reduce NO, PGE2, TNF- α , IL-6 and IL-1 β production in RAW264.7 cells exposed to LPS (Li et al., 2014). Li et al. (2017) also isolated a closely related sterol, cerevisterol 6-cinnamate (120) from the same fungus. Finally, the cerebroside (116) was reported to attenuate cisplatin-induced nephrotoxicity in LLC-PK1 cells and inhibits the effect on angiogenesis in HUVECs at concentration 25 μ M (Lee et al., 2015).

Several other fungi that have been used in Asian traditional medicine and presently under evaluation and this work is steadily yielding new molecules. A good way to expand such activities in the future

would be to study the relatives of the Asian species in other parts of the world for comparison. There is, after all, no reason to assume that, e.g. the *Ganoderma* and *Hericium* species of Latin America and Africa would be less creative with regard to the production of secondary metabolites just because they are less popular in the folk medicine of these geographic areas.

3.3. New metabolites that have been obtained from random screening approaches

Historically, most known fungal metabolites have been discovered during the course of screening programs aimed at novel antibiotics discovery. In this approach, suspensions of pathogenic organisms are tested in cell-based assays like serial dilution assays for susceptibility of growth towards fungal and microbial extracts. Other types of biological assays are not well-suited for testing of crude extracts because those contain ubiquitous compounds, such as linoleic acid which are frequently present in large amounts in the crude samples and cause false positive hits or cytotoxic effects that disguise interesting activities in assays based on mammalian cell lines. Therefore, pre-fractionation of the crude extracts prior to screening may constitute a valid alternative, but it is extremely time and work consuming and can hardly be carried out at high throughput without automation. A pragmatic approach can be to perform a thorough dereplication of the crude samples by HPLC-DAD/MS and look for new chemistry in parallel, and then isolate potentially new compounds that are detected in the crude extracts and make them available for testing in a pure compound library. It is also worth mentioning that the major advances that have been made in fungal taxonomy over the years can also play an important role in the discovery of new bioactive fungal metabolites. For many years, it has been known that secondary metabolite production and taxonomy may be closely aligned within narrow phylogenetic lineages in many organism groups (Karwehl and Stadler, 2017). A striking example are the recent studies on Basidiomycota from Thailand, where very high percentages of novel species were encountered, and concurrent investigations of the secondary metabolites of these species have already resulted in a very high hit rate of new metabolites from new species (Hyde et al., 2018). The advantage of combining classical and modern expertise on taxonomy to establish correlations between biological and chemical diversity within the fungal kingdom is the elimination of redundancies like duplicates and well-studied taxa and known producers of toxins while giving priority to putatively new species and other hitherto untapped taxa (Karwehl and Stadler, 2017). In our laboratory, the thorough taxonomic characterization of the strains prior to the screening has led to a substantial increase of the rate of new compound discovery. Several new compounds have been recently reported by employing a classical screening approach, following preselection by molecular phylogeny and chemotaxonomy. Some examples are given below.

3.3.1. Triterpenoids and cyathane diterpenoids

Terpenoids are fairly common among mushroom metabolites with sesquiterpenoids, diterpenoids and triterpenoids being the most commonly isolated metabolites from Basidiomycota. These fungi even produce numerous terpenoid carbon skeletons that have so far been found in neither plants nor Ascomycota and specifically occur in certain genera or families (Schüffler, 2018). One example are the cyathanes, which are the characteristic diterpenoids of the Bird's nest fungi (Nidulariaceae) and in particular the genus *Cyathus* (Anke and Oberwinkler, 1977; Ayer and Taube, 1972; Ayer et al., 1978).

We will focus here on recently discovered metabolites that have been published over the past five years. Substituted cyathane diterpenoids named pyristriatin A (121) and B (122) (Fig. 8) from a *Cyathus* species, for which the name *C. pyristriatus* was later proposed (Hyde et al., 2016) were recently reported by Richter et al. (2016). These pyristriatins, which exhibited moderate antimicrobial and weak

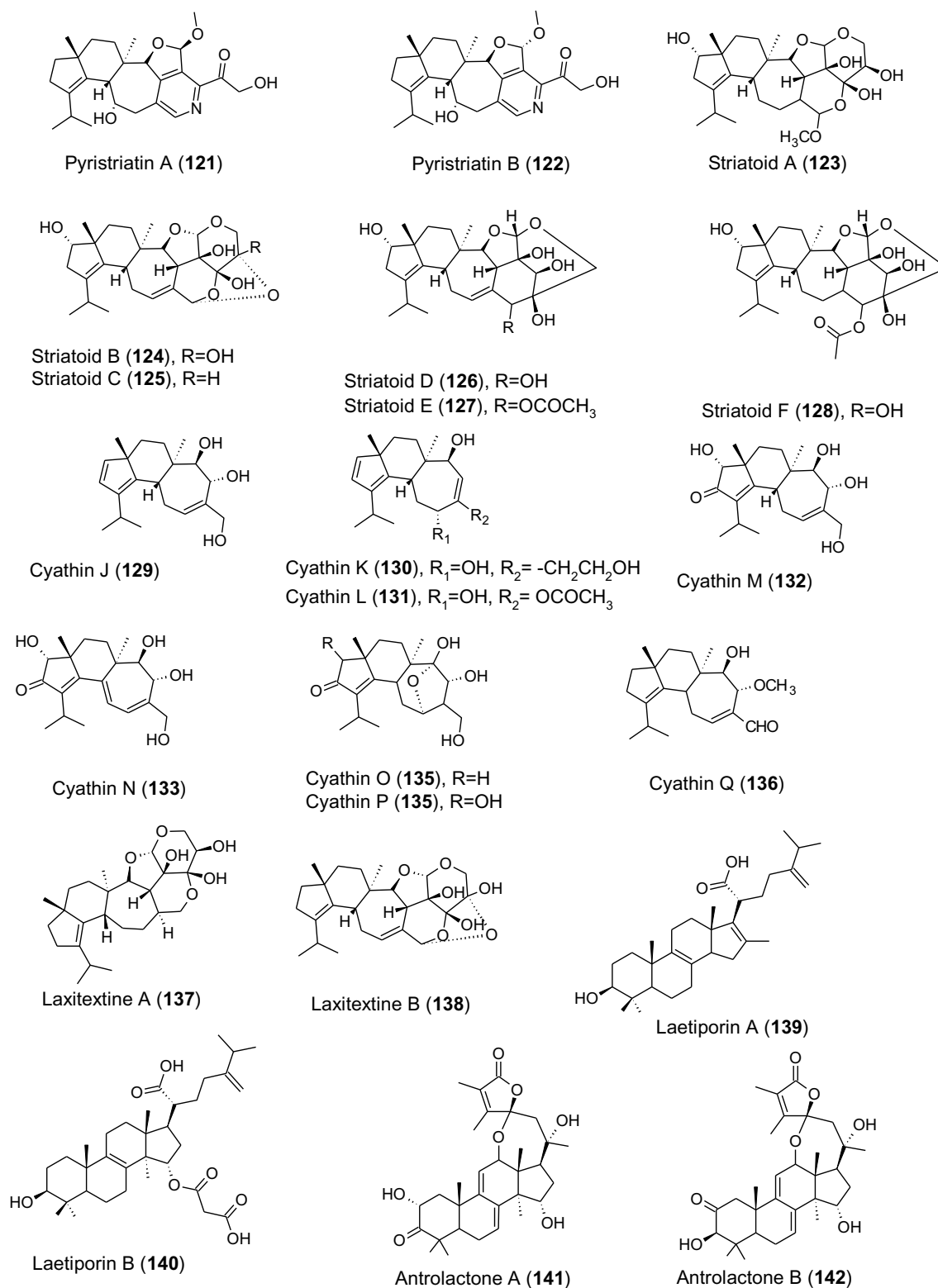


Fig. 8. Chemical structures of compounds isolated from random screening of different Basidiomycota.

cytotoxic activity, are the first terpenoids featuring a pyridine ring. Furthermore, highly oxygenated polycyclic cyathane-xylosides, named striatoids A–F (**123–128**), were isolated from cultures of a closely related species, *Cyathus striatus*. These striatoids showed dose-dependently enhanced nerve growth factor (NGF)-mediated neurite outgrowth in rat pheochromocytoma (PC-12) cells (Bai et al., 2015). To illustrate the frequent occurrence of this class of compounds in the

genus *Cyathus*, structurally related diterpenes were also isolated from *Cyathus gansuensis*. These compounds, which were named cyathins J–P (**129–135**), exhibited moderate inhibitory activity against nitric oxide (NO) production in lipopolysaccharide-activated macrophages (Wang et al., 2014). A similar compound, cyathin Q (**136**) was isolated from another *Cyathus* species, *Cyathus africanus*. This compound was reported to induce hallmarks of apoptotic events in HCT116 cells,

including caspase activation, cytochrome c release, poly (ADP-ribose) polymerase (PARP) cleavage, and depolarization of the mitochondrial inner transmembrane potential (He et al., 2016). Other cyathanes named laxitextines A (137) and B (138) with activity against Gram positive bacteria including methicillin resistant *Staphylococcus aureus* (MRSA) were reported to occur in cultures of *Laxitextum incrustatum* (Mudalungu et al., 2016). Interestingly, the genus *Laxitextum* belongs to the Hericiaceae and is very closely related to the medicinal mushrooms of the genus *Hericium*, which also predominantly produce cyathanes in their cultures (see Fig. 4 and section 3.2.4).

Triterpenes are a predominant class of secondary metabolites, above all in the wood-inhabiting polypore species, where they often are present in the basidiomes in large quantities. Therefore, many representatives of this class of molecules have already been reported in the last century (Liu, 2014; Ríos et al., 2012; Weete et al., 2010). However, as will be demonstrated here, the Basidiomycota are by far not exhausted with respect to the discovery of novel derivatives. For instance, the lanostane-type triterpenoids laetiporins A (139) and B (140) were isolated from a *Laetiporus* sp. originating from Kenya along with some known congeners, which showed cytotoxic activity against various human cancer cell lines. Laetiporin A (139) in particular, which features an unusual methylation at C-16, showed significant cytotoxic activity against L929, HeLa (KB-3-1), A431, MCF-7, PC-3 and A549 cell lines (Chepkirui et al., 2017). The spiro-lanostanes, antrolactones A (141) and B (142) from the ethanol extracts of the polypore *Antrodia heteromorpha* showed inhibitory effects on receptor activator of nuclear factor-kappaB ligand-induced osteoclastogenesis (Kwon et al., 2016). Fomitopsins D–F (143–145, Fig. 9) from *Fomitopsis feei* exhibited activity against *Bacillus cereus*. Fomitopsin D also showed activity against herpes simplex virus type 1 (HSV-1) (Masahiko et al., 2017). From a methanol extract of the fruiting bodies of a basidiomycete named “*Fomes officinalis*” (currently valid name: *Laricifomes officinalis*), eight 24-methyl-lanostane triterpenes named officimalonic acids A–H (146–153) were isolated. Officimalonic acids D, E, G and H are antioxidants, showing inhibitory effects on nitric oxide production in lipopolysaccharide-induced RAW264.7 cells in the range of 5.1–8.9 μM . Moreover, officimalonic acids E, G and H exhibited moderate cytotoxicity against H460, HepG2 and BGC-823 human cell lines (Han et al., 2016). Unusual pregnenolone type triterpenes named aethiopinolones A–E (154–158) were found in rather large quantities (total production rates ca. 50 mg/litre) in solid state fermentations of *Fomitiporia aethiopica* originating from Kenya (Chepkirui et al., 2018b). This type of triterpenes is almost unprecedented in fungi. Even though these compounds exhibited only weak cytotoxic activities against various human cancer cell lines (being otherwise inactive in biological systems), their biotechnological production may provide an alternative access to therapeutic drugs such as contraceptives and hydrocortisone that have a similar carbon skeleton

3.3.2. Sesquiterpenoids

Basidiomycota are also intricate producers of sesquiterpenoids. In fact, sesquiterpene synthases appear to be the most abundant class of natural products scaffold generating enzymes in Basidiomycota (Schmidt-Dannert, 2015, 2016). Therefore, it comes as no surprise that a manifold sesquiterpenoids have been isolated in recent years (Abraham, 2001).

A number of antioxidant spirobenzofuran-derived sesquiterpenoids (159–161; Fig. 10) have been isolated from the culture broth of “*Coprinus echinosporus*” (currently valid name *Coprinopsis echinospora*), a fungus commonly found on dung. Compounds 51 and 53 showed only weak antioxidant activity in the ABTS assay, with IC_{50} values in the 50 μM range (Ki et al., 2015). Another Asian species known for its antioxidant properties, the Enoki mushroom, (previously referred to in the literature under the European name, *Flammulina velutipes*, but recently recognised to represent an own species named *F. filiformis*, by Wang et al., 2018a) also cherished for its culinary value, has long been known

to produce the enokipodines (Ishikawa et al., 2001). However, a recent investigation of a wild specimen of this mushroom led to the identification of two new seco-cuparane sesquiterpenes, named flammufuranone A (162) and B (163); as well as 13 new sesquiterpenes (164–176), among which are the flammuspiroones A–J (164–173), and flammulipenoid F (176) with nor-eudesmane, spiroaxane, cadinane, and cuparane skeletons. Only a few of these metabolites (163, 164 and 166) exhibited moderate inhibition of DPP-4 (Dipeptidylpeptidase-4) and HMG-CoA reductase and none of the derivatives showed any signs of cytotoxicity (Tao et al., 2016a). A recent investigation of solid cultures of the edible abalone mushroom, *Pleurotus cystidiosus*, has found nine novel clitocybulol derivatives (Fig. 10 clitocybulols G (177) and L (178) depicted) with moderate inhibitory activity against protein tyrosine phosphatase-1B (PTP1B), an important regulator related to obesity (Tao et al., 2016b). Yet another edible mushroom, the gray shag, *Coprinopsis cinerea*, has been studied for its secondary metabolite profile (Otaka et al., 2017), due to its role as a model basidiomycete for the study of fruiting body development and mating types (Muraguchi et al., 2015). The study found two novel norsesquiterpenoids, Hitoyol A (179), with a unique exo-tricyclo[5.2.1.0^{2,6}]decane skeleton, and B (180), with a novel 4-cyclopentene-1,3-dione skeleton. Hitoyol B (180) displayed weak anti-malarial activity against *Plasmodium falciparum* with an IC_{50} value of 59 μM (Otaka et al., 2017). On a more recent occasion, *C. cinerea* was found to produce three further cuparene-like sesquiterpenoids, hitoyopodin A (181), featuring a benzoxabicyclo[3.2.1]octane core, and its unnamed hydroxy derivatives (182–183). The metabolites showed moderate cytotoxic activity against HL-60 cells with IC_{50} values in the 3 to 16 μM range and 181 exhibited antiplasmodial activity against *P. falciparum*, IC_{50} of 6.7 μM (Otaka et al., 2018). A chemical investigation of a *Deconica* species from Thailand led to the discovery of five cuparene-type sesquiterpenoids, deconins A–E (184–188; Fig. 11), of which four show a the common scaffold to be extended by mevalonic acid. Mevalonic acid is known to be the precursor of all terpenes synthesized in the HMG-CoA reductase pathway. It has, however, never been observed as a substituent of another terpene skeleton (Surup et al., 2015). The crust-like polypore *Perenniporia maackiae* is one of the causes of white-rot in deciduous trees (Jang et al., 2014) and was therefore extensively studied for its production of secondary metabolites. In a 2018 study, seven novel drimane sesquiterpenoids (189–195) were isolated from solid-state cultures of the same species. Compounds 189, 190, and 194 displayed cytotoxic activities against six carcinoma cells (ACHN, HCT-15, MDA-MB-231, NCI-H23, NUGC-3, and PC-3 cells), with IC_{50} values ranging from 1.2 to 6.0 μM (Kwon et al., 2018). The genus *Stereum*, which is fairly widespread among the lignicolous mushrooms has been the origin of many bioactive sesquiterpenoids, such as the sterostreins, known for their antimalarial activity (Isaka et al., 2011). Recently, three novel sterostreins, sterostrein R (196), S (197), and sterostrein T (198) have been extracted from submerged cultures of *Stereum* sp. YMF1.1686 isolated in China, Yunnan Province (Tian et al., 2016).

3.3.3. Mixed terpenoids

The same research group also studied another *Stereum* species, *Stereum insigne* CGMCC5.57, and isolated a novel dihydrobenzofuran (199; Fig. 12), as well as six known metabolites, which constitute the first secondary metabolites from this species (Tian et al., 2017). The false turkey-tail mushroom, *Stereum ostrea*, previously mentioned for its sterostreins, also produces ostalactones A–C (200–202), novel β - and ϵ -lactones. The scaffold of 200 and 201 is characterized by a β -lactone containing a fused bicyclic core structure, while ostalactone C (202) possesses a 2-oxepinone ring system, making it a potential biosynthetic precursor of 200 and 201. Ostalactones A (200) and B (201) also exhibited moderate activity against human pancreatic lipase with IC_{50} values of 9.0 and 3.2 μM , respectively (Kang and Kim, 2016). This comes as no surprise, as β -lactones have been known to inhibit the human pancreatic lipase by blocking the hydrolysis of triglycerides via

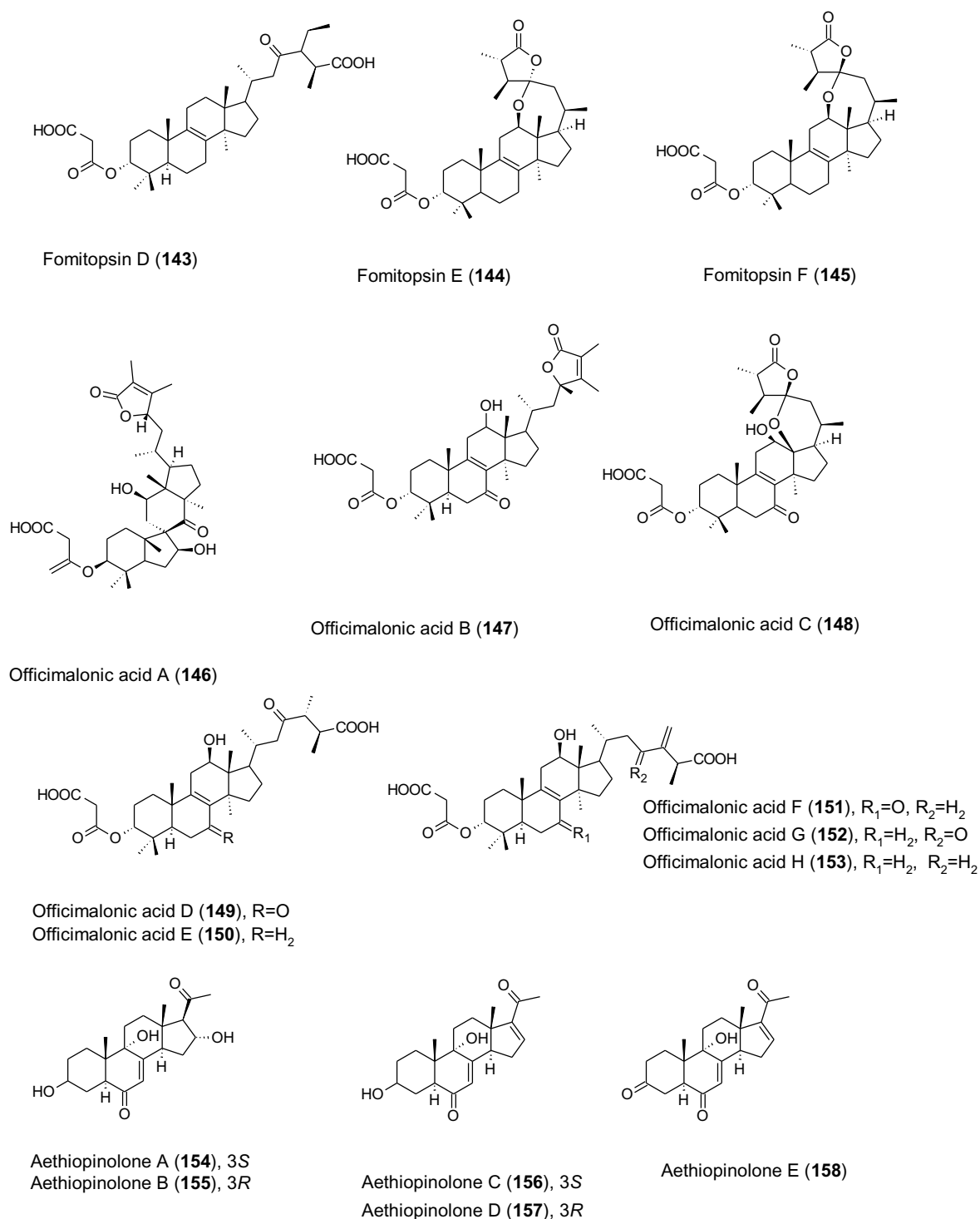


Fig. 9. Chemical structures of compounds isolated from random screening of different Basidiomycota.

covalent modification of the serine residues in the active site (Borgström, 1988; Hadváry et al., 1988; Kang and Kim, 2016). Another known pancreatic lipase inhibitor is the β -lactone, vibrallactone A (203), isolated from *Borostereum vibrans* (Liu et al., 2006). Since then, a number of vibrallactones have been isolated. In the meantime, vibrallactone R (204), which features a γ -lactone, and vibrallactone S (205), with an 2(7H)-oxepinone, which includes an unusual 3,6-substituted oxepin-2(7H)-one ring system, unknown in the vibrallactone/fomannoxin family, have been isolated from a stercaceous mushroom "BY1" together with methyl seco-fomannoxinate (206), which displays

a 2-methylprop-1-enyl ether moiety (Schwenk et al., 2016). Additional vibrallactones U–W (207–209) have been isolated again from *Borostereum vibrans*, but they did, however, not display any cytotoxicity, and their further bioactivities remain to be evaluated (Duan et al., 2018). A different wood degrader is the polypore *Cryptoporus volvatus*, which typically infects rotting conifers after an attack by the pine bark beetle (Davis et al., 2012). Investigating this fungal species for its cytotoxic constituents in the past, the group of Asakawa isolated several cytotoxic cryptoporic acids (Hashimoto and Asakawa, 1998). More recently, Zhou et al. (2016b) isolated four novel isocryptoporic acid (ICA)

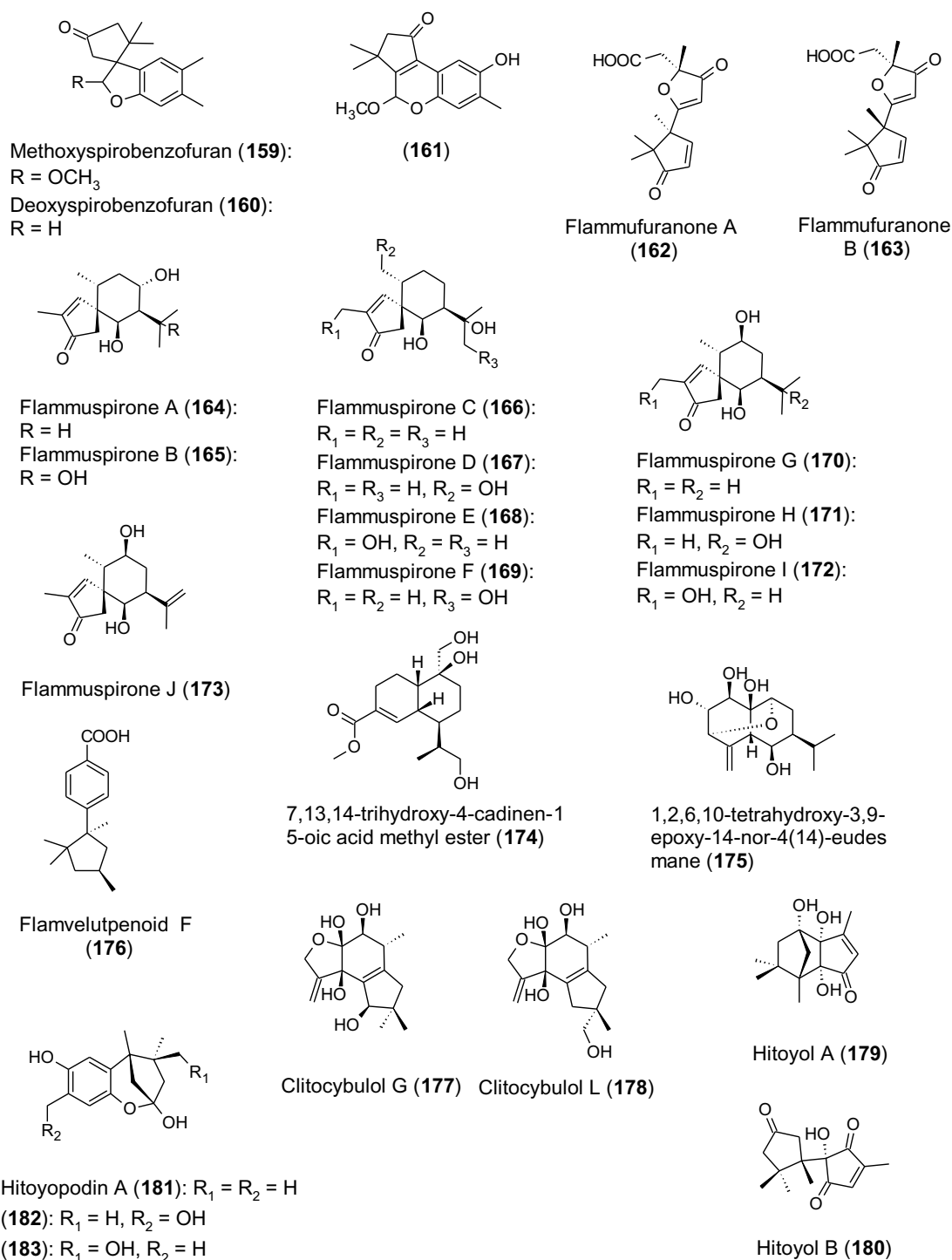


Fig. 10. Chemical structures of sesquiterpenoids isolated from random screening of different Basidiomycota.

derivatives, ICA-B trimethyl ester (**210**), ICA-E (**211**), ICA-E penta-methyl ester (**212**), and ICA-G (**213**). Only **213** exhibited stronger cy-totoxic activities with IC₅₀ values in the range of *cis*-platin (Zhou et al., 2016b). A polypore infecting the mangrove plant *Ceriops tagal* as endo-phyte was isolated and identified as *Corioloopsis* sp. The investigation of its secondary metabolites production on solid rice medium led to the discovery of six novel unnamed furan derivatives (**214-219**); as well as two novel furan-carboxylic acids (**220-221**) (Chen et al., 2017b). *Ho-henbuehelia grisea*, the producing organism of the earlier mentioned antibiotic pleurotin (**222**), was recently found to also produce the anti-viral (HCV) metabolite 4-hydroxypleurogrisein (**223**), as well as nine

other novel pleurotin derivatives (**224-232**). The new heterocycle pleurothiazole (**231**) and most of the other compounds exhibited moderate to weak antimicrobial activity (Sandargo et al., 2018a, b).

3.3.4. Polyketides and other metabolite classes

Polyketides are a fairly diverse group of natural products, their common denominator, however, is their biosynthetic machinery (Cox and Simpson, 2009). In recent years, a number of secondary metabo-lites of (partial) polyketide origin have been isolated from Basidiomy-cota. The exobasidiomycete *Acaromyces ingoldii*, isolated from the Chinese South Sea, was reported to produce two novel secondary

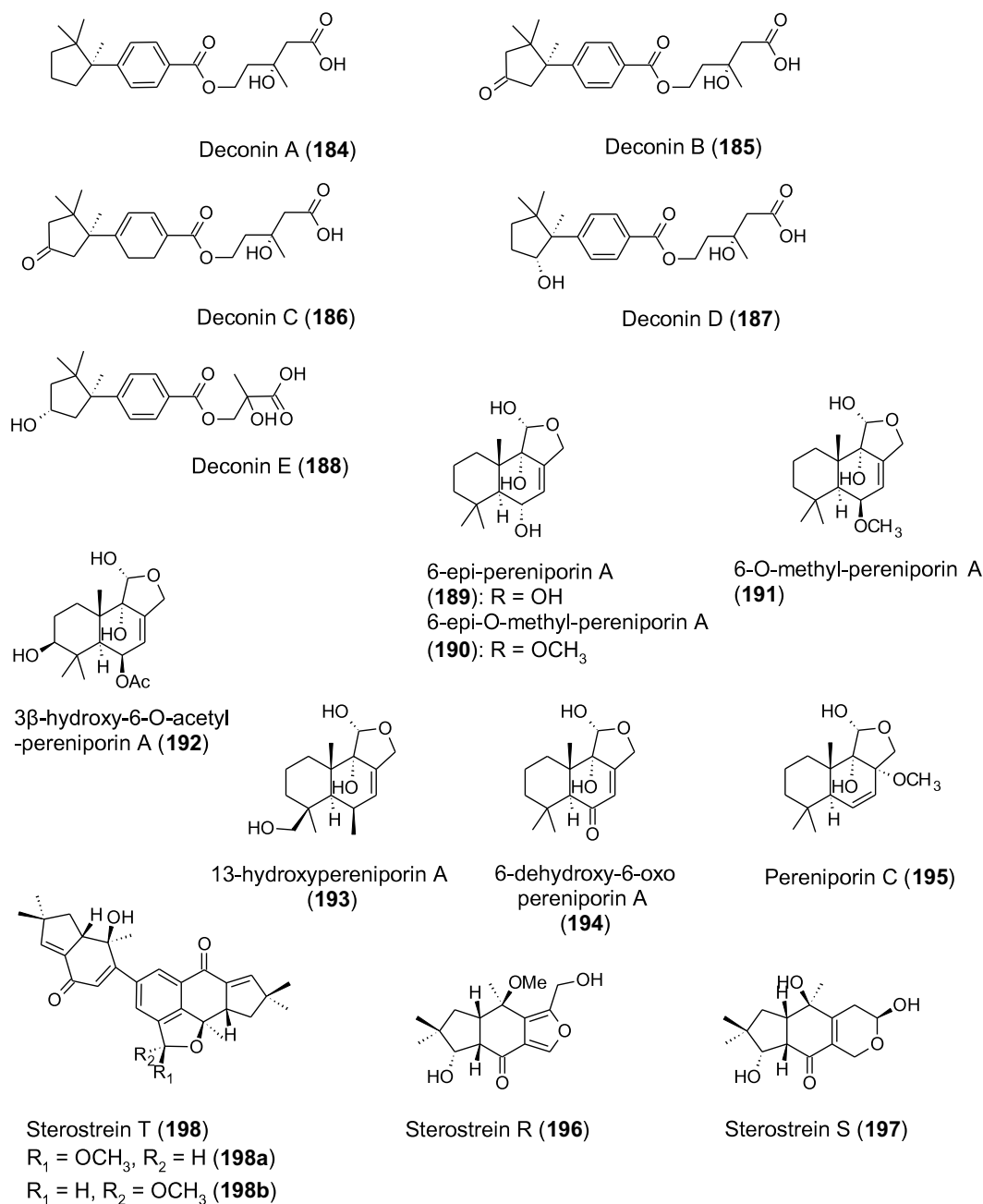


Fig. 11. Chemical structures of sesquiterpenoids isolated from random screening of different Basidiomycota.

metabolites, the naphtha-[2,3-b]pyrandione analogue, acaromycin A (**233**; Fig. 13) and its thiazole analogue, acaromyester A (**234**). Acaromycin A (**233**) showed moderate cytotoxic activities against the breast cancer cell line MCF-7 with an IC₅₀ value of 6.7 μM (Gao et al., 2016). The polyporeaceous mushroom *Lentinus strigellus* was found to produce four novel lentinoids A-D (**235–238**). These lentinoids belong to a group of compounds, which are characterized by an isoprenyl residue attached to an oxygenated cyclohexenyl ring and may be of mixed biosynthetic origin (Vásquez et al., 2018). Earlier the very same fungus was found to produce three novel benzopyran derivatives (**239–241**) as well as an isopanepoxydone derivative (**242**), with anti-parasitic activity (Julca-Canto et al., 2016). The saprotrophic species *Phlebiopsis gigantea* is commonly used as a biocontrol agent to prevent root rot caused by *Heterobasidion*. This has drawn attention to the fungus's secondary metabolome, and a recent study investigated the production

of secondary metabolites by *P. gigantea*. Five cyclopentanoid compounds, of which three were novel diarylcyclopentenones, phlebiopsins A-C (**243–245**), and a new p-terphenyl (**246**), were isolated from cultures of *P. gigantea*. For methyl-terfestatin A (**246**) this was the first report as a naturally occurring compound. The compounds did not show any significant antifungal activities against *Heterobasidion* species, hence their natural function in the biocontrol interactions between *P. gigantea* and *Heterobasidion* species remains obscure (Kälviä et al., 2018).

The ectomycorrhizal mushroom *Hygrophorus abieticola*, associated with *Abies alba*, was found to contain 4-oxo fatty acids named pseudo-hygrophorones A¹² (**247**) and B¹² (**248**) in its fruiting bodies. These are the first naturally occurring alkyl cyclohexenones of a fatty acid-polyketide metabolic origin. (Otto et al., 2016). The fruiting bodies also contained the alkyl cyclopentenone hygrophorone B¹² (**249**), of which the asymmetric total synthesis has been described (Otto et al., 2015).

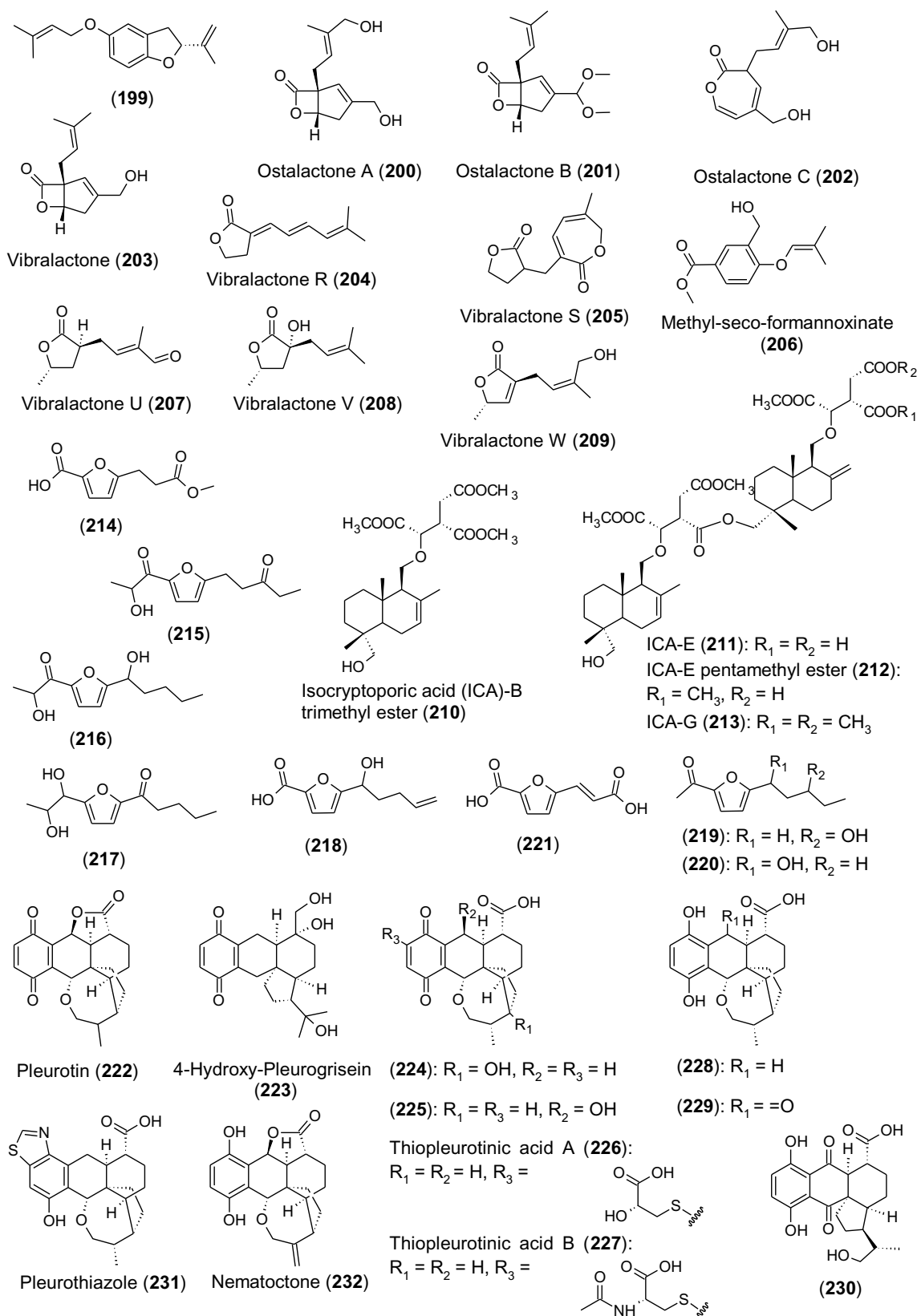


Fig. 12. Chemical structures of mixed terpenoids isolated from random screening of different Basidiomycota.

Both, pseudohyphorones A¹² (247) and B¹² (248), and hyphorone B¹² (249) showed moderate activities against the phytopathogens *Phytophthora infestans*, *Botrytis cinerea*, and *Septoria tritici* (Otto et al., 2016).

3.3.5. Alkaloids

In recent years, a number of alkaloids have been discovered in Basidiomycota. Most recently, Lohmann et al. (2018a) published two unique, red diketopiperazine alkaloids, rosellins A (250) and B (251);

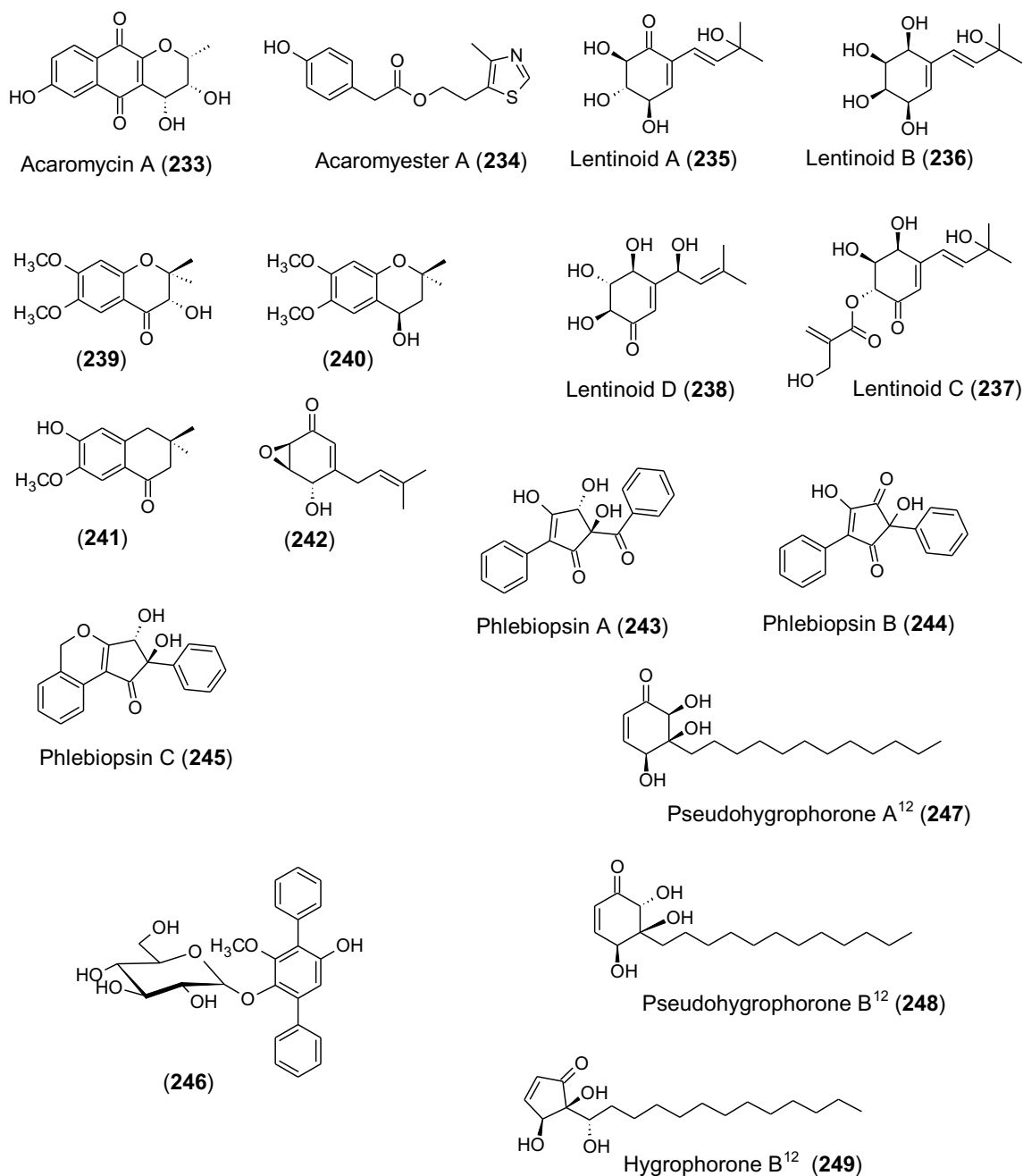


Fig. 13. Chemical structures of various polyketides isolated from random screening of different Basidiomycota.

Fig. 14), isolated from the fruiting bodies of the mushroom *Mycena rosella*. Root exposure of rosellin A (250) to *Lepidium sativum* led to a bleaching of its leaves (Lohmann et al., 2018a). *Mycena* is a genus of small saprotrophic mushrooms and known for a range of toxic species. The fruiting bodies of *Mycena cyanorhiza*, for example, contain the widely known hallucinogen psilocybin (252) and *Mycena pura* the toxic muscarine (253) (Allen et al., 1991). Another unusual *Mycena* species, the bleeding fairy helmet (*M. haematopus*), was reported to produce the pyrroloquinoline alkaloid, haematopodin (254) (Baumann et al., 1993). This compound was later shown to be a direct degradation product of haematopodin B (255) (Peters et al., 2008). The same species was recently found to produce four additional pyrroloquinoline alkaloids, i.e., the yellow mycenaflavins A (256), B (257), and C (258), and the purple mycenaflavin D (259) in its fruiting bodies. Structurally, they are highly related to haematopodin and the mycenaflavins (Peters et al., 2008;

Peters and Spiteller, 2007). Mycenaflavin D (259) is the first known dimeric pyrroloquinoline alkaloid with a C–C bridge between the two pyrroloquinoline units, possibly responsible for its purple color (Lohmann et al., 2018b). Yet another *Mycena* species, the blackedge bonnet (*M. pelianthina*), joins the group of pyrroloquinoline alkaloid producing *Mycena*. Its pelianthinarubins A (260) and B (261) are red pyrroloquinoline alkaloids featuring an S-hercynine moiety, so far unknown to pyrroloquinoline alkaloids, whether from marine organisms or other *Mycena* species (Pulte et al., 2016). *Mycena*, however, is not the only genus within the Basidiomycota producing alkaloids. Recently, three novel pyrrole alkaloids, the phlebopines A–C (262–264), were isolated from the fruiting bodies of *Phlebotus portentosus* (Sun et al., 2018). Two rather unusual alkaloids, schizines A (265) and B (266), are the first naturally occurring iminolactones to be mentioned and have been isolated from fruiting bodies of *Schizophyllum commune*; both

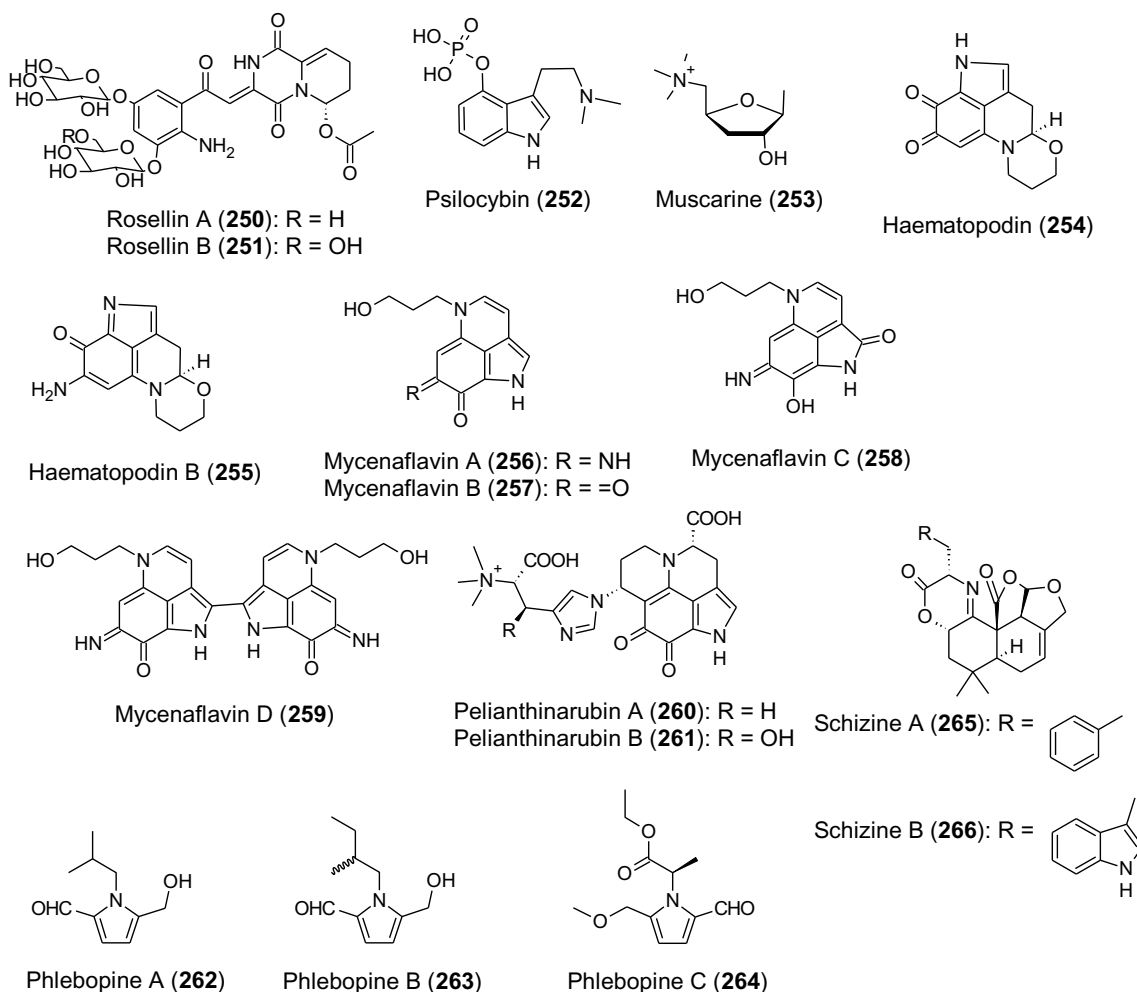


Fig. 14. Chemical structures of various alkaloids isolated from random screening of different Basidiomycota.

showing cytotoxic activity against different cancer cell lines (Liu et al., 2015). While some of the alkaloids showed cytotoxic or antimicrobial activities, for many the bioactivity remains to be revealed. Nevertheless, a role in the fungal defense system cannot be excluded (Spiteller, 2008).

4. Recent discoveries in chemical ecology of Basidiomycota

4.1. Chemical defense

Just as plants, fungi are very creative in their defense against other organisms. (Spiteller, 2015) While for many of the earlier mentioned novel secondary metabolites (chapter 3) the biological role remains unknown, most can also be attributed to one of the three currently known chemical defense strategies, the constitutive chemical defense. A constitutive chemical defense relies on permanently, readily available metabolites, as either toxins, such as the amatoxins (Fig. 15) antimicrobials, like the antifungal strobilurins (chapter 3.1.2) or the recently isolated anti-staphylococcal calopins (267-269) from fruiting bodies of the bitter rooting bolete *Caloboletus radicans* (Tareq et al., 2018), or like nematicides, such as the laccanthrilic acids A-C (270-272) produced by different *Laccaria* spp. (Schrey et al., 2019), or bitter tasting agents, like many alkaloids (chapter 3.3.5; see Spiteller, 2015). The second strategy of chemical defence includes the generation of bioactive compounds from inactive precursors that can be induced, e.g. by injury of the basidiomes. Instead of permanently keeping bioactive metabolites at hand, some Basidiomycota store precursor forms of their

warfare, and within seconds upon being attacked, convert these precursor metabolites into active chemicals (Spiteller, 2008). Only recently Caspar and Spiteller (2015) discovered in fruiting bodies of *Marasmius oreades* that upon injury cyanohydrin (273) decomposes to HCN and glyoxylic acid (274), as means of a wound-activated defense. Through feeding experiments, they established glycine (275) to be the biosynthetic precursor of the cyanohydrin (273) of glyoxylic acid (274) prompting a radically different way of cyanogenesis in fungi, compared to plants. (Caspar and Spiteller, 2015). Unlike constitutive or wound-activated defense, an induced chemical defense (the third strategy of chemical defence employed by fungi) is a slower process, which starts with the expression or upregulation of the biosynthetic genes for defensive secondary metabolites. (Spiteller, 2008) As of yet, this defense strategy is only known in mycelia of Basidiomycota in co-cultivation with other fungi. (Kettering et al., 2004) A recent example for this is the stereous mushroom BY1. Brandt et al. (2017) identified a double-bond shifting polyketide synthase (PPS1) belonging to a previously unknown clade of polyketide synthases, which is upregulated upon mycelial injury and catalyzes the entire *de novo* synthesis of the antilarval polyenes 18-methyl-19-oxoicosaoctanoic acid (276) and 20-methyl-21-oxodocosanoic acid (277). (Brandt et al., 2017)

4.2. Chemical communication in the ectomycorrhiza

Besides warfare, fungi are known to produce secondary metabolites in order to establish symbioses with various organisms. For Basidiomycota in particular, this is a common phenomenon for the

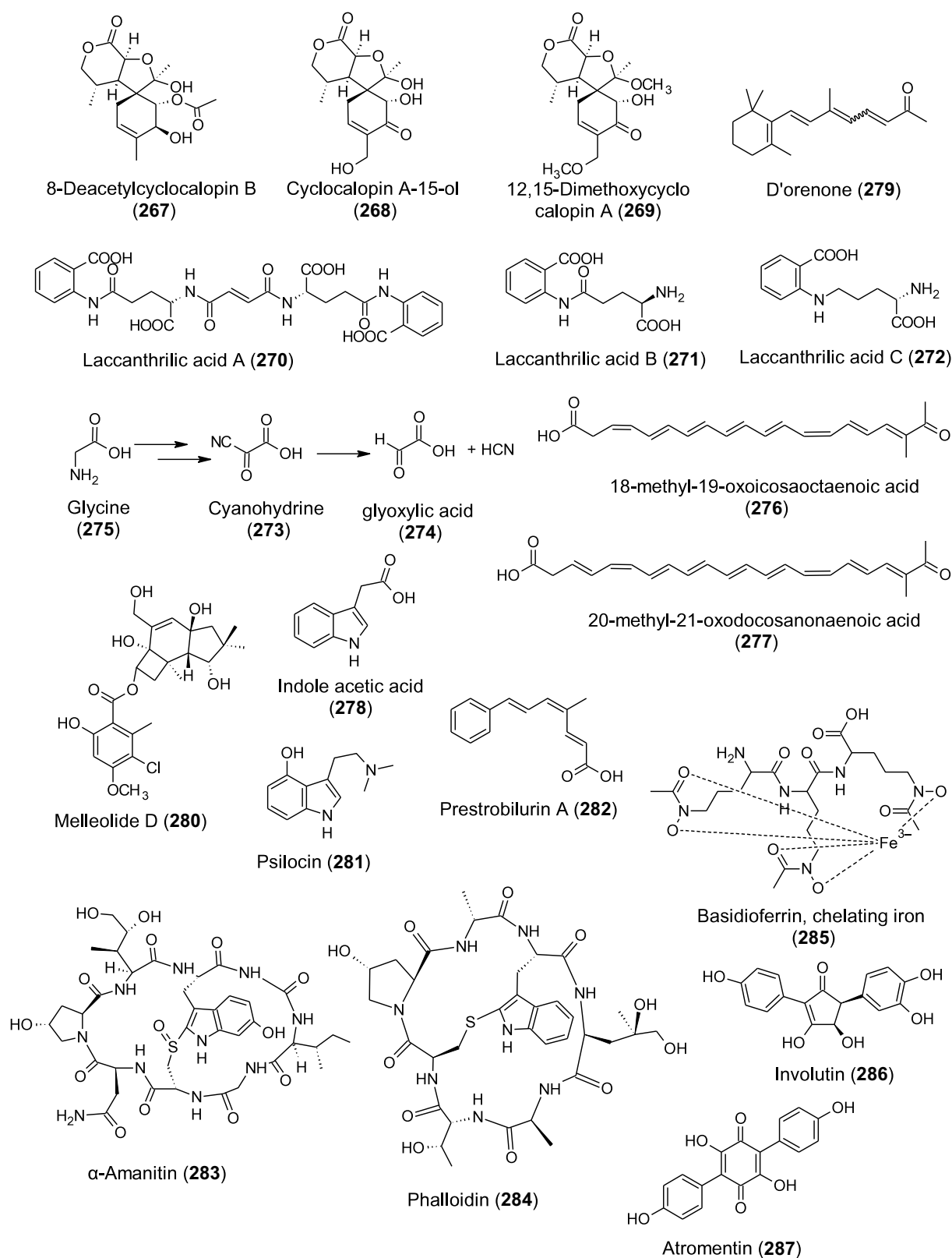


Fig. 15. Chemical structures of various metabolites isolated from different Basidiomycota.

establishment of ectomycorrhiza (Spiteller, 2015). However, only few Basidiomycota, such as *Laccaria bicolor*, were shown to produce phytohormones, like the auxin indole-3-acetic acid (IAA; 278), in order to modify the root morphology of their host plants. (Vayssières et al., 2015) The pine tree associated fungus *Tricholoma vaccinum* has been

assumed to live in a mutual symbiosis with its host tree, *Picea abies*. Wagner et al. (2016) now discovered that the secondary metabolite, D'orenone (279), is produced by a third-party, belonging to the soil-borne Zygomycota. This compound can promote hyphal branching and the production and release of indole acetic acid (IAA, 278), i.e., the

phytohormone responsible for cell differentiation and growth in plants, by *T. vaccinum*. Likewise, D'orenone (279) also had stimulating effects on the lateral root length and hypertrophy of root cortex cells of spruce seedlings of the host tree. (Wagner et al., 2016) These findings only give a glimpse on the complexity of such chemical interactions.

Growth and fruiting body formation of the ectomycorrhizal mushroom also largely depends on the fungi's microbiome, however, little is also known about microbial interactions on its fruiting bodies. It was only recently shown in a study for *Tricholoma matsutake*, how different bacteria can promote or slow down growth of this pine mushroom and its fruiting bodies. In addition, the bacteria also indirectly influenced the fungus by suppressing moulds, which would otherwise have infected the fruiting bodies (Oh et al., 2018). In co-cultivation of associated bacteria with *Tricholoma*, growth promotion could be related to soluble chemicals transmitted via the media. Growth inhibition by other bacteria, was demonstrated not only to be due to soluble chemicals but also volatile metabolites (Oh and Lim, 2018; Oh et al., 2018) Even though individual compounds have not been identified yet, such dual antagonism culture studies, also between two competing fungi, and the analysis of their VOC or DOC profiles are just coming up, and much can be expected in the near future (Hiscox et al., 2018).

5. Genomics and molecular biology of secondary metabolite biosynthesis in Basidiomycota

The first completed whole genome sequence of *Saccharomyces cerevisiae* strain S288C was a milestone in fungal genomics and biology (Goffeau et al., 1996). Thereafter, the genome of the fission yeast *Schizosaccharomyces pombe* (Wood et al., 2002) was sequenced, followed by the pathogen *Cryptococcus neoformans* (Loftus et al., 2005), and the wood-degrading saprotroph, *Phanerochaete chrysosporium* (Martinez et al., 2004), which were the first species of the Basidiomycota of which a genome sequence became available. Concurrently with Ascomycota that have become model organisms in fungal biology like *Magnaporthe grisea* (Dean et al., 2005) and *Aspergillus nidulans* (Galagan et al., 2005), the genome of the plant pathogenic rust fungus, *Ustilago maydis* (Kämper et al., 2006) was also completed early on in the history of fungal genomics. However, in the following years, the Ascomycota were very much favored by the mycological community because they turned out to be easier to handle, owing to their less complicated genetics. For instance, with the purpose of understanding evolutionary history, a comparative genomic and transcriptomic approach has first been used for the fission yeasts of the genus *Schizosaccharomyces* by Rhind et al. (2011).

5.1. Fungal genome databases and identification of secondary metabolites genes

By realizing the importance of fungal genomics, in 2000 the Whitehead Institute/MIT center for genome research—now the Broad Institute, set up the Fungal Genome Initiative (FGI, <https://www.broadinstitute.org/fungal-genome-initiative>) with the purpose to sequence the genomes of fungi throughout the kingdom, ensuing a series of databases which have been launched by mycologists to accelerate the pace of fungal genomics (Table 1); access of these fungal genome data and functions are listed. The selection of organisms followed various criteria, but a major goal was to achieve a broad phylogenetic diversity and to include strains and specimens from various lineages of the fungal kingdom. The increasing availability of genome sequences has recently led to the discovery of various secondary metabolite biosynthetic genes from various fungi by genome mining strategies, using the computational tools listed in Table 2. The presumptive function of genes can be predicted by performing an “hmmsearch” from Hidden Markov Model (HMMER, <http://hmmer.org/>) (Eddy, 1998) of target protein sequences using the Pfam (Finn et al., 2016) database as query sequences. In order to uncover the respective metabolites, the predicted protein sequences

Table 1
List of fungal genome databases.

No.	Database	Website	Function	Reference
1	TIGR	http://www.tigr.org/tbd/fungal	Collection of species-specific databases that use a highly refined protocol to analyze EST sequences	(Galagan et al., 2005)
2	Ensembl Fungi	http://fungi.ensembl.org/index.html	Offering integrated access to genome-scale data from non-vertebrate species of scientific interest developed using the Ensembl genome annotation and visualization platform.	(Kersey et al., 2010)
3	FGI	https://www.broadinstitute.org/fungal-genome-initiative	Fungal Genome Initiative	(Haas et al., 2011)
4	FungiDB	http://FungiDB.org	FungiDB provides a data-mining interface to the comparative and functional genomic data of multiple species of fungi that differs from the species-focused resources of SGD, CGD and AspGD and provides an integrated query system as part of the WDK and GUS database structure.	(Stajich et al., 2012)
5	JGI	https://genome.jgi.doe.gov/programs/fungi/index.jsf	Analysis and dissemination of fungal genome sequences and other 'omics' data by providing interactive web-based tools.	(Grigoriev et al., 2014)
6	MIPS	http://mips.gsf.de	support both national and European sequencing and functional analysis projects, develops and maintains automatically generated and manually annotated genome-specific databases, develops systematic classification schemes for the functional annotation of protein sequences, and provides tools for the comprehensive analysis of protein sequences	(Mewes et al., 2002)
7	Genomes Online database	http://www.genomesonline.org	Provides a seamless interface with the Integrated Microbial Genomes (IMG) system and supports and promotes the Genomic Standards Consortium (GSC) Minimum Information standards	(Mukherjee et al., 2017)
8	FGSC	http://www.fgsc.net	provides access to clones and other experimental resources in conjunction with several fungal genome projects	(Galagan et al., 2005)

Table 2
Computational tools for identification of metabolic genes clusters from fungi. Abbreviations: a: Nonribosomal peptide synthetase; b: Polyketide synthase; c: Prenyltransferase.

No.	Computational tool	Input to software	Cluster core	Reference
1	antiSMASH	DNA sequences or annotated nucleotide file in GenBank or EMBL format	Many signature enzymes	(Blin et al., 2017)
2	SMURF	Protein sequences and chromosomal coordinates of genes	NRPS ^a , PKS ^b , NRPS/PKS, DMATS ^c	(Khalidi et al., 2010)
3	CASSIS/SMIPS	CASSIS: DNA sequences and corresponding annotation with start position, stop position and strand orientation of each gene and list of genes serving as 'anchors' for clusters SMIPS: protein sequences or an InterProScan output file Also required: tools MEME and FIMO for motif prediction in promoter sequences	NRPS, PKS, DMATS	(Wolf et al., 2015)
4	FunGeneClusters	Gene annotation files and transcriptome data	NRPS, PKS, DMATS	(Vesth et al., 2016)
5	MIDDAS-M	DNA and protein sequences and transcriptome data	Unrestricted	(Umemura et al., 2013)
6	C-Hunter	Ordered sequences of genes and GO annotations	Unrestricted	(Xi et al., 2007)
7	NRPS predictor	Protein sequences	NRPS	(Röttig et al., 2011)

could be heterologously expressed in hosts, such as *Aspergillus niger* (Boecker et al., 2018).

5.2. Fungal gene clusters and identification strategies

Fungi tend to cluster genes encoding biosynthetic pathways within their genome, and in particular, terpene synthases are frequently part of biosynthetic clusters that include additional genes such as cytochrome P450 monooxygenases for modification of the terpene backbone. Most of the earlier studies have been conducted with Ascomycota: For instance, the trichothecene biosynthesis cluster has been studied in great detail by engineering *Saccharomyces cerevisiae* for *de novo* production using cDNAs derived from the original producer, *Fusarium graminearum* Tri5 and Tri4 (Tokai et al., 2007). Another well-studied example is the botrydial biosynthesis cluster from *Botrytis cinerea*, which comprises five genes named BcBOT1 - BcBOT5 (Pinedo et al., 2008). For Basidiomycota, Agger et al. (2009) were the first to describe the functional characterization of six sesquiterpene synthases (Cop1 - Cop6) and two terpene oxidizing cytochrome P450 monooxygenases (Cox1 - Cox2) from "*Coprinus cinereus*" (current correct name *Coprinopsis cinerea*). The genes were cloned and, except for Cop5, functionally expressed in *Escherichia coli* and/or *Saccharomyces cerevisiae*.

An exception from this rule was found during studies on the sesquiterpenoids of the melleolide type (see Fig. 15), whose biosynthesis is catalyzed by the protoilludene synthase in the first committed step. This synthase was among the first ones to be identified from Basidiomycota and a sequence comparison of the isolated 6-protoilludene synthase revealed a rather distant relationship to other known fungal terpene synthases (derived from Ascomycota), the protoilludene synthase was partially purified from *Armillaria gallica* and corresponding cDNAs were expressed in *E.coli* (Engels et al., 2011). The characterization of the ArmA adenylation domain, which is also related to melleolide biosynthesis in *Armillaria mellea* implied that the genus *Armillaria* has a highly diverse secondary metabolism (Misiek et al., 2011). Following this, two years later a heterologously produced *Armillaria* polyketide synthase ArmB was found to produce orsellinic acid (OA) in vitro and also performs a cross-coupling activity, which forms OA esters with the various protoilludane sesquiterpenoid alcohols, leading to the different melleolides produced by *Armillaria* spp. (Lackner et al., 2013). A variety of melleolides, such as melleolide D (280), consist of a chlorinated orsellinic acid moiety, which was shown to be synthesized by five parallelized flavin-dependent *A. mellea* halogenases (ArmH1 to ArmH5), which were heterologously produced in *Escherichia coli*. All five enzymes are responsible for the transfer of a single chlorine atom onto the melleolide backbone (Wick et al., 2016).

The seven-gene diterpene pleuromutilin biosynthesis cluster from *Clitopilus pseudopinsitus* and *C. passeckerianus* was identified and later on reconstructed in *Aspergillus oryzae*, giving a significant increase (over 2000%) in production of pleuromutilin (1) (Alberti et al., 2017; Bailey et al., 2016; Yamane et al., 2017). This great technology may in the future significantly facilitate the production of this highly important precursor of marketed antibiotics. The biosynthesis cluster of erinacines has been characterized containing three cytochrome P450s (*EriA*, *EriC* and *EriI*), one GGPPS (*EriE*), two prenyltransferases (*EriF* and *EriG*) and a UDP-glycosyltransferase (*EriJ*) (Yang et al., 2017).

Genomic and transcriptomic data implied that the triterpene cyclases of Basidiomycota is being coregulated during tissue-developing stages, rather than to cluster with genes encoding downstream tailoring enzymes. For instance, cytochrome P450 genes in the medicinal mushroom "*Ganoderma lucidum*" (taxonomy probably not correct as the study was carried out in China where this European species was never cultured) shown to be co-expressed with the lanosterol synthase gene and upregulated in the transition from mycelia to primordia (Chen et al., 2012). CYP5150L8 has been characterized as the first cytochrome P450 monooxygenases from *Ganoderma*, which is responsible for the biosynthesis of ganoderic acids. Its function was reconstituted both in

vivo and *in vitro* assay in *Saccharomyces cerevisiae* (Wang et al., 2018b).

Aside from terpenoids, other classes of metabolites have also been targeted and the biosynthesis was elucidated. One such example is the recent discovery of psilocybin biosynthesis. The alkaloid psilocybin (252) serves as a prodrug of its dephosphorylated psychotropic analog, psilocin (281, Fig. 15). Decarboxylation of tryptophan is performed by the enzyme PsiD which represents a new class of fungal l-tryptophan decarboxylases. A P450 monooxygenase, PsiH, introduces the hydroxy function, followed by a phosphotransferase (PsiK), and a SAM-dependant methyltransferase (PsiM), which catalyzes the N-methyl transfer in a final biosynthetic step (Fricke et al., 2017).

Strobilurins and the related oudemansins are produced by a number of different species of Basidiomycota and have long served as lead compounds for the development of the agricultural β -methoxyacrylate fungicides (see chapter 3.1.2), however until recently, the biosynthesis remained obscure. In a 2018 study, the strobilurin biosynthetic gene cluster (BGC) was identified in *Strobilurus tenacellus* and *S. lutea* (formerly known as *Bolinea lutea*, Ascomycota). The BGC was shown to encode for a highly reducing polyketide synthase with very unusual C-terminal hydrolase and methyltransferase domains. The expression in *Aspergillus oryzae* lead to the isolation of prestrobilurin A (282). The oxidative rearrangement, which leads to the β -methoxyacrylate toxophore, is achieved either by a flavin-dependent oxidase, encoded by the gene *str9*. In the last steps, two SAM-dependent methyltransferases, encoded by *str2* and *str3*, complete the synthesis (Nofiani et al., 2018).

For the cyclopeptide omphalotin A (20), which displays strong and selective activity against plant-pathogenic nematodes (see above 3.1.3), two biosynthesis genes OphMA and OphP were identified by mining the genome of *Omphalotus olearius* in two independent studies by Ramm et al. (2017) and Van der Velden et al. (2017). The authors postulated a hitherto unprecedented biosynthesis mechanism for a ribosomally synthesized and posttranslationally modified peptide (RiPP) in which the modifying enzyme delivers its own precursor peptide. This mechanism is much different from NRPS biosynthesis of other fungal cyclopeptides and is so far unparalleled in fungi.

The highly toxic amatoxins, produced by different *Amanita* and *Galerina* species, have been shown in the past to be ribosomally synthesized as proproteins and not by NRPS (Walton et al., 2012). The genes for α -amanitin (Ama1) and phalloidin (Pha1) belong to a large family of related genes, consisting of highly conserved nucleotide sequences flanked by a hypervariable “toxin” region, which is again flanked by invariant proline residues. In the case of phalloidin (284), the cleavage of the proprotein was conducted by a serine protease in the prolyl oligopeptidase (POP) subfamily, discharging the linear hepta-/octapeptide (Walton et al., 2012) For α -amanitin (Fig. 15) post-translational processing, it was shown that a specific POP, *Gmpop5*, was responsible for catalyzing the hydrolysis at an internal Pro to deliver the C-terminal 25-mer from the 35-mer propeptide and transpeptidation at the second Pro to generate the cyclic octamer (Luo et al., 2014).

An example of an unprecedented class (type VI) of fungal siderophore synthetases, is the nonribosomal peptide synthetase CsNPS2. Identified in *Ceriporiopsis subvermispota*, and expressed in *A. nidulans*, this seven-domain NRPS catalyzes *in vitro* the formation of the first trimeric hydroxamate siderophore basidioferrin (285) Orthologous genes can be found across various Basidiomycota and appear to be widespread (Brandenburger et al., 2017). Other siderophore biosynthetic genes were characterised from, e.g., *Ustilago* (Yuan et al., 2001; Winterberg et al., 2010) and *Omphalotus* (Welzel et al., 2005).

The ectomycorrhizal fungus *Paxillus involutus* was found to secrete an Fe³⁺ reducing pigment, named involutin (286), in order to facilitate the oxidative decomposition of lignocellulose, assisting its host plant in nutrient acquisition (Shah et al., 2015). Through early feeding experiments, it was known for involutin to be tyrosine-derived (Gill and Steglich, 1987). In a recent study, Braesel et al. (2015) could constitute a biosynthesis scheme, identifying atromentin (287) as a precursor, synthesized by highly similar tridomain synthetases: InvA1, InvA2, and

InvA5. Also, an additional atromentin synthetase, InvA3, was found to gain activity after a domain swap replacing its native thioesterase domain with that of InvA5. (Braesel et al., 2015). The atromentin synthetase and the corresponding gene cluster had actually already been characterized in a previous study by Schneider et al. (2008) on the related species, *Tapinella panuoides*. These pulvinic acids have recently been proven by Tauber et al. (2016, 2017) to be directly involved in chemical defence reactions during the course of dual culturing studies involving *Paxillus involutus*, *Serpula lacrymans* and bacteria. They are being elicited in response to the presence of bacteria and inhibit bacterial motility.

Taking advantages of gene clustering in fungi, several computational modes have been developed to identify metabolic gene clusters (Table 2). However, it is not clear whether they work well in all Basidiomycota because there are still too few examples of elucidated pathways for known products. Gene clusters can also be identified by manually walking genome sequence \pm 20 kb of predicted secondary metabolites genes with expected borders that clusters are predicted by existence of big gaps between genes or existence of several successive genes that are not related to natural product biosynthesis (Wawrzyn et al., 2012a). The study of Quin et al. (2014) revealed that antiSMASH 2.0 identified four of the eleven manually identified putative terpene synthases in the genome of *Omphalotus olearius* (Wawrzyn et al., 2012b). Similarly, five out of eighteen manually predicted terpene synthase sequences were identified in *Stereum hirsutum* (Quin et al., 2013). By comparing the results from algorithms platform and manually screening, we conclude that maybe because of the intricacy and variability of fungal gene clusters, these tools undervalued size of gene clusters. However, numerous secondary metabolites biosynthesis pathways have been characterized from Basidiomycota, which calls for algorithms to be trained more accurately. Currently, when considering to study secondary metabolite gene clusters in Basidiomycota, using a combination of algorithms platform and manual annotation is recommended.

In summary, the tools for exploitation of the secondary metabolite biosynthesis are readily available, and it is even possible to produce some of the metabolites using heterologous hosts, but the vast majority of the unique compounds treated in this review still remain to be targeted. An interesting strategy that could arise from these prerequisites in the future could be to express the numerous genes and gene clusters that are steadily being detected in the genomes of slow-growing species or even mycorrhizal fungi, for which no means of cultivation has so far been established, using heterologous expression. Almost concurrently with the present paper, a review by Lin et al. (2019) has been published, which gives further details on the state of the art and includes additional examples. We highly recommend this paper for further reading.

6. Biotechnology of products from Basidiomycota

6.1. Current products of industrial importance from Basidiomycota

6.1.1. Products for pharmaceutical applications

As was mentioned in previous sections, the strobilurins inspired synthetic agrochemical fungicides and the illudins led to the prodrug irofulven currently under phase II clinical trials by Oncology Venture but the only example of a currently marketed product of pharmaceutical importance derived from a basidiomycete (*Pleurotus passepck-erianus*) is pleuromutilin (see chapter 1 and Kavanagh et al., 1951). The first semisynthetic pleuromutilin analog retapamulin, was developed by GSK under the tradename Altargo. More recently, potent RNA polymerase II inhibitors produced by several *Amanita* species have been investigated as anti-body drug conjugates, like the amanitins with very promising results in pre-clinical studies (Flygare et al., 2013; Pahl et al., 2018). The material for such studies is either isolated from collected fruiting bodies of the mycorrhizal species, *Amanita phalloides*, which is

to our knowledge not cultivable, or from cultures of *Galerina* species (Muraoka et al., 1999). Curiously, there is one single paper on a species named *Amanita exitialis* (Zhang et al., 2005) which has been reported to grow in axenic culture on agar and used to produce amatoxins. The authors reported $728.3 \pm 43.8 \mu\text{g/g}$ (dry matter) of α -amanitin and $60.0 \pm 20.7 \mu\text{g/g}$ (dry matter) of β -amanitin, which represents about 10% of the total dry weight in the fruiting bodies. Unfortunately, this report has so far apparently not resulted in any follow-up studies, and the results presented also appear quite questionable because no other species in the sect. Phalloideae of *Amanita* that is known to contain amanitins has ever been established in axenic culture. On the other hand, species of the saprotrophic genus *Galerina* are often readily able to grow in culture and should be regarded as the better option to obtain amanitins in sufficient amounts to support a sustainable biotechnological production process.

6.1.2. Complex products from mycelia and fruiting bodies

Currently the bulk of commercial products derived from Basidiomycota are complex preparations from fruiting bodies or the fruiting bodies itself and or mycelia as well as fractions and preparations of submerged or solid state fermentations. Beside their use as edible mushrooms, different preparations from medicinal mushrooms are used due to the beneficial effects attributed to them. Due to the growing demand, the industrial production of different mushrooms gets more and more important. Fig. 16 shows the production increase from 1960 to 2002 (Cheung, 2008) with a market value of over U.S.\$40 billion in 2001 and a reported market value of U.S.\$45 billion (Chang, 2006a) for mushroom products overall and U.S.\$18 billion for dietary supplements derived from medicinal mushrooms in 2012 (Chang, 2006a; Cheung, 2008; Wasser, 2014). For some of these numbers the original source is not stated (Wasser, 2014). The paper by Chang (2006b) seems to be the most reliable and most cited source for such numbers. In 1997 Asia contributed 74.4% to the total production, Europe 16.3%, North America 7% and Africa and Latin America together less than 1% but numbers from non-Asian countries are increasing (Cheung, 2008). Beside the usage as nutrient and valuable protein and vitamin source, a large portion is used for the production of medicinal mushroom products, which are to 80-85% derived from either, cultivated or wild grown and collected fruiting bodies. Only around 15% of these medicinal products are derived from mycelia and the smallest portion of these products stems from culture filtrates (Cheung, 2008).

Medicinal mushrooms are thought to have beneficial effects in

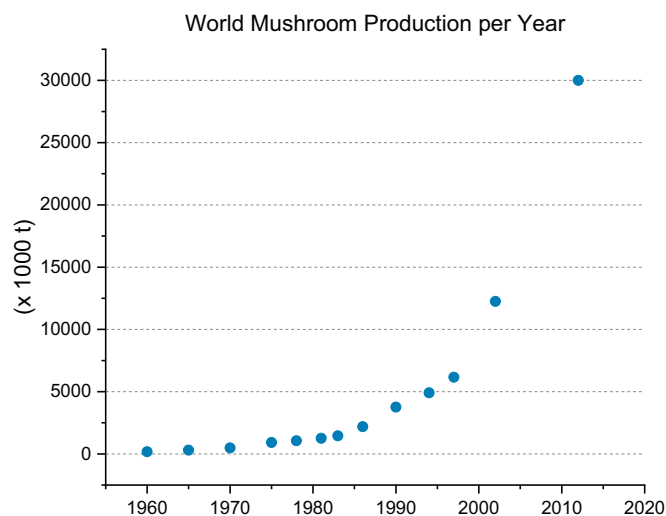


Fig. 16. Illustration of increase in mushroom production from 1960 to 2012. The numbers are adapted from Chang, 2006a, Cheung, 2008 and Wasser, 2014.

Table 3 List of some important medicinal mushroom species used in Traditional Asian Medicine and biological activities or health claims related to them. The most important activity is stated in bold.

Species	Pharmacological activity															
	Antifungal	Antiinflammatory	Anticancer	Antiviral	Antibacterial	Blood pressure regulation	Cardiotonic	Cholesterol lowering	Antidiabetic	Immunomodulatory	Kidney tonic	Hepatoprotective	Nerve tonic	Sexual potentiating	Antiasthmatic	
<i>Agaricus bisporus</i>			X							X	X					
<i>Agaricus subrufescens</i>			X								X					
<i>Schizophyllum commune</i>		X								X						
<i>Grifola frondosa</i>			X	X	X	X			X		X					O
<i>Trametes versicolor</i>			X	X	X											
<i>Hericium erinaceus</i>			X							X			X			X
<i>Ganoderma spp.</i>		X	X	X	X	X	X			X	X	X	X	X	X	X
<i>Lentinula edodes</i>		X	X	X	X	X		X	X	X	X	X	X	X	X	X
<i>Pleurotus ostreatus</i>			X	O	O			X		X						O
<i>Vohwariella yobvacea</i>			O	O	O											O

about 130 medicinal indications (Wasser, 2014), but notably, most of them have not been standardised and proven for efficacy following the rules of the Federal Drug Administration (FDA) or other agencies that are responsible for registration of classical, “ethical” prescription drugs. Many of them are sold over the counter, e.g. as nutraceuticals or “herbal” medicines. Table 3 is a list of the most important indications in combination with a list of the most important medicinal mushrooms and their products derived from them (Cheung, 2008; Lindequist et al., 2005; Turlo, 2014; Wasser, 2014). The majority of these mushroom-derived products are extracts containing complex polysaccharide fractions of different composition. Trade names of these products are Lentinan, a polysaccharide fraction isolated from *Lentinula edodes*, Schizophyllan (SPG, Sonfilan or Sizofilan), a polysaccharide fraction isolated from *Schizophyllum commune*, Grifolan, a polysaccharide fraction isolated from *Grifola frondosa*, Krestin, a protein-polysaccharide complex isolated from *Trametes versicolor*, and Ganopoly, a polysaccharide extract from *Ganoderma lucidum* (Lindequist et al., 2005; Turlo, 2014; Wasser, 2014). The activity of these and other fungal extracts seems to be mostly related to the immunomodulatory activities of the glucans and glycans derived from these, clinical trials and animal studies have been undertaken. For example, Krestin is a prescription drug in Japan for the treatment of cancer. Research on the mode of action of these partially complex mixtures is ongoing, a complete evaluation of available literature regarding Krestin (*Trametes versicolor*) concluded that the product may have positive effects upon disease and survival outcomes based on clinical trials with non-small cell lung cancer (Lindequist et al., 2005; Turlo, 2014; Wasser, 2014). These products are being sold all over Asia as “mycopharmaceuticals” and can meanwhile even be obtained via the Internet as nutraceuticals in the Western World. However, despite the fact that some products even showed efficacy in clinical trials, most of them will hardly be approved by the European and American agencies as ethical drugs because they fail to meet the criteria, in particular with respect to standardisation.

Notably, there are also some glycolipids that are being used in areas other than pharmaceuticals, such as the glycolipids from *Ustilago maydis* that are being under investigation as biosurfactants (Spoeckner et al., 1999). Their biosynthesis has recently been elucidated (Hewald et al., 2006), and they are now being produced by submerged fermentation in kg scale (Günther et al., 2017). A new class of glycolipids has also been obtained from cultures of the tropical species *Dacryopinax spathularia* (Dacrymycetales) and can be produced in gram per liter scale in bioreactors (Stadler et al., 2014). These compounds are highly effective natural preservatives and have recently been licensed by the German company Lanxess, who started their production at industrial scale.

6.2. Methods used for production of biologically active metabolites from Basidiomycota

6.2.1. Traditional mushroom cultivation

Traditionally, fungi have been cultured on solid substrates suitable for farming without sophisticated equipment according to their biological and nutritional requirements for fruiting body formation. These procedures have been improved and intensified due to the rising demands for nutritional and pharmaceutical purposes. A good overview on common cultivation techniques and further reading can be found in the book by Cheung (2008). For example, *Agaricus bitorquis* and *A. bisporus* are cultivated using composted material available locally. This material is then pasteurized to remove unwanted bacteria and treated in a special manner to be used further on in indoor cultivations. The quality of this compost enhances the number of harvests possible. Cultivation of *Lentinula edodes* in commercial scale is usually done in sterilized plastic bags filled with hardwood sawdust and other supplements, which are inoculated with the mycelium and put for fruiting body formation after colonization of the sawdust mixture at 16–18°C. The cultivation of *Pleurotus sajor-caju* can be done on solid substrate consisting mainly of cotton seed hull, water hyacinth and/or rice or

cereal straw. The fruiting body formation is triggered by white light. *Volvariella* is cultured indoor for industrial purposes on cotton wastes. *Agaricus subrufescens* is cultured on rice straw or bagasse enriched with air-dried cattle dung and poultry manure and some fertilizers to enhance growth. The exact composition varies depending on the local availability of raw material. Methods for the cultivation of “*Ganoderma lucidum*” and other species of *Ganoderma* have been developed in China. The fungus is grown on saw-dust bags or wood logs. Sterilized wood logs deliver the best quality of fruiting bodies. More detailed explanations are provided by Cheung (2008), Savoie and Mata (2016) and Smith et al. (2002). The products achieved with this method are the fruiting bodies of the respective fungus, the quality and composition of these varies depending on the source of substrate, the number of harvests the way the mushrooms are cultivated and many other factors. The same is true for the mushrooms collected in the nature. Therefore, more reproducible and controllable production processes, especially for pharmaceutical purposes are required (Lindequist et al., 2005; Smith et al., 2002; Turlo, 2014; Wasser, 2002).

6.2.2. Solid phase cultivation in bioreactors

The traditional production of mushrooms described above usually takes several months and the quality of the material obtained is prone to variations. To reduce the required time for biomass production two different technologies have been developed which allow, aside from media composition, the control of several physical process parameters like temperature, aeration and pH for optimized growth of the organism of choice. One possibility is the growth of the organism in a submerged liquid culture, which does not resemble the environment of the fungus in nature at all. Another possibility is the cultivation on sterilized solid substrates inside of static or mixed chambers with reduced amount of water, compared to submerged liquid cultivations, which allows for a nature like growth of the mycelium on the substrate (Berovic and Podgornik, 2016). The advantage using a solid substrate fermentation is the absence of free water in the cultivation chamber, which reduces the required volume for the distribution of nutrients. The control of parameters like aeration, CO₂ stripping, pH and temperature in certain ranges enhances and promotes the fast growth of the mycelium. Traditionally complex substrates have been used for fungal cultivations in solid substrate fermentations, which resemble those from chapter 6.1. The advantage of these systems is the fast growth of the fungal mycelia due to ideal biochemical conditions that can be achieved using ground and more or less homogeneous substrates according to the requirements of the fungus. Additionally, mixing of the substrate is possible in certain reactor types, which leads to new germination points inside the substrate bed and thereby increases colonization speed of the solid substrate. To optimize these processes and to address issues with upscaling, heat removal, mixing etc. several different types of reactors have been constructed, a good overview is given in Arora et al. (2018), Durand (2003) and Musoni et al. (2015). Tray reactors contain for example shelf like installations, which contain the substrate and are inoculated with the organism. These shelves inside the reactor are in some cases perforated and a nutrient containing liquid is dropping from top to the bottom. Other reactor types contain a packed static bed, which is forcefully aerated. The disadvantage of these reactors is the inhomogeneous growth of the organism (Musoni et al., 2015) and the resulting problems in aeration, pH and nutrient gradients and removal of heat. Rotating drum reactors of various types mix the substrate during the course of the cultivation and create thereby a more homogeneous environment. Problems arising with this design can be the constant mechanical disruption of the mycelium and upscaling issues when removing heat and supplying sufficient oxygen (Arora et al., 2018; Durand, 2003). There have been special developments for organism specific purposes in each of the above-mentioned reactor types but only tray reactors seem to be further developed for industrial production for pharmaceuticals. One example is the “PlaFractor™” a patented technology based on equipment which has originally been used

for soy sauce fermentation (“koji” fermentation), (Suryanarayan, 2003). This is, to best of our knowledge, the only example of a solid-phase cultivation process, which has been cited as source of a FDA approved natural product: lovastatin (Barrios-González and Miranda, 2010) but this approval could not be confirmed by investigating the original publication by Suryanarayan (2003) or the company homepage of Biocon India (<https://www.biocon.com/>). There are several reports where solid-substrate fermentation is used for the production of small molecules like antibiotics, alkaloids and toxins with promising outcomes regarding product titers (Robinson et al., 2001; Subramaniyam & Vimala, 2012). The general conclusion nevertheless is that the derived products, due to problems associated with reproducibility of in-homogeneous cultivations and complicated downstream processing of the solids, are not fulfilling the high standards required for pharmaceutical use of the derived products in humans and further development for process standardization and understanding is necessary (Arora et al., 2018; Durand, 2003; Musoni et al., 2015; Robinson et al., 2001). For the majority of the organisms listed in Table 3 methods for mycelia generation in solid-substrate fermenters have been developed. For an overview about processes and literature we recommend Berovic & Podgornik (2016).

6.2.3. Submerged liquid cultivation in bioreactors

Submerged liquid cultivation of Basidiomycota for pharmaceutical purposes will be the method of choice when dealing with medicinal mushrooms since the necessary process reproducibility and the therefore required process monitoring and control is only achievable with this reactor type. There is consent in literature that the necessary product quality and reproducibility of different charges of the same product can be only achieved with bioreactors suitable for this cultivation method (Cheung, 2008; Lindequist et al., 2005; Turło, 2014; Wasser, 2014). The task of the bioreactor is the measurement, control and maintenance of all important physical parameters, which have been identified and optimized experimentally. The base of the experiment is the culture media, which delivers nutrients and oxygen to the fungus according to its requirements. Due to the tight control, reproducible cultivations can be achieved which allows for a high batch to batch comparability even over years. Material obtained from such cultivations is suitable for the investigation of beneficial effects from medicinal mushroom products in clinical studies.

The reason for the preferred use of submerged liquid cultivation over solid substrate fermentations is that despite promising results regarding product yields, which can be achieved with solid substrate fermentations in bioreactors, the use of submerged liquid cultivations allows a much higher level of implementation of process analytical tools as well as process control strategies resulting from on-line data acquisition, which cannot be achieved with solid-state fermenters due to lacking online analytics. This high standard of control and process understanding is due to the decades of studies and developments, which have been undertaken to characterize and model bioprocesses in submerged liquid bioreactors. An overview about available online and at-line analytical technology as well as critical parameters and future directions in process modelling and knowledge based control is found (Formenti et al., 2014; Rodríguez-Duran et al., 2016; Schügerl, 2001). This enhanced process understanding is important due to the in 2004 released PAT-Guidance³, which is the collaborative work of several FDA departments (CDER = Center for Drug Evaluation and Research, CVM = Center for Veterinary Medicine, ORA = Office of Regulatory Affairs) with the purpose to continuously improve the patient safety when using pharmaceutical products derived from complex and difficult to understand bioprocesses using complex substrates and whole cell catalysts. The PAT-initiative is supported by the European Medicines Agency

(EMA), the Japanese Ministry for Health, Labor and Welfare (MHLW) and by the guidelines of the International Conference on Harmonization (ICH). For further reading we recommend Food and Drug Administration-FDA (2004) and Rathore et al. (2010).

The first reports known to us of submerged cultivations of Basidiomycota date to 1966 (Gregory et al., 1966) where several hundred species of Basidiomycota have been cultured in shake flask to evaluate their biological activity. The majority of the reports dealing with novel secondary metabolites from Basidiomycota state submerged liquid cultivation as method for production of these compounds as well as media for cultivation of all major medicinal mushrooms have been developed (Cheung, 2008; Elisashvili, 2012; Turło, 2014) which will facilitate and ease future work and further investigations of these interesting organisms. One thing which has to be kept in mind and which adds additional complexity to these fungal cultivations is the fact that under most circumstances the Basidiomycota grow as mycelium clumps in the liquid phase and secrete polysaccharides into the surrounding media. This growth pattern is leading to nutrient gradients from the surface of these pellets to the core, which can strongly influence the regulation and the productivity of the respective organism. Additionally the secretion of polysaccharides, which is regularly observed in submerged liquid cultivations, can change the rheology of the culture liquid completely and reduces thereby the mixing efficiency and the oxygen and nutrient supply to the core-cells. There have been intense investigations with Ascomycota to understand and address these issues and to model the underlying principles (Anteck et al., 2016; Hille et al., 2009; Krull et al., 2013) but the general outcome is that these effects rely totally on the organism and the applied physical and biochemical culture conditions and a general strategy to predict possible outcomes regarding productivity and culture rheology is currently not available. Promising onsets with ascomycete cultures, which are probably transferable to Basidiomycota, are the addition of particles into the liquid phase which enhance desired growth-patterns of the organism on those. In addition, variations in the osmolality seem to influence such cultivations beneficially and are transferable into bioreactor scale. Nevertheless the common consensus is, that more work has to be done and especially methodologies for faster possibly automated measurement and analysis of such effects on the morphology of the investigated organism has to be developed in order to speed up understanding of these phenomena (Anteck et al., 2016; Krull et al., 2013; Wucherpfennig et al., 2010; Wucherpfennig et al., 2013; Žnidaršič and Pavko, 2001).

6.3. Biotechnological processes to produce pharmaceutically relevant compounds

6.3.1. Overview about statistical methods to improve productivity of fungal cultivations

Once a biologically active product is promising enough for further development usually, the production from natural sources is hampered by low titers. To increase the produced amounts of compound one can optimize either the producer itself or the physical and biochemical conditions. Reports on genetic work with Basidiomycota are rather limited although a few examples exist (Xiao and Zhong, 2016). Due to the fact that strain optimization will mostly rely on random mutagenesis therefore we will focus here only on a short general overview about process- rather than strain optimization since the applied methodology does not differ from development of processes involving bacteria or Ascomycota. Application of such methodologies is also in accordance with the PAT-initiative since it increases process understanding and reduces thereby the risk of unexpected outcomes. We briefly report on the few examples of existing work on process development with Basidiomycota for single molecule production using statistical and computational methods.

Starting point of process development is usually the development of a suitable medium (carbon-, nitrogen-, phosphate source), inoculation

³ PAT = Process Analytical Technology) of the FDA, see (<https://www.fda.gov/downloads/drugs/guidances/ucm070305.pdf>)

density and other factors, which can be accessed using shake flask experiments (Singh et al., 2017). Classically these factors have been investigated changing one parameter or factor at the time (OFAT) which is time consuming and will not unravel interactions between factors. These experiments are done by removing, replacing or exchanging media components and process parameters. When no prior knowledge about the strain requirement exists, e.g. from literature or preliminary screenings, such experiments can be yet quite helpful to develop an experimental knowledge base for statistical methods for media optimization (Singh et al., 2017).

The investigation of all factors of interest on all levels of interest using a so called “full factorial” experimental design unravels the interactions of lower order (factor influenced by other factor) and also higher order interactions (factor influenced by interaction and interaction influenced by interaction). Such designs deliver the best results in terms of resolution of interactions but are laborious. It requires in case of four factors on two levels $2^4 = 16$ experiments. This number increases fast when the number of factors or the number of levels increases e.g. 5 factors on two levels require $2^5 = 32$ experiments, $2^6 = 64$ experiments..., $2^{10} = 1024$ and so on. To reduce the amount of experiments so called “fractional factorial” experimental designs can be used. These designs allow, under the assumption that in most cases only direct interactions are of importance and higher order interactions can be neglected, a reduction of the number of the experiments. Therefore specifically designed experimental plans are used, which omit those experiments that unravel higher order interactions between factors, at the cost of resolution. This means the lower the amount of experiments the higher the chance to confound first order interactions with higher order ones (Montgomery, 2013; Singh et al., 2017). These plans and the evaluation of the results have to be carefully adapted on the purpose, the required accuracy and also the expected outcome of the experiments. Using specific carefully designed experimental plans, the statistically designed experiments allow for reduction of the number of these experiments and the discovery of interactions of such parameters (Montgomery, 2013; Singh et al., 2017).

A detailed explanation of the underlying statistical principles and possible methodologies is beyond the scope of this review and we refer to Montgomery (2013) for further reading. Usually a predefined experimental design is adapted to the purposes required by adjusting concentration boundaries, central points according to the evaluation method (Mandenius and Brundin, 2008; Montgomery, 2013; Singh et al., 2017). This adjustment is crucial to the outcome of the experiment and requires expert knowledge about the process to be optimized. Usually these experiments are carried out in a certain experimental space and evaluated using statistical software, which allows then for graphical and numerical illustration of results (Mandenius and Brundin, 2008; Montgomery, 2013; Singh et al., 2017). Further optimization from there can be achieved using response surface methods (RSM) and more recent literature also describes and compares the application of artificial neural networks (ANN) and genetic algorithms (GA) to such optimization problems (Mandenius and Brundin, 2008; Montgomery, 2013; Singh et al., 2017; Weuster-Botz, 2000). Since such experiments carried out in shake flasks usually do not consider factors like pH, pO_2 composition of the gas phase effects of stirring and different temperatures they do not necessarily match results obtained in bioreactors (Singh et al., 2017). Therefore, an early transfer into a system which closely resembles that later used for production purposes can be useful although experiments in bioreactors usually reduce the number of throughput tremendously due to the complexity of the setup. Essential for a successful and meaningful experimental outcome when using Basidiomycota is from our experience to standardize all steps as much as possible and try to achieve the highest possible reduction of variance in the single experiments since small variations can have big effects on the experimental output.

There are only a few examples dealing with Basidiomycota and advanced bioprocess engineering. To the best of our knowledge, no data

have been published from Glaxo Smith Kline describing the production process of the retapamulin precursor pleuromutilin with *Clitopilus passeckerianus* CP2. There are a number of reports dealing with the optimization of pleuromutilin with “*Pleurotus mutilus*” (currently valid name: *Clitopilus scyphoides*). Khaouane et al. (2012) used a central composite design and neural network as well as particle swarm optimization to find optimal pleuromutilin production conditions. Their estimated optimal process parameters were stirrer speed 258 vs. 242 rpm, 26.78°C vs. 26.88°C and pH 5.98 vs pH 6.06. The obtained product titers with these changes were 7900 µg/g biomass and 10149 µg/g biomass, respectively, which differed only slightly from the estimated ones. They further modeled the bioprocess using feed forward neural networks

(Khaouane et al., 2013). Lu et al. (2011) used response surface methodology and artificial neural networks to optimize triterpene production (without stating which triterpenes). Malinowska et al. (2009) used a central composite rotational design and response surface methodology to optimize polysaccharide and biomass production.

7. Conclusion and outlook

The current review demonstrates that the Basidiomycota have by far not been exhaustively exploited for novel biologically active molecules. The recent progress in analytical techniques, as well as in genomics, transcriptomics and biotechnological process development now substantially facilitates the evaluation of these fascinating organisms, which show a very high biodiversity and a very interesting ecology. In fact, only very few genera and species have so far been explored systematically for secondary metabolite production and even fewer species were subjected to straightforward biotechnological process development. Many new compounds were recently obtained in the course of collaborations of chemists and biotechnologists with taxonomists who also still dispose of skills in classical microbiology that are often necessary to obtain cultures of the rather slow-growing species that remain totally untapped. Furthermore, there is a great chance to find new molecules in the endemic species from the tropics, which remain widely unstudied in particular in those countries where capacities for mycology yet remain to be built. Interdisciplinary and international collaborations on this topic should therefore be strengthened further in the future.

Acknowledgment

We gratefully acknowledge the help of Prof. Dr. Meike Piepenbring (Frankfurt) who has provided some of the images we used in Fig. 2. Birthe Sandargo is grateful to the Deutsche Forschungsgemeinschaft for a PhD grant. Clara Chepkirui and Lillibeth Chaverra Muñoz are grateful for PhD stipends from the German Academic Exchange Service (DAAD) and Tian Cheng is indebted to the China Scholarship Council (CSC) for a PhD stipend.

References

- Abraham, W.-R., 2001. Bioactive sesquiterpenes produced by fungi: are they useful for humans as well? *Curr. Med. Chem.* 8, 583–606. <https://doi.org/10.2174/0929867013373147>.
- Agger, S., Lopez-Gallego, F., Schmidt-Dannert, C., 2009. Diversity of sesquiterpene syntheses in the basidiomycete *Coprinus cinereus*. *Mol. Microbiol.* 72, 1181–1195. <https://onlinelibrary.wiley.com/doi/full/10.1111/j.1365-2958.2009.06743.x>.
- Alberti, F., Khairudin, K., Venegas, E., Davies, J.A., Hayes, P.M., Willis, C.L., Bailey, A.M., Foster, G.D., 2017. Heterologous expression reveals the biosynthesis of the antibiotic pleuromutilin and generates bioactive semi-synthetic derivatives. *Nat. Commun.* 8 (1), 1831. <https://www.nature.com/article/s/s41467-017-01659-1>.
- Allen, J.W., Merlin, M.D., Jansen, K.L.R., 1991. An ethnomycological review of psychoactive Agarics in Australia and New Zealand. *J. Psychoactive Drugs* 23, 39–69. <https://doi.org/10.1080/02791072.1991.10472573>.
- Anke, T., 1995. The antifungal strobilurins and their possible ecological role. *Canad. J. Botany* 73 (S1), 940–945.
- Anke, T., Oberwinkler, F., 1977. The striatins—new antibiotics from the basidiomycete

- Cyathus striatus* (Huds. ex Pers.) Willd. J. Antibiot. 30, 221–225. <https://doi.org/10.7164/antibiotics.30.22>.
- Antecka, A., Bizukojc, M., Ledakowicz, S., 2016. Modern morphological engineering techniques for improving productivity of filamentous fungi in submerged cultures. World J. Microbiol. Biotechnol. 32, 1–9. <https://doi.org/10.1007/s11274-016-2148-7>.
- Arora, S., Rani, R., Ghosh, S., 2018. Bioreactors in solid state fermentation technology: design, applications and engineering aspects. J. Biotechnol. 269, 16–34. <https://doi.org/10.1016/j.jbiotec.2018.01.010>.
- Ayer, W.A., Taube, H., 1972. Metabolites of *Cyathus helena*. Tetrahedron Lett. 13, 1917–1920. [https://doi.org/10.1016/S0040-4039\(01\)84751-1](https://doi.org/10.1016/S0040-4039(01)84751-1).
- Ayer, W.A., Yoshida, T., Van Schie, D.M., 1978. Diterpenoid metabolites of *Cyathus africanus* Brodie. Can. J. Chem. 56, 2197–2199. <https://doi.org/10.1139/v78-345>.
- Bai, R., Zhang, C., Yin, X., Wie, J., Gao, J., 2015. Striatoids A–F, cyathane diterpenoids with neurotrophic activity from cultures of the fungus *Cyathus striatus*. J. Nat. Prod. 78, 783–788. <https://doi.org/10.1021/np501030r>.
- Bailey, A.M., Alberti, F., Kilaru, S., Collins, C.M., de Mattos-Shipley, K., Hartley, A.J., Hayes, P., Griffin, A., Lazarus, C.M., Cox, R.J., Willis, C.L., O'Dwyer, K., Spence, D.W., Foster, G.D., 2016. Identification and manipulation of the pleuromutilin gene cluster from *Clitopilus passeckerianus* for increased rapid antibiotic production. Sci. Rep. 6, 25202.
- Barrios-González, J., Miranda, R.U., 2010. Biotechnological production and applications of statins. Appl. Microbiol. Biotechnol. 85, 869–883. <https://doi.org/10.1007/s00253-009-2239-6>.
- Baumann, C., Bröckelmann, M., Fugmann, B., Steffan, B., Steglich, W., Sheldrick, W.S., 1993. Haematopodin, an unusual pyrrolquinoline derivative isolated from the fungus *Mycena haematopus*, Agaricales. Angew. Chem. Int. Ed. 32, 1087–1089. <https://doi.org/10.1002/ange.199310871>.
- Berovic, M., Podgornik, B.B., 2016. Cultivation of Medicinal Fungi in Bioreactors. In: Petre, M. (Ed.), Mushroom Biotechnology-Developments and Applications. Elsevier Inc., London, pp. 155.
- Bills, G.F., Gloer, J.B., 2016. Biologically active secondary metabolites from the Fungi. Microbiol. Spectr. 4, 1–32. <https://doi.org/10.1128/microbiolspec.FUNK-0009-2016>.
- Blin, K., Wolf, T., Chevrette, M.G., Lu, X., Schwalen, C.J., Kautsar, S.A., Suarez Duran, H.G., de Los Santos, E.L.C.L.C., Kim, H.U., Nave, M., Dickschat, J.S., Mitchell, D.A., Shelest, E., Breitling, R., Takano, E., Lee, S.Y., Weber, T., Medema, M.H., 2017. antiSMASH 4.0-improvements in chemistry prediction and gene cluster boundary identification. Nucl. Acids Res. 45 (W1), W36–W41. <https://academic.oup.com/nar/article/45/W1/W36/3778252>.
- Boecker, S., Grätz, S., Kerwat, D., Adam, L., Schirmer, D., Richter, L., Schütze, T., Petras, D., Süßmuth, R.D., Meyer, V., 2018. *Aspergillus niger* is a superior expression host for the production of bioactive fungal cyclodepsipeptides. Fungal Biol. Biotechnol. 5, 7. <https://fungalinbiotech.biomedcentral.com/articles/https://doi.org/10.1186/s40694-018-0051-8>.
- Borgström, B., 1988. Mode of action of tetrahydrolipstatin: a derivative of the naturally occurring lipase inhibitor lipstatin. Biochim. Biophys. Acta (BBA)/Lipids Lipid Metab. 962, 308–316. [https://doi.org/10.1016/0005-2760\(88\)90260-3](https://doi.org/10.1016/0005-2760(88)90260-3).
- Braesel, J., Götz, S., Shah, F., Heine, D., Tauber, J., Hertweck, C., Tunlid, A., Stallforth, P., Hoffmeister, D., 2015. Three redundant synthetases secure redox-active pigment production in the basidiomycete *Paxillus involutus*. Chem. Biol. 22, 1325–1334. <https://doi.org/10.1016/j.chembiol.2015.08.016>.
- Brandenburger, E., Gressler, M., Leonhardt, R., Lackner, G., Habel, A., Hertweck, C., Brock, M., Hoffmeister, D., 2017. A highly conserved basidiomycete peptide synthetase produces a trimeric hydroxamate siderophore. Appl. Environ. Microbiol. 83. <https://doi.org/10.1128/AEM.01478-17>.
- Brandt, P., García-Altare, M., Nett, M., Hertweck, C., Hoffmeister, D., 2017. Induced chemical defense of a mushroom by a double-bond-shifting polyene synthase. Angew. Chem. Int. Ed. 56, 5937–5941. <https://doi.org/10.1002/anie.201700767>.
- Büchel, E., Mayer, A., Martini, U., Anke, H., Sterner, O., 1998. Structure elucidation of omphalotin, a cyclic dodecapeptide with potent nematocidal activity isolated from *Omphalotus olearius*. Pesticide Sci. 54, 309–311. [https://doi.org/10.1002/\(SICI\)1096-9063\(199811\)54:3<309::AID-PS834>3.0.CO;2-O](https://doi.org/10.1002/(SICI)1096-9063(199811)54:3<309::AID-PS834>3.0.CO;2-O).
- Caspar, J., Spittler, P., 2015. A free cyanohydrin as arms and armour of *Marasmius or-eades*. ChemBioChem 16, 570–573. <https://doi.org/10.1002/cbic.201402453>.
- Chang, S.-T., 2006a. The world mushroom industry: Trends and technological development. Int. J. Med. Mushrooms 8, 297–314. <https://doi.org/10.1615/IntJMedMushr.v8.i4.10>.
- Chang, S.-T., 2006b. The need for scientific validation of culinary-medicinal mushrooms products. Int. J. Med. Mushrooms 8, 187–195. <https://doi.org/10.1615/IntJMedMushr.v8.i2.100>.
- Chen, H.P., Liu, J.K., 2017. Secondary metabolites from higher fungi. Progr. Chem. Org. Nat. Prod. 106, 1–201.
- Chen, S., Xu, J., Liu, C., Zhu, Y., Nelson, D.R., Zhou, S., Li, C., Wang, L., Guo, X., Sun, Y., Luo, H., Li, Y., Song, J., Henrissat, B., Levasseur, A., Qian, J., Li, J., Luo, X., Shi, L., He, L., Xiang, L., Xu, X., Niu, Y., Li, Q., Han, M.V., Yan, H., Zhang, J., Chen, H., Lv, A., Wang, Z., Liu, M., Schwartz, D.C., Sun, C., 2012. Genome sequence of the model medicinal mushroom *Ganoderma lucidum*. Nat. Commun. 3, 913. <https://doi.org/10.1038/ncomms1923>.
- Chen, C., Tzeng, T., Chen, C., Ni, C., Lee, L., Chen, W., Shiao, Y., Shen, C., 2016. Erinacine S, a rare sesterterpene from the mycelia of *Hericium erinaceus*. J. Nat. Prod. 79, 438–441. <https://doi.org/10.1021/acs.jnatprod.5b00474>.
- Chen, L., Li, Z., Yao, J., Peng, Y., Huang, R., Feng, T., Liu, J., 2017a. Isoindolinone-containing meroterpenoids with α -glucosidase inhibitory activity from mushroom *Hericium caput-medusae*. Fitoterapia. 122, 107–114. <https://doi.org/10.1016/j.fitote.2017.08.017>.
- Chen, L.-L., Wang, P., Chen, H.-Q., Guo, Z.-K., Wang, H., Dai, H.-F., Mei, W.-L., Chen, L.-L., Wang, P., Chen, H.-Q., Guo, Z.-K., Wang, H., Dai, H.-F., Mei, W.-L., 2017b. New furan derivatives from a mangrove-derived endophytic fungus *Corioliopsis* sp. J5. Molecules 22, 261. <https://doi.org/10.3390/molecules22020261>.
- Chen, L., Yao, J., Chen, H., Zhao, Z., Li, Z., Feng, T., Liu, J., 2018. Hericinoids A–C, cyathane diterpenoids from culture of mushroom *Hericium erinaceus*. Phytochem. Lett. 27, 94–100. <https://doi.org/10.1016/j.phytolet.2018.07.006>.
- Chepkirui, C., Richter, C., Matasyoh, J.C., Stadler, M., 2016. Monochlorinated calocerins A–D and 9-oxostrobilurin derivatives from the basidiomycete *Favolaschia calocera*. Phytochemistry 132, 95–101. <https://doi.org/10.1016/j.phytochem.2016.10.001>.
- Chepkirui, C., Matasyoh, J.C., Decock, C., Stadler, M., 2017. Two cytotoxic triterpenes from cultures of a Kenyan *Laetiporus* sp. (Basidiomycota). Phytochem. Lett. 20, 106–110. <https://doi.org/10.1016/j.phytolet.2017.04.009>.
- Chepkirui, C., Cheng, T., Matasyoh, J.C., Decock, C., Stadler, M., 2018a. Phelligrinid L, a new spiro [furan-2,1'-indine]-3-one derivative and other nematocidal and antimicrobial metabolites from *Sanghuangporus* sp. (Hymenochaetaeaceae, Basidiomycota) from Kenya. Phytochemistry Lett. 25, 141–146. <https://doi.org/10.1016/j.phytolet.2018.04.022>.
- Chepkirui, C., Sum, W.C., Cheng, T., Matasyoh, J.C., Decock, C., Stadler, M., 2018b. Aethiopinolones A–E, new pregnenolone type steroids from the East African basidiomycete *Fomitiporia aethiopica*. Molecules 23, 369. <https://doi.org/10.3390/molecules23020369>.
- Cheung, P.C.K., 2008. Overview of mushroom cultivation and utilization as functional foods. In: Mushrooms as Functional Foods. John Wiley & Sons, Inc., Hoboken, USA, pp. 1.
- Cox, R.J., Simpson, T.J., 2009. Chapter 3 fungal type I polyketide synthases. Methods Enzymol. 459, 49–78. [https://doi.org/10.1016/S0076-6879\(09\)04603-5](https://doi.org/10.1016/S0076-6879(09)04603-5).
- Dai, Y.C., Zhou, L.W., Hattori, T., Cao, Y., Stalpers, J.A., Ryvarde, L., Buchanan, P., Oberwinkler, F., Hallenberg, N., Liu, P.G., Wu, S.H., 2017. *Ganoderma lingzhi* (Polyporales, Basidiomycota): the scientific binomial for the widely cultivated medicinal fungus Lingzhi. Mycol. Progr. 16, 1051. <https://doi.org/10.1007/s11557-017-1347-4>.
- Davis, R.M., Sommer, R., Menge, J.A., 2012. Field Guide to Mushrooms of Western North America. University of California Press.
- De Silva, D.D., Rapior, S., Sudarman, E., Stadler, M., Xu, J., Aisyah, S.A., Hyde, K.D., 2013. Bioactive metabolites from macrofungi: Ethnopharmacology, biological activities and chemistry. Fungal Divers. 62, 1–40. <https://doi.org/10.1007/s13225-013-0265-2>.
- Dean, R.A., Talbot, N.J., Ebbole, D.J., Farman, M.L., Mitchell, T.K., Orbach, M.J., Thon, M., Kulkarni, R., Xu, J.-R.R., Pan, H., Read, N.D., Lee, Y.-H.H., Carbone, I., Brown, D., Oh, Y.Y., Donofrio, N., Jeong, J.S., Soanes, D.M., Djonovich, S., Kolomiets, E., Rehmeier, C., Li, W., Harding, M., Kim, S., Lebrun, M.-H.H., Bohnert, H., Coughlan, S., Butler, J., Calvo, S., Ma, L.-J.J., Nicol, R., Purcell, S., Nusbaum, C., Galagan, J.E., Birren, B.W., 2005. The genome sequence of the rice blast fungus *Magnaporthe oryzae*. Nature 434 (7036), 980–986. <https://www.nature.com/articles/nature03449>.
- Ding, J., Li, Z., Feng, T., Liu, J., 2018. Inonotolides A–C, isopimarane diterpenoid lactones from *Inonotus sinensis*. Fitoterapia 127, 410–412. <https://doi.org/10.1016/j.fitote.2018.04.006>.
- Duan, K.-T., Li, Z.-H., Wang, W.-X., Chen, H.-P., Sun, H., Huang, R., Feng, T., Liu, J.-K., 2018. Vibrallactones U–W, three vibrallactone derivatives from cultures of the basidiomycete *Boreostereum vibrans*. J. Asian Nat. Prod. Res. 18, 1–7. <https://doi.org/10.1080/10286620.2018.1461844>.
- Durand, A., 2003. Bioreactor designs for solid state fermentation. Biochem. Eng. J. 13, 113–125. [https://doi.org/10.1016/S1369-703X\(02\)00124-9](https://doi.org/10.1016/S1369-703X(02)00124-9).
- Eddy, S.R., 1998. Profile hidden Markov models. Bioinformatics 14, 755–763. <https://academic.oup.com/bioinformatics/article/14/9/755/259550>.
- Elisashvili, V., 2012. Submerged cultivation of medicinal mushrooms: bioprocesses and products. Int. J. Med. Mushrooms 14, 211–239. <https://doi.org/10.1615/IntJMedMushr.v14.i3>.
- Engels, B., Heinig, U., Grothe, T., Stadler, M., Jennewein, S., 2011. Cloning and characterization of an *Armillaria gallica* cDNA encoding protoilludin synthase, which catalyzes the first committed step in the synthesis of antimicrobial melleolides. J. Biol. Chem. 286, 6871–6878. <http://www.jbc.org/content/286/9/6871.long>.
- Finn, R.D., Coghill, P., Eberhardt, R.Y., Eddy, S.R., Mistry, J., Mitchell, A.L., Potter, S.C., Punta, M., Qureshi, M., Sangrador-Vegas, A., Salazar, G.A., Tate, J., Bateman, A., 2016. The Pfam protein families database: towards a more sustainable future. Nucleic. Acids. Res. 44 (D1), D279–D285. <https://academic.oup.com/nar/article/44/D1/D279/2503120>.
- Flygare, J.A., Pillow, T.H., Aristoff, P., 2013. Antibody-drug conjugates for the treatment of cancer. Chem. Biol. Drug Des. 81, 113–121. <https://doi.org/10.1111/cbdd.12085>.
- Food and Drug Administration-FDA, 2004. Guidance for Industry PAT — A Framework for Innovative Pharmaceutical Development, Manufacturing, and Quality Assurance. <https://www.fda.gov/downloads/drugs/guidances/ucm070305.pdf> (accessed 9.28.18).
- Formenti, L.R., Nørregaard, A., Bolic, A., Hernandez, D.Q., Hagemann, T., Heins, A.L., Larsson, H., Mears, L., Mauricio-Iglesias, M., Krühne, U., Gernaey, K.V., 2014. Challenges in industrial fermentation technology research. Biotechnol. J. 9, 727–738. <https://doi.org/10.1002/biot.201300236>.
- Fricke, J., Blei, F., Hoffmeister, D., 2017. Enzymatic synthesis of psilocybin. Angew. Chem. Int. Ed. 56, 12352–12355. <https://doi.org/10.1002/anie.201705489>.
- Galagan, J.E., Henn, M.R., Ma, L.J., Cuomo, C.A., Birren, B., 2005. Genomics of the fungal kingdom: insights into eukaryotic biology. Genome Res. 15, 1620–1631. <https://genome.cshlp.org/content/15/12/1620.long>.
- Gao, X.-W., Liu, H.-X., Sun, Z.-H., Chen, Y.-C., Tan, Y.-Z., Zhang, W.-M., Gao, X.-W., Liu, H.-X., Sun, Z.-H., Chen, Y.-C., Tan, Y.-Z., Zhang, W.-M., 2016. Secondary metabolites from the deep-sea derived fungus *Acaromyces ingoldii* FS121. Molecules 21, 371.

- <https://doi.org/10.3390/molecules21040371>.
- Gill, M., Steglich, W., 1987. Pigments of fungi (Macromycetes). *Fortschr. Chem. Org. Naturst.* 51, 1–317.
- Goffeau, A., Barrell, B.G., Bussey, H., Davis, R.W., Dujon, B., Feldmann, H., Galibert, F., Hoheisel, J.D., Jacq, C., Johnston, M., Louis, E.J., Mewes, H.W., Murakami, Y., Philippsen, P., Tettelin, H., Oliver, S.G., 1996. Life with 6000 genes. *Science* 274 (5287), 563–567. <http://science.sciencemag.org/content/274/5287/546.long>.
- Gregory, A.F.J., Healy, E.M., Agersborg, H.P.K., Warren, G.H., 1966. Studies on antitumor substances produced by basidiomycetes. *Mycologia* 58, 80–90.
- Grigoriev, I.V., Nikitin, R., Haridas, S., Kuo, A., Ohm, R., Otilar, R., Riley, R., Salamov, A., Zhao, X., Korzeniewski, F., Smirnova, T., Nordberg, H., Dubchak, I., Shabalov, I., 2014. MycoCosm portal: gearing up for 1000 fungal genomes. *Nucl Acids Res.* 42 (Database issue), D699–D704. <https://academic.oup.com/nar/article/42/D1/D699/1058210>.
- Günther, M., Zibek, S., Rupp, S., 2017. Fungal glycolipids as biosurfactants. *Curr. Biotech.* 6, 205–218. <https://doi.org/10.2174/2211550105666160822170256>.
- Haas, B.J., Zeng, Q., Pearson, M.D., Cuomo, C.A., Wortman, J.R., 2011. Approaches to fungal genome annotation. *Mycology* 2 (3), 118–141. <https://www.ncbi.nlm.nih.gov/pmc/articles/PMC3207268/>.
- Hadváry, P., Lengsfeld, H., Wolfer, H., 1988. Inhibition of pancreatic lipase in vitro by the covalent inhibitor tetrahydrolipstatin. *Biochem. J.* 256, 357–361. <https://doi.org/10.1042/bj2560357>.
- Han, J., Li, L., Zhong, J., Tohtatou, Z., Ren, Q., Han, L., Huang, X., Yuan, T., 2016. Officialmalonic acids A–H, lanostane triterpenes from the fruiting bodies of *Fomes officinalis*. *Phytochemistry* 130, 193–200. <https://doi.org/10.1016/j.phytochem.2016.05.004>.
- Hartley, A.J., de Mattos-Shipley, K., Collins, C.M., Kilaru, S., Foster, G.D., Bailey, A.M., 2009. Investigating pleurotulin producing basidiomycetes and related *Clitopilus* species. *FEMS Microbiol. Lett.* 297, 24–30. <https://doi.org/10.1111/j.1574-6968.2009.01656.x>.
- Hashimoto, T., Asakawa, Y., 1998. Biologically active substances of Japanese inedible mushrooms. *Heterocycles* 47, 1067–1110. [https://doi.org/10.3987/REV-97-SR\(N\)6](https://doi.org/10.3987/REV-97-SR(N)6).
- Hawksworth, D.L., 2005. Reflections on changing names and related nomenclatural issues in edible and medicinal mushrooms. *Int. J. Med. Mushrooms* 7, 29–38. <https://doi.org/10.1615/IntJMedMushr.v7.i2.50>.
- He, L., Han, J., Li, B., Huang, L., Ma, K., Chen, Q., Liu, X., Bao, L., Liu, H., 2016. Identification of a new cyathane diterpene that induces mitochondrial and autophagy-dependent apoptosis and shows a potent in vivo anti-colorectal cancer activity. *Eur. J. Med. Chem.* 111, 183–192. <https://doi.org/10.1016/j.ejmech.2016.01.056>.
- Hewald, S., Linne, U., Scherer, M., Marahel, M.A., Kämper, J., Bötker, M., 2006. Identification of a gene cluster for biosynthesis of mannosylerythritol lipids in the basidiomycetous fungus *Ustilago maydis*. *Appl. Environ. Microbiol.* 72, 5469–5477. <https://doi.org/10.1128/AEM.00506-06>.
- Hille, A., Neu, T.R., Hempel, D.C., Horn, H., 2009. Effective diffusivities and mass fluxes in fungal biopellets. *Biotechnol. Bioeng.* 103, 1202–1213. <https://doi.org/10.1002/bit.22351>.
- Hiscox, J., O'Leary, J., Boddy, L., 2018. Fungus wars: basidiomycete battles in wood decay. *Stud. Mycol.* 89, 117–124. <https://doi.org/10.1016/j.simyco.2018.02.003>.
- Hoffmeister, D., Stadler, M., 2015. Fungal natural products - the mushroom perspective. *Front. Microbiol.* 6, 127. <https://doi.org/10.3389/fmicb.2015.00127>.
- Huang, S., Kuo, P., Hwang, T., Chan, Y., Chen, C., Wu, T., 2013. Three novel sesquiterpenes from the mycelium of *Phellinus linteus*. *Tetrahedron Lett.* 54, 3332–3335. <https://doi.org/10.1016/j.tetlet.2013.04.027>.
- Hyde, K.D., Hongsanan, S., Jeewon, R., Bhat, D.J., McKenzie, E.H.C., Jones, E.B.G., Phookamsak, R., Ariyawansa, H.A., Boonmee, S., Zhao, Q., Zhu, L., 2016. Fungal diversity notes 367–491: taxonomic and phylogenetic contributions to fungal taxa. *Fungal Divers* 80, 1–270. <https://doi.org/10.1007/s13225-016-0373-x>.
- Hyde, K.D., Norphanphou, C., Chen, J., Dissanayake, A.J., Doilom, M., Hongsanan, S., Jayawardena, R.S., Jeewon, S., Perera, R.H., Thongbai, B., Wanasinghe, D.N., Wisitrasameewong, K., Tibpromma, S., Stadler, M., 2018. Thailand's amazing diversity – up to 96% of fungi in northern Thailand may be novel. *Fungal Divers.* 93, 215–239. <https://doi.org/10.1007/s13225-018-0415-7>.
- Isaka, M., Srisanoh, U., Choowong, W., Boonpratuang, T., 2011. Sterostreins A–E, new terpenoids from cultures of the basidiomycete *Stereum ostrea* BCC 22955. *Org. Lett.* 13, 4886–4889. <https://doi.org/10.1021/ol2019778>.
- Isaka, M., Yangchum, A., Supothina, S., Boonpratuang, T., Choeyklin, R., Kongsaeere, P., Prabpai, S., 2015. Aromadendrane and cyclofarnesane sesquiterpenoids from cultures of the basidiomycete *Inonotus* sp. BCC 23706. *Phytochemistry* 118, 94–101. <https://doi.org/10.1016/j.phytochem.2015.08.011>.
- Isaka, M., Sappan, M., Supothina, S., Srichomthong, K., Komwijit, S., Boonpratuang, T., 2017. Alliicane sesquiterpenoids from submerged cultures of the basidiomycete *Inonotus* sp. BCC 22670. *Phytochemistry* 136, 175–181. <https://doi.org/10.1016/j.phytochem.2017.01.018>.
- Ishii, H., Fraaije, B.A., Sugiyama, T., Noguchi, K., Nishimura, K., Takeda, T., Amano, T., Hollomon, D.W., 2001. Occurrence and molecular characterization of strobilurin resistance in cucumber powdery mildew and downy mildew. *Phytopathology* 91, 1166–1171. <https://doi.org/10.1094/PHYTO.2001.91.12.1166>.
- Ishikawa, N.K., Fukushi, Y., Yamaji, K., Tahara, S., Takahashi, K., 2001. Antimicrobial cuparene-type sesquiterpenes, enokipodins C and D, from a mycelial culture of *Flammulina velutipes*. *J. Nat. Prod.* 64, 932–934. <https://doi.org/10.1021/np000593r>.
- Jang, Y., Jang, S., Lee, J., Lee, H., Lee, H., Lee, Y.M., Hong, J.-H., Min, M., Lim, Y.W., Kim, C., Kim, J.-J., 2014. Wood decay fungi in South Korea: Polytypes from Seoul. *Mycobiology* 42, 140–146. <https://doi.org/10.5941/MYCO.2014.42.2.140>.
- Jong, S.C., Birmingham, J.M., 1992. Medicinal benefits of the mushroom *Ganoderma*. *Adv. Appl. Microbiol.* 37, 101–134. [https://doi.org/10.1016/S0065-2164\(08\)70253-3](https://doi.org/10.1016/S0065-2164(08)70253-3).
- Julca-Canto, M., Aguilar-Pérez, M.M., Rios, N., Sousa, J.P.B., Cubilla-Rios, L., 2016. Additional new natural products produced by *Leninus strigellus*: a biotechnological approach. *Tetrahedron Lett.* 57, 650–653. <https://doi.org/10.1016/j.tetlet.2015.12.104>.
- Kai, W., Li, B., Weiping, Ke M., Han, J., Wang, W., Yin, W., Liu, H., 2015. Lanostane triterpenes from the Tibetan medicinal mushroom *Ganoderma leucocontextum* and their inhibitory effects on HMG-CoA reductase and α -glucosidase. *J. Nat. Prod.* 78, 1977–1989. <https://doi.org/10.1021/acs.jnatprod.5b00331>.
- Kälvö, D., Menkis, A., Broberg, A., Kälvö, D., Menkis, A., Broberg, A., 2018. Secondary metabolites from the root rot biocontrol fungus *Phlebiopsis gigantea*. *Molecules* 23, 1417. <https://doi.org/10.3390/molecules23061417>.
- Kämper, J., Kahmann, R., Bötker, M., Ma, L.-J.J., Brefort, T., Saville, B.J., Banuett, F., Kronstad, J.W., Gold, S.E., Müller, O., Perlin, M.H., Wösten, H.A., de Vries, R., Ruiz-Herrera, J., Reynaga-Peña, C.G., Snetselaar, K., McCann, M., Pérez-Martín, J., Feldbrügge, M., Basse, C.W., Steinberg, G., Ibeas, J.I., Holloman, W., Guzman, P., Farman, M., Stajich, J.E., Sentandreu, R., González-Prieto, J.M., Kennell, J.C., Molina, L., Schirawski, J., Mendoza-Mendoza, A., Greiling, D., Münch, K., Rössel, N., Scherer, M., Vranes, M., Ladendorf, O., Vincon, V., Fuchs, U., Sandrock, B., Meng, S., Ho, E.C., Cahill, M.J., Boyce, K.J., Klose, J., Klosterman, S.J., Deelstra, H.J., Ortiz-Castellanos, L., Li, W., Sanchez-Alonso, P., Schreier, P.H., Häuser-Hahn, I., Vaupel, M., Koopmann, E., Friedrich, G., Voss, H., Schlüter, T., Margolis, J., Platt, D., Swimmer, C., Gnirke, A., Chen, F., Vysotskaia, V., Mannhaupt, G., Güldener, U., Münsterkötter, M., Haase, D., Oesterheld, M., Mewes, H.-W.W., Mauceli, E.W., DeCaprio, D., Wade, C.M., Butler, J., Young, S., Jaffe, D.B., Calvo, S., Nusbaum, C., Galagan, J., Birren, B.W., 2006. Insights from the genome of the biotrophic fungal plant pathogen *Ustilago maydis*. *Nature*. 444 (7115), 97–101. <https://www.nature.com/articles/nature05248>.
- Kang, H.S., Kim, J.P., 2016. Ostalactones A-C, β - and ϵ -lactones with lipase inhibitory activity from the cultured basidiomycete *Stereum ostrea*. *J. Nat. Prod.* 79, 3148–3151. <https://doi.org/10.1021/acs.jnatprod.6b00647>.
- Karwehl, S., Stadler, M., 2017. Exploitation of fungal biodiversity for discovery of novel antibiotics. *Curr. Top. Microbiol. Immunol.* 398, 303–338. https://doi.org/10.1007/82_2016_496.
- Kavanagh, C.F., 1947. Chemical determination of pleurotin, an antibacterial substance from *Pleurotus griseus*. *Archives Biochem.* 15, 95–98. www.jstor.org/stable/87818.
- Kavanagh, F., Hervey, A., Robbins, W.J., 1951. Antibiotic substances from basidiomycetes: VIII. *Pleurotus mutilis* (Fr.) Sacc. and *Pleurotus passeckerianus* Pilat. *Proc. Natl. Acad. Sci.* 37, 570–574. <https://doi.org/10.1073/pnas.37.9.570>.
- Kavanagh, F., Hervey, A., Robbins, W.J., 1952. Antibiotic substances from basidiomycetes: IX. *Drosophila subatrata* (Batsch Ex Fr.) Quel. *Proc. Natl. Acad. Sci.* 38, 555–560. <http://www.jstor.org/stable/88450>.
- Kawagishi, H., Shimada, A., Shirai, R., Okamoto, K., Ojima, F., Sakamoto, H., Ishiguro, Y., Furukawa, S., 1994. Erinacines A, B and C, strong stimulators of nerve growth factor (NGF)-synthesis, from the mycelia of *Hericium erinaceum*. *Tetrahedron Lett.* 35, 1569–1572. [https://doi.org/10.1016/S0040-4039\(00\)76760-8](https://doi.org/10.1016/S0040-4039(00)76760-8).
- Kersey, P.J., Lawson, D., Birney, E., Derwent, P.S., Haimel, M., Herrero, J., Keenan, S., Kerhornou, A., Koscielny, G., Kähäri, A., Kinsella, R.J., Kulesha, E., Maheswari, U., Megy, K., Nuhn, M., Proctor, G., Staines, D., Valentin, F., Vilella, A.J., Yates, A., 2010. Ensembl Genomes: extending Ensembl across the taxonomic space. *Nucleic Acids Res.* 38 (Database issue), D563–D569. https://academic.oup.com/nar/article/38/suppl_1/D563/3112227.
- Kettering, M., Sterner, O., Anke, T., 2004. Antibiotics in the chemical communication of fungi. *Z. Naturforsch.* 59C, 816–823. <https://doi.org/10.1515/znc-2004-11-1209>.
- Khalidi, N., Seifuddin, F.T., Turner, G., Haft, D., Nierman, W.C., Wolfe, K.H., Fedorova, N.D., 2010. SMURF: Genomic mapping of fungal secondary metabolite clusters. *Fungal Genet. Biol.* 47 (9), 736–741. <https://www.sciencedirect.com/science/article/pii/S1087184510001052?via=ihub>.
- Khaouane, L., Si-Moussa, C., Hanini, S., Benkortbi, O., 2012. Optimization of culture conditions for the production of pleurotulin from *Pleurotus mutilis* using a hybrid method based on central composite design, neural network, and particle swarm optimization. *Biotechnol. Bioprocess Eng.* 17, 1048–1054. <https://doi.org/10.1007/s12257-012-0254-4>.
- Khaouane, L., Benkortbi, O., Hanini, S., Si-Moussa, C., 2013. Modeling of an industrial process of pleurotulin fermentation using feed-forward neural networks. *Braz. J. Chem. Eng.* 30, 105–116. <https://doi.org/10.1590/S0104-66322013000100012>.
- Ki, D.W., Kim, D.W., Hwang, B.S., Lee, S.W., Seok, S.J., Lee, I.K., Yun, B.S., 2015. New antioxidant sesquiterpenes from a culture broth of *Coprinus echinosporus*. *J. Antibiot. (Tokyo)*. <https://doi.org/10.1038/ja.2014.158>.
- Kirk, P.M., Cannon, P.F., Minter, D.W., Stalpers, J.A., 2008. *Insworth & Bisby's Dictionary of the Fungi, 10th ed.* CAB International, Wallingford (Oxon).
- Knauer, S., Biersack, B., Zoldakova, M., Effenberger, K., Milius, W., Schobert, R., 2009. Melanoma-specific ferrocene esters of the fungal cytotoxin illudin M. *Anticancer Drugs* 20, 676. <https://doi.org/10.1097/CAD.0b013e32832e056a>.
- Kobayashi, Y., Asada, Y., Ino, C., Hirotsu, M., 2010. Oral cavity composition containing *Phellinus linteus*-derived sesquiterpene derivatives. *Japanese Patent JP2010047512*.
- Kokubun, T., Scott-Brown, A., Kite, G.C., Simmonds, M.S.J., 2016. Protoilludane, illudane, illudalane, and norilludane sesquiterpenoids from *Granulobasidium vellereum*. *J. Nat. Prod.* 79, 1698–1701. <https://doi.org/10.1021/acs.jnatprod.6b00325>.
- Krull, R., Wucherpfennig, T., Esfandabadi, M.E., Walisko, R., Melzer, G., Hempel, D.C., Kampen, I., Kwade, A., Wittmann, C., 2013. Characterization and control of fungal morphology for improved production performance in biotechnology. *J. Biotechnol.* 163, 112–123. <https://doi.org/10.1016/j.jbiotec.2012.06.024>.
- Kubo, M., Liu, Y., Ishida, M., Harada, K., Fukuyama, Y., 2014. A new spiroindene pigment from the medicinal fungus *Phellinus ribis*. *Chem. Pharm. Bull.* 62, 122–124. <https://doi.org/10.1248/cpb.c13-00722>.
- Kwon, J., Lee, H., Yoon, Y.D., Hwang, B.Y., Guo, Y., Kang, J.S., Kim, J., Lee, D., 2016.

- Lanostane triterpenes isolated from *Antrodia heteromorpha* and their inhibitory effects on RANKL-induced osteoclastogenesis. *J. Nat. Prod.* 79, 1689–1693. <https://doi.org/10.1021/acs.jnatprod.6b00207>.
- Kwon, J., Lee, H., Seo, Y.H., Yun, J., Lee, J., Kwon, H.C., Guo, Y., Kang, J.S., Kim, J.J., Lee, D., 2018. Cytotoxic dirmane sesquiterpenoids isolated from *Perenniporia maackiaae*. *J. Nat. Prod.* 81, 1444–1450. <https://doi.org/10.1021/acs.jnatprod.8b00175>.
- Lackner, G., Bohnert, M., Wick, J., Hoffmeister, D., 2013. Assembly of melleolide antibiotics involves a polyketide synthase with cross-coupling activity. *Chem. Biol.* 20, 1101–1106. <https://doi.org/10.1016/j.chembiol.2013.07.009>.
- Lakornwong, W., Kanokmedhakul, K., Kanokmedhakul, S., Kongsaree, P., Prabpai, S., Sibounnavong, P., Soyontong, K., 2014. Triterpene lactones from cultures of *Ganoderma* sp. KM01. *J. Nat. Prod.* 77, 1545–1553. <https://doi.org/10.1021/np400846k>.
- Lee, S.R., Jung, K., Noh, H.J., Park, Y.J., Lee, H.L., Lee, K.R., Kang, K.S., Kim, K.H., 2015. A new cerebroside from the fruiting bodies of *Hericium erinaceus* and its applicability to cancer treatment. *Bioorg. Med. Chem. Lett.* 25, 5712–5715. <https://doi.org/10.1016/j.bmcl.2015.10.092>.
- Li, W., Zhou, W., Lee, D., Shim, S.H., Kim, Y., Kim, Y.H., 2014. Hericirine, a novel anti-inflammatory alkaloid from *Hericium erinaceum*. *Tetrahedron Lett.* 55, 4086–4090. <https://doi.org/10.1016/j.tetlet.2014.05.117>.
- Li, W., Zhou, W., Cha, J.Y., Kwon, S.U., Baek, K.H., Shim, S.H., Lee, Y.M., Kim, Y.H., 2015. Sterols from *Hericium erinaceum* and their inhibition of TNF- α and NO production in lipopolysaccharide-induced RAW 264.7 cells. *Phytochemistry* 115, 231–238. <https://doi.org/10.1016/j.phytochem.2015.02.021>.
- Li, W., Lee, S.H., Jang, H.D., Ma, J.Y., Kim, Y.H., 2017. Antioxidant and anti-osteoporotic activities of aromatic compounds and sterols from *Hericium erinaceum*. *Molecules* 22, 108. <https://doi.org/10.3390/molecules22010108>.
- Liermann, J.C., Opatz, T., Kolshorn, H., Antelo, L., Hof, C., Anke, H., 2009. Omphalotins E–I, five oxidatively modified nematocidal cyclopeptides from *Omphalotus olearius*. *Eur. J. Org. Chem.* 8, 1256–1262. <https://doi.org/10.1002/ejoc.200801068>.
- Lin, H.C., Hewage, R.T., Lu, Y.C., Chooi, Y.H., 2019. Biosynthesis of bioactive natural products from Basidiomycota. *Organ. Biomol. Chem.* <https://doi.org/10.1039/C8OB02774A>. (in press).
- Lindequist, U., Niedermeyer, T.H.J., Jülich, W.D., 2005. The pharmacological potential of mushrooms. *eCAM* 2, 285–299. <https://doi.org/10.1093/ecam/neh107>.
- Liu, D., 2014. A review of ergostane and cucurbitane triterpenoids of mushroom origin. *Nat. Prod. Res.* 28, 1099–1105. <https://doi.org/10.1080/14786419.2014.900767>.
- Liu, D.Z., Wang, F., Liao, T.G., Tang, J.G., Steglich, W., Zhu, H.J., Liu, J.K., 2006. Vibrallactone: A lipase inhibitor with an unusual fused β -lactone produced by cultures of the basidiomycete *Boreostereum vibrans*. *Org. Lett.* 8, 5749–5752. <https://doi.org/10.1021/ol062307u>.
- Liu, J., Shimizu, K., Tanaka, A., Shinobu, W., Ohnuki, K., Nakamura, T., Kondo, R., 2012. Target proteins of ganoderic acid DM provides clues to various pharmacological mechanisms. *Sci. Rep.* 2, 905. <https://doi.org/10.1038/srep00905>.
- Liu, X., Frydenvang, K., Liu, H., Zhai, L., Chen, M., Olsen, C.E., Christensen, S.B., 2015. Iminolactones from *Schizophyllum commune*. *J. Nat. Prod.* 78, 1165–1168. <https://doi.org/10.1021/np500836y>.
- Loftus, B.J., Fung, E., Roncaglia, P., Rowley, D., Amedeo, P., Bruno, D., Vamathevan, J., Miranda, M., Anderson, I.J., Fraser, J.A., Allen, J.E., Bosdet, I.E., Brent, M.R., Chiu, R., Doering, T.L., Donlin, M.J., D'Souza, C.A., Fox, D.S., Grinberg, V., Fu, J., Fukushima, M., Haas, B.J., Huang, J.C., Janbon, G., Jones, S.J., Koo, H.L., Krzywinski, M.I., Kwon-Chung, J.K., Lengeler, K.B., Maiti, R., Marra, M.A., Marra, R.E., Mathewson, C.A., Mitchell, T.G., Pertele, M., Riggs, F.R., Salzberg, S.L., Schein, J.E., Shvartsbeyn, A., Shin, H., Shumway, M., Specht, C.A., Suh, B.B., Tenney, A., Utterback, T.R., Wickes, B.L., Wortman, J.R., Wye, N.H., Kronstad, J.W., Lodge, J.K., Heitman, J., Davis, R.W., Fraser, C.M., Hyman, R.W., 2005. The genome of the basidiomycetous yeast and human pathogen *Cryptococcus neoformans*. *Science*. 307 (5713), 1321–1324. <http://science.sciencemag.org/content/307/5713/1321.long>.
- Lohmann, J.S., von Nussbaum, M., Brandt, W., Müllbradt, J., Steglich, W., Spiteller, P., 2018a. Rosellin A and B, two red diketopiperazine alkaloids from the mushroom *Mycena rosella*. *Tetrahedron* 74, 5113–5118. <https://doi.org/10.1016/J.TET.2018.06.049>.
- Lohmann, J.S., Wagner, S., von Nussbaum, M., Pulte, A., Steglich, W., Spiteller, P., 2018b. Mycenaflavin A, B, C, and D: Pyrroloquinoline alkaloids from the fruiting bodies of the mushroom *Mycena haematopus*. *Chem. Eur. J.* 24, 8609–8614. <https://doi.org/10.1002/chem.201800235>.
- Lu, Z.M., Lei, J.Y., Xu, H.Y., Shi, J.S., Xu, Z.H., 2011. Optimization of fermentation medium for triterpenoid production from *Antrodia camphorata* ATCC 200183 using artificial intelligence-based techniques. *Appl Microbiol Biotechnol.* 92, 371–379. <https://doi.org/10.1007/s00253-011-3544-4>.
- Luo, H., Hong, S.-Y., Sgambelluri, R.M., Angelos, E., Li, X., Walton, J.D., 2014. Peptide macrocyclization catalyzed by a prolyl oligopeptidase involved in α -amanitin biosynthesis. *Chem. Biol.* 21, 1610–1617. <https://doi.org/10.1016/J.CHEMBIOL.2014.10.015>.
- Luo, Q., Di, L., Dai, W., Lu, Q., Yan, Y., Yang, Z., Li, R., Cheng, Y., 2015a. Applanatumin A, a new dimeric meroterpenoid from *Ganoderma applanatum* that displays potent antifibrotic activity. *Org. Lett.* 17, 1110–1113. <https://doi.org/10.1021/ols03610b>.
- Luo, Q., Wang, X., Dia, L., Yan, Y., Lu, Q., Yang, X., Hu, D., Cheng, Y., 2015b. Isolation and identification of renoprotective substances from the mushroom *Ganoderma lucidum*. *Tetrahedron* 71, 840–845. <https://doi.org/10.1016/j.tet.2014.12.052>.
- Ma, K., Ren, J., Han, J., Bao, L., Li, L., Yao, Y., Sun, C., Zhou, B., Liu, H., 2014. Ganoboninketals A–C, antiplasmodial 3,4-seco-27-norlanostane triterpenes from *Ganoderma boninense*. *Pat. J. Nat. Prod.* 77, 1847–1852. <https://doi.org/10.1021/np5002863>.
- Malinowska, E., Krzyczkowski, W., Herold, F., Lapienis, G., Ślusarczyk, J., Suchocki, P., Kuraś, M., Turło, J., 2009. Biosynthesis of selenium-containing polysaccharides with antioxidant activity in liquid culture of *Hericium erinaceum*. *Enzym. Microb. Technol.* 44, 334–343. <https://doi.org/10.1016/j.enzmictec.2008.12.003>.
- Mandenius, C.-F., Brundin, A., 2008. Biocatalysts and bioreactor design. *Biotechnol. Prog.* 2008 (24), 1191–1203. <https://doi.org/10.1021/bp.67>.
- Martinez, D., Larrondo, L.F., Putnam, N., Gelpke, M.D., Huang, K., Chapman, J., Helfenbein, K.G., Ramaiya, P., Detter, J.C., Larimer, F., Coutinho, P.M., Henrissat, B., Berka, R., Cullen, D., Rokhsar, D., 2004. Genome sequence of the lignocellulose degrading fungus *Phanerochaete chrysosporium* strain RP78. *Nat. Biotechnol.* 22 (6), 695–700. <https://www.nature.com/articles/nbt967>.
- Masahiko, I., Chinthanom, P., Srichomthong, K., Thummarukharoen, T., 2017. Lanostane triterpenoids from fruiting bodies of the bracket fungus *Fomitopsis feei*. *Tetrahedron Lett.* 58, 1758–1761. <https://doi.org/10.1016/j.tetlet.2017.03.066>.
- Mayer, A., Kilian, M., Hoster, B., Sterner, O., Anke, H., 1999. In-vitro and in-vivo nematocidal activities of the cyclic dodecapeptide omphalotin A. *Pesticide. Sci.* 55, 27–30. [https://doi.org/10.1002/\(SICI\)1096-9063\(199901\)55:1<27::AID-PS854>3.0.CO;2-K](https://doi.org/10.1002/(SICI)1096-9063(199901)55:1<27::AID-PS854>3.0.CO;2-K).
- McMorris, T.C., Anchel, M., 1963. The structures of the basidiomycete metabolites illudin S and illudin M. *J. Am. Chem. Soc.* 85, 831–832. <https://doi.org/10.1021/ja00889a052>.
- Mewes, H.W., Frishman, D., Güldener, U., Mannhaupt, G., Mayer, K., Mokrejs, M., Morgenstern, B., Münsterkötter, M., Rudd, S., Weil, B., 2002. MIPS: a database for genomes and protein sequences. *Nucl. Acids Res.* 30 (1), 31–34. <https://www.ncbi.nlm.nih.gov/pmc/articles/PMC99165/>.
- Misiek, M., Braesel, J., Hoffmeister, D., 2011. Characterisation of the ArmA adenylation domain implies a more diverse secondary metabolism in the genus *Armillaria*. *Fungal Biol.* 115 (8), 775–781. <https://www.sciencedirect.com/science/article/pii/S1878614611000985?via%3Dihub>.
- Mohr, K.I., 2017. History of antibiotics research. *Curr. Top. Microbiol. Immunol.* 398, 237–272. https://doi.org/10.1007/822016_499.
- Montgomery, D.C. (Ed.), 2013. *Design and Analysis of Experiments*, Eight ed. John Wiley and Sons, Inc., Hoboken.
- Mudalungu, C.M., Richter, C., Wittstein, K., Abdalla, M.A., Matasyoh, J.C., Stadler, M., Süßmuth, R.D., 2016. Laxitextines A and B, cyathane xyloides from the tropical fungus *Laxitextum incrustatum*. *J. Nat. Prod.* 79, 894–898. <https://doi.org/10.1021/acs.jnatprod.5b00950>.
- Mukherjee, S., Stamatis, D., Bertsch, J., Ovchinnikova, G., Verezemskaja, O., Isbandi, M., Thomas, A.D., Ali, R., Sharma, K., Kyrpidis, N.C., Reddy, T.B., 2017. Genomes Online Database (GOLD) v.6: data updates and feature enhancements. *Nucl. Acids Res.* 45 (D1), D446.
- Muraguchi, H., Umezawa, K., Niikura, M., Yoshida, M., Kozaki, T., Ishii, K., Sakai, K., Shimizu, M., Nakahori, K., Sakamoto, Y., Choi, C., Ngan, C.Y., Lindquist, E., Lipzen, A., Tritt, A., Haridas, S., Barry, K., Grigoriev, I.V., Pukkila, P.J., 2015. Strand-specific RNA-Seq analyses of fruiting body development in *Coprinopsis cinerea*. *PLoS One* 10, e0141586. <https://doi.org/10.1371/journal.pone.0141586>.
- Muraoka, S., Fukamachi, N., Mizumoto, K., Shinozawa, T., 1999. Detection and identification of amanitins in the wood-rotting fungi *Galerina fasciculata* and *Galerina helvoliceps*. *Appl. Environ. Microbiol.* 65, 4207–4210.
- Musoni, M., Destain, J., Thonart, P., Bahama, J.-B., Delvigne, F., 2015. Bioreactor design and implementation strategies for the cultivation of filamentous fungi and the production of fungal metabolites: from traditional methods to engineered systems. *Biotechnol. Agron. Soc. Environ.* 19, 430–442.
- Nofiani, R., de Mattos-Shipley, K., Lebe, K.E., Han, L.-C., Iqbal, Z., Bailey, A.M., Willis, C.L., Simpson, T.J., Cox, R.J., 2018. Strobilurin biosynthesis in basidiomycete fungi. *Nat. Commun.* 9 (1), 3940. <https://www.nature.com/articles/s41467-018-06202-4>.
- Nord, C., Menkis, A., Broberg, A., 2015. Cytotoxic illudane sesquiterpenes from the fungus *Granulobasidium vellereum* (Ellis and Cragin) Jülich. *J. Nat. Prod.* 78, 2559–2564. <https://doi.org/10.1021/acs.jnatprod.5b00500>.
- Novak, R., 2011. Are pleuromutilin antibiotics finally fit for human use? *Ann. NY Acad. Sci.* 1241, 71–81. <https://doi.org/10.1111/j.1749-6632.2011.06219.x>.
- Oh, S.-Y., Lim, Y.W., 2018. Root-associated bacteria influencing mycelial growth of *Tricholoma matsutake* (pine mushroom). *J. Microbiol.* 56, 399–407. <https://doi.org/10.1007/s12275-018-7491-y>.
- Oh, S.Y., Kim, M., Eimes, J.A., Lim, Y.W., 2018. Effect of fruiting body bacteria on the growth of *Tricholoma matsutake* and its related molds. *PLoS One* 13, e0190948. <https://doi.org/10.1371/journal.pone.0190948>.
- Otaka, J., Hashizume, D., Masumoto, Y., Muranaka, A., Uchiyama, M., Koshino, H., Futamura, Y., Osada, H., 2017. Hitoyal A and B, two norsesterpenoids from the basidiomycete *Coprinopsis cinerea*. *Org. Lett.* 19, 4030–4033. <https://doi.org/10.1021/acs.orglett.7b01784>.
- Otaka, J., Shimizu, T., Futamura, Y., Hashizume, D., Osada, H., 2018. Structures and synthesis of hitoyopodins: bioactive aromatic sesquiterpenoids produced by the mushroom *Coprinopsis cinerea*. *Org. Lett.* 20, 6294–6297. <https://doi.org/10.1021/acs.orglett.8b02788>.
- Otto, A., Porzel, A., Schmidt, J., Wessjohann, L., Arnold, N., 2015. A study on the biosynthesis of hygrophorone B12 in the mushroom *Hygrophorus abieticola* reveals an unexpected labelling pattern in the cyclopentenone moiety. *Phytochemistry* 118, 174–180. <https://doi.org/10.1016/j.phytochem.2015.08.018>.
- Otto, A., Porzel, A., Schmidt, J., Brandt, W., Wessjohann, L., Arnold, N., 2016. Structure and absolute configuration of pseudohygrophorones A¹² and B¹², alkyl cyclohexenone derivatives from *Hygrophorus abieticola* (Basidiomycetes). *J. Nat. Prod.* 79, 74–80. <https://doi.org/10.1021/acs.jnatprod.5b00675>.
- Pahl, A., Lutz, C., Hechler, T., 2018. Amanitins and their development as a payload for antibody-drug conjugates. *Drug Discov. Today Technol.* 30, 85–89. <https://doi.org/10.1016/j.ddtec.2018.08.005>.
- Paukner, S., Riedl, R., 2018. Pleuromutilins: potent drugs for resistant bugs—mode of action and resistance. *Cold Spring Harb. Perspect. Med.* 7, a027110. <https://doi.org/10.1101/2018.08.005>.

- 10.1101/cshperspect.a027110.
- Peng, X., Liu, J., Wang, C., Li, X., Shu, Y., Zhou, L., Qiu, M., 2014. Hepatoprotective effects of triterpenoids from *Ganoderma cochlear*. J. Nat. Prod. 77, 737–743. <https://doi.org/10.1021/np400323u>.
- Peters, S., Spitteller, P., 2007. Mycenarubins A and B, Red pyrroloquinoline alkaloids from the mushroom *Mycena rosea*. Eur. J. Org. Chem. 2007, 1571–1576. <https://doi.org/10.1002/ejoc.200600826>.
- Peters, S., Jaeger, R.J.R., Spitteller, P., 2008. Red pyrroloquinoline alkaloids from the mushroom *Mycena haematopus*. Eur. J. Org. Chem. 2008, 319–323. <https://doi.org/10.1002/ejoc.200700739>.
- Pinedo, C., Wang, C.M., Pradier, J.M., Dalmats, B., Choquer, M., Pêcheur, P., Morgant, G., Collado, I.G., Cane, D.E., Viaud, M., 2008. Sesquiterpene synthase from the botrydial biosynthetic gene cluster of the phytopathogen *Botrytis cinerea*. ACS Chem. Biol. 3, 791–801. <https://pubs.acs.org/doi/abs/10.1021/cb800225v>.
- Poulsen, S.M., Karlsson, M., Johansson, L.B., Vester, B., 2001. The pleuromutilin drugs tiamulin and valnemulin bind to the RNA at the peptidyl transferase centre on the ribosome. Mol. Microbiol. 41, 1091–1099. <https://doi.org/10.1046/j.1365-2958.2001.02595.x>.
- Premnath, P., Reck, M., Wittstein, K., Stadler, M., Wagner-Döbler, I., 2018. Screening for inhibitors of mutacin synthesis in *Streptococcus mutans* using fluorescent reporter strains. BMC Microbiol. 8, 24. <https://doi.org/10.1186/s12866-018-1170-3>.
- Prince, W.T., Ivezic-Schoenfeld, Z., Lell, C., Tack, K.J., Novak, R., Obermayr, F., Talbot, G.H., 2013. Phase II clinical study of BC-3781, a pleuromutilin antibiotic, in treatment of patients with acute bacterial skin and skin structure infections. Antimicrob. Agents Chemother. 57, 2087–2094. <https://doi.org/10.1128/AAC.02106-12>.
- Pulte, A., Wagner, S., Kogler, H., Spitteller, P., 2016. Peliathinarubins A and B, red pyrroloquinoline alkaloids from the fruiting bodies of the mushroom *Mycena pelianthina*. J. Nat. Prod. 79, 873–878. <https://doi.org/10.1021/acs.jnatprod.5b00942>.
- Qing, R., Lu, X., Han, J., Aisa, H.J., Yuan, T., 2017. Triterpenoids and phenolics from the fruiting bodies of *Inonotus hispidus* and their activations of melanogenesis and tyrosinase. Chin. Chem. Lett. 28, 1052–1056. <https://doi.org/10.1016/j.ccl.2016.12.010>.
- Quin, M.B., Flynn, C.M., Wawrzyn, G.T., Choudhary, S., Schmidt-Dannert, C., 2013. Mushroom hunting by using bioinformatics: application of a predictive framework facilitates the selective identification of sesquiterpene synthases in Basidiomycota. ChemBiochem. 14, 2480–2491. <https://onlinelibrary.wiley.com/doi/abs/10.1002/cbic.201300349>.
- Quin, M.B., Flynn, C.M., Schmidt-Dannert, C., 2014. Traversing the fungal terpenome. Nat. Prod. Rep. 31, 1449–1473. <https://pubs.rsc.org/en/Content/ArticleLanding/2014/NP/C4NP00075G#divAbstract>.
- Ramm, S., Krawczyk, B., Mühlenweg, A., Poch, A., Mösler, E., Süßmuth, R.D., 2017. A self-sacrificing N-methyltransferase is the precursor of the fungal natural product omphalotin. Angew. Chem. Int. Ed. 56, 9994–9997. <https://doi.org/10.1002/anie.201703488>.
- Rathore, A.S., Bhambure, R., Ghare, V., 2010. Process analytical technology (PAT) for biopharmaceutical products. Anal. Bioanal. Chem. 398, 137–154. <https://doi.org/10.1007/s00216-010-3781-x>.
- Rhind, N., Chen, Z., Yassour, M., Thompson, D.A., Haas, B.J., Habib, N., Wapinski, I., Roy, S., Lin, M.F., Heiman, D.I., Young, S.K., Furuya, K., Guo, Y., Pidoux, A., Chen, H.M., Robbertse, B., Goldberg, J.M., Aoki, K., Bayne, E.H., Berlin, A.M., Desjardins, C.A., Dobbs, E., Dukaj, L., Fan, L., FitzGerald, M.G., French, C., Gujja, S., Hansen, K., Keifenheim, D., Levin, J.Z., Mosher, R.A., Müller, C.A., Pfiffner, J., Priest, M., Russ, C., Smialowska, A., Swoboda, P., Sykes, S.M., Vaughn, M., Vengrova, S., Yoder, R., Zeng, Q., Allshire, R., Baulcombe, D., Birren, B.W., Brown, W., Ekwall, K., Kellis, M., Leatherwood, J., Levin, H., Margalit, H., Martienssen, R., Nieduszynski, C.A., Spatafora, J.W., Friedman, N., Dalggaard, J.Z., Baumann, P., Niki, H., Regev, A., Nusbaum, C., 2011. Comparative functional genomics of the fission yeasts. Science 332 (6032), 930–936. <http://science.sciencemag.org/content/332/6032/930.long>.
- Richter, C., Wittstein, K., Kirk, P.M., Stadler, M., 2015. An assessment of the taxonomy and chemotaxonomy of *Ganoderma*. Fungal Divers 71, 1–15. <https://doi.org/10.1007/s13225-014-0313-6>.
- Richter, C., Helaly, S.E., Thongbai, B., Hyde, K.D., Stadler, S., 2016. Pyristriatins A and B: pyridino-cyathane antibiotics from the basidiomycete *Cyathus cf. striatus*. J. Nat. Prod. 79, 1684–1688. <https://doi.org/10.1021/acs.jnatprod.6b00194>.
- Ríos, L., Andujar, I., Recio, M.C., Giner, R.M., 2012. Lanostanoids from fungi: a group of potential anticancer compounds. J. Nat. Prod. 75, 2016–2044. <https://doi.org/10.1021/np300412h>.
- Robinson, T., Singh, D., Nigam, P., 2001. Solid-state fermentation: a promising microbial technology for secondary metabolite production. Appl. Microbiol. Biotechnol. 55, 284–289. <https://doi.org/10.1007/s002530000565>.
- Rodríguez-Duran, L.V., Torres-Mancera, M.T., Trujillo-Roldán, M.A., Valdez-Cruz, N.A., Favela-Torres, E., Saucedo-Castañeda, G., 2016. Standard instruments for bioprocess analysis and control. In: Larroche, C., Sanromán, M.A., Du, G., Pandey, A. (Eds.), Current Developments in Biotechnology and Bioengineering: Bioprocesses, Bioreactors and Controls. Elsevier, Amsterdam.
- Röttig, M., Medema, M.H., Blin, K., Weber, T., Rausch, C., Kohlbacher, O., 2011. NRPSpredictor2—a web server for predicting NRPS adenylation domain specificity. Nucl. Acids Res. 39 (Web Server issue), W362–367. https://academic.oup.com/nar/article/39/suppl_2/W362/2506164.
- Rupic, Z., Rascher, M., Kanaki, S., Köster, R.W., Stadler, M., Wittstein, K., 2018. Two new cyathane diterpenoids from mycelial cultures of the medicinal mushroom *Hericium erinaceus* and the rare species, *Hericium flagellum*. Int. J. Mol. Sci. 19, 740. <https://doi.org/10.3390/ijms19030740>.
- Sandargo, B., Thongbai, B., Praditya, D., Steinmann, E., Stadler, M., Surup, F., 2018a. Antiviral 4-hydroxypleuroisatin and antimicrobial pleurotin derivatives from cultures of the nematophagous basidiomycete *Hohenbuehelia grisea*. Molecules 23, 2697. <https://doi.org/10.3390/molecules23102697>.
- Sandargo, B., Thongbai, B., Stadler, M., Surup, F., 2018b. Cysteine-derived pleurotin congeners from the nematode-trapping basidiomycete *Hohenbuehelia grisea*. J. Nat. Prod. 81, 286–291. <https://doi.org/10.1021/acs.jnatprod.7b00713>.
- Sauter, H., Steglich, W., Anke, T., 1999. Strobilurins: evolution of a new class of active substances. Angew. Chem. Int. Ed. 38, 1328–1349. [https://doi.org/10.1002/\(SICI\)1521-3773\(19990517\)38:10<1328::AID-ANIE1328>3.0.CO;2-1](https://doi.org/10.1002/(SICI)1521-3773(19990517)38:10<1328::AID-ANIE1328>3.0.CO;2-1).
- Savoie, J.-M., Mata, G., 2016. Growing *Agaricus bisporus* as a contribution to sustainable agricultural development. In: Petre, M. (Ed.), Mushroom Biotechnology—Developments and Applications. Elsevier, London.
- Schmidt-Dannert, C., 2015. Biosynthesis of terpenoid natural products in fungi. Springer. Adv. Biochem. Eng. Biotechnol. 148, 19–61. https://doi.org/10.1007/10_2014_283.
- Schmidt-Dannert, C., 2016. Biocatalytic portfolio of Basidiomycota. Curr. Opin. Chem. Biol. 31, 40–49. <https://doi.org/10.1016/j.cbpa.2016.01.002>.
- Schneider, P., Bouhired, S., Hoffmeister, D., 2008. Characterization of the atromentin biosynthesis genes and enzymes in the homobasidiomycete *Tapinella panuoides*. Fungal Genet. Biol. 45, 1487–1496. <https://doi.org/10.1016/j.fgb.2008.08.009>.
- Schober, R., Biersack, B., Knauer, S., Ocker, M., 2008. Conjugates of the fungal cytotoxin illudin M with improved tumour specificity. Bioorg. Med. Chem. 16, 8592–8597. <https://doi.org/10.1016/j.bmc.2008.08.015>.
- Schober, R., Knauer, S., Seibt, S., Biersack, B., 2011. Anticancer active illudins: recent developments of a potent alkylating compound class. Curr. Med. Chem. 18, 790–807. <https://doi.org/10.2174/092986711794927766>.
- Schrey, H., Harz, P., Müller, F.J., Rupic, Z., Stadler, M., Spitteller, P., 2019. Nematicidal anthranilic acid derivatives from *Laccaria* species. Phytochemistry. <https://doi.org/10.1016/j.phytochem.2019.01.008>. (in press).
- Schöffler, A., 2018. Secondary metabolites of basidiomycetes. In: The Mycota Vo. IX. Physiology and Genetics. Springer, Cham, pp. 231–275. https://doi.org/10.1007/978-3-642-00286-1_10.
- Schügerl, K., 2001. Progress in monitoring, modeling and control of bioprocesses during the last 20 years. J. Biotechnol. 85, 149–173. [https://doi.org/10.1016/S0168-1656\(00\)00361-8](https://doi.org/10.1016/S0168-1656(00)00361-8).
- Schwenk, D., Brandt, P., Blanchette, R.A., Nett, M., Hoffmeister, D., 2016. Unexpected metabolic versatility in a combined fungal fomonoxin/vibrallactone biosynthesis. J. Nat. Prod. 79, 1407–1414. <https://doi.org/10.1021/acs.jnatprod.6b00147>.
- Shah, F., Schwenk, D., Nicolás, C., Persson, P., Hoffmeister, D., Tunlid, A., 2015. Involutin is an Fe³⁺ reductant secreted by the ectomycorrhizal fungus *Paxillus involutus* during Fenton-based decomposition of organic matter. Appl. Environ. Microbiol. 81, 8427–8433. <https://doi.org/10.1128/AEM.02312-15>.
- Singh, V., Haque, S., Niwas, R., Srivastava, A., Pasupuleti, M., Tripathi, C.K.M., 2017. Strategies for fermentation medium optimization: an in-depth review. Front. Microbiol. 7. <https://doi.org/10.3389/fmicb.2016.02087>.
- Smith, J.E., Rowan, N.J., Sullivan, R., 2002. Medicinal mushrooms: a rapidly developing area of biotechnology for cancer therapy and other bioactivities. Biotechnol. Lett. 24, 1839–1845. <https://doi.org/10.1023/A:1020994628109>.
- Solomon, P.W., Alexander, L.W., 1999. Therapeutic effects of substances occurring in higher basidiomycetes mushrooms: a modern perspective. Crit. Rev. Immunol. 19, 65–96. <https://doi.org/10.1615/CritRevImmunol.v19.i1.30>.
- Spitteller, P., 2008. Chemical defence strategies of higher fungi. Chem. Eur. J. 14, 9100–9110. <https://doi.org/10.1002/chem.200800292>.
- Spitteller, P., 2015. Chemical ecology of fungi. Nat. Prod. Rep. 32, 971–993. <https://doi.org/10.1039/c4np00166d>.
- Spoekner, S., Wray, V., Nimtz, M., Lang, S., 1999. Glycolipids of the smut fungus *Ustilago maydis* from cultivation on renewable resources. Appl. Microb. Biotechnol. 51, 33–39. <https://doi.org/10.1007/s002530051359>.
- Stadler, M., Bitzer, J., Köpcke, B., Reinhardt, K., Moldenhauer, J., 2014. Long chain glycolipids useful to avoid perishing or microbial contamination of materials. U.S. Patent Application 14/124,429.
- Stajich, J.E., Harris, T., Brunk, B.P., Brestelli, J., Fischer, S., Harb, O.S., Kissinger, J.C., Li, W., Nayak, V., Pinney, D.F., Stoekert, C.J., Roos, D.S., 2012. FungiDB: an integrated functional genomics database for fungi. Nucl. Acids Res. 40 (Database issue), D675–D681. <https://academic.oup.com/nar/article/40/D1/D675/2903526>.
- Sternor, O., Etzel, W., Mayer, A., Anke, H., 1997. Omphalotin, A new cyclic peptide with potent nematicidal activity from *Omphalotus olearius* II. Isolation and structure determination. Nat. Prod. Lett. 10, 33–38. <https://doi.org/10.1080/10575639708043692>.
- Subramaniyam, R., Vimala, R., 2012. Solid state and submerged fermentation for the production of bioactive substances: a comparative study. Int. J. Sci. Nat. 3, 480–486.
- Sun, Z., Hu, M., Sun, Z., Zhu, N., Yang, J., Ma, G., Xu, X., Sun, Z., Hu, M., Sun, Z., Zhu, N., Yang, J., Ma, G., Xu, X., 2018. Pyrrole alkaloids from the edible mushroom *Phlebotus portentosus* with their bioactive activities. Molecules 23, 1198. <https://doi.org/10.3390/molecules23051198>.
- Surup, F., Thongbai, B., Kuhnert, E., Sudarman, E., Hyde, K.D., Stadler, M., 2015. Deconins A-E: Cuparenic and mevalonic or propionic acid conjugates from the basidiomycete *Deconica* sp. 471. J. Nat. Prod. 78, 934–938. <https://doi.org/10.1021/np501014>.
- Suryanarayan, S., 2003. Current industrial practice in solid state fermentations for secondary metabolite production: the Biocon India experience. Biochem. Eng. J. 13, 189–195. [https://doi.org/10.1016/S1369-703X\(02\)00131-6](https://doi.org/10.1016/S1369-703X(02)00131-6).
- Tanasova, M., Sturla, S.J., 2012. Chemistry and biology of acylfulvenes: sesquiterpene-derived antitumor agents. Chem. Rev. 112, 3578–3610. <https://doi.org/10.1021/cr2001367>.
- Tang, W., Liu, J.W., Zhao, W.M., Wei, D.Z., Zhong, J.J., 2006. Ganoderic acid T from *Ganoderma lucidum* mycelia induces mitochondria mediated apoptosis in lung cancer cells. Life Sci. 80, 205–211. <https://doi.org/10.1016/j.lfs.2006.09.001>.
- Tao, Q.Q., Ma, K., Bao, L., Wang, K., Han, J.J., Zhang, J.X., Huang, C.Y., Liu, H.W., 2016a.

- New sesquiterpenoids from the edible mushroom *Pleurotus cystidiosus* and their inhibitory activity against α -glucosidase and PTP1B. *Fitoterapia* 111, 29–35. <https://doi.org/10.1016/j.fitote.2016.04.007>.
- Tao, Q.Q., Ma, K., Yang, Y., Wang, K., Chen, B., Huang, Y., Han, J., Bao, L., Liu, X.-B., Yang, Z., Yin, W.-B., Liu, H., 2016b. Bioactive sesquiterpenes from the edible mushroom *Flammulina velutipes* and their biosynthetic pathway confirmed by genome analysis and chemical evidence. *J. Org. Chem.* 81, 9867–9877. <https://doi.org/10.1021/acs.joc.6b01971>.
- Tareq, F.S., Hasan, C.M., Rahman, M.M., Hanafi, M.M.M., Colombi Ciacchi, L., Michaelis, M., Harder, T., Tebben, J., Islam, M.T., Spittler, P., 2018. Anti-staphylococcal capilopins from fruiting bodies of *Calobolus radicans*. *J. Nat. Prod.* 81, 400–404. <https://doi.org/10.1021/acs.jnatprod.7b00525>.
- Tauber, J.P., Schroeckh, V., Shelest, E., Brakhage, A.A., Hoffmeister, D., 2016. Bacteria induce pigment formation in the basidiomycete *Serpula lacrymans*. *Environ. Microbiol.* 18, 5218–5227. <https://doi.org/10.1111/1462-2920.13558>.
- Tauber, J.P., Gallegos-Monterrosa, R., Kovács, Á.T., Shelest, E., Hoffmeister, D., 2017. Dissimilar pigment regulation in *Serpula lacrymans* and *Paxillus involutus* during interkingdom interactions. *Microbiology* 164, 65–77. <https://doi.org/10.1099/mic.0.000582>.
- Tederso, L., Bahram, M., Pölme, S., Kóljalg, U., Yorou, N.S., Wijesundera, R., Ruiz, L.V., Vasco-Palacios, A.M., Thu, P.Q., Suija, A., Smith, M.E., Abarenko, K., 2014. Global diversity and geography of soil fungi. *Science* 346, 1256688. <https://doi.org/10.1126/science.1256688>.
- Tello, S.A., Silva-Flores, P., Agerer, R., Halbwachs, H., Beck, A., Persoh, D., 2014. *Hygrocybe virginea* is a systemic endophyte of *Plantago lanceolata*. *Mycol. Prog.* 13, 471–475. <https://doi.org/10.1007/s11557-013-0928-0>.
- Thongbai, B., Rapior, S., Wittstein, K., Hyde, K.D., Stadler, M., 2015. *Hericium erinaceus*, an amazing medicinal mushroom. *Mycol. Prog.* 14, 1–23. <https://doi.org/10.1007/s11557-015-1105-4>.
- Tian, M.-Q., Liu, R., Li, J.-F., Zhang, K.-Q., Li, G.-H., 2016. Three new sesquiterpenes from the fungus *Stereum* sp. YMF1.1686. *Phytochem. Lett.* 15, 186–189. <https://doi.org/10.1016/j.phytol.2016.01.006>.
- Tian, M.-Q., Wu, Q.-L., Wang, X., Zhang, K.-Q., Li, G.-H., 2017. A new compound from *Stereum insignis* CGMCC5.7. *Nat. Prod. Res.* 31, 932–937. <https://doi.org/10.1080/14786419.2016.1255889>.
- Tokai, T., Koshino, H., Takahashi-Ando, N., Sato, M., Fujimura, M., Kimura, M., 2007. *Fusarium* Tri4 encodes a key multifunctional cytochrome P450 monooxygenase for four consecutive oxygenation steps in trichothecene biosynthesis. *Biochem. Biophys. Res. Commun.* 353 (2), 412–417. <https://www.sciencedirect.com/science/article/pii/S0006291X06026866?via%3Dihub>.
- Turlo, J., 2014. The biotechnology of higher fungi - current state and perspectives. *Folia Biol. Oecologica* 10, 49–65. <https://doi.org/10.2478/fobio-2014-0010>.
- Umemura, M., Koike, H., Nagano, N., Ishii, T., Kawano, J., Yamane, N., Kozono, I., Horimoto, K., Shin-ya, K., Asai, K., Yu, J., Bennett, J.W., Machida, M., 2013. MIDDAS-M: motif-independent de novo detection of secondary metabolite gene clusters through the integration of genome sequencing and transcriptome data. *PLoS one* 8 (12), e84028. <https://journals.plos.org/plosone/article?id=10.1371/journal.pone.0084028>.
- Vaghefi, N., Hay, F.S., 2016. Genotypic diversity and resistance to azoxystrobin of *Cercospora beticola* on processing table beet in New York. *Plant Dis.* 100, 1466–1473. <https://doi.org/10.1094/PDIS-09-15-1014-RE>.
- Van Der Velden, N.S., Kälin, N., Helf, M.J., Piel, J., Freeman, M.F., Künzler, M., 2017. Autocatalytic backbone N-methylation in a family of ribosomal peptide natural products. *Nature Chem. Biology* 13, 833–835. <https://doi.org/10.1038/nchembio.2393>.
- Vásquez, R., Rios, N., Solano, G., Cubilla-Rios, L., Vásquez, R., Rios, N., Solano, G., Cubilla-Rios, L., 2018. Lentinoids A–D, new natural products isolated from *Lentinus strigellus*. *Molecules* 23, 773. <https://doi.org/10.3390/molecules23040773>.
- Vayssières, A., Pěničák, A., Felten, J., Kohler, A., Ljung, K., Martin, F., Legué, V., 2015. Development of the poplar *Laccaria bicolor* ectomycorrhiza modifies root auxin metabolism, signaling, and response. *Plant Physiol.* 169, 890–902. <https://doi.org/10.1104/pp.114.255620>.
- Vesth, T.C., Brandl, J., Andersen, M.R., 2016. FunGeneClusterS: predicting fungal gene clusters from genome and transcriptome data. *Synth. Syst. Biotechnol.* 1 (2), 122–129. <https://www.sciencedirect.com/science/article/pii/S2405805X15300017X?via%3Dihub>.
- Wagner, K., Krause, K., David, A., Kai, M., Jung, E.M., Sammer, D., Kniemeyer, O., Boland, W., Kothe, E., 2016. Influence of zygomycete-derived D'orenone on IAA signalling in *Tricholoma*-spruce ectomycorrhiza. *Environ. Microbiol.* 18, 2470–2480. <https://doi.org/10.1111/1462-2920.13160>.
- Walton, J.D., Luo, H., Hallen-Adams, H., 2012. Ribosomally encoded cyclic peptide toxins from mushrooms. In: *Methods in Enzymology*, 1st ed. Elsevier, Amsterdam. <https://doi.org/10.1016/B978-0-12-394291-3.00025-3>.
- Wang, B., Han, J., Xu, W., Chen, Y., Liu, H., 2014. Production of bioactive cyathane diterpenes by a Bird's nest fungus *Cyathus ganuensis* growing on cooked rice. *Food Chem.* 152, 169–176. <https://doi.org/10.1016/j.foodchem.2013.11.137>.
- Wang, K., Bao, L., Qi, Q., Zhao, F., Ma, K., Pei, Y., Liu, H., 2015a. Erinacerins C–L, isoindolin-1-ones with α -glucosidase inhibitory activity from cultures of the medicinal mushroom *Hericium erinaceus*. *J. Nat. Prod.* 78, 146–154. <https://doi.org/10.1021/np5004388>.
- Wang, K., Bao, L., Ma, K., Liu, N., Huang, Y., Ren, J., Wang, W., Liu, W., 2015b. Eight new alkaloids with PTP1B and α -glucosidase inhibitory activities from the medicinal mushroom *Hericium erinaceus*. *Tetrahedron* 71, 9557–9563. <https://doi.org/10.1016/j.tet.2015.10.068>.
- Wang, X.L., Xu, K.P., Long, H.P., Zou, H., Cao, X.Z., Zhang, K., Hu, J.Z., He, S.J., Zhu, G.Z., He, X.A., Xu, P.S., Tan, G.S., 2016. New isoindolinones from the fruiting bodies of *Hericium erinaceum*. *Fitoterapia* 111, 58–65. <https://doi.org/10.1016/j.fitote.2016.04.010>.
- Wang, P.M., Liu, X.B., Dai, Y.C., Horak, E., Steffen, K., Yang, Z.L., 2018a. Phylogeny and species delimitation of *Flammulina*: taxonomic status of winter mushroom in East Asia and a new European species identified using an integrated approach. *Mycol. Progr.* 17, 1013–1030.
- Wang, W.F., Xiao, H., Zhong, J.J., 2018b. Biosynthesis of a ganoderic acid in *Saccharomyces cerevisiae* by expressing a cytochrome P450 gene from *Ganoderma lucidum*. *Biotechnol. Bioeng.* 115, 1842–1854. <https://doi.org/10.1002/bit.26583>.
- Wasser, S.P., 2002. Medicinal mushrooms as a source of antitumor and immunomodulating polysaccharides. *Appl. Microbiol. Biotechnol.* 60, 258–274. <https://doi.org/10.1007/s00253-002-1076-7>.
- Wasser, S.P., 2014. Medicinal mushroom science: current perspectives, advances, evidences, and challenges. *Biomed. J.* 37, 345–356. <https://doi.org/10.4103/2319-4170.138318>.
- Wawrzyn, G.T., Bloch, S.E., Schmidt-Dannert, C., 2012a. Discovery and characterization of terpeneoid biosynthetic pathways of fungi. *Methods Enzymol.* 515, 83–105. <https://www.sciencedirect.com/science/article/pii/B9780123942906000057?via%3Dihub>.
- Wawrzyn, G.T., Quin, M.B., Choudhary, S., Lopez-Gallego, F., Schmidt-Dannert, C., 2012b. Draft genome of *Omphalotus olearius* provides a predictive framework for sesquiterpenoid natural product biosynthesis in Basidiomycota. *Chem. Biol.* 19, 772–783.
- Weete, J.D., Abril, M., Blackwell, M., 2010. Phylogenetic distribution of fungal sterols. *PLoS ONE* 5, 10899–10904. <https://doi.org/10.1371/journal.pone.0010899>.
- Welzel, K., Einfeld, K., Antelo, L., Anke, T., Anke, H., 2005. Characterization of the ferriochrome A biosynthetic gene cluster in the homobasidiomycete *Omphalotus olearius*. *FEMS Microbiol. Letters* 249, 157–163.
- Weuster-Botz, D., 2000. Experimental design for fermentation media development: statistical design or global random search? *J. Biosci. Bioeng.* 90, 473–483. [https://doi.org/10.1016/S1389-1723\(01\)80027](https://doi.org/10.1016/S1389-1723(01)80027).
- Wick, J., Heine, D., Lackner, G., Misiek, M., Tauber, J., Jagusch, H., Hertweck, C., Hoffmeister, D., 2016. A fivefold parallelized biosynthetic process screens chlorination of *Armillaria mellea* (honey mushroom) toxins. *Appl. Environ. Microbiol.* 82, 1196–1204. <https://doi.org/10.1128/AEM.03168-15>.
- Wieland, H., Hallermayer, R., 1941. Über die Giftstoffe des Knollenblätterpilzes. VI. Amanitin, das Hauptgift des Knollenblätterpilzes. *Justus Liebigs Annal. Chem.* 548 (1), 1–8. <https://doi.org/10.1002/jlac.19415480102>.
- Wilkinson, S., 1961. The history and chemistry of muscarine. *Quart. Rev. Chem. Soc.* 15, 153–171. <https://pubs.rsc.org/en/content/articlelanding/1961/qr/q9611500153>.
- Winterberg, B., Uhlmann, S., Linne, U., Lessing, F., Marahiel, M.A., Eichhorn, H., Kahrmann, R., Schirawski, J., 2010. Elucidation of the complete ferriochrome A biosynthetic pathway in *Ustilago maydis*. *Mol. Microbiol.* 75, 1260–1271.
- Wittstein, K., Rascher, M., Ruppig, Z., Löwen, E., Winter, B., Köster, R.W., Stadler, M., 2016. Corallocin A-C, nerve growth and brain-derived neurotrophic factor inducing metabolites from the mushroom *Hericium coralloides*. *J. Nat. Prod.* 79, 2264–2269. <https://doi.org/10.1021/acs.jnatprod.6b00371>.
- Wolf, T., Shelest, V., Nath, N., Shelest, E., 2015. CASSIS and SMIPS: promoter-based prediction of secondary metabolite gene clusters in eukaryotic genomes. *Bioinformatics* 32 (8), 1138–1143.
- Wood, V., Gwilliam, R., Rajandream, M.A.A., Lyne, M., Lyne, R., Stewart, A., Sgouros, J., Peat, N., Hayes, J., Baker, S., Basham, D., Bowman, S., Brooks, K., Brown, D., Brown, S., Chillingworth, T., Churcher, C., Collins, M., Connor, R., Cronin, A., Davis, P., Feltwell, T., Fraser, A., Gentles, S., Goble, A., Hamlin, N., Harris, D., Hidalgo, J., Hodgson, G., Holroyd, S., Hornsby, T., Howarth, S., Huckle, E.J., Hunt, S., Jagels, K., James, K., Jones, L., Jones, M., Leather, S., McDonald, S., McLean, J., Mooney, P., Moule, S., Mungall, K., Murphy, L., Niblett, D., Odell, C., Oliver, K., O'Neil, S., Pearson, D., Quail, M.A., Rabinowitz, E., Rutherford, K., Rutter, S., Saunders, D., Seeger, K., Sharp, S., Skelton, J., Simmonds, M., Squares, S., Stevens, S., Stevens, K., Taylor, K., Taylor, R.G., Tivey, A., Walsh, S., Warren, T., Whitehead, S., Woodward, J., Volckaert, G., Aert, R., Robben, J., Grymonprez, B., Weltjens, I., Vanstreels, E., Rieger, M., Schäfer, M., Müller-Auer, S., Gabel, C., Fuchs, M., Dusterhöft, A., Fritzc, C., Holzer, E., Moestl, D., Hilbert, H., Borzym, K., Langer, I., Beck, A., Lehrach, H., Reinhardt, R., Pohl, T.M., Eger, P., Zimmermann, W., Wedler, H., Wambutt, R., Purnelle, B., Goffeau, A., Cadieu, E., Dréano, S., Gloux, S., 2002. The genome sequence of *Schizosaccharomyces pombe*. *Nature*. 415 (6874), 871–880. <https://www.nature.com/articles/nature724>.
- Wu, G.S., Lu, J.J., Guo, J.J., Li, Y.B., Tan, W., Dang, Y.Y., Zhong, Z.F., Xu, Z.T., Chen, X.P., Wang, Y.T., 2012. Ganoderic acid DM, a natural triterpenoid, induces DNA damage, G1 cell cycle arrest and apoptosis in human breast cancer cells. *Fitoterapia* 83, 408–414. <https://doi.org/10.1016/j.fitote.2011.12.004>.
- Wucherfennig, T., Kiep, K.A., Driouch, H., Wittmann, C., Krull, R., 2010. Morphology and rheology in filamentous cultivations. In: Laskin, A., Gadd, G., Sariaslani, S. (Eds.), *Advances in Applied Microbiology*. Elsevier, Amsterdam, pp. 89–136. [https://doi.org/10.1016/S0065-2164\(10\)72004-9](https://doi.org/10.1016/S0065-2164(10)72004-9).
- Wucherfennig, T., Lakowitz, A., Krull, R., 2013. Comprehension of viscous morphology-Evaluation of fractal and conventional parameters for rheological characterization of *Aspergillus niger* culture broth. *J. Biotechnol.* 163, 124–132. <https://doi.org/10.1016/j.jbiotec.2012.08.027>.
- Xiao, H., Zhong, J., 2016. Production of useful terpenoids by higher-fungus cell factory and synthetic biology approaches. *Trends Biotechnol.* 34, 242–255. <https://doi.org/10.1016/j.tibtech.2015.12.007>.
- Yamane, M., Oikawa, A., Liu, C., Ozaki, T., Takeuchi, I., Tsukagoshi, T., Tokiwano, T., Gomi, K., Minami, H., 2017. Biosynthetic machinery of diterpene pleuromutilin isolated from basidiomycete fungi. *ChemBiochem* 18 (23), 2317–2322. <https://doi.org/10.1002/cbic.201700434>.
- Yang, Y.L., Zhang, S., Ma, K., Xu, Y., Tao, Q., Chen, Y., Chen, J., Guo, S., Ren, J., Wang,

- W., Tao, Y., Yin, W.B., Liu, H., 2017. Discovery and characterization of a new family of diterpene cyclases in bacteria and fungi. *Angew. Chem. Int. Ed. Engl.* 56 (17), 4749–4752. <https://doi.org/10.1002/anie.201700565>.
- Yaoita, Y., Danbara, K., Kikuchi, M., 2005. Two new aromatic compounds from *Hericium erinaceum*. *Chem. Pharm. Bull.* 53, 1202–1203. <https://doi.org/10.1248/cpb.53.1202>.
- Yi, G., Sze, S.H., Thon, M.R., 2007. Identifying clusters of functionally related genes in genomes. *Bioinformatics* 23 (9), 1053–1060. <https://academic.oup.com/bioinformatics/article/23/9/1053/271923>.
- Yin, R., Zhao, Z., Chen, H., Yin, X., Ji, X., Dong, Z., Li, Z., Feng, T., Liu, T., 2014. Tremulane sesquiterpenes from cultures of the fungus *Phellinus igniarius* and their vascular-relaxing activities. *Phytochem. Lett.* 10, 300–303. <https://doi.org/10.1016/j.phytochem.2014.10.019>.
- Ying, Y., Zhang, L., Zhang, X., Bai, H., Liang, D., Ma, L., Shan, W., Zhan, Z., 2014. Terpenoids with alpha-glucosidase inhibitory activity from the submerged culture of *Inonotus obliquus*. *Phytochemistry* 108, 171–176. <https://doi.org/10.1016/j.phytochem.2014.09.022>.
- Yuan, W.M., Gentil, G.D., Budde, A.D., Leong, S.A., 2001. Characterization of the *Ustilago maydis* sid2 gene, encoding a multidomain peptide synthetase in the ferrichrome biosynthetic gene cluster. *J. Bacteriol.* 183, 4040–4051.
- Zhang, P., Chen, Z.H., Hu, J.S., Wei, B.Y., Zhang, Z.G., Hu, W.Q., 2005. Production and characterization of Amanitin toxins from a pure culture of *Amanita exitialis*. *FEMS Microbiol Lett* 252, 223–228. <https://doi.org/10.1016/j.femsle.2005.08.049>.
- Zhang, Z., Zhu, Z., Ma, Z., Li, H., 2009. A molecular mechanism of azoxystrobin resistance in *Penicillium digitatum* UV mutants and a PCR-based assay for detection of azoxystrobin-resistant strains in packing- or store-house isolates. *Int. J. Food Microbiol.* 131, 157–161. <https://doi.org/10.1016/j.ijfoodmicro.2009.02.015>.
- Zhang, Z., Liu, R., Tang, Q., Zhang, J., Yang, Y., Shang, X., 2015. A new diterpene from the fungal mycelia of *Hericium erinaceus*. *Phytochemistry Lett.* 11, 151–156. <https://doi.org/10.1016/j.phytol.2014.12.011>.
- Zhao, F., Mai, Q., Ma, J., Xu, M., Wang, X., Cui, T., Qiu, F., Han, G., 2015. Triterpenoids from *Inonotus obliquus* and their antitumor activities. *Fitoterapia* 101, 34–40. <https://doi.org/10.1016/j.fitote.2014.12.005>.
- Zhao, R.L., Li, G.J., Sánchez-Ramírez, S., Stata, M., Yang, Z.L., Wu, G., Dai, Y.C., He, S.H., Cui, B.K., Zhou, J.L., Wu, F., He, M.Q., Moncalvo, J.M., Hyde, K.D., 2017. A six-gene phylogenetic overview of Basidiomycota and allied phyla with estimated divergence times of higher taxa and a phyloproteomics perspective. *Fungal Divers* 84, 43–74.
- Zhou, F., Nian, Y., Yan, Y., Gong, Y., Luo, Q., Zhang, Y., Hou, B., Zuo, Z., Wang, S., Jiang, H., Yang, J., Cheng, Y., 2015. Two new classes of T-type calcium channel inhibitors with new chemical scaffolds from *Ganoderma cochlear*. *Org. Lett.* 17, 3082–3085. <https://doi.org/10.1021/acs.orglett.5b01353>.
- Zhou, L.W., Vlasák, J., Decock, C., Assefa, A., Stenlid, J., Abate, D., Wu, S.H., Dai, Y.C., 2016a. Global diversity and taxonomy of the *Inonotus linteus* complex (Hymenochaetales, Basidiomycota): *Sanghuangporus* gen. nov., *Tropicoporus ex-centrodendri* and *T. guanacastensis* gen. et spp. nov., and 17 new combinations. *Fungal Divers* 77, 335–347. <https://doi.org/10.1007/s13225-015-0335-8>.
- Zhou, L.-Y., Yu, X.-H., Lu, B., Hua, Y., Zhou, L.-Y., Yu, X.-H., Lu, B., Hua, Y., 2016b. Bioassay-guided isolation of cytotoxic isocryptoporic acids from *Cryptoporus volvatus*. *Molecules* 21, 1692. <https://doi.org/10.3390/molecules21121692>.
- Žnidaršič, P., Pavko, A., 2001. The morphology of filamentous fungi in submerged cultivations as a bioprocess parameter. *Food Technol. Biotechnol.* 39, 237–252.